UNIVERSITAT DE BARCELONA

Study and characterization of the *Drosophila wg*[1]-enhancer in development, regeneration and tumorigenesis

Elena Gracia Latorre

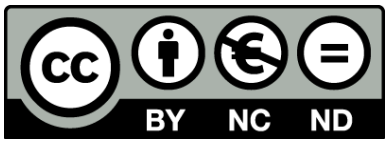

Study and characterization of the *Drosophila wg*^{1}-enhancer in development, regeneration and tumorigenesis

Elena Gracia Latorre

PhD thesis 2023

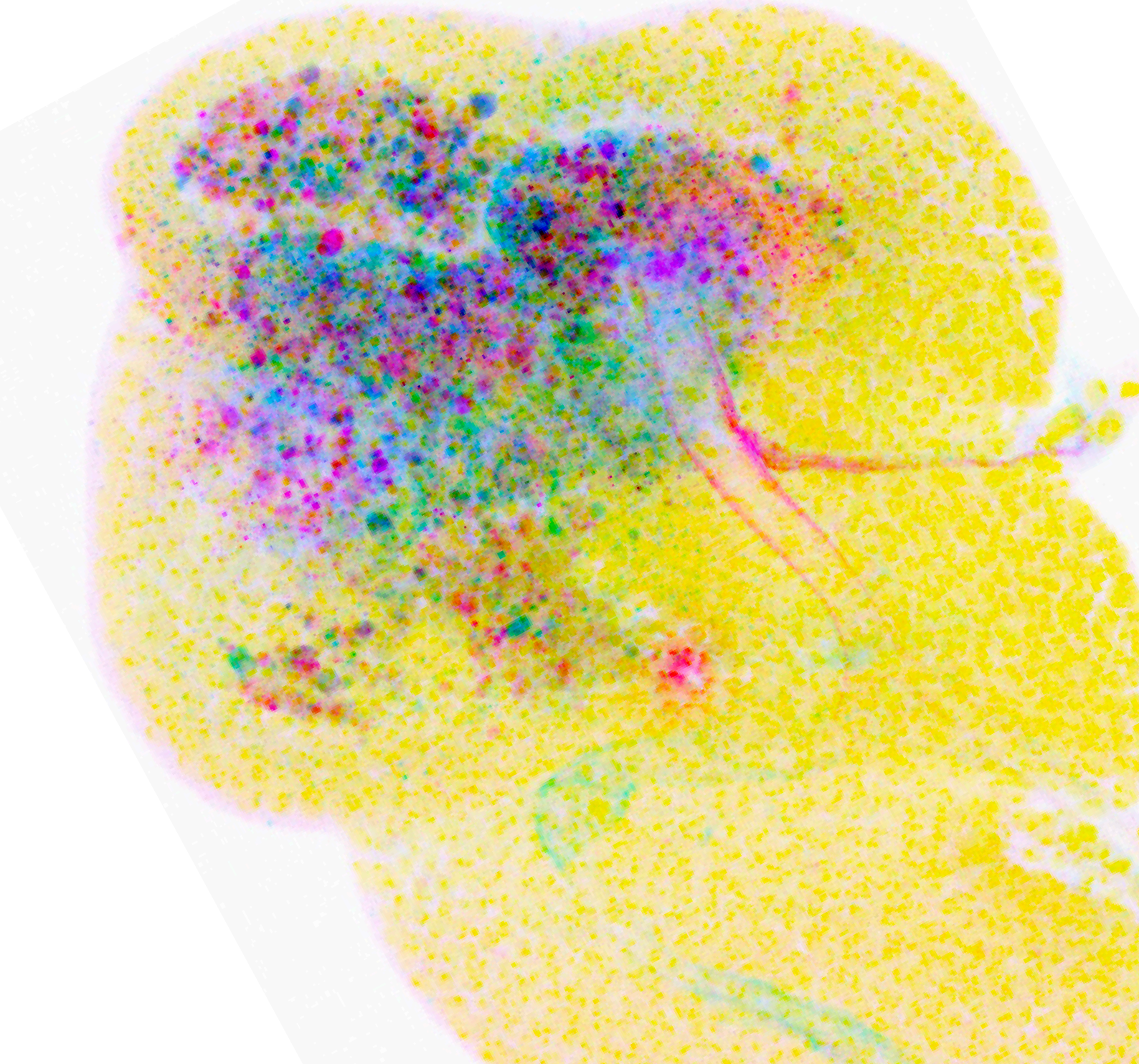

Programa de Doctorat de Genètica
Facultat de Biologia
Universitat de Barcelona

Study and characterization of the *Drosophila wg*[1]-enhancer in development, regeneration and tumorigenesis

Memòria presentada per l'

Elena Gracia Latorre

Per a optar al grau de Doctora per la Universitat de Barcelona

Development and Growth Control Laboratory
Institute for Research in Biomedicine (IRB Barcelona)
Parc científic Barcelona

Barcelona, Abril 2023

Director:	Estudiant:	Tutor:
Dr Marco Milán	Elena Gracia Latorre	Dr Florenci Serras

Acknowledgements

Primer de tot em vull disculpar per que aquest agraïments seran un barreja de llengües que portarà més d'un mal de cap.

Le quiero dar las gracias a Marco por darme la oportunidad de realizar el doctorado en el laboratorio y por ejercer de mentor en todo este proceso. Pero sobre todo le quiero dar las gracias por mostrar tanta humanidad en los momentos tan duros que a veces me ha tocado pasar durante este periodo. También le quiero dar las gracias a Mercedes por escuchar pacientemente todos los dramas de mi vida, aunque muchos de ellos no fueran tan dramáticos como yo me pensaba.

También les quiero dar las gracias a Lara y a Mariana, por estar allí cuando tenía una duda, por escuchar mis problemas y por todos los consejos que me han dado al largo de este proceso.

Amanda, Berta, KG and Aish, I would like to thank you for bringing joy to my last year of PhD. I know many times I was in my own world isolated and stressed, but your histories and dramas have made my last year much easier and more fun. Thank you to remember me that there is life out there. You are wonderful guys.

No soy la persona más fácil del mundo, muchas veces parezco distante y que no me importa el resto del mundo, por eso os quiero dar las gracias a vosotras, Dani, Elena Gaspar y Emma, por que supisteis ver más allá de esto y tener la paciencia de conocerme. Dani, eres una de las personas más fuertes y capaces que he conocido nunca, me has inspirado a ser mejor científica, y de mayor espero ser un poco más como tú. Elena Gaspar, creo que, tanto a ti como a mí, los años del doctorado nos han resultado especialmente duros. Que siempre hayas sido capaz de seguir sonriendo y alegrando a los demás es una capacidad que no todo el mundo tiene, y por eso creo que el futuro te depara cosas maravillosas, por que te lo mereces. Y nuestro pollito Emma, apareciste de sopetón y te convertiste en nuestra amiga. Gracias por todas las cervezas que nos hicimos después de karv, por todas las risas y las historias que nos contamos. Creo que eres una persona muy lista y capaz, la cual podrá hacer lo que quiera. Siempre recordaré vuestros momentos de locura en el lab y de como en los momentos más duros siempre encontrabais la risa.

Y si, lo siento, tienes tu propio parágrafo, por que la verdad es que eres única Elena Fusari. Eres la felicidad hecha persona. Nunca había conocido a nadie como tu que literalmente

llevara la felicidad a los demás. Me alegro mucho de que vinieras al lab y de conocerte, me alegra mucho que te hayas convertido en mi amiga y de que estes presente en mi vida. Eres fantástica y una de las personas más maravillosas que he conocido nunca, de verdad. También quiero darte las gracias por que la mitad de mis stocks los pude hacer por que tu encontraste la virgen que a mí no me salía y sí, aunque suene mal, era necesario mencionar lo de los stocks.

Vili, en tu no només he trobat la meva parella, sinó que també he trobat el meu millor amic (si, ho sé, molt clixé). Moltes gràcies per estar al meu costat en tot aquest procés, gràcies per fer l'imbècil amb mi sempre que ho he necessitat i gràcies per la paciència que has demostrat tenir sempre. T'has convertit en el meu suport més gran i en una persona imprescindible. I si, els teus stats de "wisdom", carisma i constitució són millors que els meus, ho reconec. Mil gràcies per sempre estar aquí, per cuidar-me i per tot el que has compartit amb mi.

També et volia donar les gràcies a tu, mare. T'estic immensament agraïda de què m'hagis ensenyat el valor que té l'educació. Tu vas ser qui va passar hores i hores amb mi ajudant-me a aprendre les taules de multiplicar, les normes gramaticals o llegint "manolito gafotas". Així que moltes gràcies, per què vas establir les bases per a que jo hagi arribat fins aquí. També et vull donar les gràcies per que sé que encara que tu i jo som molt diferents i que moltes vegades em trobes tossuda i molt quadriculada, sempre em demostres lo molt que m'estimes. Jo també t'estimo molt mare.

Moltes gràcies sista per estar sempre allí per mi. Sincerament, no se que hauria fet sense tu. Gràcies, per que de veritat crec que m'has fet més humana, que m'has ajudat a entendre la gent i a comunicar-me millor. Ets la meva germana gran, així que estic una mica esbiaixada, però ets la millor, així de simple i pla. Només em queda dir-te que "simio no hiere a simio, simio protege a simio". Gràcies per que sempre m'has protegit.

Esta tesis está dedicada a mi padre. Pare, tú eras la persona que más ganas tenía que estuviera aquí conmigo en la defensa de mi tesis, pero ya no estás. Perderte ha sido lo más duro que me ha pasado jamás, y muchas veces aún lloro como una niña pequeña cuando pienso en ti. Tu me enseñaste el amor por los libros, me enseñaste la importancia de demostrar nuestro amor a aquellos que queremos, me enseñaste a ser curiosa y me hiciste una persona fuerte e independiente. Te quiero mucho y te echo mucho de menos. Siempre te voy a llevar conmigo.

Abstract

Enhancers are the master regulators of gene expression. Genes rely on them to be differentially expressed in different tissues, developmental time points or contexts. In recent years, it has been reported that although there are enhancers specific for development, many developmental enhancers are "reused" in regeneration and tumorigenesis. One of these enhancers is wg^{1}, the first ever allele described of *wg*. wg^{1} encodes an enhancer that has been described to participate in the development of the wing disc and its deletion induces the emergence of completely functional adult flies that only lack wings. Furthermore, recent reports have shown that wg^{1} is also involved in regeneration and tumorigenesis. However, a controversy exists among the authors on whether wg^{1} contributes to the three processes. Moreover, the lack of a proper characterization of wg^{1} makes it difficult to understand how wg^{1} may differently contribute to these different processes. Hence, the main aim of this thesis is to characterize wg^{1} and to understand how it performs its functions differentially in development, regeneration and tumorigenesis.

In this thesis, we have identified a highly robust regulatory mechanism that ensures the specification and growth of the wing not only during normal development but also under stress conditions. We have narrowed down the long wing-specific enhancer to a 1.8-kb-long enhancer comprising two highly conserved regulatory modules that act in a redundant manner to guarantee the expression of Wingless (Wg) and the specification of the wing. In later stages, the same modules are reused in the injured tissue to trigger Wg and Wnt6 expression and allow regeneration. Besides, the same enhancer is aberrantly used in CIN-induced tumours to drive the expression of Wg and Wnt6 and drive the tumoral overgrowth. Furthermore, we have unveiled that the enhancer mediates these two activities through the use of distinct molecular mechanisms. Whereas Hedgehog, EGFR and JAK/STAT signalling regulate Wg expression in early primordia, JNK activation in injured tissues induce Wg expression to promote compensatory proliferation while driving tissue overgrowth in tumoral tissues.

In addition, in the regenerative tissue, we have detected the presence of a cell population with enlarged nuclei and resistance to cell death inputs. Assessing different hallmarks of senescent we have been able to conclude that these cells are senescent and persist along the regeneration. Besides, we have shown that the establishment of the cell cycle arrest in the senescent population is independent of p53.

Resum

Els potenciadors són els principals reguladors de l'expressió genètica. Els gens depenen d'aquests per ser expressats diferencialment en diferents teixits, punts del desenvolupament o contextos. En els últims anys s'ha vist que tot i que hi ha potenciadors específics per al desenvolupament, molts d'ells són "reutilitzats" en regeneració i càncer. Un d'aquests potenciadors és *wg*^{1}, el primer al·lel descrit de *wg*. *wg*^{1} conté un potenciador que s'ha descrit que participa en el desenvolupament del disc d'ala i que de fet, la seva deleció indueix l'aparició de mosques adultes completament funcionals que només els hi manquen les ales. A més, informes recents han demostrat que el *wg*^{1} també està implicat en regeneració i càncer. No obstant això, existeix controvèrsia entre els autors sobre si *wg*^{1} contribueix realment als tres processos. A més a més, la manca d'una caracterització adequada de *wg*^{1} dificulta entendre com aquest pot contribuir de manera diferent en els tres processos. Per tant, l'objectiu principal d'aquesta tesi és caracteritzar *wg*^{1} i entendre com realitza les seves funcions de forma diferent en el desenvolupament, la regeneració i en els tumors.

En aquesta tesi, hem identificat un mecanisme regulador molt sòlid que garanteix l'especificació i el creixement de l'ala no només durant el desenvolupament normal, sinó també en condicions d'estrès. Hem reduït el potenciador específic de l'ala a una seqüència d'1,8 kb de llarg que comprèn dos mòduls reguladors altament conservats que actuen de manera redundant per garantir l'expressió de Wingless (Wg) i l'especificació de l'ala. En etapes posteriors els mateixos mòduls es reutilitzen en el teixit lesionat per activar l'expressió Wg i Wnt6 i permetre la regeneració. A més, el mateix potenciador s'utilitza de manera aberrant en tumors CIN per induir l'expressió de Wg i Wnt6 e impulsar el creixement tumoral. A més a més, hem descobert que *wg*^{1} executa aquestes dues activitats mitjançant l'ús de diferents mecanismes moleculars. Mentre que la senyalització de Hedgehog, EGFR i JAK/STAT regula l'expressió de Wg en etapes primerenques, l'activació de JNK en teixits lesionats indueix l'expressió de Wg per promoure la proliferació compensatòria mentre que en el teixit tumoral promou el sobrecreixement del teixit.

Per últim, en el teixit regeneratiu hem detectat la presència d'una població cel·lular de nuclis grans resistent als senyals de mort cel·lular. Avaluant diferents marcadors associats a la senescència hem pogut concloure que aquestes cèl·lules són sen senescents i que persisteixen al llarg de la regeneració. A més, hem demostrat que l'establiment de l'aturada del cicle cel·lular en la població senescent és independent de p53.

Table of contents

Figures Index v
Table Index ix
Abbreviations x

Introduction 1

Enhancers, the master regulators of gene expression 4

Transcriptional factors and the activity of enhancers 4
Chromatin accessibility and the activity of enhancers 7
3D genome and the activity of enhancers 9
Enhancers and development 11

***Drosophila* as a model organism 15**

The development of the wing 18

The landscape of the wing disc 18
Embryonic origin of the wing disc 20
Establishment of the Anterior-Posterior axis 22
Wing fate specification vs notum formation: the establishment of the Proximo-Distal axis 23
Establishment of the Dorsal-Ventral axis 25

Regeneration in the wing disc 28

Principles of regeneration 28
Steps of regeneration 28
Chromatin dynamics, enhancers and regeneration 32
Drosophila wing disc as a regeneration model 34
The JNK pathway, the key of regeneration and tumorigenesis 38

Tumorigenesis in the wing disc 42

Chromosomal instability and cancer 42
Enhancers in the context of tumorigenesis 44
Drosophila wing disc as a chromosomal instability tumoral model 47

The *wg*^{1}-enhancer 51

Objectives 55

Results 59

Chapter 1: The *wg*^{1}-enhancer in development 61

wg^{1} deletion induces a wing to notum transformation 61
wg^{1} drives Wg expression and wing fate specification 62
wg^{1} contains an early *wg*-enhancer 68
The molecular mechanisms behind *wg*^{1}-enhancer regulation 69
wg^{1} is positively regulated by Hh and negatively by EGFR 70
JAK/STAT keeps Wg and EGFR apart allowing the specification of the wing 74

Looking for other wing fate specification enhancers 78
wg^{1}-enhancer is composed of two *cis*-regulatory modules 79
Gamma and *Gamma*-590 modules recapitulates *wg*^{1} expression pattern 79
Gamma comprises *wg*^{1} positive regulation while *Beta* acts as a regulator 81
Beta and *Gamma* together are the minimal functional enhancer 84

wg^{1} comprises three enhancers in one 87

Chapter 2: The *wg*^{1} enhancer in regeneration 89

wg^{1} enhancer respond to damage inputs 89
Beta and *Gamma* modules drive regeneration 94
Wnt6 is necessary for wing regeneration 97

Chapter 3: The *wg*^{1} enhancer in tumorigenesis 98

wg^{1} is expressed in CIN tumours 99
Beta and *Gamma* modules drive tumorigenesis 99
Wnt6 contributes to CIN-induced overgrowth 101

Chapter 4: Senescence in the regenerative discs 103

Big nuclei cells are detached from the healthy epithelium 104
Big nuclei cells avoid apoptosis 106

Big nuclei cells are senescent 108
Big nuclei cells are arrested in G2 109
Big nuclei cells secrete molecules from the SASP 111
Big nuclei cells present an abnormal Endoplasmic Reticulum and Golgi apparatus 114
Big nuclei cells present an increased senescence-associated beta-galactosidase activity 116
Big nuclei cells present accumulation of altered mitochondria 118
Big nuclei cells present nuclear changes 120

G2 arrest does not rely on p53 and p21 123
The cell cycle regulates the ability of cells to die 125
Senescent cells persist over time in the regenerating tissue 129

Discussion 131

***wg*^{1}, a key enhancer in the development, regeneration and tumorigenesis of the wing disc 134**

wg^{1} inter-enhancer redundancy 134
wg^{1} intra-enhancer redundancy 136
Developmental regulation of *wg*^{1}-enhancer by Hh, EGFR and JAK/STAT 139
Role of *wg*^{1}-enhancer in regeneration and tumorigenesis 143
wg^{1}, a pleiotropic or tissue-specific enhancer? 147
Role of Wnt6 in regeneration and tumorigenesis 151

Senescence in the regenerating wing disc 152

Stg and Trbl mediate the cell cycle arrest in the senescent population 153
Exploring possible candidates to mediate cell death resistance in the senescent population 154
Senescent cells in the regenerative tissue, a friend or a foe? 158

Conclusions 163

Materials and Methods 167

Fly maintenance, husbandry and *Drosophila* lines 169
Expression of reporter lines in development 171
Tissue injury models 172

Egr-induced cell death 172
Sal-lexA/LexO-rpr cell death induction 172
Ionizing Radiation (IR) treatment 172
DSS feeding protocol 172

Standard induction of CIN 172
Immunohistochemistry 173
DNA synthesis 174
TUNEL 174
SA-β-galactosidase assay 175
Analysis of sequence conservation 175
Generation of lacZ-reporter lines 175
Prediction of transcription factor binding sites 175
Generation of *Gamma* and *Gamma-590* reporters carrying mutations in the Ci binding site 176
Generation of *wg*^{1}-reporter carrying mutations in AP1 binding sites 176
Generation of *wg*^{1}-enhancer deletions with the CRISPR/Cas9 technique 177
Molecular characterisation of deletions 178
Primers 178
Quantifications 181
Wing to notum transformation 181
Adult wing regeneration 181
Wing disc size upon CIN 181
Wingless signal intensity 181
Cleaved-Dcp1 signal intensity 182
Mitotic activity 182
EdU incorporation 182
Gut regeneration 182

Microscopy 183
Statistics and reproducibility 183

References 185

Annex 219

Publications 223

Figures Index

Introduction

Figure 1. An overview of the transcription mechanism. 4

Figure 2. Factors that affect TFs binding to the DNA. 6

Figure 3. Models of chromatin accessibility. 7

Figure 4. Models of enhancer-promoter interaction 10

Figure 5. Models of enhancer redundancy. 12

Figure 6. Enhancer state. 14

Figure 7. *Drosophila* imaginal discs. 15

Figure 8. *Drosophila* genetic tools. 17

Figure 9. Regions and compartments of the wing disc and adult wing. 19

Figure 10. The embryonic origin of the wing disc 21

Figure 11. Establishment of the Anterior-Posterior Axis. 22

Figure 12. Wing fate specification vs notum formation. 24

Figure 13. Disc growth is essential for the wing fate specification. 25

Figure 14. Establishment of the Dorsal-Ventral Axis. 26

Figure 15. Regeneration types. 29

Figure 16. The steps of regeneration. 31

Figure 17. Enhancer accessibility in the regenerative tissue. 34

Figure 18. Overview of regeneration in the *Drosophila* wing disc. 37

Figure 19. The JNK pathway. 40

Figure 20. The hallmarks of cancer. 42

Figure 21. Enhancers in the context of tumorigenesis. 46

Figure 22. CIN derived tumorigenesis in the *Drosophila* wing disc. 49

Results

Chapter 1: The *wg[1]*-enhancer in Development.

Figure 23. *wg[1]* deletion induces a wing loss and a notum duplication. 62

Figure 24. *wg[1]* drives early Wg expression. 64

Figure 25. *wnt6KO* does not recapitulate *Δwg[1]* phenotype. 66

Figure 26. Ectopic Wg, but not Wnt6, is capable to induce an ectopic wing formation. 67

Figure 27. *wg[1]*-enhancer recapitulates early *wg-lacZ* expression. 68

Figure 28. Early Wg regulation by the Hh, EGFR and JAK/STAT pathways. 69

Figure 29. Ci and ETS binding sites are present in the *wg[1]*-enhancer sequence. 70

Figure 30. Hh positively regulates *wg[1]*-enhancer. 72

Figure 31. EGFR pathway repress *wg[1]*-enhancer activity to the ventral area of the disc. 73

Figure 32. JAK/STAT activity is not affected by *wg[1]* deletion. 74

Figure 33. JAK/STAT represses *wg[1]*-enhancer. 75

Figure 34. JAK/STAT depletion induces a notum duplication paired with a vestigial wing. 76

Figure 35. Impact of Hh and JAK/STAT signalling depletion in males. 78

Figure 36. Neither the sequence of *spdFlag* nor *wnt6-intron* recapitulate early Wg expression. 79

Figure 37. *Gamma* module recapitulates *wg[1]* expression pattern. 80

Figure 38. *Gamma* comprises all the regulatory cues while *Beta* only comprises EGFR. 83

Figure 39. *β* and *γ* act together to induce the wing fate specification. 85

Figure 40. *wg[1]* comprises three enhancers in one. 86

Figure 41. Three distinct overlapping enhancers are required for the development of notum, eyes and wings. 87

Chapter 2: The *wg[1]* enhancer in Regeneration.

Figure 42. AP1 binding sites present in the sequence of *wg[1]*-enhancer. 90

Figure 43. *wg*^{1}-enhancer respond to damage inputs. 91

Figure 44. Mutation of AP1 binding sites prevents *wg*^{1} response to damage. 92

Figure 45. *wg*^{1}-enhancer responds to a different damage input. 93

Figure 46. *wg*^{1}-enhancer responds to radiation. 94

Figure 47. Only *Beta* and *Gamma* respond to damage. 95

Figure 48. Deletion of *Beta*, *Gamma* or both reduce Wg expression and the regenerative capacity. 96

Figure 49. Wnt6 depletion impairs regeneration. 97

Chapter 3: The *wg*^{1} enhancer in Tumorigenesis.

Figure 50. *wg*^{1}-enhnacer respond to CIN. 98

Figure 51. Mutation of AP1 binding sites prevents *wg*^{1}*-lacZ* expression. 90

Figure 52. Only *Beta* and *Gamma* respond to CIN. 100

Figure 53. Blockage of JNK activity reduce the expression of the enhancer in CIN tissues. 100

Figure 54. Deletion of *Beta*, *Gamma* or both reduce Wg expression and prevents tumoral growth. 101

Figure 55. Wnt6 depletion impairs tumoral growth. 102

Chapter 4: Senescence in the regenerative discs.

Figure 56. Big nuclei cells are observed in *egr*-expressing discs. 103

Figure 57. Big nuclei cells are detached from the main epithelium. 105

Figure 58. Big nuclei show misslocalized DE-Cadherin. 106

Figure 59. Big nuclei cells are not dying despite showing caspase activity. 107

Figure 60. Hallmarks of Senescence. 108

Figure 61. Big nuclei cells do not proliferate. 109

Figure 62. Big nuclei cells are arrested at G2. 110

Figure 63. Big nuclei cells produce Dilp8. 112

Figure 64. Big nuclei cells express molecules from the SASP. 113

Figure 65. Big nuclei cells present altered exosomes. 114

Figure 66. Big nuclei cells present an altered endoplasmic reticulum. 115

Figure 67. Big nuclei cells present an altered Golgi apparatus. 116

Figure 68. Big nuclei cells present SA-β-gal activity. 117

Figure 69. Big nuclei cells present altered mitochondria. 118

Figure 70. Big nuclei cells present high levels of ROS. 119

Figure 71. Big nuclei cells present nuclear changes. 121

Figure 72. HP1 is not altered in big nuclei cells. 122

Figure 73. Senescent cells do not present p53 activity. 123

Figure 74. Senescent cells do not present *dacapo* expression. 124

Figure 75. Stg and Trbl regulate G2-M cell cycle progression. 125

Figure 76. Cell cycle arrest prevents cell death. 127

Figure 77. Trbl overexpression impairs regeneration. 128

Figure 78. Senescent cells persist over time in the regenerative tissue. 129

Discussion

Figure 79. The developmental enhancer *wg*^{1} is reused in regeneration and tumorigenesis. 133

Figure 80. Upd prevent the activity of En. 142

Figure 81. The Wnt cluster is conserved in other winged species. 147

Figure 82. Enhancers overlapping *wg*^{1}. 148

Figure 83. *wg*^{1} deletion does not affect the regenerative capacity of the gut. 150

Table Index

Results

Table 1. Genomic coordinates. 63

Materials and Methods

Table 2. *Drosophila* lines 169

Table 3. List of primary and secondary antibodies. 173

Table 4. Oligonucleotides 178

Annex

Table Annex 1. Ci and ETS predicted binding sites are present in the wg^{1}-enhancer sequence. 221

Table Annex 2. AP1 predicted binding sites present in the wg^{1}-enhancer sequence. 222

Abbreviations

ΔBRV118: BRV118 deletion
Δwg[1]: wingless[1] deletion
3D: three-dimensional
A/P: Anterior-Posterior
A: anterior
A: Anterior
abd-A: abdominal-A
abd-B: abdominal-B
AiP: apoptosis-induced compensatory proliferation
Aos: Argos
Ap: Apterous
AP-1: Activator Protein-1
Apt: apontic
Ask1: apoptosis signal regulating kinase-1
Bcd: Bicoid
Bcl-2: B-cell lymphoma 2
Bmp: *bone morphogenetic proteins*
bp: base pairs
BS: Binding Sites
Bsk: Basket
CDC: chromosome dosage compensation
c-Dcp-1: cleaved-Death caspase 1
Cdk: Cyclin-dependent kinase
CDKi: Cyclin-dependent kinase inhibitor
Ci: Cubitus interruptus
CIN: Chromosomal Instability
Cyc: Cyclin
D/V: Dorsal-Ventral
D: Dorsal
D: Dorsal
Dcp-1: Death caspase-1
DDR: DNA damage response
DE-Cadh: DE-Cadherin
Diap-1: associated inhibitor of apoptosis 1
Dilp8: *Drosophila* Insulin-like peptide 8
Dist.: Distal
Dl: Delta
Dlg: disc large
Dll: Distal-less
DNA: Deoxyribonucleic acid
Doc: Dorsocross
Dome: Domeless
Dpp: Decapentaplegic
drICE: Death related ICE-like caspase
Dronc: Death regulator Nedd2-like caspase
DRRE: damage-responsive regulatory elements
DSB: double-strand break
DV: Dorso-Ventral
eDRRE: emerging DRRE
EdU: 5-ethynyl-2'-deoxyuridine
EGFR: Epidermal Growth Factor Receptor
egr: *eiger*
En: Engrailed
ER: Endoplasmic Reticulum
eRNA: enhancer RNA

esg: *escargo*t
Esq: *escargot*
Ex: expanded
FACS: Fluorescence-activated Cell Sorting
FasIII: Fasciclin III
ftz-f1: transcription factor 1
Gal80^{ts}*:* thermosensitive allele of Gal80
GC3Ai: GFP Caspase-3-like protease activity indicator
GFP: Green Fluorescent Protein
GFPn::lacZ*:* GFP fused with β-galactosidase
GOF: Gain of function
gRNA: guide RNA
Grnd: Grindelwal
H3K27ac: Histone 3 Lysine 27 acetylation
H3K27me3: Histone 3 Lysine 27 tri-methylation
H3K4me1: Histone 3 Lysine 4 mono-methylation
HDR: homology-directed repair
Hep: Hemipterous
Hh: Hedgehog
hid: *head involution defective*
HP1: heterochromatin protein 1
ICS: intestinal stem cell
iDRRE: increasing DRRE
IL-6: interleukin-6
Iro-C: Iroquois complex
JAK/STAT: Janus Kinase/ Signal Transducer and Activator of Transcription
JNK: c-Jun N-terminal kinase
Lamp1: Lysosomal-associated membrane protein 1
lncRNA: long noncoding RNA
LOF: Loss of function
LP: Limb primordium
M: Mitosis
MAPK: mitogen-activated protein kinase
MiDAS: Mitochondrial dysfunction-associated senescence
Mkk4: MAP kinase kinase 4
MMP1: Matrix metalloproteinase 1
Msn: Misshapen
mtDNA: mitochondria DNA
Mud: Mushroom body defect
MyrT: MyrTomato
N: Notch
NHEJ: non-homologous end-joining
Nub: Nubbin
P/D: Proximo-Distal
P: Posterior
PAM: protospacer adjacent motif
PcG: Polycomb group
pH2Av: phosphorylated histone 2Av
pH3: phosphorylated histone 3
PM: peripodial membrane
Pol-II: RNA Polymerase II
Prox.: Proximal
Ptc: Patched
Puc: Puckered
PWM: Position wight matrix
Rb: Retinoblastoma

RFP: Red Fluorescent Protein
rn: *rotund*
RNA: Ribonucleic acid
RNAi: RNA interference
Rod: *rough deal*
ROS: reactive oxygen species
rpr: reaper
RSRE: regeneration signal response enhancers
SAC: Spindle Assembly Checkpoint
SAHF: senescence-associated heterochromatin foci
sal: *spalt*
SAPS: Senescence-Associated Secretory Phenotype
SA-βgal: senescence-associated beta-galactosidase
Scr: Sex Combs reduced
scrib: scribble
sd: scalloped
SE: Super enhancers
Ser: Serrate
Slrp: Slipper
sna: *snail*
Stg: String
TAD: topologically associating domain
Tak-1: TGFβ-associated kinase 1
TF: Transcriptional Factor
TFBS: Transcriptional Factor Binding Site
TNF- α: Tumour necrosis factor-α
Trbl: Tribbles
TREE: tissue regeneration enhancer elements
Trx: thioredoxin
TrxG: Trithorax group
Tsh: Teashirt
tub-gal80^{ts}: tubulin-gal80^{thermosensitive}
UAS: upstream activating sequences
ubx: *ultrabithorax*
Upd: Unpaired
UPR: Unfolded Protein Response
V: Ventral
vg: *vestigial*
Vn: Vein
Vn::aos: Vein::Argos
Wg: Wingless
wg^{1}: *wingless^{1}*
Wgn: Wengen
Wnd: Wallenda
Yki: Yorki
Zld: Zelda
α: Alpha
β: Beta
β-gal: β-galactosidase
γ: Gamma
γ-590: Gamma-590
γ-630: Gamma-630
γδ: GammaDelta
δ: Delta

Introduction

Most genes play multiple roles in different organs, time points and contexts. In other words, most genes are pleiotropic (Paaby & Rockman, 2013; Stern, 2000). A good example of a pleiotropic gene in *Drosophila* is *wingless* (*wg*), which is required in the early stages of development to ensure the proper segmentation of the embryo, but it is also required in many other tissues, such as the wing disc (reviewed in Bejsovec, 2018; Swarup & Verheyen, 2012). *wg* contributes not only to the development, but also to the regeneration and the tumorigenesis of the wing disc (Dekanty et al., 2012; Smith-Bolton et al., 2009). Genes rely on enhancers to be differentially expressed in different tissues, developmental time points or contexts. Therefore, enhancers are the master regulators of gene expression (Catarino & Stark, 2018; Shlyueva et al., 2014). In recent years, there has been a boom in understanding how enhancers are regulating the specific and precise spatiotemporal expression of a gene. The study of enhancers in development, regeneration and tumorigenesis has allowed us to see that although there are enhancers specific for each of these processes, sometimes the enhancers in development are "reused" in regeneration and tumorigenesis (reviewed in Goldman & Poss, 2020; Hanahan, 2022; Maurya, 2021; Vizcaya-Molina et al., 2020). One of these enhancers is wg^{1}, the first ever allele described of *wg*. wg^{1} encodes an enhancer that has been described to participate in the development of the wing disc and its deletion induces the emergence of completely functional adult flies that only lack wings (Sharma & Chopra, 1976). Although it was thought that wg^{1} only contributed to the development of the wing, recent reports have shown that wg^{1} is also involved in regeneration (Harris et al., 2016) and tumorigenesis (Dekanty et al., 2012). However, a controversy exists among the authors on whether wg^{1} contributes to the three processes. Furthermore, the lack of characterization of wg^{1} makes it difficult to understand how it may differently contribute to the three processes. Hence, the main aim of this thesis is to characterize wg^{1} and to understand how it performs its functions differentially in development, regeneration and tumorigenesis.

Enhancers, the master regulators of gene expression

Gene expression is a tightly regulated process that requires many elements to properly function. The first step of gene expression is the transcription of the genomic DNA to RNA by the RNA Polymerase II (Pol-II). Thus, Pol-II is recruited to the transcription start site (TSS) of a gene, also known as the core promoter, to start the transcription. However, the levels of transcription achieved by the promoter are often weak, and enhancers are required to fully achieve the proper expression levels (Catarino & Stark, 2018). Enhancers, or *cis*-regulatory modules, are non-coding DNA regions that, when bound by tissue-specific transcriptional factors (TFs), increase the level of transcription of an associated gene, independently of their orientation or distance to the gene (Jindal & Farley, 2021; Shlyueva et al., 2014; Spitz & Furlong, 2012). The binding of the TF along with other protein-protein interactions leads to the recruitment of cofactors and the transcriptional machinery that, consequently, activate gene expression (Figure 1)(Clapier et al., 2017; S. Kim & Wysocka, 2023). Other factors such as chromatin accessibility, TFs binding mechanism or the 3D structure of the DNA affects the output of the enhancer activity. Some of these aspects are explored in the following sections.

Transcriptional factors and the activity of enhancers

Enhancers by themselves cannot induce gene expression, they require the binding of TFs to be capable to recruit the transcription machinery and induce gene expression. Thus, to understand enhancers it is essential to understand the role of TFs. In fact, it is the combination of tissue-specific enhancers with the expression of lineage-specific TFs that governs the transcription of linage-specific genes in the proper place and time (Buecker & Wysocka, 2012; S.

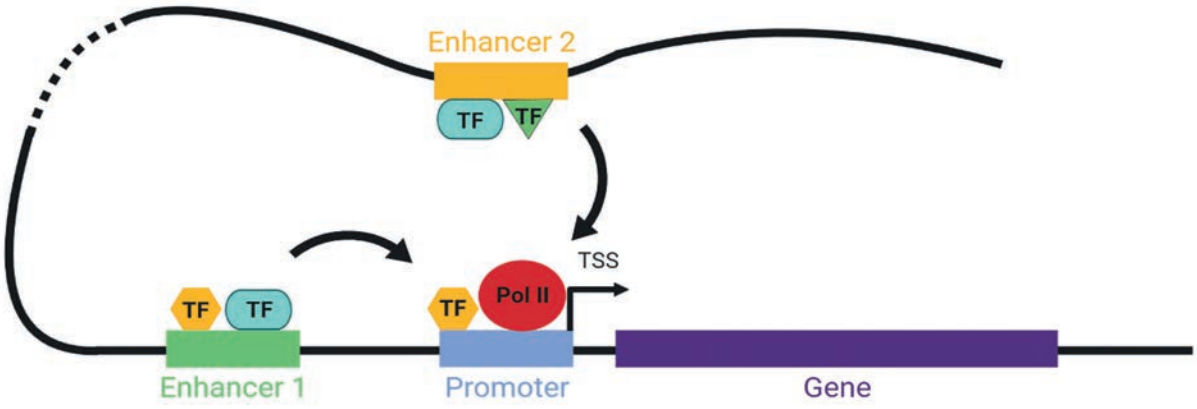

Figure 1. An overview of the transcription mechanism. Cartoon depicting the mechanism by which enhancers regulate gene transcription. Proximal and distal enhancers recruit TFs and cofactors to activate the Pol-II, located in the promoter of the target gene, and activate transcription. The chromatin generates loops to bring enhancers and the promoter into spatial proximity.

Kim & Wysocka, 2023; M. Levine, 2010; Spitz & Furlong, 2012). Furthermore, it is important to note that TFs can act as either as activators or repressors (Reiter et al., 2017).

TFs bind to short DNA sequences within the enhancer called motifs or TF binding sites (TFBSs) that typically are 6-12 bp long. Usually, enhancers contain clusters of different TFBSs. The composition, disposition, orientation and spacing of the TFBSs within the enhancer are called enhancer grammar (Jindal & Farley, 2021; Spitz & Furlong, 2012). These elements are crucial to understand how TFs interact among them and with the DNA. For example, it is known that to ensure proper patterns of expression during development high- and low-affinity binding sites are required. In fact, increasing the affinity of a low-affinity motif leads to ectopic expression or loss of tissue specificity (Farley et al., 2016; Jindal et al., 2022; Lim et al., 2022). It is thought that low-affinity binding sites confer tissue specificity by the necessary interaction with other TFs, ensuring a combinatorial control of gene expression (Berger et al., 2008; Farley et al., 2016). Furthermore, it has been proposed that these differences in affinity could be important also to determine how enhancers respond to different TFs concentrations (S. Kim & Wysocka, 2023). Moreover, the position and the distance between TFs are crucial for these TF-TF interactions to occur. A change in the order or an increase in the spacing can disrupt this interaction and lead to changes in gene expression (Farley et al., 2016; King et al., 2020; Scully et al., 2000; Swanson et al., 2010). Finally, the orientation of the TFs also influences the grammar of the enhancer. Orientation refers to its relative position respect to the TFBS sequence. This determines at which strain the TF binds and, therefore, whether the TF could interact with other proteins or not (Figure 2A)(Cave et al., 2005; Farley et al., 2016; King et al., 2020; Senger et al., 2004).

Three models of how TFs interact with enhancers have been proposed: the enhanceosome model, the billboard model, and the TF-collective model (Jindal & Farley, 2021; Spitz & Furlong, 2012). In the enhanceosome model, the TFs bind to the enhancer in a cooperative manner in specifically arranged motifs. The position of the motifs is fixed and requires the binding of all the TFs are required to allow the activity of the enhancer (Figure 2B)(Merika & Thanos, 2001). However, no developmental enhancer as rigid has been described. By contrast, in the billboard model, each TF is recruited independently via its own binding motif. In this model motif spicing and orientation have little importance and the position of the TFBSs is flexible. In other words, there are no constraints on how TFBSs are arranged, their presence within the enhancer is the only requirement. Besides, it only requires a subset of TFs joining to be active at a given time (Figure 2B)(Arnosti & Kulkarni, 2005). Interestingly, no example of

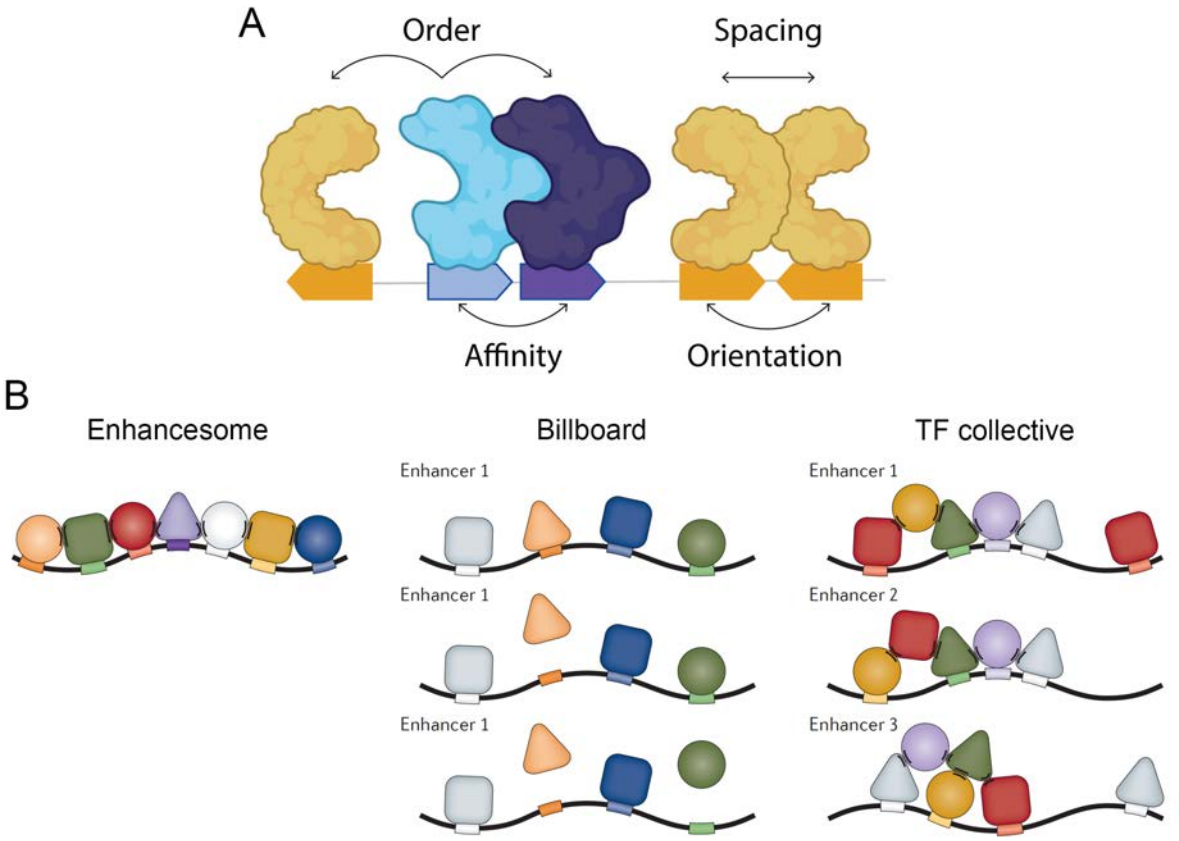

Figure 2. Factors that affect TFs binding to the DNA. A) Cartoon depicting the features of the enhancer grammar. Those features are the order of the TFBS, the binding affinity, the orientation of the TFBS or the spacing between the TFBSs. Adapted from Jindal and Farley, 2021. **B)** Cartoon depicting the three models of TF binding. Enhancesome model (left): all the TFs are essential for the activity of the enhancer. Billboard model (centre): the enhancer only requires a subset of TFs to show activity. TF collective model (right): the TFs binding occurs in the absence of any consistent motif grammar and the same combination of TFs can activate different enhancers. Adapted from Spitz and Furlong 2012.

an active enhancer without any organization of the TFBSs has been described yet. Finally, the TF-collective model proposes that the binding occurs in the absence of any consistent motif grammar. Instead, in this model, the binding of the TFs to the enhancer is based on the protein-protein interactions established among the TFs. The authors propose that the binding is initiated by a TF with a high affinity for its motif. The binding of this TF triggers the recruitment of the rest of the TFs via protein-protein interactions. Consequently, very little or no grammar is required for the binding and, there is extensive grammar flexibility. This makes that the same set of TFs can bind and activate different enhancers (Figure 2B)(Junion et al., 2012). Most probably, in reality, enhancers most likely share aspects of all three models, being the two first models in the extremes of the spectrum.

Nevertheless, a binding event does not always correlate with activity. In fact, there is evidence that there are non-functional bindings that most probably simply reflect the accessibility of chromatin (John et al., 2011; X. Y. Li et al., 2011) .

Chromatin accessibility and the activity of enhancers

Enhancer activity and gene expression are tightly linked to DNA accessibility. DNA is organized in the chromatin, a dynamic structure that helps to pack the entire genome and at the same time regulates gene transcription by regulating the accessibility to enhancers and genes. The basic unit of the chromatin is the nucleosome, a group of 8 histones that is wrapped by 147bp of DNA, acting as a gatekeeper to prevent binding from TFs and other molecules. Hence, active enhancers, that require the binding of the TFs, are found in accessible or nucleosome-depleted areas (Klemm et al., 2019; Venkatesh & Workman, 2015). Hence, chromatin accessibility is a key requirement for gene regulation, making this a tightly regulated process with many players.

One of the main players involved in chromatin accessibility are the TFs. Three different models have been proposed for how these proteins contribute to chromatin accessibility: collaborative binding, TF-TF interactions and pioneer factors (Reiter et al., 2017). The collaborative model postulates a passive collaboration between the TFs that leads to the eviction of the nucleosome by mass action. According to this model, contacts among the TFs are not required, and it relays in the affinity of the TFs by their motifs (Figure 3A)(Deplancke et al., 2016). On the contrary, in the TF-TF interaction model, direct protein-protein interactions are necessary

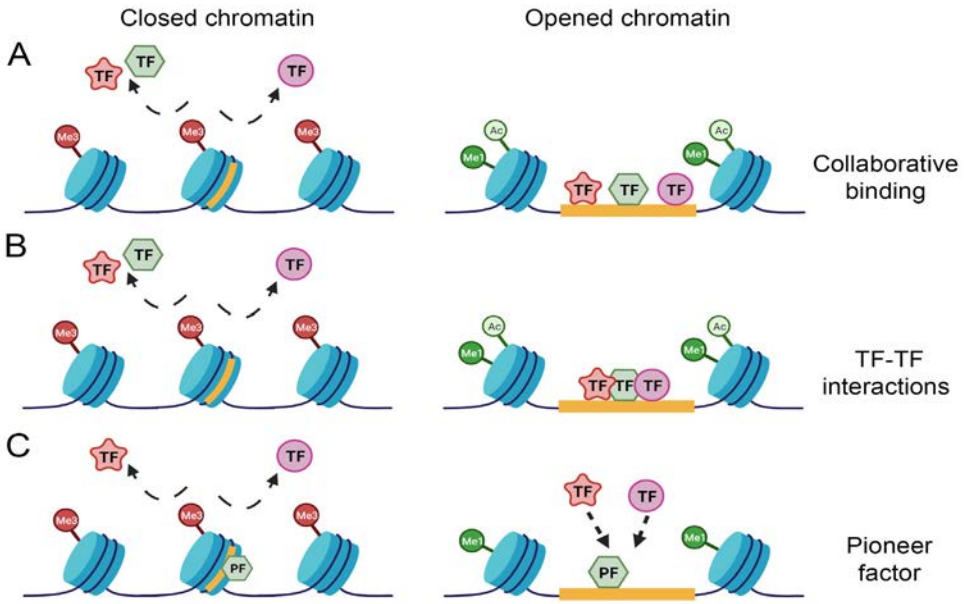

Figure 3. Models of chromatin accessibility. Cartoon depicting the three models of chromatin accessibility. **A)** Collaborative binding model. The TFs passively act together to induce the eviction of the nucleosome. **B)** TF-TF interaction model. Interactions between the TFs are necessary to induce the eviction of the nucleosome. **C)** Pioneer factor model. The binding of the pioneer factor to the closed chromatin forces the nucleosome eviction, allowing the binding of other TFs.

to evict the nucleosome and allow the binding to the DNA. It is thought that the interaction between TFs can increase their affinity for their motifs (Figure 3B)(Reiter et al., 2017). Finally, in the pioneer factor model is proposed that there are specific TFs capable of directly binding to closed chromatin on their own, inducing the eviction of the nucleosome and then allowing the binding of other TFs (Figure 3C)(Zaret & Carroll, 2011). Independently of the model, the binding of TFs to the enhancer leads to the recruitment of different cofactors. Among these cofactors, several contribute to the post-transcriptional modification of the histone tails and the recruitment of chromatin remodelers that contribute to accessing the chromatin and maintaining it open (Catarino & Stark, 2018; Reiter et al., 2017).

Modification of histone tails is a key element of enhancer activity. As mentioned above, some of the cofactors recruited by the TFs have the capacity to modify the neighbouring histones. These modifications directly impact the binding between the histone core and the DNA, thus facilitating or hindering the eviction of the nucleosome (Clapier et al., 2017; S. Kim & Wysocka, 2023; P. Zhang et al., 2016). The most common histone modifications found in enhancers are three: the acetylation of H3K27 (H3K27ac), the mono-methylation of H3K4 (H3K4me1) and the tri-methylation of H3K27 (H3K27me3). While active enhancers are marked with H3K27ac and H3K4me1, silenced chromatin is associated with H3K27me3 (Y. Guo et al., 2021; P. Zhang et al., 2016). Whereas it is clear that histone acetylation loosens the interaction between the DNA and the nucleosome, hence facilitating nucleosome eviction (Zentner & Henikoff, 2013), the function of methylation on chromatin accessibility seems more diverse. In fact, histone methylation does not affect the interaction between the histone core and the DNA. Instead, methylation interferes with the interactions between chromatin-binding factors and DNA (P. Zhang et al., 2016). In addition, histones can also undergo phosphorylation, adenosine diphosphate (ADP)-ribosylation, glycosylation, sumoylation, and ubiquitylation. These modifications can interfere with the interaction between the nucleosome and the DNA or even target nucleosomes for its degradation (reviewed in P. Zhang et al., 2016).

Another crucial regulator of chromatin status and gene activity are the chromatin remodelers. The chromatin remodelers can be separated into two main groups with antagonistic functions. On one side, there is the Polycomb group (PcG), formed by the Polycomb Repressive Complexes PCR1 and PCR2, that impairs the accessibility to the chromatin, therefore, repressing gene expression. On the other side the Trithorax group (TrxG), which comprises a more diverse group of protein complexes such as the SWI/SNF or the ISWI complex, is in charge to mediate chromatin accessibility and allow gene expression. Therefore, these proteins or-

chestrate the expression of key developmental genes by modifying the chromatin accessibility, thus determining the fate, identity and plasticity of cells (Katsuyama & Paro, 2011; Kuroda et al., 2020; Schuettengruber et al., 2017). However, we cannot think about histone remodelers as independent elements from histone modifications. In fact, there is increasing evidence that these two mechanisms interact with each other (Swygert & Peterson, 2014; P. Zhang et al., 2016). A good example is the NuRD remodeler complex, which has been demonstrated that can mediate gene repression by its ATP-dependent chromatin remodelling capacity or by its histone deacetylase activities (Tong et al., 1998; Xue et al., 1998). Another example is PRC2, which catalyses the tri-methylation of H3K27 (Aranda et al., 2015).

In addition to all these mechanisms, accessibility to the DNA is also mediated by its methylation state. CpG islands, regions of the DNA with a high concentration of phosphate-linked cytosine-guanine pairs than the rest of the genome, are mostly found in promoters (Saxonov et al., 2005). Methylation of these islands mediates gene expression by impairing the binding of TFs and other transcriptional activators (Moore et al., 2013). On the contrary, the role of methylation in enhancers is not that clear. On average, enhancers present a lower CpG density and present variable levels of methylation. Nevertheless, studies suggest that active enhancers on average display less methylation than silenced enhancers, suggesting the existence of mechanisms to keep active enhancers methylation free (reviewed in Angeloni & Bogdanovic, 2019).

3D genome and the activity of enhancers

For many years the genome has been understood and studied as a linear molecule. Therefore, it was difficult to understand how enhancers, which can be hundreds to tens of thousands of bases away from the promoter, could regulate gene expression. Consequently, in recent years the flat perspective of the genome has been left behind and it has begun to be understood and studied as a three-dimensional (3D) structure. These studies have shown that DNA 3D structure is another layer in the regulation of gene expression (Rowley & Corces, 2016).

The genome is organised in large regulatory domains called topologically associating domains (TADs), which bring distant regulatory elements to proximity (Dekker & Heard, 2015; Dixon et al., 2016). Moreover, these domains are separated by topological boundaries that favour the interaction of enhancers with genes within the domain and limit interactions with genes from other TADs (Figure 4A)(Dixon et al., 2012; Sexton et al., 2012; Symmons et al.,

2014). These boundaries are often delineated by a cluster of binding motifs for insulator proteins such as the CTCF (Phillips-Cremins et al., 2013; Rao et al., 2014).

Four different models have been proposed to explain how enhancers and promoters reach each other: the looping model, the tracking (or scanning or sliding) model, the linking (or changing) model and the conformational model. The looping model is the clear favourite. This model proposes that two regions of DNA (e.g., the enhancer and the promoter) would physically interact with each other via protein-protein interaction, triggering the formation of a loop. In this model, Cohesin extrudes the loop of chromatin until its advance is blocked by CTCF bound to DNA. Therefore, during the extrusion, the promoter and the enhancer are brought to close spatial proximity (Figure 4B). On the other hand, the tracking model proposes that upon its binding at the enhancer, the Pol-II begins to pull the enhancer towards the promoter following the DNA sequence. It is proposed that along the way the Pol-II would

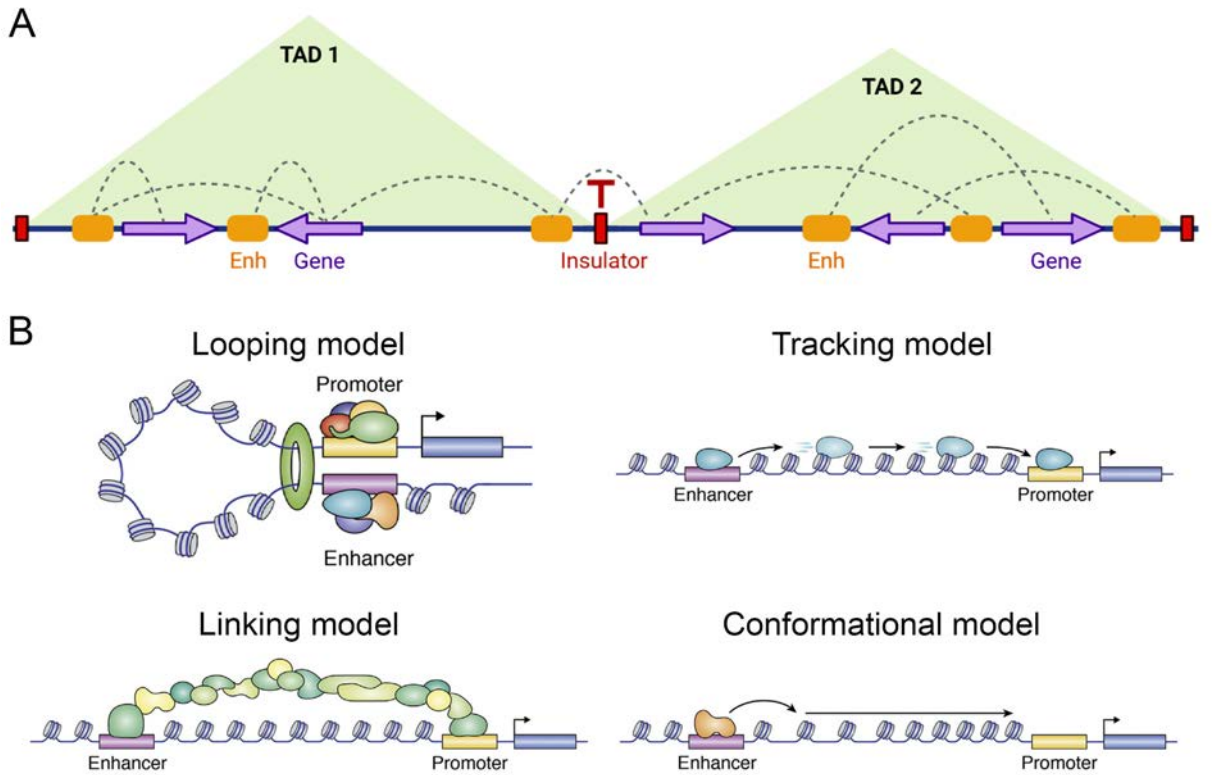

Figure 4. Models of enhancer-promoter interaction. A) Representation of enhancer-promoter interactions (dashed grey lines) that occur within a TAD domain. The interactions between enhancers and promoters from different TADs are prevented by the insulators. **B)** Models of enhancer-promoter interactions. In the looping model (up-left) Choesin induces the formation of a loop that brings the enhancer and promoter to close spatial proximity. Tracking model (up-right): the Pol-II binds to an enhancer and tracks along chromatin pulling the chromatin with it. Linking model (down-left): the TFs and other proteins bind to form a bridge that links the enhancer with the promoter. Conformational model (down-right): chromatin conformational changes initiated in the enhancer propagate to the promoter, leading to alterations in the promoter structure. Adapted from Popay and Dixon, 2022.

transcribe parts of the DNA sequence, thus giving rise to long noncoding RNAs (lncRNAs; Figure 4B). On the contrary, the linking model proposes that a protein-protein oligomers bridge is formed between the enhancer and the promoter (Figure 4B). Finally, the conformational model proposes that conformational changes in the chromatin initiated in the enhancer are propagated from it to the promoter, leading to alterations in the promoter structure such as the decompaction of chromatin (Figure 4B)(Furlong & Levine, 2018; Popay & Dixon, 2022).

As stated above, TADs encourage the formation of contacts between enhancers and promoters within the same TAD while blocking the interaction between enhancers and promoters of different TADs. Indeed, disruption of TADs boundaries can result in ectopic enhancer-promoter interactions that lead to aberrant gene expression (Franke et al., 2016; Hanssen et al., 2017). Nevertheless, some studies have shown that TAD disruption does not always lead to ectopic enhancer-promoter interactions and that upon global loss of TADs, minor changes in gene expression have been detected (Despang et al., 2019; Kubo et al., 2021; Nora et al., 2017). This suggests the existence of other mechanisms to guarantee the correct interaction between enhancers and promoters. Indeed, in the same TAD different enhancers and promoters can be found and many times enhancers skip the closest promoter to specifically interact with more distal promoters (Akalin et al., 2009; Kikuta et al., 2007), supporting the idea of additional regulatory mechanisms. In fact, it has been described that the presence of tethering elements, CpG islands or specific interactions between TFs, among other mechanisms, favour specific enhancer-promoter interactions (reviewed in Pachano et al., 2022).

Enhancers and development

Developmental biology is the study of how a heterogeneous organism is formed; how a single cell, the zygote, can generate a whole organism with different cells and organs with utterly different gene expression profiles, shapes, sizes and functionality. One of the most fascinating facts is that all these different cells, with very different functions and gene expression profiles, share the same genome. As introduced above, is the combinatory effect of cell type-specific TFs, enhancers, chromatin landscape and 3D genome structure that determines the different gene expression profiles of all these cells. Many genes present expression in different organs or tissues and at different developmental stages (Paaby & Rockman, 2013; Stern, 2000). Hence, most genes present different enhancers to be capable to induce its different patterns of expression in the different tissues and developmental stages. Therefore, each enhancer regulates a specific spatiotemporal activity of the gene (Spitz & Furlong, 2012). Nev-

ertheless, it has been described that some enhancers present a very similar spatiotemporal activity, showing redundant interactions within the genome (Figure 5A and B)(Kvon et al., 2021; Osterwalder et al., 2018; Zeitlinger et al., 2007). Five kinds of interaction between enhancers have been proposed: redundant, synergetic, additive, subadditive and repressive interactions (S. Kim & Wysocka, 2023; Kvon et al., 2021; Spitz & Furlong, 2012). In redundant interactions, each enhancer by itself can cover the transcription activation required. In other words, the deletion of one of the enhancers does not show a strong effect on the level of transcription, because the other enhancer is capable to cover it. It is necessary to delete both enhancers to see a drastic reduction of the transcriptional levels (Figure 5C). On the contrary, in synergetic or additive interactions it is essential for the contribution of all the enhancers to achieve a full level of transcription. In these two models, each enhancer has a certain level of activity on its own. The difference between both interactions is that in the additive interaction, the activity of enhancers adds, while in the synergetic interaction, the combination of both enhancers

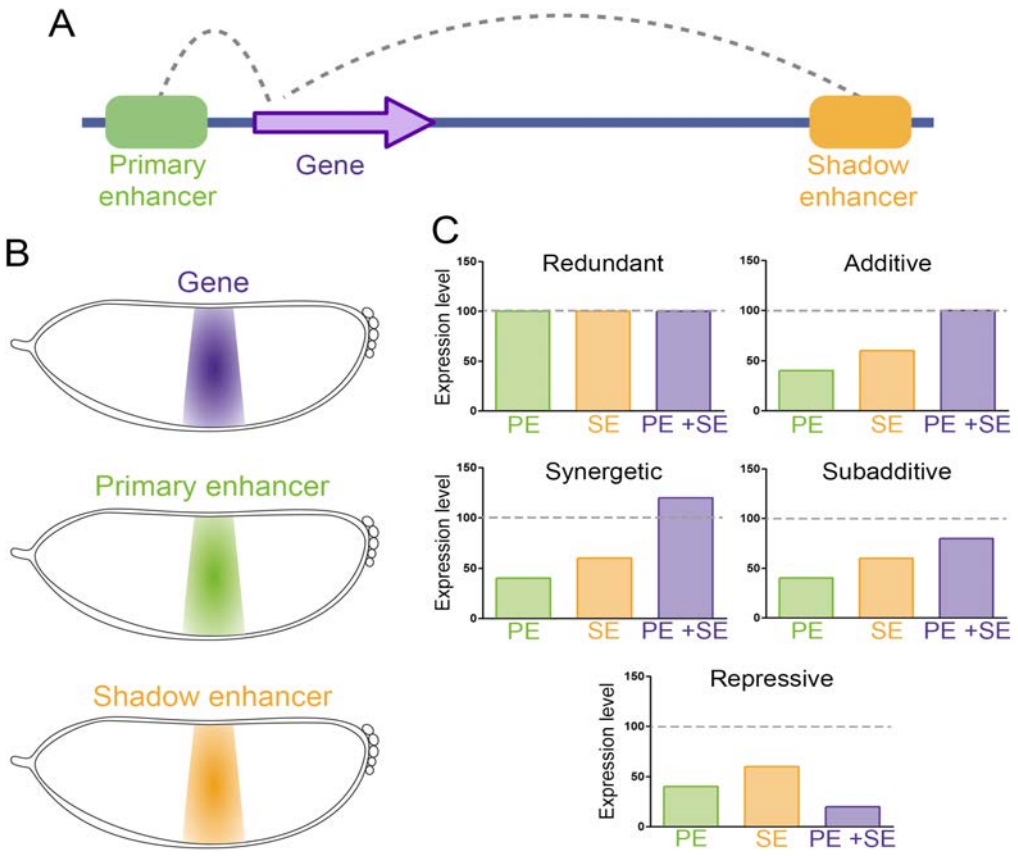

Figure 5. Models of enhancer redundancy. A) Cartoon depicting the interactions of the primary and shadow enhancer with the gene. **B)** Cartoon of a Drosophila embryo showing the same spatiotemporal activity of the primary and shadow enhancer and the gene. **C)** Models of interaction between the primary (PE) and the shadow (SE) enhancer. In green (PE) and orange (SE) the individual activity of each enhancer is represented and in purple (PE+SE) the activity resulting from the interaction of both enhancers. The dashed line represents the theoretical activity that both enhancers should present if they interacted in an additive way.

multiplies (Figure 5C)(S. Kim & Wysocka, 2023; Kvon et al., 2021). On the contrary, in the sub-additive model, although the interactions between both enhancers increase the overall activity, the increase is not as high as we would expect (Figure 5C). Finally, the interactions between the enhancer can have a repressive nature, leading to a reduction in their activity (Figure 5C) (Kvon et al., 2021). Sometimes these enhancers are called shadow enhancers and they are often conserved in the genome (Kvon et al., 2021; Lagha et al., 2012; Osterwalder et al., 2018). This suggests that these secondary enhancers have another role beyond simply conferring robustness in front of genetic variation. It has been proposed that these overlapping between enhancers could serve as a mechanism to ensure gene expression in front of stressing conditions (Frankel et al., 2010) or to express more precise and sharp expression patterns (Lagha et al., 2012; Perry et al., 2011), for example. However, further research is needed to clarify how different enhancers interact among them. In fact, it has been observed that among interacting enhancers there are specific enhancers that drive the majority of transcription, suggesting a certain degree of hierarchy among them (Carleton et al., 2017; Shin et al., 2016).

Gene expression and enhancer activity changes over time. For a long time, enhancers have been understood as a simple on-and-off switch, but recently this view of the enhancer activity has been challenged. In recent years it has been shown that enhancers are present in the genome in multiple varieties of regulatory states and that there is a transition between these states during development (reviewed in Calo & Wysocka, 2013; Heinz et al., 2015). Although we can roughly separate the enhancers between active and inactive enhancers, among the inactive enhancers important differences exist. Therefore, it is better to classify enhancers according to their state. Hence, we can find four different kinds of enhancers according to their state: active, silenced, repressed and primed or poised (Bozek & Gompel, 2020). Active enhancers are characterized by a high degree of accessibility (they are nucleosome depleted). Besides, they present a high density of TFs and cofactors binding to them. Moreover, the Pol-II is also bound to the enhancer and it transcribes the enhancer to enhancer RNA (eRNA), which is proportional to the degree of activity of the enhancer (Mikhaylichenko et al., 2018; Sartorelli & Lauberth, 2020). They are associated with genes that present active transcription and they are associated with the histone marks H3K4me and H3K27ac (Figure 6)(Creyghton et al., 2010; Rada-Iglesias et al., 2011). By contrast, silenced enhancers are sequestered in compacted chromatin and associated with the repressive markers H3K27me3 and PRC2 (Figure 6) (Schuettengruber et al., 2017; Simon & Kingston, 2009). For a long time, enhancer accessibility was a synonym of enhancer activity, but in recent years, with the description of repressed

and poised enhancers, this has been challenged. On another note, TFs can act both as activators or repressors, and it is the final balance between the two that determines the activity of enhancers. Repressed enhancers are accessible enhancers that are occupied by TFs but repressing TFs outperform activating TFs. These enhancers are associated with the histone marks H3K4me and present little or no labelling of H3K27ac (Figure 6)(Bozek et al., 2019; Spitz & Furlong, 2012). Finally, primed or poised enhancers are a group of enhancers that despite being accessible, although not as much as an active enhancer, do not present activity. Both primed and poised enhancers are associated with the histone mark H3K4me, and neither of them presents H3K27ac. The difference is that poised enhancers also present the repressor histone mark H3K27me3 while primed enhancers do not (Figure 6)(Creyghton et al., 2010; Rada-Iglesias et al., 2011; Zentner et al., 2011). It is thought that this state exists to allow the rapid activation of the enhancers along development (Blanco et al., 2020; Spitz & Furlong, 2012). This seems to be very, important especially in embryogenesis, where the differentiation events occur very fast (Creyghton et al., 2010; Crispatzu et al., 2021; Rada-Iglesias et al., 2011).

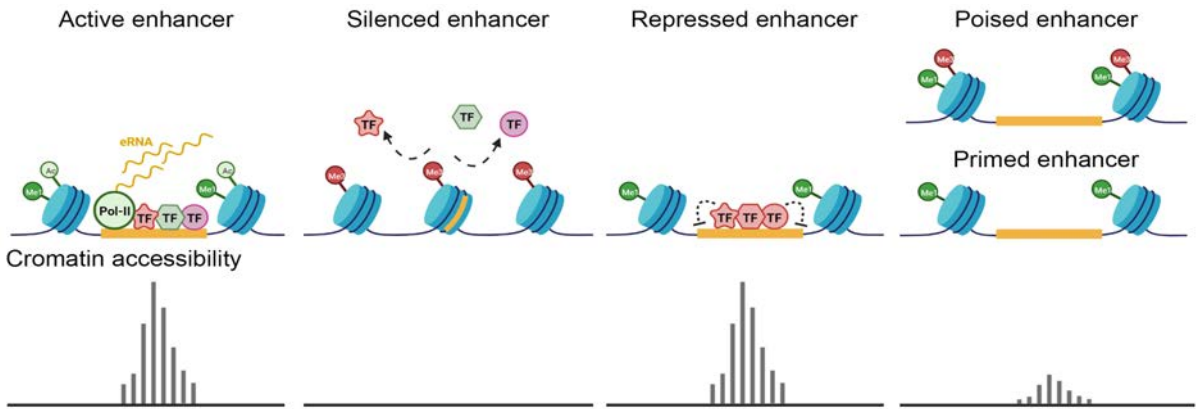

Figure 6. Enhancer state. Upper panel: cartoon depicting the chromatin marks and chromatin characteristics reported for each enhancer state. Lower panel: cartoon depicting the chromatin accessibility of each enhancer state.

Drosophila as a model organism

The conservation of core structural and functional genes across species has allowed the use of model organisms to improve our knowledge of development, regeneration and tumorigenesis.

For many years, *Drosophila melanogaster,* commonly known as the fruit fly, has been used as a model organism. Two main reasons exist for *Drosophila* to be a good model. The first one is that 75% of human genes involved in disease have an ortholog in *Drosophila.* The second is that many of the core genes are single-copied, thus *Drosophila* presents a low genetic redundancy (Adams et al., 2000; Singh & Irvine, 2012). This added to other factors such as the low cost, the rapid generation of new individuals and the great variety of genetic tools available has made *Drosophila* a very attractive model to address multiple biological questions. In fact, it has been used to study development, regeneration and tumorigenesis for many years (Enomoto et al., 2018; Fox et al., 2020; Gerlach & Herranz, 2020; Hariharan & Serras, 2017; Milán et al., 2014; Singh & Irvine, 2012).

Drosophila is a holometabolous insect. This kind of insect undergoes a complete metamorphosis cycle that compresses four different stages: the embryo, larva, pupa, and imago (or adult). At 25 ºC the cycle takes 10 days while at 18 ºC it takes 20 days (Figure 7A). As shown in Figure 7B, the *Drosophila* larva is very different from the adult. The larva presents a collection of tissues called imaginal discs that are responsible for giving rise to the adult structures such

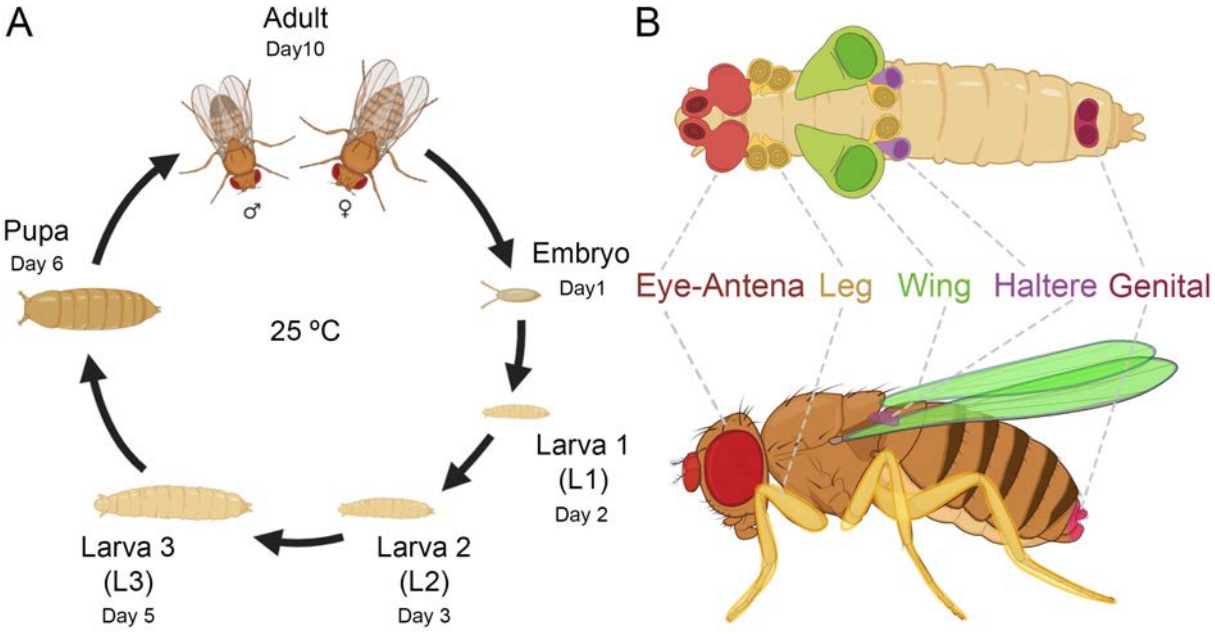

Figure 7. *Drosophila* imaginal discs. A) Cartoon depicting the life cycle of *Drosophila* at 25 ºC. **B)** Cartoon depicting the imaginal discs in the larvae and the adult structures that they give rise to.

as the wings, the legs, the eye or the genitalia, among others. In total, the larva presents 19 imaginal discs, all presented in pairs with the exception of the genital disc (Figure 7B).

One of the main tools used for the genetic manipulation of *Drosophila* is the Gal4/UAS transactivation system. This system relays on the activity of the yeast Gal4 transcriptional activator expressed under the control of a tissue-specific promoter or enhancer. When the Gal4 is expressed, it binds to the Upstream Activator Sequence (UAS), triggering the expression of the transgene under the UAS control (Figure 8A)(Brand & Perrimon, 1993). Therefore, this binary expression system allows the selective activation of transgenes in a tissue-specific manner. In addition, the use of a thermosensitive allele of Gal80 ($Gal80^{ts}$), allows the regulation of gene expression in specific time windows (Figure 8A)(McGuire et al., 2003). In addition, the LexA/lexO system allows the tissue-specific expression of transgenes in a similar way as the Gal4/UAS system. In this system, LexA plays the role of the Gal4 while LexO plays the role of the UAS. Moreover, the function of the system in specific windows of time also can be modulated by $Gal80^{ts}$ (Figure 8B)(Santabárbara-Ruiz et al., 2015). The fact that these systems function independently, allows the simultaneous expression of several transgenes in a different subset of cells.

Another technique that in recent years has been implemented in the vast majority of laboratories is the CRISPR/Cas9 technology for a targeted edition of the genome. This technique allows the targeting not only of genes but also other genomic elements such as enhancers. This technique can be used to disrupt, delete, replace, tag and edit different genomic elements, allowing their functional study. The technique is based on the use of two different elements: an endonuclease called Cas9, which cuts the DNA, and an RNA molecule called guide RNA (gRNA), which recognizes the specific sequence of the genome that is targeted. The sequence of the gRNA usually is 20 bp long and is complementary to the sequence that it targets. Besides, it requires a 3-bp protospacer adjacent motif (PAM) immediately 3' of the target sequence to allow the function of the endonuclease. Hence, the gRNA interacts with the Cas9 to guide it to the sequence that has to be edited. Upon binding, Cas9 generates a double-strand break (DSB) to the DNA, which activates the DNA repair machinery. On one side, the non-homologous end-joining (NHEJ) repair machinery tries to fix the DSB by simply ligating together the broken ends of the DNA. This allows the formation of small deletions or insertions. On the other side, the homology-directed repair (HDR) machinery, which requires a donor DNA template, allows the precise modification of the sequence. The use of donor templates allows the precise modification of the sequence. Therefore, depending on the expected

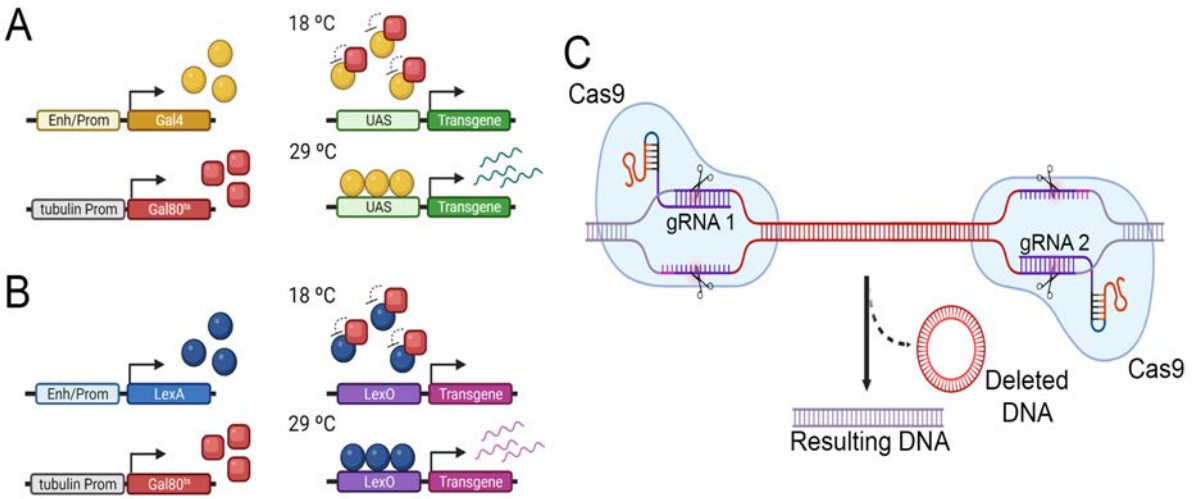

Figure 8. *Drosophila* genetic tools. A and B) Cartoon depicting the mechanism of action of the Gal4/UAS system **(A)** and the LexA/lexO system **(B)**. At 18ºC both systems are repressed by the Gal80^{ts}, but at 29ºC the Gal80^{ts} can no longer repress them and transcription takes place. **C)** Cartoon depicting how the CRISPR/Cas9 technology can be implemented to induce the deletion of the desired sequence. The two gRNAs are designed to flank the sequence to delete.

result, we can take advantage of the different DNA repair mechanisms and design strategies to induce the desired modification. Indeed, to induce specific deletions it can be implemented the design of two different flanking gRNAs in order to induce the deletion of the sequence in between the gRNAs for lack of repair (Figure 8C)(Bassett & Liu, 2014; Gratz et al., 2015). This technique has been used in this thesis to induce different deletions of the *wg*^{1} enhancer.

The development of the wing

The landscape of the wing disc

In this thesis, we use the *Drosophila* imaginal wing disc as a model of development, regeneration and tumorigenesis. The wing disc is a sac-like structure composed by a monolayer of epithelial cells that originate from a group of cells that invaginate from the embryonic ectoderm (Ruiz-Losada et al., 2018). At early stages, the wing epithelium is observed as a monolayer of cuboidal epithelial cells. As the wing disc grows, the epithelium diverges in morphology giving rise to two different populations. On one hand, cells on one side flatten, forming a thin squamous epithelium called the peripodial membrane (PM). These cells barely contribute to the adult structures, but they play a crucial role during metamorphosis enabling the wing eversion and participating in the thorax fusion (Figure 9A)(Pastor-Pareja et al., 2004; Tripura et al., 2011). On the other hand, cells of the other side elongate apico-basally as their density increase, forming a monolayer of pseudostratified cells that compose the disc proper (DP; Figure 9A). The cells of the epithelium are linked to each other through the cell-cell junctions near the apical side, easily recognizable through a DE-cadherin staining (Badouel & McNeill, 2009). At the same time, all the cells are attached to the basal membrane, composed of different proteins such as Laminin or Perlecan, that wraps up the entire disc (Tripathi & Irvine, 2022). The DP is the main responsible to give rise to the adult structures and it is divided into regions according to the structure that will form in the adult. Even if the wing disc is called like that because it will give rise to the adult blade, it also gives rise to the body wall (or notum), the pleura and the hinge, the structure that joins and articulates the wing blade to the body wall (Figure 9A and B)(Bryant, 1975; Tripathi & Irvine, 2022).

Despite the division of the wing disc into regions, the disc presents a second level of organization: the compartments. The compartments are cell populations that do not mix during development and that are crucial for wing development (Garcia-Bellido et al., 1973). The different expression of selective genes is what confer specificity and identities to the compartments. Hence, that disc is divided along the Anterior-Posterior (A/P) axis into the anterior (A) and posterior (P) compartments; and along the Dorsal-Ventral (D/V) axis into de dorsal (D) and ventral (V) compartments (Figure 9C). In the middle of the two compartments, it takes place the formation of the corresponding boundary of the axis (the A/P boundary or the D/V boundary). These boundaries act as developmental organizers that lead to the patterning and the growth of the disc. These compartments are still present in the adult wing. For instance,

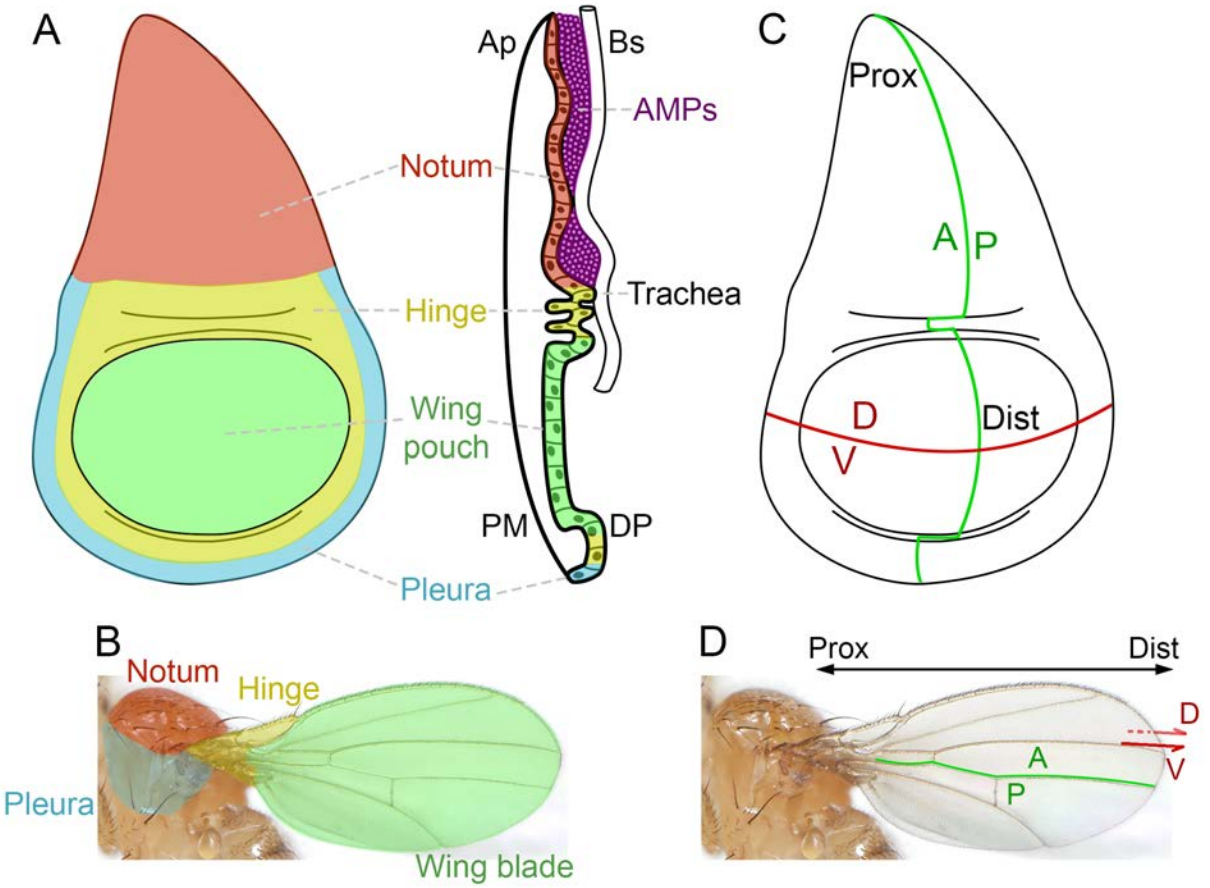

Figure 9. Regions and compartments of the wing disc and adult wing. A and B) Cartoon depicting the different regions of the wing disc (A) and the adult wing (B). A frontal (left) and a lateral (right) view of the wing disc are shown in A. **C and D)** Cartoon depicting the different compartments of the wing discs (C) and the adult wing (D).

the A and P compartments are located above and below the fourth vein, respectively (Figure 9D). On the other hand, during the eversion of the wing in metamorphosis, the wing disc folds and the dorsal and ventral surfaces of the wing blade become attached. This results in the D and V compartments occupying each one a face of the wing blade (Figure 9D). Additionally, a third axis is established during the development of the disc: the Proximo-Distal (P/D) axis. This axis is not defined by the compartments but by the different regions of the disc, being the notum the most proximal region and the wing pouch the most distal (Figure 9C). Interestingly, the D/V boundary is considered the most distal part of the disc because it gives rise to the wing margin (Figure 9C and D)(Tripathi & Irvine, 2022). We will discuss the formation of the compartments in the following sections.

In addition to the epithelial cells, the wing disc also contains other kinds of cells. Indeed, under the notum the adult muscle precursor cells, or AMPs, can be found, the cell population that gives rise to the flight muscles (Figure 9A)(Bate et al., 1991; Fernandes et al., 1991). Interestingly, the proliferation and patterning of AMPs depend on signals coming from

the main epithelium (Everetts et al., 2021; Gunage et al., 2014a; Hatori & Kornberg, 2020). In addition to AMPs, neurons and the associated glial cells can be also found in the wing disc. These cells form the sensory bristles in the notum and along the anterior edge of the wing (Gómez-Skarmeta et al., 2003; F. Huang et al., 1991). Finally, tightly associated to the disc we found the trachea which provides oxygen to the disc. Interestingly, its patterning also depends on the epithelium (Figure 9A)(Du et al., 2018; Hatori & Kornberg, 2020; Roy et al., 2014).

Embryonic origin of the wing disc

The origin of the wing disc has been traced back to the embryonic stages 11-13 and it shares its origin with the leg disc (Bate & Martinez Arias, 1991; B. Cohen et al., 1993; Requena et al., 2017). At the 11th embryonic stage from the epidermis of the embryo it appears a group of cells that can be distinguished by their distinct cellular morphology (Bate & Martinez Arias, 1991; Mandaravally Madhavan & Schneiderman, 1977) and their expression of Distal-less (Dll; Figure 10)(B. Cohen et al., 1993; S. M. Cohen, 1990). This group of cells is the limb primordium (LP, or imaginal disc primordium), the precursor of the leg and wing disc (B. Cohen et al., 1993; Requena et al., 2017). Dll expression is triggered by Wingless (Wg) which is expressed along D/V stripes in the anterior compartment of each segment (S. M. Cohen, 1990). At the same time, Dll expression is repressed in more dorsal and ventral cells by Decapentaplegic (Dpp) and Epidermal Growth Factor Receptor (EGFR), respectively (Figure 10)(Goto & Hayashi, 1997). LP outbreak is only observed in the first, second and third thoracic segments (T1, T2 and T3, Figure 10) but not in the abdominal segments even though the abdominal segments present the same Wg, Dpp and EGFR expression. The main responsible of blocking the LP development in the abdominal segments are the *abdominal* (*abd-A* and *abd-B*) and *ultrabithorax* (*ubx*) Hox genes that repress Dll transcription. The lack of activity of Hox genes in the abdominal segments allows the outbreak of the LP there (Carroll et al., 1995; Gebelein et al., 2002; Vachon et al., 1992).

Hereunder, at stage 12, Dpp becomes expressed in a lateral strip just dorsal to the LP that forms a gradient that promotes wing disc fate in the most dorsal cells from the LP (Figure 10)(Goto & Hayashi, 1997; Hamaguchi et al., 2004). Conversely, EGFR coming from ventral cells blocks wing disc fate in the most ventral cells from the LP while promoting leg disc fate instead (Figure 10)(Kubota et al., 2000). At the same time, Dpp promotes Wg local downregulation, favouring wing disc fate over leg disc (Kubota et al., 2003). So, those cells exposed to high levels of Dpp and low levels of Wg and EGFR will lose Dll expression and activate the expression

of wing disc promoter genes *snail* (*sna*), *escargot* (*esg*) and *vestigial* (*vg*; Figure 10)(Fuse et al., 1996; Requena et al., 2017; Williams et al., 1991). This phenomenon only occurs in the T2 and T3 segments but not at T1, where wing disc fate is repressed by Sex Combs reduced (Scr; Figure 10)(Carroll et al., 1995). Hence, those cells of the LP at T2 and T3 segments expressing *vg* migrate dorsally to form the wing and the halter disc, respectively (Figure 10)(Williams et al., 1991). In the T3 segment, Ubx represses wing disc fate and instead promotes halter disc fate. Hence, the lack of Ubx causes the halters to become wings, giving place to four-winged flies (Carroll et al., 1995; Lewis, 1978).

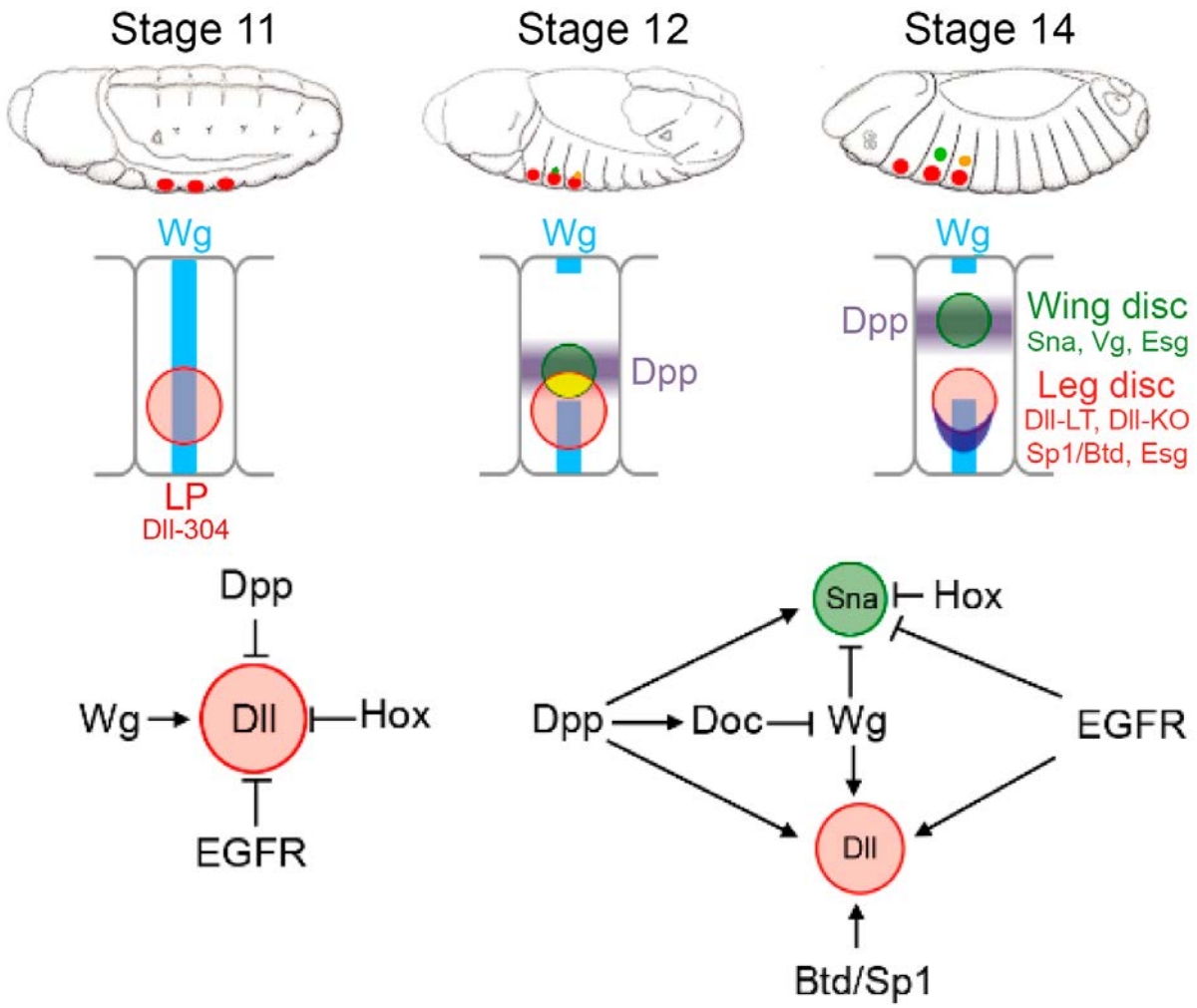

Figure 10. The embryonic origin of the wing disc. A) Cartoon showing the main steps of the embryonic origin of the wing (green) and haltere (orange) imaginal discs. A group of cells expressing Sna, Esg and Vg start to migrate dorsally from the limb primordia (red), giving rise to the wing (green) and halter (orange) discs in the second and third thoracic segments respectively. Ubx represses wing disc fate and instead promotes halter disc fate in the third thoracic segment. The leg disc (red) is localized ventrally and can be identified by the expression of Dll. **B)** Schematic representation of the different genetic inputs that control the specification of the wing disc in the embryo. Adapted from Ruiz-Losada et al., 2018.

Establishment of the Anterior-Posterior axis

The establishment of the A/P axis of the wing disc is inherited from the embryo and starts even before the formation of the wing primordium (Wieschaus & Gehring, 1976). The compartmentalization of the wing disc starts with the posterior-specific expression of Engrailed (En)(Kornberg, 1981) that is first established during the embryonic segmentation (Figure 11A)(Perrimon, 1994) and then maintained by the posterior cells of the wing disc by stable inheritance of the chromatin state (DeVido et al., 2008). The key player to establish the A/P axis in the wing disc is the Hedgehog (Hh) pathway. On one side, En induces Hh expression by the posterior cells of the wing disc (Guillen et al., 1995; Tabata et al., 1992), but it can exert its function there because En prevents its activity by repressing the expression of Cubitus interruptus (Ci), the transcriptional factor of the pathway (Eaton & Kornberg, 1990). On the other hand, anterior cells cannot express Hh because Ci represses its expression there (Apidianakis et al., 2001; Bejarano & Milán, 2009; Méthot & Basler, 1999). This results in the activation of the Hh pathway in a narrow strip of cells along the anterior side of the A/P boundary. In this strip Hh is capable to stabilize Ci and activate the transcription of *dpp* morphogen, the fly homolog of bone morphogenic proteins BMP2 and BMP4 (Figure 11B)(Méthot & Basler, 1999; Zecca et al., 1995). From there, Dpp is expressed and spreads along the anterior and posterior

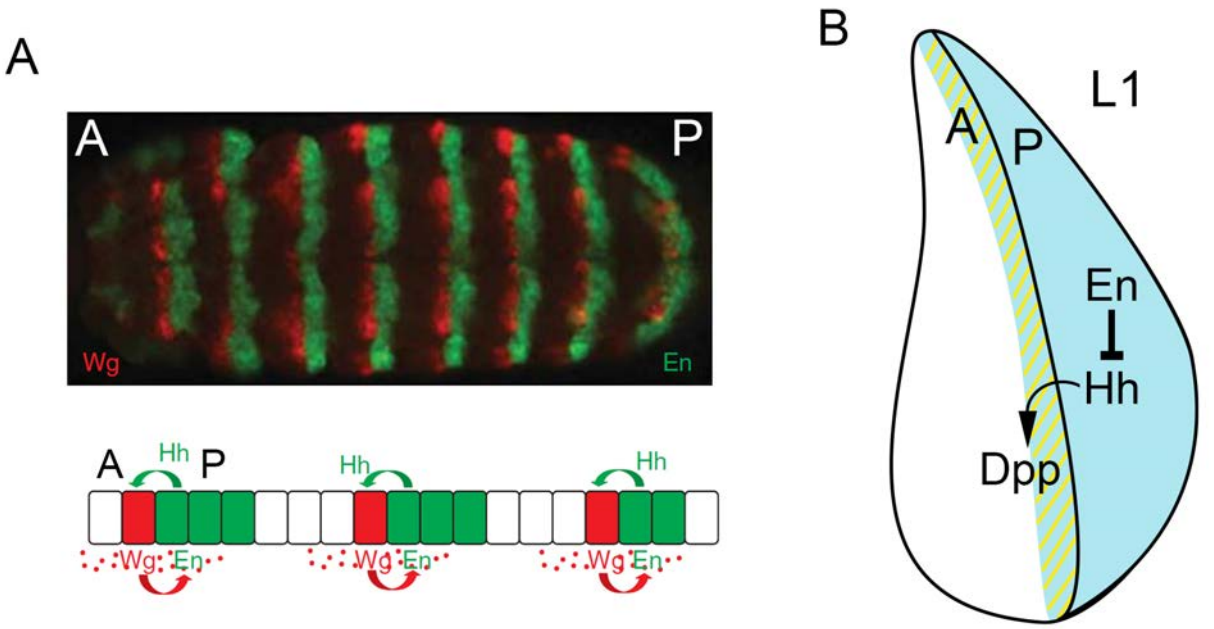

Figure 11. Establishment of the Anterior-Posterior Axis. A) *Drosophila* embryo stained for Wg (red) and En (green). Wg is expressed anteriorly (A) and En posteriorly (P) in the embryo. Adapted from Swarup and Verheyen, 2012. **B)** Cartoon depicting the establishment of the A/P boundary in the wing disc at the first instar. In the posterior (P) compartment En represses the activity of Hh. Hh only can be active in a narrow strip (yellow strip shadowing) in the anterior compartment (A), where it triggers the expression of Dpp, establishing the formation of the A/P boundary.

compartments, forming a gradient that declines as the distance from the boundary increases (Lecuit et al., 1996; Nellen et al., 1996; Teleman & Cohen, 2000). From there, Dpp establishes a gradient-dependent gene expression that will be crucial for the proper wing patterning (Calleja et al., 2002; De Celis, 2003) and growth (Barrio & Milán, 2017; P. S. Bosch et al., 2017; Burke & Basler, 1996).

Wing fate specification vs notum formation: the establishment of the Proximo-Distal axis

Although the wing disc is called that way because it gives rise to this structure, as previously mentioned, it also gives rise to the notum or body wall. During the second instar, both the specification of the notum and the wing take place. Prior to their differentiation, no overt territorial subdivisions exist, and the first clear differentiation along the proximo-distal axis is the formation of both structures.

The specification of the wing fate takes place when Hh coming from the posterior compartment activates Wg expression in a small group of cells in the ventral anterior edge of the disc (Figure 12A)(Ng et al., 1996). Expression of Wg is fundamental to trigger the wing fate specification. Consistently, the lack of Wg in the wing disc at the second instar induces the appearance of adults that lack wings and present a mirror duplication of the notal structures (Morata & Lawrence, 1977; Ng et al., 1996; Sharma & Chopra, 1976). For the wing to be specified Wg has to perform two functions. Before Wg is expressed, the wing presents a ubiquitous expression of Teashirt (Tsh), a transcriptional factor that contributes to the development of the notum and hinge. Thus, on the one hand, Wg represses *tsh* to allow the specification of the wing (Wu & Cohen, 2002; Zirin & Mann, 2007). On the other hand, shortly after the repression of *tsh,* Wg triggers Nubbin (Nub) expression, the first marker of the wing pouch (Ng et al., 1995, 1996; Zirin & Mann, 2007).

At the same time that the wing specification occurs, it also takes place the specification of the notum. The notum fate starts with the secretion of Vn, the ligand of the EGFR pathway, in the most proximal part of the disc (Simcox et al., 1996; S. H. Wang et al., 2000). Initially, Vn expression is triggered by Dpp coming from the peripodial membrane (Paul et al., 2013) but later on it generates a positive feedback loop to keep its own expression through development (Golembo et al., 1996; S. H. Wang et al., 2000). The activation of the EGFR pathway leads to the expression of the three transcriptional factors members of the Iroquois complex (Iro-C),

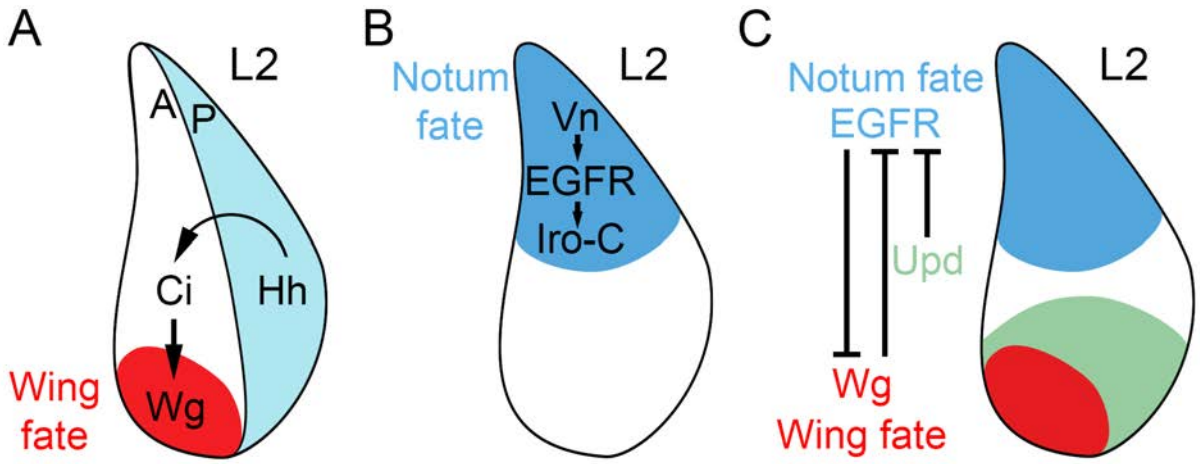

Figure 12. Wing fate specification vs notum formation. A) Cartoon depicting the wing fate specification at the second instar (L2). Hh coming from the posterior (P) compartment triggers the expression of Wg in the anterior (A) compartment through its TF Ci. Expression of Wg in the ventral anterior edge of the wing triggers the specification of the wing. **B)** Cartoon depicting the specification of the notum at the second instar (L2). Vn triggers the activation of the EGFR pathway, leading to the activation of the Iroquois complex (Iro-C) that triggers the specification of the notum. **C)** Cartoon depicting Wg and EGFR (Vn) mutual negative regulation at the second instar (L2). The JAK/STAT pathway (Upd) contributes to restricting EGFR activity to the proximal area of the disc, allowing Wg expression.

Araucan, Caupoplican and Mirror, the responsible to trigger the notum fate specification (Figure 12B)(Diez Del Corral et al., 1999; S. H. Wang et al., 2000; Zecca & Struhl, 2002b).

Hence, in the second instar, the expression of Vn in the most proximal part and the expression of Wg in the ventral region triggers the specification of the notum and the wing, respectively. Importantly, Vn and Wg signalling antagonize each other (Figure 12C). In fact, in *wg* mutants, *vn* expression spreads distally and adults emerge without wings and a mirror duplication of the notal structures. By contrast, repression of EGFR signalling or overexpression of Wg in most proximal parts leads to a notum to wing transformation (Baonza et al., 2000; Klein & Arias, 1998; S. H. Wang et al., 2000). In fact, it is so important that these two signals remain separate that the discs feature two mechanisms to ensure this. On one side, JAK/STAT activity can be detected in the most ventral part of the disc and has been shown that is crucial to keep Vn expression restricted to the most proximal part, allowing Wg to trigger the specification of the wing (Figure 12C). In fact, when JAK/STAT activity is depleted at the second instar, Vn expands towards the most proximal regions and a duplication of the notal structures can be observed (Recasens-Alvarez et al., 2017). On the other side, Notch contributes to the formation of the wing pouch by keeping the distance between Vn and Wg by inducing the growth of the disc and physically separating them (Figure 13). In fact, before its role in the D/V boundary formation, Notch drives growth in the very early disc. A failure of Notch activity at this stage results in smaller discs that produce adults that show the wing to notum transformation phe-

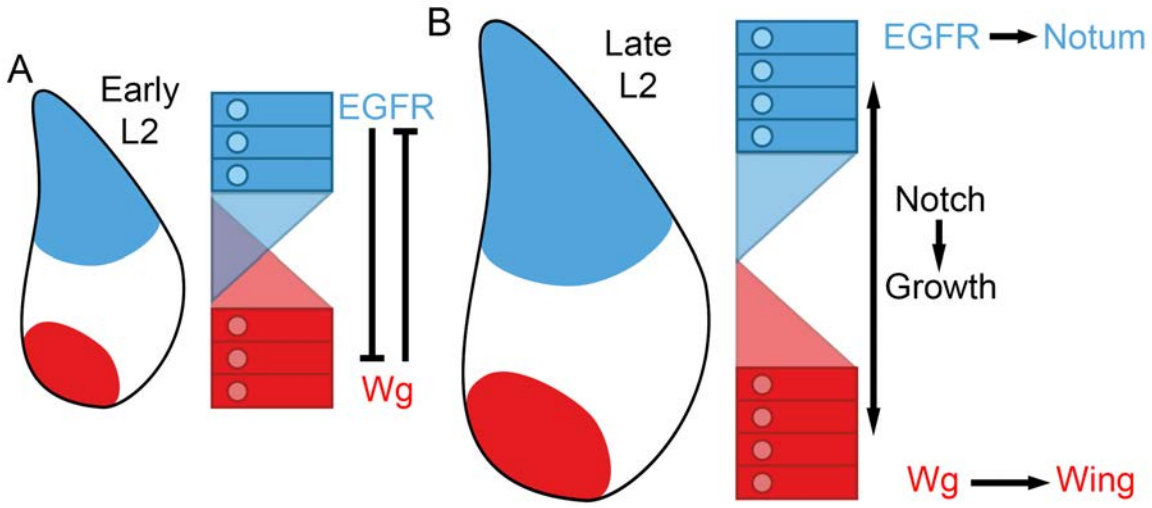

Figure 13. Disc growth is essential for the wing fate specification. Cartoon depicting how Notch regulates the growth of the early disc and allows the specification of the wing. In the early stages, both EGFR (blue) and Wg (red) signallings are too close and the specification of the wing cannot take place because EGFR represses Wg **(A)**. Notch induces the growth of the disc, putting distance between both signals and allowing the specification of the wing **(B)**.

notype (Couso & Arias, 1994; Rafel & Milán, 2008). Hence, in the absence of Notch, Vn and Wg signals are too close and Vn antagonizes Wg activity, preventing the specification of the wing. This phenotype can be rescued by the overexpression of growth promoters or cell cycle regulators. By contrast, the expression of growth inhibitors such as Hippo phenocopies the wing to notum transformation phenotype induced by the absence of Notch (Rafel & Milán, 2008). This is a clear example where growth and fate specification are tightly coupled to generate a correct shape and sized structure.

Establishment of the Dorsal-Ventral axis

Immediately after the differentiation between the body wall and the wing pouch occurs, the establishment of the Dorsal-Ventral axis takes place. The process starts when EGFR signalling triggers the expression of Apterous (Ap) in dorsal cells (Figure 14A)(S. H. Wang et al., 2000; Zecca & Struhl, 2002b, 2002a). In turn, Ap triggers the expression of Serrate (Ser), a ligand of the Notch (N) pathway, in the dorsal compartment. At the same time, ventral cells express Delta (Dl), another ligand of Notch, leading to an asymmetric activation of Notch at both sides of the boundary. This triggers the expression of Wg morphogen and allows the formation of the D/V boundary (Figure 14A)(Couso et al., 1995; De Celis et al., 1996; Diaz-Benjumea & Cohen, 1995; J. Kim et al., 1995). From there Wg establishes a gradient-dependent gene expression that will be crucial for the wing. Remarkably, at the third instar disc, the expression pattern of Wg and its function drastically differs from the one observed at the second instar. At

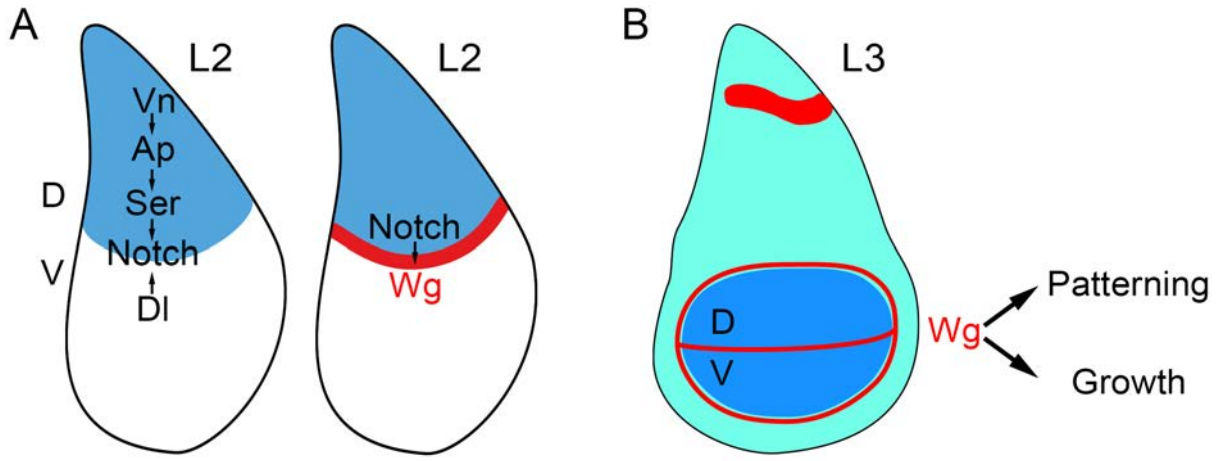

Figure 14. Establishment of the Dorsal-Ventral Axis. A) Cartoon depicting the establishment of the D/B boundary. In the second instar, Vn promotes the expression of Ap, which triggers the expression of Ser in the dorsal (D) compartment. The expression of Ser in the D compartment and Dl in the ventral (V) compartment triggers the expression of Notch between both compartments, leading to the expression of Wg and the establishment of the D/V boundary. **B)** Cartoon showing the expression of Wg in the late third instar (L3) wing disc. In the third instar, Wg promotes the patterning and the growth of the disc.

the second instar, Wg is expressed in a small group of cells in the ventral anterior edge of the disc and its only function is to trigger the specification of the wing pouch (Ng et al., 1996). By contrast, at later stages Wg expresses along the D/V boundary and from there it drives wing patterning (Couso & Arias, 1994; Neumann & Cohen, 1997; Zecca et al., 1996) and growth (Baena-Lopez et al., 2009; Barrio & Milán, 2020; Couso & Arias, 1994; Neumann & Cohen, 1997). Consistently, depletion of Wg activity at the latter stages results in smaller wings, although the wing blade always remains (Barrio & Milán, 2020; Zecca et al., 1996). Only depletion of Wg at early stages results in adults with an absence of wings and duplication of the notal structures (Ng et al., 1996). In addition to the D/V boundary, expression of Wg can also be observed in two concentric rings in the hinge and in a broad stripe in the notum (Figure 14B)(Swarup & Verheyen, 2012). On one hand, Wg on the hinge regulates hinge size (Neumann & Cohen, 1996). Interestingly, depletion of Wg in the hinge results in hinge growth defects that turn out in a nonautonomous reduction in blade size most probably because the hinge no longer can conduct the proper tensions during pupariation to ensure the elongation of the wing (Barrio & Milán, 2020). On the other hand, Wg from the notum is required for the proper development of the flight muscles of the adult fly (Everetts et al., 2021; Gunage et al., 2014; Sudarsan et al., 2001). Although there are other members of the Wnt family that are expressed in the wing disc in the same cells as Wg, such as *wnt4* and *wnt6* (Gieseler et al., 2001; Janson et al., 2001; J. J. S. Yu et al., 2020), they barely contribute to the development of the wing discs (Barrio & Milán, 2020; Doumpas et al., 2013; Herr & Basler, 2012). As presented here, Wg expression in

the wing disc is a dynamic process that requires tight regulation to ensure it functions at the proper place and time. Enhancers can be a very good tool to understand the dynamic regulation of Wg over time.

Regeneration in the wing disc

Principles of regeneration

Regeneration is the capacities to reconstruct a tissue or an organ to its original size, shape and function and to restore its proper homeostasis after damage. Interestingly, the regenerative capacity greatly varies among species. Whereas some animals can regenerate an entire individual from a small piece (e.g., hydra or planarians), others can barely regenerate (e.g., birds or mammalians)(Bely & Nyberg, 2010; Iismaa et al., 2018). Not just among species, but also within the same individual the regenerative potential greatly varies depending on the organ or the developmental stage (Seifert et al., 2012). Furthermore, when we talk about regeneration, this can range from the regeneration of a part of a cell, as in the case of the neuronal axon repair, to the recovery of tissues, organs, entire structures such as an arm, or the regeneration of the hole body from a small piece (Figure 15A). Although in all cases we talk about regeneration, the different levels of performance require different mechanisms and the complexity among them greatly varies. For example, in the case of organ regeneration it will not just be necessary to orchestrate the proliferation of different cell populations, but also have to integrate a sense of total organ size to stop growing when size is restored. By contrast, whole-body regeneration, apart from this, requires spatial patterning and the establishment of a polarity within the individual (e.g., head vs tail)(Bely & Nyberg, 2010; Slack, 2017).

Regeneration can be classified into two main groups: epimorphosis and morphallaxis. In epimorphosis regeneration requires proliferation. The regenerative capacity of this kind of regeneration relies on the blastema formation, a mass of undifferentiated cells with a high proliferative capacity and capable to give rise to the missing structures (Figure 15B). On the other hand, in morphallaxis there is a spatial reorganization of the remanent part without proliferation nor the formation of the blastema, giving rise to a smaller but well-patterned individual (Figure 15B). However, subsequently, it has been shown that regeneration is a much more complex process and many times both kinds of regeneration occur at the same time. This kind of regeneration was called intercalary growth and occurs in organisms such as planarians or *Drosophila* imaginal discs (Agata et al., 2007; Elchaninov et al., 2021; Repiso et al., 2013).

Steps of regeneration

Despite the different capacity to regenerate of different organisms and the high variability of regenerative types, it seems that regeneration presents some conserved steps: sensing

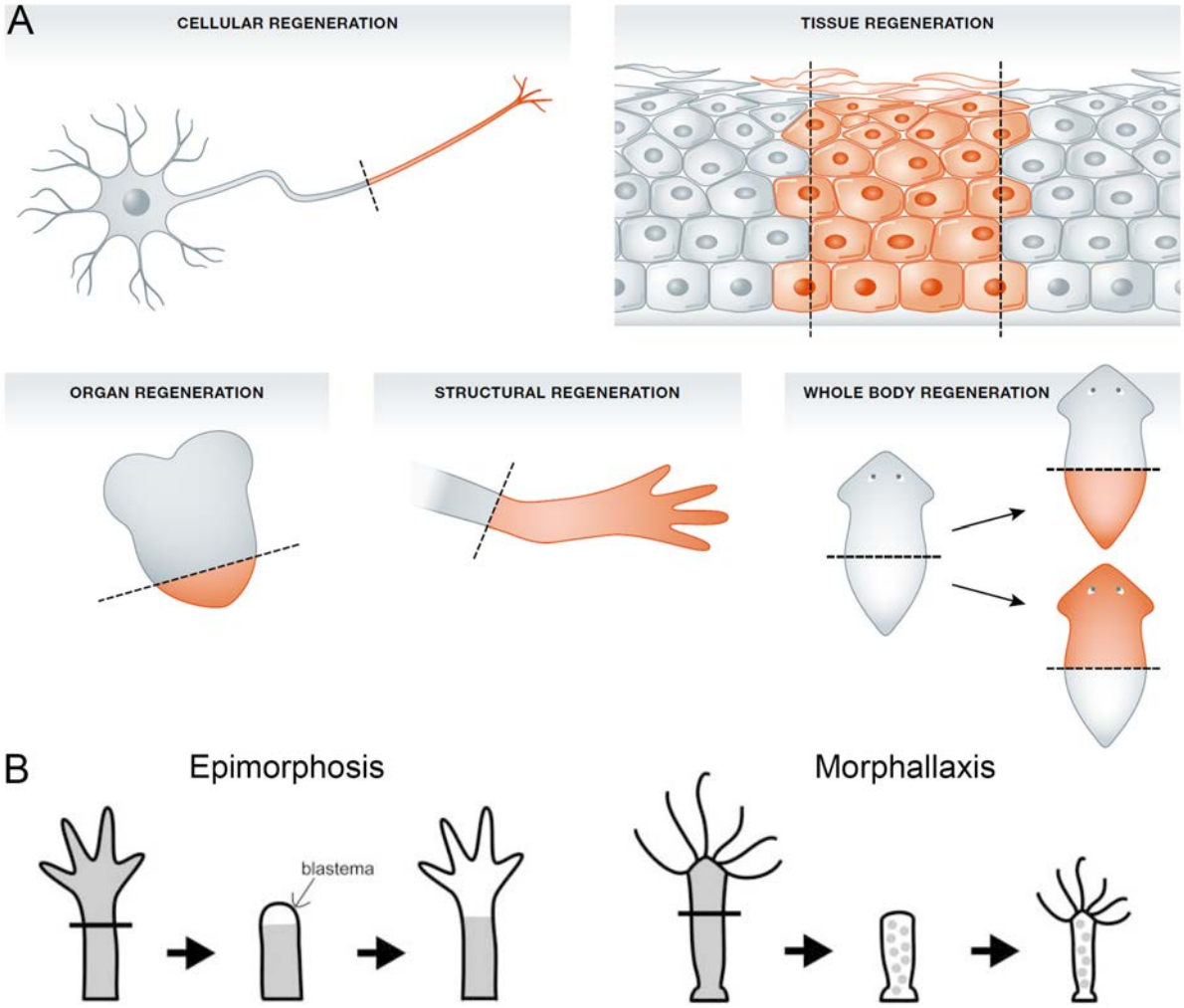

Figure 15. Regeneration types. A) Cartoon depicting the five types of regeneration. Adapted from Slack, 2017. **B)** Cartoon depicting classical examples of Epimorphosis and Morphallaxis regeneration. On the left: the limb regeneration in amphibians, where the origin of new cells is the blastema, a classic example of Epimorphosis. On the right: the Hydra regeneration, where a direct rearrangement of pre-existing cells gives rise to a smaller but well-patterned individual, a classic example of Morphallaxis. Adapted from Agata et al., 2007.

and signalling of the damage, production of new cells and morphogenesis (Figure 16)(Bideau et al., 2021). Minutes after the damage, damaged cells release reactive oxygen species (ROS) and calcium waves that signal to the nearby tissue to start regeneration (Love et al., 2013; Pirotte et al., 2015; Serras, 2022). Interestingly, these signals also induce apoptosis too (Mittal et al., 2014). This is important because apoptosis promotes regeneration through apoptosis-induced compensatory proliferation (AiP)(Fan & Bergmann, 2008; Tseng et al., 2007). At the same time, injury triggers the recruitment of the innate immune system that releases cytokines that are sensed as pro-regenerative signals (Figure 16A)(Dipietro et al., 2021; Godwin et al., 2013; Petrie et al., 2015). Consequently, all these signals lead to the formation of the blastema and the production of new cells.

Four main sources of new cells have been described: stem cells, dedifferentiation of cells, transdifferentiation or compensatory hyperplasia. Depending on the organism or the organ of study the source of new cells can vary (reviewed in Stocum, 2012). For example, in planarians, the source of new cells is a group of stem cells called neoblast that self-renew and differentiate in the new cell types required (Figure 16B)(reviewed in Reddien, 2013). By contrast, in axolotl's limb or in zebrafish heart and fin regeneration has been observed the dedifferentiation of cells to a less differentiated state that allows them to proliferate and redifferentiate into their parent cell type (Figure 16B)(Jopling et al., 2010; Sandoval-Guzmán et al., 2014; Sehring et al., 2022). A similar phenomenon occurs in *Drosophila* imaginal discs or in the newt iris where a poll of cells dedifferentiate in order to re-enter the cell cycle and proliferate. However, in this case, the cells differentiate into a different type of cell than the original one, hence cells undergo transdifferentiation (Figure 16B)(Henry & Tsonis, 2010; Repiso et al., 2013). The last kind of source of new cells is compensatory hyperplasia. In this kind of regeneration, already differentiated cells simply divide while they maintain their differentiated structure and function. A good example of this is the regeneration of the liver in mammalians where, after a hepatectomy, hepatocytes divide to regenerate the tissue while they continue performing their function (Figure 16B)(reviewed in Michalopoulos & DeFrances, 1997).

Finally, the last step of regeneration is morphogenesis. This step is crucial to recover the proper shape, size and function of the damaged tissue. This step is highly complex because at the same time it has to coordinate the positional memory of the remaining tissue, the cell differentiation, the patterning of the regenerated region and the innervation of the tissue. For this, molecular mechanisms crucial for development became essential to achieve a proper regeneration of the missing structure (Figure 16C)(Bideau et al., 2021). Importantly, it is essential that as regeneration completes, all these programs return to their pre-injury state to assure the proper functioning of the regenerated structure (Goldman & Poss, 2020).

Interestingly, in recent years it has been proposed that senescent cells, that usually has been associated with ageing and age-related diseases (Calcinotto et al., 2019; Muñoz-Espín & Serrano, 2014), are present in the damaged tissue and that they could play a positive role in the regeneration process (reviewed in Antelo-Iglesias et al., 2021; Wilkinson & Hardman, 2020). In fact, it seems that senescent cells promote the closure of the wound in mice damage skin (Demaria et al., 2014), positively regulates the regeneration of the fin in zebrafish (Da Silva-Álvarez et al., 2020) or the limb in axolotls (Q. Yu et al., 2022; Yun et al., 2015). Nevertheless, more research is needed to understand their role in each developmental stage and whether they truly have a positive impact on regeneration.

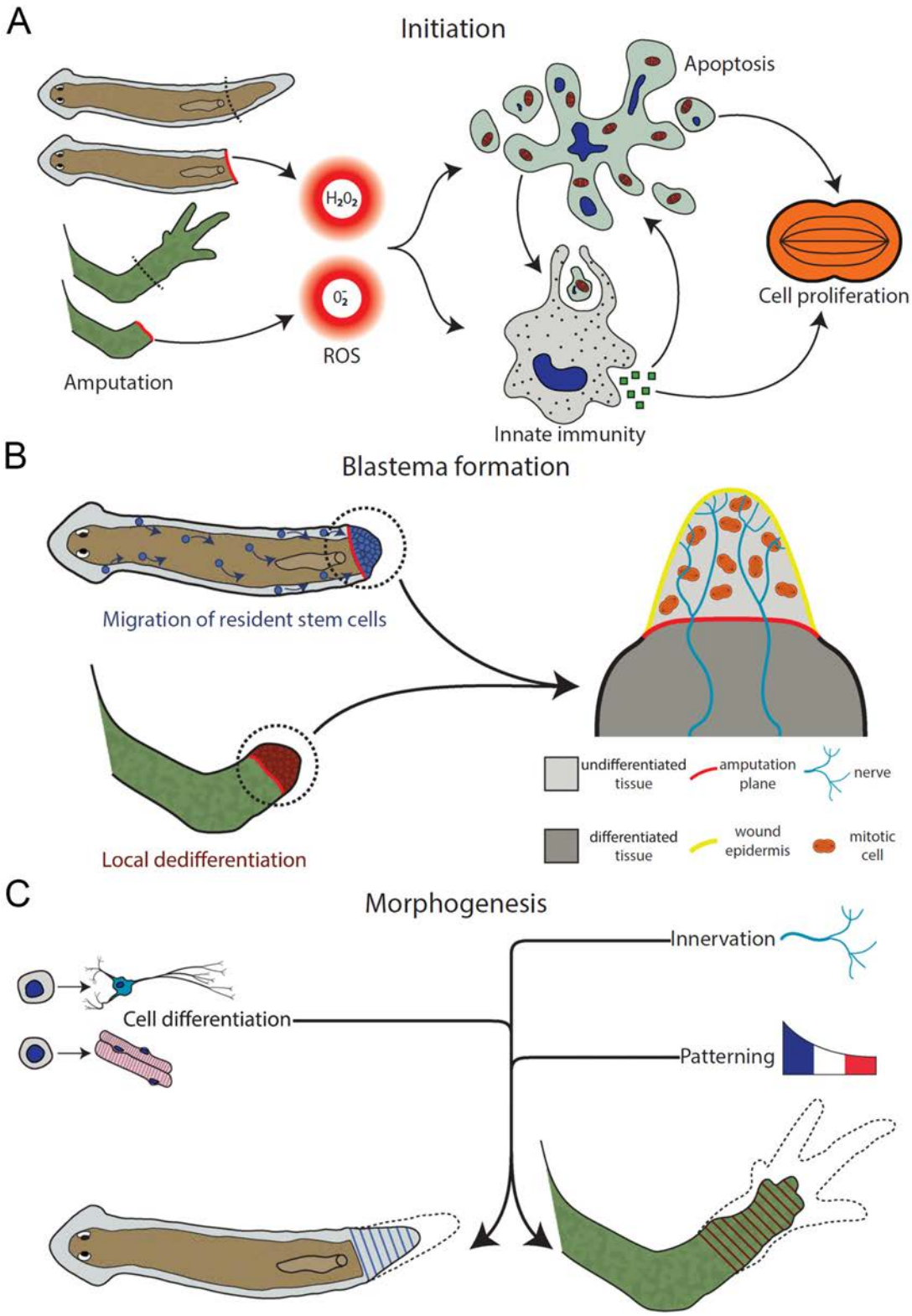

Figure 16. The steps of regeneration. A) Initiation of regeneration. The damage induces the release of ROS at the wound site, triggering apoptosis and the recruitment of the immune system. The pro-inflammatory cytokines released by the immune system also trigger apoptosis. Dying cells trigger apoptosis-induced proliferation (AiP) in the nearby tissue. **B)** Formation of the blastema, a group of undifferentiated cells that proliferate to regenerate the lost structure. **C)** Morphogenesis. It is the last step of regeneration and leads to the formation of a functional structure. Cellular differentiation, re-innervation and re-patterning are the main aspects of morphogenesis. Adapted from Bideau et al., 2021.

Chromatin dynamics, enhancers and regeneration

Although it is clear that a high regenerative capacity confers a clear evolutionary advantage, it remains a mystery why some species are such good regenerators and others are not, especially because it seems that the molecular and cellular basis of regeneration are conserved. Recent reports have shown that although there are some genes specific for regeneration, mostly what occurs during regeneration is that there is a reactivation of genes crucial during development that perform proliferative, migratory or morphogenic functions (Goldman & Poss, 2020; Vizcaya-Molina et al., 2020). Good examples of these are the *bone morphogenetic proteins* (*bmp*) or *wnt* genes that are required for both, development and regeneration (Guenther et al., 2015; D. Li et al., 2022). It has been hypothesized that the chromatin landscape could be responsible to determine the regenerative capacity of an organism. Thus, organisms capable to induce reprogramming of their chromatin landscape could up-regulate those genes essential for regeneration and would be capable of properly regenerating. By contrast, those organisms where chromatin would be fully repressed, could not allow the expression of genes involved in regeneration. This hypothesis would not only explain the different regeneration potentials between organisms, but also the variability in the regenerative capacity of the same organism at different stages (Goldman & Poss, 2020; Katsuyama & Paro, 2011; Vizcaya-Molina et al., 2020). Hence, the difference in the regenerative capacity among species or within an organism would not be due to the genes present in their genome, but the accessibility to them. This idea is supported by the fact that upon damage it has been reported a change in the chromatin accessibility (Vizcaya-Molina et al., 2018; W. Wang et al., 2020). This will be discussed a little further below.

Two of the most important protein complexes that regulate chromatin accessibility during development and regeneration are the PcG and TrxG groups. Therefore, both genes are crucial to determine the fate, identity and plasticity of cells (Katsuyama & Paro, 2011; Schuettengruber et al., 2017). In fact, the lack of epigenetic repression by depletion of PcG proteins in wounded mouse skin helps to mediate the up-regulation of genes involved in regeneration (Shaw & Martin, 2009). Although these proteins rely on the core of chromatin accessibility and gene regulation, their study is hard due to their pleiotropic effects. Furthermore, we have to take into consideration that PcG and TrxG are not the only regulators of chromatin accessibility and that there are others molecules that contribute such as histone modification enzymes and non-coding RNAs (Kaikkonen & Adelman, 2018; P. Zhang et al., 2016), among others.

Although it is clear that chromatin accessibility is essential to allow the expression of genes, the master regulators of gene expression are the enhancers. Hence, the reactivation of developmental genes during regeneration relay on them, putting enhancers as central elements of regeneration (reviewed in Goldman & Poss, 2020; Vizcaya-Molina et al., 2020; Yang & Kang, 2019). As stated above, there are very few genes specific for regeneration, and most of them are reused from development. Thus, in recent years, many authors have focused their efforts to find enhancers that specifically drive gene expression in response to damage. Many authors have referred to them in very different terms such as tissue regeneration enhancer elements (TREEs), damage-responsive regulatory elements (DRREs) or regeneration signal response enhancers (RSREs). Still, hereafter we are going to refer to them as DRREs. As matter of fact, two main kinds of enhancers have been described to participate in regeneration: emerging and increasing DRREs (Figure 17A). The emerging DRREs (eDRREs) correspond to those enhancers that only get accessible in response to damage. Within the eDRREs, we can find those that have been used in other tissues or in another developmental time, so the authors named them reused eDRREs (Figure 17A), and those which are specific from regeneration, the novel eDRREs (Figure 17A)(Vizcaya-Molina et al., 2018). A good example of reused eDRREs are *Raldh2 CR2* and *Wt1 CR4* epicardial enhancers in mice. These enhancers are expressed during the early stages of heart formation and later on, they are reused upon injury in the adult heart (G. N. Huang et al., 2012). By contrast, an example of novel eDRRE would be the *leptin B* enhancer in zebrafish. Indeed, it plays a role in regeneration, but it does not seem to contribute to development (Kang et al., 2016). On the other hand, increasing DRREs (iDRREs) are those enhancers that are already accessible in the non-damaged tissue, but become more accessible after damage, indicating an increase in activity (Figure 17A)(Vizcaya-Molina et al., 2018). An example of iDRRE would be the regulatory elements of *transcription factor 1* (*ftz-f1*) and *apontic* (*apt*). Those elements are already accessible during the development of the wing disc, but upon damage they become more accessible (Harris et al., 2020). Hence, the accessibility of the enhancers is crucial to be capable to regenerate injured structures. Indeed, some authors have shown that it exists a loss of regenerative potential over time that is linked to the epigenetic silencing of DRREs (Figure 17B)(Harris, 2022). Indeed, in *Drosophila* imaginal wing discs there is a loss of its regenerative capacity over time that seems linked to the accessibility to the DRREs. In fact, in this study, they compare the accessibility of DRREs after damage at early and later stages. Although DRREs become more accessible upon damage at early and late stages when compared to control, we can see that the DRREs at later stages become less accessible upon damage respect to early damaged discs (Harris et al., 2020). Results pointing towards the same

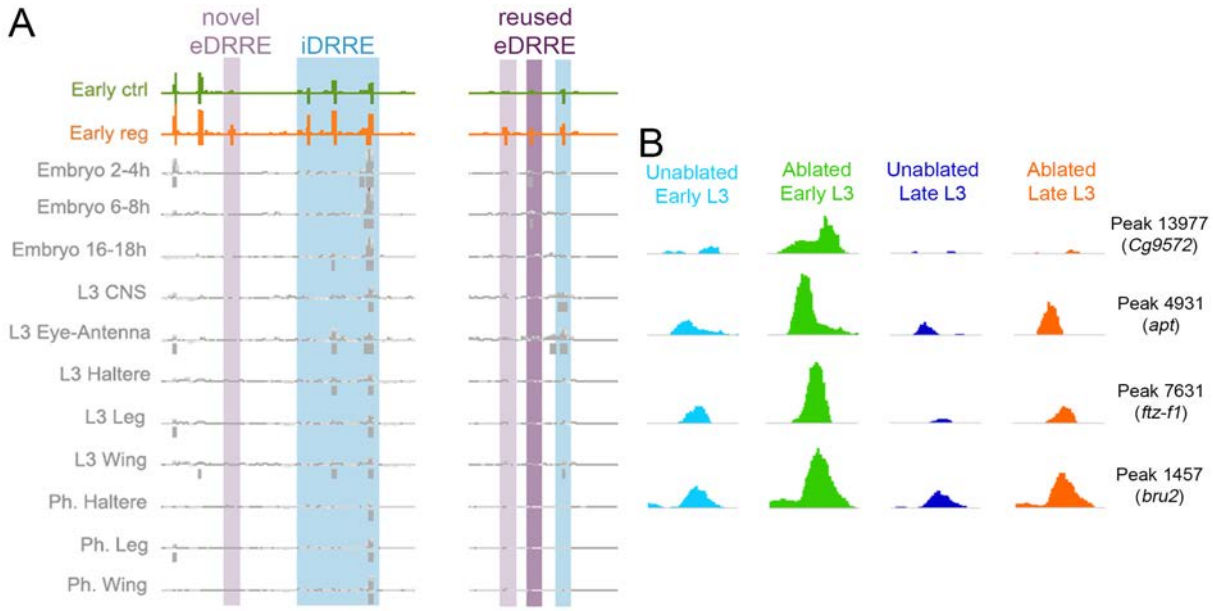

Figure 17. Enhancer accessibility in the regenerative tissue. A) Examples of damage-responsive regulatory elements (DRREs). Three kinds of DRREs are present in the regenerative tissue: increasing DRREs (iDRRE, blue), those enhancers that are already accessible in the non-damaged tissue, but become more accessible after damage; reused emerging DRREs (reused eDRRE, dark purple), those enhancers that only get accessible in response to damage but are accessible in other tissues; and novel emerging DRREs (novel eDRRE, light purple), those enhancers that only get activate in the regenerative tissue. Adapted from Vizcaya-Molina et al., 2018. **B)** Examples of enhancer accessibility upon damage in early and late stage wing discs. Notice that at later stages although the enhancers become more accessible, they do not become as accessible as in the early stages. Adapted from Harris et al., 2020. In both cases, the accessibility to the DNA has been determined through the assay for transposase-accessible chromatin with sequencing (ATAC-Seq). The accessibility is represented as peaks. The higher they are, the higher the accessibility to the DNA.

direction were obtained in mice, where the capacity to regenerate the mechanosensitive hair cells in the ear is lost over time due to the silencing of the hair cell enhancer network (Tao et al., 2021). Thus, it is clear that enhancers play a key role in regeneration and that their study can help us to improve our comprehension of how regeneration is regulated.

Drosophila wing disc as a regeneration model

Drosophila imaginal discs have been a model for the study of regeneration for many years basically due to their capacity to undergo compensatory proliferation upon damage (Huh et al., 2004; Pérez-Garijo et al., 2009; Ryoo et al., 2004; Smith-Bolton et al., 2009). due to the fact that it has been an organism studied for many years by geneticists, it exists a large number of genetic tools that allow easy manipulation of gene expression (reviewed in Fox et al., 2020). It is important to notice that not all the regions of the wing disc present the same potential to regenerate. Indeed, while the pouch presents a robust regenerative potential, the notum regenerates very poorly (R. Martín & Morata, 2018). Therefore, the regenerative studies in the wing disc have focused their attention on the wing pouch.

Immediately after damage, there is a wave of calcium and ROS that triggers the sensing of damage (Figure 18)(Narciso et al., 2015; Restrepo & Basler, 2016; Santabárbara-Ruiz et al., 2015). Interestingly, upon damage calcium is released from the endoplasmic reticulum and migrates within the mitochondria, inducing a loss of potential of the mitochondrial membrane and increasing the membrane permeability, therefore enhancing ROS production (Khan et al., 2017). Furthermore, calcium and ROS can propagate to the neighbouring cells through the gap junctions (Narciso et al., 2015; Razzell et al., 2013) or extracellularly (Serras, 2016; Thiagarajah et al., 2017), respectively, propagating their effects. These two molecules are essential to the start of regeneration and interfering with any of them leads to problems in tissue repair (Khan et al., 2017; Restrepo & Basler, 2016; Santabárbara-Ruiz et al., 2015). Thus, the waves of calcium and ROS, on one hand, will recruit haemocytes into the wound (Fogarty et al., 2016) while on the other hand, ROS induces the activation of the MAP kinases c-Jun-N Terminal kinase (JNK) and p38, the main orchestrators of wing regeneration (Santabárbara-Ruiz et al., 2015). The activation of JNK and p38 by ROS is mediated by the apoptosis signal regulating kinase-1 (Ask1). Upon oxidative stress, Ask1 dissociates from the inhibitory protein thioredoxin (Trx). Interestingly, in the presence of high levels of ROS, Ask1 strongly activates JNK and induces cell death. By contrast, in the nearby tissue, where ROS levels are lower, Ask1 gets still activated by ROS but also phosphorylated by Akt1, leading to activation of p38 and lower activation of JNK. This promotes the survival of the nearby tissue allowing regeneration (Santabárbara-Ruiz et al., 2019). Indeed, it is so crucial that JNK feeds back on ROS production to modulate the duration of the response (Khan et al., 2017). In addition, a recent report has shown that upon damage JNK activates the expression of Ets21C, a transcriptional factor essential to mantain the transcription of genes fundamental for regeneration even when the activity of JNK declines at the end of regeneration (Worley et al., 2022). Consistently, depletion of Ets21C in damaged discs impairs the regeneration of the wing (Khan et al., 2017; Worley et al., 2022).

JNK is at the epicentre of regeneration. In fact, JNK regulates tissue remodelling (Bergantiños et al., 2010; M. Bosch et al., 2005; Mattila et al., 2005), stimulates proliferation (Bergantiños et al., 2010; Crucianelli et al., 2022; Mattila et al., 2005; Ryoo et al., 2004), regulates cell plasticity (Klebes et al., 2005; Lee et al., 2005) and drives delay in response to damage (Cao et al., 2022; Colombani et al., 2012). It is so crucial that the majority of cells that form the blastema and will give rise to the regenerated wing, come from cells where JNK was activated (M. Bosch et al., 2008). Indeed, the activation of the JNK pathways leads to the activation of several pathways essential to drive growth in regeneration. Interestingly, the pathways re-

quired for regeneration seem to be the same ones that regulate growth at development (Vizcaya-Molina et al., 2020). Among the pathways that are activated in response to damage, we can find the JAK/STAT pathway, which gets activated by both, JNK and p38 (Ahmed-de-Prado et al., 2018; Katsuyama et al., 2015; Santabárbara-Ruiz et al., 2015), and the Hippo pathway, that is inhibited upon damage due to the changes in cell tension, resulting in an increased Yorki (Yki) activity that promotes growth (Grusche et al., 2011; Sun & Irvine, 2011). In addition to the upregulation of these pathways, an increase in *wg* expression has also been observed in response to damage (Harris et al., 2016; F. A. Martín et al., 2009; Pérez-Garijo et al., 2004; Ryoo et al., 2004; Smith-Bolton et al., 2009). Interestingly there is no consensus on the role of these molecules regarding proliferation. While some authors claim that Wg promotes proliferation in the regenerative tissue (Harris et al., 2016; Ryoo et al., 2004; Smith-Bolton et al., 2009), others authors claim that compensatory proliferation can take place independently of Wg (Díaz-García & Baonza, 2013; Herrera et al., 2013; Pérez-Garijo et al., 2009). Thus, further research is needed to comprehend the role of Wg in regeneration.

Apart from growth, repatterning of the damaged tissue is essential to recover the proper functionality of the organ. Upon damage, there is a loss of patterning expression genes such as *vg*, that is not recovered until the regenerative growth is complete, or even the loss of the compartment boundaries (Díaz-García & Baonza, 2013; Smith-Bolton et al., 2009). Although the boundaries are recovered shortly after the injury (Smith-Bolton et al., 2009), it has been reported that some cells can change their fate and adopt new compartment identities, something impossible in development (Herrera & Morata, 2014). Similarly, cells from the veins and interveins or cells from the hinge can change their fate to pouch cells in order to contribute to the regeneration process (Herrera et al., 2013; Repiso et al., 2013; Verghese & Su, 2016; Worley et al., 2022). These fate changes are facilitated by the regulation of chromatin modifiers downstream of JNK (Blanco et al., 2010; Klebes et al., 2005; Lee et al., 2005; Tian & Smith-Bolton, 2021). Moreover, the regulation of these chromatin modifiers could explain why regeneration sometimes is associated to transdetermination (Klebes et al., 2005; Lee et al., 2005).

Regeneration is a process that takes time. In fact, the imaginal wing discs present mechanisms to delay the development of the larvae in order to allow regeneration. One of these mechanisms is the release of the *Drosophila* Insulin-like peptide 8 (Dilp8) induced by JNK and Yki in the damaged disc. This peptide travels and signals to the prothoracic gland, and prevents the production of the Ecdysone hormone, the responsible to induce pupariation (Garelli et al., 2015; Katsuyama et al., 2015). Interestingly, it has been proposed that Dilp8 contribute to

the ending of regeneration. Specifically, it has been proposed that upon the restoration of the epithelial barrier in regeneration, Dilp8 would be sequestered inside the disc and could not be capable to signal to the prothoracic gland, therefore Ecdysone would be no longer repressed and metamorphosis would take place (DaCrema et al., 2021). Not just Dilp8 but also retinoids can induce delay by inhibiting the transcription of the gene encoding PTTH and therefore preventing Ecdysone release (Halme et al., 2010). Additionally, in damage or tumoral discs, JNK induces the production of Unpaired 3 (Upd3), a cytokine ligand of the JAK/STAT pathway that has been reported to act directly on the prothoracic gland to suppress Ecdysone and drive delay (Cao et al., 2022; Romão et al., 2021).

So far, we have been talking about the mechanisms that kick in in response to damage, but one important feature of wing disc regeneration that we have not mentioned is that its regenerative ability decreases over time (Smith-Bolton et al., 2009). Multiple factors have been identified as possible causes of this loss of potential. For example, upon damage there is a reorganization of the chromatin accessibility, making DRREs accessible in order to induce the

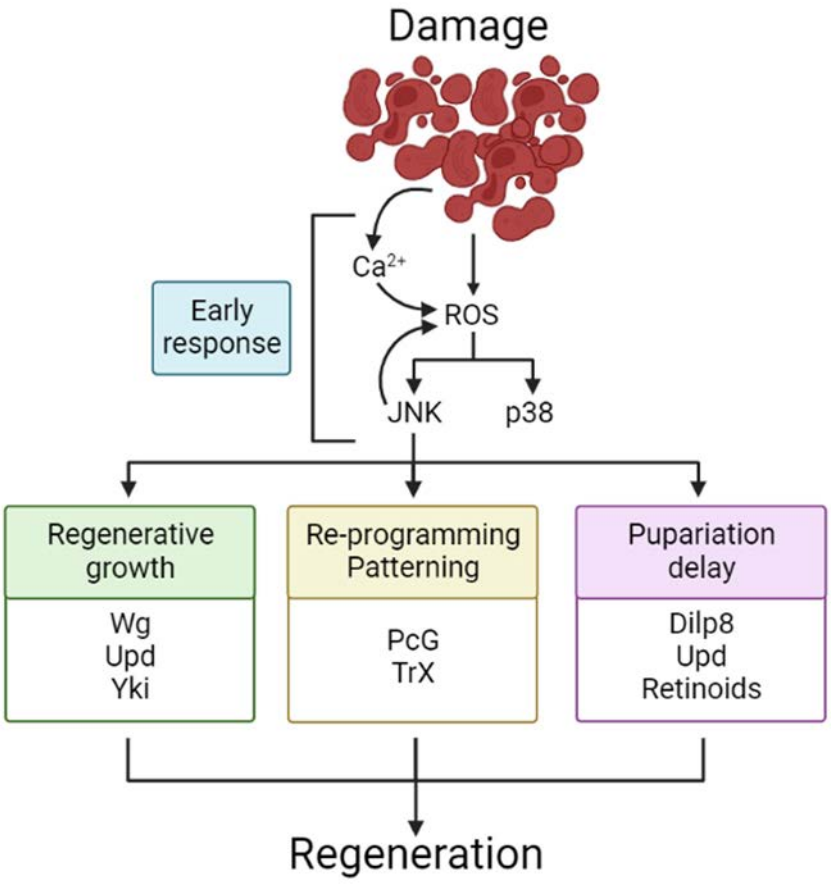

Figure 18. Overview of regeneration in the *Drosophila* wing disc. Schematic representation of the steps that take place in the regenerating wing disc and some of the players that participate in each of these steps.

expression of the many genes required for regeneration (Vizcaya-Molina et al., 2018). Interestingly, at later stages of development, although DRREs get more accessible upon damage, the capacity of response does not seem to be as strong as at the early stages. This suggests that at later stages there is an epigenetic silencing of the DRREs that limits the capacity to induce the expression of regenerative genes in response to damage, thus limiting the regenerative capacity (Harris et al., 2020). In addition to the chromatin landscape changes that decrease the regenerative potential over time, changes in regenerative capacity often correlate with significant changes in systemic hormone signalling. Consistently, an increase of Ecdysone in the later stages of development impairs regeneration by the upregulation of *broad* and downregulation of *chimno.* Interestingly, the upregulation of Chinmo is able to rescue the expression levels of Wg and other important regenerative genes in late damaged discs, enhancing the regenerative capacity of the disc (Narbonne-Reveau & Maurange, 2019). It is highly probable that Chimno helps cells to have a more dedifferentiated state, conferring them plasticity and proliferative potential. Moreover, it most probably performs its function through the downregulation of PcG, as it happens in eye disc tumours, suggesting that Chimno could play a role in modelling the chromatin state (Jiang et al., 2018).

The JNK pathway, the key of regeneration and tumorigenesis

The JNK pathway is a branch of the mitogen-activated protein kinase (MAPK) pathway (Pearson et al., 2001). This pathway plays a central role in a multitude of physiological and non-physiological processes. For example, JNK is crucial in the dorsal closure of the embryo (Ríos-Barrera & Riesgo-Escovar, 2013), in the thoracic closure during pupariation (Agnès et al., 1999; Zeitlinger & Bohmann, 1999) or in the testis, where promotes the self-renewal of the somatic cyst stem cells (Herrera & Bach, 2021). As shown above, JNK orchestrates regeneration. On one side, JNK triggers the expression of the proapoptotic genes *head involution defective* (*hid*) and *reaper* (*rpr*), leading to the activation of the caspase cascade and finally to death. At the same time, JNK also induces the expression of a vast repertoire of molecules required for many different processes during regeneration. Interestingly, at the same time that JNK induces cell death, also promotes proliferation and regeneration by triggering the secretion of promitotic molecules such as Wg (reviewed in Pinal et al., 2019). Besides that, JNK also seems to be involved in the elimination of loser cells during cell competition (reviewed in La Marca & Richardson, 2020; Morata & Calleja, 2020). JNK is also a central player in tumorigenesis where it can act as both a friend and a foe. Indeed, similarly as occurs in cell competition, JNK can mediate the elimination of those cells that are no longer fit for the tissue, acting as a tumour

suppressor. However, in tumoral cells that are resistant to cell death, JNK plays the opposite role. In these cells, JNK mediates a continuous release of molecules that play a protumoral role, such as Wg, that induces the overgrowth of the tumour (reviewed in Igaki & Miura, 2014; La Marca & Richardson, 2020; Pinal et al., 2019). In the following section, we will discuss in more detail the role of JNK in tumorigenesis.

The main ligand of the pathway is Eiger (Egr), the *Drosophila* homolog of the Tumour necrosis factor-α (TNF-α)(Igaki et al., 2002; Moreno et al., 2002). Egr can activate the JNK cascade by binding any of the two receptors of the pathway, Wengen (Wgn)(Kanda et al., 2002) and Grindelwal (Grnd)(Andersen et al., 2015). The activation of the receptors leads to the activation of the JNKKKK Misshapen (Msn), that in turn activates the JNKKK TGFβ-associated kinase 1 (Tak-1)(Igaki & Miura, 2014). Three more JNKKK can be found: Ask1, Slipper (Slrp) and Wallenda (Wnd). Depending on the stimuli that lead to the activation of the JNK pathway, it is more prompted that one of the JNKKK gets specifically activated. For example, in the dorsal closure, it seems that is Slpr the JNKKK that gets activated (Ríos-Barrera & Riesgo-Escovar, 2013), while Ask1 gets intracellularly activated due to ROS imbalances induced upon damage (Figure 19A)(Santabárbara-Ruiz et al., 2015) or by chromosomal instability (Muzzopappa et al., 2017). Then the cascade continues by the activation of the JNKK Hemipterous (Hep)(Glise et al., 1995) or MAP kinase kinase 4 (Mkk4) that triggers the activation of the only JNK, Basket (Bsk)(Riesgo-Escovar et al., 1996; Sluss et al., 1996). Bsk is capable to phosphorylate and activate a number of TFs, though the best know TFs are Jun proto-oncogene (Jun, also known as Jra) and Fos proto-oncogene (Fos, also known as Kay), which together make up the heterodimeric Activator Protein-1 (AP-1). AP-1 transcriptionally upregulates numerous target genes that are involved in proliferation, wound closure, cell migration, apoptosis, etc (Figure 19A) (reviewed in Igaki, 2009).

Many different inputs can lead to the activation of JNK, triggering a large response to which many different elements contribute. Interestingly, many of these elements in turn regulate JNK, generating a series of feedback loops essential for JNK function. For example, JNK induces the expression of Puckered (Puc), a phosphatase that dephosphorylates Bsk. Therefore, Puc establishes a negative feedback loop that is essential to modulate the activity of the pathway (Figure 19B)(Martín-Blanco et al., 1998). Another feedback loop occurs between the JNK pathway and the caspase cascade. As mentioned above, the activation of the JNK triggers the transcription of *hid* and *rpr,* which are at the top of the caspase cascade. Once activated, they block the Death-associated inhibitor of apoptosis 1 (Diap-1), which in turn is blocking the

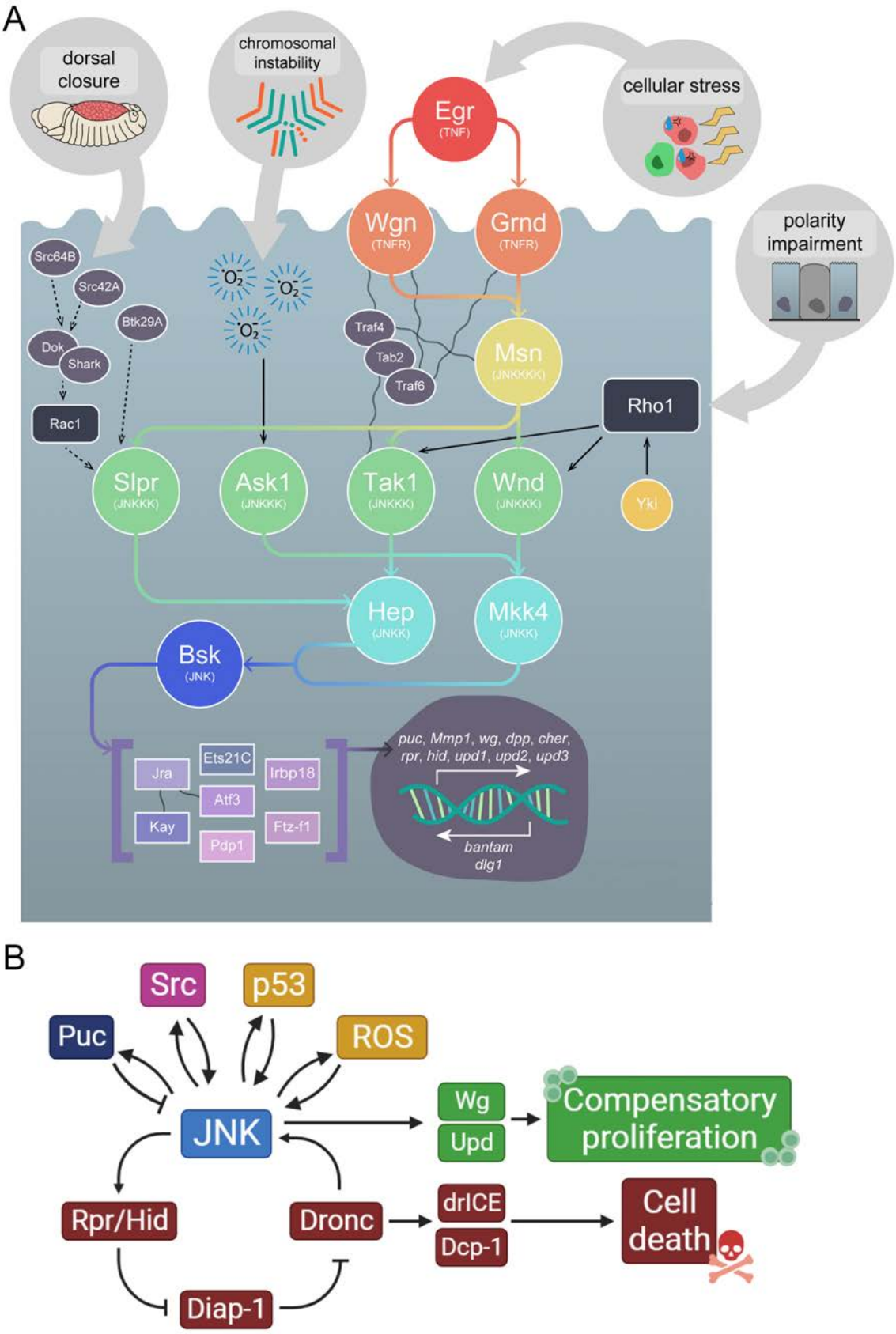

Figure 19. The JNK pathway. A) Cartoon depicting the JNK pathway. Different stimuli can differentially activate the JNK cascade. The cascade converges in the activation of Bsk, which activates the TFs of the pathway. Thus, the activation of the JNK pathway culminates in the transcription of different JNK targets such as the promitotic molecules Wg or the proapoptotic genes *rpr* and *hid*. Adapted from La Marca and Richardson, 2020. **B)** Cartoon depicting the different feedback loops of the JNK pathway.

initiator caspase Death regulator Nedd2-like caspase (Dronc). Hence, when Hid and Rpr are active, Dronc is no longer repressed and can activate the effector caspases Death caspase-1 (Dcp-1) and Death related ICE-like caspase (drICE), which trigger cell death (Figure 19B)(Fuchs & Steller, 2011). Interestingly, has been proposed that Dronc is capable to trigger the activity of the JNK pathway, although is not very well established how (Figure 19B)(Rudrapatna et al., 2013; Shlevkov & Morata, 2012). Another positive feedback loop essential for the JNK activity is the one established between JNK and ROS. Interestingly, this is a common feedback loop in both regeneration and tumorigenesis (Figure 19B)(Khan et al., 2017; Muzzopappa et al., 2017; Pinal et al., 2018). Similarly to the ROS feedback loop, JNK also establishes a feedback loop with p53 in regeneration (Shlevkov & Morata, 2012). Finally, it seems that JNK also a positive establishes a feedback loop with the proto-oncogene Src, a critical molecule that directs actin remodelling to promote invasion (Figure 19B)(Rudrapatna et al., 2014).

Tumorigenesis in the wing disc

Chromosomal instability and cancer

According to the World Health Organization, in 2018 cancer was the second leading cause of death worldwide, making cancer a global problem. Consequently, cancer is one of the most researched topics in the world. Although the general public often understands cancer as a single disease, cancer comprises more than 100 distinct diseases, that can originate from almost any cell type and organs of the body. The main characteristic of these cells is that they present an unrestrained proliferative capacity and they can invade the adjoining tissue and metastasize to distant organs (Stratton et al., 2009). All tumours are characterized by the fact that many steps are required to pass from a healthy to a tumoral one, it is a progressive transformation. Interestingly, although heterogeneity is found among tumours, all of them obtain common capabilities that allow tumour progression. These capabilities or hallmarks were described by Hanahan and Weinberg initially as six: evasion of apoptosis, self-sufficiency

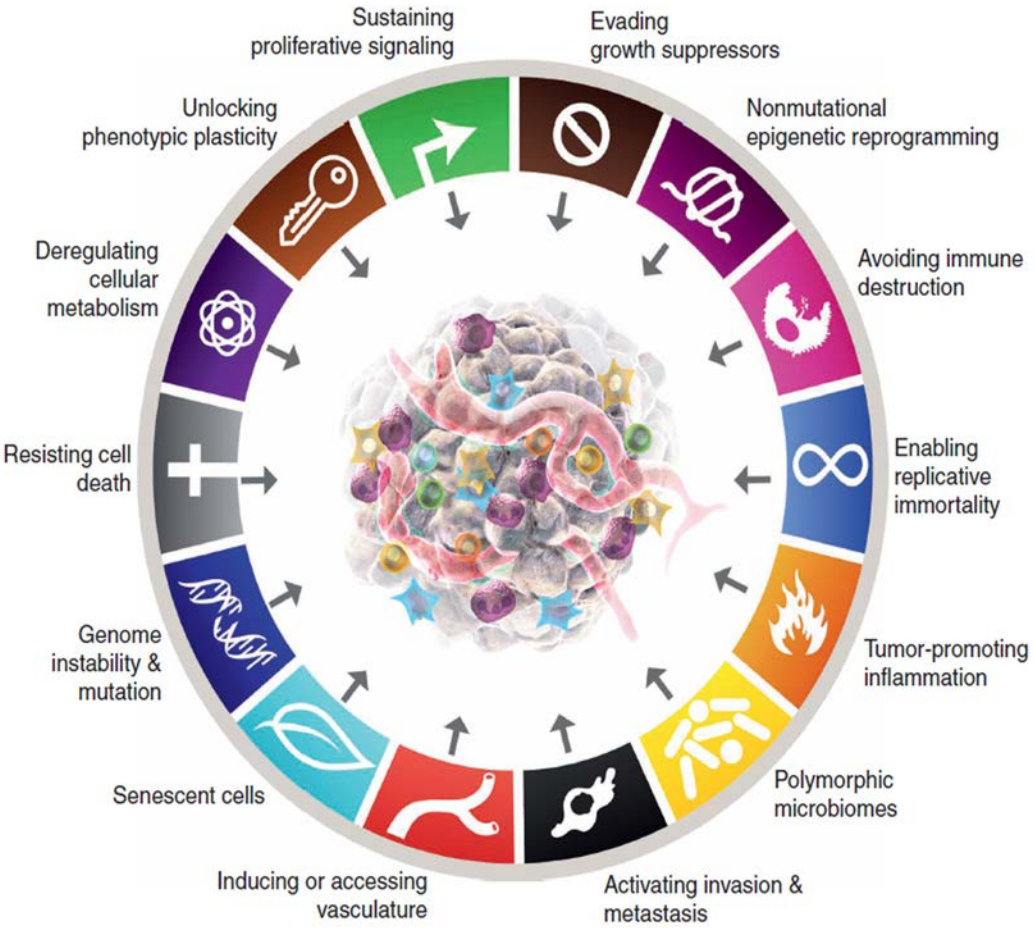

Figure 20. The hallmarks of cancer. Cartoon showing the hallmarks of cancer. Adapted from Hanahan, 2022.

in growth signals, insensitivity to anti-growth signals, limitless replicative potential, sustained angiogenesis, and tissue invasion and metastasis (Hanahan & Weinberg, 2000). Since then, researchers have continued investigating and new hallmarks of cancer as crucial as the deregulation of the cellular metabolism, the avoidance of the immune system, the tumour-promoting inflammation, the senescent cells present in tumours or the unlocking phenotypic plasticity, have been added to the list (Figure 20)(Hanahan, 2022; Hanahan & Weinberg, 2000). Among the hallmarks of cancer, in our laboratory, we are especially interested in genome instability.

Genomic instability is present in almost all cancers and it is defined as the increased tendency for DNA mutations and other genetic changes. Genomic instability is highly complex and includes nucleotide, microsatellite, and chromosomal instabilities. Although all these factors contribute to inducing genomic instability, chromosomal instability is the predominant form of genomic instability, and many times is referred to as a hallmark of cancer (S. Guo et al., 2023; Wei et al., 2016). Thus, in recent years our laboratory has focused its efforts to improve our understanding of the role of chromosomal instability in tumour formation and progression.

Chromosomal instability (CIN) is defined as the dynamic change in the chromosome number or structure as a result of ongoing chromosome segregation errors through consecutive cell divisions. Changes can vary from the loss or gain of an entire chromosome to just a fragment. Consequently, CIN leads to aneuploidy, a state where the cell presents an imbalanced (or non-euploid) number of chromosomes (Bakhoum & Cantley, 2018). It is estimated that 90% of solid cancers and 50% of hematopoietic cancer present some level of aneuploidy (Vasudevan et al., 2021). Despite it is clear the implication of CIN on tumours, the causal relationship between CIN and tumorigenesis remains controversial (Sen, 2000). In fact, in mice models, induction of CIN is insufficient to trigger tumour formation by itself, and it is required the mutagenesis of tumour suppressive genes, such as p53, to allow the development of a tumour (Holland & Cleveland, 2009; M. Li et al., 2010). Nevertheless, it is clear that CIN impacts tumour development and malignancy. Indeed, there is evidence of a clear correlation between high degrees of aneuploidy and CIN with disease progression and poor prognosis. Patients that present tumours with high levels of CIN have a shorter lifespan than those patients that present tumours chromosomally stable (Andor et al., 2016; Hieronymus et al., 2018; van Dijk et al., 2021). Moreover, it has been reported that metastatic cells present higher levels of CIN and aneuploidy, showing a clear correlation between CIN and tumour malignancy (Bakhoum et al., 2018). On top of that, it has been shown that tumoral heterogeneity derived from CIN

contributes to enhance the cell adaptability in front of deleterious cues and contributes to developing drug resistance (Carloni et al., 2023; Lukow & Sheltzer, 2022).

Enhancers in the context of tumorigenesis

Among the newest hallmarks of cancer, two of them are highly related to enhancers: the nonmutational epigenetic reprogramming and the unlocking of phenotypic plasticity (Hanahan, 2022).

Many tumours are associated with a disruption in the differentiation state of the cells, showing transcriptional signatures more typical of less differentiated states. Therefore, these cells present increased phenotypic plasticity. This less differentiated state could be due to de-differentiation (when the tumoral origin is from a differentiated cell), blockage of differentiation (when the tumoral origin is from a progenitor or a stem cell) or transdetermination (when cells change their cell fate to a new one)(Hanahan, 2022). Therefore, in general, tumours present a loss of expression of genes that trigger cell fate specification and a gain of expression of growth-promoting genes, most probably related with the fact that as a cell differentiates it loses its proliferative potential. In fact, forced differentiation helps to impair tumour progression and malignancy (Claps et al., 2016; Ordóñez-Morán et al., 2015; Tan & Barker, 2015). Therefore, everything indicates that the acquisition of a more plastic state is an essential feature of tumorigenic cells.

The acquisition of the phenotypic plasticity of the cells is highly related to changes in the epigenome since the silencing of more differentiating genes and the reactivation of growth-promoting genes require changes in the chromatin landscape. Recent reports have shown that genes that organize, modulate and maintain chromatin architecture, in other words, genes that regulate gene expression, often are mutated in tumours (Baylin & Jones, 2016; Flavahan et al., 2017). Consequently, changes in the epigenome and the chromatin landscape lead to changes in gene expression. Nevertheless, both gain and loss of function of both PcG and TrxG have been associated with tumour development (reviewed in Pasini & Di Croce, 2016; Schuettengruber et al., 2017). This indicates that the role of these mutations is highly dependent on the cellular context and the tumour type. Not just the chromatin remodelers but the histone modification enzymes are often mutated too (reviewed in Zhao & Shilatifard, 2019). For example, mutations in the histone acetyltransferase CREBBP have been found in gastric and colorectal, epithelial, ovarian, lung and esophageal cancer (Miremadi et al., 2007). In addition, tumoral cells present an aberrant DNA methylation pattern. Indeed, many tu-

mours show a general hypomethylated state while maintaining a subset of target genes, such as tumour suppressor genes, hypermethylated (reviewed in Nishiyama & Nakanishi, 2021). Therefore, despite the complex biology behind epigenetic regulation in tumoral cells, the fact that these genes are often mutated in tumours indicates that these changes can be beneficial for the cancer cell. Indeed, it seems that epigenomic changes contribute to the heterogeneity of the tumour, hence, contributing to tumour development and malignant progression (Hanahan, 2022). Furthermore, we do not have to forget that TFs, responsible for enhancer activity, are mutationally activated in tumours. Therefore, mutations in these key proteins or in their regulators can affect both enhancer activity and accessibility (I. Sur & Taipale, 2016).

As mentioned above, tumours undergo a series of epigenomic changes that lead to major changes in gene expression that drive the cell to a less differentiated state by the downregulation of cell fate-specifying genes and the upregulation of growth-promoting genes. Therefore, since enhancers are the main responsible for gene expression, it is easy to conclude that they are the prime targets of the epigenetic modifications that occur during tumorigenesis (Kron et al., 2014; Maurya, 2021). Indeed, there is a loss of activity in enhancer nearby cell fate-specifying genes and a gain in nearby growth-associated genes (Akhtar-Zaidi et al., 2012; Aran et al., 2013; Heyn et al., 2016). Interestingly, enhancers associated with cancer also exhibit tumour type-specificity (I. Sur & Taipale, 2016). A good example of this is the *myc* gene. Although *myc* is expressed in many tumours, in each of them its expression is driven by a different enhancer. For example, while in pancreatic cancer *myc* expression is driven by a super-enhancer nearby its transcription termination site, in colorectal cancer *myc* expression is driven by a super-enhancer upstream of *myc* (Figure 21A)(Hnisz et al., 2013). In tumours it has been observed de novo formation of super enhancers (SEs). SEs are a large cluster of enhancers with a high density of TFs and cofactors that drives a strong transcription of key developmental genes (Hnisz et al., 2013; Pott & Lieb, 2015). By contrast, in tumours, SEs drive high levels of expression of key oncogenes (Figure 21B)(Tang et al., 2020; Thandapani, 2019). Although there is a "reuse" of enhancers associated with growth-promoting genes in tumoral cells, there are also some enhancers that seem to be specific to tumoral cells. For instance, in mice, there is a highly conserved enhancer upstream of the *myc* gene whose deletion prevents tumoral formation without affecting regular development (I. K. Sur et al., 2012). The fact that this enhancer is highly conserved but does not contribute to development suggests that it could be involved in regeneration. Thus, this regeneration enhancer would be aberrantly reused in tumoral cells to drive proliferation.

In addition to changes in the epigenome, enhancer's activity can be affected by somatic mutations. For instance, enhancer copy number alteration can affect their activity (Figure 21C) (X. Zhang et al., 2016). Indeed, these kinds of mutations seem to accumulate over time, sug-

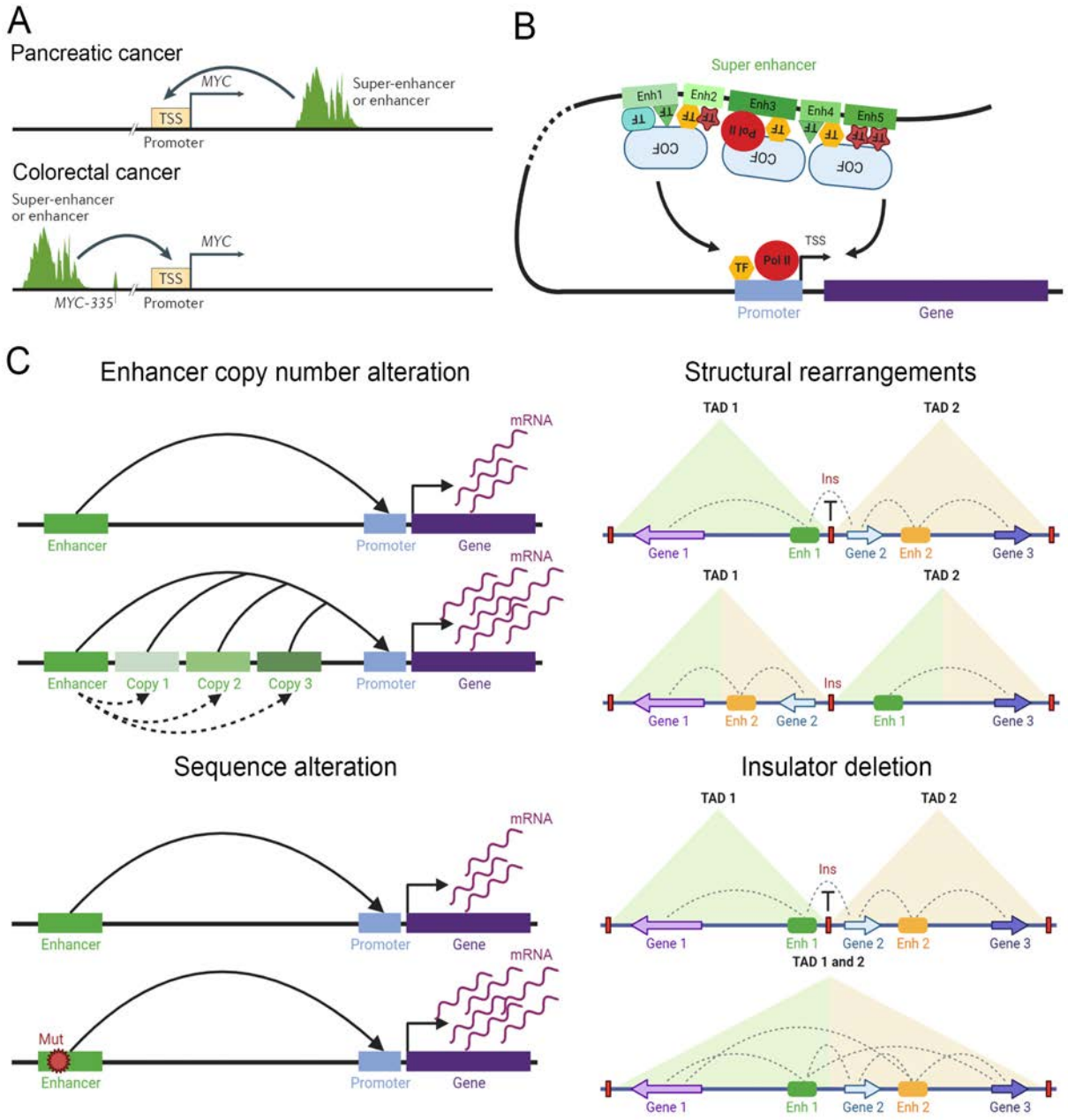

Figure 21. Enhancers in the context of tumorigenesis. A) Different types of cancer use different enhancers to drive the expression of the same gene. Example of two different Super Enhancers regulating the expression of myc in pancreatic and colorectal cancer. Adapted from Sur and Taipale, 2016. **B)** Representation of a super enhancer regulating the expression of a gene. Notice that the super enhancer is composed of a cluster of smaller enhancers. **C)** Somatic mutations that occur during tumorigenesis and that can alter the activity of the enhancers. Top-left: enhancer copy number alteration. The duplication of the enhancer can alter the level of transcription of the target gene. Top-right: Structural rearrangements such as chromosomal inversions or deletion can bring to close proximity enhancers to oncogenic genes that previously were separated in different TADs, leading to aberrant gene expression. Bottom-right: the elimination of insulators leads to the merging of different TADs, promoting aberrant interactions between genes and enhancers from the two TADs.

gesting that they are positively selected (D. Herranz et al., 2014; Hsu et al., 2013). Moreover, translocations and structural rearrangements are also typical events in tumoral cells. It has been described that sometimes these rearrangements reposition enhancers next to key oncogenic genes, leading to aberrant gene expression (Figure 21C)(Cauwelier et al., 2006; Northcott et al., 2014; Taub et al., 1982). In addition, aberrant enhancer-promoter interactions in tumoral cells also can be promoted by mutations or deletions of the insulators sequence of the TADs (Figure 21C)(Hnisz et al., 2016; Katainen et al., 2015). Finally, enhancers can also suffer mutations inside their sequence such as small deletions, small insertions or single base mutations. These mutations can change the TF binding affinity, eliminate a TFBS of the enhancer or even generate new TFBS, altering the activity of the enhancer (Figure 21C)(Herz, 2016).

Finally, recent reports have shown that many mutations that predispose to cancer are localized in enhancers (Maurano et al., 2012; Schaub et al., 2012). In general, these mutations have small effects on the binding capacity of TFs, leading for example to a slight increase in the transcription of the gene for example. These mutations do not completely activate or inactivate their respective enhancers, and they require additional somatic mutations to allow cancer formation (I. Sur & Taipale, 2016).

Drosophila wing disc as a chromosomal instability tumoral model

For the last few decades *Drosophila* has been used as a tumoral model. This is possible because 75% of all the human disease-causing have a homolog in *Drosophila* (Singh & Irvine, 2012; Ugur et al., 2016). In fact, the first tumour suppressor gene was found in *Drosophila* (reviewed in Watson et al., 1994). Moreover, many pathways involved in human cancer are conserved in flies (Brumby & Richardson, 2005; Gonzalez, 2013). All this, added to the massive quantity of sophisticated genetic tools available to manipulate the *Drosophila* genome, has made *Drosophila* a very attractive model to study tumour formation and progression (Enomoto et al., 2018; H. Herranz et al., 2016). Furthermore, to study tumorigenesis in *Drosophila*, the use of imaginal discs has been quite common because their epithelium is quite similar, both morphologically and biochemically, to the epithelium of mammals (Richardson & Portela, 2018; Wodarz & Näthke, 2007). This is relevant because approximately 90% of human cancer present an epithelial origin (Hanahan & Weinberg, 2000).

In our laboratory, we have been using the *Drosophila* wing disc to model CIN-induced tumours for many years. As stated above, chromosomal instability is defined as a high rate of change in the chromosome number or structure as a result of missegregation events during

mitosis. Due to its relevance for the future of the cell, mitosis is a highly regulated process. Prior to chromosome segregation, two distinct pols are formed in the cell established by the centrosomes. Centrosomes are in charge of the formation of the mitotic spindle, inducing the synthesis of microtubules and directing them to join the chromosomes to separate the sister chromatids in the two daughter cells. All this process is tightly controlled by the Spindle Assembly Checkpoint (SAC). This is the mechanism in charge to ensure that the chromosomes are properly placed and attached to the spindle microtubules in order to prevent errors in their segregation (reviewed in Musacchio & Salmon, 2007). Hence, errors in any of these steps can lead to the induction of CIN (Dekanty & Milán, 2013; Gerlach & Herranz, 2020; M. S. Levine & Holland, 2018). In fact, different laboratories use the mutation or depletion of one or more of these genes to induce CIN (Basto et al., 2008; Da Silva et al., 2013; Dekanty et al., 2012; Mirkovic et al., 2019).

In our laboratory, we have been using the depletion of SAC genes such as *bub3* or *rough deal* (*rod*) to induce chromosomal instability. Interestingly, as it occurs in mice, the depletion of SAC genes by itself is not sufficient to drive tumorigenesis. On the contrary, induction of CIN triggers the extrusion of the cell from the epithelium (delamination) and its death through the activation of the JNK pathway, eliminating the aneuploid cells from the tissue and ensuring tissue homeostasis (Figure 22A)(Castellanos et al., 2008; Dekanty et al., 2012). However, when apoptosis is blocked at different levels of the caspase cascade, aneuploid cells delaminate from the epithelium and are maintained in the tissue leading to the formation of tumours. Thus, this results in the formation of two different cell populations. On one side there is the growing epithelium, which presents low levels of aneuploidy and has a high proliferative potential. On the other side, the delaminated population presents high levels of aneuploidy and JNK activity (Figure 22B)(Dekanty et al., 2012; Dekanty & Milán, 2013).

The delaminated population is mostly composed of senescent cells arrested at G2 with a highly secretory profile (Clemente-Ruiz et al., 2016; Joy et al., 2021). Both senescence and the secretome are mediated by JNK and are essential for tumour progression (Clemente-Ruiz et al., 2016; Dekanty et al., 2012; Joy et al., 2021). Among the molecules secreted by senescent cells, there is the promitotic molecule Wg that signals to the growing epithelium promoting proliferation and tumour growth (Dekanty et al., 2012). Nevertheless, this proliferation leads to an increase in CIN and, therefore, aneuploidy, causing its delamination. Thus, it exists a cross-feeding interaction between the main epithelium and the delamination population that is essential for the tumoral progression (Figure 22B)(Muzzopappa et al., 2017). In fact, Wg

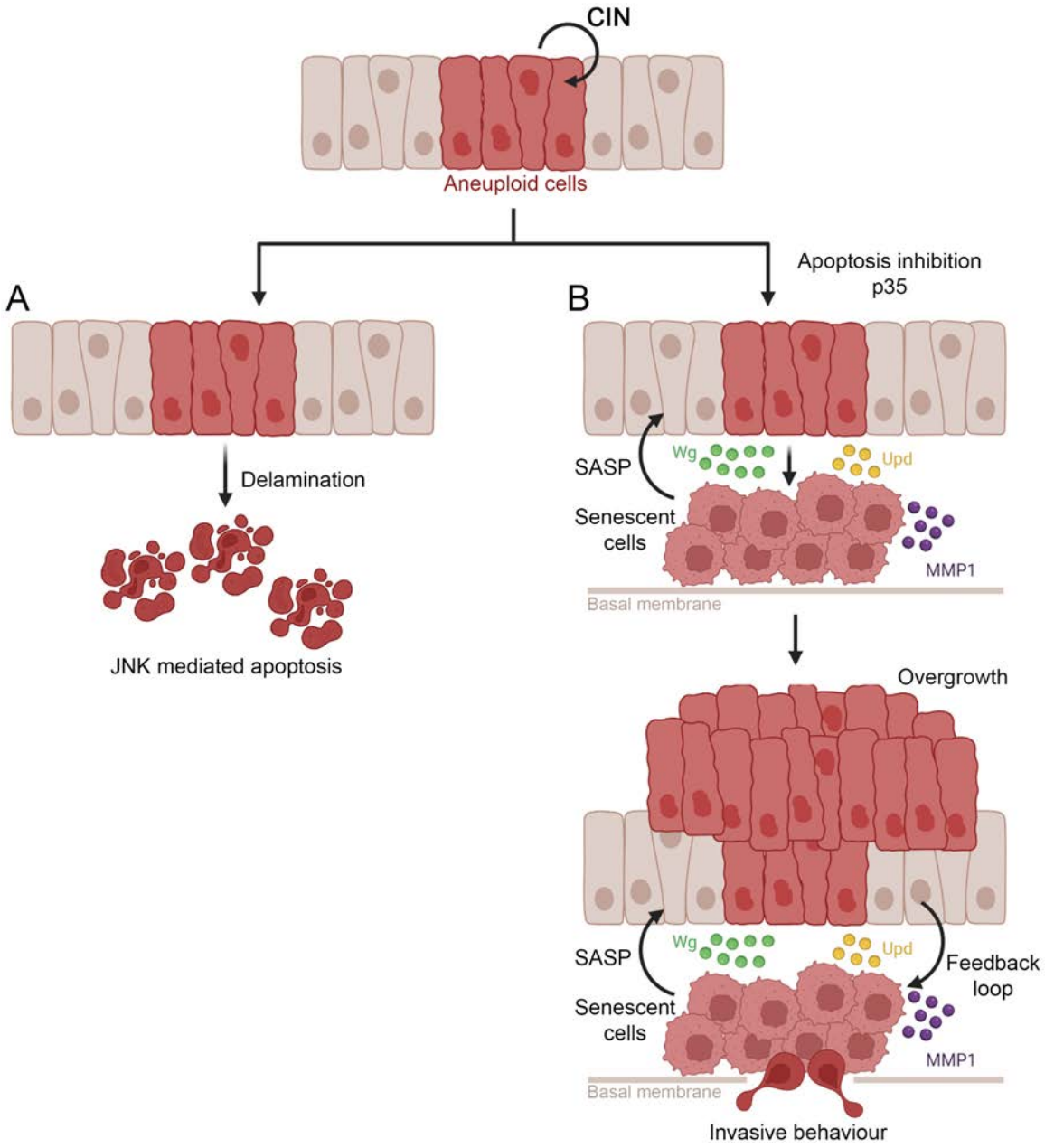

F**igure 22. CIN derived tumorigenesis in the *Drosophila* wing disc. A)** Aneuploid cells generated by the induction of CIN (though SAC genes depletion) delaminate from the epithelium and enter into JNK mediated apoptosis. **B)** Blockage of apoptosis via p35 prevents the JNK mediated apoptosis and allows this group of cells to become senescent. The senescent population secrets molecules from the SASP such as the promitotic molecule Wg, which induces the overgrowth, or MMP1, a metalloprotease that degrades the basal membrane and allows the invasion of neighbouring tissues, and Upds which, among other things, induce developmental delay.

depletion drastically reduces tumoral growth and the number of delaminated cells (Dekanty et al., 2012; Muzzopappa et al., 2017). In addition to Wg, the delaminated population also secrete the pro-inflammatory molecule Upd3. This molecule signals to the Ringland inducing a delay in pupariation, giving the tumour time to continue growing and finally resulting in lethality for the animal (Romão et al., 2021). Moreover, the delaminated population produces

MMP1, a metalloprotease that degrades the basal membrane, allowing the migration of these cell population (Benhra et al., 2018; Dekanty et al., 2012). Interestingly, it seems that cell migration is not just mediated by JNK, which modulates the actin-myosin cytoskeleton, but also relays on the EGFR/Erk pathway and the caspases (Figure 22B)(Benhra et al., 2018).

Although the senescent population is crucial for tumour development, these cells are subjected to high levels of stress (Clemente-Ruiz et al., 2016; Joy et al., 2021). In fact, the genome of *Drosophila* consists only of four chromosomes that present a highly compacted genome, thus even small gains or losses of a chromosome lead to big imbalances that drive stress in the cells (Milán et al., 2014). Indeed, the delaminated population presents a near-saturation functioning of autophagy and accumulation of dysfunctional mitochondria that lead to an increase in ROS levels, among other stresses (Joy et al., 2021). Interestingly, the cells present mechanisms to try to buffer the effects of CIN such as the dosage compensation mechanism, the DNA-damage repair machinery or the activation of p38 (Clemente-Ruiz et al., 2016).

The *wg*^{1}-enhancer

The first ever described allele of the *wg* gene was *wg*^{1} (Sharma, 1973; Sharma & Chopra, 1976). *wg*^{1} is a hypomorphic mutation of *wg* that induces the lack of wings and a mirror duplication of the body wall. However, despite the highly pleiotropic effects of Wg in the development, the phenotype of *wg*^{1} flies is remarkably restricted to the absence of wings (Bejsovec, 2018; Swarup & Verheyen, 2012). Interestingly, the penetrance of the phenotype was variable and flies showing the absence of one or both wings could be observed, or on some occasions, completely normal flies with two regular wings also could be observed. (Morata & Lawrence, 1977; Sharma & Chopra, 1976). However, the absence of wing and the notum duplication was not the only effect observed in the *wg*^{1} flies. In fact, similarly to the wing phenotype, *wg*^{1} flies also presented an absence of the halter and a duplication of the structures of the scutellum with variable penetrance (Morata & Lawrence, 1977; Sharma & Chopra, 1976). In the beginning, it was thought that *wg*^{1} was a gene, but a few years later Dr Baker discovered that the phenotype was a result of a small deletion placed between the *wg* and *wnt6* genes (Baker, 1987). This fact suggested the idea that *wg*^{1} comprises a regulatory element in its sequence that contribute to the early expression of *wg* in the wing and halter, thus participating in the specification of the wing fate in early discs. Indeed, Dr Ng and colleagues showed that flies carrying the *wg*^{1} deletion did not exhibit expression of Nub, a specific marker of the wing pouch. Besides, at later stages, they observed a mirror duplication of the notum in late *wg*^{1} discs (Ng et al., 1996). Consistently, as reported by the laboratory of Dr Campbell, in *wg*^{1} early discs it can be observed the absence of *wg* mRNA expression coupled with an expansion of Vn, the molecule that confers notal identity, towards the ventral part of the discs (S. H. Wang et al., 2000). Altogether, these data reinforce the idea that *wg*^{1} contains a regulatory element that regulates *wg* early expression. However, in recent years, it has been reported that the penetrance of the phenotype in flies carrying the deletion has drastically reduced (Harris et al., 2016), questioning whether this deletion is responsible for the mutant phenotype. Furthermore, it has never been properly shown whether *wg*^{1} truly comprises a *wg* enhancer or how regulates *wg* expression in development.

In recent years it has been shown that *wg*^{1} can have a role further away from development. Dr Schubiger's laboratory showed that the leg disc could suffer Wg-dependent leg-to-wing transdetermination upon damage. Interestingly, the expression of ectopic Wg in the damaged area colocalized with the expression of *BRV118-lacZ* reporter, a reporter whose sequence partially overlaps with the *wg*^{1} sequence, starting at 23 bp after *wg*^{1} sequence and

extending 567 bp longer. Thus, it could be that *wg*^{1} might be mediating the expression of ectopic Wg upon damage in the leg disc. As expected, in *wg*^{1} flies the expression of ectopic Wg was drastically reduced upon damage (Schubiger et al., 2010). Consistently with Schubiger data, the laboratory of Dr Hariharan showed expression of the *BRV118* reporter colocalizing with ectopic Wg expression in the damaged discs. As expected, in the *wg*^{1} damaged wing disc they could not detect *wg* nor *wnt6* expression, indicating that *wg*^{1} mediates the upregulation of both genes upon damage (Harris et al., 2016). In addition, it was confirmed that the burst in the expression of *BRV118* upon damage correlates with an increase in the accessibility of the chromatin of its locus (Harris et al., 2020; Vizcaya-Molina et al., 2018). However, they could not detect the expression of the *BRV118* reporter at the different stages of development of the wing disc. Nevertheless, they could detect the expression of the *BRV118* reporter in different tissues upon damage. Therefore, the authors suggested that *BRV118*, hence *wg*^{1}, is a damage-responsive element that mediates Wg expression upon damage in several tissues (Harris et al., 2016). Indeed, a recent publication has shown that adult *wg*^{1} flies subjected to brain damage regenerate much worse than control flies (Simões et al., 2022). Furthermore, Dr Hariharan's laboratory reported a decrease in the enhancer activity over time mediated by the PcG proteins (Harris et al., 2016). This is consistent with the progressive loss of the *BRV118* locus accessibility observed over time (Harris et al., 2020). Interestingly, the activity of *BRV118* is mediated by the JNK pathway in the regenerative discs. Oddly, the authors reported that while they were capable to detect *BRV118* expression in *disc large* (*dlg*) tumoral discs, they were not capable to detect *BRV118* expression in *yki* tumoral discs (Harris et al., 2016). On the other hand, observations made by our laboratory showed that *BRV118* expression is detected in CIN tumours. Moreover, Wg ectopic expression and tumoral overgrowth were rescued in *wg*^{1} discs (Dekanty et al., 2012). Similarly, in *expanded (ex)* hyperplasic eye discs, upregulation of Wg upon *ex* depletion seems to be regulated by *wg*^{1}. In fact, hyperplasic overgrowth induced by *ex*-depletion was partially rescued in *wg*^{1} mutant eye discs (Pellock et al., 2007). Thus, it seems that there are contradictions between the different authors in the possible role of *wg*^{1} in the processes of development, regeneration and tumorigenesis.

wg^{1} has always been described as a highly tissue-specific allele since its main phenotype is winglessness. However, this not seems the only effect that this small deletion induces. In fact, Sharma and Chopra reported that sometimes the *wg*^{1} flies could present a stringer phenotype showing a partial or complete lack of the notal structures, suggesting that *wg*^{1} also could have a role in the notum (Sharma & Chopra, 1976). Moreover, *wg*^{1} flies also showed a

defect in the ventral part of the eye (Ma & Moses, 1995; Morata & Lawrence, 1977). Indeed, different authors have used the *wg*^{1} allele to study the function of Wg in the eye development and in the progression of the eye furrow (Ma & Moses, 1995; Pellock et al., 2007; Singh et al., 2006). Moreover, *wg*^{1} also has been used to study the function of Wg not just in the eye disc, but also in the brain. Indeed, it seems that *wg*^{1} contributes to the expression of *wg* during the formation of the synapsis in the neuromuscular junction (Ataman et al., 2008; Y. Huang et al., 2018) and in the differentiation of the glia and neurons in adult flies (Kerr et al., 2014). Furthermore, it has been used in adult brain models of disease. In fact, in Huntington's Disease model, *wg*^{1} deletion contributes to the expansion of the life span of the affected flies by depleting Wg expression (Dupont et al., 2012). *wg*^{1} also has been used in adult brain regeneration studies (Simões et al., 2022). Finally, it has been reported that *wg*^{1} also leads to minor effects on the leg (Held, 1993). Therefore, all these reports show us that *wg*^{1} contributes to more than just wing formation. Thus, it seems that *wg*^{1}, instead of having just a tissue-specific function, presents a more pleiotropic activity. Nevertheless, part of the data comes from indirect observations instead of a direct study of the *wg*^{1} allele. Therefore, further research is required to understand the role of *wg*^{1} in each of these processes.

As shown above, there are still holes in our knowledge about *wg*^{1}. Although there is evidence that *wg*^{1} participates in the development, regeneration and tumorigenesis of the wing disc, it exists controversy among the different authors on whether it contributes to the three processes. Furthermore, the lack of a proper characterization of *wg*^{1} makes it difficult to understand how *wg*^{1} may differently contribute to these different very relevant processes. In addition, it seems that *wg*^{1} could be involved in the development and in the stress response of other tissues. Hence, is the goal of this thesis to try to address these issues.

Objectives

Drosophila wg, the founding member of the Wnt family, is a highly pleiotropic gene that participates in many processes such as development, regeneration and tumorigenesis in different organs. On the contrary, wg^{1}, the first ever identified allele of *wg*, presents a remarkably restricted phenotype to the absence of wings. Interestingly, recent reports have shown that it is also implicated in the regeneration and tumorigenesis of the wing disc. However, it exists controversy among the different authors on whether it contributes to the three processes. Furthermore, the lack of proper characterization of the wg^{1} difficult to understand how wg^{1} may differently contribute to the different processes. Therefore, the main aim of this thesis is to characterize wg^{1} and understand how it contributes to the development, regeneration and tumorigenesis of the wing disc. Furthermore, it has been proposed that wg^{1} could regulate the expression of both, *wg* and *wnt6,* so we want to further understand how each of these genes contributes to each process. Finally, the data suggest the idea that wg^{1} also could present a function in other tissues, therefore we would like to test whether it is the case.

To further address the main goal of this thesis, the characterization of wg^{1} and understanding how it differentially contributes to the development, regeneration and tumorigenesis, we have we have proposed the following goals:

(1) Development:

- To determine how the wg^{1}-enhancer triggers wing development by controlling early Wg expression.

- To characterize the molecular mechanism behind Wg early expression.

- To define the minimal enhancer required.

(2) Regeneration:

- To determine whether wg^{1}-enhancer is involved in regeneration.

- To determine the minimal region required for Wg expression during regeneration.

- To characterize whether expression of the wg^{1}-enhancer is regulated by JNK in regeneration or by other mechanisms.

- To determine whether Wg is truly required during regeneration or not.

- To determine the role of Wnt6 in regeneration.

(3) Tumorigenesis:

- To determine whether the *wg*^{1}-enhancer is involved in tumorigenesis.

- To determine the minimal region required for Wg expression during tumorigenesis.

- To characterize whether expression of the *wg*^{1}-enhancer is regulated by JNK in tumorigenesis or by other mechanisms.

- To determine the role of Wnt6 in tumorigenesis.

Results

Chapter 1: The *wg*^{1}-enhancer in development

wg^{1} deletion induces a wing to notum transformation

wg is a highly pleiotropic gene that participates in several developmental processes in *Drosophila* (Bejsovec, 2018; Swarup & Verheyen, 2012). It was first discovered through a hypomorphic mutation called *wg*^{1} (Sharma, 1973). That induces a lack of the wing and a duplication of the body wall or notum (Morata & Lawrence, 1977; Sharma & Chopra, 1976). Interestingly, this phenotype is primarily restricted to the absence of the wing in contrast to the pleiotropic effects of *wg* mutations (Van Den Heuvell et al., 1993). That is because the *wg*^{1} phenotype is caused by a 2.416 bp deletion located approximately 8 kb downstream of the *wg* gene (named hereafter as *Δwg*^{1} for simplicity; Figure 23A, Table 1)(Baker, 1987). Surprisingly, the original penetrance of the *wg*^{1} deletion was not complete, with only the 40% of the heminotas (half of a notum) presenting the phenotype. However, after five cycles of selection the penetrance of the phenotype was increased up to 70% (Sharma & Chopra, 1976). Engagingly, recent reports have shown that the penetrance has decreased even lower that 40% (below 20%; Harris et al., 2016). As reported by Morata and Lawrence (1977), the decrease in the penetrance of the phenotype over time can be counterbalanced by outcrossing the line. Therefore, we decided to backcross the *Δwg*^{1}-carrying line twice with the *w*^{1118} line in order to remove potential genetic suppressors and recover the penetrance of the stock. Surprisingly, upon the backcrossing of the *Δwg*^{1} line, were no longer capable to obtain homozygous flies. To assess whether the penetrance of the phenotype was recovered, we decided to cross the *Δwg*^{1} flies with flies carrying the *BRV118* deletion (Schubiger et al., 2010). *BRV118* sequence partially overlaps with the *wg*^{1} sequence, starting 23 bp after *wg*^{1} sequence and extending 567 bp longer (Figure 23A, Table 1). Interestingly, the penetrance of the wing to notum transformation in *Δwg*^{1}*/ΔBRV118* flies was up to 81%, presenting most of the flies the complete lack of both wings or the lack of one wing and the subsequent notum duplication (Figure 23B and C). Surprisingly, the penetrance of the phenotype was not 100%, suggesting that there might be other regulatory elements driving the wing specification. For that reason, we decided to cross *wg*^{1} mutated flies with flies carrying larger chromosomal deficiencies comprehending the *wnt* cluster where *wg* and *wg*^{1} are located (Figure 23A, Table 1). In most transheterozygotic conditions, the penetrance was over 90% (Figure 23B), indicating that probably there are other regulatory elements in this region, such as shadow enhancers, that contribute to the specification of the wing. This will be further discussed in other sections of this thesis.

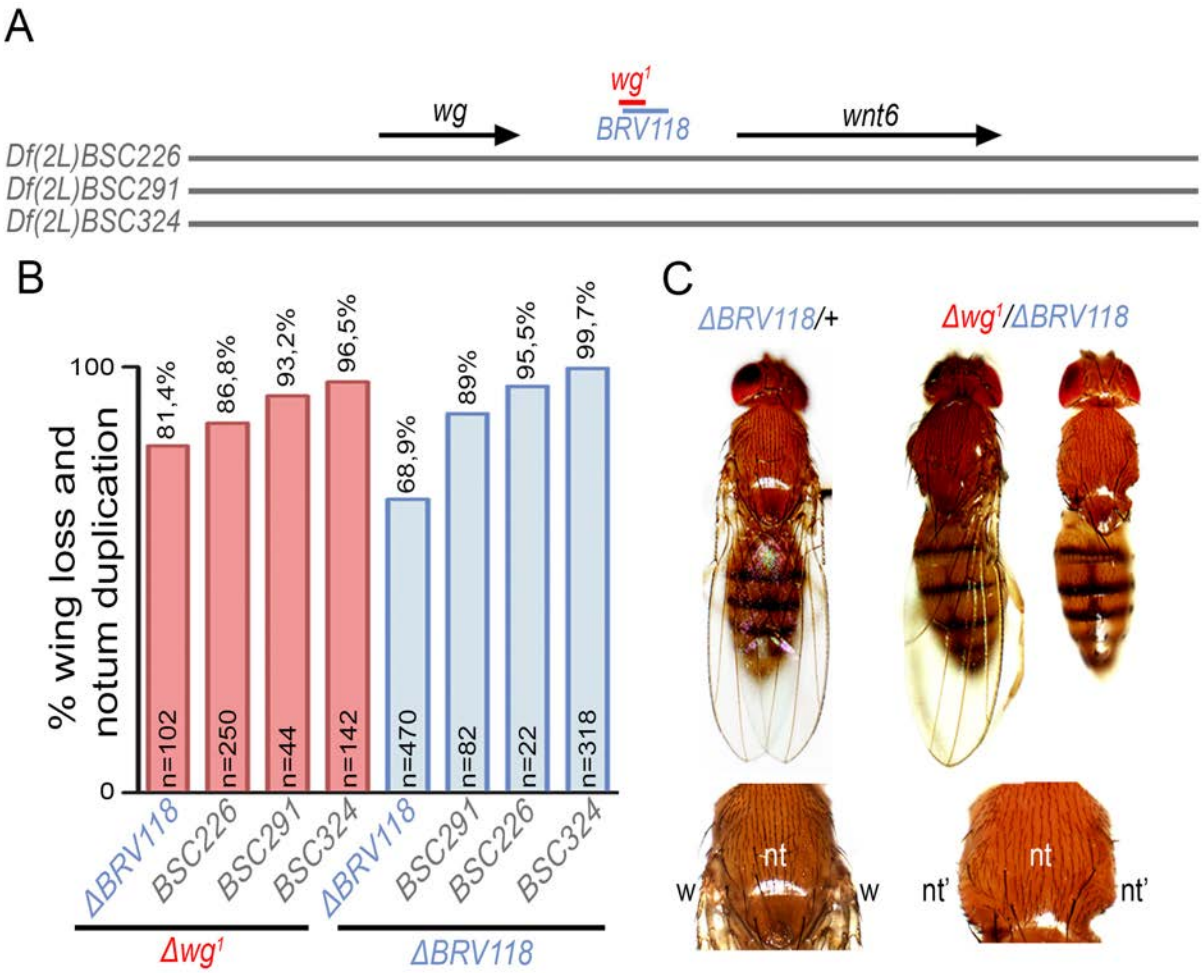

Figure 23. *wg¹* deletion induces a wing loss and a notum duplication. A) Cartoon depicting the genomic localization of and *BRV118* sequence between *wg* and *wnt6* genes and the different deficiencies that cover the region. **B)** Histogram showing the presence of flies that present the absence of wings and duplication of the notal structures of the indicated genotypes. The number of scored heminota (n) and the exact percentage is shown in the histogram. **C)** Examples of wing to notum transformation in adult flies of the indicated genotypes. The wing (w), the notum (n) and duplicated notum (n') are labelled in the magnification.

wg¹ drives Wg expression and wing fate specification

The next step was to unveil the mechanism by which *wg¹* controls wing fate specification. As previously mentioned, *wg¹* is localized within a cluster of the wnt family that contains the *wg* gene (Figure 23, Table 1). Wg is crucial in many steps of wing development, but early in development (in second instar, L2), Wg is expressed in a ventral anterior wedge triggering the specification of the wing fate in these cells (Figure 24A). The cells producing Wg are the ones that give rise to the wing pouch, the precursor of the wing blade (Couso et al., 1993; Ng M et al., 1996). Later on, in third instar (L3), Wg pattern expression changes, and it is expressed in a strip at the DV boundary, two concentric rings at the hinge, and a strip in the notum (Figure 24A'). At this stage Wg is reported to promote wing growth (Baena-Lopez et al., 2009; Barrio

wg^{1}-enhancer genomic positions

	FlyBase 1.6 Chrm 2L:		
wg Region	**Start Number:**	**End Number:**	**Base Pairs:**
wg gene	7.307.159	7.316.265	9.106
wnt6	7.333.714	7.352.542	18.828
wg^{1}	7.324.252	7.326.668	2.416
BRV118	7.324.275	7.327.235	2.960
BRV-A	7.324.275	7.325.250	975
BRV-B	7.325.250	7.326.235	985
BRV-C	7.326.172	7.327.303	1.131
Alpha	7.323.135	7.324.749	1.614
Beta	7.324.770	7.325.443	673
Gamma	7.325.445	7.326.565	1.120
Gamma-590	7.325.993	7.326.565	572
Gamma-630	7.325.445	7.325.993	548
Delta	7.326.565	7.327.855	1.290
*Df(2L)BSC226 (**Center**)*	7.249.632	7.366.119	116.487
*Df(2L)BSC291 (**Left**)*	7.042.642	7.366.119	323.477
*Df(2L)BSC324 (**Right**)*	7.249.633	7.718.010	468.377
BRV-AC59 Hariharan Deletion ABC	7.324.259	7.327.303	3.044
Spd^{flg}	7.297.496	7.298.924	1.428
Spd^{flg} *Ci Binding*	7.298.788	7.298.799	11
wnt6 intron	7.338.026	7.339.980	1.954
wnt6 Ci Binding	7.298.789	7.298.802	13

Table 1. Genomic coordinates. Table containing information on the genomic position of the regions analysed in this work around, overlapping or within *wg*^{1}.

& Milán, 2020; Diaz-Benjumea & Cohen, 1995) and to drive notum patterning (Phillips & Whittle, 1993). Interestingly, second instar wing disc (L2) of *Δwg*^{1}*/ΔBRV118* flies showed no Wg expression. Furthermore, the expression of Tsh, an early notal marker repressed by Wg at early stages (Wu & Cohen, 2002; Zirin & Mann, 2007), has expanded all over the disc, while in early wild type discs Tsh could not be detected in the region of Wg expression (Figure 24A and B). At later stages, the wing pouch (easily identified by the absence of Tsh, Figure 24A') could not be

detected in the majority of *Δwg¹/ΔBRV118* discs. Instead, we could detect the mirror duplication of the notal structures (Figure 24B'). These results suggest that *wg¹* contains a regulatory sequence that triggers early Wg expression, driving wing fate specification. Interestingly, as also shown in Figure 23, the absence of Wg in second instar *Δwg¹/ΔBRV118* wing discs and the absence of wing pouch and notum duplication at later stages did not occur in all cases. A small percentage of early discs presented Wg expression in the ventral anterior wedge, and those who went through wing disc specification gave rise to complete normal late L3 discs (Figure 24C and C'). This is coherent with the fact that the penetrance of the adult phenotype was not 100% (Figure 23B). Furthermore, the fact that *Δwg¹/ΔBRV118* escapers present a wild type-like wing disc and fully formed adult wings reinforces the idea that *wg¹* plays a role in early and not later stages of the wing disc development where we could observe a normal Wg expression pattern (Figure 24C'). Moreover, if *wg¹* would have an effect in later stages of wing development, we should observe abnormalities in later stage wing discs and in the adult wing, but they are completely normal (Figure 24C').

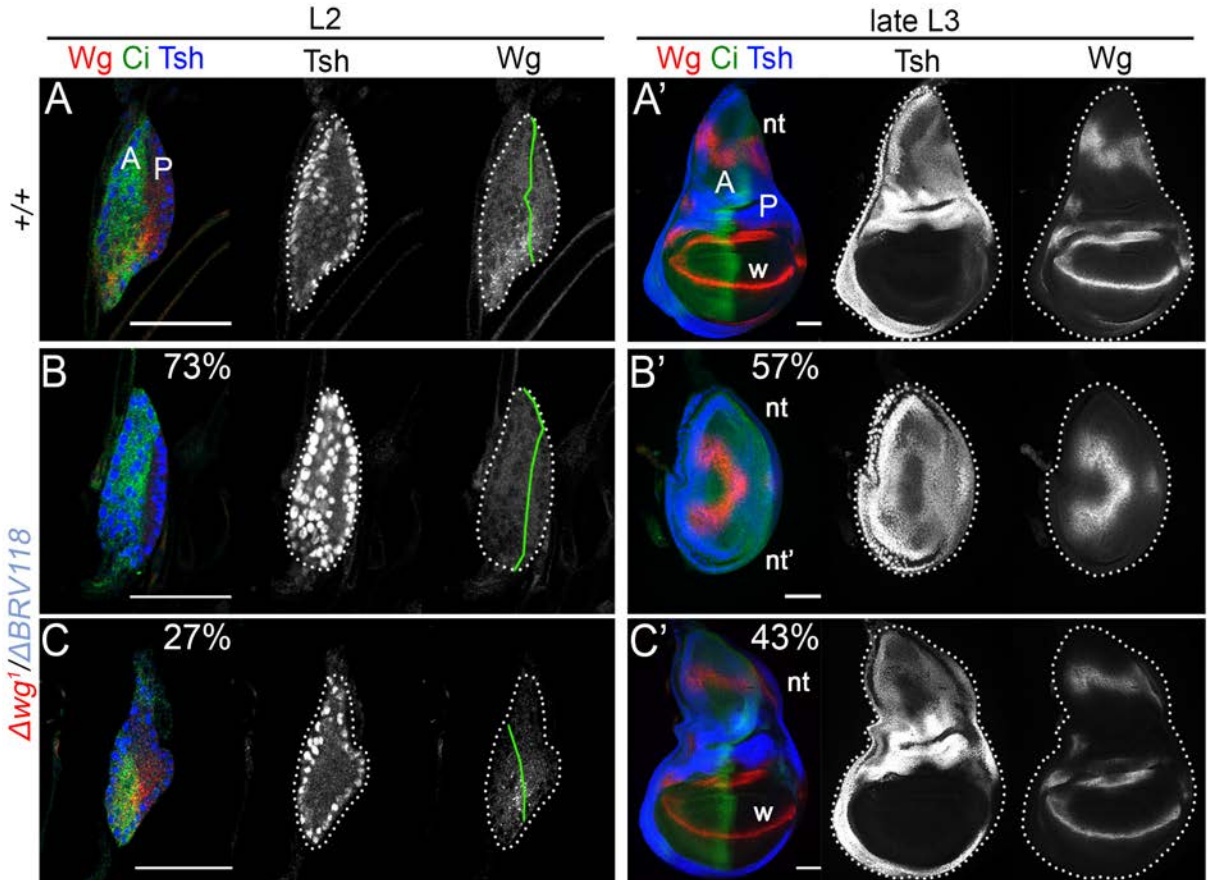

Figure 24. *wg¹* drives early Wg expression. Second (L2) and third (L3) instar larvae of the indicated genotypes stained for Wg (red and white), Ci (green) and Tsh (blue and white). Disc contour and AP boundary are labelled by white and green lines, respectively. The wing pouch (w), the notum (n) and duplicated notum (n') are labelled. Scale bar: 50 µm. In B and C percentages of the affected and wild-type like discs are shown.

As stated above, *wg*^{1} is located between two *wnt* genes, *wg* and *wnt6* (Figure 25A, Table 1). Interestingly, *wnt6* presented the same pattern of expression as Wg not only in later discs (Janson et al., 2001; J. J. S. Yu et al., 2020), where it was reported to potentiate Wg-driven tissue growth (Barrio & Milán, 2020), but also at early stages where the wing fate specification takes place (Figure 25B). This made us wonder whether *wnt6* could be contributing to the *Δwg*^{1} phenotype. To further assess the contributions of both genes to the wing fate specification, we decided to cross flies carrying *Δwg*^{1} or *ΔBRV118* deletions with different *wg* and *wnt6* alleles. Upon transheterozygous conditions of *Δwg*^{1} or *ΔBRV118* with *wg*^{CX4} (a null allele of wg where the first coding exon is deleted; Figure 25A; Van Den Heuvell et al., 1993) we could observe the presence of adults showing the wing to notum phenotype (23,6% and 33,3% penetrance, respectively; Figure 25C). However, the penetrance of the phenotype was lower than the one obtained for *Δwg*^{1}*/ΔBRV118* flies (81%). On the other hand, when we crossed *Δwg*^{1} or *ΔBRV118* with *wg*^{CX3} (a 17 kb-long insertion between *wg* and *wg*^{1}; Figure 25A; Van Den Heuvell et al., 1993) we could observe that the penetrance of the phenotype in the offspring (52,1% and 78,9%, respectively) was higher than the one obtained in transheterozygous conditions with *wg*^{CX4} (Figure 25C). However, the penetrance was still lower than the penetrance obtained for *Δwg*^{1}*/ΔBRV118* flies (compare Figures 23B and 25C). The low penetrance of transheterozygous conditions of *Δwg*^{1} or *ΔBRV118* with *wg*^{CX4} could be explained most probably by potential interactions in trans between *wg*^{1} and the *wg* promoter of the homologous chromosome, in other words, the *wg*^{1} enhancer on the chromosome bearing the *wg*^{CX4} allele could activate the wild type *wg* gene present in the other chromosome (Figure 25D). In contrast, trans interactions between *wg*^{1} and the *wg* promoter could be impaired in *wg*^{CX3} transheterozygotes due to the 17 kb-long insertion. This insertion increases the distance between *wg*^{1} and the *wg* promoter in cis. Besides, it may be altering the 3D structure of the DNA disrupting the interaction in trans of *wg*^{1} and the *wg* promoter (Figure 25D). Therefore, in *wg*^{CX3} transheterozygotes, *wg*^{1} might not be capable to interact with *wg* promoter in cis neither in trans, preventing early Wg expression and inducing the wing to notum phenotype. Even then, we can speculate that some trans events may happen because the penetrance is lower than in *Δwg*^{1}*/ΔBRV118* flies. On the other hand, interactions in *wg*^{CX4} transheterozygotes between *wg*^{1} and *wg* promoter may happen, triggering early Wg expression and inducing the specification of the wing. Differently, when we analysed the role of *wnt6* in wing specification using *wnt6KO* flies (a null allele of *wnt6* where the first coding exon is deleted (Figure 25A)(Doumpas et al., 2013) either in homozygosis, in transheterozygosis with *Δwg*^{1}*/ΔBRV118* or over large chromosomal deficiencies, all the adults emerged with a complete normal pair of wings (Figure 25C). These results

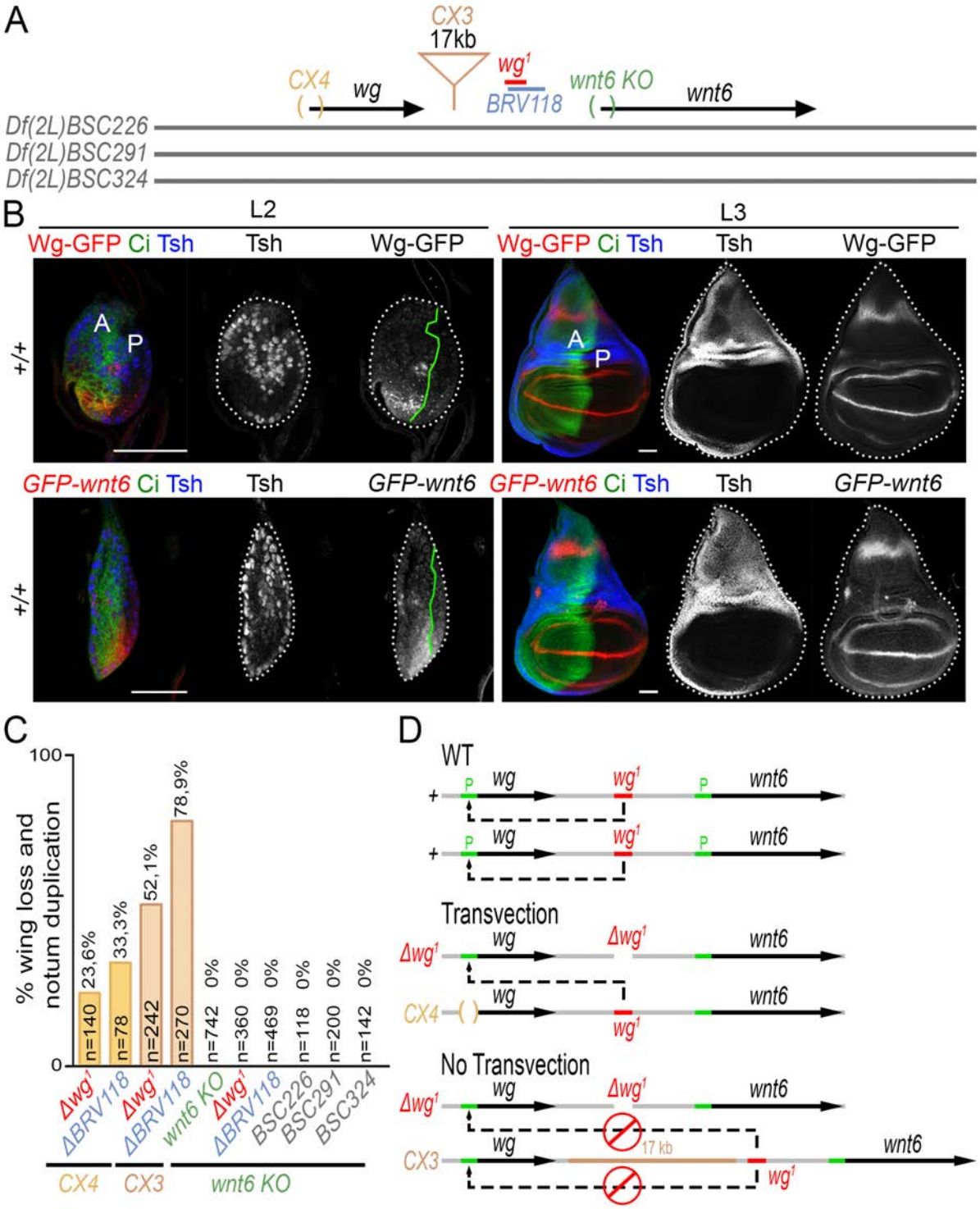

Figure 25. *wnt6KO* does not recapitulate *Δwg¹* phenotype. A) Cartoon depicting the genomic localization of *wg¹* and *BRV118* sequences between *wg* and *wnt6* genes and the different deficiencies and mutations present in the region. **B)** Second (L2) and third (L3) instar larvae of the indicated genotypes stained for Wg-GFP or *GFP-wnt6* (red and white), Ci (green) and Tsh (blue and white). Disc contour and AP boundary are labelled by white and green lines, respectively. Scale bar: 50 µm. **C)** Histogram showing the presence of flies that present the absence of wings and duplication of the notal structures of the indicated genotypes. The number of scored heminota (n) and the exact percentage is shown in the histogram. **D)** Cartoon depicting the possible interaction in trans of *wg¹* with *wg* promoter in transheterozygous conditions of *Δwg¹* over wg^{CX4} and wg^{CX3} alleles.

indicate that is Wg, and not Wnt6, the protein that is required for wing fate specification. This is supported by the fact that only Wg ectopic expression under the *dpp-gal4* driver (Staehling-Hampton et al., 1994), but not Wnt6, was capable to induce the outbreak of a second wing pouch in the notum labelled by Nub (Figure 26), a very well-established marker of the wing pouch (Ng et al., 1995, 1996). Altogether, these results indicate that the genomic region comprised within the wg^{1} deletion is necessary to trigger early Wg expression and to drive wing fate specification suggesting the presence of a wing-specific enhancer in this region.

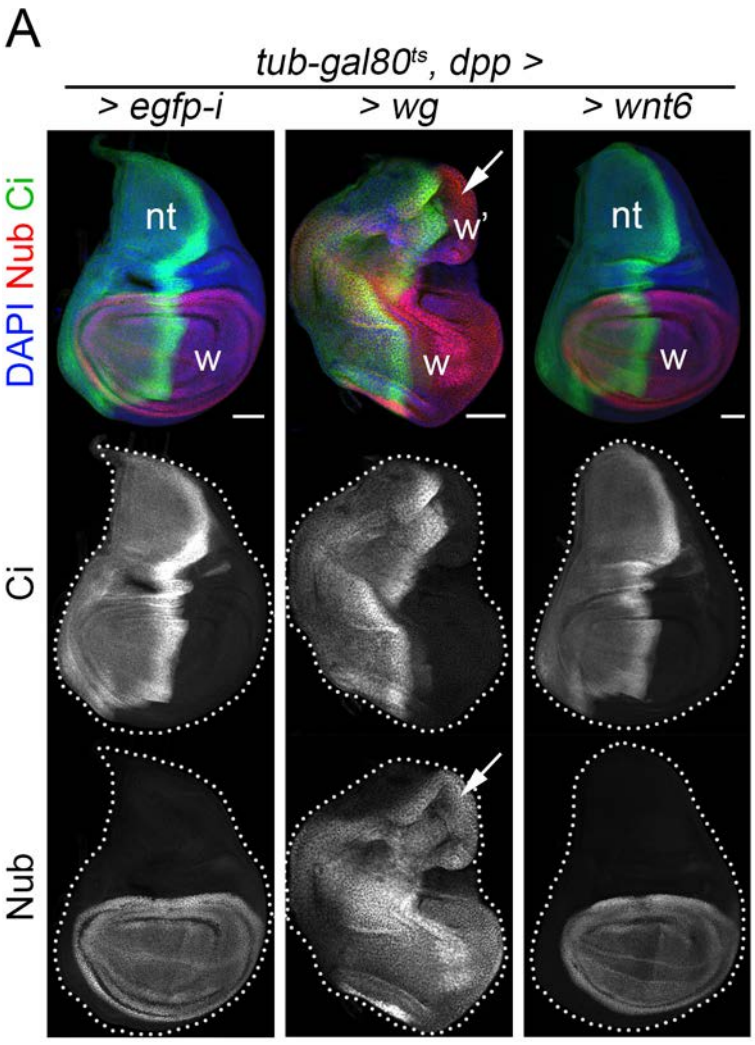

Figure 26. Ectopic Wg, but not Wnt6, is capable to induce an ectopic wing formation. A) Third instar wing discs expressing the indicated transgenes under the control of the *dpp-gal4* driver and stained for Nub (red or white), Ci (green or white) and DAPI (blue). Disc contours are labelled by a white line. The wing pouch (w) and notum (nt) region are labelled and the induction of an ectopic wing (w') by Wg ectopic expression is marked by an arrow. Scale bar: 50 µm.

wg[1] contains an early *wg*-enhancer

Our previous results suggest the presence of an enhancer within the *wg*[1] deletion. To further address this, we decided to generate a transgenic *lacZ* reporter of *wg*[1] to see whether this genomic region is capable to drive β-gal expression or not. The promoter of this *lacZ* construct is too weak to drive expression by itself, so we will only detect β-gal expression in case *wg*[1] contains an enhancer that promotes the transcription. As expected, we could detect β-gal expression in *wg*[1]*-lacZ* discs (Figure 27C), confirming that the *wg*[1] region comprises an enhancer. Furthermore, we were interested in whether our *wg*[1] reporter would be capable to recapitulate Wg pattern expression or not. Interestingly, we could see that *wg*[1]*-lacZ* recapitulates the early *wg-lacZ* expression in the ventral anterior wedge of the wing disc but not its late expression (compare Figures 27B and C). This result reinforces the idea that *wg*[1] is an early enhancer of *wg*. Moreover, while Wg pattern expression is very dynamic during wing development (Figures 27A and B), *wg*[1]*-lacZ* expression pattern persists over time in the anterior wedge of the wing pouch, although we saw that the expression levels decreased over time (Figure 27C). This result agrees with the ATAC data from Hariharan laboratories that show that

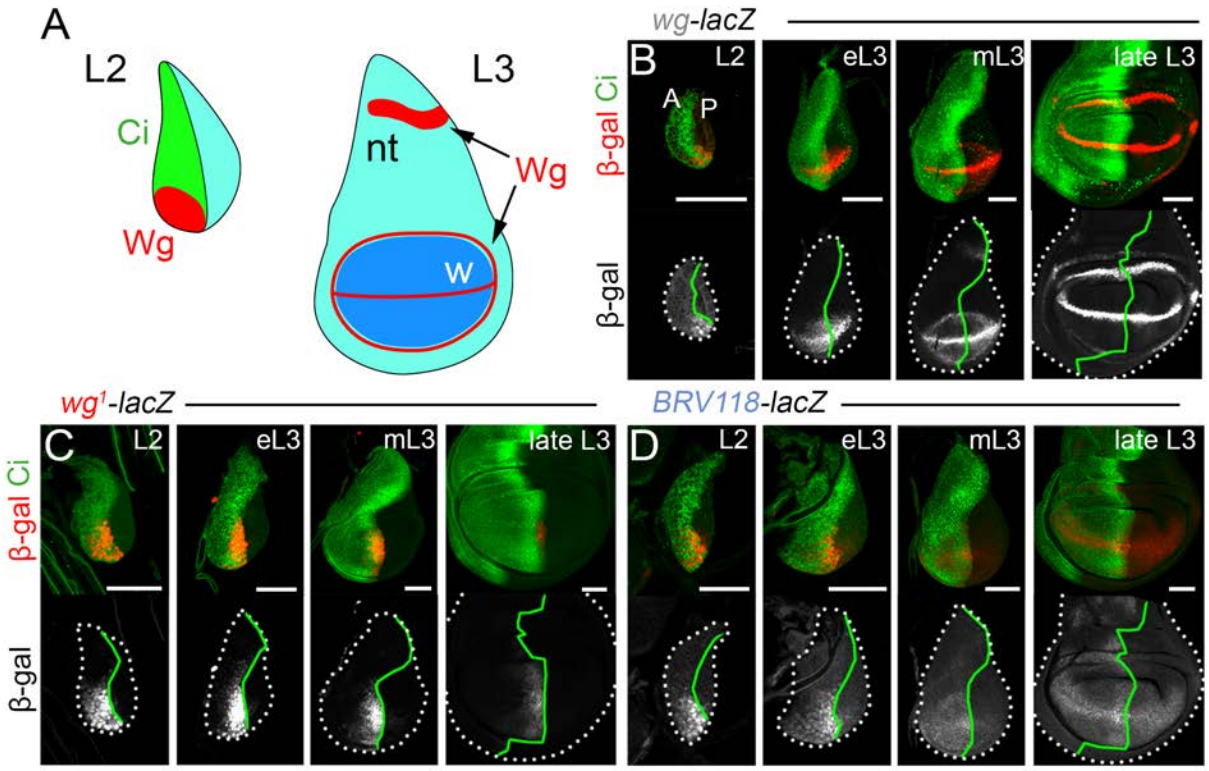

Figure 27. *wg*[1]-enhancer recapitulates early *wg-lacZ* expression. A) Cartoon depicting the expression of Wg at early (L2) and latter (L3) stages of wing development. **B to D)** Second (L2), early (eL3), mid (mL3) and late (late L3) third instar wing discs of larvae bearing the *wg-lacZ* enhancer trap (B) and the *wg*[1]*-lacZ* (C) or *BRV118-lacZ* (D) reporters. All discs were stained for β-galactosidase (red or white) and Ci (green). Disc contour and AP boundary are labelled by white and green lines, respectively. Scale bar: 50 µm.

despite the *BRV118*-enhancer accessibility decrease over time, at later stages the enhancer is still accessible (Harris et al., 2020). Interestingly, when we analysed the expression of the overlapping *BRV118* reporter (*BRV118-lacZ*)(Schubiger et al., 2010) we could see that it perfectly recapitulated *wg*- and *wg*^{1}*-lacZ* early expression but not their late expression (Figure 27D). This difference between the *wg*^{1}- and *BRV118-lacZ* expression pattern could be a consequence of the additional 567 bp of *BRV118*. Altogether, these results confirm the presence of an enhancer in the *wg*^{1} region that drives the early expression of Wg in second instar wing discs.

The molecular mechanisms behind *wg*^{1}-enhancer regulation

The next question that we wanted to address was which were the molecular mechanisms behind the regulation of the *wg*^{1}-enhancer. As mentioned in the introduction, in the early wing disc there are three main pathways that participate in the establishment of the Proximo-Distal axis and the specification of the wing and the notum fates. On one hand, Hh coming from the posterior cells induce the expression of Wg in the ventral anterior wedge through its transcriptional factor Ci (Ng et al., 1996)(Figure 28A). By the other hand, EGFR pathway activity in the most proximal part of the disc it is crucial to trigger the notum specification and restrict the wing fate to the ventral part of the disc (S. H. Wang et al., 2000)(Figure 28B). Finally, the JAK/STAT pathway also contributes to the establishment of the wing pouch restricting EGFR activity to the most proximal part of the disc (Recasens-Alvarez et al., 2017)

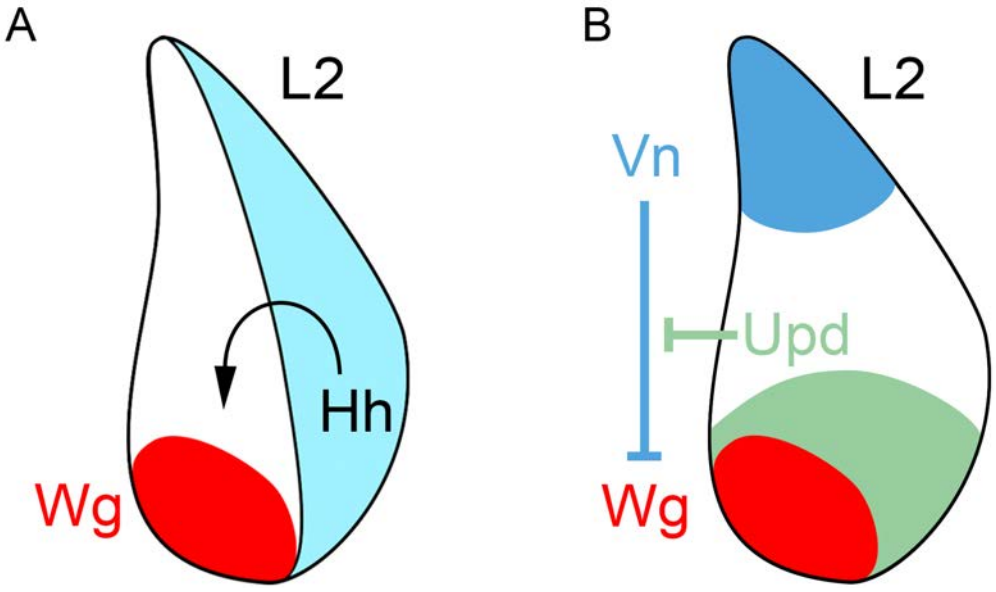

Figure 28. Early Wg regulation by the Hh, EGFR and JAK/STAT pathways. A) Cartoon depicting Wg positive regulation by Hh at early stages. **B)** Cartoon depicting Wg negative regulation by the EGFR pathway (Vn) at early stages. The JAK/STAT pathway (Upd) prevents EGFR expansion toward the ventral area of the disc, allowing Wg expression.

(Figure 28B). Therefore, we wanted to know whether these pathways exerted their function through the *wg*[1]-enhancer.

wg[1] is positively regulated by Hh and negatively by EGFR

The first thing we did was to look in the sequence of *wg*[1] for bioinformatically predicted TFBSs for Ci (the TF of the Hh pathway)(Von Ohlen et al., 1997) and ETS-family transcriptional factors Pointed and Yan (the TFs of the EGFR pathway)(O'Neill et al., 1994; Rebay & Rubin, 1995). To do so, we looked for Position weight matrixes (PWM) for Ci and ETS in 2020-all organisms 42, and MEME v12.21 Fly Factor Survey collection (Figure 29A and B; TF column in Table Annex 1). PWM are a commonly used to represent TF motifs where the nucleotides are

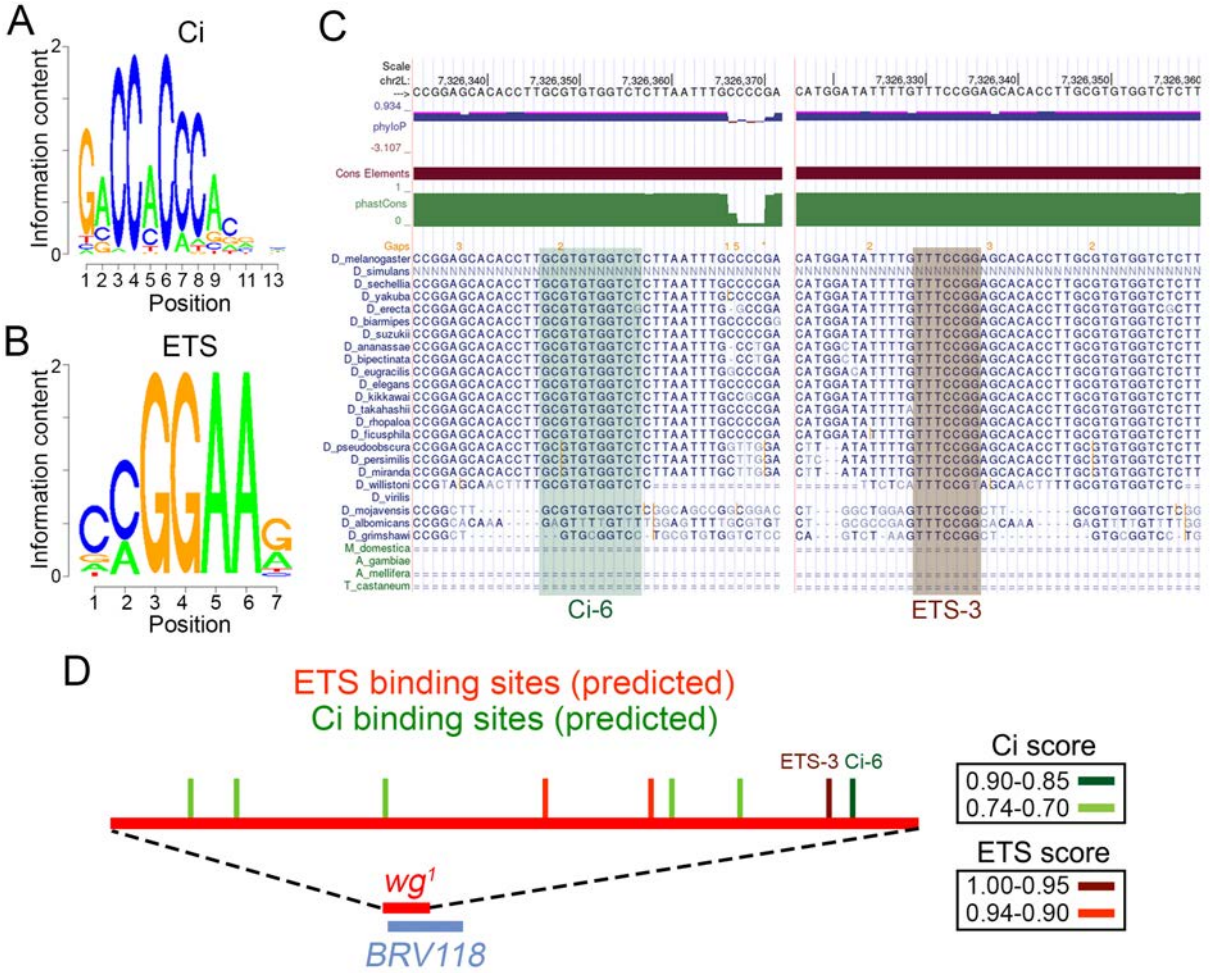

Figure 29. Ci and ETS binding sites are present in the *wg*¹-enhancer sequence. A and B) Examples of PWMs of Ci (A) and ETS (B). **C)** Conservation of the most relevant Ci and ETS binding sites by multiple alignments of 27 insect species. Purple and green tracks show measurements of evolutionary conservation using two methods (phastCons and phyloP) from the PHAST package (http://compgen.cshl.edu/phast/), for all 27 species. Conserved elements (brown) identified by phastCons are also displayed. Data are taken from the UCSC genome browser (https://genome-euro.ucsc.edu/index.html). **D)** Cartoon depicting the presence of bioinformatically predicted Ci (in green) and ETS (in red) binding sites within *wg*¹ sequence. The score of each binding site is shown in the table at left.

weighted accordingly to the tolerance of the TF. In other words, it represents the probability to find a particular nucleotide in a specific position of the binding site. Even though TFs present a preference for a specific combination of nucleosides, they can tolerate slight variations in the target binding site. This is represented in the PWM. Then, using the Matscan software 41, we looked for predicted binding sites in the *wg*^{1} region that would match the Ci and ETS PWMs. Each prediction produced a MatScan score that told us how close was the sequence to the given PWM. Moreover, to give robustness to the prediction of our binding sites, we added a second layer of complexity analysing the conservation degree of Ci and ETS binding sites by multiple alignments of our sequence (*D. melanogaster*) with other 26 insect species (Figure 29C; cons.max column in Table Annex 1). The MatScan and Conservation scores were confronted to calculate the final score (score.max in Table Annex 1) of each binding site. Higher the value of the score, higher the probability that the predicted binding site is real. Predicted binding sites that overlapped using the same position weight matrix were merged (both average and maximum values are shown in Table Annex 1). By colour coding our table, for concrete score ranges, we saw that in many cases different PWMs of the same TF pointed the presence of a binding site in the same localization. For simplicity, we merged these binding sites and represented them as representative binding sites in our figures. As expected, several binding sites of both pathways were found in the *wg*^{1} region (Figure 29D; Table Annex 1) indicating that most probably those TFs can bind to our enhancer and regulate its activity.

We next performed gain of function (GOF) and loss of function (LOF) experiments to further assess the impact of Hh and EGFR pathways in *wg*^{1}*-lacZ* expression. For this, we used the *sd-gal4* driver, which is ubiquitously expressed in all the disc at early stages (Figure 30F) (Rafel & Milán, 2008), to express the transgenes of interest. First, we analysed the impact of the Hh pathway, which induces Wg expression at the early stages of wing development (Ng et al., 1996), in the expression *wg*^{1}*-lacZ*. The first thing we did was to induce a GOF of the Hh pathway by overexpressing its ligand Hh (Varjosalo & Taipale, 2007). Even though we expected to observe an expansion or an increase of the enhancer expression at early stages, we could not detect any difference with respect to the control (compare Figures 30A and B). Most probably this is because early wild type discs are so small that Hh already reaches the totality of the disc and, therefore, overexpressing Hh makes no difference. However, at later stages, we could observe a clear expansion of the enhancer expression through the A compartment (labelled by Ci) and an increase of its intensity (compare Figures 30A' and B'). Consistently, in the posterior compartment, where Ci is repressed by En (Eaton & Kornberg, 1990), we did not detect expres-

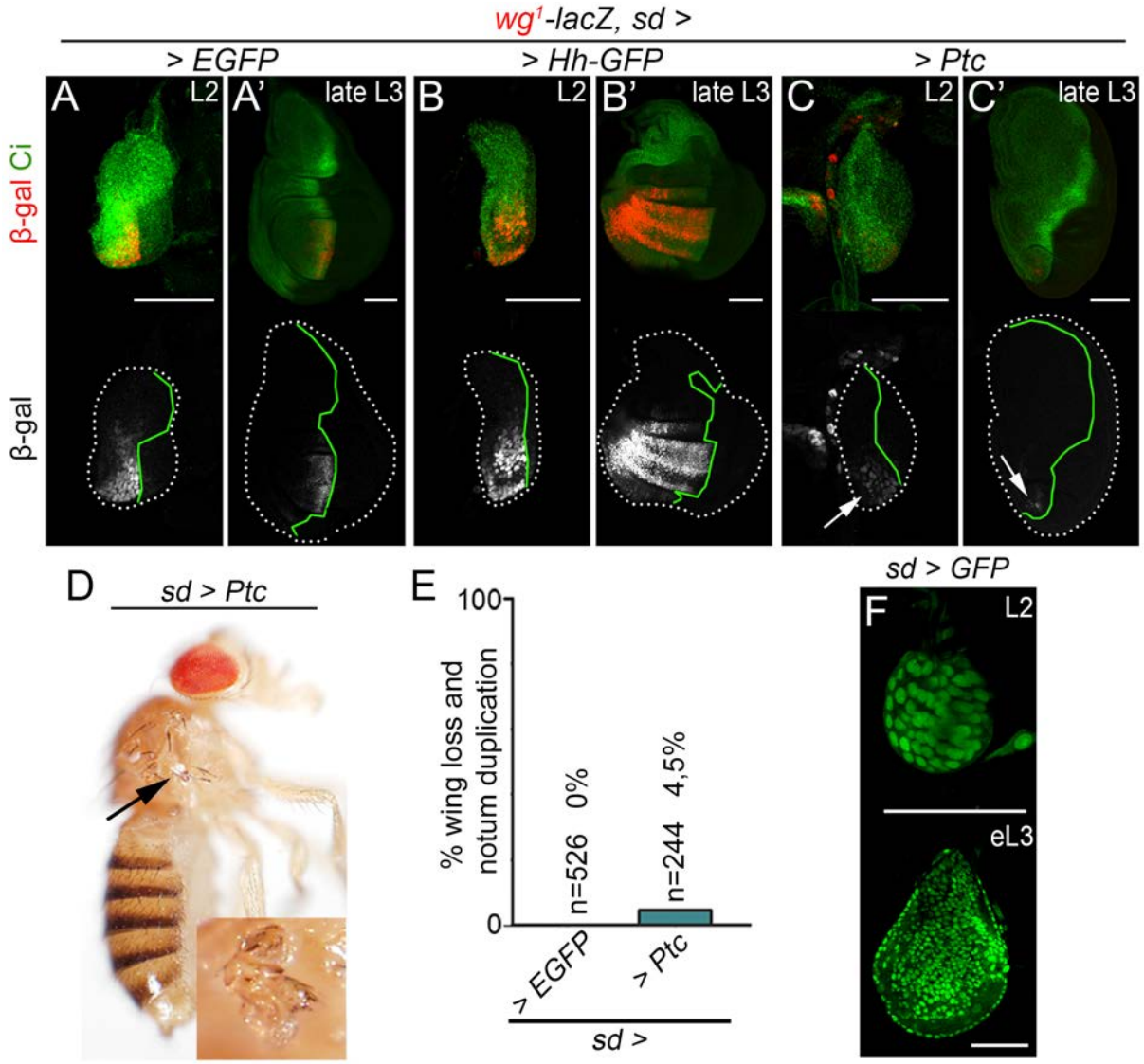

Figure 30. Hh positively regulates *wg¹*-enhancer. A to C) Second (L2) and late third (L3) instar wing discs of flies carrying the *wg¹-lacZ* reporter and expressing the indicated transgene under the control of the *sd-gal4* driver. Discs are were stained for β-galactosidase (red or white) and Ci (green). Disc contour and AP boundary are labelled by white and green lines, respectively. Arrows in C) point to the low expression of the *wg¹-lacZ* reporter. **D)** Most representative adult flid obtained upon Ptc overexpression under the control of the *sd-gal4* driver. The arrow points to a vestigial wing (see the magnification). **E)** Histogram showing the presence of flies that present the absence of wings and duplication of the notal structures of the indicated genotypes. The number of scored heminota (n) and the exact percentage is shown in the histogram. **F)** Second (L2) and early third (eL3) instar wing disc expressing GFP (green) under the control of the *sd-gal4* driver. Scale bar: 50 µm.

sion of the enhancer. On the other hand, when we induced a LOF by overexpressing Patched (Ptc, the receptor of the pathway which is known to block Hh activity upon overexpression) (Johnson et al., 1995), as expected, we could detect a reduction of the enhancer expression both at early and late stages (Figures 30C and C'). Surprisingly, *wg¹-lacZ* expression was not wholly abolished upon Ptc overexpression and a small atrophic wing pouch could be observed (Figure 30C'), suggesting that Hh signalling is not an absolute requirement for Wg expression

in early discs. Consistently, most adult flies that overexpress Ptc showed a small vestigial wing (Figure 30D) and just a very small proportion showed a complete absence of the wing and a notum duplication (Figure 30E). The presence of these vestigial wings is most probably due to the decrease of the promitotic molecule Dpp produced by the blockage of Hh signalling (Barrio & Milán, 2017; Restrepo et al., 2014). Thereupon, we can conclude that Hh signalling positively regulates *wg*^{1} even though our data suggest that there is a Hh-independent regulation of the enhancer.

Next, we focused our attention on the EGFR signalling, which has been described to restrict Wg expression to the ventral area of the disc (S. H. Wang et al., 2000), where our enhancer is expressed. Hence, we would expect that a LOF of the EGFR pathway all over the disc would allow our enhancer activity to expand towards the most proximal parts. To test this hypothesis, we decided to overexpress the chimeric protein Vein::Argos (Vn::aos), a chimeric protein between Vn and the antagonistic ligand Argos that acts as an inhibitor of the EGFR pathway (Schnepp et al., 1998). As expected, at early stages, we could detect an expansion of the enhancer expression towards the most proximal parts of the disc (compare Figures 31A and C). Interestingly, at later stages we could observe that Vn::aos overexpression induced different phenotypes. While in some cases the absence of EGFR signalling induced a complete lack of notal structures (Figure 31D), in other cases we could observe an expansion of the pouch towards the notum paired with an expansion of the enhancer expression (Figure

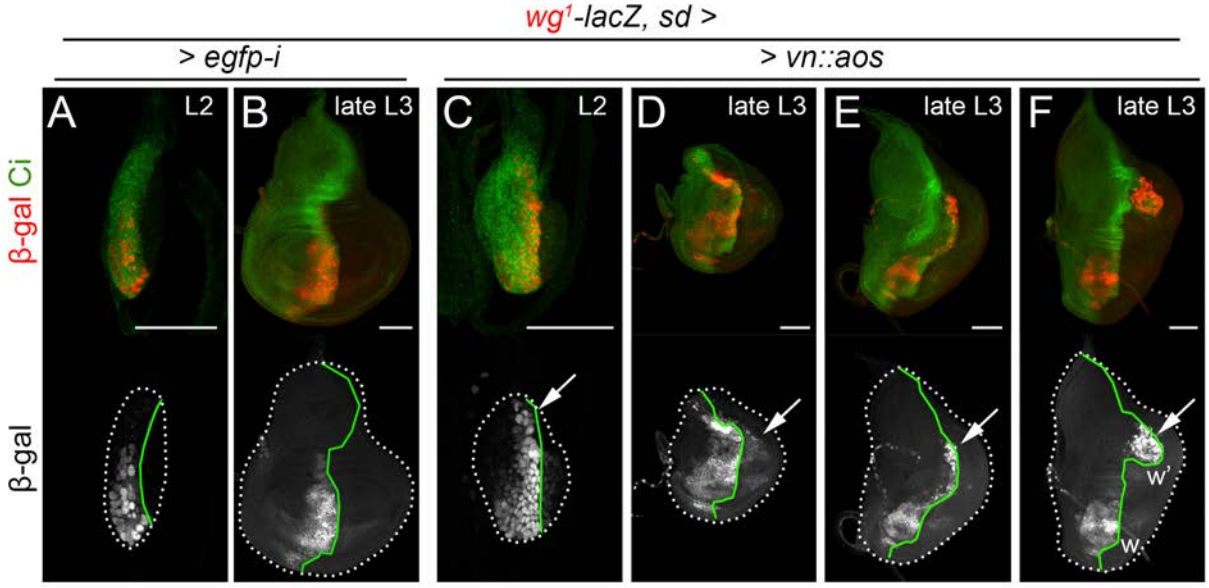

Figure 31. EGFR pathway repress *wg*^{1}-enhancer activity to the ventral area of the disc. A-F) Second (L2) and late third (L3) instar wing disc of flies carrying the *wg*^{1}*-lacZ* reporter and expressing the indicated transgene under the control of the *sd-gal4* driver. Discs are were stained for β-galactosidase (red or white) and Ci (green). Disc contour and AP boundary are labelled by white and green lines, respectively. Arrows C to F point to the ectopic expression of *wg*^{1}*-lacZ* reporter. Scale bar: 50 µm.

31E). Besides, in some cases, we could observe the formation of an ectopic wing pouch in the notum that presented *wg¹-lacZ* expression (Figure 31F). This data confirms that *wg¹*-enhancer is restricted to the ventral part of the disc by the action of the EGFR pathway. Furthermore, our data suggest that the formation of an ectopic pouch requires the activity of the *wg¹*-enhancer. Interestingly, upon Vn::aos overexpression we could detect expression of the enhancer in the posterior compartment at early and late stages (Figure 31C and D). This will be discussed in further sections of this thesis. Altogether, these results indicate that at early stages the *wg¹*-enhancer is positively regulated by Hh and negatively regulated by EGFR.

JAK/STAT keeps Wg and EGFR apart allowing the specification of the wing

JAK/STAT activity is fundamental at early stages to restrict EGFR activity to the most proximal part of the disc, allowing the expression of Wg in the ventral part, enabling the specification of the wing (Recasens-Alvarez et al., 2017). As previously shown, upon *wg¹* deletion the pouch does not specify and there is a mirror duplication of the notum (Figure 24B). Hence, in the adult we can observe an absence of the wing and a notum duplication (Figures 23B and C). If JAK/STAT activity was not affected by the absence of Wg in *wg¹* mutants, the activity of EGFR would still be restricted to the most proximal part of the disc and, therefore, it causes the absence of the wing but not a notum duplication. To assess if the absence of Wg at early stag-

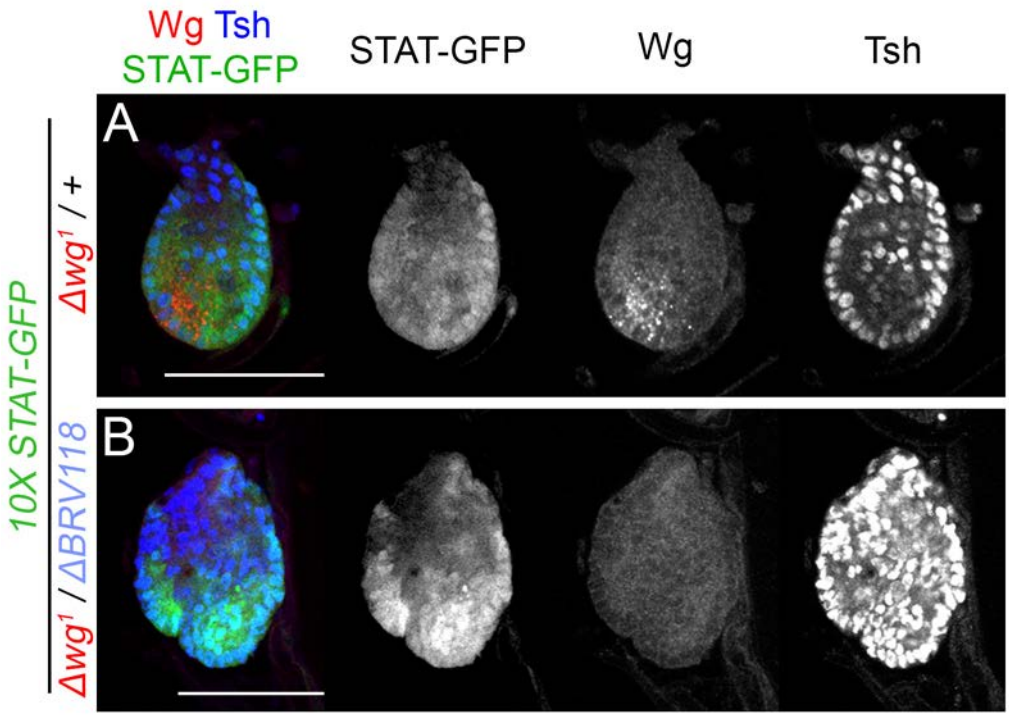

Figure 32. JAK/STAT activity is not affected by *wg¹* deletion. A-B) Second instar wing disc of *Δwg¹/+* and *Δwg¹/ΔBRV118* flies carrying the *10X STAT-GFP* reporter. Discs are were stained for STAT-GFP (green or white), Wg (red or white) and Tsh (blue or white). Scale bar: 50 µm.

es produced by *wg*[1] mutation could be affecting the JAK/STAT activity, we used the *STAT-GFP* reporter line. This reporter consists of a GFP controlled by 10 tandem repeats of a sequence that contains Stat92E binding sites (the TF of the JAK/STAT pathway)(Bach et al., 2007). Hence, those cells that present JAK/STAT activity will be GFP positive. Therefore, we would not expect to detect JAK/STAT activity in *wg*[1] mutants. Surprisingly, we could observe a regular JAK/STAT activity in all early *wg*[1] mutant discs analysed (Figure 32B). This result makes clear that Wg is not regulating JAK/STAT activity in early discs. Moreover, it made us wonder how could we observe notum duplication if JAK/STAT activity was still present in *wg*[1] mutants repressing EGFR activity to the most proximal part of the disc.

To further address the role of JAK/STAT in wing specification, we wanted to analyse the effect of JAK/STAT activity depletion in the expression of our enhancer reporter *wg*[1]*-lacZ*. To do so, we expressed an *RNA-i* against *domeless* (*dome*), the receptor of the pathway (Brown et al., 2001), under the control of the *sd-gal4* driver. As previously described by our laboratory, at early stages, upon *dome* depletion EGFR signalling activity domain expands and represses Wg, preventing the specification of the wing (Recasens-Alvarez et al., 2017). Moreover, our previous results show that EGFR activity repress the expression of our enhancer to the most ventral part of the disc. Therefore, we would suppose that upon *dome* depletion EGFR would expand

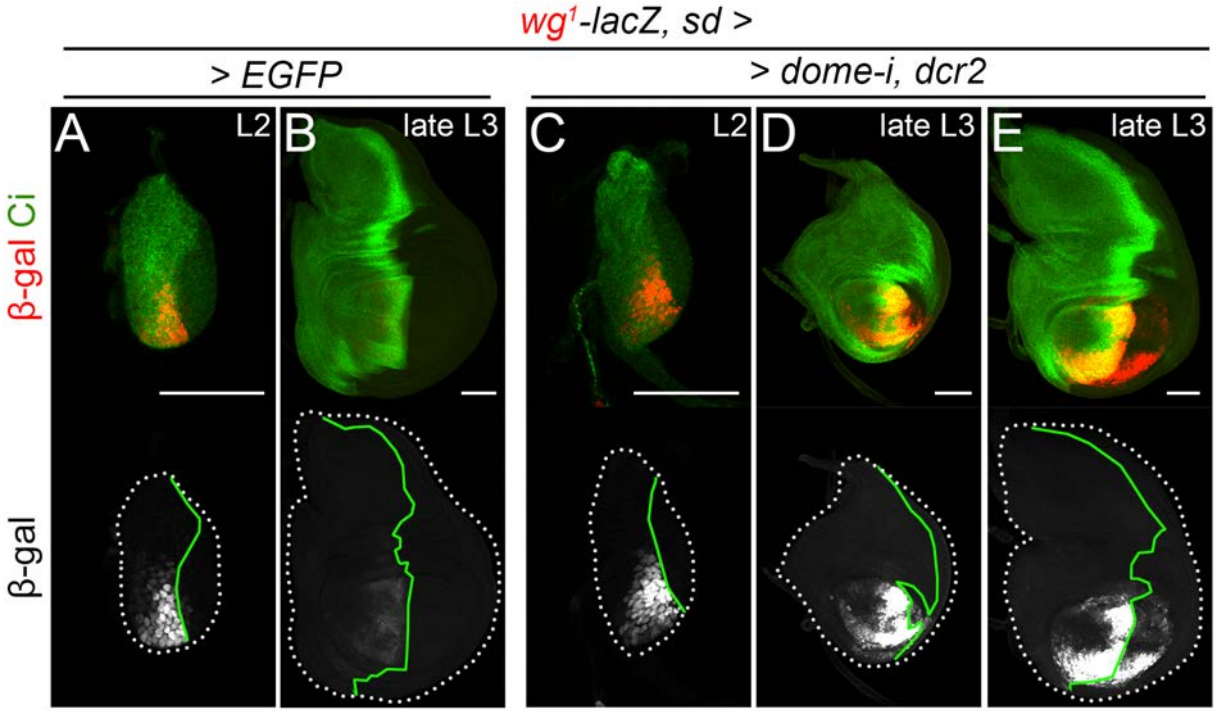

Figure 33. JAK/STAT represses *wg*[1]-enhancer. A-E) Second (L2) and late third (L3) instar wing disc of flies carrying the *wg*[1]*-lacZ* reporter and expressing the indicated transgene under the control of the *sd-gal4* driver. Discs were stained for β-galactosidase (red or white) and Ci (green). Disc contour and AP boundary are labelled by white and green lines, respectively. Scale bar: 50 µm.

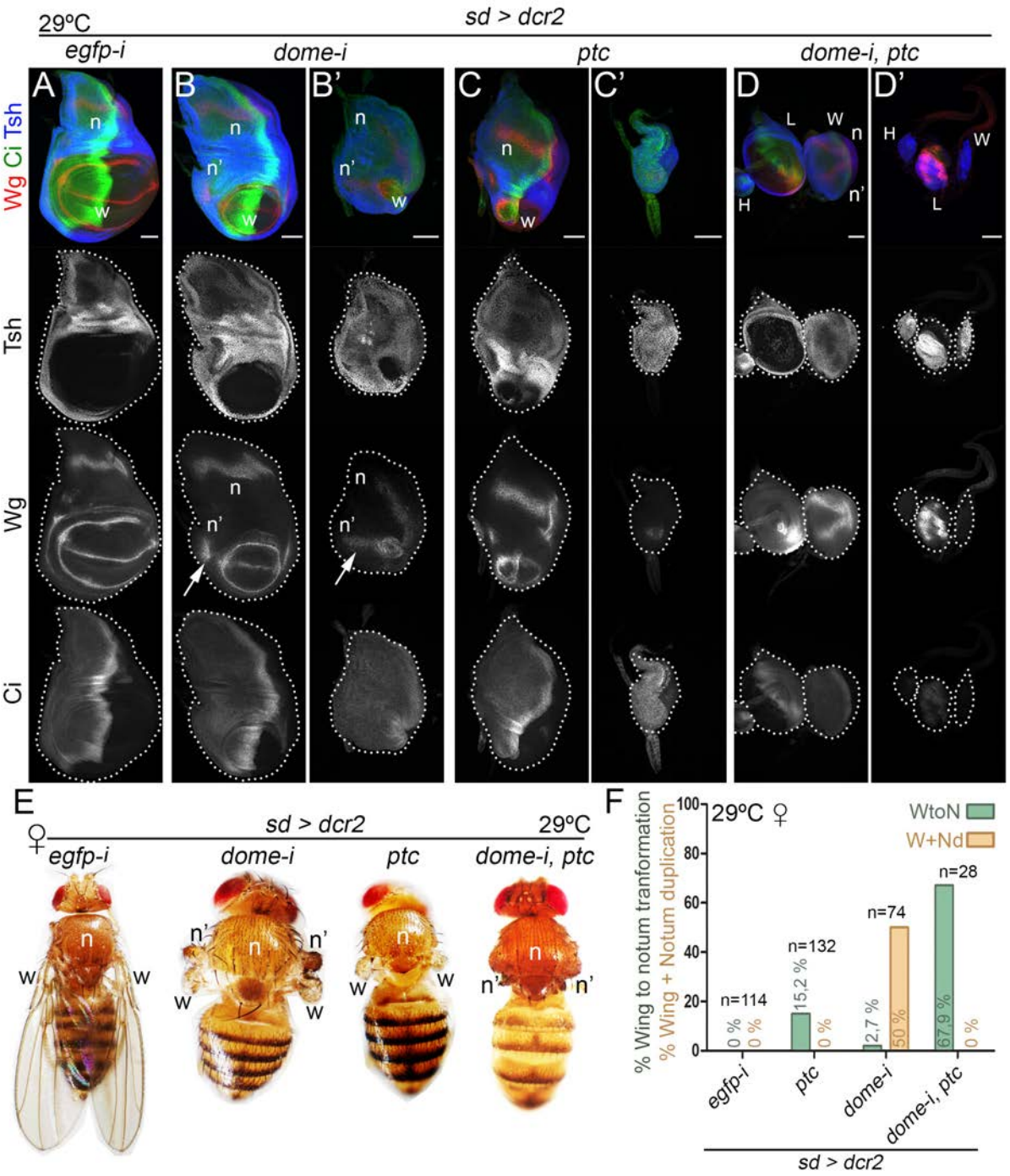

Figure 34. JAK/STAT depletion induces a notum duplication paired with a vestigial wing. A-D') Late third instar wing disc of flies expressing the indicated transgene under the control of the *sd-gal4* driver. Each condition shows a week and a strong phenotype. Discs were stained for Wg (red or white), Tsh (blue or white) and Ci (green or white). Disc contours are labelled by a white line. The wing (w), notum (n) and duplicated notum (n') are labelled. Arrows in B and B' point to ectopic Wg expression. **D-D')** Wing (W), leg (L) and haltere (H) imaginal discs are indicated. Scale bar: 50 µm. **E)** Most representative adult flies obtained of the indicated transgene under the control of the *sd-gal4* driver. The wing (w), notum (n) and duplicated notum (n') are labelled. **F)** Histogram showing the presence of flies that present the absence of wings and duplication of the notal structures (WtoN, wing to notum transformation) or a vestigial wing with a notum duplication W-Nd, Wing+Notum duplication) of the indicated genotypes. The number of scored heminota (n) and the exact percentage are shown in the histogram. Experiments were performed at 29ºC.

and the activity of *wg*^{1}-enhancer would be decreased and even more repressed to the ventral part of the disc. Interestingly, when we analysed early *wg*^{1}*-lacZ* expression in *dome-i* discs, we could not detect any difference between our samples and the wild type discs (compare Figures 33A and C). Contrary to what we expected, at later stages, we could see that the expression of the enhancer was increased in *dome-i* discs (Figures 33D and E), somehow suggesting that JAK/STAT activity could be repressing *wg*^{1}-enhancer activity. Furthermore, we could detect high expression of the enhancer in the posterior compartment (Figure 33E), fact that will be discussed in further sections of this thesis. Interestingly, we were never capable to obtain discs that showed a complete absence of the wing pouch. However, ectopic notal structures could be detected near the atrophic wing pouch (Figures 34B and B' arrows). Consistently, when we analysed adult flies that expressed the *dome-i* transgene we could see that many of them showed a vestigial wing together with a duplication of the notum, and just some sporadic wing to notum transformation events were detected (Figures 34E and F). Remarkably, upon expression of *dome-i* together with the blockage of the Hh pathway by Ptc overexpression, we could no longer detect the vestigial wing paired with the partial notum duplication but instead, we detected a complete wing to notum transformation (Figures 34D, E and F). Moreover, the penetrance of the wing to notum phenotype in flies in which we have depleted both, JAK/STAT and the Hh pathway, is much higher than when we just deplete Hh (Figure 34F). Interestingly, in all conditions we could observe a strong and a weak phenotype (Figures 34B to D'). That could be explained by the fact that our driver, *sd-gal4*, is localized in the X chromosome. In *Drosophila* males, that only present a single X chromosome, it exists a mechanism called chromosome dosage compensation (CDC) to equalize the level of X-linked genes to autosomes, which are present in two copies (Laverty et al., 2010). Hence, male X chromosome will have double the transcription than a female X chromosome. In our case, the CDC will enhance expression of the *sd-gal4* transgene in males respect to females. Therefore, we can suppose that the weak phenotypes belong to females while the strong ones to males. This idea is reinforced by the fact that when we raised our flies at 29ºC, temperature at which the GAL4/UAS system is more active, we could only obtain adult females (Figure 34B). Instead, when we performed the same experiments at 25ºC we were capable to obtain males that presented stronger phenotypes and females that presented weaker phenotypes (Figure 35). Significantly, when we analysed males raised at 25ºC we could detect that some of the flies lacked an heminota (Figure 35, *ptc* and *dome-i*). That matches with some of the strong wing disc phenotypes obtained at 29ºC, where we could observe very small wing discs that present a complete or partial loss of Wg (Figures 34C' and D'). Altogether, our data indicates that JAK/STAT could be acting as a

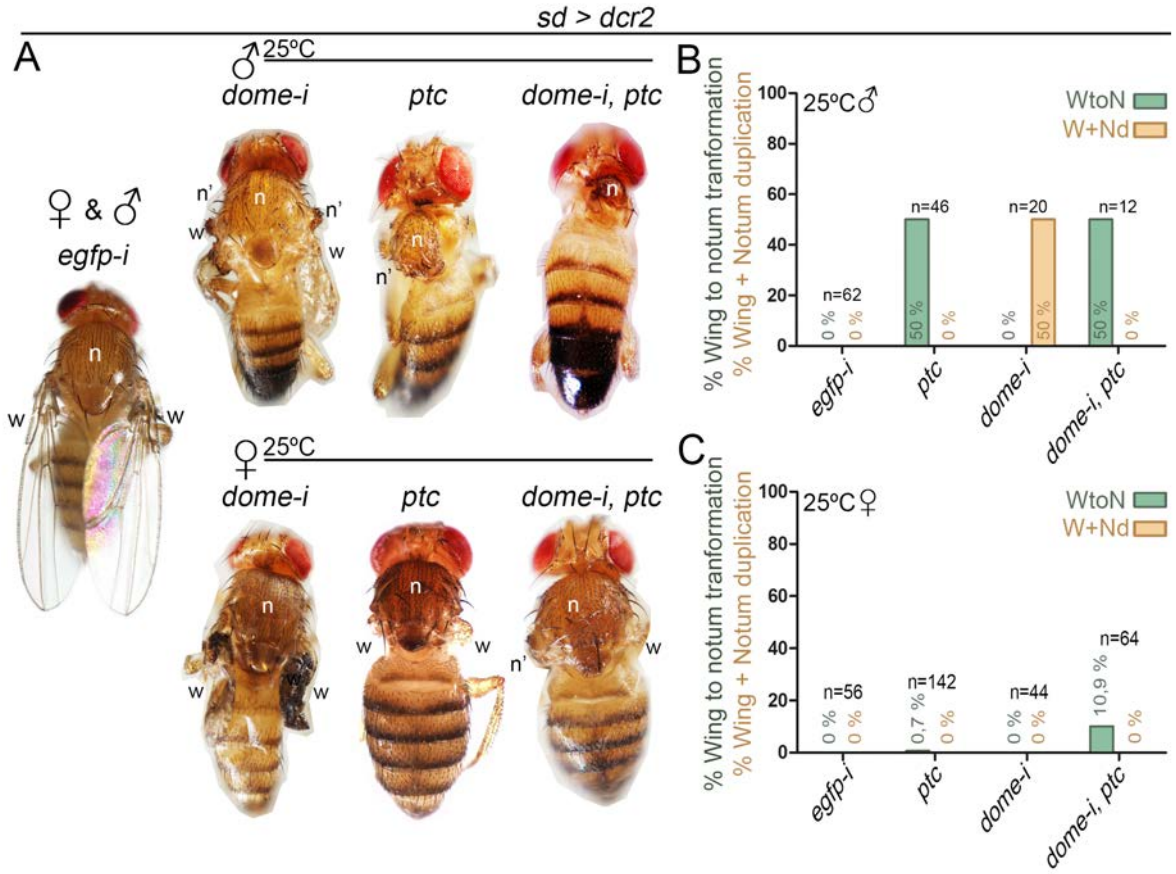

Figure 35. Impact of Hh and JAK/STAT signalling depletion in males. A) Most representative male and female adult flies obtained of the indicated transgene under the control of the *sd-gal4* driver. The wing (w), notum (n) and duplicated notum (n') are labelled. **B-C)** Histogram showing the presence of flies that present the absence of wings and duplication of the notal structures (WtoN, wing to notum transformation) or a vestigial wing with a notum duplication W-Nd, Wing+Notum duplication) of the indicated genotypes for males (B) and females (C). The number of scored heminota (n) and the exact percentage are shown in the histogram. Experiments were performed at 25ºC.

safety belt between EGFR and Wg activity, repressing both EGFR activity and Wg expression, respectively to the most proximal and ventral part of the disc, therefore allowing the normal development of the notum and the wing pouch.

Looking for other wing fate specification enhancers

As previously mentioned, the penetrance of wg^{1} deletion is not 100% (Figure 23B). This indicates the presence of other regulatory elements capable of driving Wg expression at early stages. Therefore, taking advantage of the fact that Hh regulates early Wg expression, we tried to look for other possible enhancers by looking for high-score Ci binding sites in other regions close to the *wg* and *wnt6* genes. Two possible candidates were found, one in the *SpdFlag wg* allele and the other in the first intron of the *wnt6* gene (Figure 36A; Table 1). While the *wnt6-intron-LacZ* reporter showed no expression (Figure 36C), the *spdFlag* was sufficient to drive

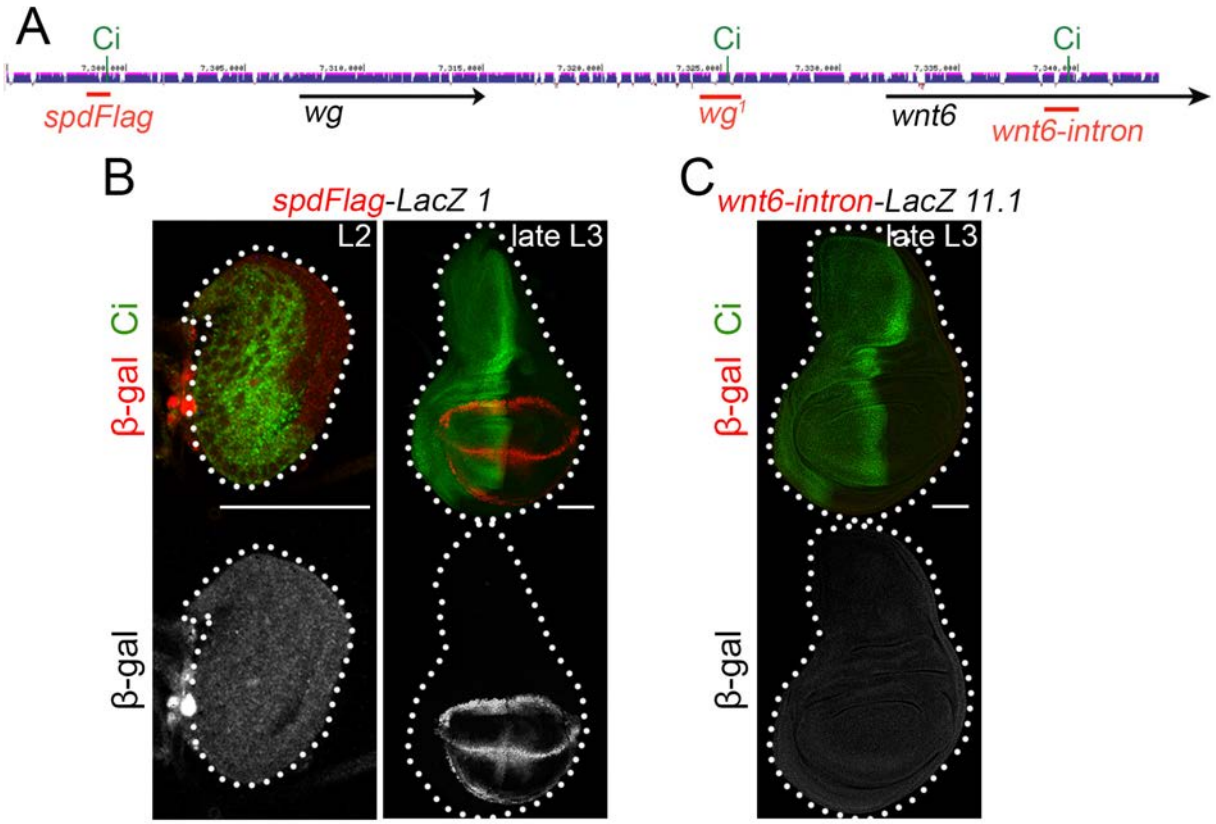

Figure 36. Neither the sequence of *spdFlag* nor *wnt6-intron* recapitulate early Wg expression. A) Cartoon depicting the genomic localization of the two enhancers candidates with respect to *wg¹*, *wg* and *wnt6*. Purple track show measurements of evolutionary conservation. The high-score Ci binding sites are indicated. **B-C)** Second (L2) and late third (late L3) instar wing discs of larvae bearing the indicated reporter. All discs were stained for β-galactosidase (red or white) and Ci (green). Disc contours are labelled by a white line. Scale bar: 50 µm.

lacZ expression (Figure 36B). Nevertheless, *spdFlag* was only capable to drive expression at later stages, and this expression did not recapitulate the *wg*^{1}*-lacZ* expression pattern (Figure 36B). Therefore, we can conclude that neither of the sequences contributes to the early wing fate specification.

wg^{1}-enhancer is composed of two *cis*-regulatory modules

Gamma and *Gamma*-590 modules recapitulates *wg*^{1} expression pattern

Next, we wanted to find the minimal functional enhancer necessary to drive the wing specification. To do so, we analyse the conservation of the *wg*^{1} sequence among other *Drosophila* species to divide the enhancer into conservated modules. Four main modules were found in a 4.7-kb-long region containing *wg*^{1}: *Alpha* (*α*), *Beta* (*β*), *Gamma* (*γ*) and *Delta* (*δ*; Figure 37A). From each of these fragments, we generated a *lacZ* reporter and we analysed its expression pattern to see whether they were capable to recapitulate *wg*^{1}*-lacZ* pattern expression or not at early and later stages. The first thing we noticed was that despite *Alpha* did not

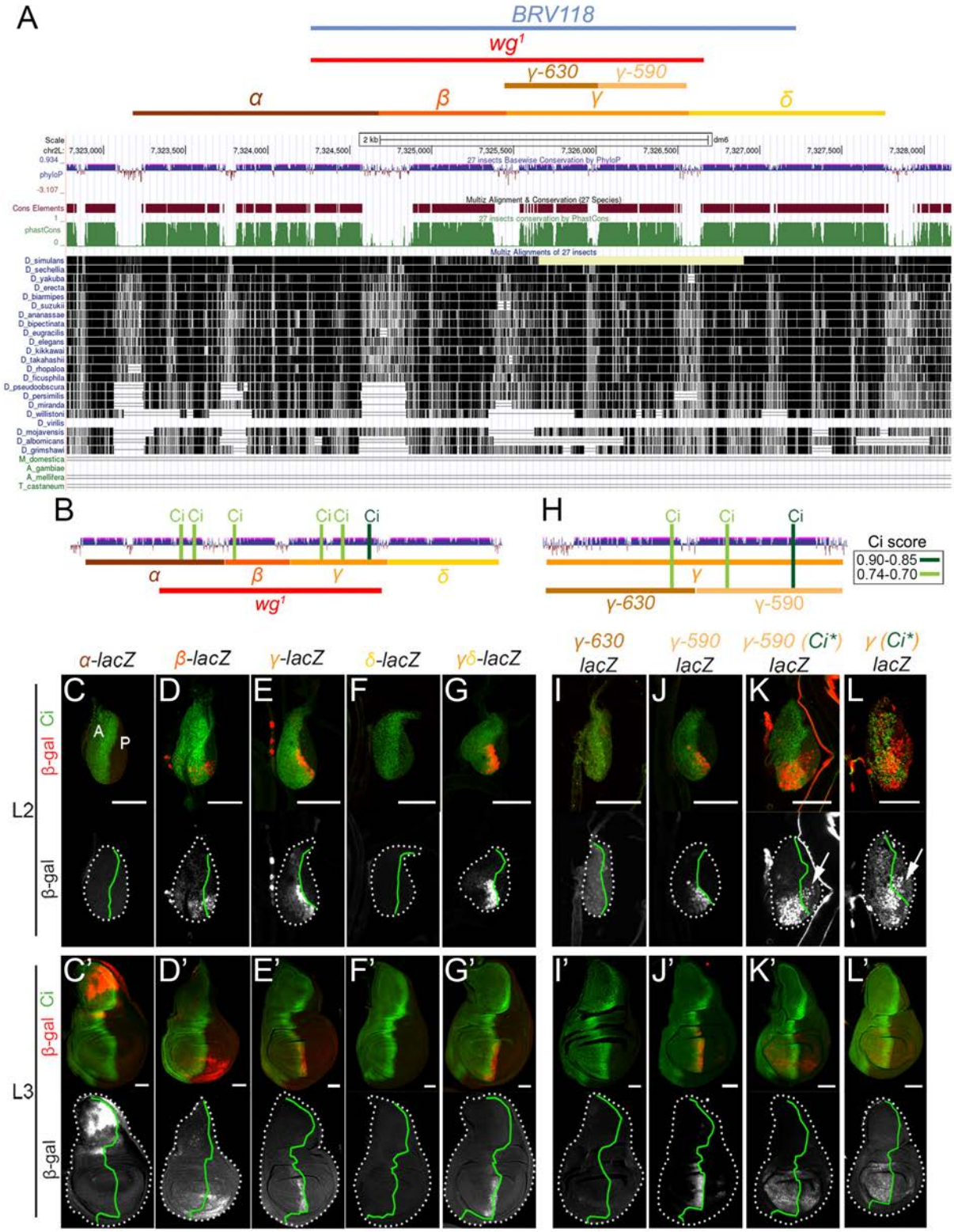

Figure 37. *Gamma* module recapitulates *wg¹* expression pattern. A) Cartoon depicting the different modules spanning the *wg¹*-enhancer and their conservation as shown by multiple alignments of 27 insect species. Purple and green tracks show measurements of evolutionary conservation using two methods (phastCons and phyloP) from the PHAST package (http://compgen.cshl.edu/phast/), for all 27 species. Conserved elements (brown) identified by phastCons are also displayed. Data are taken from the UCSC genome browser (https://genome-euro.ucsc.edu/index.html). **B and H)** Cartoon depicting the different modules spanning the *wg¹*-enhancer and the bioinformatically predicted Ci (in green) and ETS (in red) binding sites. The scores are shown in the table at left. **C-G and I-L)** Second (L2) and late third (L3) instar wing discs of larvae bearing the indicated reporter. All discs were stained for β-galactosidase (red or white) and Ci (green). Disc contour and AP boundary are labelled by white and green lines, respectively. Scale bar: 50 µm.

show expression at the early stages, in later stages it presented expression in the notum (Figures 37C and C'). Remarkably, *Delta* was not capable to induce *lacZ* expression in neither early nor later stages of the wing development (Figures 37F and F'). On the contrary, the *Gamma* module, which contains a high-score Ci binding site (Figure 37B), perfectly reproduced *wg^{1}-lacZ* pattern expression at early and later stages (discussed later in the text, Figures 37E and E'). Interestingly, it has been proposed the presence of a silencing element in the *Delta* module of the enhancer (Harris et al., 2016), therefore we decided to analyse whether *Gamma* expression could be altered when *Delta* was present. Oddly, no differences in the expression pattern or expression levels were detected between *Gamma-* and *GammaDelta-lacZ* (*γδ-lacZ*) constructs, suggesting that there is not a silencing element in *Delta* (compare Figures 37E and E' with G and G'). On the other hand, *Beta* showed expression at both early and later stages in the ventral part of the disc, but was not capable of resembling *wg^{1}-lacZ* pattern expression in the ventral anterior wedge of the wing disc. Instead, it showed mostly a posterior expression (Figures 37D and D') even though it includes a Ci binding site in its sequence (Figure 37B).

Interestingly, two conserved modules were present in *Gamma.* Hence, we decided to divide it into two sub-modules: *Gamma-630* (*γ-630*) and *Gamma-590* (*γ-590*), which contained the highest-score Ci binding site (Figure 37H). While the *Gamma-630* module was not capable to drive *lacZ* expression, suggesting that it is not functional, the *Gamma-590* module perfectly recapitulated the expression pattern of *Gamma* and *wg^{1}* (Figures 37I to J'). Interestingly, mutation of the highest-score Ci binding site in the *590* module compromised its pattern expression, allowing its expression in the posterior compartment (Figure 37K and K'). Yet, we could still observe expression of the reporters in the ventral anterior wedge in early discs (Figures 37K and L), somehow suggesting that lower score Ci binding sites in the region are functionally relevant for Wg regulation. Similar results were obtained when the same Ci binding site was mutated into the *Gamma-lacZ* reporter (Figures 37L and L'). Overall, our data indicates that *Gamma-590* is the minimal required region to recapitulate *wg^{1}-lacZ* pattern expression. Moreover, it seems that the highest-score Ci binding site present in this module is fundamental for the proper expression of the enhancer.

Gamma comprises *wg^{1}* positive regulation while *Beta* acts as a regulator

To further understand the functionality of *Beta* and *Gamma* within the *wg^{1}*-enhancer, we analysed the response of *Beta-* and *Gamma-lacZ* reporters to the different molecular actors that we have shown to play a role in *wg^{1}* regulation. First, we analysed the response of

Beta and *Gamma* to the alteration of the Hh activity. As expected, upon Hh overexpression we saw an expansion of *Gamma* towards the anterior compartment and higher expression levels (Figure 38H), as previously seen in the *wg[1]-lacZ* late discs. This is consistent with the presence of several Ci binding sites in the sequence of *Gamma* (Figure 38A). Moreover, *Gamma-lacZ* expression was completely abolished upon Ptc overexpression (Figure 38I), indicating that Hh is an absolute requirement for the activity of *Gamma.* By contrast, *Beta-lacZ* expression was not expanded toward the anterior compartment upon Hh overexpression (Figure 38C) despite the presence of a low-score Ci binding site in its sequence (Figure 38A). Oddly, upon Ptc overexpression, *Beta-lacZ* expression was lost (Figure 38D). This would indicate that *Beta* may have a certain capacity to respond to Hh activity though it seems that it is not its main regulator. Another possible explanation is that due to the drastic reduction of the wing pouch generated by the depletion of Hh, we are no longer capable to detect the posterior expression of *Beta*.

Next, we analysed the effect of EGFR activity depletion in *Beta* and *Gamma*. Interestingly, both were expanded to the most proximal region of the disc upon Vn::Aos overexpression and higher levels of expression were detected (Figures 38E and J, arrows). This is consistent with the presence of ETS binding sites in both, *Beta* and *Gamma* (Figure 38A). Surprisingly, in this context, we could detect the expression of *Gamma* in the posterior compartment (Figure 38J) but this expression colocalized with pyknotic nuclei (Figure 38J'), indicating that probably this expression is more related to cell death than to developmental inputs. That would be further discussed in the following sections of this thesis. Consistently with these results, previous results showed that upon EGFR depletion *wg[1]-lacZ* expression was suddenly detected in the posterior compartment (Figure 31C to E). Even though there are some pyknotic nuclei positive for *wg[1]* in the posterior compartment, many of them are healthy, therefore *wg[1]-lacZ* posterior expression could be mainly explained by the loss of suppression of *Beta* upon EGFR depletion. Altogether, these results indicate that both, *Beta* and *Gamma,* respond to the EGFR activity and that EGFR represses the activity of *wg[1]*-enhancer through both modules.

Finally, we tested the effect of JAK/STAT activity depletion. While *dome-i* overexpression did not significantly impact *Beta-lacZ* expression (Figure 38F), the effect in *Gamma-lacZ* reporter was dramatic. Upon *dome-i* overexpression expression of *Gamma-lacZ* reporter was remarkably enhanced not just across the anterior compartment but also through the posterior compartment (Figure 38K and K'). Interestingly, the effect observed in the *Gamma-lacZ* reporter was the same one as the observed for *wg[1]-lacZ*, indicating that JAK/STAT performs its *wg[1]* regulation through *Gamma* and not *Beta*. Altogether, our data suggest that *wg[1],* hence Wg,

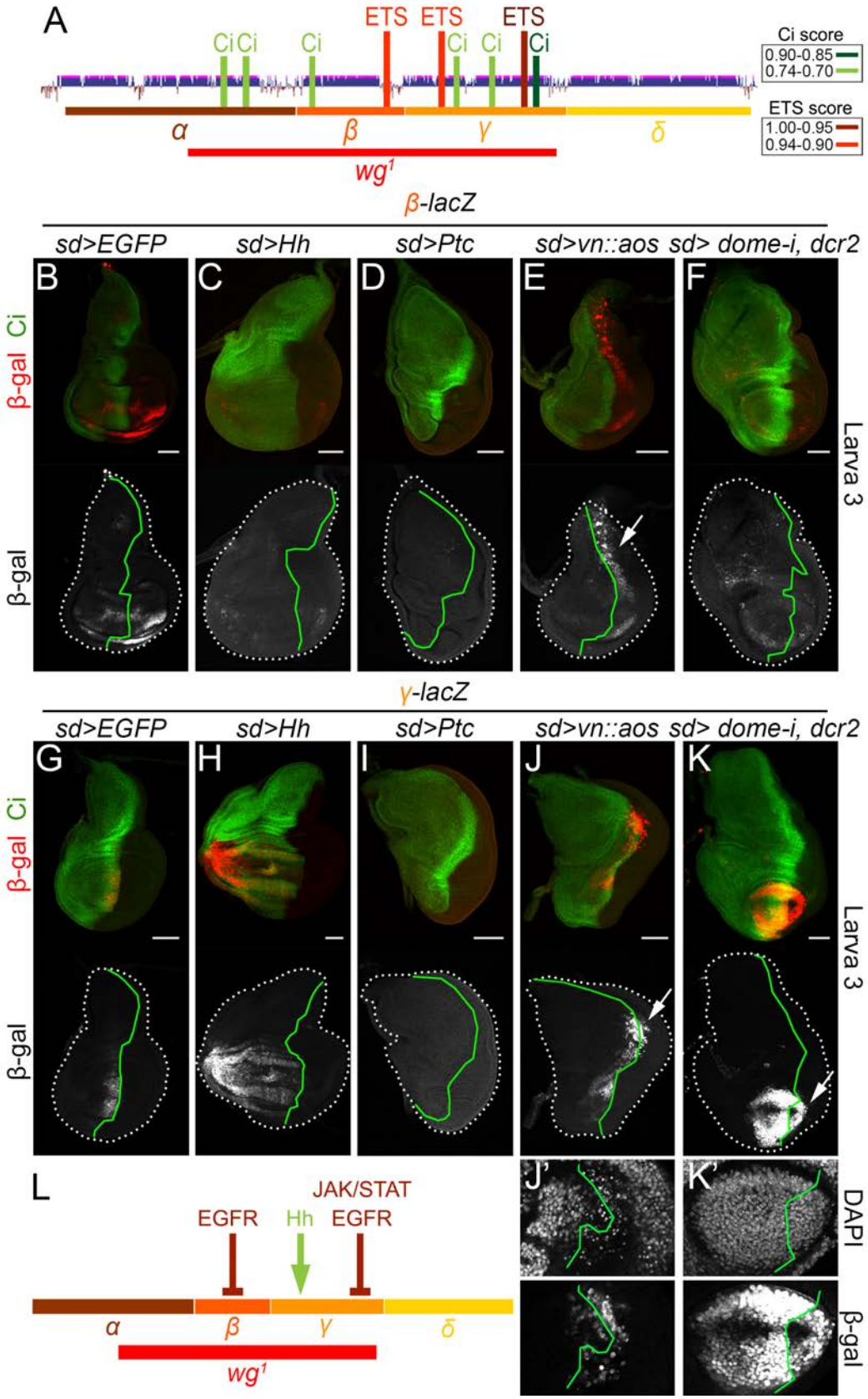

Figure 38. *Gamma* comprises all the regulatory cues while *Beta* only comprises EGFR. A) Cartoon depicting the different modules spanning the *wg*¹-enhancer and the bioinformatically predicted Ci (in green) and ETS (in red) binding sites. The scores are shown in the table at left. **B-K)** Late third instar wing disc of flies carrying the *β-lacZ* (B to F) or *γ-lacZ* (G-K) reporters and expressing the indicated transgene under the control of the *sd-gal4* driver. Discs were stained for β-galactosidase (red or white) and Ci (green). Disc contour and AP boundary are labelled by white and green lines, respectively. Arrows at E, J and K point to the ectopic expression of reporters. **J' and K')** Higher magnification of the regions of discs showing *Gamma* posterior expression. Scale bar: 50 µm. L) Cartoon showing the regulation of *Beta* and *Gamma* by the Hh, EGFR and JAK/STAT pathways.

is regulated by two modules: *Gamma,* which is positively regulated by Hh and negatively by EGFR and JAK/STA, and *Beta,* which acts a regulatory module that respond to EGFR repression (Figure 38L).

Beta and *Gamma* together are the minimal functional enhancer

Despite expression data is very useful and can give us plenty of information, it is always necessary to experimentally confirm the biological relevance of what expression data tells us. To do so, we generated different targeted deletions of *Gamma* and *Beta* using the CRISPR/Cas9 technique (Figures 39A and B). First, we targeted the high-score Ci binding site present in *Gamma-590* because its mutation caused a loss of the characteristic pattern of the reporter (Figures 37K and L). Remarkably, the loss of this Ci binding site (*Δ Ci BS*) did not induce the expected the loss of the wing and notum duplication. The same happened when we deleted the 590-bp-long module within *Gamma* (*Δγ-590*), and only when we deleted the totality of *Gamma* in homozygosis (*Δγ*), we could obtain flies showing the wing to notum phenotype. However, the penetrance was remarkably low, only 0.39%. As expected, upon *Beta* deletion (*Δβ*) in homozygosis we did not obtain any fly presenting a wing to notum transformation (Figure 39C). Just upon deletion of both *Beta* and *Gamma* (*Δβγ*) we could obtain flies presenting the wing to notum phenotype with a high penetrance (Figures 39C and D). Interestingly, the penetrance of the phenotype in homozygosis or transheterozygosis with *BRV118* deletion was very similar to the one obtained upon wg^{1} deletion in transheterozygosis with *BRV118* deletion (79% in *Δβγ/Δβγ*, 86% in *Δβγ/ΔBRV118*, and 81.4% in Δwg^{1}*/ΔBRV118* flies; Figure 39C). As expected, early Wg expression was completely lost in *Δβγ* homozygous disc, and Tsh was all over the disc. Consequently, mature *Δβγ* homozygous discs showed a lack of wing pouch and a notum mirror duplication (Figure 39E). Interestingly, *Gamma* deletion over larger wg^{1}-related deletions increased the penetrance of the phenotype, although it was still low (12% in *Δγ/Δβγ* flies, and 37% in *Δγ/ΔBRV118* flies; Figure 39C). Similar results were obtained when we crossed *Δγ-590* flies with *ΔBRV118 (Δγ-590/ΔBRV118*) where 1.65% of the flies showed the phenotype (Figure 39C). The fact that the penetrance of the phenotype in *Δγ* transheterozygotes is higher than the one in *Δγ-590* transheterozygotes points to a potential role of the *Gamma-630* module in the regulation of Wg despite its inability to drive *lacZ* expression. Whether it contributes to transcriptional factor binding or another function remains as an open question. On the other hand, as expected, when we crossed *Beta* deletion with larger wg^{1}-related deletions we could not detect even a single adult showing the wing to notum phenotype (Figure 39C). Altogether, these results unveil *Beta* and *Gamma* together as the minimal functional enhancer. Despite

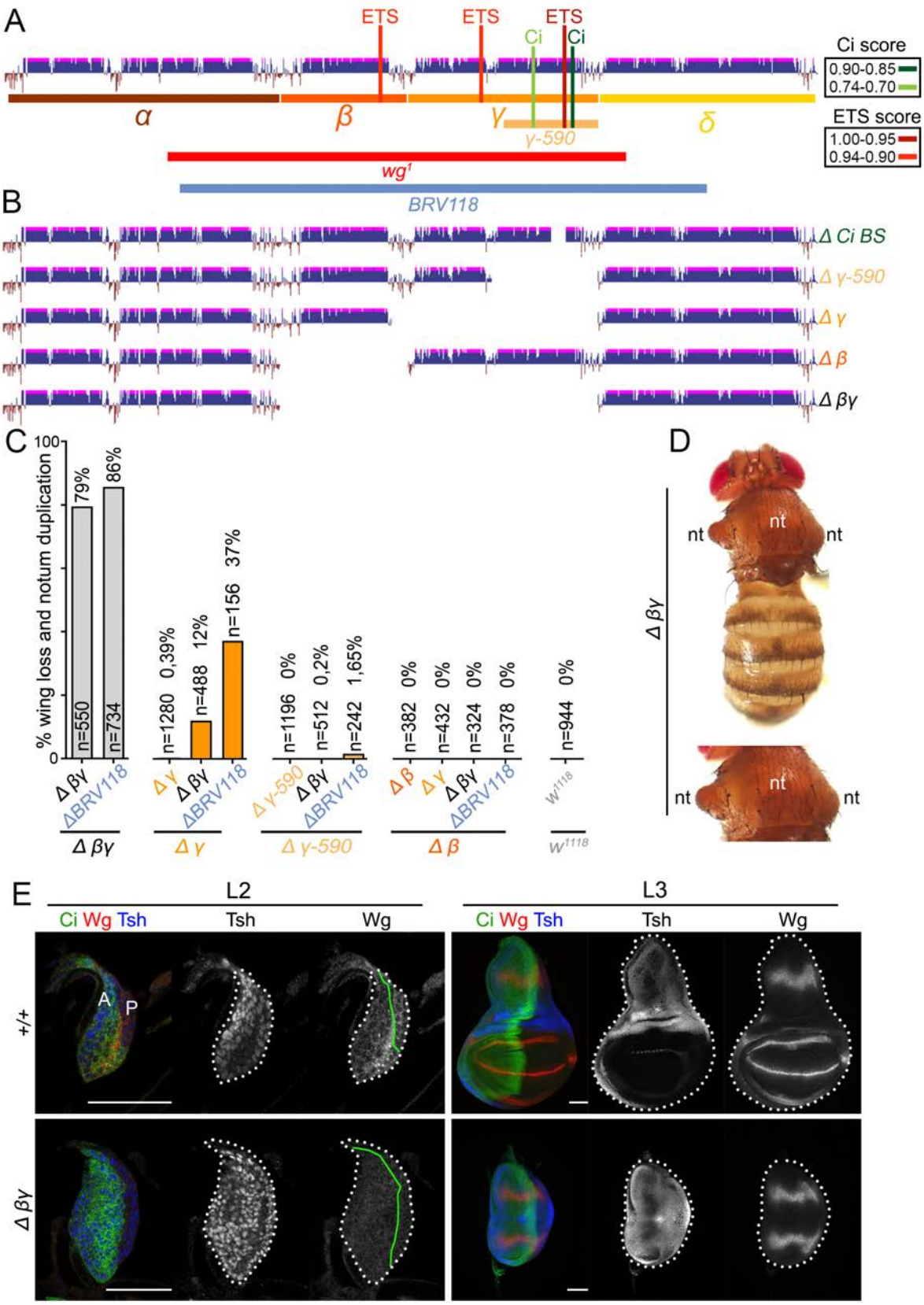

Figure 39. *Beta* and *Gamma* act together to induce the wing fate specification. A) Cartoon depicting the different modules spanning the *wg¹*-enhancer and the bioinformatically predicted Ci (in green) and ETS (in red) binding sites. The scores are shown in the table at left. **B)** CRISPR/Cas9-induced deletions generated in the *wg¹* sequence. **C)** Histogram showing the presence of flies that present the absence of wings and duplication of the notal structures of the indicated genotypes. The number of scored heminota (n) and the exact percentage is shown in the histogram. **D)** Example of wing to notum transformation of a *Δβγ* adult fly. The notum (nt) and duplicated notum (nt') are labelled. **E)** Second (L2) and third (L3) instar larvae of the indicated genotypes stained for Wg (red and white), Ci (green) and Tsh (blue and white). Disc contour and AP boundary are labelled by white and green lines, respectively. Scale bar: 50 µm.

this, the fact that a wing to notum phenotype is observed only in transheterozygous conditions of *Gamma* deletion over bigger deletion and not in *Δβ* transheterozygotes suggests that *Gamma* module acts as the main driver of Wg expression. Whether *Beta* contributes to tran-

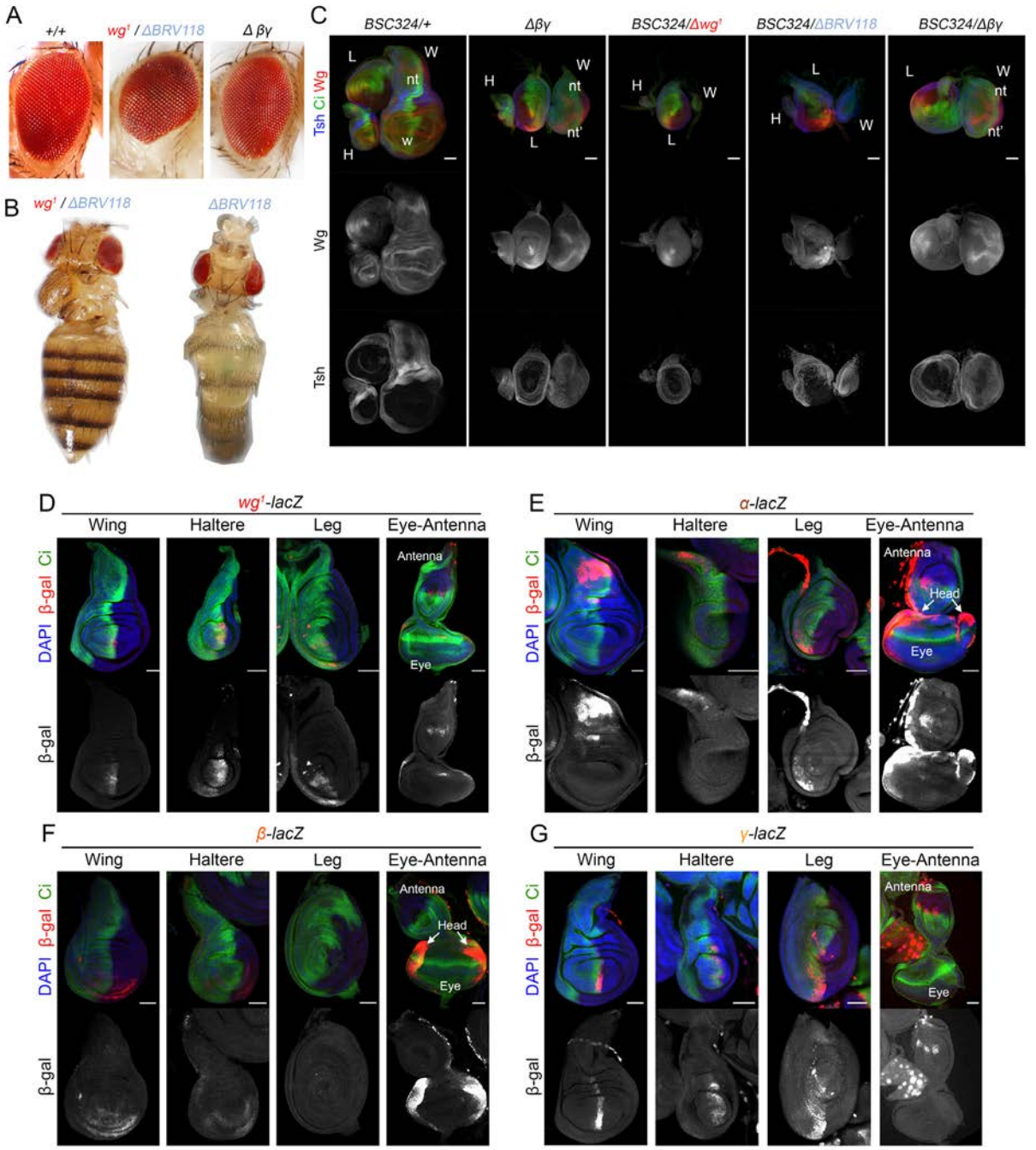

Figure 40. *wg¹* comprises three enhancers in one. A) Adult eyes of individuals of the indicated genotypes. **B)** Examples of loss of notum structures in *Δwg¹/ΔBRV118* or *ΔBRV118* homozygous flies. This phenotype was not observed in *Δβγ* homozygous flies. **C)** Late third instar discs of the indicated genotypes stained for Wg (red and white), Ci (green) and Tsh (blue and white). The wing pouch (w), the notum (n) and duplicated notum (n') are labelled. Wing (W), leg (L) and haltere (H) imaginal discs are indicated. **D-G)** Late third instar wing discs of larvae bearing the indicated reporter. All discs were stained for β-galactosidase (red or white), Ci (green) and DAPI (blue). Scale bar: 50 µm.

scriptional factor or co-factors binding, enhancer-promoter interactions or response to other molecular pathways remains to be further investigated. Nevertheless, our results demonstrate the functional redundancy of *Gamma* and *Beta* in Wg expression and wing specification.

wg^{1} comprises three enhancers in one

The phenotypical characteristic most important of *wg*^{1} flies is the absence of wings coupled with the duplication of notal structures. However, *wg*^{1} deletion also generates defects in the shape of the eye (Figure 40A)(Morata & Lawrence, 1977). Consistently, *wg*^{1}*-lacZ* expression was detected in the eye-antennal disc (Figure 40D). Interestingly, *Alpha*- and *Beta-lacZ* were capable to recapitulate *wg*^{1}*-lacZ* expression in the eye-antennal disc while *Gamma* presented no expression (Figures 40E to G) suggesting that *Alpha* and *Beta* modules are responsible for the eye phenotype. Furthermore, sometimes adults that presented a complete loss of one or both notal structures emerged (Figures 40B)(Sharma & Chopra, 1976). Consistently, tiny wing discs that present a complete loss of Wg were observed in *wg*^{1}*/BSC324* or *ΔBRV118/BSC324* flies while in *Δβγ/BSC324* or *Δβγ* homozygous flies showed a regular notum duplication with its characteristic Wg notal expression (Figure 40C). These results suggest that Wg from the notum would contribute to the growth of the notum. Moreover, the *Alpha* module drove *lacZ* expression in the notum of the developing wing disc (Figure 40E). Expression of *Alpha* in the notum together with the fact that we only could detect absence of notal structures

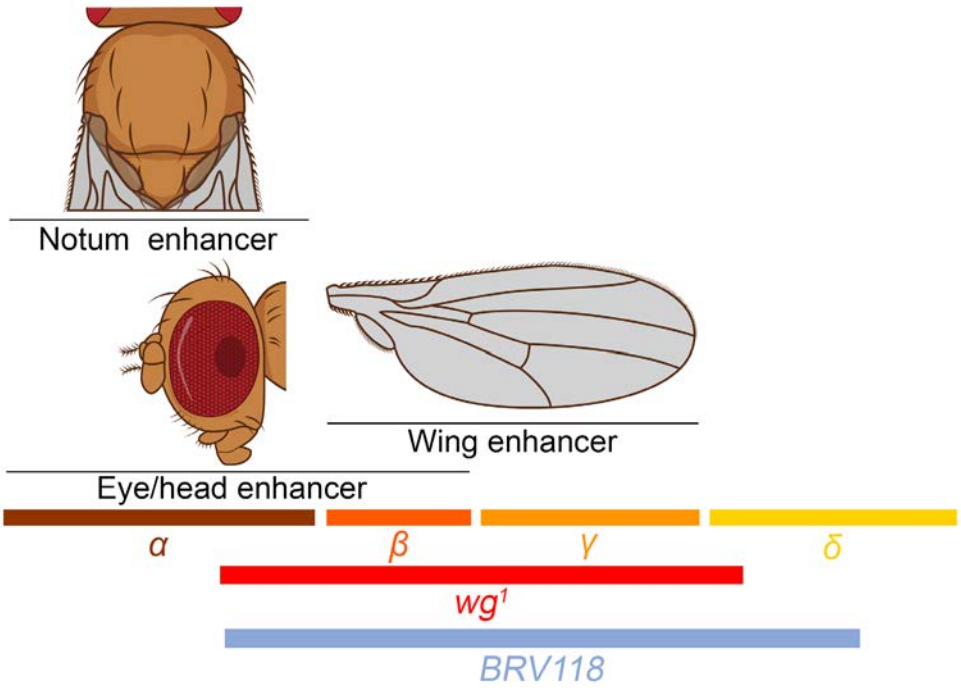

Figure 41. Three distinct overlapping enhancers are required for the development of notum, eyes and wings. Cartoon showing the localisation of the notum, eye/head and wing enhancers in relation to *wg*^{1}.

in *wg*^{1} mutants (that partially overlaps with the *Alpha* module) but not in *Δβγ* flies suggests that the *Alpha* module comprises an enhancer responsible for Wg expression in the notum. Altogether, these results point to the presence of three overlapping enhancers in the *wg*^{1} region (Figure 41).

Chapter 2: The *wg[1]* enhancer in regeneration

The role of *wg[1]*-enhancer in homeostatic conditions is to drive wing fate specification at the early stages of wing development. Interestingly, our data and the literature show that the enhancer is kept accessible at later stages even though it seems that does not play a role in wing development any longer (Harris et al., 2020). To answer why the enhancer is still active in later stages we would have to turn our attention to the regeneration field. It has been reported that *wg[1]*-enhancer respond to damage inputs by becoming more accessible (Harris et al., 2020; Vizcaya-Molina et al., 2018) and contributing to Wg and Wnt6 expression (Harris et al., 2016). Despite the consensus about the role of Wg in wing development, the role of Wg in regeneration is still controversial. While some authors argue that Wg plays a role at later stages in response to damage by inducing compensatory cell proliferation in the nearby cells and allowing regeneration (Harris et al., 2016; Ryoo et al., 2004; Smith-Bolton et al., 2009), other authors claim that regeneration can take place independently of Wg (Díaz-García & Baonza, 2013; Herrera et al., 2013; Pérez-Garijo et al., 2009).In addition, despite the fact that it is known that Wnt6 is expressed in response to damage (Harris et al., 2016), very little is known about its role in regeneration. The fact that these two molecules contribute to wing development (Baena-Lopez et al., 2009; Barrio & Milán, 2020; Diaz-Benjumea & Cohen, 1995), have made it difficult to study these molecules in regeneration due to the incapacity to circumvent their developmental role. Henceforth, we find in our collection of reporters and CRISPR/Cas9-targeted deletions of the *wg[1]*-enhancer a very good tool to bypass the developmental effects of Wg and Wnt6 depletion, allowing the revisiting of the role of Wg, Wnt6 and *wg[1]*-enhancer in regeneration. In addition, we want to uncover the possible role of the new enhancer modules in regeneration.

wg[1] enhancer respond to damage inputs

JNK is one of the main pathways that gets activated upon injury (Bergantiños et al., 2010; Bosch et al., 2005; Khan et al., 2017) and it is very well accepted that Wg expression upon injury is triggered by JNK (Pérez-Garijo et al., 2004; Ryoo et al., 2004; Smith-Bolton et al., 2009). Therefore, as previously described, we looked for bioinformatically predicted AP1 binding sites (the transcriptional factor of the JNK pathway formed by Jun and Fos)(Igaki, 2009) in *wg[1].* As expected, taking into account the PWMs for AP1 (Figure 42A) and the conservation among different insect species (Figure 42B), several binding sites were found in *wg[1]* and many of them with a very high score (Figure 42C and Table Annex 2).

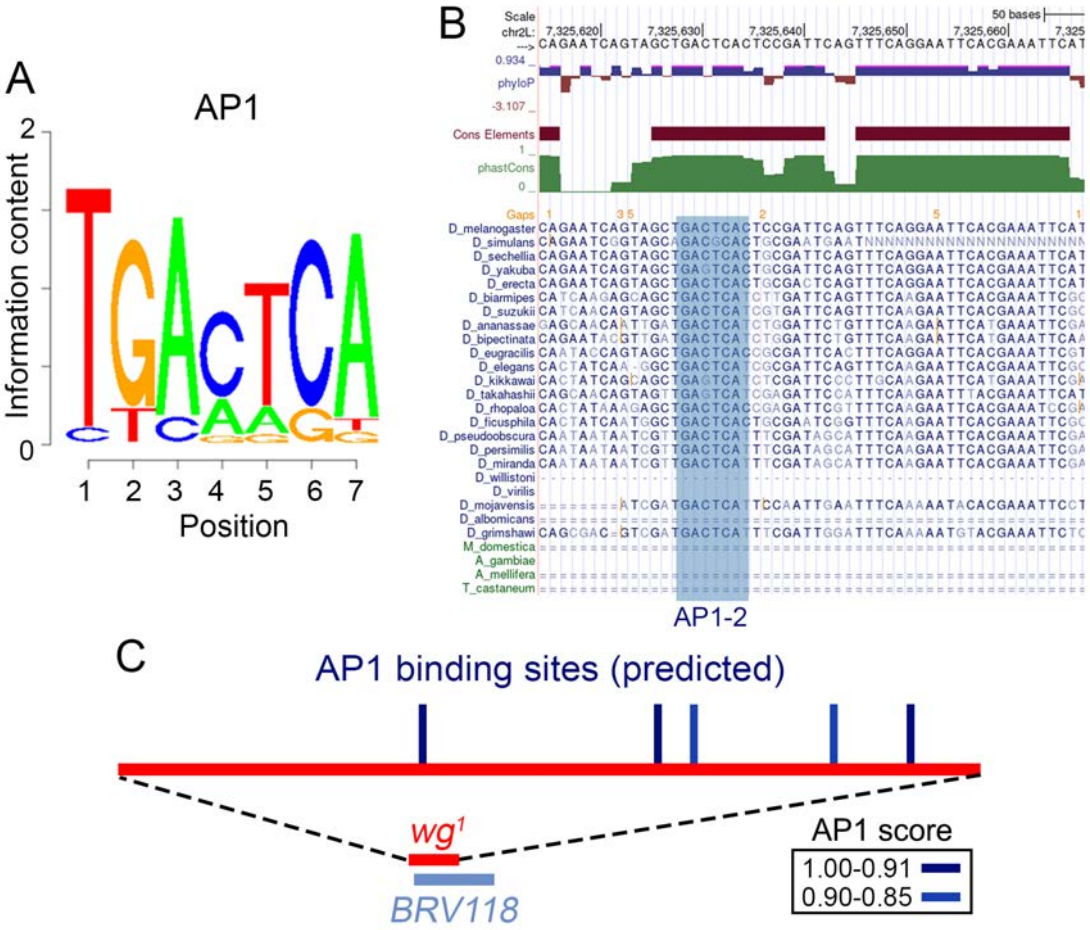

Figure 42. AP1 binding sites present in the sequence of *wg¹*-enhancer. A) Examples of PWMs of AP1. **B)** Conservation of the most relevant AP1 binding sites by multiple alignments of 27 insect species. Purple and green tracks show measurements of evolutionary conservation using two methods (phastCons and phyloP) from the PHAST package (http://compgen.cshl.edu/phast/), for all 27 species. Conserved elements (brown) identified by phastCons are also displayed. Data are taken from the UCSC genome browser (https://genome-euro.ucsc.edu/index.html). **C)** Cartoon depicting the presence of bioinformatically predicted AP1 (in blue) binding sites within *wg¹* sequence. The score of each binding site is shown in the table.

To study the role of Wg, Wnt6 and *wg¹*-enhancer in regeneration we used the genetic ablation system established by Dr Hariharan's laboratory. This system is based on the overexpression of the proapoptotic gene *egr*, *Drosophila* TNF-α homolog and ligand of the JNK pathway (Igaki et al., 2002; Moreno et al., 2002), under the control of the *rotund-gal4* (*rn-gal4*) driver which comprises the wing pouch. When Egr binds to its receptor it triggers the JNK cascade, leading to the cell death of most of the cells of the pouch (the future wing blade). Moreover, a temperature-sensitive version of Gal80 (*tub-gal80^{ts}*), which represses Gal4 activity at 18ºC but not at 29ºC, was used to switch on and off *egr* expression, allowing us to induce cell death for a specific window of time (Smith-Bolton et al., 2009). More specifically, we induced *egr* overexpression by moving flies from 18ºC to 29ºC for 16 h at early L3 stage (day 7 at 18 ºC; Figure 43A). So, we analysed the capacity of response of *wg¹-lacZ,* Wg and Wnt6 after 16h of

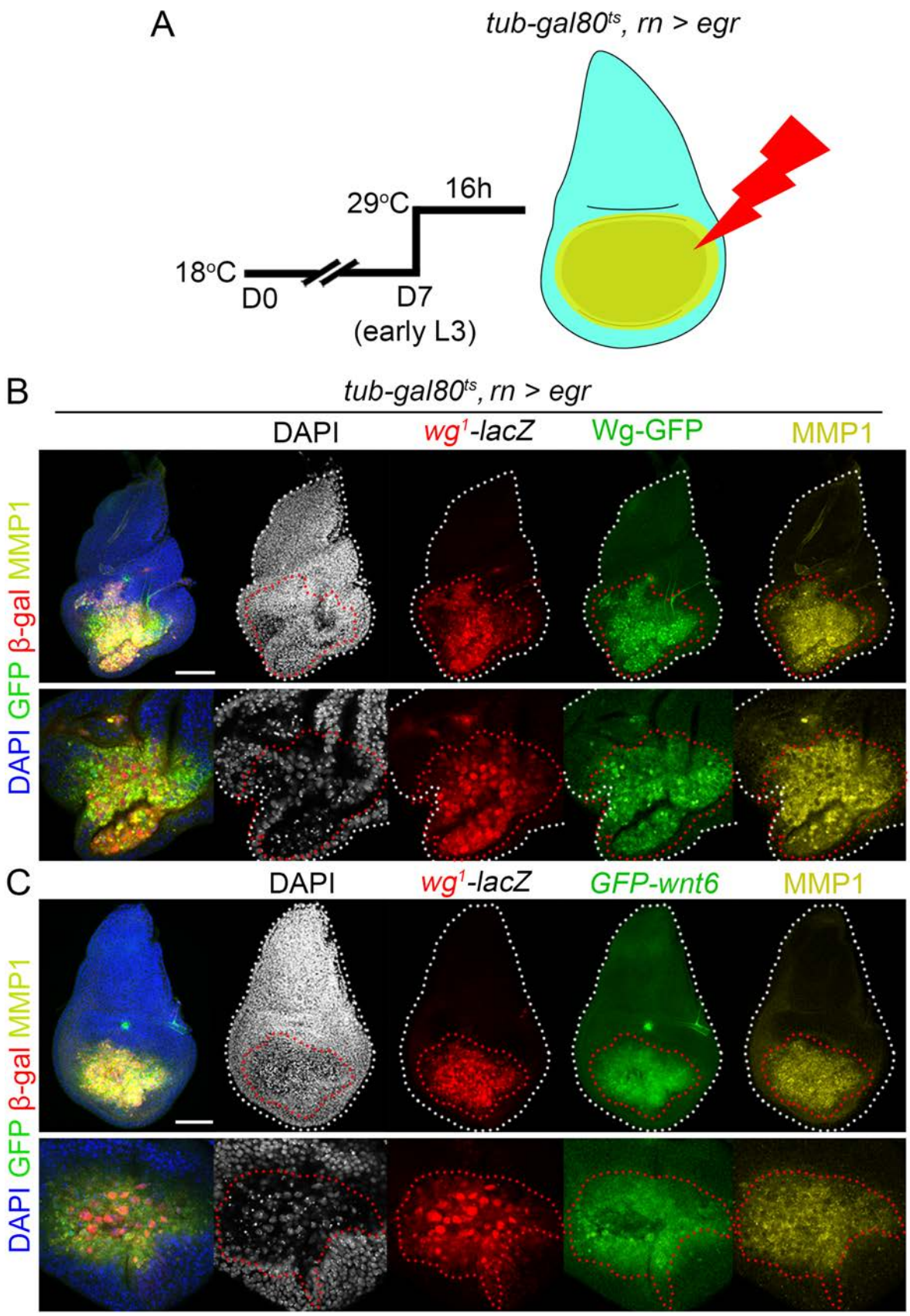

Figure 43. *wg*¹-enhancer respond to damage inputs. A) Schematic representation of the Eiger-dependent wing ablation systems. Larvae were raised at 18 °C for 7 days (D7) and switched to 29 °C for 16 h to visualise gene expression. **B-C)** Early third instar wing discs of larvae bearing the indicated reporters, after 16 h of *egr* induction under the control of the *rn-gal4* driver and stained for *wg*¹*-lacZ* expression (antibody to β-galactosidase in red), Wg-GFP (green, B), *GFP-Wnt6* (green, C), MMP1 (yellow), and DAPI (blue or white). Wing disc contours are labelled by a white line and cells expressing the *wg*¹-enhancer by a red line. Higher magnification of the wing pouch is shown in lower panels. Scale bar: 50 µm.

egr overexpression. A robust ectopic activation of *wg¹-lacZ,* endogenous Wg-GFP fusion protein and *GFP-wnt6* reporter was detected in response to *egr*-induced cell death. Interestingly, *wg¹-lacZ* reporter colocalized with both Wg-GFP and *GFP-wnt6* expression suggesting that *wg¹* could be regulating the expression of both genes. Remarkably, *wg¹-lacZ* also colocalizes with MMP1 (Figures 43B and C), a very well accepted target gene of JNK pathway in *Drosophila* (Uhlirova & Bohmann, 2006). These results, together with the presence of AP1 binding sites in the sequence of *wg¹*, suggest that upon damage Wg and Wnt6 expression is activated by the JNK pathway through the *wg¹*-enhancer. In addition, β-gal expression upon *egr* overexpression was drastically reduced when mutating four of the most important AP1 binding sites in

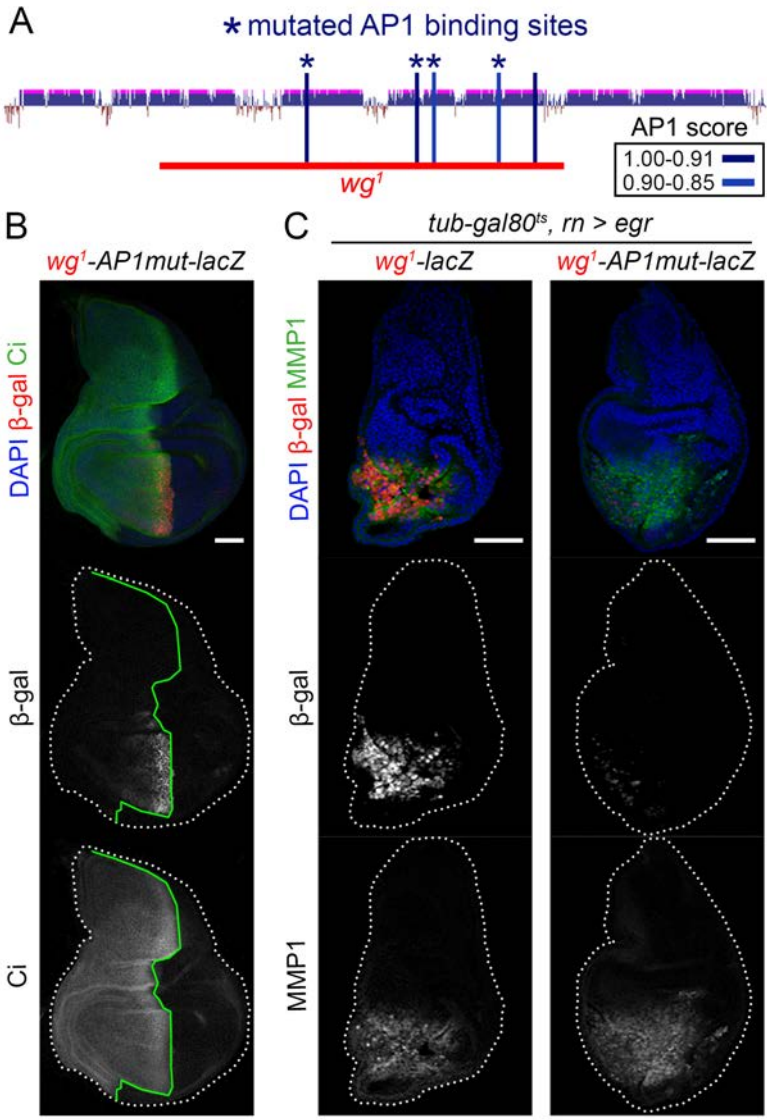

Figure 44. Mutation of AP1 binding sites prevents *wg¹* response to damage. A) Cartoon depicting the mutated AP1 binding sites into *wg¹*-enhancer. The score of each binding site is shown in the table. **B)** Developmental expression of the *wg¹-AP1mut-lacZ* reporter in a late third instar wing discs stained for β-galactosidase (red and white), Ci (green and white), and DAPI (blue). **C)** Early third instar wing discs of larvae bearing the *wg¹-lacZ* or the *wg¹-AP1mut-lacZ* reporter after 16 h of egr induction under the control of the *rn-gal4* driver and stained for β-galactosidase (red and white), MMP1 (green and white), and DAPI (blue). Disc contour and AP boundary are labelled by white and green lines, respectively. Scale bar: 50 µm

the *wg*^{1}-enhancer (Figures 44A and C, Table Annex 2). Importantly, the mutation of these AP1 binding sites does not affect the developmental expression of *wg*^{1}-enhancer (Figure 44B). This confirms that *wg*^{1} expression upon damage is driven by JNK.

Since JNK regulates Wg expression, it can be argued that the β-gal expression that we detected upon *egr* overexpression could be a mere consequence of JNK activity instead of a consequence of cell death. For that reason, in order to prove that *wg*^{1} activation is a general response to damage, we decided to use different mechanisms to induce cell death. First, we used the genetic ablation system established by the Dr Serras's laboratory. This system is based on the LexA/lexO binary system, and allows us to overexpress the pro-apoptotic gene *reaper* (*lexO-rpr*) under the control of the *spalt-lexA* (*sal-lexA*) driver, which is expressed in the central region of the wing pouch (Figure 45A). Rpr is at the top of the caspase cascade; hence, its overexpression triggers cell death. Importantly, the salE/Pv-LHG transgene includes a Gal80 thermosensitive form of LexA, allowing the conditionally expression of *rpr.* Therefore, *rpr* expression is supressed at 18ºC while it gets activates at 29ºC (Santabárbara-Ruiz et al., 2015).

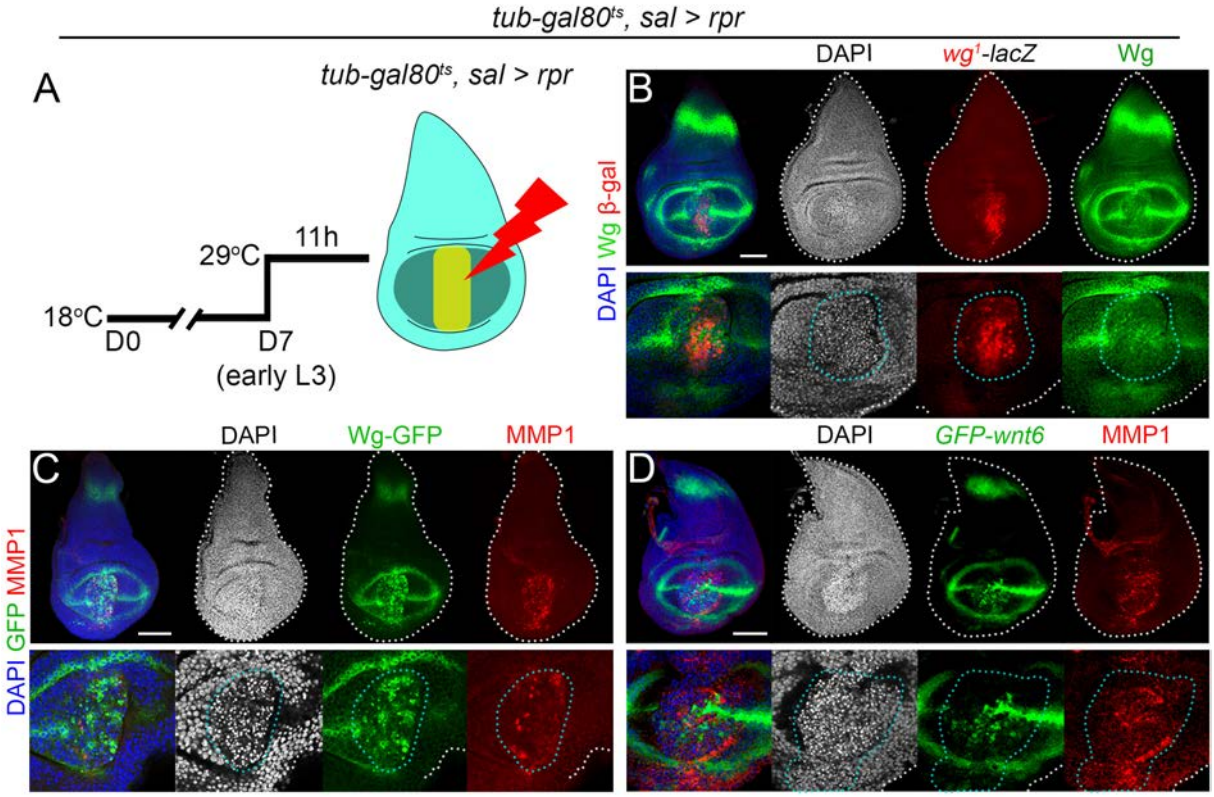

Figure 45. *wg*^{1}-enhancer responds to a different damage input. A) Schematic representation of the Reaper-dependent wing ablation systems. Larvae were raised at 18 °C for 7 days (D7) and switched to 29 °C for 11 h to visualise gene expression. **B-D)** Early third instar wing discs of larvae bearing the indicated reporters, after Rpr expression under de control of *sal-lexA* driver and stained for *wg*^{1}*-lacZ* expression (antibody to β-galactosidase in red, B), Wg (green, B), Wg-GFP (green, C), *GFP-Wnt6* (green, D), MMP1 (red, C and D), and DAPI (blue or white). Wing disc contours are labelled by a white line and pyknotic cells by a cyan line. Higher magnification of the wing pouch is shown in lower panels. Scale bar: 50 µm.

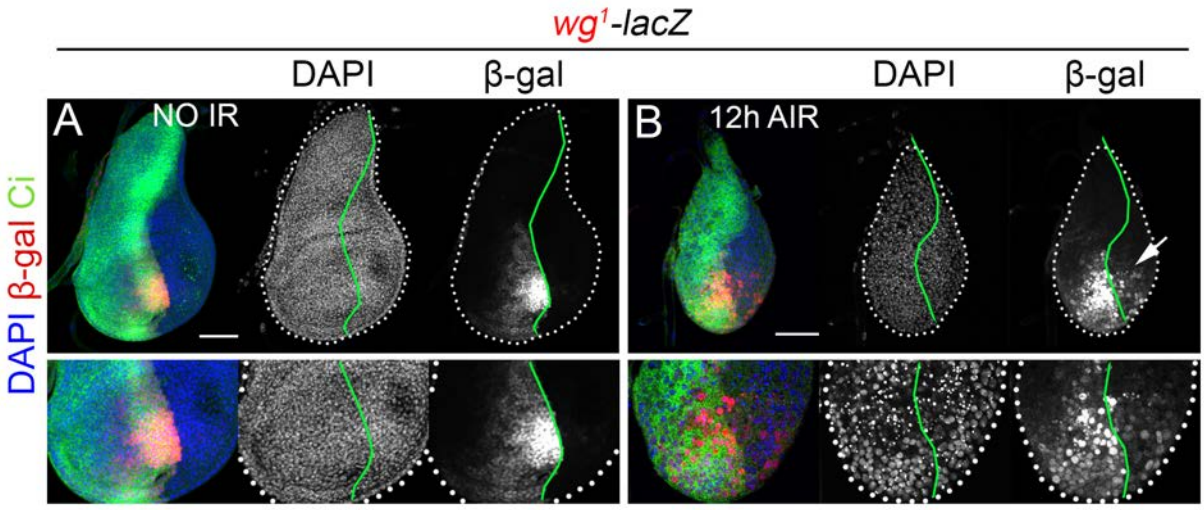

Figure 46. *wg*¹-enhancer responds to radiation. Expression of the *wg*¹-*lacZ* reporter in control (A) or irradiated (B) discs. Irradiated discs were subject to 45 Gy of radiation and dissected 12 h after the irradiation (12h AIR). All discs were stained for β-galactosidase (red or white), Ci (green), and DAPI (blue or white). Disc contour and AP boundary are labelled by white and green lines, respectively. Higher magnification of the wing pouch is shown in lower panels. Scale bar: 50 µm.

More specifically, we induced *rpr* overexpression by moving flies from 18ºC to 29ºC for 11 h at early L3 stage (day 7 at 18 ºC; Figure 45A). As expected, upon *rpr* overexpression we detected a robust expression of *wg*¹-*lacZ*, GFP-Wg and *GFP-wnt6* (Figures 45B to D). In addition, we detected a robust *wg*¹-*lacZ* expression in discs of larvae subjected to 45 Gys of irradiation (Figure 46B). Therefore, we can conclude that activation of *wg*¹-enhancer is a general feature of regeneration processes.

Beta and *Gamma* modules drive regeneration

We wanted to study more in depth the contribution of the *wg*¹-enhancer and its modules to regeneration. First, we analysed which modules of the *wg*¹-enhancer were capable to respond to *egr* overexpression. Interestingly, only *Beta* and *Gamma* responded to *egr* expression and its expression colocalized with MMP1 (Figure 47B). This is consistent with the fact that while *Beta* and *Gamma* present high score predicted AP1 binding sites, the ones predicted in *Alpha* presented a much lower score (Figure 47B and Table Annex 2). Interestingly, when we tested the response of both *Gamma* sub-modules, *Gamma-630 and -590,* to *egr* overexpression, both modules were capable to respond to *egr* induction, in contrast to what happened in development (Figure 47C).

Next, we functionally tested the capacity of *Beta* and *Gamma* modules to induce Wg expression using the CRISPR/Cas9 deletions previously generated. Consistently, Wg expression was reduced in disc homozygous for *Beta* (*Δβ*) or *Gamma* (*Δγ*) deletions and the reduction was

even stronger when both modules were deleted (*Δβγ*; Figures 48A and B). These findings indicate that *Beta* and *Gamma* present functionally independent roles in mediating Wg expression in response to JNK. Interestingly, Wg expression after Egr expression was detected even upon deletion of *Beta* and *Gamma* modules, pointing to the presence of other possible regulators of Wg expression in response to damage. Remarkably, the reduction of Wg expression was coupled with a reduction of the proliferative capacity of the disc in response to damage, measured by pH3 staining (a marker of mitosis) and EdU incorporation (a marker of the S-phase; Figures 48B to D). Consistently, when we allowed the adult wings to regenerate putting the larvae back at 18ºC after 16 h of cell death induction (Figure 48E), we saw a drastic reduction

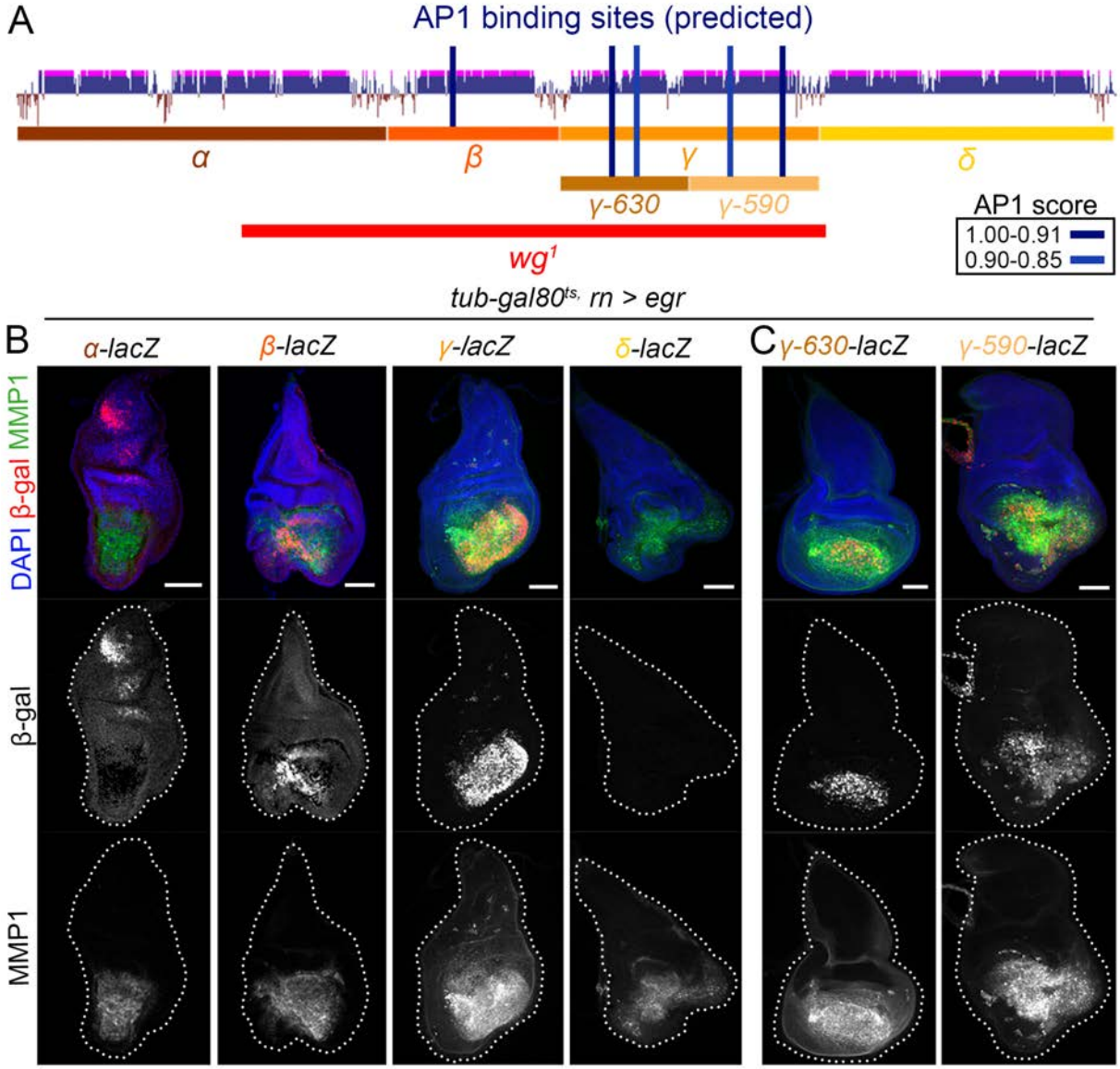

Figure 47. Only *Beta* and *Gamma* respond to damage. A) Cartoon depicting the different modules spanning the *wg¹*-enhancer and the bioinformatically predicted AP1 (in blue) binding sites. The scores are shown in the table at left. **B-C)** Early third instar wing discs of larvae bearing the indicated reporter after 16 h of egr induction under the control of the *rn-gal4* driver. All discs were stained for β-galactosidase (red or white), MMP1 (green or white) and DAPI (Blue). Disc contours are labelled by a white line. Scale bar: 50 μm.

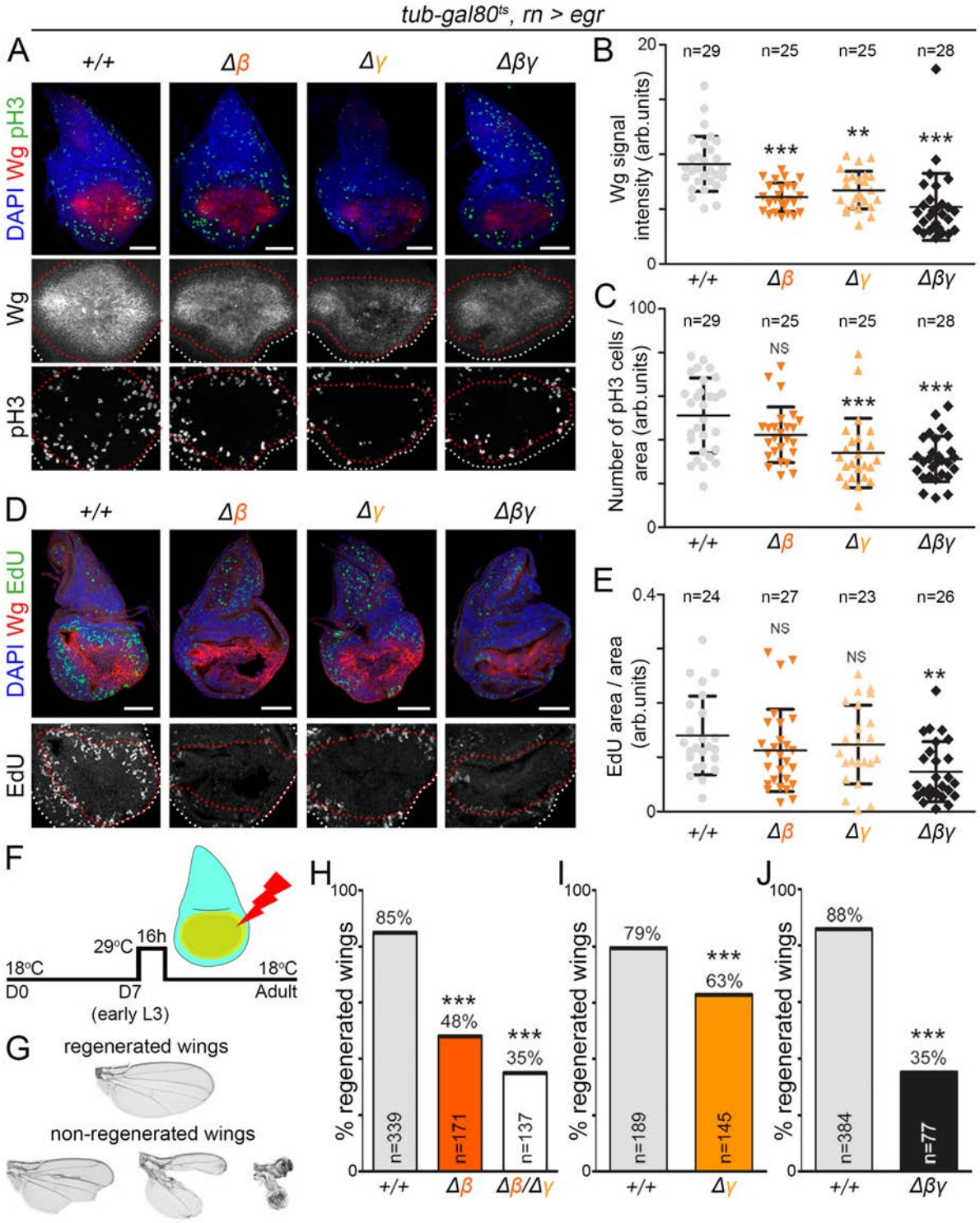

Figure 48. Deletion of *Beta*, *Gamma* or both reduce Wg expression and the regenerative capacity. A and D) Early third instar wing discs of the indicated genotypes after 16 h of egr induction under the control of the *rn-gal4* driver. Discs were stained for Wg (red or white), pH3 (green or white, A), EdU (green or white, D) and DAPI (blue). Higher magnification of the wing pouch is shown in lower panels. Wing disc contours are labelled by a white line and Wg staining by a red line. Scale bar: 50 µm. **B, C and E)** Scattered plots representing Wg signal intensity (in arbitrary units, B), number of pH3-positive cells per area (in arbitrary units, C), and EdU incorporation per area (in arbitrary units, E) of the indicated genotypes. The number of scored wing discs is shown and the area where mitotic activity or EdU was quantified (in B, C and E) is labelled by a red line in A and D. Mean and SD are shown. **F)** Schematic representation of the Eiger-dependent wing ablation and regeneration system. Larvae were raised at 18 °C for 7 days (D7), switched to 29 °C for 16 h and put back at 18 °C until adulthood to allow regeneration. **G)** Examples of the resulting fully regenerated and non-regenerated adult wings. **H-J)** Histograms plotting the percentages of fully regenerated wings of individuals of the indicated genotypes. The number of scored wings and the percentage of regenerated wings are shown. All statistical tests (Anova in A, C and E, logistic regression/Wald test statistic in H to J) are two-tailed and, in case of more than two conditions, Dunnett's multiple comparison correction against a common control was performed. Statistically significant differences are shown: NS, $p > 0.05$; **$p < 0.01$; ***$p < 0.001$.

on the regenerative capacities of those flies where *Beta, Gamma* or both modules were deleted, the effect being stronger when both modules were deleted (Figures 48F to G). The use of *Beta* and *Gamma* deletions, that do not generate any wing phenotype by themselves, have allowed us to overcome the developmental effect generated by Wg depletion that makes the study of Wg in regeneration difficult, allowing us to address its solely effect in the regenerative capacity. That said, these results demonstrate that Wg is a mitogenic molecule essential for wing regeneration.

Wnt6 is necessary for wing regeneration

Our previous results showed that Wnt6 is expressed in response to *egr* overexpression. To further analyse its role, we depleted its expression using an RNAi against it (*wnt6-i*). Then, we analysed the mitotic activity after 16 h of cell death induction or we put the larvae back to 18ºC to allow the wings to regenerate. Surprisingly, both the mitotic activity and the percentage of regenerated wings was decreased when *wnt6* was depleted (Figure 49). These results indicate that Wnt6 contributes to regeneration. This is surprising considering the little contribution of Wnt6 in wing development (Barrio & Milán, 2020; Doumpas et al., 2013). Further experiments are required to know how Wnt6 exerts its function.

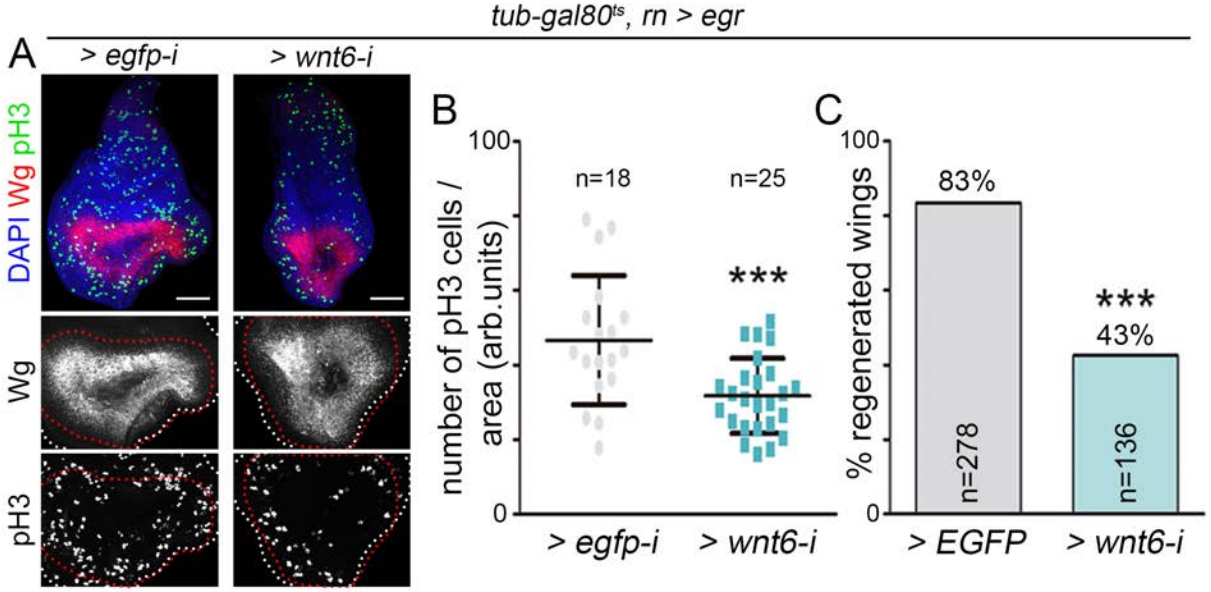

Figure 49. Wnt6 depletion impairs regeneration. A) Early third instar wing discs of the indicated genotypes after 16 h of egr induction under the control of the *rn-gal4* driver. Discs were stained for Wg (red or white), pH3 (green or white), and DAPI (blue). Higher magnification of the wing pouch is shown in lower panels. Wing disc contours are labelled by a white line and Wg staining by a red line. Scale bar: 50 µm. **B)** Scattered plot representing number of pH3-positive cells per area (in arbitrary units) of the indicated genotypes. The number of scored wing discs (n) is shown and the area where mitotic activity was quantified (in B) is labelled by a red line in A. Mean and SD are shown. **C)** Histograms plotting the percentages of fully regenerated wings of individuals of the indicated genotypes. The number of scored wings (n) and the percentage of regenerated wings are shown. All statistical tests (Anova in B, logistic regression/Wald test statistic in C) are two-tailed. Statistically significant differences are shown: ***p < 0.001.

Chapter 3: The *wg*^{1} enhancer in tumorigenesis

Development, regeneration and tumorigenesis have many shared genes at the core of their regulation. It has been shown that Wg is a key component of *Drosophila* wing development, regeneration and tumorigenesis (Baena-Lopez et al., 2009; Barrio & Milán, 2020; Dekanty et al., 2012; Diaz-Benjumea & Cohen, 1995; Ryoo et al., 2004; Smith-Bolton et al., 2009; Song et al., 2019). Actually, this is not a unique feature of the *Drosophila* wing disc, but it also plays a key role in the development, regeneration, and tumours of vertebrates (Aros et al., 2021; Deng et al., 2018; Majidinia et al., 2018). In fact, in tumours, it is common to observe the upregulation of genes involved in the early stages of development. This upregulation is linked to a reactivation of the enhancers associated with growth (Kron et al., 2014; Maurya, 2021). Therefore, the aim of this section is to analyse the capacity of *wg*^{1}-enhancer to drive Wg expression and tumoral growth in tissues subjected to chromosomal instability (CIN). In addition, we want to use the *lacZ* reporters and CRISPR/Cas9 tools generated in this work to further address the contribution of the different enhancer modules in CIN tumours.

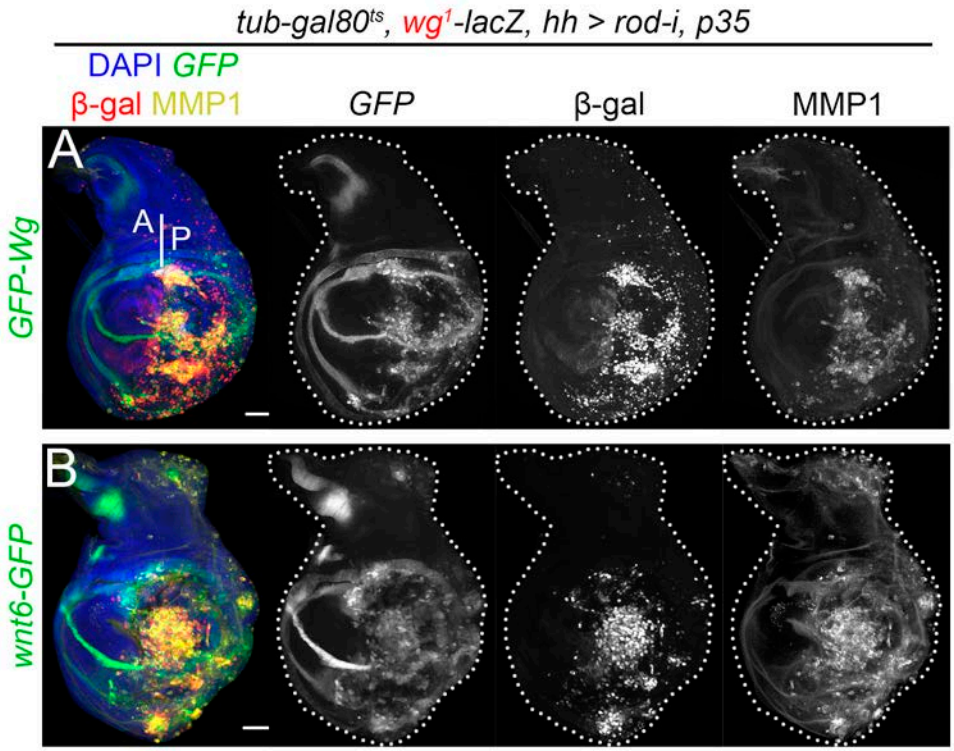

Figure 50. *wg*¹-enhnacer respond to CIN. A and B) Third instar wing discs of larvae bearing the indicated reporters, after CIN induction under the control of the *hh-gal4* driver and stained for *wg*¹*-lacZ* expression (antibody to β-galactosidase in red or white), Wg-GFP (green or white, A), *GFP-Wnt6* (green or white, B), MMP1 (yellow or white), and DAPI (blue). Wing disc contours are labelled by a white line. Anterior and posterior compartments are indicated. Scale bar: 50 µm.

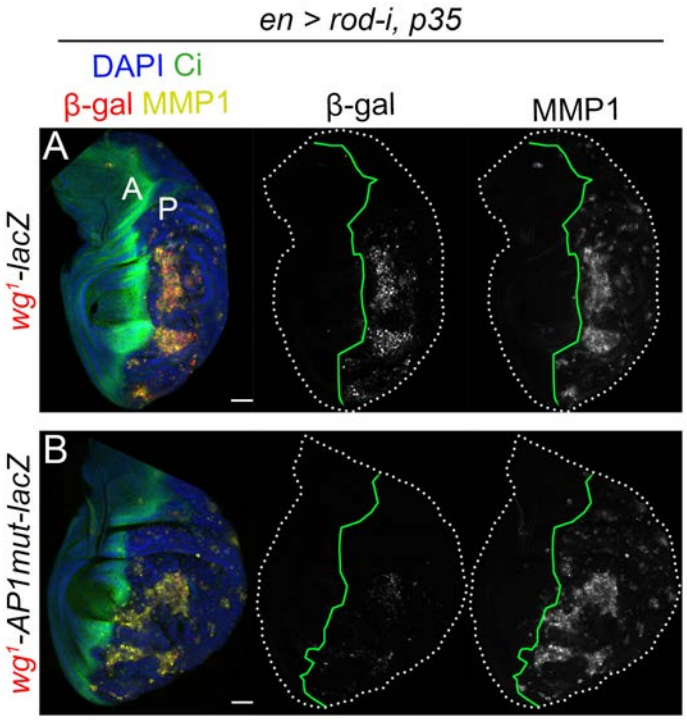

Figure 51. Mutation of AP1 binding sites prevents *wg¹*-lacZ expression. A and B) Third instar wing discs of larvae bearing the *wg¹-lacZ* (A) or *wg¹-AP1mut-lacZ* (B) reporter, after CIN induction under the control of the *en-gal4* driver and stained for β-galactosidase (in red or white), Ci (green), MMP1 (yellow or white), and DAPI (blue). Disc contour and AP boundary are labelled by white and green lines, respectively. Scale bar: 50 µm.

wg¹ is expressed in CIN tumours

As previously reported by our laboratory, in tissues subjected to CIN, JNK triggers Wg ectopic expression, leading to massive tissue overgrowth (Dekanty et al., 2012). Interestingly, not only Wg but also Wnt6 was expressed in CIN tissues and colocalized with both *wg¹-lacZ* and MMP1 expression (Figure 50). This result suggests that Wg and Wnt6 expression in CIN tissues could be regulated by JNK through the *wg¹*-enhancer. Consistently, expression of *wg¹-lacZ* reporter was drastically reduced in CIN tissues when four of the most important AP1 binding sites were mutated, even though MMP1 levels remained the same (Figure 51).

Beta and *Gamma* modules drive tumorigenesis

We wanted to study more in depth the contribution of the *wg¹*-enhancer modules to regeneration. First, we tested the capacity of each module to drive *lacZ* expression in CIN tissues. As expected, only *Beta* and *Gamma* were active in CIN tissues, and both *630-* and *590-Gamma* submodules were expressed too (Figure 52). Consistently, *wg¹-, Beta-,* and *Gamma-lacZ* expression levels were reduced upon the overexpression of a dominant negative form of Bsk (JNK kinase in *Drosophila*), confirming that both modules were regulated by JNK in CIN tissues (Figure 53).

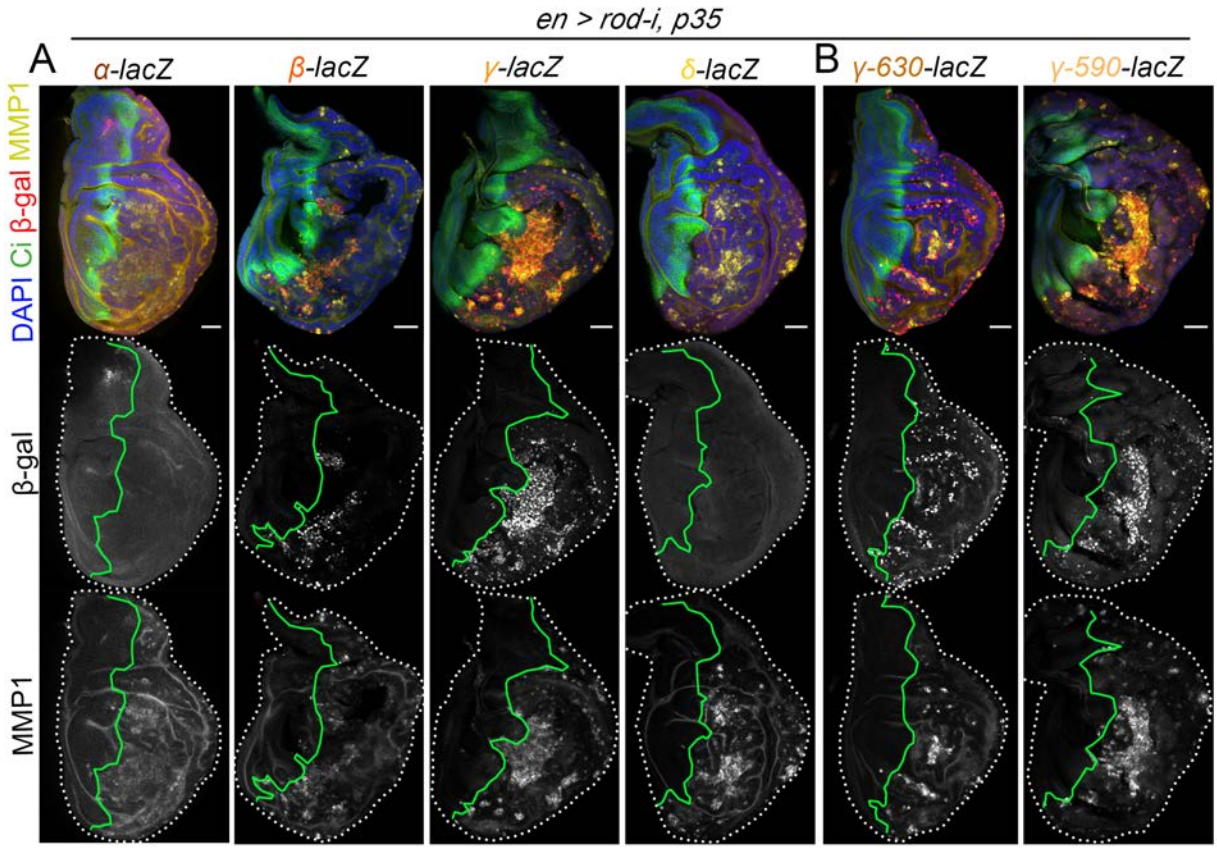

Figure 52. Only *Beta* and *Gamma* respond to CIN. A and B) Third instar wing discs of larvae bearing the indicated reporters, after CIN induction under the control of the *en-gal4* driver and stained for β-galactosidase (in red or white), Ci (green), MMP1 (yellow or white), and DAPI (blue). Disc contour and AP boundary are labelled by white and green lines, respectively. Scale bar: 50 µm.

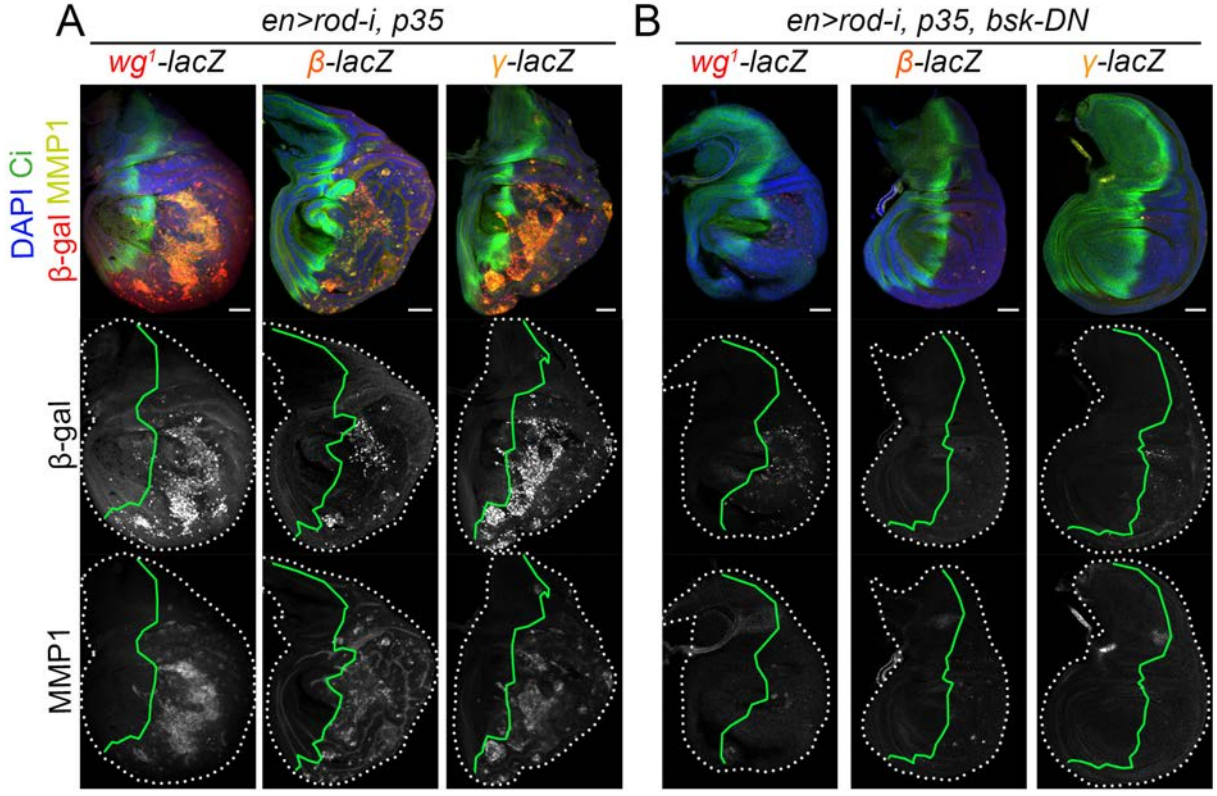

Figure 53. Blockage of JNK activity reduce the expression of the enhancer in CIN tissues. A and B) Third instar wing discs of larvae bearing the indicated reporters, after CIN induction under the control of the *en-gal4* driver (A) or with JNK activity blocked by *bsk-DN* (B). Discs were stained for β-galactosidase (in red or white), Ci (green), MMP1 (yellow or white), and DAPI (blue). Disc contour and AP boundary are labelled by white and green lines, respectively. Scale bar: 50 µm.

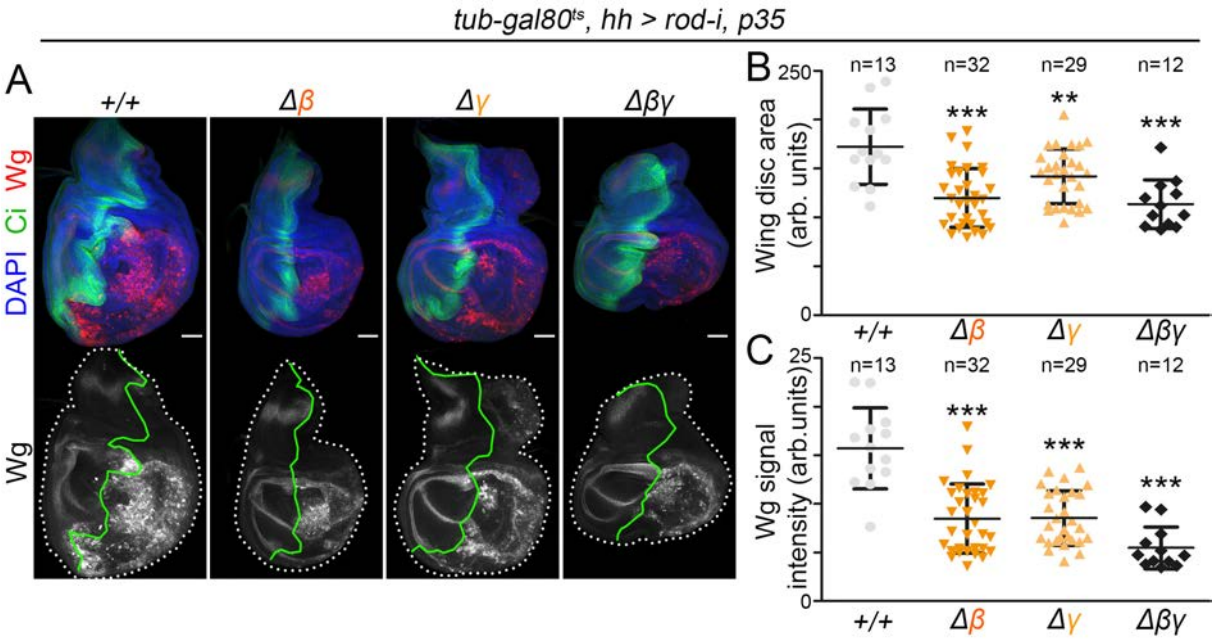

Figure 54. Deletion of *Beta*, *Gamma* or both reduce Wg expression and prevents tumoral growth. A) Third instar wing discs of the indicated genotype, after CIN induction under the control of the *hh-gal4* driver. Discs were stained for Wg (in red or white), Ci (green), and DAPI (blue). Disc contour and AP boundary are labelled by white and green lines, respectively. Scale bar: 50 µm. **B and C)** Scattered plots representing wing disc area (in arbitrary units, B), and Wg signal intensity (in arbitrary units, C) of the indicated genotypes. The number of scored wing discs, mean and SD are shown. Two-tiled Anova statistical test was performed with Dunnett's multiple comparison correction against a common control. Statistically significant differences are shown: **p < 0.01; ***p < 0.001.

Next, we assessed the capacity of *Beta* and *Gamma* to trigger Wg in CIN tissues and lead to tissue overgrowth using the CRISPR/Cas9 deletions previously generated in this work. As expected, in CIN tissues deletion of *Beta* (*Δβ*) or *Gamma* (*Δγ*) in homozygosis drastically reduced the levels of Wg expression, directly impacting the overgrowth capacity. The effects were even stronger when both modules were deleted together (*Δβγ*; Figure 54). Similar results were previously obtained in the laboratory in CIN discs with a full deletion of the *wg*^{1}-enhancer (Dekanty et al., 2012).

Wnt6 contributes to CIN-induced overgrowth

Since we observed that Wnt6 was also expressed in CIN tissues (Figure 50B), we wanted to dissect its functional role in sustaining tumour growth. Remarkably, by using a null allele of *wnt6* (*wnt6KO*) we saw a drastic reduction in the capacity of CIN tissue to overgrowth (Figure 55). How Wnt6 contributes to the overgrowth of CIN tissues is still an open question. On the other hand, the fact that *GFP-wnt6* expression colocalizes with *wg*^{1}*-lacZ* and MMP1 (Figure 50B) expression suggest that in CIN tissues Wnt6 would be regulated by JNK through *wg*^{1}-enhancer. However, further experiments are required to confirm this hypothesis.

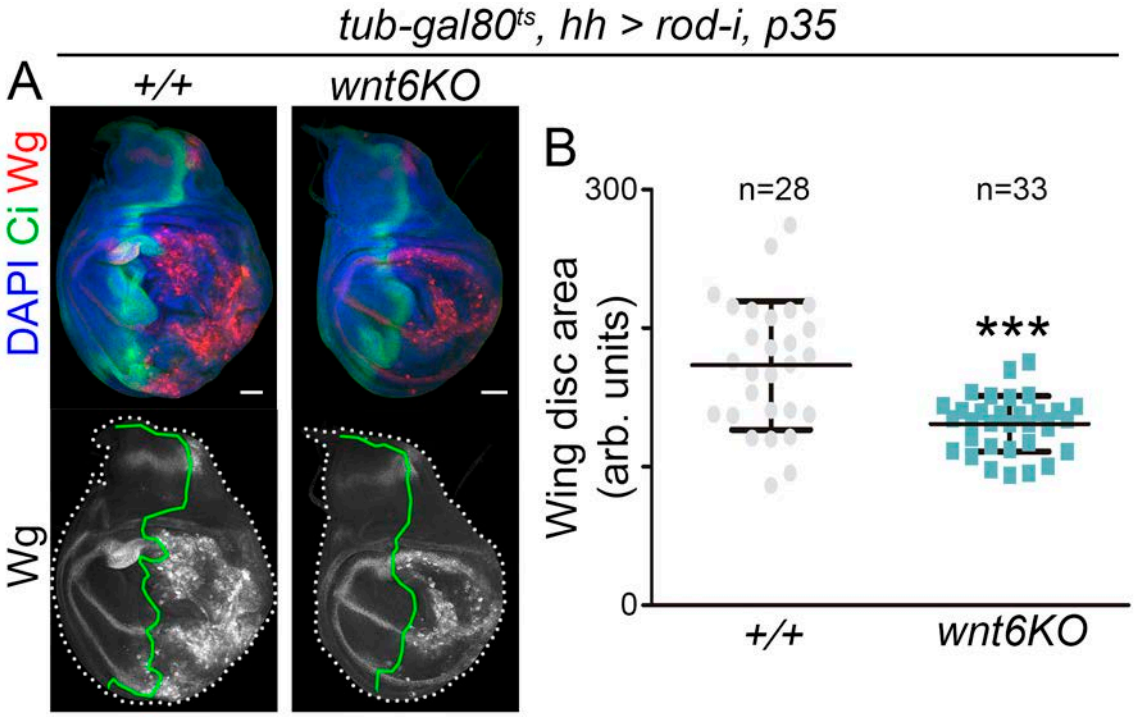

Figure 55. Wnt6 depletion impairs tumoral growth. A) Third instar wing discs of the indicated genotype, after CIN induction under the control of the *hh-gal4* driver. Discs were stained for Wg (in red or white), Ci (green), and DAPI (blue). Disc contour and AP boundary are labelled by white and green lines, respectively. Scale bar: 50 µm. B) Scattered plots representing wing disc area (in arbitrary units) of the indicated genotypes. The number of scored wing discs, mean and SD are shown. Two-tiled Anova statistical test was performed. Statistically significant differences are shown: ***p < 0.001.

Chapter 4: Senescence in the regenerative discs

Analysing the expression of the *wg¹-lacZ* reporter in *egr*-expressing discs, we noticed the presence of abnormal big nuclei cells (Figure 56A, arrows). Their enlarged nuclei size could be easily noticed when comparing them with nuclei of healthy cells in the control discs, where these big nuclei cells could not be found (Figure 56B). This result suggests that big nuclei cells appear after ectopically inducing *egr* expression. Since these cells are expressing Egr, they

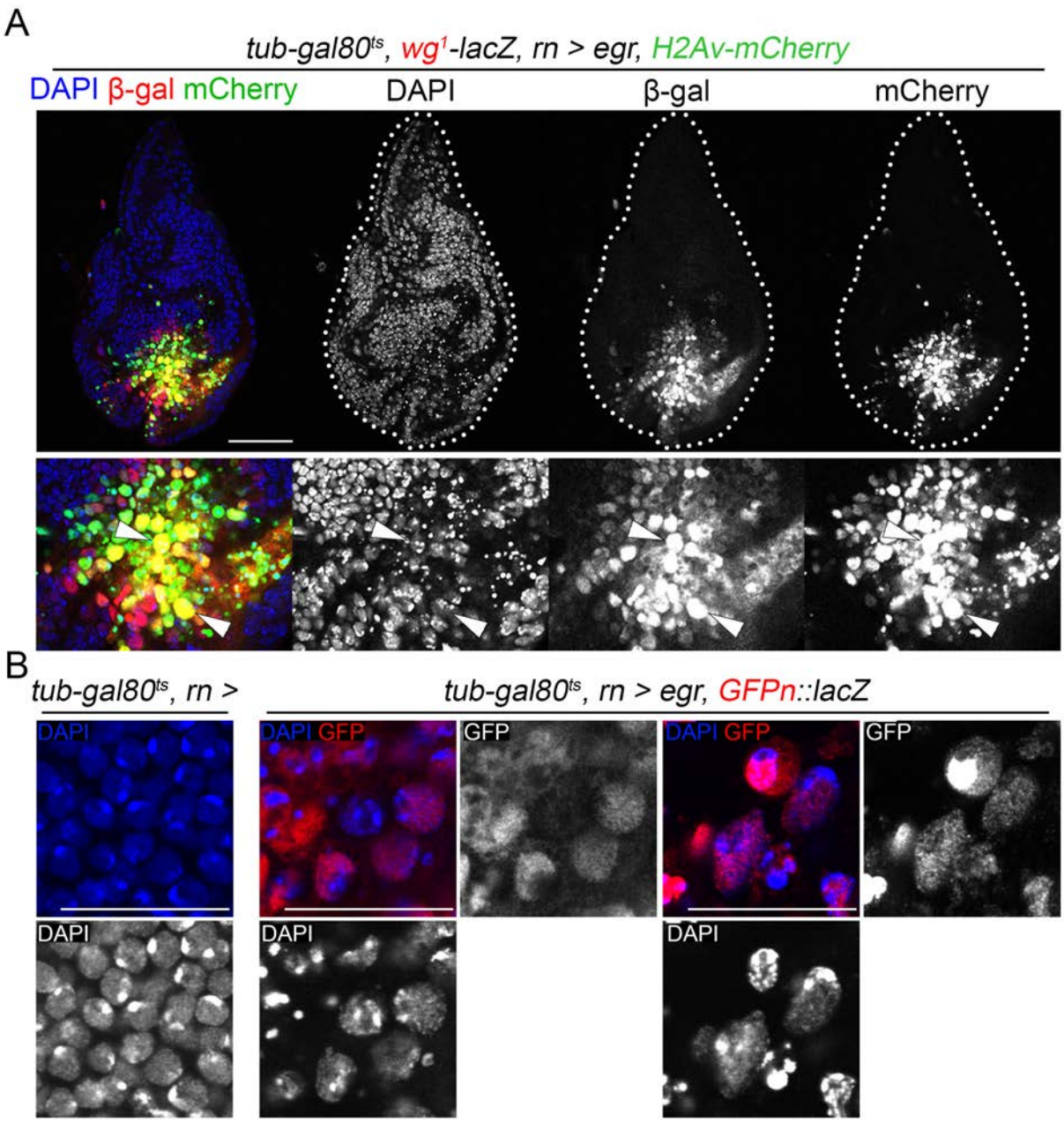

Figure 56. Big nuclei cells are observed in *egr*-expressing discs. A) Early third instar wing discs of larvae bearing the indicated reporters, after 16 h of egr induction under the control of the *rn-gal4* driver and stained for *wg¹-lacZ* expression (antibody to β-galactosidase in red or white), H2Av-mCherry (green or white) and DAPI (blue or white). Arrowheads point to big nuclei cells expressing *wg¹-lacZ* and H2Av-mCHerry. Wing disc contours are labelled by a white line. Higher magnification of the wing pouch is shown in lower panels. Scale bar: 50 µm. B) 63X magnification of non-damaged (*rn >*) and damaged (*rn > egr*) discs stained for GFP (red or white) and DAPI (blue or white). Scale bar: 20 µm.

should die. Remarkably, they did not look like dying cells (they were not pyknotic), but they did not look as healthy cells either. It is the aim of this section to characterize the nature of this population of cells.

Big nuclei cells are detached from the healthy epithelium

The first thing we wanted to understand was whether this cell population was part of the main epithelium or not. To analyse the architecture of the main epithelium we expressed, under the control of *rn-gal4* driver, MyrTomato (MyrT), a fluorescent protein expressed in the cellular membrane, and a GFP fused with β-galactosidase (*GFPn::lacZ*), that labels the nucleus, both in control and damage conditions. Upon *egr* expression, we could observe a large number of pyknotic nuclei mainly on the apical side of the epithelium. Some big nuclei cells could be observed apically, but most of them were found more basally (Figure 57B, apical and basal planes). Besides, as previously reported in the literature, upon *egr* expression we could observe the loss of the pseudostratified architecture of the disc when compared with control (compare Figure 57A and B, orthogonal YZ and XZ planes)(Smith-Bolton et al., 2009). Another observation we could make was that in *egr*-expressing discs, the integrity of the membrane seemed affected. While in controls the membrane was well delimited by MyrT, in *egr*-expressing discs it was impossible to properly visualize the membrane by MyrT labelling. Similar results were obtained when we analysed the expression of Fasciclin III (FasIII), another membrane protein (Figure 57C). These results suggest that the integrity of the cellular membrane or of its proteins is affected upon *egr* induction. If the membrane proteins are affected, most probably the cell-cell interactions will be also affected, reinforcing the idea that most probably these big nuclei cells are no longer attached to the main epithelium.

Next, we analysed the expression of DE-Cadherin (DE-Cadh), a protein of the adherens junctions near the apical side of the disc (Badouel & McNeill, 2009). While in controls we only can detect DE-Cadherin expression apically, in *egr*-expressing discs we observed that its expression is disrupted (compare Figure 58A and B, apical and basal planes), consistent with the MyrT and FasIII data. Interestingly, we could detect some small discrete miss-localized DE-cadherin puncta in basally localized big nuclei cells (Figure 58B orthogonal YZ and XZ planes). Altogether, these results indicate that the expression of *egr* disrupts the main epithelium and leads to the appearance of these big nuclei cells that are not part of the main epithelium.

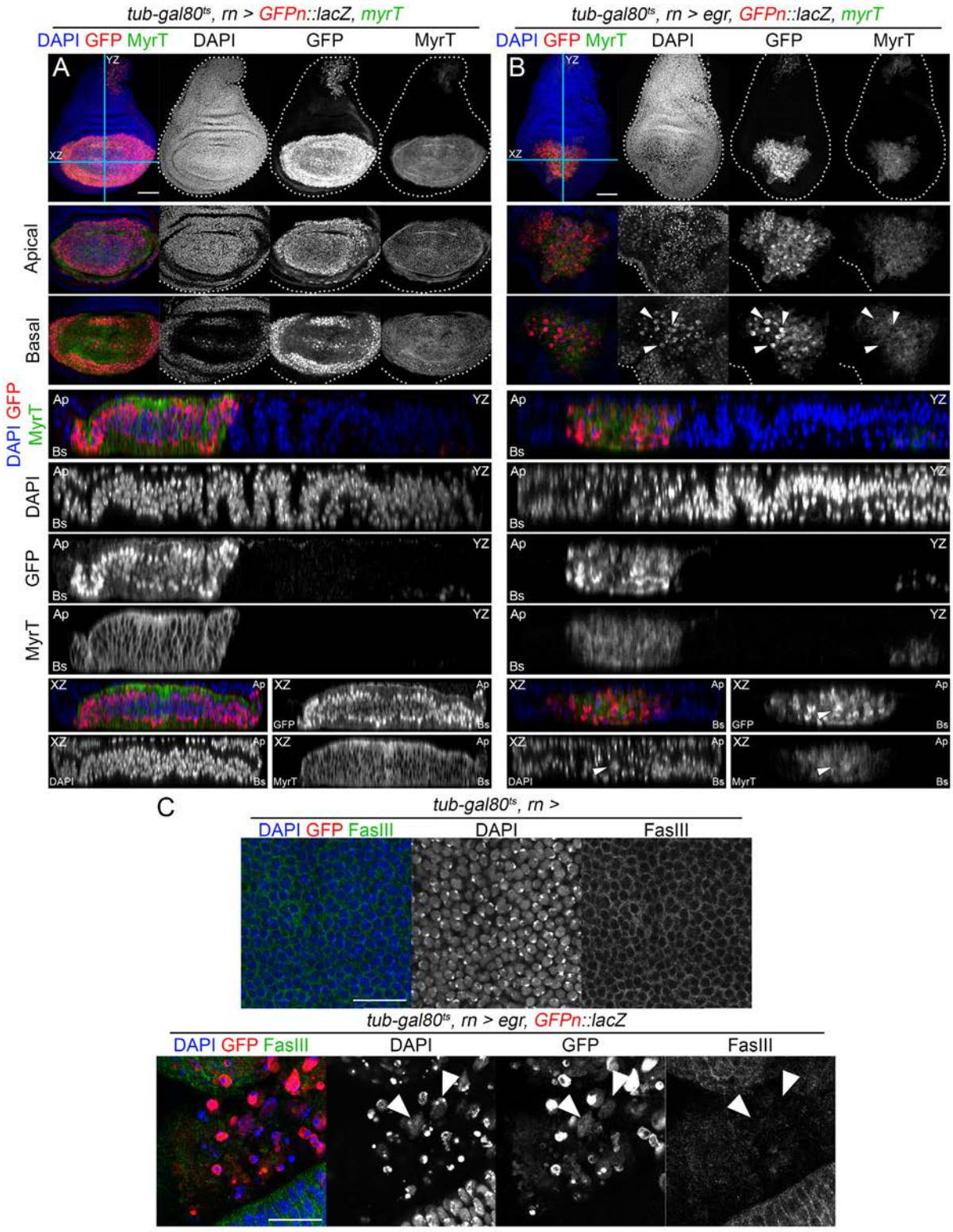

Figure 57. Big nuclei cells are detached from the main epithelium. A and B) Early third instar wing discs of the indicated genotype stained for GFP (red or white), MyrT (green or white) and DAPI (blue or white). Upper panels show a Z-projection of the full disc. Single apical and basal planes of the pouch are shown in middle panels. Orthogonal projections of YZ and XZ planes are shown in lower panels. The apical (Ap) and basal (Bs) planes of the projection are indicated. Arrowheads point to big nuclei cells. Wing disc contours are labelled by a white line. Scale bar: 50 µm. **C)** 63X magnification of non-damaged (*rn >*) and damaged (*rn > egr*) discs stained for GFP (red or white), FasIII (green or white) and DAPI (blue or white). Scale bar: 20 µm.

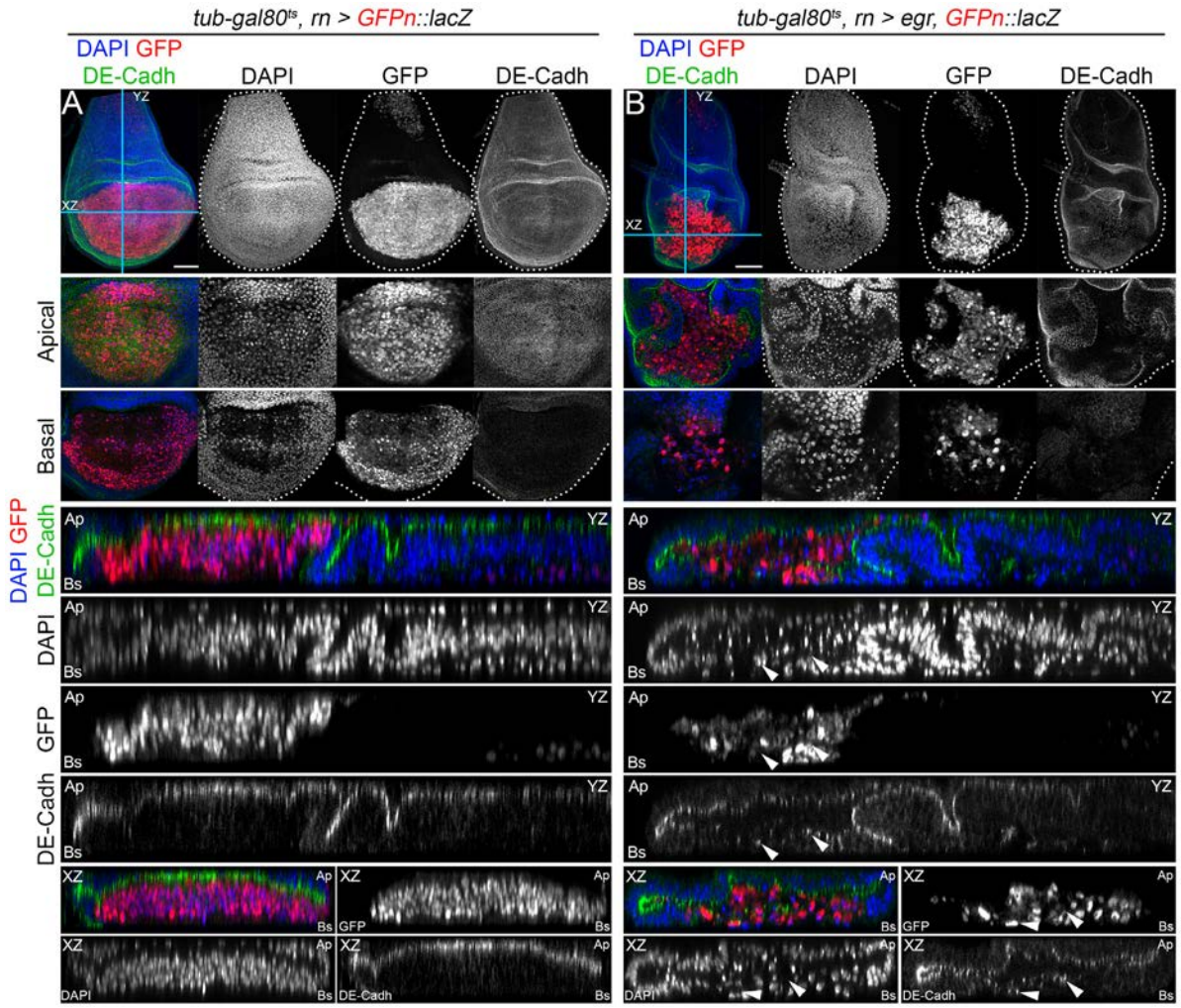

Figure 58. Big nuclei show misslocalized DE-Cadherin. A and B) Early third instar wing discs of the indicated genotype stained for GFP (red or white, B), DE-Cadherin (DE-Cadh, green or white) and DAPI (blue or white). Upper panels show a Z-projection of the full disc. Single apical and basal planes of the pouch are shown in middle panels. Orthogonal projections of YZ and XZ planes are shown in lower panels. The apical (Ap) and basal (Bs) planes of the projection are indicated. Arrowheads point to misslocalized DE-Cadherin. Wing disc contours are labelled by a white line. Scale bar: 50 µm.

Big nuclei cells avoid apoptosis

As previously described, *egr* overexpression leads to JNK activation that triggers the caspases, hence, activating programmed cell death (Igaki et al., 2002; Moreno et al., 2002). Interestingly, as seen in figure 56B, despite expressing *egr*, our big nuclei cells do not look like dying cells (they are not pyknotic). Therefore, we decided to perform a TUNEL assay, a well-established technique to label dying cells, to know whether these cells were dying or not. As expected, upon *egr* induction we could observe a massive number of pyknotic cells that were TUNEL-positive (Figure 59B). In control discs we could detect some TUNEL-positive cells, but while in controls pyknotic cells were found only basally, in the *egr*-expressing disc we could find them in all planes, but especially apically (compare Figure 59A and B orthogonal planes

YZ). Surprisingly, our big nuclei cells were TUNEL-negative, although they did present caspase activity as seen by the GC3Ai reporter signal (a reporter that displays GFP signal only when caspase activity is present)(Schott et al., 2017). Altogether, these results show that upon *egr* overexpression the caspase cascade is triggered and there is a massive amount of cell death. Interestingly, despite caspase cascade activation, there is a population of *egr*-expressing cells with enlarged nuclei size that appear resistant to cell death resistant, being negative for TUNEL staining and pyknosis. How these cells stay alive even if they present caspase activity, still remains a mystery and further research would be necessary to unveil the mechanism by which these cells resist apoptosis.

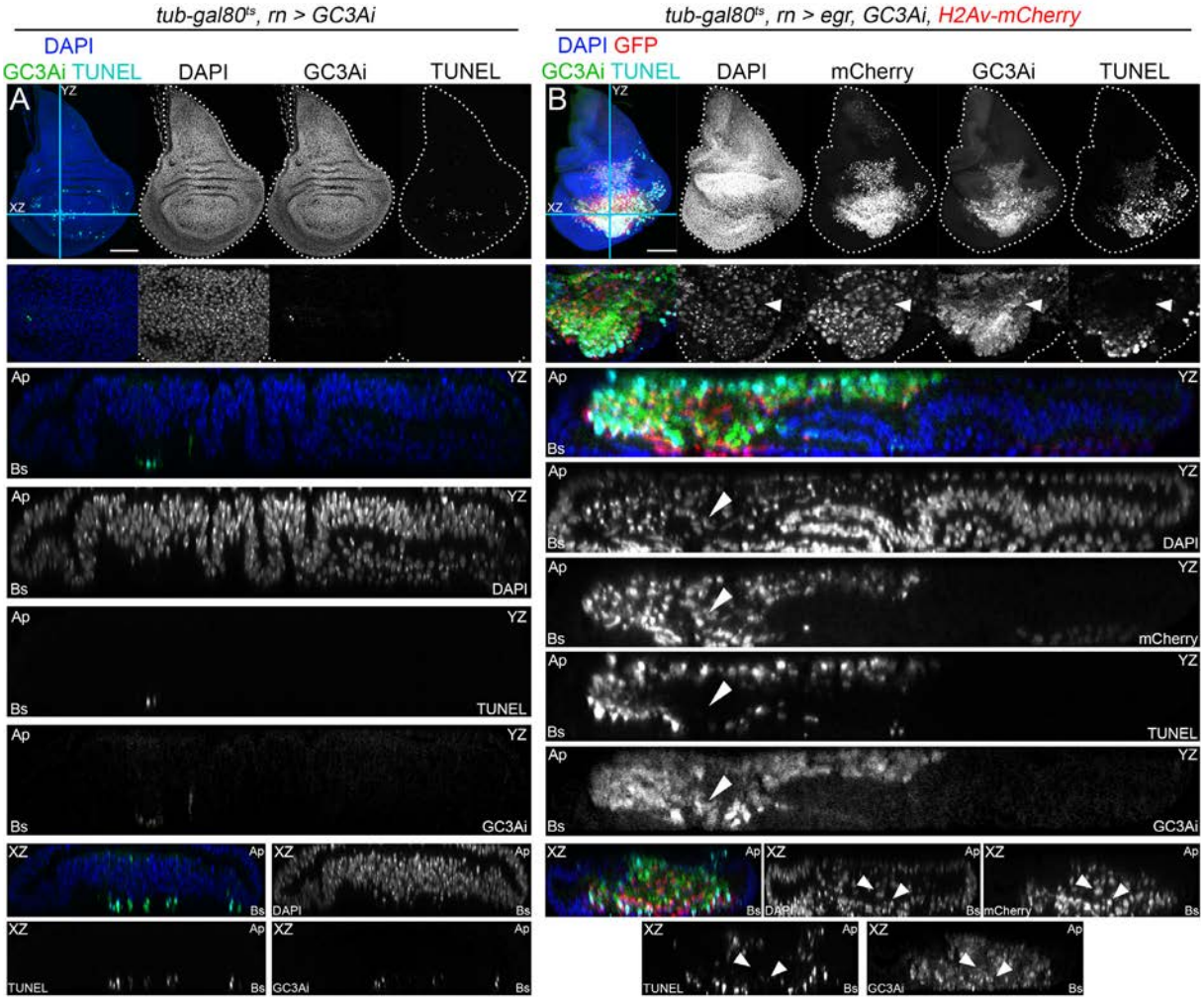

Figure 59. Big nuclei cells are not dying despite showing caspase activity. A and B) Early third instar wing discs of the indicated genotype stained for GFP (red or white, B), caspase sensor GC3Ai (green or white), TUNEL (cyan or white), and DAPI (blue or white). Upper panels show a Z-projection of the full disc. Magnifications of single apical and basal planes of the pouch are shown in middle panels. Orthogonal projections of YZ and XZ planes are shown in lower panels. The apical (Ap) and basal (Bs) planes of the projection are indicated. Arrowheads point to big nuclei cells positive for caspase activity and negative for TUNEL. Wing disc contours are labelled by a white line. Scale bar: 50 µm.

Big nuclei cells are senescent

Senescent cells are cells that enter a permanent and stable cell cycle arrest upon different damage or stress stimuli and do not respond to mitogenic or apoptotic signals. Moreover, these cells are highly metabolically active and secret a complex mix of molecules, known as the Senescence-Associated Secretory Phenotype (SASP), which affect the nearby tissue (González-Gualda et al., 2021). Different stimuli induce different types of senescence, making the phenotype associated to senescence highly heterogeneous and variable. This makes it hard to establish universal markers to identify senescence. For this reason, it is required to characterize several markers to establish that a cell is senescent (Figure 60)(González-Gualda et al., 2021; Hernandez-Segura et al., 2018). The previous results show that upon *egr* induction a population of cell with an enlarged nuclei size appears and that these cells, despite presenting caspase activity, are not dying. Remarkably, these are characteristics of senescent cells (Childs et al., 2014; Funayama & Ishikawa, 2007; Soto-Gamez et al., 2019). These results point towards the possibility that these cells could be senescent.

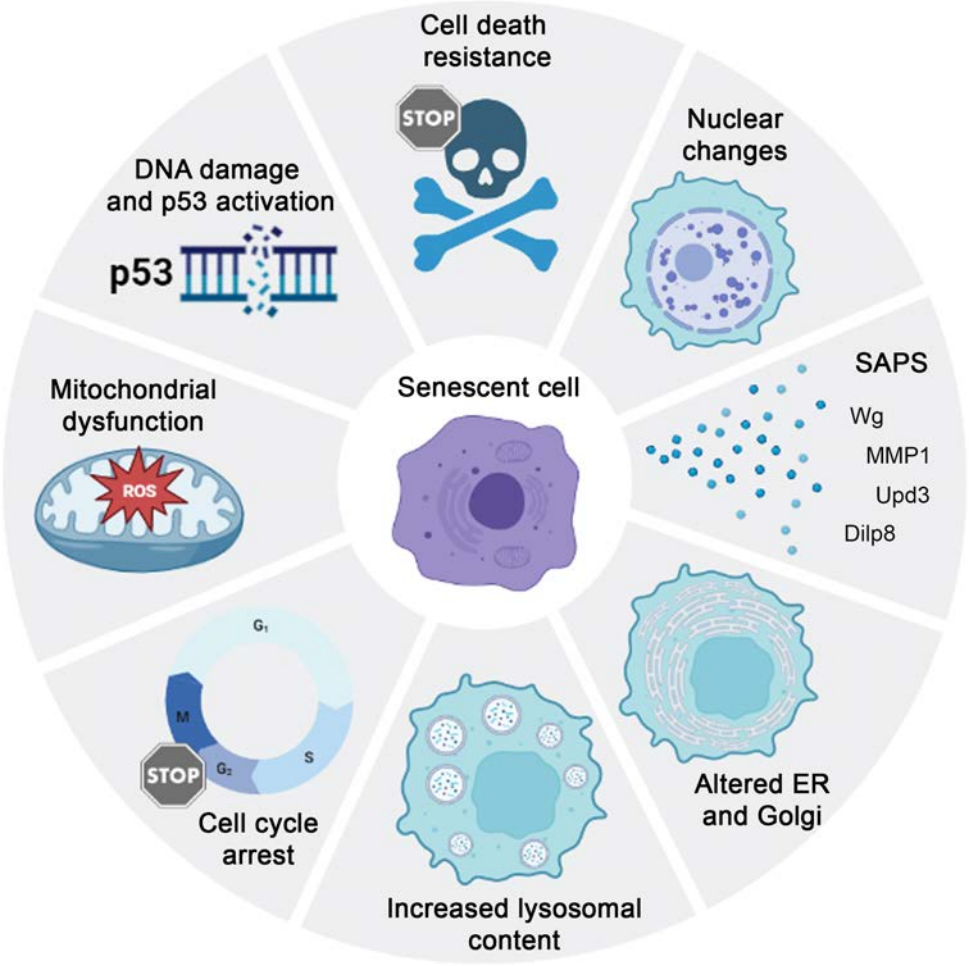

Figure 60. The hallmarks of senescence. Cartoon depicting some of the typical characteristics of senescent cells.

Interestingly, in recent years it has been proposed that senescent cells, that usually has been associated with ageing and age-related diseases (Calcinotto et al., 2019; Muñoz-Espín & Serrano, 2014), are present in the damaged tissue and that they could play a positive role in the regeneration process (reviewed in Antelo-Iglesias et al., 2021; Wilkinson & Hardman, 2020). In fact, it seems that senescent cells promote the closure of the wound in mice damage skin (Demaria et al., 2014), positively regulates the regeneration of the fin in zebrafish (Da Silva-Álvarez et al., 2020) or the limb in axolotls (Q. Yu et al., 2022; Yun et al., 2015). This reinforces the idea that the big nuclei population that we observe in the regenerative disc could be senescent.

It is the aim of this section to check different senescence-associated markers to test whether the big nuclei population is indeed senescent.

Big nuclei cells are arrested in G2

One of the most important characteristics of senescent cells is the cell cycle arrest (Gire & Dulic, 2015; Kumari & Jat, 2021). Thus, to determine whether these cells were arrested or not, we decided to monitor their mitotic activity, by labelling the phosphorylation of histone 3

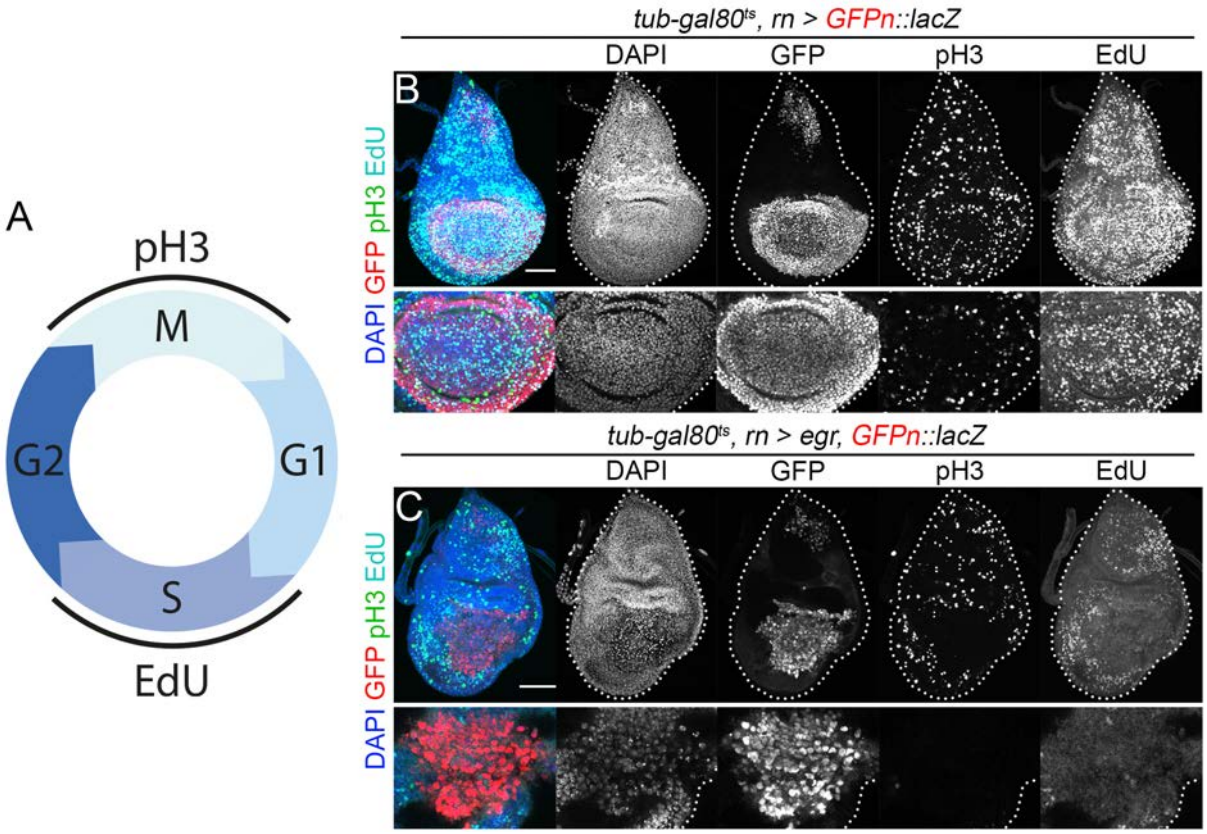

Figure 61. Big nuclei cells do not proliferate. A) Cartoon showing the cell cycle phase labelled by pH3 and EdU. **B and C)** Early third instar wing discs of the indicated genotype stained for GFP (red or white), pH3 (green or white), EdU (cyan or white), and DAPI (blue or white). Wing disc contours are labelled by a white line. Higher magnification of the wing pouch is shown in lower panels. Scale bar: 50 µm.

(pH3), event that occurs during mitosis (M), and their capacity to undergo through S phase by monitoring EdU (5-ethynyl-2'-deoxyuridine) incorporation in the DNA, which will occur during active DNA synthesis in S phase (Figure 61A). While in control discs we could observe EdU- and pH3-positive cells all over the disc, in *egr*-expressing discs we could not observe neither EdU- nor pH3-positive cells in the wing pouch (compare Figures 61B and C). Remarkably, when we focused on the big nuclei population, we observed that these cells were negative for both, EdU and pH3 (Figure 61B, magnification). Therefore, the fact that they do not present neither M nor S markers suggest that they are not proliferating.

Since the big nuclei cells seemed to be stalled in the cell cycle, we wondered at which stage they were arrested. Traditionally, the cell cycle arrest was thought to happen at G1 in mammals. However, in the past years, different reports have shown an increased relevance of G2 arrest in senescence (Gire & Dulic, 2015; Kumari & Jat, 2021) not just in mammals, but also in *Drosophila*. Recent reports have shown the presence of cells stalled in G2 upon damage

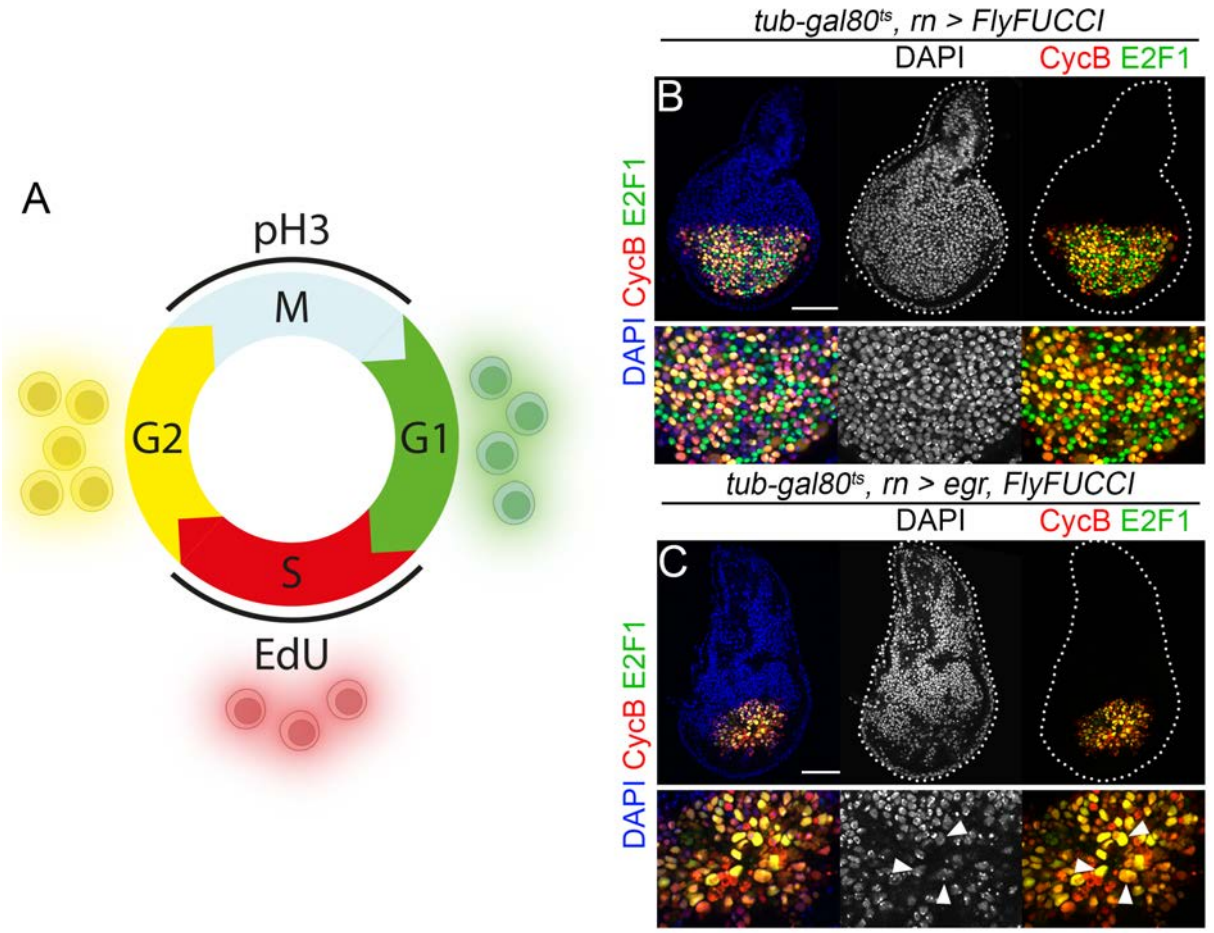

Figure 62. Big nuclei cells are arrested at G2. A) Cartoon depicting the functioning of FlyFUCCI system. **B and C)** Early third instar wing discs of the indicated genotype stained for CycB-RFP (CycB, red), E2F1-EGFP (E2F1, green), and DAPI (blue or white). Wing disc contours are labelled by a white line. Higher magnification of the wing pouch is shown in lower panels. Arrowheads point to big nuclei cells arrested at G2. Scale bar: 50 µm.

(Cosolo et al., 2019; Ruiz-Losada et al., 2022) and the presence of senescent cells arrested in G2 in CIN tumours (Joy et al., 2021). To test whether our cell population was arrested at G1 or G2 we used the FlyFUCCI system, a technique developed by Dr Edgar's laboratory that allows us to differentiate between the different stages of the cell cycle. This technique is based on fluorochrome-tagged degrons from Cyclin B (RFP) and E2F1 (GFP) that are degraded at the end of mitosis and at the onset of the S phase, respectively. Thus, when a cell presents GFP signal it means that it is in G1; if it presents RFP, it is in the S phase; and, when it presents both (GFP and RFP) it is in G2 (Figure 62A)(Zielke et al., 2014). While in control discs we could observe cells in all phases of the cycle (Figure 62B), when we focused on the big nuclei population we could see that most of the cells were arrested in G2 (Figure 62C). Altogether, these results indicated that our big nuclei population is arrested in G2. FACS analysis is required to confirm the G2 arrest, but our results point towards the same direction as the recent reports previously mentioned.

Big nuclei cells secrete molecules from the SASP

The senescence-associated secretory phenotype, or SASP, is the secretion of a complex mix of molecules by the senescent cells. Among these molecules, we can find pro-inflammatory cytokines and chemokines, growth factors, angiogenic factors, and matrix metalloproteinases (MMPs). It should be noted that the SASP composition varies depending on the senescence stimulus, the cell type or the duration of senescence (Coppé et al., 2010; González-Gualda et al., 2021; Hernandez-Segura et al., 2018). For example, senescent cells in regenerative tissue have been shown to secrete several MMPs and growth factors (Demaria et al., 2014; Jun & Lau, 2010) while age-associated or therapy-induced senescent cells are mainly associated with inflammatory factors (Demaria et al., 2017). What is clear is that senescent cells contribute to either tissue homeostasis or dysfunction in nearby tissue through the SASP molecules. Despite the importance of the SASP in senescent, it is too interspecific and heterogeneous to be used as a senescent marker by itself. Just a few factors are shared between the different senescence types, making a universal SASP signature difficult to establish (González-Gualda et al., 2021; Hernandez-Segura et al., 2018).

It should be noted that SASP is not exclusive to mammals. In fact, *Drosophila* senescent cells also produce SASP molecules. Indeed, it has been reported that *Drosophila* senescent cells produce the pro-inflammatory molecule Upd (Nakamura et al., 2014; Romão et al., 2021), the *Drosophila* homologue of interleukin-6 (IL-6)(Harrison et al., 1998), the ECM degrading en-

zymes MMP1 (Joy et al., 2021; Nakamura et al., 2014), the pro-mitotic molecule Wg (Dekanty et al., 2012; Joy et al., 2021) and Dilp8 (Joy et al., 2021; Romão et al., 2021), among others. Thus, we tested the expression of some of these molecules in our big nuclei population. First, we tested the expression of Dilp8, a peptide that has been reported to be expressed upon damage and delay development (Colombani et al., 2012; Garelli et al., 2015; Katsuyama et al., 2015). As expected, when we assessed Dilp8 expression in *egr*-expressing discs, we saw high levels of expression in the big nuclei population (Figure 63). Similar results were obtained when we analysed MMP1 (assessed by an MMP1-GFP reporter)(Q. Wang et al., 2010) and Wg expression (Figures 64). Hence, these results indicate that big nuclei cells produce molecules from the SASP, suggesting once again that they could be senescent. These observations are consistent with the fact that in *Drosophila*, the main pathway regulating senescence and the SASP is JNK (Ito & Igaki, 2016; Joy et al., 2021) and that our big nuclei population present a high activation of JNK as a consequence of Egr overexpression. It is also consistent with previous

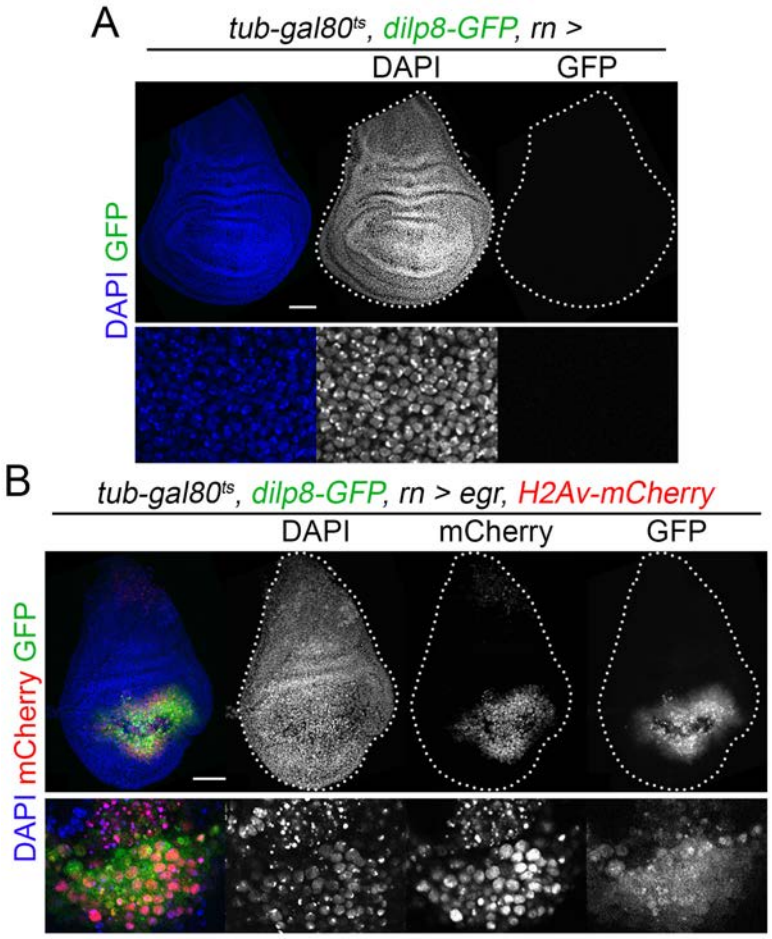

Figure 63. Big nuclei cells produce Dilp8. A and B) Early third instar wing discs of the indicated genotype bearing the *dilp8-GFP* reporter and stained for GFP (green or white), H2Av-mCherry (red or white, B), and DAPI (blue or white). Wing disc contours are labelled by a white line. Higher magnification of the wing pouch is shown in lower panels. Scale bar: 50 µm.

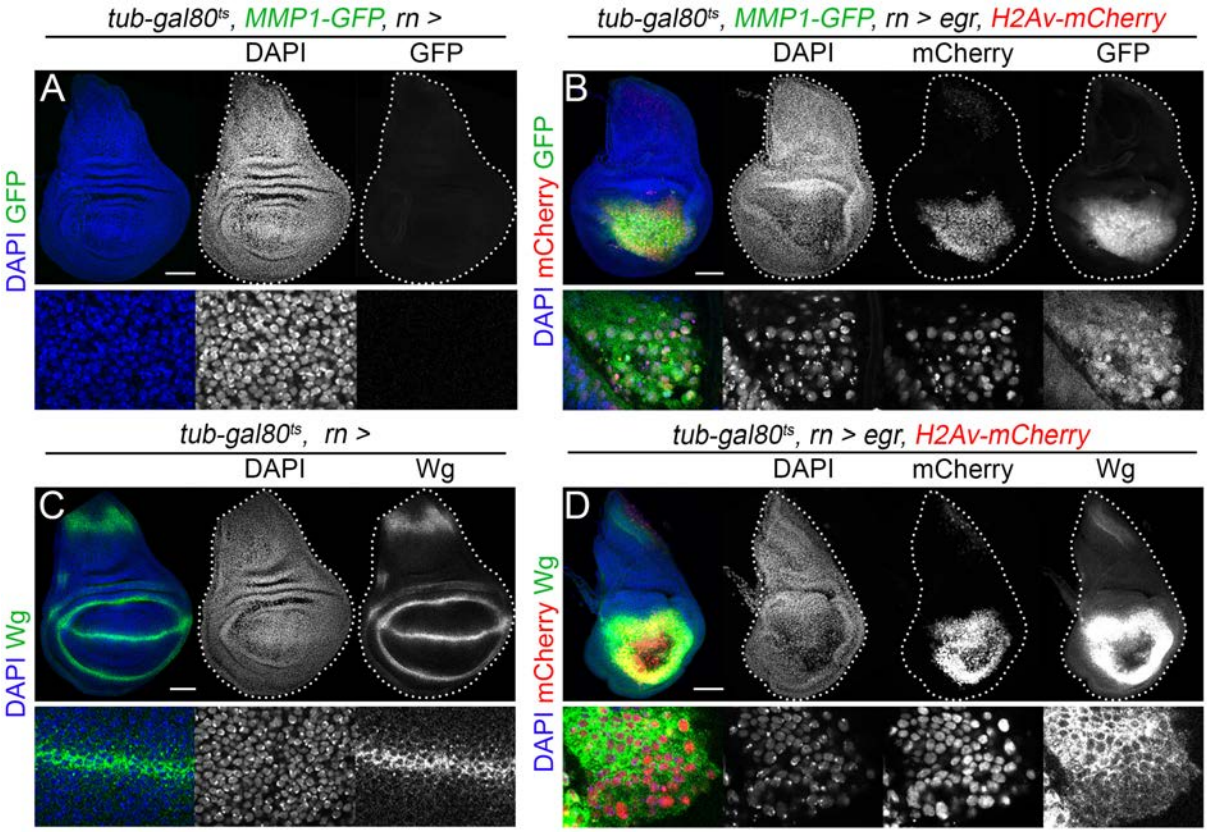

Figure 64. Big nuclei cells express molecules from the SASP. A and B) Early third instar wing discs of the indicated genotype bearing the *MMP1-GFP* reporter and stained for GFP (green or white), H2Av-mCherry (red or white, B), and DAPI (blue or white). **C and D)** Early third instar wing discs of the indicated genotype and stained for Wg (green or white), H2Av-mCherry (red or white, D), and DAPI (blue or white). Wing disc contours are labelled by a white line. Higher magnification of the wing pouch is shown in lower panels. Scale bar: 50 µm.

reports showing that, upon different damage inputs, JNK is trigger and induces the production of these molecules (Katsuyama et al., 2015; McClure et al., 2008; Ryoo et al., 2004). Therefore, it would be interesting to see whether these molecules would be secreted by cells with similar characteristics to our cell population in other damage models.

In addition to SASP, senescent cells can communicate with nearby tissue through other mechanisms such as the release of ROS (Kuilman & Peeper, 2009), cytoplasmic bridges (Biran et al., 2015) or extracellular vesicles, such as exosomes (Takasugi et al., 2017). Indeed, in senescent cells, the biogenesis of exosomes and their release is enhanced (Lehmann et al., 2008; Takasugi et al., 2017). Thus, we decided to check the state of the exosome compartment in our cell population using the exosome reporter CD63-mCherry (Fan et al., 2020). We could observe that, while control discs presented a perinuclear expression with some stronger localized punctate expression (Figure 65A), in the big nuclei population of our damaged discs, the perinuclear pattern was lost and, in many cases, higher expression levels were detected (Figure 65B). These results show a clear alteration of the exosomes and suggest an increase

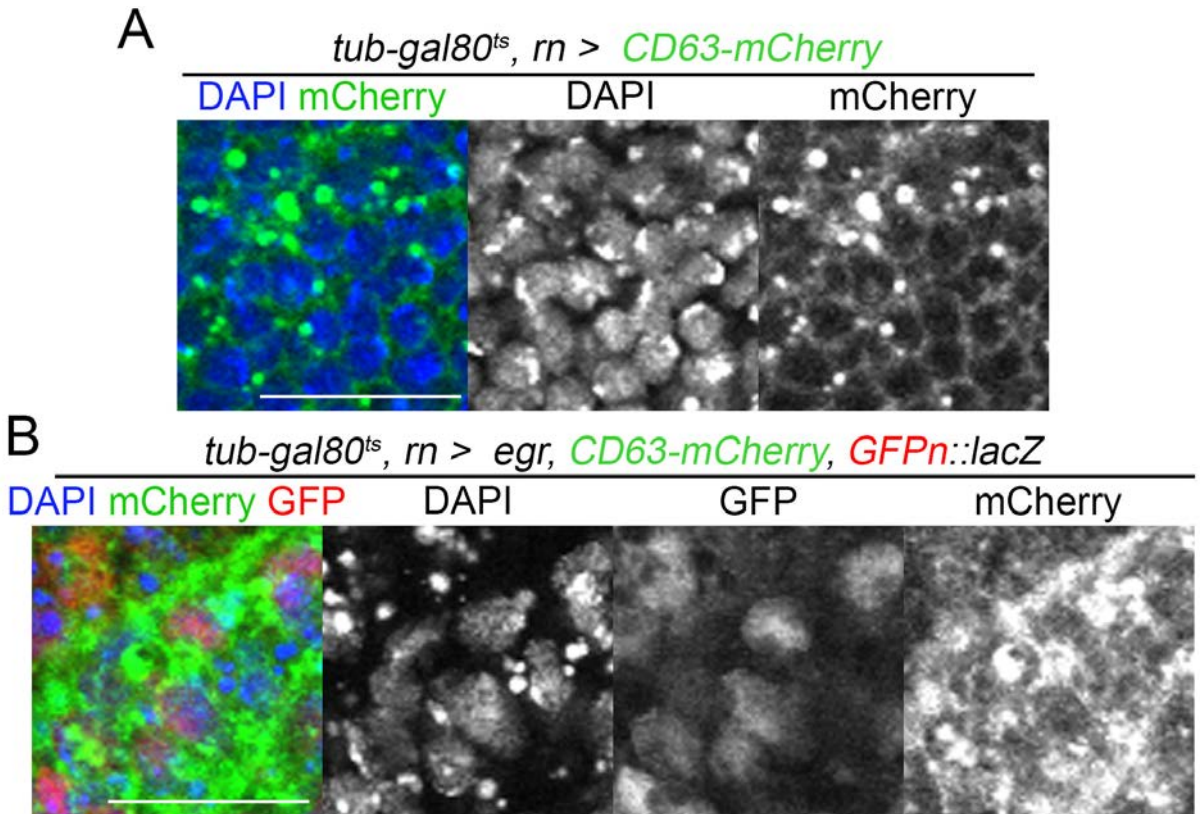

Figure 65. Big nuclei cells present altered exosomes. A and B) Magnification of non-damaged (*rn >*) and damaged (*rn > egr*) discs bearing the exosome reporter *CD63-mCherry*. Discs were stained for mCherry (green or white), GFP (red or white, B), and DAPI (blue or white). Scale bar: 20 µm.

in the exosome biomass although further research would be required to know whether this is due to an increase in their biogenesis. What is clear is that most probably these exosomes are contributing to the observed SASP and to the signalling to the nearby tissue. Altogether, our results show that the big nuclei population present an increased release of molecules characteristic of the SASP and an altered exosomal network, a key characteristic of senescent cells.

Big nuclei cells present an abnormal Endoplasmic Reticulum and Golgi apparatus

Senescent cells present an increased protein synthesis due to the SASP. Moreover, senescent cells present high levels of ROS, which oxidizes proteins and induces their misfolding. The sum of these two factors leads to the accumulation of misfolded protein aggregates and proteotoxic stress (Höhn et al., 2017; Pluquet et al., 2015). To cope with this situation, the Endoplasmic Reticulum (ER) initiates the unfolded protein response (UPR), leading to a reduction in protein synthesis, enlargement and shape change of the ER, and export of misfolded proteins (Cormenier et al., 2018; Druelle et al., 2016). Besides, due to the SASP, there is an increase not only in protein production, but also in protein secretion. Indeed, it has been reported that the Golgi apparatus, the central organelle of the secretory pathway, presents an enlarged and expanded morphology in senescent cells (Despres et al., 2019).

To address the state of the ER and Golgi apparatus in the big nuclei population, we performed imaging analysis using markers specific for both organelles. First, we used the ER membrane marker tdTomato–Sec61β (Summerville et al., 2016) to assess the possible changes in the ER morphology. While in control we could observe a clear perinuclear labelling of the ER (Figure 66A), in the big nuclei population we detected a loss of perinuclear labelling and a general decrease of the intensity (Figure 66B), indicating anomalies in the ER. Then, we used the TagRFP-T-tagged galactosyltransferase reporter (GalT-RFP) to label the Golgi apparatus (Zhou et al., 2014). Similarly to the ER, the Golgi apparatus marker in control discs presented a perinuclear expression but with some stronger localized punctate expression (Figure 67A). By contrast, the perinuclear expression was lost in the big nuclei population and, the localized stronger expression was no longer observed in the punctate pattern of the controls but rather

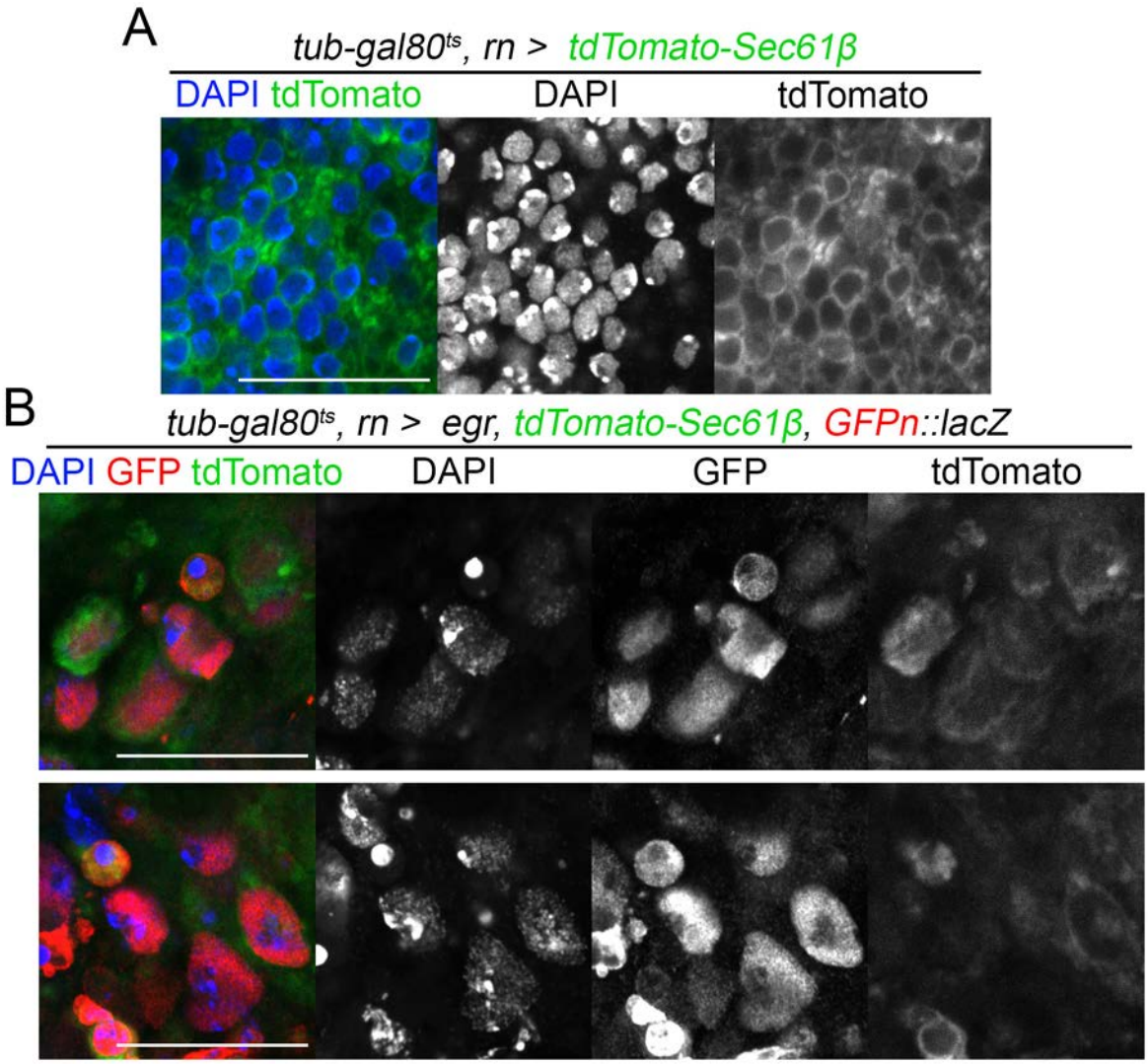

Figure 66. Big nuclei cells present an altered endoplasmic reticulum. A and B) 63X magnification of non-damaged (*rn >*) and damaged (*rn > egr*) discs bearing the endoplasmic reticulum reporter *tdTomato-Sec61β*. Discs were stained for mCherry (green or white), GFP (red or white, B), and DAPI (blue or white). Scale bar: 20 µm.

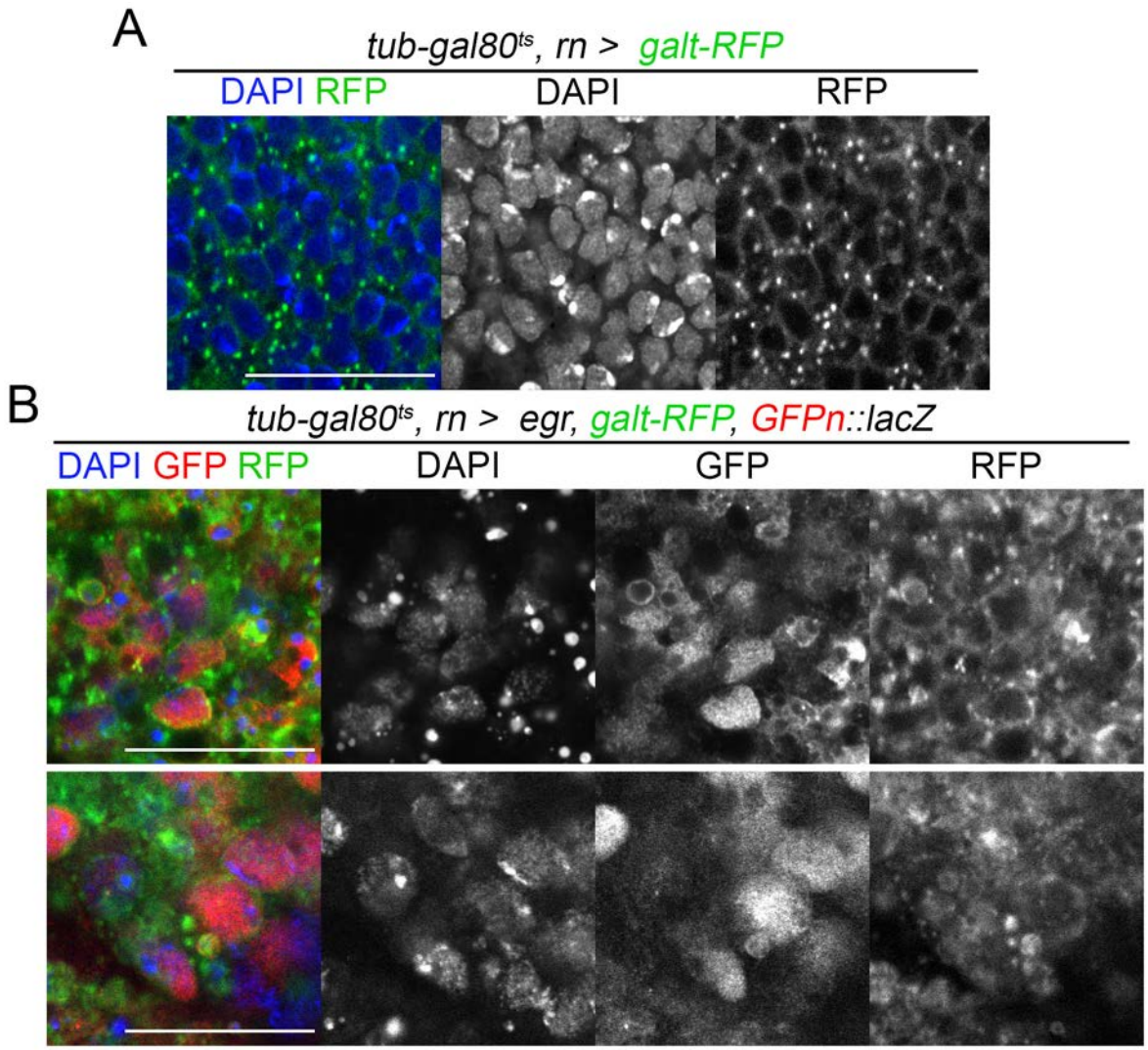

Figure 67. Big nuclei cells present an altered Golgi apparatus. A and B) 63X magnification of non-damaged (*rn >*) and damaged (*rn > egr*) discs bearing the Golgi reporter *galt-RFP*. Discs were stained for RFP (green or white), GFP (red or white, B), and DAPI (blue or white). Scale bar: 20 µm.

in aggregates (compare RFP expression Figure 67A and B). This result suggests an alteration of the Golgi apparatus in the big nuclei cells. Thus, our results indicate that both, the ER and the Golgi apparatus present structural abnormalities most probably due to the stress induced by the enhanced protein synthesis and secretion required by the SASP, again reinforcing the hypothesis that these big nuclei cells are senescent.

Big nuclei cells present an increased senescence-associated beta-galactosidase activity

The senescent state is characterized by an increase in the lysosomal content and its proteins (Cho & Hwang, 2012). One of the lysosomal enzymes that is up-regulated in senescent cells is the senescence-associated beta-galactosidase (SA-βgal) enzyme. The measurement of

the activity of this enzyme is one of the most used approaches to assess the increase of the lysosomal content (Dimri et al., 1995; Kurz et al., 2000) and it is a well-established marker for senescence. In fact, the increase in SA-βgal activity has been proven useful in detecting senescent cells not just in mammalians but also in *Drosophila* (Joy et al., 2021; Nakamura et al., 2014). As expected, when we analysed our big nuclei population, we could see that these cells presented SA-βgal activity (Figure 68B). This result indicate that our cells present an increased lysosomal content and point towards the direction that these cells are senescent. However, we have to take into account that increased SA-βgal activity is not exclusive of senescent cells (Kopp et al., 2007). Therefore, other methodologies to assess the lysosomes content increase such as the Lysotraker probes, or the analysis of other enhanced lysosomal proteins, such as Lysosomal-associated membrane protein 1 (Lamp1)(Barral et al., 2022), should be considered to further confirm this result.

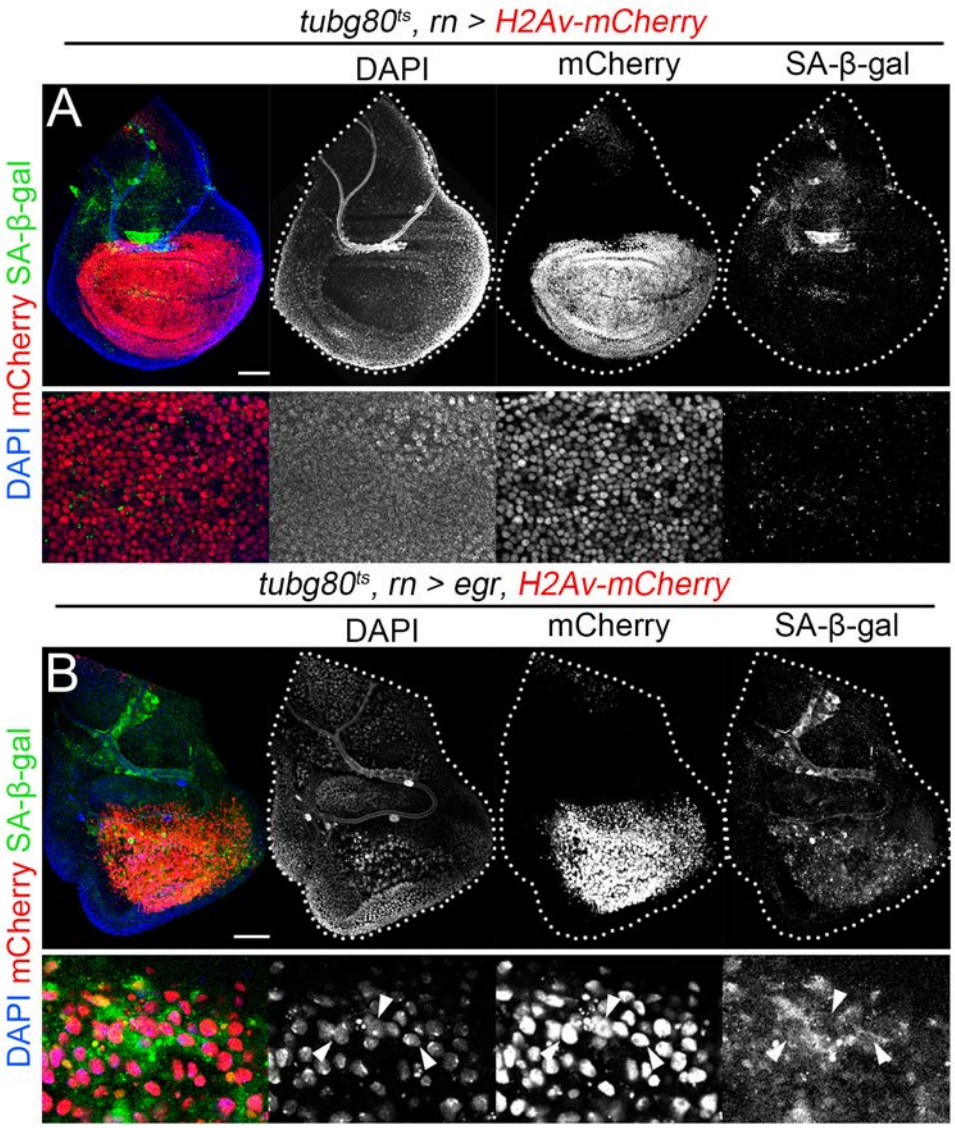

Figure 68. Big nuclei cells present SA-β-gal activity. A and B) Early third instar wing discs of the indicated genotype stained for H2Av-mCherry (red or white), SA-β-gal (green or white) and DAPI (blue or white). Wing disc contours are labelled by a white line. Higher magnification of the wing pouch is shown in lower panels. Arrowheads point to big nuclei cells presenting SA-β-gal activity. Scale bar: 50 µm.

Big nuclei cells present accumulation of altered mitochondria

A characteristic of senescent cells is the accumulation of mitochondria (reviewed in Miwa et al., 2022; Vasileiou et al., 2019). The main reason for this is that in senescent cells mitophagy is reduced, leading to the accumulation of old dysfunctional mitochondria (Korolchuk et al., 2017). Moreover, the mitochondrial dynamics are altered. Senescent cells present an increased fusion and reduced fission, which result in elongated and branched mitochondria that hinder mitophagy (Dalle Pezze et al., 2014; Lee et al., 2007; Yoon et al., 2006). However, these mitochondria present a decreased membrane potential leading to an increased production of ROS (Passos et al., 2007), electron transport chain defects (Ziegler et al., 2015), dysregulated mitochondrial calcium homeostasis (Wiel et al., 2014) and leakage of mitochondrial enzymes (Studencka & Schaber, 2017), among other things. Indeed, mitochondrial ROS can aggravate cellular senescence by enhancing the DNA damage and the DNA damage response signalling pathway (DDR)(Passos et al., 2010). Remarkably, alteration of the mitochondrial homeostasis can induce by itself the establishment of cellular senescence (Wiley et al., 2016). All these facts point to mitochondria as a key element for senescence.

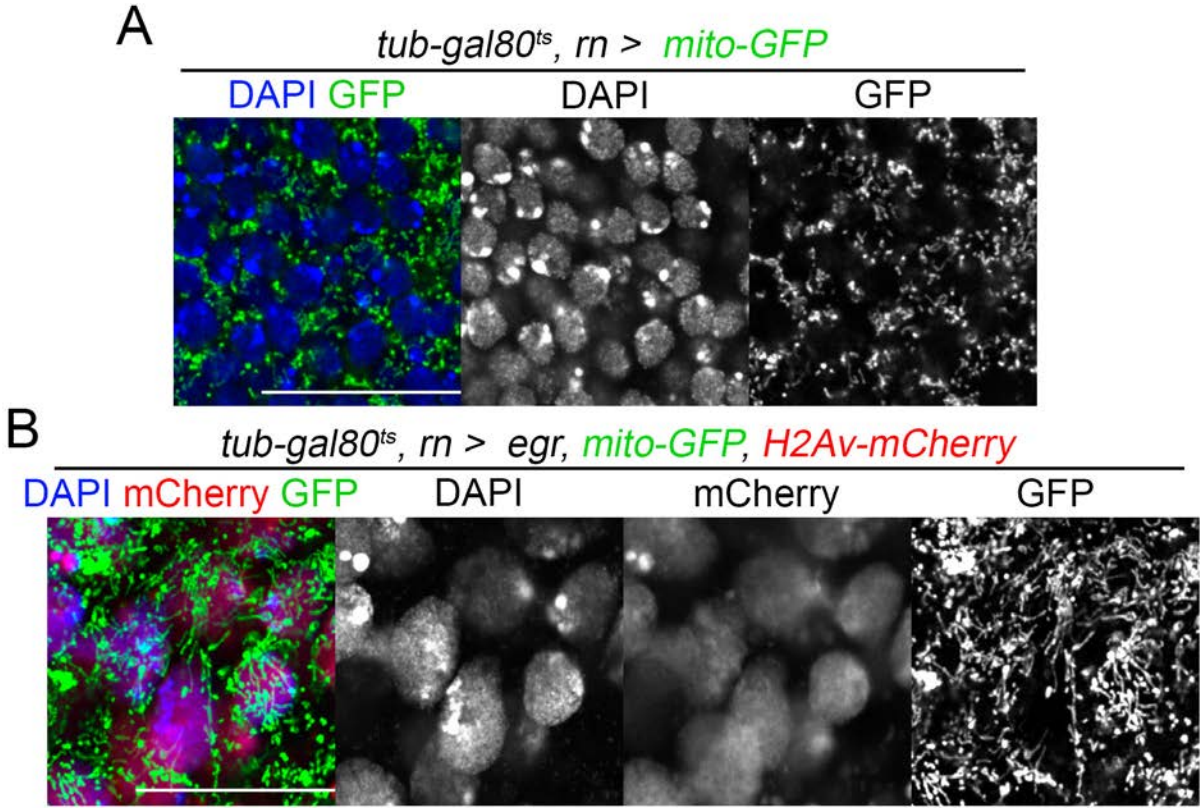

Figure 69. Big nuclei cells present altered mitochondria. A and B) 63X magnification of non-damaged (*rn >*) and damaged (*rn > egr*) discs bearing the mitochondrial reporter *mito-GFP*. Discs were stained for GFP (green or white), H2Av-mCherry (red or white, B), and DAPI (blue or white). Scale bar: 20 µm.

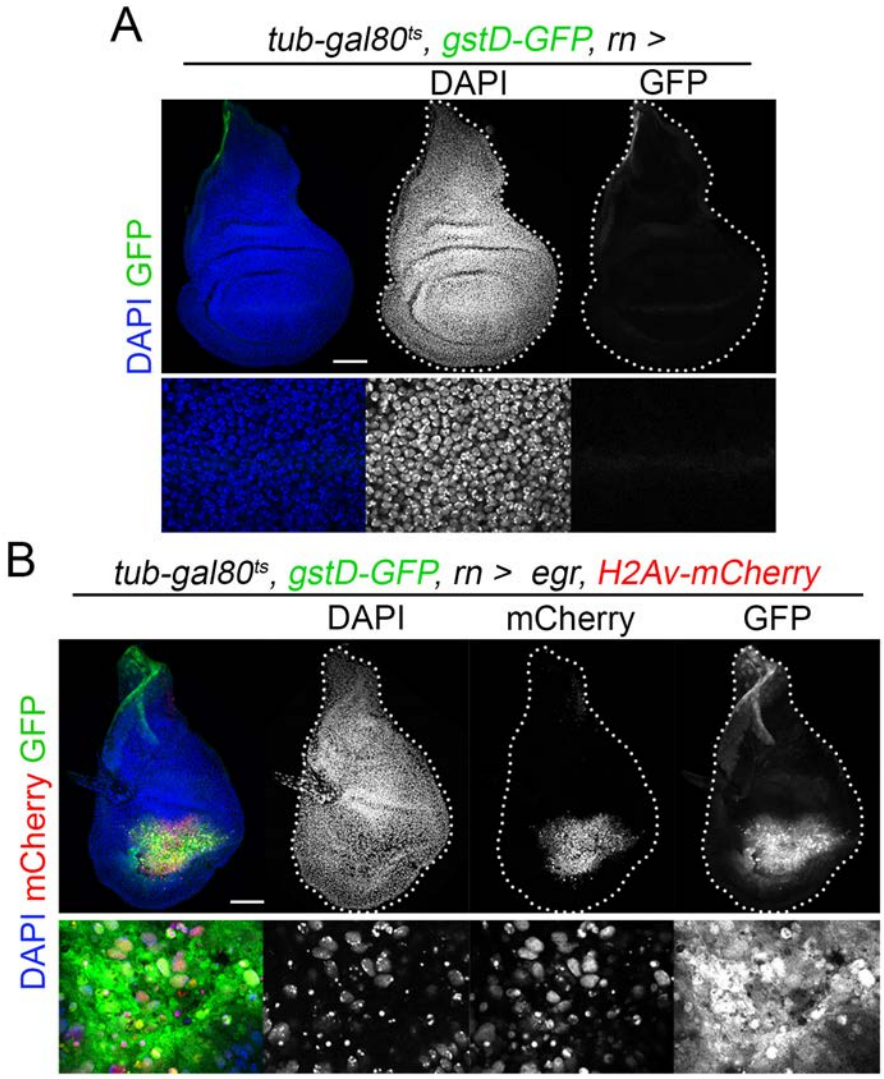

Figure 70. Big nuclei cells present high levels of ROS. A and B) Early third instar wing discs of the indicated genotype bearing the ROS reporter *gstD-GFP.* Discs were stained for GFP (green or white), H2Av-mCherry (red or white, B), and DAPI (blue or white). Wing disc contours are labelled by a white line. Higher magnification of the wing pouch is shown in lower panels. Scale bar: 50 µm.

To study the state of mitochondria in our cell population we used the *mito-GFP* reporter to label them. Upon damage, we could detect an increase in the mitochondrial biomass in the big nuclei population when compared with controls (Figures 69A and B). Moreover, a clear elongated and branched mitochondria structure could be detected along with an increase in the reticular mitochondrial network (Figure 69B), pointing to a possible alteration in the mitochondrial dynamics. Besides, the increase in mitochondrial biomass could be an indicator that mitophagy is failing too. All these results point to the loss of mitochondrial homeostasis and, therefore, a possible loss of its membrane potential and an increase in ROS production. Consistently, when we analysed the presence of ROS in the big nuclei population by using the *gstD-GFP* reporter, a reporter that induces GFP expression upon oxidative stress (Sykiotis &

Bohmann, 2008), we detected a strong GFP expression in big nuclei cells (Figure 70). Altogether, these results suggest that in the big nuclei population mitochondrial dynamics and mitophagy are altered, leading to the accumulation of unhealthy mitochondria and boosting the production of ROS, as happens in senescent cells.

Big nuclei cells present nuclear changes

A common marker of senescent is the loss of LaminB1, an essential protein of the nuclear lamina (Freund et al., 2012; Shimi et al., 2011). The destabilization of the nuclear lamina leads to other nuclear changes such as the loss of condensation of heterochromatin or the leaking of the DNA to the cytoplasm (Adams et al., 2013; Cruickshanks et al., 2013). It has been proposed that to counterbalance the general decondensation of constitutive heterochromatin, in an effort to silence proliferation genes, the cell rearranges the chromatin and forms dense structures known as senescence-associated heterochromatin foci (SAHFs). SAHFs can be recognized by intense DAPI nuclear foci enriched in repressive epigenetic marks (Chandra et al., 2012; Narita et al., 2003) and heterochromatin-forming proteins, such as heterochromatin protein 1 (HP1)(Narita et al., 2003; Zhang et al., 2005). It should be noted that while the loss of LaminB1 is a common marker of senescence, the presence of SAHFs is not accepted as a universal marker.

First, we analysed the expression of Lamin in the big nuclei cell population. As expected, a complete or partial loss of Lamin expression was observed in our cell population (Figure 71B). In contrast, in control discs all cells presented an intact nuclear envelope (Figure 71A). Consistently, we could observe that the loss of Lamin went together with a loss of DNA condensation in the big nuclei population (assessed by the reduction of DAPI signalling; compare Figures 71C and D). Moreover, upon magnification of the nuclei of our cell population, denser DAPI areas could be detected, suggesting the presence of SAHFs (Figure 71D'). This was supported by a more homogeneous DAPI labelling in control nuclei (Figure 71C'). By contrast, when we analysed the expression of HP1-RFP in our cell population, we could not detect major differences with control discs (Figure 72), most probably due to the low magnification of our images. Altogether our results indicate that big nuclei cells present a reduction of Lamin and decondensation of the DNA, both characteristics of senescent cells. Although our results suggest the presence of SAHFs too, microscopy techniques that allow a higher resolution would be required to confirm their presence.

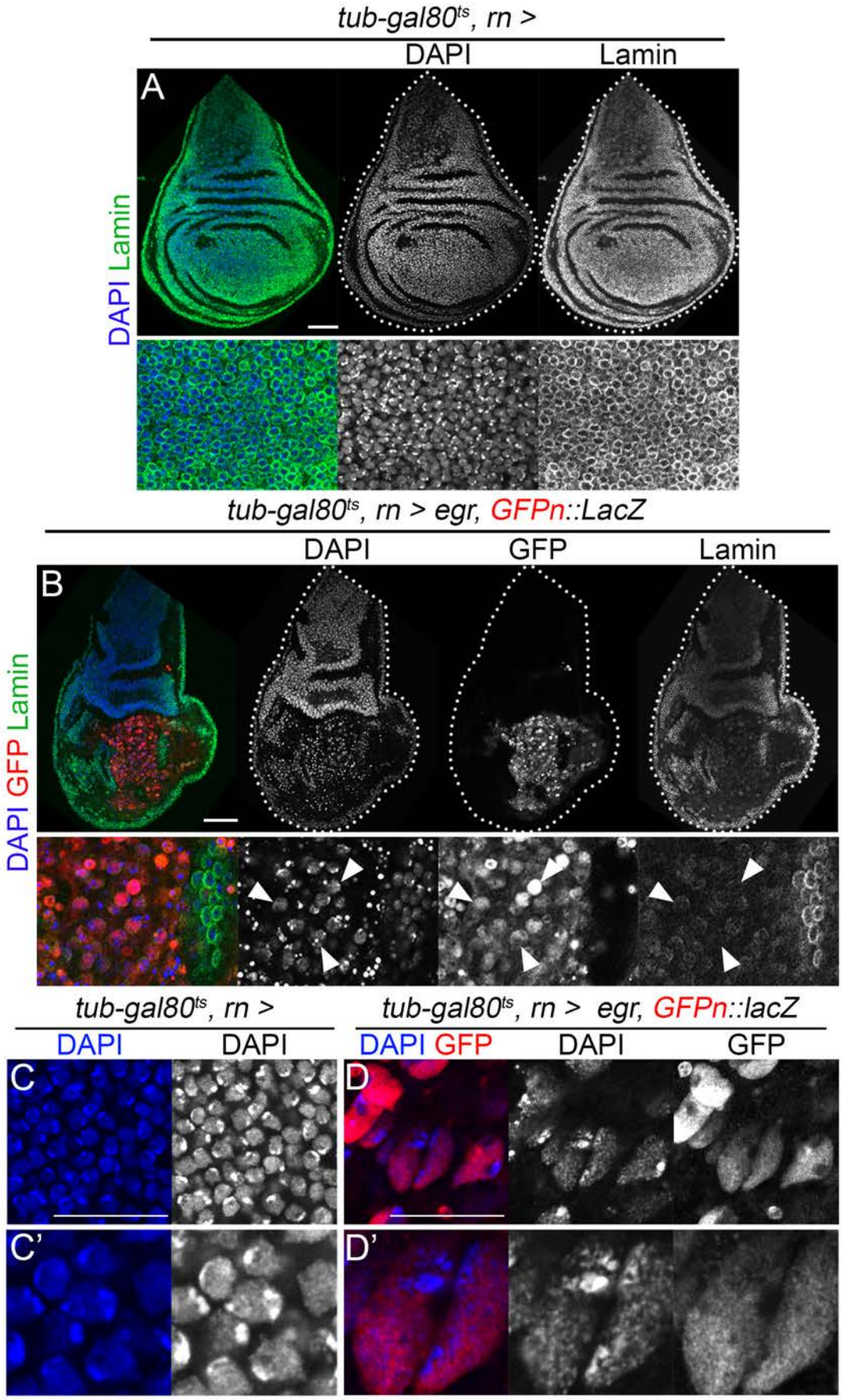

Figure 71. Big nuclei cells present nuclear changes. A and B) Early third instar wing discs of the indicated genotype and stained for Lamin (green or white), GFP (red or white, B), and DAPI (blue or white). Wing disc contours are labelled by a white line. Higher magnification of the wing pouch is shown in lower panels. Arrowheads point to big nuclei cells that show a partial or complete loss of the nuclear envelope. Scale bar: 50 µm. **C and D)** 63X magnification of non-damaged (*rn >*) and damaged (*rn > egr*) discs stained for GFP (red or white, D), and DAPI (blue or white). Scale bar: 20 µm. C' and D') Higher magnification from C and D.

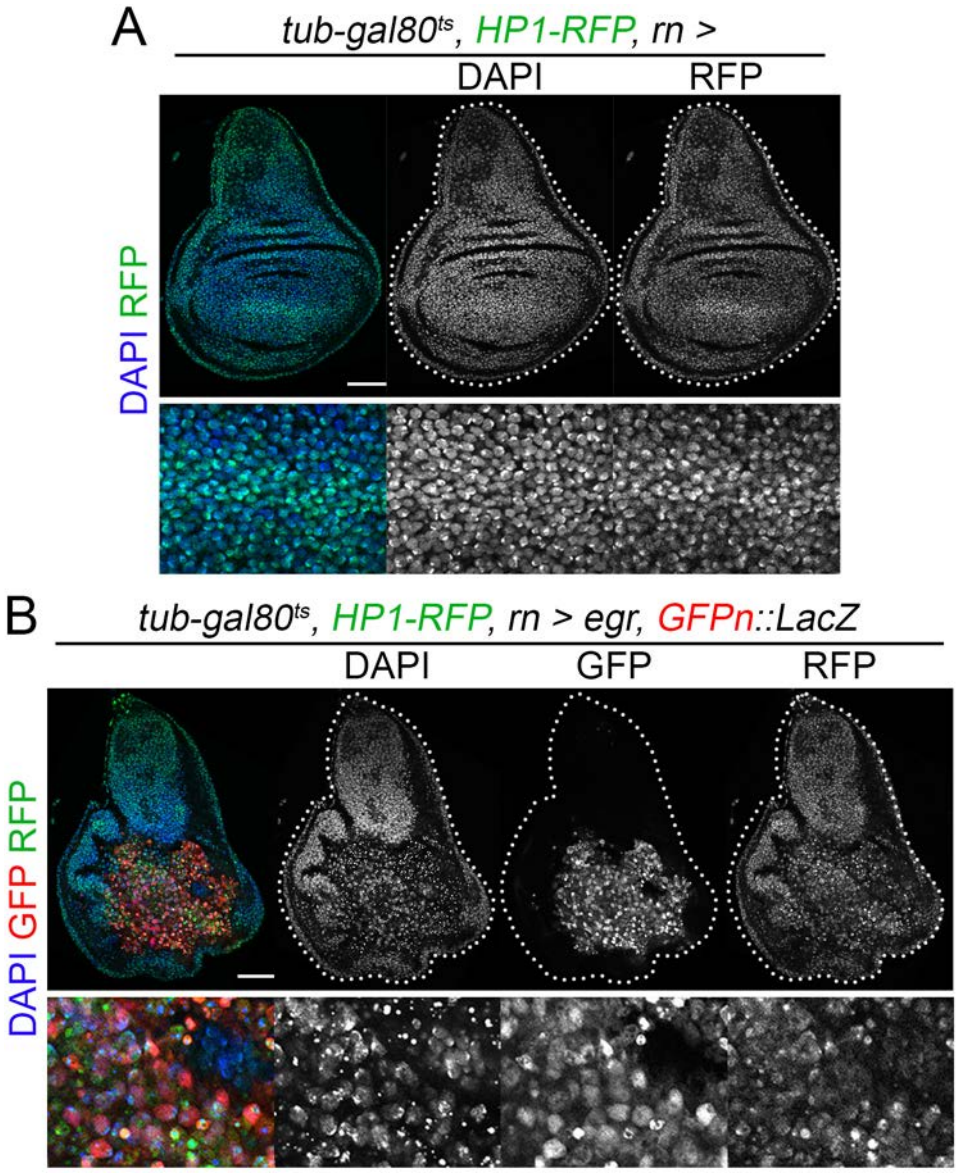

Figure 72. HP1 is not altered in big nuclei cells. A and B) Early third instar wing discs of the indicated genotype bearing the fusion protein HP1-RFP. Discs were stained for RFP (green or white), GFP (red or white, B), and DAPI (blue or white). Wing disc contours are labelled by a white line. Higher magnification of the wing pouch is shown in lower panels. Scale bar: 50 µm.

As mentioned above, senescence is a complex and highly heterogeneous cellular state that varies depending on the triggering stimuli. Therefore, it is required to characterize several markers to establish whether a cell is senescent or not. In this section, we have analysed several of these markers that have allowed us to conclude that the big nuclei cells present in *egr*-expressing discs are senescent. From these results two new questions arise: first, which pathways are implicated in the establishment of senescence and cell death resistance; and second, which is the role that senescent cells play in the regenerative tissue. In the following sections, we are going to show the steps we took to start to answer these questions.

G2 arrest does not rely on p53 and p21

In mammalians, the two main players in the establishment of the cell cycle arrest are p53, known as the 'Guardian of the genome', and p21, a Cyclin-dependent kinase inhibitor (CDKi). Thus, different stimuli lead to the activation of p51/p21 pathway, which arrest the cell cycle in G1 (Gire & Dulic, 2015; Kumari & Jat, 2021). Due to the relevance of these two proteins, we decided to check whether they were responsible for the establishment of senescence and cell cycle arrest in our cell population.

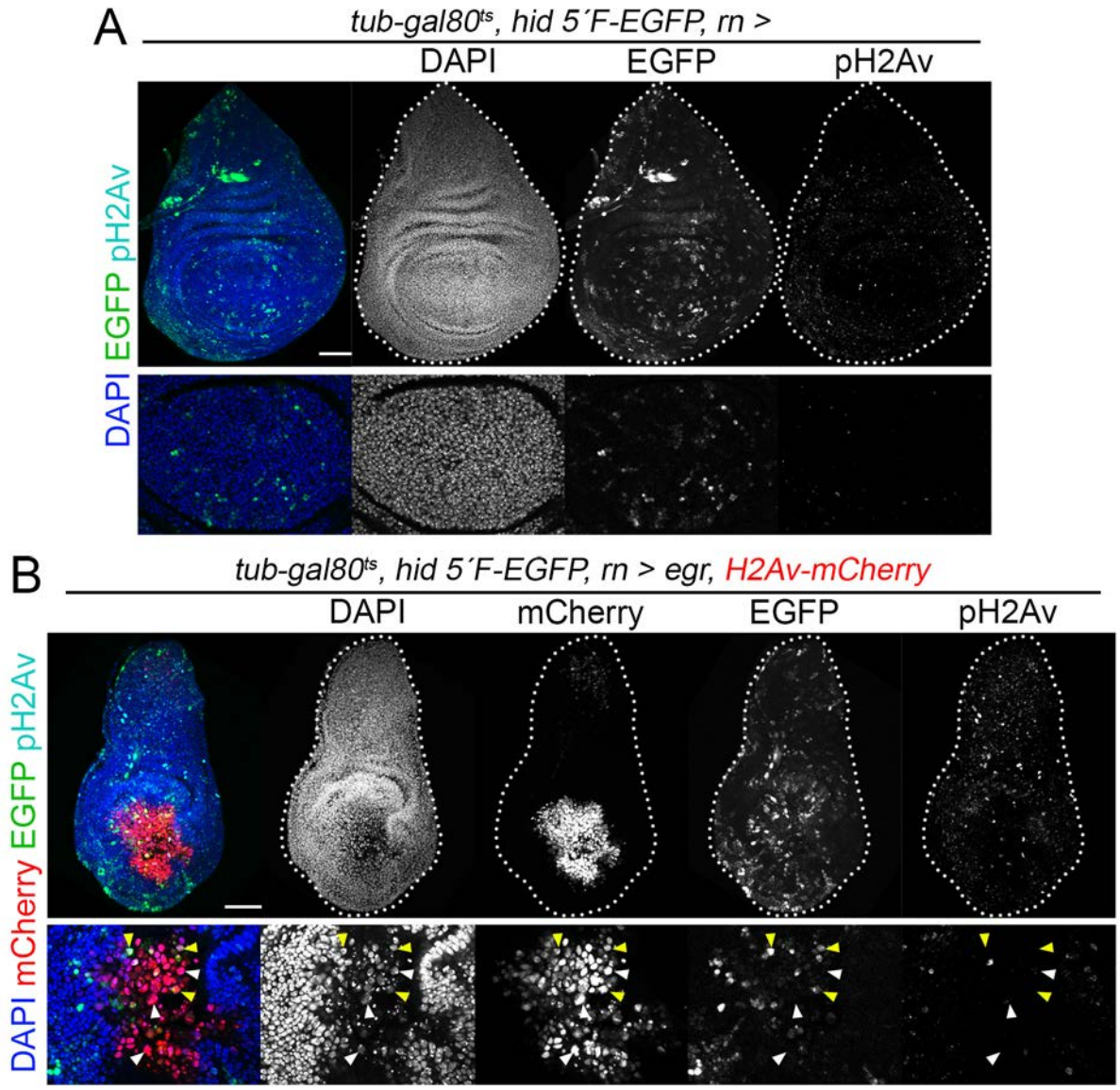

Figure 73. Senescent cells do not present p53 activity. A and B) Early third instar wing discs of the indicated genotype bearing the reporter of p53 activity *hid 5'F-RGFP*. Discs were stained for EGFP (green or white), H2Av-mCherry (red or white, B), pH2Av (cyan or white), and DAPI (blue or white). Wing disc contours are labelled by a white line. Higher magnification of the wing pouch is shown in lower panels. White arrowheads point to senescent cells that do not present p53 activity and yellow arrowheads to the ones that does. Scale bar: 50 µm.

First, we wanted to assess the activity of *Drosophila* ortholog of p53 (Dp53)(Ollmann et al., 2000) in our cells using the *hid 5´F-EGFP* reporter. This reporter consists of the *EGFP* sequence under the control of the *hid* promoter that contains binding sites for Dp53. Therefore, EGFP expression is only detected when there is p53 activity (Tanaka-Matakatsu et al., 2009). Random EGFP expression was detected in both control and *egr*-expressing discs at similar levels (Figure 73). Surprisingly, just a few random big nuclei cells showed p53 activity (Figure 73B, yellow arrows) while the majority of the big nuclei population did not (Figure 73B, white arrows). Consistently, we could not detect in the big nuclei cells neither the phosphorylation of H2Av (pH2Av; Figure 73B), a wildly used senescent marker associated with the DNA damage response (DDR) and the activation of p53 (Pospelova et al., 2009; Rodier et al., 2011), nor the

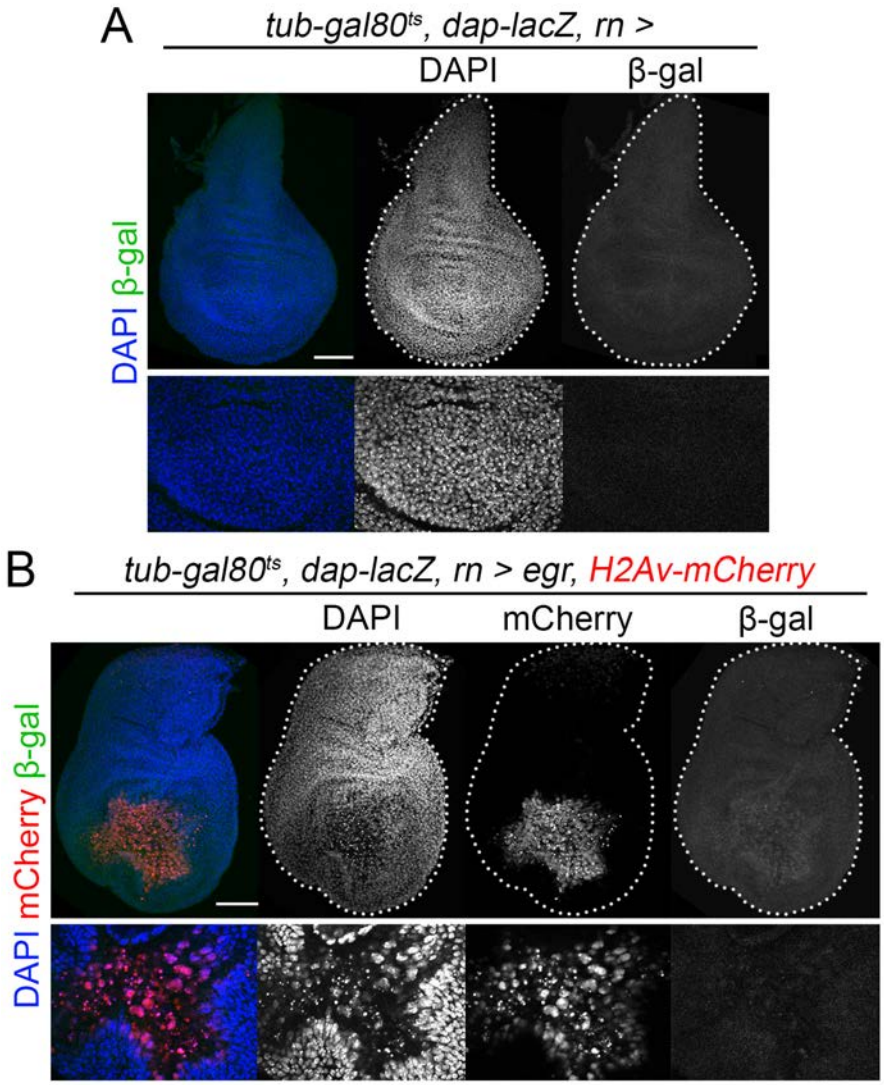

Figure 74. Senescent cells do not present dacapo expression. A and B) Early third instar wing discs of the indicated genotype bearing the *dap-lacZ* reporter. Discs were stained for anti-β-galactosidase (green or white), H2Av-mCherry (red or white, B), and DAPI (blue or white). Wing disc contours are labelled by a white line. Higher magnification of the wing pouch is shown in lower panels. Scale bar: 50 µm.

expression of the *Drosophila* p21 ortholog Dacapo (Dap; Figure 74B)(De Nooij et al., 1996; Lane et al., 1996), a CDKi that is a transcriptional target of p53 (El-Deiry et al., 1993). Altogether these results indicate that the cell cycle arrest is not mediated by the p53/p21 pathway. This is consistent with the fact that the cell cycle arrest that we detected occurs at G2 and not at the G1 phase, where p53/p21 induce the arrest.

The cell cycle regulates the ability of cells to die

Our previous data show that when we induce damage upon *egr* overexpression there is a group of cells that avoid apoptosis and become senescent. Interestingly, our data show that the cell cycle arrest is not mediated by p53/p21. Two questions arise from these results. The first one is how these cells establish senescence if it is not through the p53/p21 axis. The second one is which is the molecular mechanism by which these cells survive. Interestingly, two different papers shed some light on these matters. First, Dr Estella's laboratory reported that cell cycle stalling prevents cells from dying upon irradiation (Ruiz-Losada et al., 2022).

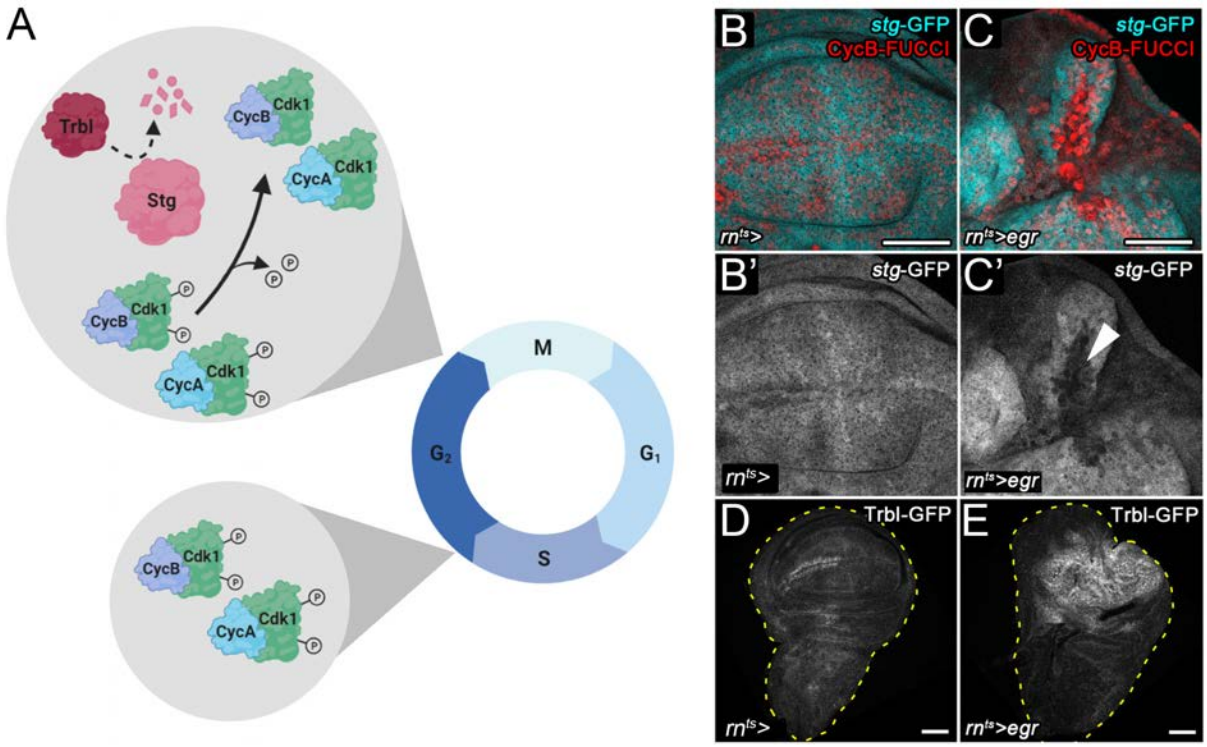

Figure 75. Stg and Trbl regulate G2-M cell cycle progression. A) Cartoon showing how Stg and Trbl regulate the G2-M transition. During the G2 phase, Cyc-CDK complexes accumulate but the phosphorylation inactivates them. To allow G2-M phase transition, the phosphatase Stg has to remove the phosphates. This event can be prevented by Trbl, which mediates Stg degradation. **B to E)** Early third instar discs of the indicated genotype stained for CycB-FUCCI (red, B and C) and stg-GFP (cyan or white, B to C') or Trbl-GFP (white, D and E). CycB-FUCCI is used to label G2 stall cells (B and C). White arrowhead points toward G2 stall cells that do not present Stg expression in egr-expressing discs (C'). egr-expressing discs show an up-regulation of Trbl in the wounded area (E). B to E) Images modified from Cosolo et al., 2019.

Second, Dr Classen's laboratory reported the presence of cells stalled at G2 in *egr*-expressing discs (Cosolo et al., 2019). During the G2 phase, Cyclins A (CycA) and B (CycB) accumulate and form complexes with Cyclin-dependent kinase 1 (Cdk1). However, these complexes are not active, and they require the phosphatase Cdc25/String (Stg) to remove the phosphate residues from the Cdk1 active domain and progress from G2 to M phase (Edgar & O'Farrell, 1989, 1990; Follette & O'Farrell, 1997). By contrast, Tribbles (Trbl) prevents the cell cycle progression by mediating Stg degradation (Figure 75A)(Großhans & Wieschaus, 2000; Mata et al., 2000; Seher & Leptin, 2000). Thus, in *egr*-expressing discs they observed that stalled cells presented a down-regulation of Stg and an up-regulation of Trbl, preventing the activation of Cdk1 and blocking the progression from G2 to M phase. Hence, the cells were stalled at G2 (Figure 75B)(Cosolo et al., 2019). Consistently, previous data from our laboratory showed that in CIN tumours the arrest of the senescent population was mediated by JNK that induced the down-regulation of Stg and the up-regulation of Trbl (data not published).

As previously mentioned, upon *egr* expression the apoptotic caspase cascade is activated and most cells dye, while a small proportion of them get stall and become senescent. Interestingly, while the majority of dying cells are localized apically, senescent cells identified by the increased nuclear size are more basally localized (Figure 76A). When we forced the arrest of the cells at G2 in damaged discs by over-expressing *trbl*, we detected a drastic decrease of pyknotic nuclei and an increase of senescent cells both apically and basally localized (Figure 76B). Moreover, the decrease in dying cells was accompanied by a reduction in the presence of the active form of effector caspase Dcp-1 (c-Dcp-1) respect to control damaged discs (Figure 76B and F). Interestingly, the disc architecture remained highly altered (Figure 76B). Surprisingly, despite the rescue of the cell death, when we analysed the capacity of *trbl*-expressing discs to regenerate fully normal wings (Figure 77A), we saw that it was drastically reduced when compared to controls (Figure 77B). Altogether, these results show that Trbl over-expression can prevent apoptosis, allowing cells to become senescent. However, despite the capacity of Trbl to prevent cell death, its overexpression is not improving regeneration but it rather had the opposite effect. A possible explanation might be that Trbl is acting as a dam, preventing caspase activity. Hence, when discs are put back at 18ºC to allow regeneration, *trbl* expression is stopped and can no longer prevent caspase activity. Therefore, those cells that have been expressing *egr* massively die when *trbl* expression is stopped because caspase activity no longer is prevented. Independently, this result does not mean that senescence is not playing a positive role in regeneration. In fact, in both zebrafish and axolotl regeneration models have

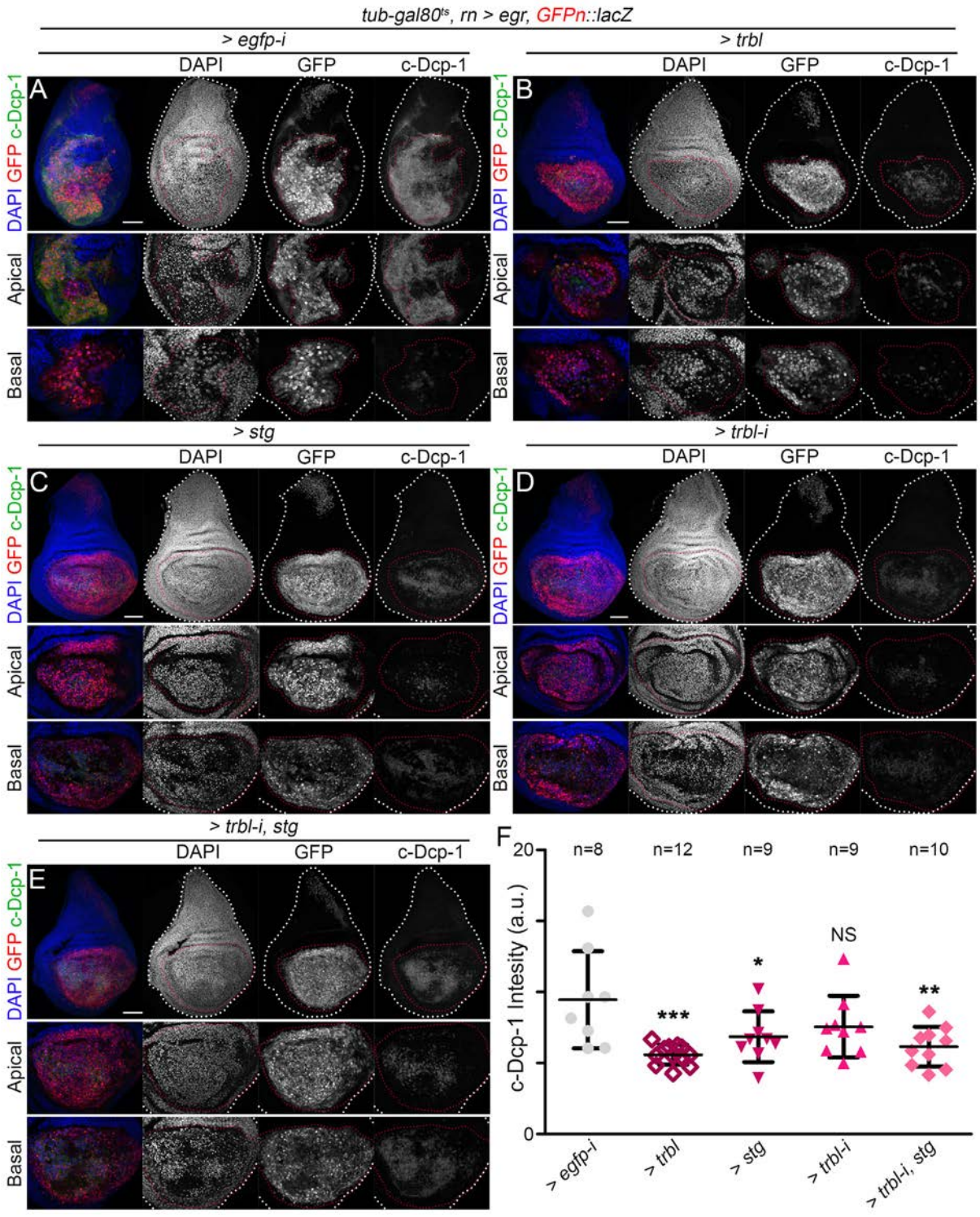

Figure 76. Cell cycle arrest prevents cell death. A to E) Early third instar wing discs of the indicated genotype after 16 h of *egr* expression under the control of *rn-gal4* driver. Discs were stained for GFP (red or white), cleaved-Dcp-1 (c-Dcp1, green or white), and DAPI (blue or white). Wing disc contours are labelled by a white line and GFP-expressing cells by a red line. Magnifications of single apical and basal planes of the pouch are shown in lower panels. Scale bar: 50 µm. **F)** Scattered plot representing cleved-Dcp-1 signal intensity (in arbitrary units) of the indicated genotypes. Two-tailed Anova test with Dunnett's multiple comparison correction against a common control was performed .The number of scored wing discs, mean and SD are shown. Statistically significant differences are shown: NS, $p > 0.05$; * $p < 0.05$; **$p < 0.01$; ***$p < 0.001$.

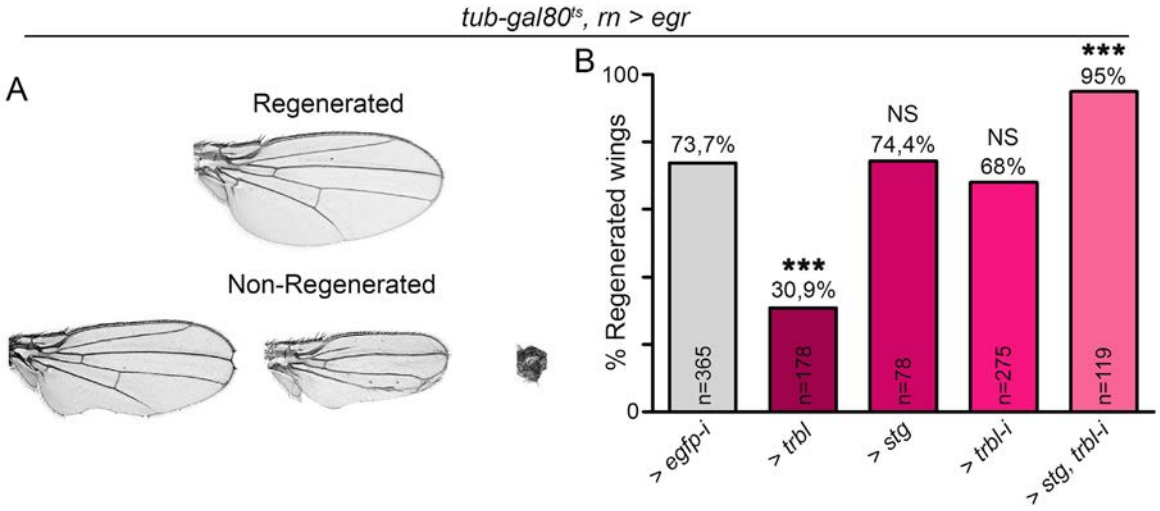

Figure 77. Trbl overexpression impairs regeneration. A) Examples of the resulting fully regenerated and non-regenerated adult wings. **B)** Histograms plotting the percentages of fully regenerated wings of individuals of the indicated genotypes. The number of scored wings and the percentage of regenerated wings are shown. Chi squared test was performed. Statistically significant differences are shown: NS; ***p < 0.001.

been observed the presence of senescent cells contribute to the regeneration of the tissue (Da Silva-Álvarez et al., 2020; Q. Yu et al., 2022; Yun et al., 2015). Indeed, in both models, depletion of the senescence population impairs regeneration (Da Silva-Álvarez et al., 2020; Q. Yu et al., 2022). Therefore, it is possible that in our model senescent cells play the same role. However, a different approach would be necessary to confirm this hypothesis.

By contrast, when we forced the cell cycle progression by *stg* over-expression (Figure 76C) or by inducing a knockdown of *trbl* (Figure 76D), or both (Figure 76E), we observed the presence of wild-type-like discs that did not present senescence-like cells. Despite the regular architecture, cell death was still present in the tissue, but apoptotic cells were extruded from the main epithelium and were mainly basally localized (Figures 76C and D). Interestingly, c-Dcp-1 levels were reduced too, but not as much as when we over-expressed *trbl* (Figure 76F). Consistently, when we analysed the regenerative capacity of these discs, they presented the same or better capacity to regenerate a complete normal wing than control discs (Figure 77B). These results suggest that forcing cell cycle progression would prevent cells from dying and establishing senescence. Although these results point towards this direction, the fact that these discs in terms of architecture look like wild type discs, and not like *egr*-expressing discs, may indicate that Stg could be preventing the activity of the JNK pathway. If this would be true, these discs would not be considered wounded and, therefore, the resulting wings would not be regenerated wings but wings arising from normal development. However, the fact that high levels of pyknotic cells can still be observed basally suggests that in some cells JNK ac-

tivity could exceed Stg activity and therefore apoptosis would occur normally. Therefore, to maintain tissue integrity, these cells would be extruded from the main epithelium. Although these results are promising, further experiments are required to properly understand the role of cell cycle arrest in resistance to cell death and to confirm the speculations presented in this section.

Senescent cells persist over time in the regenerating tissue

Although we do not know yet the function of the senescent cells in regeneration, it is clear that they do play a role. A study performed on axolotls demonstrated that upon amputation of their limb, senescent cells appeared and were required over time to properly regenerate the amputated limb (Yun et al., 2015). Therefore, it would be expected that in our tissue senescent cells would be maintained over time to contribute to the regeneration of the wing disc. To analyse the presence of senescent cells in the regenerating disc over time, we conducted the regular genetic ablation protocol by overexpressing *egr* for 16 h at day 7. After 16 h, the discs were immediately dissected (R0) or put back at 18 ºC to allow regeneration and

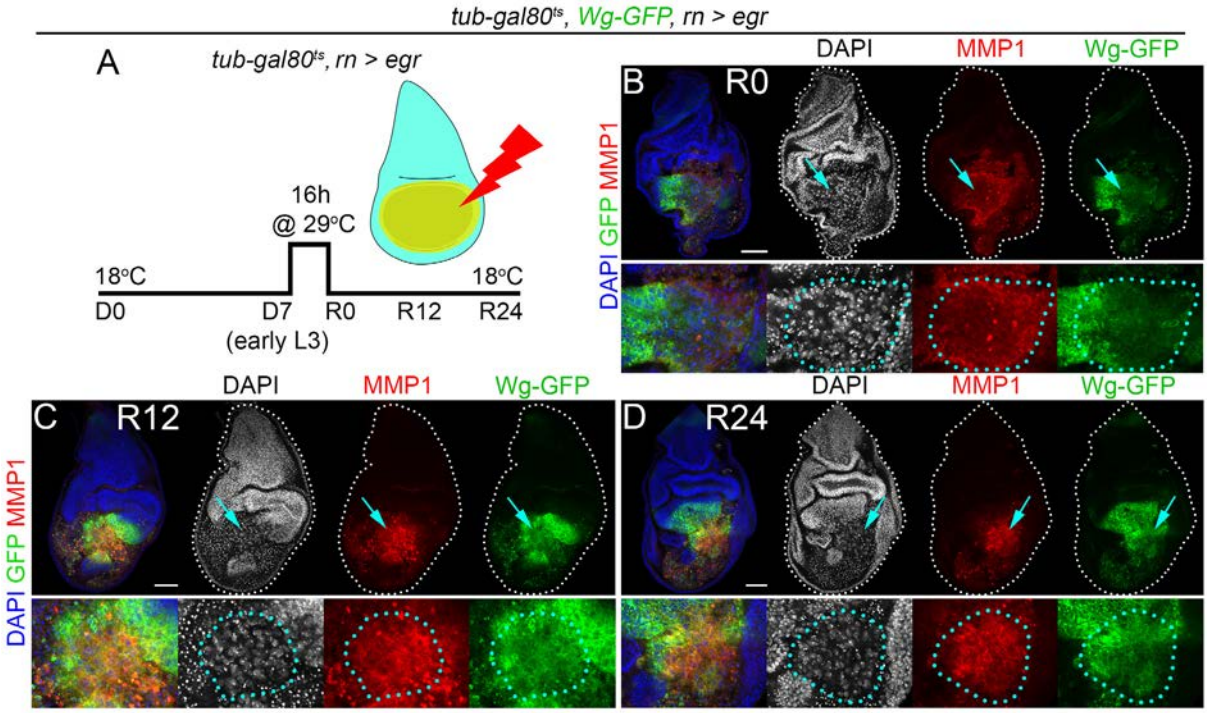

Figure 78. Senescent cells persist over time in the regenerative tissue. A) Schematic representation of the Eiger-dependent wing ablation systems. Larvae were raised at 18 °C for 7 days (D7) and switched to 29 °C for 16 h to induce *egr* expression. Discs were dissected immediately after the 16 h induction (R0) or place back at 18 ºC and dissected 12 h (R12) or 24 h (R24) later. **B-D)** Early third instar wing discs of larvae bearing the indicated reporters dissected at regenerating points R0, R12 and R24. Discs were stained for MMP1 (red), Wg-GFP (green), and DAPI (blue or white). Wing disc contours are labelled by a white line and cyan arrows point to the senescent cells. Higher magnification of the wing pouch is shown in lower panels where senescent cells are circled by a cyan line. Scale bar: 50 µm.

dissect the discs 12 h (R12) and 24 h (R24) after the end of *egr* induction (Figure 78A). As previously reported in the sections above, after 16 h of induction we could detect senescent cells that were expressing molecules from the SASP (Figure 78B). Surprisingly, senescent cells were detected even 12 h and 24 h after *egr* induction (Figures 78C and D). Importantly, even after 24 h of regeneration, senescent cells were still secreting MMP1 and Wg (Figure 78D), reinforcing the idea that senescent cells play a long-term role in regeneration. Altogether, these results indicates that senescent cells are present in the tissue at least for the first 24 h of regeneration and suggest that they participate in the process through the secretion of different molecules. Although more experiments are required to clarify whether senescent cells play a positive or a negative role in regeneration, these results are promising and open the door to new research lines.

Discussion

The main goal of this thesis was to characterize *wg*^{1}-enhancer and understand how differentially contributes to the development, regeneration and tumorigenesis of the wing disc. Here we have proved that *wg*^{1} deletion contains an enhancer that is required at the early stages of the wing development to drive the expression of Wg and trigger the specification of the wing. Moreover, we have narrowed down the wing-specific enhancer to a 1.8-kb-long enhancer comprising two highly conserved regulatory modules, *Beta* and *Gamma,* that act in a redundant manner. Whereas *Gamma* acts as a driving module integrating the positive signals from the Hh pathway and the repressing inputs of the EGFR and JAK/STAT pathways, *Beta* seems to act as a regulatory module, comprising the repressing signals of the EGFR pathway. The combinatorial effects of the three pathways contribute to triggering and restricting the expression of Wg to the ventral anterior edge of the early disc, restricting the specification of the wing to this area (Figure 79A). Furthermore, we have been capable to show that the eye and notum phenotypes of the flies carrying the *wg*^{1} deletion are not present in flies carrying the deletion of *Beta* and *Gamma*, that only present the wing phenotype, indicating the presence of an overlapping enhancer that drives Wg expression in the notum and the eye.

In later stages, the same modules used for the specification of the wing are reused in the injured wing disc to promote regeneration. Upon damage, JNK triggers the activity of the

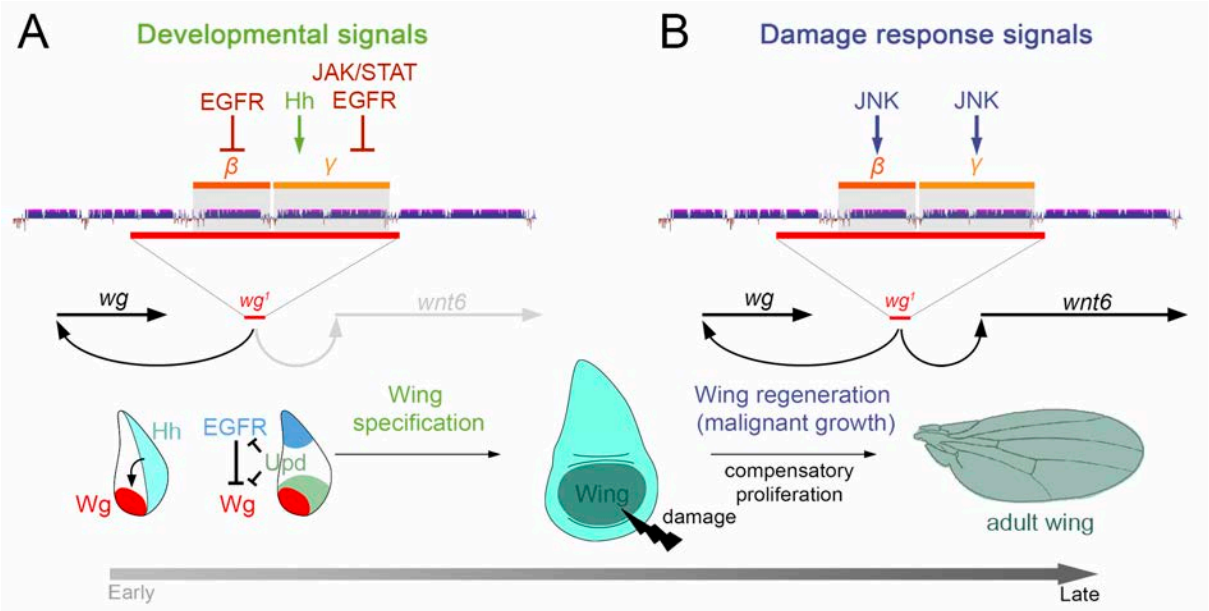

Figure 79. The developmental enhancer *wg'* is reused in regeneration and tumorigenesis. Cartoon depicting the role of *Beta* and *Gamma* in early (A) and later stages (B). While at early stages the enhancer drives Wg expression to trigger the specification of the wing (A), at later stages *Beta* and *Gamma* drive wing regeneration and malignant growth through the expression of both Wg and Wnt6. Wnt6 has no major role in wing specification even though it is expressed during development in the same expression pattern as Wg. Furthermore, while the activity of the enhancer is positively regulated by the Hh and negatively by the EGFR and JAK/STAT pathways at early stages (A), during regeneration and tumorigenesis the activity of the enhancer is driven by JNK (B).

enhancer through both *Beta* and *Gamma*, leading to the expression of Wg and Wnt6. Interestingly, the regenerative tissue requires both Wg and Wnt6 to drive compensatory proliferation and allow regeneration (Figure 79B). The shared use of this enhancer in the specification of the wing disc and regeneration unravels a highly evolutionary robust mechanism to ensure the development of the wing not only during normal development but also under stress conditions. However, the same enhancer is aberrantly used in CIN-induced tumours to drive the expression of Wg and Wnt6 which are responsible for the tumoral overgrowth. Consistently, the deletion of the enhancer prevents tumoral overgrowth (Figure 79B).

In addition, in the regenerative tissue, we detected the presence of a cell population with enlarged nuclei and resistance to cell death inputs. Assessing different hallmarks of senescence we have been able to conclude that these cells are senescent and persist along the regeneration. Besides, we have shown that the establishment of the cell cycle arrest is independent of p53. Which are the pathways implicated in the establishment of senescence and cell death resistance or which is the role of the senescent cells in the regenerative tissue are two questions that remain open.

In this section, we will discuss the open questions that have remained both in the *wg[1]*-enhancer and senescence sections.

wg[1], a key enhancer in the development, regeneration and tumorigenesis of the wing disc

wg[1] inter-enhancer redundancy

In this thesis, we have focused on the characterization of *wg[1]*, the first *wg* allele to be discovered (Sharma, 1973; Sharma & Chopra, 1976). We have shown that the sequence of *wg[1]* contains an enhancer responsible to drive the expression of Wg in the early stages of development and trigger the specification of the wing fate (Figures 23, 24 and 27). However, when we analysed the penetrance of the *Δwg[1]* phenotype, in other words, the absence of wing and duplication of the notum, we saw that it was around 80% (Figure 23). Consistently, 73% of *Δwg[1]/ΔBRV118* early discs did not present Wg expression, while the other 27% of the early discs showed Wg expression (Figure 24). These results suggest the presence of a shadow enhancer that contributes to triggering the expression of Wg in the early stages. Shadow enhancers are redundant enhancers that display overlapping spatiotemporal activity. Indeed,

these shadow enhancers seem to be a mechanism of redundancy to guarantee gene expression in front of genetic and environmental perturbations (reviewed in Kvon et al., 2021). A study performed in *Drosophila* embryos showed that many developmental genes were controlled by two or more enhancers with overlapping activities (Kvon et al., 2014). Besides, the presence of shadow enhancers also has been described in zebrafish (Ertzer et al., 2007), mice (Hörnblad et al., 2021; Jeong et al., 2006; Osterwalder et al., 2018) and humans (Allan et al., 1995; Zhou & Sigmund, 2008), indicating that it is a fairly common mechanism to ensure gene expression in different species. Moreover, the presence of a secondary enhancer driving the expression of Wg is reinforced by the fact that the penetrance of the Δwg^{1} phenotypes decreases over time as reported by Dr Morata and Lawrence (1977). This progressive loss of the phenotype over time suggests that in flies where the wg^{1}-enhancer has been deleted, it has somehow favoured the interaction between the *wg* promoter and the shadow enhancer. This ensures the expression of *wg* despite the absence of the wg^{1}-enhancer and thus guarantees the specification of the wing, an organ that confers a clear advantage for the fly.

Our understanding of how these two enhancers could be regulating the expression of *wg* is still unknown. As exposed in the introduction, several models have been proposed to explain the different kinds of interactions observed among shadow enhancers (Figure 5)(reviewed in Kim & Wysocka, 2023; Kvon et al., 2021). The fact the deletion of the wg^{1}-enhancer does not present a penetrance of 100% indicates that the shadow enhancer positively regulates the expression of *wg*, suggesting that the interaction among the enhancers has an additive nature. To know whether this additive nature is synergic, subadditive or simply additive, more experiments would be required. Nevertheless, the fact that the penetrance of the Δwg^{1} phenotype is around 80% suggests a clear hierarchical interaction between both enhancers where, in normal conditions, the activation of *wg* is mainly driven by the wg^{1}-enhancer. Indeed, several cases of hierarchical interactions among enhancers have been reported (Carleton et al., 2017; Shin et al., 2016). However, to clarify these assumptions, we would need to identify the shadow enhancer to study how both enhancers interact with each other and the *wg* promoter and how the deletion of the shadow enhancer could impact *wg* expression or wg^{1}-enhancer activity.

The fact that the penetrance of the phenotype is almost 100% when we cross Δwg^{1} flies with flies carrying the deficiency *BSC226*, *BSC291* or *BSC324* (Figure 23) suggests that most probably the shadow enhancer is comprised within the sequence of these deficiencies. Although we tried to find possible candidates by looking for high-score Ci binding sites, the TF

of the pathway responsible to trigger Wg expression, neither of the candidates was capable to recapitulate the pattern expression of the *wg*^{1}-enhancer (Figure 36). To increase the chances to find the shadow enhancer a better approach could be to include in our analysis the TFBSs of the EGFR and JAK/STAT pathway, two of the pathways that we have shown to be capable to regulate the activity of the *wg*^{1}- enhancer. Nevertheless, there is a chance that the shadow enhancers do not share the same TFBSs as the *wg*^{1}-enhancer. Indeed, some reports are showing that although the shadow enhancers present the same spatiotemporal activity as the primary enhancer, they can present different TF motifs (Cannavò et al., 2016; Staller et al., 2015; Waymack et al., 2020; Wunderlich et al., 2015). A good example is the Krüppel gene in the embryo, where its proximal and distal enhancers present different TFBSs in their sequence. While the proximal enhancer is regulated by the TFs STAT92E and Hunchback (Hb), the distal enhancer is regulated by Bicoid (Bcd) and Zelda (Zld)(Waymack et al., 2020; Wunderlich et al., 2015). However, there are many other examples of shadow enhancers that share the same TFs motif in their sequence (Barolo, 2012; Cannavò et al., 2016; Hong et al., 2008; Whitney et al., 2022). Besides, the clear requirement of Hh signalling (Ng et al., 1996) or the repressive signalling from the EGFR pathway (Baonza et al., 2000; S. H. Wang et al., 2000) makes it highly probable that the shadow enhancer shared at least a part of the TF motifs with the *wg*^{1}-enhancer.

wg^{1} intra-enhancer redundancy

The expression experiments using *lacZ* reporters for the different enhancer modules showed that the minimum sequence required to recapitulate the expression pattern of the *wg*^{1}-enhancer was a 590 bp-long sequence from the 3' region of the *Gamma* module (*Gamma-590*), a region containing a bioinformatically predicted high score Ci binding site (Figure 37). Interestingly, the mutation of this high score Ci binding site compromised the expression pattern of both *Gamma-590* and *Gamma-lacZ* reporters, showing expression in the posterior compartment (Figure 37). This identifies this Ci binding site as a crucial site for the activity of *wg*^{1}-enhancer. However, when we generated targeted deletions of the high score Ci binding site no loss of the wings and notum duplication was observed. On the contrary, the deletion of both modules *Beta* and *Gamma* was required to recapitulate the *Δwg*^{1} phenotype (Figure 39). How could this be?

A typical enhancer contains multiple binding sites for two or more TFs (Jindal & Farley, 2021; Spitz & Furlong, 2012). It has been proposed that the presence of several binding sites for the same TF confers robustness to the enhancer in front of genetic variability. Therefore,

the loss of one of these TFBSs would not affect the general output of the enhancer (Lagha et al., 2012). Indeed, the ZRS enhancer from the *sonic hedgehog* gene in mice limb development presents five ETS binding sites in its sequence. Individual deletions of the binding sites have no impact on the expression of *shh.* However, the combinatorial deletion of all the ETS binding sites leads to a reduction of *shh* expression (Lettice et al., 2012). This result suggests that the ETS binding sites act in a redundant manner within the enhancer. This would explain why, although we have deleted the high score Ci binding site, we do not observe the wing to notum phenotype: the remaining Ci binding sites in the sequence of the enhancer act redundantly to allow the enhancer activity and trigger the expression of *wg.*

Nevertheless, it remains curious that deletion of *Beta* is necessary to observe a phenotype although it only contains one predicted Ci binding site and does not recapitulate the expression pattern of either the wg^{1}*-lacZ* reporter or the endogenous Wg expression (Figures 37 and 39). Hence, could there be more reasons than the simple TF redundancy that explain the requirement to delete both *Beta* and *Gamma* to induce the wing to notum phenotype? In mice, the CD64 enhancer is crucial to induce *fgf8* expression in the midbrain-hindbrain boundary (MHB). When the enhancer is deleted *fgf8* cannot be expressed and the midbrain cannot properly develop. Interestingly, the authors showed that the CD64 enhancer was comprised of 3 functional modules named A, B and C. While the deletion of the A module did not induce any phenotype, the deletion of the B or C modules induced the loss of the midbrain. Interestingly, when the authors further studied module B, they showed that only one-third of the module was required to drive enhancer activity regardless of the third, showing intra-enhancer redundancy in the B module. Oddly, the B module is essential for the enhancer activity although its reporter is not capable to recapitulate the expression pattern of the full enhancer (Hörnblad et al., 2021). Therefore, the fact that we have to delete both *Beta* and *Gamma* (*Δβγ*) together to recapitulate the Δwg^{1} phenotype indicates that *Beta*, as it occurs for the CD64 enhancer, performs a redundant function within the enhancer even though it does not recapitulate the same expression pattern. This ensures the development of the wing in front of possible genetic variation that could affect the *Gamma* module. Whether *Beta* performs its redundant function by binding to the same TFs as *Gamma* or to other TFs still remains unknown. The fact that, even in the absence of *Gamma, Beta* is still capable of triggering the specification of the wing (Figure 39) suggests that at least in part *Beta* is capable to respond to Hh, even if our expression data do not firmly support this. Nevertheless, the fact that *Beta* presents posterior expression (Figure 37), where Hh activity cannot drive its expression, supports the idea that

there is a TF not yet identified that drives *Beta* posterior expression and contributes to the activity of the *wg[1]*-enhancer. However, the fact that we do not detect posterior expression of the *wg[1]-lacZ* reporter, which comprises both *Beta* and *Gamma* modules, suggests that *Beta* posterior activity may be inhibited by *Gamma*.

The necessity of deleting both *Beta* and *Gamma* to recapitulate the *Δwg[1]* phenotype indicates the existence of intra-enhancer redundancy between *Beta* and *Gamma*. However, we cannot ignore the fact that *Gamma* deletion, but not *Beta,* showed an increase in the penetrance of the wing to notum phenotype over larger *wg[1]*-related deletions (Figure 39). This result together with the expression data of the *Gamma-lacZ* reporter, that recapitulates *wg[1]-lacZ* pattern expression, suggests that *Gamma* has a driving role within *wg[1]*-enhancer and the specification of the wing. However, in front of the genetic variability of *Gamma*, the redundant activity of *Beta* rescues the enhancer activity, ensuring the development of the wing.

Altogether, the data suggest that early Wg expression in the wing discs presents a double inter- and intra-enhancer redundancy mechanism to guarantee its expression. Therefore, the intra-enhancer redundancy between *wg[1]*-enhancer modules together with the presence of shadow enhancers ensures the activity of the enhancer and the specification of the wing in front of genetic variation.

In addition, the identification of this wing-specific enhancer can bring some insight into the evolutionary origin of the wing. The origin of the wing is a mystery that scientists have been trying to solve since the 19th century (Alexander, 2018; Ross, 2017). Two main hypotheses were proposed to explain the origin of the wing: the paranotal (or tergal) hypothesis and the pleural origin hypothesis. While the paranotal hypothesis proposes that the wing originates from a lateral extension of the thorax (notum), the pleural origin hypothesis suggests that the wing formed from an extension of the pleura. Variations of this hypothesis argue that the formation of the wing from the pleura can be a de novo projection or can form from a pre-existing structure such as the gills (reviewed in Clark-Hachtel & Tomoyasu, 2016; Ruiz-Losada et al., 2018). Nevertheless, the most accepted hypothesis nowadays is the dual origin hypothesis proposed by Niwa and colleagues (Niwa et al., 2010). As the name indicates, the dual hypothesis defends that both the tergal and pleural tissues contribute to the origin of the wings (Clark-Hachtel & Tomoyasu, 2016; Ross, 2022). The identification of a wing-specific enhancer and the fact that its deletion results in a duplication of the notal structures (Figure 23) reinforces the proposal that the wing evolved of an extension from the dorsal thorax. Nevertheless, our re-

sults also could be compatible with the dual origin hypothesis. In fact, we cannot obviate data pointing to a contribution of the pleural tissue to the origin of the wing. Indeed, as reported by Almudi and colleagues, a genome-wide expression comparison of the mayfly gills and wing pads showed that 43% of the genes were shared, supporting the idea that ancestral thoracic gills contributed to the development of wing (Almudi et al., 2020). Furthermore, linage tracing experiments performed by Dr Estella's laboratory showed that although most of the cells of the *Drosophila* wing disc originated from the dorsal primordium of the embryo (the primordium that gives rise to the wing and haltere discs), some of the cells originated from the ventral primordium (the primordium that gives rise to the leg)(Requena et al., 2017). Therefore, the data indicates a dual origin of the wing. In fact, there are more and more reports pointing in this direction (Clark-Hachtel et al., 2013; Clark-Hachtel & Tomoyasu, 2020; Linz & Tomoyasu, 2018; Prokop et al., 2017; Requena et al., 2017). Hence, taking into consideration our data together with the data from the literature, everything points towards a dual origin of the wing.

Developmental regulation of *wg*^{1}-enhancer by Hh, EGFR and JAK/STAT

The experiments performed to understand the molecular pathways behind *wg*^{1}-enhancer activity showed that, while on one side the enhancer is positively regulated by the Hh pathway through the *Gamma* module, on the other it is negatively regulated by the EGFR through both *Beta* and *Gamma* and by the JAK/STAT pathway through *Gamma* (Figure 38).

Hh pathway positively regulates the early expression of Wg through Ci, the transcriptional factor of the pathway (Von Ohlen et al., 1997). Consistently, the Hh pathway positively regulates the activity of the *wg*^{1}-enhancer. Indeed, while Hh overexpression induces an expansion of the *wg*^{1}*-lacZ* reporter expression, Ptc upregulation, a negative regulator of the pathway, drastically diminishes its expression but does not completely abolish it (Figure 30). This indicates that although Hh positively regulates the expression of Wg and the wing fate specification, it is not an absolute requirement. Consistently, when we analysed the percentage of wing to notum transformation in flies overexpressing Ptc, we saw that most of the flies at 29ºC did not show the phenotype. On the contrary, most flies showed a vestigial wing, most probably as a consequence of the decreased Dpp activity due to the blockage of Hh signalling (Figure 34)(Barrio & Milán, 2017; Restrepo et al., 2014). Similarly, at 25ºC, where the expression of the transgene is not so strong and, therefore, males could be obtained, the percentage of flies showing wing to notum transformation increased up to 50%, supporting the previous statement that Hh is not an absolute requirement (Figure 35). Nevertheless, it must also be con-

sidered that we are working with the Gal4/UAS system instead of a mutant and, therefore, it might be that the depletion of the Hh pathway is not complete, leading to weaker phenotypes.

In addition, consistently with the literature (Baonza et al., 2000; S. H. Wang et al., 2000), we have shown that EGFR activity restricts Wg to the ventral part of the disc by suppressing the enhancer activity in the most proximal part of the disc, where EGFR activity is higher. Hence, we could only detect enhancer activity in the ventral part, where EGFR signalling does not reach. Consistently, depletion of EGFR activity at early stages showed an expanded expression of the *wg[1]-lacZ* reporter towards the more proximal regions of the discs (Figure 31). At later stages, upon EGFR depletion, the expression of the *wg[1]-lacZ* reporter was detected in the ectopic wing pouches that formed (Figure 31). Besides, EGFR mediates its regulatory activity through both *Beta* and *Gamma* (Figure 38). Oddly, in some discs, it was detected posterior expression of the enhancer upon EGFR signalling depletion (Figure 38). One of the functions of EGFR is to mediate cell survival (Baker & Yu, 2001; Bergmann et al., 1998; Crossman et al., 2018) and, indeed, *egfr*- or *erk*-deficient clones cannot survive in the wing pouch (Diaz-Benjumea & Garcia-Bellido, 1990; Diaz-Benjumea & Hafen, 1994; Zecca & Struhl, 2002). When we analysed the posterior expression of the enhancer, we could see that its expression colocalized with pyknotic cells (Figure 38). Therefore, this observation suggests that the expression of the enhancer in the posterior compartment in *egfr* depleted discs is a consequence of cell death and might be mediated by JNK activity.

Finally, we analysed the impact of the JAK/STAT pathway on the enhancer. As reported by our laboratory, at early stages JAK/STAT activity contributes to restricting EGFR activity to the most proximal part of the disc, thus preventing the repression of Wg in the most ventral part. Hence, in those discs where the activity of JAK/STAT is depleted, EGFR cannot be repressed and advances to the most distal parts of the disc, repressing Wg activity (Recasens-Alvarez et al., 2017). In *Δwg[1]* discs, apart from observing the absence of a wing, a duplication of the notum is also observed (Figure 23). That is because, in discs lacking early Wg expression, the EGFR signalling extends ventrally. This results in the duplication of the notum (S. H. Wang et al., 2000). Oddly, the *Δwg[1]* disc still showed JAK/STAT activity (Figure 32). This raises the question of how EGFR activity can advance towards more ventral part of the disc if JAK/STAT activity is still there. The fact that the notum duplication in the *Δwg[1]* disc occurs even in the presence of JAK/STAT activity suggests that JAK/STAT is not sufficient by itself to restrict the EGFR activity to the most proximal part of the disc and to do that it requires Wg. Moreover, interesting observations were made when we analysed the activity of the *wg[1]-lacZ* reporter in

discs where JAK/STAT activity was depleted. It was previously shown that JAK/STAT depletion did not directly impact the expression of Wg. However, the depletion of JAK/STAT signalling allows the advance of EGFR activity that represses Wg (Recasens-Alvarez et al., 2017). Hence, we would expect that in early discs where the activity of JAK/STAT has been depleted, the enhancer expression would be repressed by the advance of EGFR activity or at least be even more ventrally restricted than in controls. However, no difference between the expression of *wg[1]-lacZ* was detected between the control and discs where JAK/STAT activity was depleted (Figure 33). Nevertheless, in later discs, our expression data indicate that JAK/STAT represses the activity of the enhancer because upon *dome* depletion we observed an upregulation of the enhancer expression in both the anterior and posterior compartment (Figure 33), indicating that JAK/STAT represses the activity of the *wg[1]*-enhancer. Shockingly, the *Gamma* module, which only presents activity in the anterior compartment, also presented activity in the posterior compartment upon *dome* depletion. Two possibilities could explain the posterior expression of the enhancer upon the depletion of the JAK/STAT activity. The first possibility is that, as it occurs with EGFR depletion, the posterior expression of the enhancer is due to the apoptosis generated by the absence of JAK/STAT signalling. As exposed by Recasens-Alvarez and colleagues, at later stages of development JAK/STAT signalling is essential to modulate En activity in the posterior compartment. When JAK/STAT is depleted, En downregulates the expression of the antiapoptotic gene *diap-1* and the cell cycle regulator gene *cyclin A*. Therefore, JAK/STAT is required to modulate En and guarantee the correct levels of Diap-1 and CycA to prevent cells from dying and allow them to proliferate (Figure 80)(Recasens-Alvarez et al., 2017). Although it is possible that a certain extent of the enhancer signalling upon dome depletion is caused by cell death, many non-pyknotic nuclei express the reporter (Figure 38). Hence, cell death by itself would not explain the full extent of the posterior expression observed. The second option is that there is a fourth player, another pathway capable to drive the posterior expression of the enhancer. This idea would be supported by the fact that *Beta* presents posterior expression (Figure 37). Besides Hh, whose TF Ci is repressed in the posterior compartment by En (Eaton & Kornberg, 1990), the other two pathways that we know regulate the enhancer activity, EGFR and JAK/STAT, perform repressive functions. Hence, another pathway should be responsible of positively regulating the expression of *Beta* in the posterior compartment. In addition, the *Gamma* module, despite presenting expression in the anterior compartment, it expands posteriorly upon the mutation of the high-score Ci binding site (Figure 37). As mentioned above, Hh cannot be the pathway driving this posterior expression. Therefore, this supports the idea of a fourth player capable to drive the activity of the enhancer in the posterior compartment.

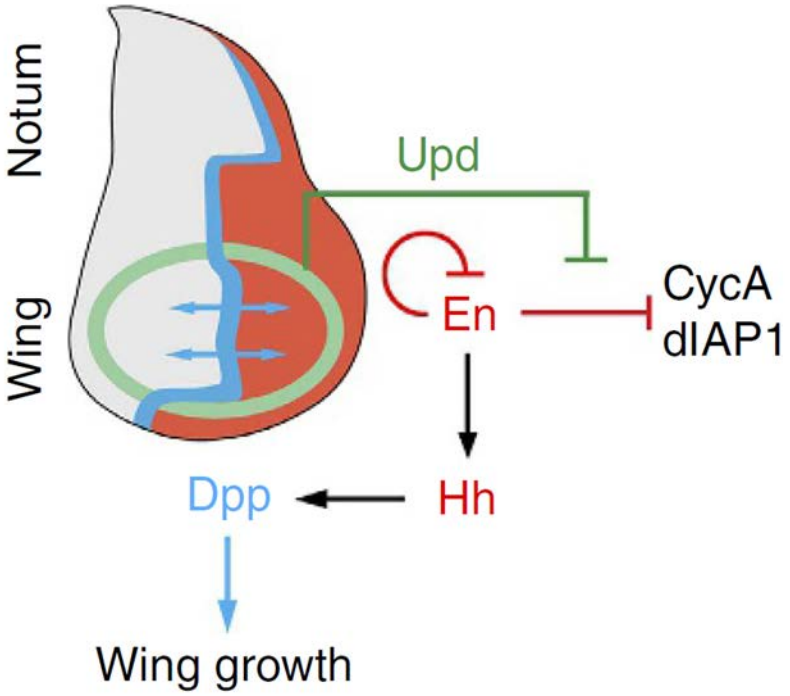

Figure 80. Upd prevent the activity of En. Cartoon depicting the role of the JAK/STAT pathway preventing the downregulation of CycA and Diap-1 by En. Blockage of En activity by JAK/STAT promotes the survival and cycling of Hh-producing cells, ensuring Dpp expression and guaranteeing Dpp-dependent wing growth. Adapted from Recasens-Alvarez et al., 2017.

Altogether, these data suggest that upon JAK/STAT depletion this fourth player could bind to the enhancer and drive expression in the posterior compartment. To test whether cell death is driving the posterior expression of the enhancer or if there is a fourth player regulating its expression, we could overexpress *diap-1* in *dome*-depleted discs. The overexpression of *diap-1* should rescue the drastic reduction in the size of the posterior compartment observed in *dome-i* discs (Recasens-Alvarez et al., 2017). If the overexpression of *diap-1* prevents the posterior expression of the enhancer, that would indicate that the posterior expression of the enhancer was triggered by cell death, as it occurs when we deplete EGFR activity. On the contrary, if even when overexpressing *diap-1* we could detect expression of the enhancer in the posterior compartment, this would suggest that the posterior expression observed in *dome-i* discs is mediated by a pathway capable to induce the expression of the enhancer posteriorly. Independently, the fact that JAK/STAT activity is capable to repress both EGFR and Wg suggests that, during the specification of the wing and notum, it acts as a safety belt between both signals to guarantee the specification of both structures. However, more experiments are required to confirm this hypothesis.

The capacity of JAK/STAT to regulate the activity of wg^{1}-enhancer could have implications further away than development. Indeed, as it has been shown in the introduction, Upds

and JAK/STAT activity is fundamental in both regeneration and tumorigenesis (reviewed in Amoyel et al., 2014; Herrera & Bach, 2019). Previous reports have shown that JAK/STAT could be regulating the spreading and activity of JNK signalling (La Fortezza et al., 2016) or the expression of Dilp8 (Katsuyama et al., 2015). Hence, it would not be so hard to think that JAK/STAT could also be regulating the expression of Wg in regeneration.

As presented here, probably there is another molecular pathway involved in the regulation of the activity of the *wg*^{1}-enhancer and the specification of the wing fate. But which are the candidates? When Harris and colleagues looked for possible candidates to regulate the activity of the enhancer in the regenerative tissue, they detected the presence of TCF binding sites, the TF of the Wnt pathway, in the sequence of the enhancer, suggesting a positive feedback loop (Harris et al., 2016). This would be supported by the observations made by Schubiger and colleagues that ectopic expression of Wg in the leg disc can activate the enhancer there (Schubiger et al., 2010). Another candidate would be Vg together with Sd. Vg lacks a DNA binding domain, so it functions as a transcriptional activator when bound to Sd (Halder et al., 1998; Simmonds et al., 1998). Furthermore, ectopic expression of *vg* in other discs triggers the formation of ectopic wings there (J. Kim et al., 1996; Simmonds et al., 1998). For these reasons, Vg stands as a possible regulator of the *wg*^{1}-enhancer. Finally, another candidate would be the targets of Dpp that spread both through the anterior and posterior compartments (Strigini & Cohen, 1999). However, this would not explain the posterior expression of the enhancer observed in *dome-i* discs. The drastic reduction of the posterior compartment in discs where JAK/STAT activity was depleted, failed to properly activate the expression of Dpp (Recasens-Alvarez et al., 2017). Hence, if the fourth player is a target of Dpp, in *dome-i* discs, where Dpp activity is drastically reduced, the Dpp target would not be expressed and, therefore, would not be capable to drive the posterior expression that we observe. In conclusion, further research is necessary to clarify whether it truly exists a fourth player that contributes to regulating the early expression of Wg and the wing fate specification.

Role of *wg*^{1}-enhancer in regeneration and tumorigenesis

During the study of the *wg*^{1}-enhancer across the different developmental stages we could notice that even after performing its developmental role at early stages, the enhancer continued to be accessible and showed a certain degree of activity (Figure 27). That was consistent with the ATAC data showing that the enhancer was still accessible during the L3 stage (Harris et al., 2020; Vizcaya-Molina et al., 2018). Why is this?

It has been shown that during regeneration many developmental enhancers are reused to drive regeneration (Suzuki & Ochi, 2020; Vizcaya-Molina et al., 2020; Yang & Kang, 2019). Indeed, our data indicate that *wg[1]* is a developmental enhancer that later in development is reused upon injury to drive regeneration in the wing disc (Figures 43, 45 and 46). As presented by Vizcaya-Molina and colleagues, *wg[1]* (or *BRV118* by defect) is an iDRRE, in other words, an enhancer that is already accessible but becomes even more accessible upon damage (Harris et al., 2020; Vizcaya-Molina et al., 2018). The fact that *wg[1]* is still active after performing its activity makes us think that it could be a primed enhancer. Primed or poised enhancers are those enhancers that, despite being accessible, are not active (Creyghton et al., 2010; Rada-Iglesias et al., 2011; Zentner et al., 2011). It is thought that this enhancer state allows a fast activation of the enhancers along development (Blanco et al., 2020; Spitz & Furlong, 2012). Therefore, it could be possible that some enhancers are kept primed to rapid respond upon damage. This idea is supported by the fact that most iDRREs in uninjured discs are free of the repressive histone mark H3K27me3 (Vizcaya-Molina et al., 2018). Besides, a recent report has shown in neonatal mice the supportive cells of the inner ear keep the enhancer network primed to be capable to regenerate upon damage. Interestingly, the primed state is lost over time together with the regenerative capacity (Tao et al., 2021). Hence, it could be possible that *wg[1]* is kept primed to allow a fast response to damage. Furthermore, it has been reported that the accessibility of the *wg[1]*-enhancer is lost over time (Harris et al., 2016, 2020). Therefore, it is possible that this loss of the primed state is paired with a loss of accessibility and a decrease in the regenerative potential. Furthermore, JNK could be contributing to the priming of the enhancer in development. It has been reported that in the developing disc, there is localised JNK expression along the A/P border in the pouch (Rankin Willsey et al., 2016), in the same exact spot where the *wg[1]-lacZ* reporter is expressed. Therefore, it could be possible that the binding of AP1 to the enhancer sequence contributes to keeping it accessible and responsive to further changes. However, the fact that the mutation of several high score AP1 binding sites does not affect the endogenous expression of the enhancer, while it does affect the expression of the enhancer in the damaged discs (Figure 44), does not support this role of AP1.

Regeneration and tumorigenesis share many molecules and pathways. Consequently, it has been proposed that cancer is a wound that does not heal (Flier et al., 1986). The same pathways involved in regeneration lead to tumour development when they are not properly regulated (La Marca & Richardson, 2020; Pinal et al., 2019). Moreover, two independent studies based on single-cell transcriptomics have shown that tumoral tissues present cell popu-

lations that resemble cell populations of the regenerative tissue. These populations seem to share the transcriptome and the gene regulatory networks (Floc'hlay et al., 2022; Worley et al., 2022). Our data on *wg*^{1}-enhancer supports these observations. Indeed, in tumoral cells, the *wg*^{1}-enhancer is aberrantly activated by continuous JNK signalling (Figure 51 and 53). In both cases, the activation of the enhancer promotes the expression of Wg and the proliferation and growth of the nearby tissue. The main difference between regeneration and tumorigenesis is the perdurance of the signalling in the tissue. While in regeneration the perdurance of these cells producing Wg is transient, in tumoral cells the blockage of apoptosis makes them remain in the tissue, turning them into a continuous source of promitotic molecules that lead to aberrant growth. Interestingly, the same phenomena seem to take place in vertebrate epithelia (Ankawa et al., 2021).

As previously shown, the *wg*^{1}-enhancer is not just involved in the expression of Wg in development, but it is also essential to triggering Wg expression in regeneration and tumorigenesis (Figures 48 and 54)(Dekanty et al., 2012; Harris et al., 2016). However, a controversy exists regarding the role of Wg as a promitotic molecule. While some authors claim that Wg promotes proliferation in the regenerative tissue (Harris et al., 2016; Ryoo et al., 2004; Smith-Bolton et al., 2009), others authors claim that compensatory proliferation can take place independently of Wg (Díaz-García & Baonza, 2013; Herrera et al., 2013; Pérez-Garijo et al., 2009). However, the study of Wg in regeneration is difficult due to the associated developmental problems that its depletion induces. Hence, extracting firm conclusions about the role of Wg in regeneration is hard. In this work, the use of CRISPR/Cas9-mediated deletions of both *Beta* (*Δβ*) and *Gamma* (*Δγ*), which have no major developmental effect by themselves, has allowed us to circumvent the developmental effect of Wg depletion and study its role in regeneration. Independent deletion of *Beta* or *Gamma* reduces the Wg levels, which translates into decreased cell proliferation and wing regeneration (Figure 48). The fact that each of the modules can reduce the expression of Wg by itself points towards a more independent role in driving Wg expression in regeneration and tumorigenesis than in development. Nevertheless, the fact that the deletion of both modules together reduces even more the levels of Wg indicates that they play a redundant role to guarantee the expression of Wg upon damage. Therefore, the use of the different deletions of the enhancer has allowed us to circumvent the developmental effects of Wg and confirm its requirement in regeneration as a promitotic molecule. This opens the door to the use of enhancers to study the role of developmental genes in regeneration circumventing the developmental effects that we would observe using other tools.

We have proven that the *wg[1]*-enhancer gets activated in the regenerative and tumoral disc in response to JNK activity (Figures 44 and 51). This is consistent with previous data showing a role of *wg[1]*-enhancer in CIN (Dekanty et al., 2012) and *dlg* (Harris et al., 2016) tumours. Oddly, the expression of the enhancer was not detected in Yki tumours (Harris et al., 2016). Overexpression of Yki by itself induces a massive overgrowth of the tissue. However, the tissue retains its normal epithelial polarity and cell-cell junctions (Staley & Irvine, 2012). Indeed, similarly to Ras tumours, Yki requires other mutations, such as loss of Mushroom body defect (Mud) or loss of polarity genes such as *scribble* (*scrib*) or *dlg*, among others, to become a neoplastic tumour (Gerlach et al., 2018; Grzeschik et al., 2010; Parra & Johnston, 2020; Sun & Irvine, 2013). Furthermore, the hyperplasia observed in Yki-overexpressing discs is mediated by its target promitotic gene *CycE* and antiapoptotic genes *diap-1* and *bantam* micro-RNA (J. Huang et al., 2005; Thompson & Cohen, 2006). Therefore, in a hyperplasic model where JNK activity is not very high and that does not mediate its overgrowth via Wg, it is expected that the *wg[1]*-enhancer is not active. Similarly, in the Ras^{V12} hyperplasia model, we would not expect to detect the activity of the enhancer. On the contrary, in the Ras^{V12} $Scrib^{-/-}$ model, where JNK is active (Igaki et al., 2006), we would expect to detect enhancer activity. For this reason, the enhancer is detected in the CIN or *dlg* tumoral models, where there is a strong JNK activity (Dekanty et al., 2012; Harris et al., 2016), but not in the Yki hyperplasia model.

Although the different deletions of the enhancers reduce the expression of Wg in regeneration and tumorigenesis, we still detect Wg expression in both cases (Figures 48 and 54). As it happens in development, this suggests the presence of shadow enhancers that play a redundant role in ensuring Wg expression in response to damage. Hence, once again, *wg[1]*-enhancer shows intra- and inter-enhancer redundancy to guarantee the expression of Wg. The redundant and shared use of the same enhancer to trigger the development of the wing and to allow the regeneration of the wing unveil the existence of a highly evolutionarily robust mechanism to ensure the development of the wing not only during normal development but also under stress conditions. Wings confer a huge developmental advantage to insects. Therefore, it is possible that other winged insects present the same or similar mechanisms to ensure the proper development of the wings during normal development and under stress conditions. *wg[1]* is localized within a Wnt cluster in the left arm of the second chromosome (Baker, 1987; Harris et al., 2016; Schubiger et al., 2010; Sharma & Chopra, 1976). Interestingly, it has been shown that this same genetic cluster is also conserved in other winged species such as *Tribolium, Apis* or *Anopheles.* Moreover, the synteny of the cluster is kept (Figure 81)(Bolognesi et al.,

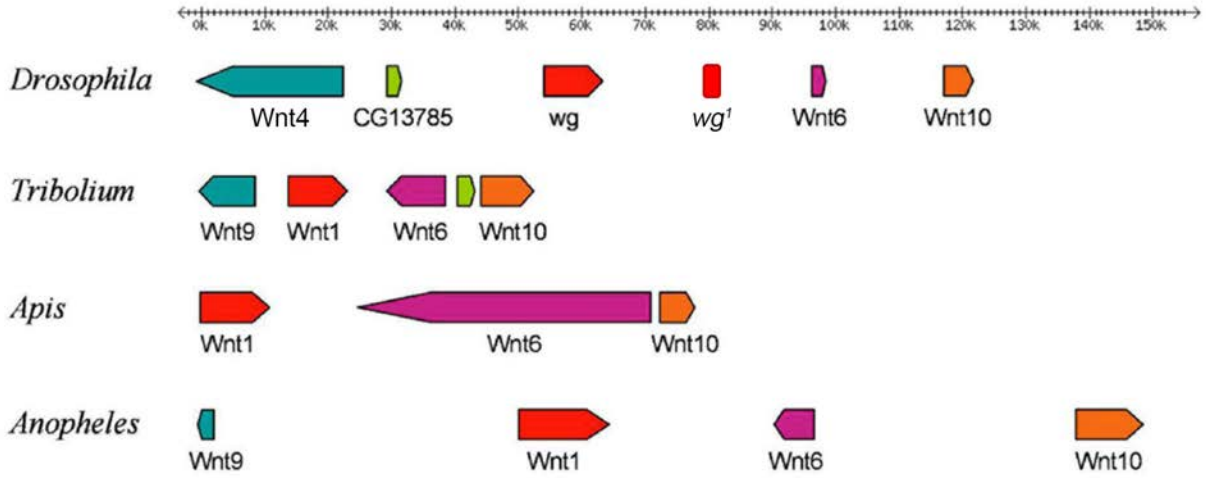

Figure 81. The Wnt cluster is conserved in other winged species. Representation of the Wnt genetic cluster conserved in *Drosophila, Tribolium, Apis* and *Anopheles*. The synteny of the cluster is kept among the four species. Adapted from Bolognesi et al., 2008.

2008). Hence, it might be possible that the *wg*^{1}-enhancer is conserved in the genome of other winged insects, ensuring the development of the wing under normal and stressful conditions.

wg^{1}, a pleiotropic or tissue-specific enhancer?

Enhancers that only perform a function in a specific tissue are the so-called tissue-specific enhancers. On the contrary, a pleiotropic enhancer is an enhancer that plays a role in multiple contexts, driving gene expression in various organs or at different time points. Interestingly, to perform its pleiotropic function, the enhancer can use the same or a different set of TFBSs (Sabarís et al., 2019). The *wg*^{1}-enhancer has always been referred to as a highly tissue-specific enhancer due to its remarkably restricted phenotype to the wing (Sharma & Chopra, 1976). However, an analysis of the data obtained during this work and from the literature challenge this view of the *wg*^{1}-enhancer.

The *wg*^{1} phenotype is characterized by the absence of wings paired with a duplication of the notum. Nevertheless, the *wg*^{1} flies also show an alteration of the ventral part of the eye (Figure 40)(Ma & Moses, 1995; Morata & Lawrence, 1977), minor effects on the leg (Held, 1993) and occasionally a partial or complete lack of the notal structures (Figure 40)(Sharma & Chopra, 1976). Consistently, when we analysed the expression of the *wg*^{1}*-lacZ* reporter, we could detect its expression in the eye-antenna, leg and notum of the wing disc (Figure 40), suggesting that the enhancer could have a role in the development of these structures. Interestingly, not all the modules of the enhancer were expressed in all the circumstances. Indeed, only *Alpha* was expressed in the notum of the wing disc, whereas both *Alpha* and *Beta* showed

expression in the eye-antenna disc in the region where Wg is endogenously expressed to repress the eye fate and give rise to the head (Figure 40)(Legent & Treisman, 2008). Oddly, only the deletion of *wg*^{1} (*Δwg*^{1}) and not *BetaGamma* deletion (*ΔβγΔ*) presented the alteration in the notum and the eye, suggesting that the expression in the notum and eye phenotypes is due to *Alpha* and not to the rest of the enhancer. Interestingly, in the *wg* 3' genomic region next to *wg*^{1} it was described the presence of two regulatory regions, *wg-2* and *wg-9* (Figure 82), capable to drive *lacZ* expression in the eye-antenna, leg and notum of the wing disc in a very similar expression pattern as the one showed by our reporters (Pereira et al., 2006). In fact, the *wg-9* region and some of the *wg-2* subdivisions, partially overlap with the *Alpha* domain of the *wg*^{1}-enhancer, suggesting that these two genomic regions are part of the same notal and eye enhancer (Figure 82)(Pereira et al., 2006). Altogether, these data seem to indicate that in the *wg* 3' genomic region, there is a cluster of partially overlapping enhancers that contribute to regulating the differential expression of *wg* in the eye-antenna, leg and notum of the wing disc. Furthermore, the data indicate that the modules *Beta* and *Gamma* compose the enhancer specifically devoted to the development of the wing. Nevertheless, we have to bear in mind that the boundaries of enhancers are not always clear and defining them is hard, especially in a genome as small as that of *Drosophila* where enhancer clusters are more common (Fujioka et al., 1999; Fujioka & Jaynes, 2012; Henriques et al., 2018; Lorberbaum et al., 2016).

The fact that the pleiotropic effect observed in *wg*^{1} deletion might be explained by the

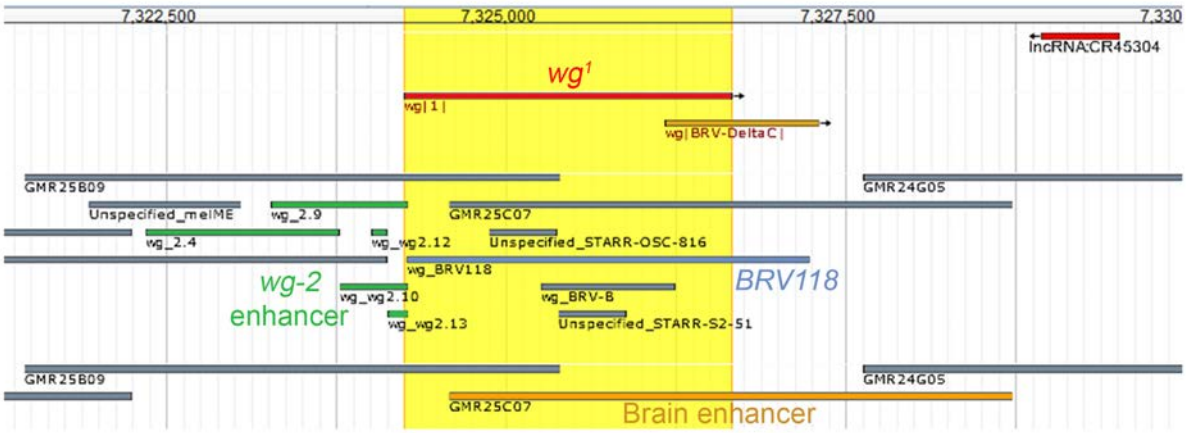

Figure 82. Enhancers overlapping *wg*¹. Screenshot of the genomic region comprising the sequence of the *wg*¹-enhancer. *wg*¹-enhancer is marked in red and the genomic region that occupies is highlighted in yellow. The sequence of *BRV118* is marked in blue, the partially overlapping fragments of the *wg-2* enhancer are marked in green and the overlapping putative brain enhancer (*GMR25C07*) is marked in orange. The screenshot has been obtained from the JBrowser from FlyBase looking at the Transcriptional Regulatory Regions from REDFly and the Putative Brain enhancers from Janelia Gal4 lines.

deletion of two distinct elements, the notal/eye enhancer and the wing enhancer composed by *Beta* and *Gamma,* argues against the fact that wg^1 is a pleiotropic enhancer. However, there is additional evidence that supports the idea that wg^1 is a pleiotropic enhancer. Firstly, it has been shown that wg^1 can be used as a *wg* null allele during the study of the adult brain. Indeed, it seems that wg^1 contributes to the expression of *wg* during the formation of the synapsis in the neuromuscular junction (Ataman et al., 2008; Y. Huang et al., 2018) and in the differentiation of the glia and neurons in adult flies (Kerr et al., 2014). Besides, in Huntington's Disease model, wg^1 deletion contributes to the expansion of the life span of the affected flies by depleting Wg expression (Dupont et al., 2012). Therefore, this data supports the idea that wg^1 might be playing a role in the adult brain. Indeed, it had been described a putative brain enhancer, GMR25C07 (REDfly_CRMs: FBlc0000493)(Jenett et al., 2012), that practically overlaps the totality of wg^1 (Figure 82). Therefore, the data suggest that wg^1 also could be a brain enhancer. Secondly, wg^1 is capable to drive *wg* expression in two different contexts, development and regeneration, by using two different sets of TFBSs. Moreover, the enhancer was capable to respond to damage in the leg (Harris et al., 2016; Schubiger et al., 2010), and to JNK ectopic activity in the haltere and eye-antenna discs, in the larval brain and the adult gut in addition to the wing disc (Harris et al., 2016). However, it is important to highlight that although the expression of the enhancer colocalized with JNK clones, many JNK clones did not show enhancer activity (Harris et al., 2016). Moreover, some of the expression patterns observed in the damaged tissue were reminiscent of the ones observed with our reporter during regular development. For example, the two dots that they observe upon damage in the larvae brain were also present in non-injured brains (Figure 40). Furthermore, the authors claimed that the enhancer showed expression in damaged adult guts, suggesting that it could be driving *wg* expression in the damaged gut (Harris et al., 2016). Wg is required to allow the expansion of the intestinal stem cells (ICSs) and allow regeneration, thus its depletion induces a lack of regeneration (Cordero et al., 2012). Therefore, it could be that the wg^1-enhancer might be regulating the expression of Wg in injured guts. Thus, we assessed the expression of the wg^1-*lacZ* reporter in the gut. However, we were not capable to detect any signal of the reporter in damaged guts (Figure 83A). Nevertheless, the gut is a hard tissue for staining, so we decided to directly assess whether the deletion of the enhancer had an impact on the regenerative capacity of the gut. To do so, we quantified the increase of ICSs that occur during the regeneration of the gut in control, $\Delta wg^1/\Delta BRV118$ and $\Delta\beta\gamma$ flies, but no differences were observed between control flies and flies carrying the enhancer deletion (Figure 83B and C). Therefore, we concluded that the increase of Wg expression in damaged guts is not driven by the wg^1-enhancer.

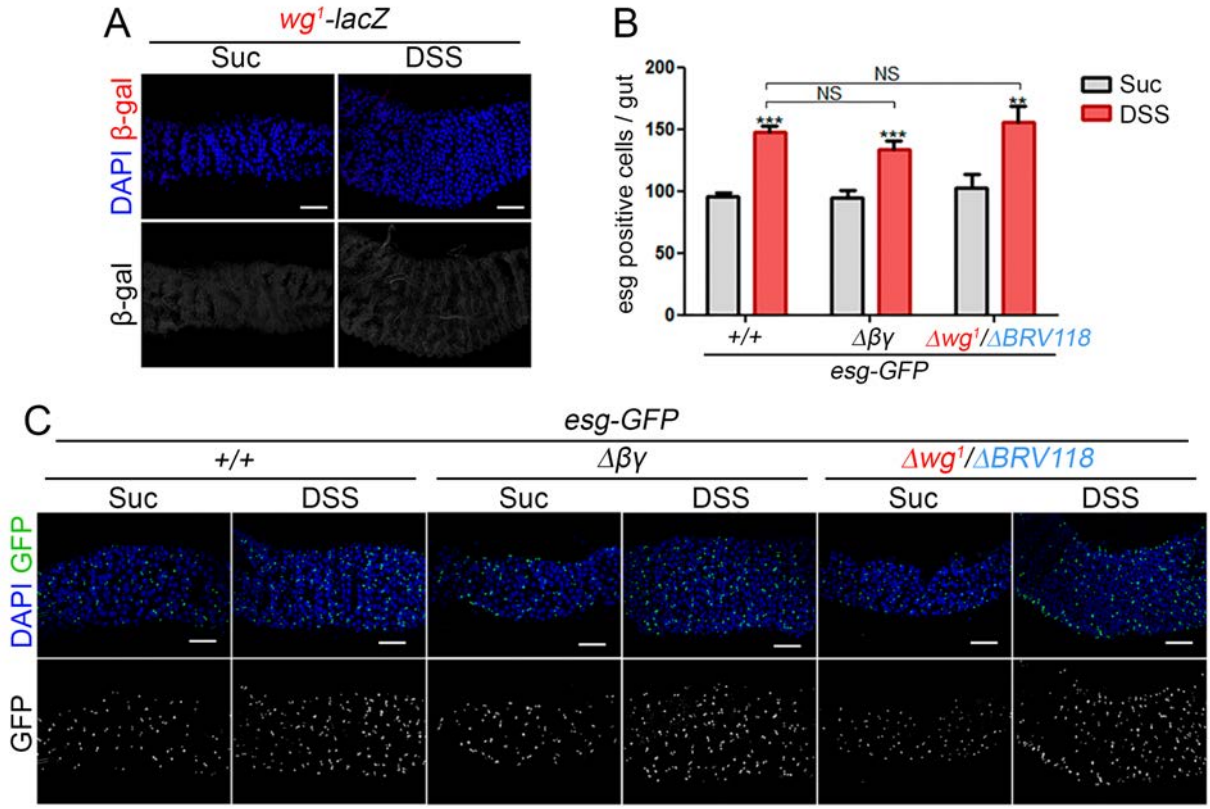

Figure 83. *wg¹* deletion does not affect the regenerative capacity of the gut. A and C) Posterior midguts of adult female flies of the indicated genotypes feed for two days with 5% sucrose or 3% of the damaging agent dextran sulfate sodium (DSS) and stained for β-galactosidase (in red or white, A), GFP (green or white, C) and DAPI (blue). Scale bar: 50 µm. **B)** Histogram showing the number of ICS (esg positive cells) per gut of flies of the indicated genotype after two days of feeding with 5% sucrose (grey) or 3% DSS (red). Two-ways ANOVA with Tukey HSD's multiple comparison test was applied when comparing the difference in means of different experimental groups and diets. Values represent mean ± sd. Statistically significant differences are shown: NS, $p > 0.05$; **$p < 0.01$; ***$p < 0.001$. C) Representative images of the guts quantified in B.

Altogether, these results suggest that the role of *wg¹* as a damage enhancer in different tissues must be carefully reassessed. Nevertheless, a recent report supports the idea of *wg¹*-enhancer as a broad damage response element as it has shown that adult *wg¹* flies subjected to brain damage regenerate much worse than control flies (Simões et al., 2022). Altogether, this data supports the idea that *wg¹* is a pleiotropic enhancer.

The fact that *wg¹* is a pleiotropic enhancer that can play functions in tissues such diverse as the imaginal discs or the adult brain is not a crazy idea. In the literature, there are many examples of very different organs using the same enhancers to drive gene expression. For example, a study performed on the mouse forebrain, heart, and liver showed that 52% of the putative enhancers were active in more than one organ (Nord et al., 2013). Even for highly tissue-specific enhancers, evidence of pleiotropy has been reported. Indeed, an enhancer of the *eve* gene, that is involved in the establishment of *eve* strips during embryogenesis,

has been reported to be expressed in ganglion mother cells, neurons and the anal plate ring (Fujioka et al., 1999). Moreover, the reuse of enhancers is not only common in physiological conditions but also during regeneration. In fact, in *Drosophila* damaged discs, 58% of the enhancers activated upon damage were also active in other tissues and/or other developmental time points (Vizcaya-Molina et al., 2018). Hence, enhancer pleiotropy is more prevalent than originally thought. It has been proposed that pleiotropic enhancers are more conserved than tissue-specific enhancers, most probably because alterations in these enhancers would alter gene and protein expression in several tissues. Indeed, a study showed that pleiotropic enhancers were twice more conserved than tissue-specific enhancers (Andersson et al., 2014). A clear example that pleiotropy potentiates conservation is the fact that limb enhancers from the mice seem to be conserved in different snake species. It was found that these limb enhancers were also enhancers from the genital tubercle. Hence, the authors suggest that these enhancers are conserved in snakes due to their role during genitalia development (Infante et al., 2015). Therefore, if wg^{1} is indeed a pleiotropic enhancer instead of a tissue-specific enhancer, is more probable to be is conserved in other species.

Role of Wnt6 in regeneration and tumorigenesis

Wnt6 is a member of the Wnt family that is expressed in the developmental wing discs in a pattern that perfectly resembles the expression of Wg both in the late (Janson et al., 2001; J. J. S. Yu et al., 2020) and early stages (Figure 25). Interestingly, experiments performed by Harris and colleagues showed that the damaged wing disc also expressed Wnt6 (Figure 43) and that its expression relied on the wg^{1}-enhancer (Harris et al., 2016). In the developmental disc, Wnt6 plays little role there because its deletion just caused minor effects in the margin of the wing (Doumpas et al., 2013). Moreover, it seems that Wnt6 is not capable of activating the canonical Wnt signalling (Herr & Basler, 2012). Consistently, when we analysed its role in the developing wing, we could not detect any major effect of Wnt6 deletion in the discs (Figure 25), supporting the idea that it is Wg, and not Wnt6, the protein that is required for wing fate specification. For this reason, it was a surprise to see that Wnt6 plays a role in the regeneration and tumorigenesis of the wing disc (Figure 79). Indeed, while the depletion of *wnt6* in the damaged disc impairs regeneration (Figure 49), in the tumoral disc prevents the tumoral overgrowth (Figure 55). How this could be?

As previously mentioned, Wnt6 has no major role neither in wing fate specification (Figure 25) nor later in wing growth (Doumpas et al., 2013). Nevertheless, it seems that Wnt6

holds a certain extent of mitogenic activity. Indeed, in discs where Wg activity is depleted, co-depletion of Wnt6 results in even smaller wings. This implies a possible promitotic role of Wnt6 (Barrio & Milán, 2020). This suggests that, in normal development, Wg drives the totality of the Wnt activity and only when it is depleted Wnt6 can bind to the receptor and activate the pathway to a certain extent. Therefore, in a situation such as the regenerative or the tumoral disc, where the demand for Wnt activity sharply increases, Wg by itself might not be sufficient and, therefore, Wnt6 could be require. However, the fact that Wnt6 cannot activate canonical Wnt signalling (Herr & Basler, 2012) is in direct conflict with this theory. Another option would be that Wnt6 performs its function through the activation of the non-canonical Wnt pathway (Wnt/PCP). Indeed, it has been shown that in the testis Wnt6 regulates cell proliferation and apoptosis through the non-canonical Wnt pathway components Rac1 and Cdc42. However, the authors report an increase in proliferation and cell death upon Wnt6 depletion (Wang et al., 2021). Hence, the role of Wnt6 observed in the testis goes in the opposite direction of our observations in the regenerative discs where *wnt6* depletion reduces proliferation.

Altogether the data our data show that *wg*^{1}-enhancer mediates its activity in regeneration and tumorigenesis through both Wg and Wnt6. However, further research is needed to clarify how Wnt6 mediates its proliferative role in these two processes.

Senescence in the regenerating wing disc

During our regeneration experiments, we unravelled the existence, upon *egr* induction, of a cell population characterized by large nuclei and resistance to cell death, both hallmarks of senescence (Figures 56 and 59). Senescence is a cellular state characterized by a stable cell cycle arrest and highly proactive secretome. However, the phenotype associated with senescence is highly heterogeneous and variable, making it hard to establish universal markers to identify it. Hence, it is required to characterize several markers to establish that a cell is senescent (González-Gualda et al., 2021; Gorgoulis et al., 2019; Hernandez-Segura et al., 2018). The analysis of several senescence hallmarks such as their cellular arrest, the release of molecules from the SASP or the presence of SA-β-gal activity, among others, allowed us to conclude that those cells were senescent (Figures 61 to 72). Moreover, the presence of senescent cells in *egr*-expressing discs has been confirmed by an independent study that has shown the presence of a cell population that presents an enhancer Gene Regulatory Network characteristic of senescent cells (Floc'hlay et al., 2022). Two main questions arise from the presence of senescent cells in regenerative tissue. Firstly, which are the pathways implicated in

the establishment of senescence and cell death resistance? Secondly, which role do senescent cells play in regenerative tissue? These are the two main questions that we will try to address in this section.

Stg and Trbl mediate the cell cycle arrest in the senescent population

In the senescence field is very accepted that the cellular arrest in senescent cells occurs at G1 and is mainly mediated by p53 and p21 (reviewed in Gire & Dulic, 2015; Kumari & Jat, 2021). However, in the *Drosophila* field a controversy exist on whether senescent cells are arrested in G1 or G2. In our CIN model, the cell cycle arrest in senescent cells occurs at the G2 phase and is mediated by JNK (Joy et al., 2021). Interestingly, the arrest is mediated by the up-regulation of Trbl and the down-regulation of Stg induced by JNK (data not published). Similarly, a previous report showed that in the *egr*-expressing discs, the progression from the G2 to the M phase is blocked by the down-regulation of Stg and an up-regulation of Trbl, inducing the stalling of the cells at G2 (Cosolo et al., 2019). Supporting the role of JNK as a crucial driver of senescence, in aged *Drosophila* midguts the establishment of age-related senescence is mediated by JNK (Takeda et al., 2018). On the contrary, the laboratory of Dr Igaki claims that in the Ras^{V12} model, the cell cycle arrest occurs at G1 and is mediated by p53/p21 (Nakamura et al., 2014). However, our laboratory has shown that while short periods of Ras^{V12} expression in the disc induce a G1-S transition, the sustained activity of Ras^{V12} induced the arrest of cells at G2 (Murcia et al., 2019). Interestingly, a later report from Dr Igaki's laboratory supports our observation. They showed that in Ras^{V12} cells the majority of cells were at G2 and not at G1. Besides, they showed that Ras^{V12} tumours expressed Trbl in addition to Dap, *Drosophila* p21 ortholog (Ito & Igaki, 2021). The main conclusion that we can obtain from these observations is that further research is required to establish whether senescence in *Drosophila* is established via JNK or p53/p21 or by a combination of both.

In our damage model, which is based on the overexpression of *egr,* JNK activity is strongly activated. By using the FlyFUCCI system we could observe that the cells were arrested at G2 (Figure 62). That was consistent with previous observations from Dr Classen's laboratory that upon *egr* overexpression cells were stalled at G2 by the downregulation of Stg and upregulation of Trbl (Cosolo et al., 2019) and the G2 arrest of senescent cells in our CIN model (Joy et al., 2021). Interestingly, the majority of senescent cells did not show p53 activity nor *dacapo* expression (*Drosophila* p21 ortholog; Figures 73 and 74). Hence, our data indicate that the G2 arrest observed in the senescent population of *egr*-expressing discs is not mediated by p53/

p21. On the contrary, it seems to be mediated directly by JNK through the down-regulation of Stg and an up-regulation of Trbl as supported by the data from Dr Classen's laboratory (Cosolo et al., 2019). Indeed, the evidence indicates that the stalled cells reported by Cosolo and colleagues are our senescent cells. Hence, the evidence indicates that in our *egr*-expressing discs, the cell cycle arrest of the senescent population at G2 is mediated by JNK through the upregulation of Trbl and the downregulation of Stg.

Exploring possible candidates to mediate cell death resistance in the senescent population

A striking fact about our senescent population is that although they present high levels of JNK activity, the cells do not die. The fact that in our model cells present scattered expression of p53 (Figure 73) suggests that in the senescent population, p53 does not play a relevant role, as it occurs in our CIN model (Joy et al., 2021). Therefore, the question arises of who might be regulating the cell apoptosis resistance in our senescent population. In this section, we will analyse several candidates that could be mediating the survival of the senescent cells in the *egr*-expressing discs.

A recent report showed that cells arrested at the G1 or G2 phase of the cell cycle, both naturally or induced, were protected from dying upon irradiation. Furthermore, forcing the cell cycle progression increased the number of dying cells in the tissue upon irradiation (Ruiz-Losada et al., 2022). Therefore, it could be that Stg and Trbl are playing a role further away than mediating the cell cycle arrest at G2. Firstly, we decided to force the arrest of the cells at G2 in damaged discs by overexpressing *trbl*. Consistently with the Ruiz-Losada report, upon the forced arrest at G2 by overexpressing *trbl,* we detected a drastic decrease in pyknotic nuclei and caspase activity. Besides, this was accompanied by an increase in senescent-like cells (Figure 76). However, when we analysed the regenerative capacity of those discs, they regenerate much worse than control wings (Figure 77). On the contrary, when we forced the cell cycle progression, the discs were pretty much like wild type discs and just a discrete number of dying cells could be observed basally (Figure 76). Furthermore, these discs presented the same or even greater regenerative capacity than control discs (Figure 77). This was consistent with previous observations from Cosolo and colleagues and they concluded that persistent stalling at G2 interferes with regeneration (Cosolo et al., 2019). However, this contradicts the observations made by Ruiz-Losada and colleagues, that reported that cycle progression increased the number of deaths (Ruiz-Losada et al., 2022). Interestingly, it was reported that in

egr-expressing eye discs cell death was prevented by the overexpression of CycE, obtaining practically wild type-like eyes. Furthermore, the authors showed that CycE can prevent JNK activity in discs overexpressing a constitutively active form of Hemipterous, the JNKK, or in Ras^{V12} tumour cells with defective mitochondria (Nakamura et al., 2014). Hence, aside from the role of CycE regulating the progression from G1 to the S phase, it seems that also could have a role in regulating the activity of JNK and its ability to induce cell death. This is pretty reminiscent of what we observe in *egr*-expressing discs where *stg* has been upregulated or *trbl* has been depleted (or both at the same time), where we obtain almost wild type discs that give rise to fully normal wings (Figure 76). Therefore, it could be that Stg would be regulating the activity of JNK and preventing the activation of the caspase cascade. Hence, the resulting wings would not be a result of a regeneration process, but a result of regular development. To test this hypothesis would be interesting to test the levels of JNK activity in the discs where cell cycle progression has been forced. It is indeed odd that in both cases, when we force the cell cycle and when we arrest it, we detect a decrease in caspase activity but the resulting wings are on different sides of the regeneration spectrum. The fact that caspase activity is decreased in damaged discs that present *trbl* overexpression suggests that Trbl may be regulating the activity of the caspases. In fact, in mammals, it has been reported that Trbl3 has the capacity to prevent cell death by sequestering the procaspase-3 in the nucleus (Shimizu et al., 2012). Nevertheless, this does not explain why wings do not regenerate when the proapoptotic input is silenced by placing flies back at 18 ºC. A possible explanation might be that while *trbl* is expressed can prevent the activity of the caspases and cell death. However, when we put back the flies at 18 ºC we not only silence the proapoptotic input, but we also silence *trbl*. Therefore, the caspase activity can no longer be stopped and cells massively die. To confirm this, it would be interesting to monitor the dynamics of cell death in control and *trbl*-expressing discs at different regenerative time points and confirm whether massive cell death occurs upon *trbl* silencing. Although more research is needed to clarify how Trbl and Stg perform their functions, it is clear that they play a role not just in cell cycle arrest but also in cell death resistance. Indeed, our data place them as key elements for senescent cells to survive proapoptotic inputs.

In mammals, the antiapoptotic members of the B-cell lymphoma 2 (Bcl-2) family play a crucial role in mediating the cell death resistance of senescent cells (reviewed in Anantram & Degani, 2019; Basu, 2022). Hence, Bcl-2 family orthologs in *Drosophila* would be clear candidates to mediate the cell death resistance in the senescent population. Indeed, *Drosophila* presents two orthologs of the Bcl-2 family: Buffy and Debcl (Igaki & Miura, 2004). Neverthe-

less, it seems that they play a little role in programmed cell death in *Drosophila*. Instead, the main drivers of *Drosophila* cell death are Reaper, Hid and Grim (reviewed in Clavier et al., 2016). Therefore, despite Bcl-2 antiapoptotic members playing a central role in mammalian senescent cell death resistance, it is hard to believe that they would play a significant role in cell death resistance in *Drosophila* senescent cells.

In recent years, increasing evidence has put mitochondria as a central element of senescence. In fact, senescent cells present a dramatic change in mitochondrial mass, dynamics, structure and function (reviewed in Abate et al., 2020; Ghosh-Choudhary et al., 2021; Martini & Passos, 2023; Miwa et al., 2022; Vasileiou et al., 2019). One of the causes that leads to the accumulation of dysfunctional mitochondria is the alteration of their dynamics. Senescent cells present an increase in fusion and a decrease in fission that result in elongated and branched mitochondria. These elongated mitochondria hinder mitophagy, resulting in their accumulation (Dalle Pezze et al., 2014; Korolchuk et al., 2017; Lee et al., 2007; Yoon et al., 2006). The accumulation of dysfunctional mitochondria in senescent cells leads to increased production of ROS that contributes to increased DNA damage and the activation of the DDR response (Passos et al., 2010). Besides, it has been shown that mitochondria also influence the molecules secreted by the SASP (Correia-Melo et al., 2016). Interestingly, mitochondria are more than just players in senescence because the disruption of their homeostasis can induce by itself the establishment of cellular senescence, the Mitochondrial dysfunction-associated senescence (MiDAS)(Lee et al., 2007; Nakamura et al., 2014; Stöckl et al., 2007; Wiley et al., 2016). Furthermore, mitochondria are also tightly linked to programmed cell death both in mammals and in *Drosophila* (Fuchs & Steller, 2015). Therefore, it is not a surprise that in recent years it has been proposed that mitochondria could be playing a role in cell death resistance in senescent cells (Abate et al., 2020; Martini & Passos, 2023). Mitochondria dynamics is a mechanism to ensure mitochondria homeostasis. On one hand, fission plays a role in segregating dysfunctional mitochondria from the entire mitochondrial network and sorting out mutant mitochondria DNA (mtDNA) copies. On the other hand, fusion is a way for the mitochondria to obtain matrix metabolites, intact mtDNA copies and mitochondrial membrane components (Twig & Shirihai, 2011). Nevertheless, it has been also shown that mitochondrial dynamics play a role in apoptosis. Indeed, fission is a requirement for apoptosis and it seems to happen prior to caspase activation (reviewed in Otera & Mihara, 2012; Suen et al., 2008). Similarly, mitochondrial fission is also essential for programmed cell death in *Drosophila* (Goyal et al., 2007). Indeed, the inhibition of the pro-fission gene *drp-1*, the main driver of fission, prevents the ac-

tivation of the apoptosis both in mammals and *Drosophila* (Abdelwahid et al., 2007; Estaquier & Arnoult, 2007; Frank et al., 2001; Goyal et al., 2007). On the other hand, it is thought that mitochondria hyperfusion might contribute to the protection against apoptosis in senescent cells, but more research is required in that regard (Martini & Passos, 2023). The mitochondria of our senescent population present a clear elongated and branched structure (Figure 69), indicating that mitochondrial dynamics might be altered. Although we do not know whether the resulting elongated mitochondria is caused by problems in fission, fusion or both, this observation makes us think that maybe apoptosis could be hampered due to the lack of mitochondrial fission. Hence, it could be that mitochondria would be playing a role in cell death resistance. Even though more experiments are required to clarify the role of mitochondria dynamics in the survival of senescent cells, they appear as a strong candidate.

Another possible candidate to mediate the cell death resistance in the senescent population is Yki. Upon damage, Yki gets expressed in the discs and mediates growth (Grusche et al., 2011; Sun & Irvine, 2011). However, Yki also presents antiapoptotic functions by mediating the expression of *bantam* microRNA and Diap-1 (J. Huang et al., 2005; Thompson & Cohen, 2006). On one side, overexpression of Diap-1 prevents the activation of the caspase cascade (Muro et al., 2002; S. L. Wang et al., 1999). On the other side, it has been shown that *bantam* prevents *hid* expression by targeting its mRNA (Brennecke et al., 2003; Moberg & Hariharan, 2003). Interestingly, a recent report from Dr Classen's laboratory has shown the expression of Yki in the stalled population that corresponds to our senescent cells (Crucianelli et al., 2022). Hence, it could be that Yki would be mediating prosurvival signalling in the senescent population. However, recent reports have shown that Yki antagonises cell cycle arrest in tumours (Gerlach et al., 2018, 2019; Ito & Igaki, 2021). More specifically it seems that it can mediate the upregulation of Stg (Gerlach et al., 2018, 2019) and the downregulation of Trbl via *bantam* (Gerlach et al., 2019; Ito & Igaki, 2021). These observations are in direct conflict with the fact that in the senescent population, the cell cycle arrest is mediated by the downregulation of Stg and the upregulation of Trbl. Therefore, the odds that Yki mediates the survival of the senescent population are low.

MAPK play an important role in senescence. Indeed, the MAPK p38 and Erk have been reported to contribute to the regulation of SASP and the cell cycle arrest. However, their role in senescent cell survival is not that clear (reviewed in Anerillas et al., 2020). For example, depending on the trigger, p38 can mediate both prosurvival and proapoptotic signals (Igea & Nebreda, 2015). We considered p38 and Erk as possible mediators of the senescent cell death

resistance because of the roles that they perform in *Drosophila.* For a long time, it has been known that Erk has the capacity to repress Hid and prevent cell death (Bergmann et al., 1998; Kurada & White, 1998). Interestingly, two independent studies showed that apoptotic cells trigger EGFR/Erk waves in their neighbouring cells promoting their survival (Gagliardi et al., 2021; Valon et al., 2021). Hence, it could be that upon damage, dying cells promote the survival of senescent cells by inducing the activity of Erk activity. Similarly, p38 performs a function during the regeneration of the *Drosophila* wing disc. Upon the damage to the disc, p38 is activated by ROS via Ask1 (Santabárbara-Ruiz et al., 2019) and, the inhibition of p38 negatively impacts the regenerative capacity of the wing (Santabárbara-Ruiz et al., 2015). Interestingly, p38 also is essential for midgut regeneration (Patel et al., 2019) and during embryonic wound repair (Scepanovic et al., 2021). Hence, it could be possible that p38 mediates the survival of the senescent cells. Staining against the phosphorylated forms of p38 and Erk would shed some light on whether they are active in the senescent population or not and, therefore, if they could be playing some role in the survival of senescent cells.

Senescent cells in the regenerative tissue, a friend or a foe?

Traditionally, senescence has been associated with ageing and age-related diseases such as cancer, arteriosclerosis or Alzheimer's disease, where it primarily plays a deleterious role (reviewed in Calcinotto et al., 2019; Cuollo et al., 2020; Lee & Schmitt, 2019; Muñoz-Espín & Serrano, 2014). Nevertheless, recent publications have shown that senescence plays a positive role during development and regeneration (reviewed in Antelo-Iglesias et al., 2021; Rhinn et al., 2019; Walters & Yun, 2020; Wilkinson & Hardman, 2020), breaking the dogma that senescence is primarily limited to age-related dysfunction and cancer.

The idea of senescence playing a role in regeneration is relatively new. The presence of senescent cells has been described in different organisms and organs. For example, in mice skin subjected to damage, it has been described that senescent cells promote the closure of the wound (Demaria et al., 2014) and prevent fibrosis (Jun & Lau, 2010). Similarly, senescent cells also prevent fibrosis in the damaged mice heart (Meyer et al., 2016; Zhu et al., 2013), in the skeletal muscle (Saito et al., 2020) or in the liver (Krizhanovsky et al., 2008). Furthermore, it has been described that senescent cells also play a role during limb regeneration in both axolotls and zebrafish (Da Silva-Álvarez et al., 2020; Q. Yu et al., 2022; Yun et al., 2015). It seems that the presence of senescent cells in the regenerating limb is transient, at least in axolotls (Yun et al., 2015), and that its depletion using senolytics, a group of drugs that spe-

cifically targets senescent cells, drastically reduce their proliferative and regenerative capacity (Da Silva-Álvarez et al., 2020; Q. Yu et al., 2022). Nevertheless, there are also examples of the negative role of senescent cells during regeneration. For instance, it has been described that senescent cells can promote fibrosis and impairment of renal function in the kidney upon transplantation (Braun et al., 2012) or after acute kidney injury by ischemia-reperfusion (Li et al., 2021; Mylonas et al., 2021). Interestingly, it has been reported the presence of senescent cells upon spinal cord injury in mice and zebrafish. However, while in zebrafish the presence of senescent cells is transient and leads to an improvement in regeneration, in mice senescent cells accumulate over time and impair regeneration by the promotion of fibrosis (Paramos-de-Carvalho et al., 2021). This suggests that the amount of time that senescent cells spend in the regenerative tissue is crucial to determine whether they play a positive or a negative role in regeneration. In fact, Antelo-Iglesias and colleagues propose that upon damage cellular senesce is induced in the tissue to promote regeneration. Hence, the elimination of senescent cells of the regenerative tissue impairs regeneration. Furthermore, they propose that the presence of senescent cells in the regenerative tissue must be transient. Indeed, the data supports that the accumulation and persistence of senescent cells over time produces a negative effect, favouring fibrosis and impairing regeneration (Antelo-Iglesias et al., 2021).

Different reports have shown that senescent cells can play both a beneficial and a detrimental role during tissue regeneration, but what role do we expect senescence plays in our regenerative model? In fact, there is evidence that senescence could be playing a positive role in the regeneration of *egr*-expressing discs. A recent report from Dr Hariharan's laboratory can shed some light on that regard. They have reported that upon *egr* overexpression in the wing discs, two specific regenerating cell populations appear within the blastema which they have named Blastema1 and Blastema2 (Worley et al., 2022). Similarly, Floc'hlay and colleagues also reported the presence of two regeneration-specific cell populations in the *egr*-expressing discs: the α and β populations (Floc'hlay et al., 2022). In fact, the β population from Floc'hlay and colleagues and the Blastema1 from Worley and colleagues are the same cell population. Moreover, the β population is composed of senescent cells (Floc'hlay et al., 2022) and it corresponds to our senescent population. Therefore, the Blastema1 population, the β population and our senescent population are the same group of cells. Interestingly, Worley and colleagues identified a transcriptional factor crucial for the function of the senescence population: Ets21C (Worley et al., 2022). Depletion of *ets21C* in the regenerating disc drastically reduces its regenerative capacity. However, the effect that they observed was not caused by the disap-

pearance of the Blastema1 population. On the contrary, the effect was caused by the lack of capacity to maintain the secretome expression over time. In the beginning, the expression of MMP1, Dilp8, or Upd3, among others, is triggered by JNK in the *egr*-expressing disc. However, Ets21C is required to maintain their expression over time, even when JNK activity has already decreased. Hence, *ets21C*-depleted discs fail to maintain the expression of the secretome. This loss of the secretome has two interesting effects. On one side, it seems that it changes the pattern of cell proliferation during regeneration. On the other side, it seems that cells in *ets21C*-depleted discs present a more advanced cellular maturity state and that they prematurely start the repatterning of the discs (Worley et al., 2022). This is consistent with the fact that senescent cells trigger the dedifferentiation of the nearby cells increasing their cellular plasticity through the SASP (reviewed in Ring et al., 2022). Therefore, in discs lacking the secretome this dedifferentiated state could not be maintained. In conclusion, although the authors did not eliminate the senescent population from regenerative tissue, they recapitulate what its elimination would cause through the depletion of the secretome. Even so, the data show that the senescent population would play a positive role during regeneration. The use of senolytics to try to specifically eliminate the senescent population from the regenerative disc would help us to clarify whether the senescent population truly plays a positive role in the regeneration of the discs.

Finally, the last question that arises from the presence of senescent cells in *egr*-expressing discs is whether the senescent cells could be found in other damage models or not. Similarly as it occurs in *egr*-expressing discs, it has been reported the presence of big nuclei cells stalled at G2 in physical injury wing discs. Besides, in these discs, the G2 stall is also mediated by JNK (Cosolo et al., 2019). Hence, it is highly possible that these cells indeed are senescent. The same authors also analysed the presence of big nuclei cells stalled at G2 in *hid*-expressing discs. However, they were not successful to detect any cell with these characteristics (Cosolo et al., 2019). Interestingly, although *hid* overexpression triggers cell death, its activation results in controlled delamination of apoptotic cells, maintaining the integrity and architecture of the epithelium (Cosolo et al., 2019; Crucianelli et al., 2022; Herrera et al., 2013). This contrast with *egr* and *rpr* models that show a complete loss of epithelial integrity and architecture (Bergantiños et al., 2010; Smith-Bolton et al., 2009). The fact that the tissue integrity is kept in *hid*-expressing discs leads to lower activation of the JNK pathway (Crucianelli et al., 2022). All these data indicates that the establishment of senescence is mediated by JNK. Therefore, the low activity of JNK in *hid*-expressing discs difficults the establishment of senescence, despite

the presence of cell death. In contrast, in the *rpr* model, a strong loss of the epithelial integrity and architecture highly activates the JNK pathway (Bergantiños et al., 2010). However, the fact that the caspase cascade is directly activated by the expression of *rpr* might difficult the survival of the cells long enough to become senescent. Finally, discs subject to irradiation present a transient arrest in G2. However, the arrest in G2 seems generalized throughout the disc and seems to serve the purpose to prevent massive cell death after irradiation (Ruiz-Losada et al., 2022). Although it could be possible that some of those cells have become senescent, it is hard to believe that all of them are senescent. Furthermore, their morphology is not indicative of senescence. In conclusion, more experiments would be required to confirm the presence of senescent cells in other regenerative models. Nevertheless, it is highly possible that upon physical damage senescent cells appear.

Conclusions

Based on the experiments carried out during the development of this thesis, we can conclude that:

1. The *wg*^{1} deletion includes an enhancer that triggers the early expression of Wg in the wing disc, allowing the specification of the wing.
2. In development, the *wg*^{1}-enhancer is positively regulated by Hh signalling and negatively by the EGFR and JAK/STAT pathways.
3. We have narrowed down the wing-specific enhancer to a 1.8-kb-long genomic region formed by the *Beta* and *Gamma* modules.
4. *Beta* and *Gamma* modules show intra-enhancer redundancy to guarantee the early expression of Wg and the specification of the wing.
5. Although Wnt6 expression is also driven by the *wg*^{1}-enhancer at the early stages of development, it does not contribute to the specification of the wing.
6. Our genetic results suggest the presence of a shadow enhancer that contributes, together with the *wg*^{1}-enhancer, to wing fate specification.
7. The *wg*^{1} deletion includes two other enhancers: a notum enhancer comprised of the *Alpha* module and an eye enhancer comprised of *Alpha* and *Beta* modules.
8. *Beta* and *Gamma* modules are activated by the JNK pathway to drive Wingless expression and mediate wing regeneration and tumorigenesis.
9. *Beta* and *Gamma* modules show intra-enhancer redundancy in regeneration and tumorigenesis, guaranteeing the expression of Wg in these processes.
10. Wnt6 contributes to wing regeneration and tumorigenesis by promoting cell proliferation.
11. The *wg*^{1}-enhancer is activated in senescent cells of regenerating wing discs.
12. Senescence in regenerating discs is not mediated by p53/p21.
13. The cell cycle interferes with the ability of cells to die.
14. Senescent cells persist overtime in the regenerative tissue.

Materials and Methods

Fly maintenance, husbandry and *Drosophila* lines

Strains of *Drosophila melanogaster* were maintained on standard medium (4% glucose, 55 g/L yeast, 0.65% agar, 28 g/L wheat flour, 4 ml/L propionic acid and 1.1 g/L nipagin) at 25 ºC in light/dark cycles of 12 h. The sex of experimental larvae was not considered relevant to this study and was not determined. The strains used are summarised in the following table (Table 3):

Table 2. *Drosophila* lines

Line	Source	Identifier
wg^{1}	Bloomington Drosophila Stock Center	RRID: BDSC_2978
ΔBRV118	(Harris et al., 2016)	RRID: BDSC_23676
Df(2L)BSC226	Bloomington Drosophila Stock Center	RRID: BDSC_9703
Df(2L)BSC291	Bloomington Drosophila Stock Center	RRID: BDSC_23676
Df(2L)BSC324	Bloomington Drosophila Stock Center	RRID: BDSC_24349
wg^{CX4}	Bloomington Drosophila Stock Center	RRID: BDSC_2980
wg^{CX3}	Bloomington Drosophila Stock Center	RRID: BDSC_2977
GFP-Wg	(Yu et al., 2020)	N/A
nlsGFP-DWnt6	(Yu et al., 2020)	N/A
$wnt6^{KO}$	(Doumpas et al., 2013)	RRID: BDSC_76311
wg^{02657} (wg-lacZ in the text)	Bloomington Drosophila Stock Center	RRID: BDSC_11205
wg^{1}-lacZ	generated in this work	N/A
BRV118-lacZ	(Schubiger et al., 2010)	N/A
sd-GAL4	Bloomington Drosophila Stock Center	RRID: BDSC_8609
UAS-EGFP	Bloomington Drosophila Stock Center	RRID: BDSC_9331
UAS-Hh-GFP	(Callejo et al., 2008)	N/A
UAS-ptc	(Callejo et al., 2008)	N/A
UAS-$egfp^{RNAi}$	Bloomington Drosophila Stock Center	RRID: BDSC_35786
UAS-vn-argos	(Wang et al., 2000)	N/A
10X STAT-GFP	Bloomington Drosophila Stock Center	N/A
UAS-dome-i	VDRC Stock Center	RRID: VDRC_106071
UAS-dcr2	Bloomington Drosophila Stock Center	RRID: BDSC_24651

α-lacZ	generated in this work	N/A
β-lacZ	generated in this work	N/A
γ-lacZ	generated in this work	N/A
δ-lacZ	generated in this work	N/A
γδ -lacZ	generated in this work	N/A
γ-630-lacZ	generated in this work	N/A
γ-590-lacZ	generated in this work	N/A
γ-590(Ci)-lacZ*	generated in this work	N/A
γ (Ci)-lacZ*	generated in this work	N/A
wg^{1}-AP1mut-lacZ	generated in this work	N/A
Δγ-Ci-BS	generated in this work	N/A
Δγ-590	generated in this work	N/A
Δγ	generated in this work	N/A
Δβ	generated in this work	N/A
Δβγ	generated in this work	N/A
rn-Gal4, tub-$Gal80^{ts}$, UAS-egr	(Smith-Bolton et al., 2009)	N/A
sal-lexA, $tubg80^{ts}$	(Santabárbara-Ruiz et al., 2015)	N/A
lexO-rpr	(Santabárbara-Ruiz et al., 2015)	N/A
UAS-$wnt6^{RNAi}$	VDRC Stock Center	RRID: VDRC_26669
hh-Gal4, tub-$Gal80^{ts}$	(Muzzopappa et al., 2017)	N/A
UAS-rod^{RNAi}	VDRC Stock Center	RRID: VDRC_16152
UAS-p35	Bloomington Drosophila Stock Center	RRID: BDSC_5073
UAS-bskDN	Bloomington Drosophila Stock Center	RRID: BDSC_6409
en-Gal4	Bloomington Drosophila Stock Center	RRID: BDSC_1973
dpp^{disk}-gal4 (dpp-Gal4 in the text) tub-$Gal80^{ts}$	(Staehling-Hampton et al., 1994)	N/A
UAS-wg-GFP	(Pfeiffer et al., 2002)	N/A
UAS-wnt6	FlyORF	RRID: F003540
spdFlag-lacZ	generated in this work	N/A
wnt6-intron-lacZ	generated in this work	N/A
$y^{1}v^{1}$P{nos-phiC31\int.NLS}X; P{CaryP}attP40	Bloomington Drosophila Stock Center	RRID: BDSC_25709

v^1; Sco / SM6a	Bloomington Drosophila Stock Center	RRID: BDSC_137
w^{1118}	Bloomington Drosophila Stock Center	RRID: BDSC_3605
tub-gal80^{ts}, rn > gal4	(Colombani et al., 2012)	N/A
UAS-H2Av-mCherry	(Yuen et al., 2022)	N/A
UAS-GFPn::lacZ	(Lavista-Llanos et al., 2002)	
UAS-MyrT	Bloomington Drosophila Stock Center	RRID: BDSC_32221
UAS-GC3Ai	(Schott et al., 2017)	N/A
UAS-FlyFUCCI	Kindly provided by Héctor Herranz	RRID: BDSC_55121
Dilp8-mimicGFP (Dilp8-GFP in the text*)*	Bloomington Drosophila Stock Center	RRID: BDSC_33079
MMP1-GFP	(Uhlirova and Bohmann, 2006)	N/A
UAS-CD63-mCherry	Bloomington Drosophila Stock Center	RRID: BDSC_91389
20XUAS-tdTomato-Sec61β	Bloomington Drosophila Stock Center	RRID: BDSC_64747
UAS-galt-RFP	Bloomington Drosophila Stock Center	RRID: BDSC_65251
UAS-mitoGFP	Bloomington Drosophila Stock Center	RRID: BDSC_8442
gstD-GFP	(Sykiotis & Bohmann, 2008)	N/A
HP1-RFP	Bloomington Drosophila Stock Center	RRID: BDSC_30562
hid 5'F-EGFP	Bloomington Drosophila Stock Center	RRID: BDSC_50750
dap-lacZ	Bloomington Drosophila Stock Center	RRID: BDSC_10406
UAS-trbl	Bloomington Drosophila Stock Center	RRID: BDSC_58493
UAS-stg	Bloomington Drosophila Stock Center	RRID: BDSC_4778
UAS-trbl^{RNAi}	Bloomington Drosophila Stock Center	RRID:BDSC_42523
esg-GFP	Bloomington Drosophila Stock Center	RRID: BDSC_83386

Expression of reporter lines in development

Flies carrying the corresponding *lacZ* reporters were allowed to lay eggs for 24 h at 25ºC. For those experiments aimed at monitoring the developmental dynamics in expression pattern, flies were allowed to lay eggs for 6 h. Flies carrying GAL4/UAS transgenes were switched to 29ºC after the egg laying or were otherwise kept at 25ºC. Second instar (L2) or early third instar (eL3), mild third instar (mL3) and late third instar (L3) larvae were dissected at day 3, 4 or 5, respectively.

Tissue injury models

Egr-induced cell death

Flies were allowed to lay eggs for 24 h (for the expression of reporter lines) or 6 h (for regeneration or timepoint experiments) at 18 ºC. Flies were allowed to lay eggs for 6 h at 18°C. Flies were kept at 18ºC until day 7 when they were switched to 29ºC to induce *eiger* expression for 16 h. Larvae were either dissected immediately after (R0) to isolate wing discs for immunostainings or were subsequently allowed to recover at 18°C for 12 h (R12) or 24 h (R24) and then dissected or left at 18ºC until adulthood. All images are R0, unless noted otherwise. Experimental flies and control individuals were grown in parallel.

Sal-lexA/LexO-rpr cell death induction

Flies were allowed to lay eggs for 24 h at 18°C. Developing animals were kept at 18ºC until day 7 when they were switched to 29ºC for 11 h and dissected immediately after to isolate wing discs for immunostainings.

Ionizing Radiation (IR) treatment

Flies were raised at 25ºC until day 3, when they were irradiated at the standard dose of 45Gy using the YXLON MaxiShot X-ray system. Flies were placed back at 25ºC and dissected 12 h after the irradiation (12h AIR) to isolate the wing discs for immunostainings.

DSS feeding protocol

4-days old adult female flies from 24-hour parallel egg-layings were collected and transferred to empty vials containing a piece of 2.5 cm x 3.75 cm chromatography paper (Bio-Rad) wet with 500 µl of 5% sucrose (control) or 3% of the DSS (Sigma Aldrich). Flies were transferred to new vials with new fresh media every day for 2 days. During this period flies were kept at 25°C. After 2 days, flies were dissected to isolate the guts for immunostaining. Experimental flies and control individuals were grown in parallel.

Standard induction of CIN

Flies were allowed to lay eggs on standard fly food for 24 h (for the expression of reporter lines) or 8 h (for the quantification of tissue size) at 25°C, larvae kept at 25°C for an additional day, switched to 29° C and dissected 4 days thereafter. Experimental flies and control individuals were grown in parallel.

Immunohistochemistry

Wing, haltere, and leg imaginal discs, brains and guts of the indicated larval stage were dissected in cold PBS, fixed in 4% formaldehyde for 20 min (or 30 min for gut fixation), washed three times in PBT (PBS1%, 0.2% Triton), blocked for 45 min in BBT (PBS1X, 0.3% BSA, 0.2% Triton, 250 mM NaCl), and incubated overnight with the primary antibodies (listed in Table 4). Discs were rinsed with BBT and incubated with secondary antibodies (listed in Table 4) and DAPI (Sigma Aldrich, 28718-90-3) for 90 min. After 4 washes with PBT, discs were kept on mounting media (80 ml glycerol + 10 ml PBS 10x + 0.8 ml N-propyl-gallate 50%). The most representative images are shown in all experiments. At least 8-15 wing discs per genotype were imaged.

Table 3. List of primary and secondary antibodies.

REAGENT	DILUTION	SOURCE	IDENTIFIER
mouse anti-dMMP1 (14A3D2)	1:50	Developmental Studies Hybridoma Bank	RRID: AB_579782
goat polyclonal anti-GFP (ab6673)	1:300	Abcam	Code: ab6673
rabbit anti-β-galactosidase (0855976)	1:600	Cappel (MP Biochemicals)	Code: 0855976
mouse anti-β-galactosidase (40.1a)	1:50	Developmental Studies Hybridoma Bank	RRID: AB_2314509
rabbit anti-phospho-Histone H3 (pH3)	1:1000	Cell Signaling	RRID: AB_331535
rat anti-Ci (2A1)	1:10	Developmental Studies Hybridoma Bank	RRID: AB_2109711
mouse anti-Wg (4D4)	1:50	Developmental Studies Hybridoma Bank	RRID: AB_528512
mouse anti-Nubbin (nub2D4)	1:50	Developmental Studies Hybridoma Bank	RRID: AB_2722119
rabbit anti-Tsh	1:100	(Wu & Cohen, 2002)	N/A
mouse anti-Fasciclin III (FasIII) (7G10)	1:50	Developmental Studies Hybridoma Bank	RRID: AB_528238
rat anti-DE-cadherin (DCAD2)	1:50	Developmental Studies Hybridoma Bank	RRID: AB_528120
mouse anti-Lamin (dmo) (ADL84.12)	1:150	Developmental Studies Hybridoma Bank	RRID: AB_528335
mouse anti-pH2Av (UNC93-5.2.1)	1:500	Developmental Studies Hybridoma Bank	RRID: AB_2618077
mouse anti-c-Dcp-1 (9578S)	1:100	Cell Signaling Technology	Code: 9578-s
Cy2 AffiniPure Donkey Anti-Rat IgG (H+L)	1:400	Jackson ImmunoResearch	Code: 712-225-150

Cy2 AffiniPure Donkey Anti-Goat IgG (H+L)	1:400	Jackson ImmunoResearch	Code: 705-225-147
Cy5 AffiniPure Donkey Anti-Mouse IgG (H+L)	1:400	Jackson ImmunoResearch	Code: 715-175-151
Cy5 AffiniPure Donkey Anti-Rabbit IgG (H+L)	1:400	Jackson ImmunoResearch	Code: 711-175-152
Cy3 AffiniPure Donkey Anti-Rat IgG (H+L)	1:400	Jackson ImmunoResearch	Code: 712-165-153
Cy3 AffiniPure Donkey Anti-Mouse IgG (H+L)	1:400	Jackson ImmunoResearch	Code: 715-165-150
Cy3 AffiniPure Donkey Anti-Rabbit IgG (H+L)	1:400	Jackson ImmunoResearch	Code: 711-165-152

DNA synthesis

Click-iT™ Plus EdU Alexa Fluor™ 647 Imaging Kit from Invitrogen (C10640) was used to measure DNA synthesis (S phase) in regenerating wing discs, following the manufacturer's indications. EdU (5-ethynyl-2´-deoxyuridine) provided in the kit is a nucleoside analogue of thymidine and is incorporated into DNA during active DNA synthesis. Time of incubation with EdU: 10 min.

TUNEL

Early L3 larvae were dissected in cold 1X PBS and fixed in 4% FA for 20 min. After fixation, three fast washes with PBT 0.3% Triton (PBS 1%, Triton X-100 0.3%) followed by four PBT 0.3% Triton 15 min-washes were performed. The samples were blocked with BBT for 1h rotating at RT and then incubated overnight with the primary antibody. Next day, three PBT 0.3% Triton fast washes were done, and samples were washed four more times with PBT 0.3% Triton for 20 min each and then incubated with secondary antibodies diluted in BBT for 90 min rotating in the dark at RT. After incubation, the samples were subjected to three rounds of fast washes with PBT 0.3% Triton and four 20 min washed with PBT 0.3%. Samples were kept in BBT blocking overnight at 4ºC. The following day, samples were permeabilized with 495 µl of 100 mM Na-Citrate and 2,5 µl of 20% TritonX for 30 min at 65ºC and then three fast washes with PBT 0.3% Triton. Then samples were incubated twice for 5 min at RT with 50 µl of Equilibration buffer. Then 51 µl of TUNEL reaction mix (50 µl of TUNEL reaction buffer Component A, 1 µl TdT Enzyme, Biotium) were added and incubated for 2 h at RT. After incubation, three PBT 0.3% Triton fast washes were done followed by 30 min of DAPI incubation at RT. Finally, three fast washes and three 10 min-washes of PBT 0.3% Triton were done. Stained tissues were kept in mounting media.

SA-β-galactosidase assay

CellEvent senescence green detection kit from Invitrogen (C10850) was used following the manufacturer's instructions. Wing discs were fixed with 4% PFA for 20 min, followed by 2 10 min-washed with 100 µl BSA 1% in PBS and then incubated in 100 µl working solution for 2 h at 37ºC in dark. Discs were rinsed four times with BBT and incubated with DAPI for 20 min. After 4 washes with PBT, discs were kept on mounting media. Dissection, mounting and imaging of the samples were performed on the same day.

Analysis of sequence conservation

Conservation of the CRMs spanning the *wg*^{1}-enhancer (*Alpha*, *Beta*, *Gamma* and *Delta*) was performed at the University of California Santa Cruz (UCSC) Genome Browser on *Drosophila melanogaster* (BDGP Release 6). In brief, multiple alignments of 27 insect species (23 *Drosophila* species, and *Musca Domestica*, *Anopheles gambiae, Apis melifera and Tribolium catsnaeum*) and measurements of evolutionary conservation used two methods (phastCons43 and phyloP) from the PHAST package (http://compgen.cshl.edu/phast/), for all 27 species. Multiz and other tools in the UCSC/Penn State Bioinformatics comparative genomics alignment pipeline (http://www.bx.psu.edu/miller_lab/) were used to generate multiple alignments. For more details, see description of methods at https://genome-euro.ucsc.edu/index.html.

Generation of lacZ-reporter lines

Different regions of the *wg*^{1}-enhancer named *Alpha* to *Delta*, *wnt6 Intron* and *SpdFlag* were amplified by PCR from genomic DNA extracted from *w*^{1118} flies, using the suitable primers detailed in Table 6. PCR products were digested with EcoRi/KpnI or KpnI/NotI restriction enzymes, gel-purified (NZYGelpure) and ligated into the pHs43nLacz vector previously digested with the same enzymes. Final constructs were checked by restriction, sequenced and sent for injection for transgenic generation in the *w*^{1118} background. At least six independent insertions per construct were analysed and shown to drive a reproducible expression pattern.

Prediction of transcription factor binding sites

Predictions of binding sites in the *wg*^{1} region were performed using the Matscan software 41. Position weight matrices were obtained from JASPAR 2020-all organisms 42, and MEME v12.21 Fly Factor Survey collection (https://meme-suite.org/meme/db/motifs). Matrix logos were plotted using the seqLogo R package (https://bioconductor.org/packages/release/

bioc/html/seqLogo.html). Conservation score was taken from the evolutionary conservation track from UCSC (https://genome.ucsc.edu/index.html) for 26 species close to *Drosophila* melanogaster (DM6). Method of computation for conservation score: phastCons 43. p-values were computed by permutation test in 1000 random genomic sequences of the same length as the analysed query sequence(s). Predicted binding sites that overlapped using the same position weight matrix were merged and presented in the tables 2 and 3, where maximum and average match score (score.max, score.avg), maximum and average conservation score (cons. max, cons.avg), and minimum and maximum permutation test p-value (pv.min, pv.max) for all individual hits within the overlapping region are shown.

Generation of *Gamma* and *Gamma-590* reporters carrying mutations in the Ci binding site

To introduce the Ci mutation in the *Gamma-LacZ* reporter, two independent PCRs were performed using the pHsnLacZ-*Gamma* as a template. The first PCR introduced the mutation GCGT**G**T**G**GTCT → GCGT**A**T**A**GTCT in the Reverse primer (see PCR1 wg-*GammaCi* mut on Table 6) and the second PCR introduced the same mutation on the Fwd primer (see PCR2 wg-*GammaCi* mut on Table 6). A third PCR was performed on the mixed PCR1 and PCR2 products using the wg-*Gamma* Fwd and wg-*Gamma* Rev primers. The final product was 1145 bp long bearing the mutation in the Ci binding site. The wg-*Gamma*-mut was digested and cloned into the pHsnLacZ vector. To obtain the *Gamma-590Cimut-LacZ* reporter, a PCR with the *Gamma590*-Fwd and *Gamma*-Rev was performed using the pHsnLacZ-*GammaCimut* construct as a template. The PCR product was digested and cloned in the pHsnLacZ vector. Final constructs were checked by restriction, sequenced and sent for injection for transgenic generation in the w^{1118} background.

Generation of wg^{1}-reporter carrying mutations in AP1 binding sites

Five AP1 binding sites were present in the wg^{1}-enhancer and AP1 binding sites 1 to 4 (Table 6) were mutated. These four AP1 binding sites were mutated introducing XbaI restriction sites in oligos. For sites 1 and 4 the following mutations were introduced: CGCGCTTATGTTTCTA**TGATT**CAGCAGCCAGATT → CGCGCTTATGTTTCTA**TCTAGA**AGCAGCCAGATT. TCTCTGCTGGCTGACG**TTTAGT**CATAAAATATTCCA→TCTCTGCTGGCTGACGT**TCTAGA**ATAAAATATTCA. The two oligos were annealed to vector pBS-wg1 followed by PCR polymerase reaction, Klenow blunt, ligation, DpnI digestion and transformation. Minipreps were checked by XbaI re-

striction. Mutations 2 and 3 were introduced performing independent PCRs using pBSK-wg1 Mut1&4 as a template. For Mutation 2 the first PCR introduced the mutation TAGC**TGACT-C**ACTC → TAGC**TCTAGA**ACTC on the Reverse primer and the second PCR introduced the same mutation on the Forward primer. A third PCR was performed on the mixed PCRs products using wg-AP1 Fwd and wg-AP1 Rev primers. For Mutation 3 the same strategy was used introducing mutation AGTC**TGACTA**ATAC → AGTC**TCTAGA**ATAC. The final vector pBSK- wg1 Mut1,2,3&4 was sequenced, digested KpnI/NotI and cloned into the pHsnLacZ vector.

Generation of *wg*^{1}-enhancer deletions with the CRISPR/Cas9 technique

gRNAs Up and Down to generate the different *wg*^{1}-enhancer deletions were cloned in the pBFv-U6.2B vector in three steps as follows:

1. gRNA_Up was designed, and sticky ends for BbsI were added to the 5' end of the Fwd (CTTC) and Rev (AAAC) oligos (see Table 6). 9.5 µl of Fwd and Rev oligos at a concentration of 100 µM were mixed with 1 µl of SSC20X, boiled for 5 mins and allowed to cool down overnight in a 1 L water bath for efficient annealing. 1 µl of 1/20 dilution of the mix was used to ligate with the pBFv-U6.2 plasmid previously digested with BbsI. Ligation was transformed into DH5Alpha competent bacteria and 3 colonies were selected for DNA miniprep and sequencing with the T3 primer.

2. gRNA-Down was designed, and sticky ends for BbsI were added to the 5' end of the Fwd (CTTC) and Rev (AAAC) oligos (see Table 6). Fwd and Rev oligos were annealed and ligated in the pBFv-U6.2B plasmid previously digested with BbsI. Ligation was transformed and 3 positive colonies were selected for checking and sequencing.

3. pBFv-U6.2-gRNA_Up was digested with EcoRI/NotI and the gRNA_Up insert was gel-purified and ligated with the pBFv-U6.2B-gRNA_Down, previously digested with EcoRI/NotI. Five colonies were selected for plasmid preparation and sequenced with the T3 primer.

One positive colony pBFv-U6.2B-gRNA_Up+Down was selected for Maxiprep and the DNA was used for injection into y1v1P{nos-phiC31\int.NLS}X; P{CaryP}attP40 (BL 25709) flies. Trangenics were identified as v+ individuals.

gRNAup+down transgenic flies were then crossed to y1 cho v1; attP40.nosCas9 / Cyo flies to generate the deletions in the germline. Five males from the progeny that carried gRNAUp+Down and the Cas9 were individually crossed with v1; Sco / SM6a (BL137) females. In

a second step, 5 to 10 males from each cross were selected and individually backcrossed with v1; Sco / SM6a females. 2-3 individuals from each established stock were used for genomic extraction and PCR checking to identify the mutant lines (see Table 6).

Molecular characterisation of deletions

To identify CRISPR mutants, genomic DNA was extracted from individuals of 10-15 different candidate lines. For this purpose, 2-3 flies from each line were squashed in 300 µL of homogenizing buffer (0.1M Tris-HCl pH 9, 0.1M EDTA, 1% SDS) and the mix incubated at 65 °C for 30 min. After incubation, 67.8 µl of KAc was added and tubes were kept on ice for 30 min. Samples were centrifuged for 10 min at 4ºC, the supernatant was transferred to a new tube and DNA was precipitated by adding 0.5 volumes of isopropanol, incubated 5 min at RT and centrifuged again for 5 min at RT. The pellet was washed with 70% EtOH and resuspended in 50 µl of TE. 1 µl was then used to perform a PCR with the suitable primers (see Table 6). PCR products from samples that showed the expected deletions were gel-purified and sent for Sanger sequencing to characterise indels.

Primers

The primers used in this thesis are summarised in the following table:

Table 4. Oligonucleotides

CTTCGGATAGGAAGGTATTGCGAC	Invitrogen	*Beta* CRISPR_Down-Fwd
AAACGTCGCAATACCTTCCTATCC	Invitrogen	*Beta* CRISPR_Down-Rev
CTTCGGCATATTGGACTGTGTTCG	Invitrogen	*Beta_Gamma* CRISPR_Up-Fwd
AAACCGAACACAGTCCAATATGCC	Invitrogen	*Beta_Gamma* CRISPR_Up-Rev
CTTCGTTCCCAATCTCAAAAGATGT	Invitrogen	*Gamma* CRISPR_Up-Fwd
AAACACATCTTTTGAGATTGGGAAC	Invitrogen	*Gamma* CRISPR_Up-Rev

CTTCGTCGAGTGCACCGATCTTCCC	Invitrogen	*Gamma* CRISPR_Down-Fwd
AAACGGGAAGATCGGTGCACTCGAC	Invitrogen	*Gamma* CRISPR_Down-Rev
CTTCTCTGGCGATCCGGGGAGCTA	Invitrogen	*Gamma*590 CRISPR_Up-Fwd
AAACTAGCTCCCCGGATCGCCAGA	Invitrogen	*Gamma*590 CRISPR_Up-Rev
CTTCTCGAGTGCACCGATCTTCCC	Invitrogen	*Gamma*590 CRISPR_Down-Fwd
AAACGGGAAGATCGGTGCACTCGA	Invitrogen	*Gamma*590 CRISPR_Down-Rev
GTC GAA ATT AAG AGA CCA CAC GCA	Invitrogen	*Gamma* Ci1mut CRISPR_Fwd
AAA CTG CGT GTG GTC TCT TAA TTT	Invitrogen	*Gamma* Ci1mut CRISPR_Rev
GCGGAATTCTAATGTTATAGTATTTCTGCT	Invitrogen	wg-*Alpha*-Fwd (EcoRI)
CCGGGTACCCTACTTTATAAATTTACATTA	Invitrogen	wg-*Alpha*-Rev (KpnI)
GCGGAATTCTTAAACCGATTTTATTACCCA	Invitrogen	wg-*Beta*-Fwd (EcoRI)
CCGGGTACCAAGGTTTTATATCTAACCTAC	Invitrogen	wg-*Beta*-Rev (KpnI)
CGGGGTACCGTTTTATTATATTTCGACAAA	Invitrogen	wg-*Gamma*-Fwd (KpnI)
ATAGTTTAGCGGCCGCTATGAGTACTTA-ACTAAATGT	Invitrogen	wg-*Gamma*-Rev (NotI)
GCGGAATTCGTAAAACAGTTTTATTTTGGG	Invitrogen	wg-*Delta*-Fwd (EcoRI)
CCGGGTACCATTTATAAACGACGTATAGTT	Invitrogen	wg-*Delta*-Rev (KpnI)

ATATGGTACCTTTTGTTTTATTATATTTCGA-CAAAATCG	Invitrogen	wg-*GammaDelta*-Fw (KpnI)
ATAAGAATGCGGCCGCACATTTCATATGT-CAACCCTTCGTTT	Invitrogen	wg-*GammaDelta*-Rev (NotI)
CGG ATC CGG GGA GCT ACG GAG TTG CGG AGC AGC GTT	Invitrogen	wg-*Gamma*590-Fwd
GGGGTACCAGGCATTGCGACAGGAGCTATG-GGAGGTTTTT	Invitrogen	wg- *Gamma*630-Fwd (KpnI)
ATAAGAATGCGGCCGCTCCCCGGATCGC-CAGATGCCCAGA	Invitrogen	wg- *Gamma*630-Rev (NotI)
CGGGGTACCAATTCTCGTGAACCTCCCAG-CACATCT	Invitrogen	spdFlag CiS2-Fwd
ATAGTTTAGCGGCCGCACTACAATTCTAGT-TAGTTT	Invitrogen	spdFlag CiS2-Fwd
CGGGTACCTGACGAATAGCCCATAGCTCTG	Invitrogen	spdFlag350 CiS2-Fwd
ATAGTTTAGCGCGGCCGCATATTAGCATGA-TAAGT	Invitrogen	spdFlag350 CiS2-Rv
GGTACCTTCAAGTTTCTTTCCCCAACCTTA-AGT	Invitrogen	wnt6-1st Intron CiBS1-Fwd
ATAGTTTAGCGGCCGCCTTTAGTTC-GCTTTTAATGC	Invitrogen	wnt6-1st Intron CiBS1-Rev
CGGGGTACCGTTTTATTATATTTCGACAAA	Invitrogen	**PCR1:** wg-*Gamma*-Fwd
AAATTAAGAGACTATACGCAAGGTGTGCTC	Invitrogen	**PCR1:** wg-*Gamma*Ci mut- Rev
GAGCACACCTTGCGTATAGTCTCTTAATTT	Invitrogen	**PCR2:** wg-*Gamma*Mut-Fwd
ATAGTTTAGCGGCCGCTATGAGTACTTA-ACTAAATGT	Invitrogen	**PCR2:** wg-*Gamma*-Rev
CGGATCCGGGGAGCTACGGAGTTG CGGAG-CAGCGTT	Invitrogen	wg-*Gamma*590-Fwd

ATAGTTTAGCGGCCGCTATGAGTACTTA-ACTAAATGT	Invitrogen	wg-*Gamma*-Rev

Quantifications

Wing to notum transformation

Each heminotum was considered an independent event. The percentage of wing to notum transformation (loss of wings and appearance of an ectopic heminotum where bristles showed reverse polarity) was calculated by dividing the number of transformed heminota by the total number of heminota (% wing to notum transformation = (n transformed heminota/n total heminota)*100). Representative pictures of the phenotype were obtained. The percentage of duplicated notum paired with a vestigial wing was calculated the same way.

Adult wing regeneration

Adult flies were collected in SH buffer (75% glycerol, 25% ethanol) and wings were dissected in water and mounted in Faure´s mounting medium. Regenerated wings were scored using Fiji Software (NIH, USA). They were considered regenerated when they were capable of reaching a regular size. No patterning problems were considered when assessing the regenerative potential. The percentage of regenerated wings was calculated by dividing the number of regenerated wings by the total number of scored wings (% regenerated wings = (n regenerated wings/n total wings)*100).

Wing disc size upon CIN

The sizes of the whole wing disc (based on DAPI staining) were measured manually using Fiji Software (NIH, USA) on Z-projection of the wing disc obtained using a Zeiss LSM780 confocal microscope at 25X glycerol immersion objective with 1.5 µm per optical section covering the entire thickness of each disc.

Wingless signal intensity

Wingless areas in the pouch of regenerating wing discs and in the pouch and hinge of the P compartment of wing discs subjected to CIN (based on the absence of Ci expression) were selected using the polygonal tool of Fiji Software (NIH, USA). Wingless intensity (in arbirtrary units, a.u.) was measured upon setting a fluorescence threshold for the corresponding channel. Image stacks were obtained using a Zeiss LSM780 confocal microscope at 40X oil

immersion objective with 1.5 µm per optical section for regenerating discs, and at 25X glycerol immersion objective with 1.5 µm per optical section for wing discs subjected to CIN. The entire thickness of each disc was covered in both cases. Maximum intensity Z-projection was performed on the stacks prior to quantification.

Cleaved-Dcp1 signal intensity

Cleaved-Dcp1 intensity (in arbirtrary units, a.u.) was measured in the totality of the disc using the Fiji Software (NIH, USA) upon setting a fluorescence threshold for the corresponding channel. Image stacks were obtained using a Zeiss LSM780 confocal microscope at 40X oil immersion objective with 1.5 µm per optical section. The entire thickness of each disc was covered in both cases. Maximum intensity Z-projection was performed on the stacks prior to quantification.

Mitotic activity

Mitosis was measured by counting mitotic cells (pH3-positive cells) present in an area slightly broader to the one of the Wg expression domain (red lines in Figures 48) of regenerating wing discs using the Fiji Software (NIH, USA). Image stacks were obtained using a Zeiss LSM780 confocal microscope under a 40X oil immersion objective with 1.5 µm per optical section to cover the entire thickness of each disc. The ratio between the number of mitotic cells and Wg area (sizes measured in arbirtrary units, a.u., using the polygonal tool on Fiji) was calculated.

EdU incorporation

The region comprising the wing pouch and hinge primordia was selected using the polygonal tool of Fiji and the area was quantified. EdU positive area within this region was measured using a Macro created in Fiji. The ratio between the areas of EdU incorporation and wing pouch and hinge regions (sizes measured in arbitrary units, a.u.) was calculated. Experiments were carried out in parallel in all the genotypes analysed and experiments were repeated three times.

Gut regeneration

Gut regeneration was measured by counting Intestinal Stem Cells (Esg-positive cells) present in in the posterior midguts of control and DSS treated flies using the Fiji Software (NIH, USA). Image stacks were obtained using a Zeiss LSM780 confocal microscope under a 40X oil

immersion objective with 1.5 µm per optical section to cover the entire thickness of the gut wall. The mean of ICS per gut was quantified (esg+ cells / gut = (esg+ cells/n total guts)). Between 30-45 posterior midguts were considered for each condition.

Microscopy

Larval discs or tissues were analysed and scanned with a LSM 780 Zeiss confocal microscope. Adult wings, nota and eyes were analysed and pictured with an Olympus MVX10 macroscope. Regenerating wings were imaged using an ECLIPSE E600 microscope coupled to a NIKON DSRi2 camera. For the orthogonal projections at Figures 57, 58 and 59 the discs were imaged at 40X oil immersion objective with 0.25 µm per optical section. The entire thickness of the disc was covered. For the magnifications at Figures 56, 57, 66, 67 and 69 the images were obtained at 63x oil immersion objective with 0.2 µm per optical section. The entire thickness of a cell was covered.

Statistics and reproducibility

The statistical analysis for comparison of means was performed by linear regression using the experimental batch as adjusting variable. Normality assumption was tested for every fitted model, applying a log2-transformation of the data when necessary. However, for clarity of representation, data are shown in the original scale. The statistical analysis for comparison of percentages of regenerated wings was performed by logistic regression using the experimental batch as adjusting variable. In both types of models, Dunnett's multiple comparisons correction was applied when comparing the means/percentages of several experimental groups with a common control. Differences were considered significant when adjusted p values were less than 0.001 (***), 0.01 (**), or 0.05 (*). Statistical analysis was carried out with the multcomp 44 R package. In gut samples two-ways ANOVA with Tukey HSD's multiple comparison test was applied when comparing the difference in means of different experimental groups and diets. Differences were considered significant when p-values were less than 0.001 (***), 0.01 (**), or 0.05 (*). All genotypes included in each histogram or scatter plot were subjected to the same experimental conditions (temperature and time of transgene induction) and analysed in parallel, and all experimental quantifications were carried out at least three times in different days. Graphical representations were performed with Graphpad Prism 9 statistical software.

References

Abate, M., Festa, A., Falco, M., Lombardi, A., Luce, A., Grimaldi, A., Zappavigna, S., Sperlongano, P., Irace, C., Caraglia, M., & Misso, G. (2020). Mitochondria as playmakers of apoptosis, autophagy and senescence. In *Seminars in Cell and Developmental Biology* (Vol. 98, pp. 139–153). Elsevier Ltd. https://doi.org/10.1016/j.semcdb.2019.05.022

Abdelwahid, E., Yokokura, T., Krieser, R. J., Balasundaram, S., Fowle, W. H., & White, K. (2007). Mitochondrial Disruption in Drosophila Apoptosis. *Developmental Cell*, *12*(5), 793–806. https://doi.org/10.1016/j.devcel.2007.04.004

Adams, M. D., Celniker, S. E., Holt, R. A., Evans, C. A., Gocayne, J. D., Amanatides, P. G., Scherer, S. E., Li, P. W., Hoskins, R. A., Galle, R. F., George, R. A., Lewis, S. E., Richards, S., Ashburner, M., Henderson, S. N., Sutton, G. G., Wortman, J. R., Yandell, M. D., Zhang, Q., … Craig Venter, J. (2000). The genome sequence of Drosophila melanogaster. *Science (New York, N.Y.)*, *287*(5461), 2185–2195. https://doi.org/10.1126/SCIENCE.287.5461.2185

Adams, P. D., Ivanov, A., Pawlikowski, J., Manoharan, I., Tuyn, J. Van, Nelson, D. M., Singh Rai, T., Shah, P. P., Hewitt, G., Korolchuk, V. I., Passos, J. F., Wu, H., & Berger, S. L. (2013). Lysosome-mediated processing of chromatin in senescence. *Journal of Cell Biology*, *202*(1), 129–143. https://doi.org/10.1083/jcb.201212110

Agata, K., Saito, Y., & Nakajima, E. (2007). Unifying principles of regeneration I: Epimorphosis versus morphallaxis. In *Development Growth and Differentiation* (Vol. 49, Issue 2, pp. 73–78). https://doi.org/10.1111/j.1440-169X.2007.00919.x

Agnès, F., Suzanne, M., & Noselli, S. (1999). The Drosophila JNK pathway controls the morphogenesis of imaginal discs during metamorphosis. *Development*, *126*(23), 5453–5462. https://doi.org/10.1242/DEV.126.23.5453

Ahmed-de-Prado, S., Diaz-Garcia, S., & Baonza, A. (2018). JNK and JAK/STAT signalling are required for inducing loss of cell fate specification during imaginal wing discs regeneration in Drosophila melanogaster. *Developmental Biology*, *441*(1), 31–41. https://doi.org/10.1016/j.ydbio.2018.05.021

Akalin, A., Fredman, D., Arner, E., Dong, X., Bryne, J. C., Suzuki, H., Daub, C. O., Hayashizaki, Y., & Lenhard, B. (2009). Transcriptional features of genomic regulatory blocks. *Genome Biology*, *10*(4). https://doi.org/10.1186/gb-2009-10-4-r38

Akhtar-Zaidi, B., Cowper-Sallari, R., Corradin, O., Saiakhova, A., Bartels, C. F., Balasubramanian, D., Myeroff, L., Lutterbaugh, J., Jarrar, A., Kalady, M. F., Willis, J., Moore, J. H., Tesar, P. J., Laframboise, T., Markowitz, S., Lupien, M., & Scacheri, P. C. (2012). Epigenomic enhancer profiling defines a signature of colon cancer. *Science (New York, N.Y.)*, *336*(6082), 736–739. https://doi.org/10.1126/SCIENCE.1217277

Allan, C. M., Walker, D., & Taylor, J. M. (1995). Evolutionary duplication of a hepatic control region in the human apolipoprotein E gene locus: Identification of a second region that confers high level and liver-specific expression of the human apolipoprotein E gene in transgenic mice. *Journal of Biological Chemistry*, *270*(44), 26278–26281. https://doi.org/10.1074/jbc.270.44.26278

Amoyel, M., Anderson, A. M., & Bach, E. A. (2014). JAK/STAT pathway dysregulation in tumors: A Drosophila perspective. In *Seminars in Cell and Developmental Biology* (Vol. 28, pp. 96–103). Elsevier Ltd. https://doi.org/10.1016/j.semcdb.2014.03.023

Anantram, A., & Degani, M. (2019). Targeting cancer's Achilles' heel: Role of BCL-2 inhibitors in cellular senescence and apoptosis. In *Future Medicinal Chemistry* (Vol. 11, Issue 17, pp. 2287–2312). Future Medicine Ltd. https://doi.org/10.4155/fmc-2018-0366

Andersen, D. S., Colombani, J., Palmerini, V., Chakrabandhu, K., Boone, E., Röthlisberger, M., Toggweiler, J., Basler, K., Mapelli, M., Hueber, A. O., & Léopold, P. (2015). The Drosophila TNF receptor Grindelwald couples loss of cell polarity and neoplastic growth. *Nature*, *522*(7557), 482–486. https://doi.org/10.1038/NATURE14298

Andersson, R., Gebhard, C., Miguel-Escalada, I., Hoof, I., Bornholdt, J., Boyd, M., Chen, Y., Zhao, X., Schmidl, C., Suzuki, T., Ntini, E., Arner, E., Valen, E., Li, K., Schwarzfischer, L., Glatz, D., Raithel, J., Lilje, B., Rapin, N., … Sandelin, A. (2014). An atlas of active enhancers across human cell types and tissues. *Nature*, *507*(7493), 455–461. https://doi.org/10.1038/nature12787

Andor, N., Graham, T. A., Jansen, M., Xia, L. C., Aktipis, C. A., Petritsch, C., Ji, H. P., & Maley, C. C. (2016). Pan-cancer analysis of the extent and consequences of intratumor heterogeneity. *Nature Medicine*, *22*(1), 105–113. https://doi.org/10.1038/nm.3984

Anerillas, C., Abdelmohsen, K., & Gorospe, M. (2020). Regulation of senescence traits by MAPKs. In *GeroScience* (Vol. 42, Issue 2, pp. 397–408). Springer. https://doi.org/10.1007/s11357-020-00183-3

Angeloni, A., & Bogdanovic, O. (2019). Enhancer DNA methylation: Implications for gene regulation. In *Essays in Biochemistry* (Vol. 63, Issue 6, pp. 707–715). Portland Press Ltd. https://doi.org/10.1042/EBC20190030

Ankawa, R., Goldberger, N., Yosefzon, Y., Koren, E., Yusupova, M., Rosner, D., Feldman, A., Baror-Sebban, S., Buganim, Y., Simon, D. J., Tessier-Lavigne, M., & Fuchs, Y. (2021). Apoptotic cells represent a dynamic stem cell niche governing proliferation and tissue regeneration. *Developmental Cell*, *56*(13), 1900-1916.e5. https://doi.org/10.1016/J.DEVCEL.2021.06.008

Antelo-Iglesias, L., Picallos-Rabina, P., Estévez-Souto, V., Da Silva-Álvarez, S., & Collado, M. (2021). The role of cellular senescence in tissue repair and regeneration. *Mechanisms of Ageing and Development*, *198*. https://doi.org/10.1016/j.mad.2021.111528

Apidianakis, Y., Grbavec, D., Stifani, S., & Delidakis, C. (2001). Groucho mediates a Ci-independent mechanism of hedgehog repression in the anterior wing pouch. *Development (Cambridge, England)*, *128*(21), 4361–4370. https://doi.org/10.1242/DEV.128.21.4361

Aran, D., Sabato, S., & Hellman, A. (2013). DNA methylation of distal regulatory sites characterizes dysregulation of cancer genes. *Genome Biology*, *14*(3). https://doi.org/10.1186/gb-2013-14-3-r21

Aranda, S., Mas, G., & Di Croce, L. (2015). Regulation of gene transcription by Polycomb proteins. *Science Advances*, *1*(11). https://doi.org/10.1126/sciadv.1500737

Arnosti, D. N., & Kulkarni, M. M. (2005). Transcriptional enhancers: Intelligent enhanceosomes or flexible billboards? In *Journal of Cellular Biochemistry* (Vol. 94, Issue 5, pp. 890–898). https://doi.org/10.1002/jcb.20352

Aros, C. J., Pantoja, C. J., & Gomperts, B. N. (2021). Wnt signaling in lung development, regeneration, and disease progression. In *Communications Biology* (Vol. 4, Issue 1). Nature Research. https://doi.org/10.1038/s42003-021-02118-w

Ataman, B., Ashley, J., Gorczyca, M., Ramachandran, P., Fouquet, W., Sigrist, S. J., & Budnik, V. (2008). Rapid Activity-Dependent Modifications in Synaptic Structure and Function Require Bidirectional Wnt Signaling. *Neuron*, *57*(5), 705–718. https://doi.org/10.1016/j.neuron.2008.01.026

Bach, E. A., Ekas, L. A., Ayala-Camargo, A., Flaherty, M. S., Lee, H., Perrimon, N., & Baeg, G. H. (2007). GFP reporters detect the activation of the Drosophila JAK/STAT pathway in vivo. *Gene Expression Patterns*, *7*(3), 323–331. https://doi.org/10.1016/j.modgep.2006.08.003

Badouel, C., & McNeill, H. (2009). Apical junctions and growth control in Drosophila. *Biochimica et Biophysica Acta*, *1788*(4), 755–760. https://doi.org/10.1016/J.BBAMEM.2008.08.026

Baena-Lopez, L. A., Franch-Marro, X., & Vincent, J. P. (2009). Wingless promotes proliferative growth in a gradient-independent manner. *Science Signaling*, *2*(91). https://doi.org/10.1126/scisignal.2000360

Baker, N. E. (1987). Molecular cloning of sequences from wingless, a segment polarity gene in Drosophila: The spatial distribution of a transcript in embryos. *EMBO Journal*, *6*(6), 1765–1773. https://doi.org/10.1002/j.1460-2075.1987.tb02429.x

Baker, N. E., & Yu, S. Y. (2001). The EGF receptor defines domains of cell cycle progression and survival to regulate cell number in the developing Drosophila eye. *Cell*, *104*(5), 699–708. https://doi.org/10.1016/S0092-8674(01)00266-5

Bakhoum, S. F., & Cantley, L. C. (2018). The Multifaceted Role of Chromosomal Instability in Cancer and Its Microenvironment. In *Cell* (Vol. 174, Issue 6, pp. 1347–1360). Cell Press. https://doi.org/10.1016/j.cell.2018.08.027

Bakhoum, S. F., Ngo, B., Laughney, A. M., Cavallo, J. A., Murphy, C. J., Ly, P., Shah, P., Sriram, R. K., Watkins, T. B. K., Taunk, N. K., Duran, M., Pauli, C., Shaw, C., Chadalavada, K., Rajasekhar, V. K., Genovese, G., Venkatesan, S., Birkbak, N. J., McGranahan, N., … Cantley, L. C. (2018). Chromosomal instability drives metastasis through a cytosolic DNA response. *Nature*, *553*(7689), 467–472. https://doi.org/10.1038/nature25432

Baonza, A., Roch, F., & Martin-Blanco, E. (2000). DER signaling restricts the boundaries of the wing field during Drosophila development. *Proceedings of the National Academy of Sciences of the United States of America*, *97*(13), 7331–7335. https://doi.org/10.1073/PNAS.97.13.7331

Barolo, S. (2012). Shadow enhancers: Frequently asked questions about distributed cis-regulatory information and enhancer redundancy. *BioEssays*, *34*(2), 135–141. https://doi.org/10.1002/bies.201100121

Barral, D. C., Staiano, L., Guimas Almeida, C., Cutler, D. F., Eden, E. R., Futter, C. E., Galione, A., Marques, A. R. A., Medina, D. L., Napolitano, G., Settembre, C., Vieira, O. V., Aerts, J. M. F. G., Atakpa-Adaji, P., Bruno, G., Capuozzo, A., De Leonibus, E., Di Malta, C., Escrevente, C., … Seabra, M. C. (2022). Current methods to analyze lysosome morphology, positioning, motility and function. *Traffic (Copenhagen, Denmark)*, *23*(5), 238–269. https://doi.org/10.1111/TRA.12839

Barrio, L., & Milán, M. (2017). Boundary Dpp promotes growth of medial and lateral regions of the Drosophila wing. *ELife*, *6*. https://doi.org/10.7554/ELIFE.22013

Barrio, L., & Milán, M. (2020). Regulation of Anisotropic Tissue Growth by Two Orthogonal Signaling Centers. *Developmental Cell*, *52*(5), 659-672.e3. https://doi.org/10.1016/j.devcel.2020.01.017

Bassett, A. R., & Liu, J. L. (2014). CRISPR/Cas9 and Genome Editing in Drosophila. In *Journal of Genetics and Genomics* (Vol. 41, Issue 1, pp. 7–19). https://doi.org/10.1016/j.jgg.2013.12.004

Basto, R., Brunk, K., Vinadogrova, T., Peel, N., Franz, A., Khodjakov, A., & Raff, J. W. (2008). Centrosome Amplification Can Initiate Tumorigenesis in Flies. *Cell*, *133*(6), 1032–1042. https://doi.org/10.1016/j.cell.2008.05.039

Basu, A. (2022). The interplay between apoptosis and cellular senescence: Bcl-2 family proteins as targets for cancer therapy. In *Pharmacology and Therapeutics* (Vol. 230). Elsevier Inc. https://doi.org/10.1016/j.pharmthera.2021.107943

Bate, M., & Martinez Arias, A. (1991). The embryonic origin of imaginal discs in Drosophila. *Development (Cambridge, England)*, *112*(3), 755–761. https://doi.org/10.1242/DEV.112.3.755

Bate, M., Rushton, E., & Currie, D. A. (1991). Cells with persistent twist expression are the embryonic precursors of adult muscles in Drosophila. *Development (Cambridge, England)*, *113*(1), 79–89. https://doi.org/10.1242/DEV.113.1.79

Baylin, S. B., & Jones, P. A. (2016). Epigenetic determinants of cancer. *Cold Spring Harbor Perspectives in Biology*, *8*(9). https://doi.org/10.1101/cshperspect.a019505

Bejarano, F., & Milán, M. (2009). Genetic and epigenetic mechanisms regulating hedgehog expression in the Drosophila wing. *Developmental Biology*, *327*(2), 508–515. https://doi.org/10.1016/J.YDBIO.2009.01.006

Bejsovec, A. (2018). Wingless signaling: A genetic journey from morphogenesis to metastasis. *Genetics*, *208*(4), 1311–1336. https://doi.org/10.1534/genetics.117.300157

Bely, A. E., & Nyberg, K. G. (2010). Evolution of animal regeneration: re-emergence of a field. In *Trends in Ecology and Evolution* (Vol. 25, Issue 3, pp. 161–170). https://doi.org/10.1016/j.tree.2009.08.005

Benhra, N., Barrio, L., Muzzopappa, M., & Milán, M. (2018). Chromosomal Instability Induces Cellular Invasion in Epithelial Tissues. *Developmental Cell*, *47*(2), 161-174.e4. https://doi.org/10.1016/j.devcel.2018.08.021

Bergantiños, C., Corominas, M., & Serras, F. (2010). Cell death-induced regeneration in wing imaginal discs requires JNK signalling. *Development*, *137*(7), 1169–1179. https://doi.org/10.1242/dev.045559

Berger, M. F., Badis, G., Gehrke, A. R., Talukder, S., Philippakis, A. A., Peña-Castillo, L., Alleyne, T. M., Mnaimneh, S., Botvinnik, O. B., Chan, E. T., Khalid, F., Zhang, W., Newburger, D., Jaeger, S. A., Morris, Q. D., Bulyk, M. L., & Hughes, T. R. (2008). Variation in Homeodomain DNA Binding Revealed by High-Resolution Analysis of Sequence Preferences. *Cell*, *133*(7), 1266–1276. https://doi.org/10.1016/j.cell.2008.05.024

Bergmann, A., Agapite, J., Mccall, K., & Steller, H. (1998). The Drosophila Gene hid Is a Direct Molecular Target of Ras-Dependent Survival Signaling. In *Cell* (Vol. 95).

Bideau, L., Kerner, P., Hui, J., Vervoort, M., & Gazave, E. (2021). Animal regeneration in the era of transcriptomics. In *Cellular and Molecular Life Sciences* (Vol. 78, Issue 8, pp. 3941–3956). Springer Science and Business Media Deutschland GmbH. https://doi.org/10.1007/s00018-021-03760-7

Biran, A., Perelmutter, M., Gal, H., G.A. Burton, D., Ovadya, Y., Vadai, E., Geiger, T., & Krizhanovsky, V. (2015). Senescent cells communicate via intercellular protein transfer. *Genes & Development*, *29*(8), 791. https://doi.org/10.1101/GAD.259341.115

Blanco, E., González-Ramírez, M., Alcaine-Colet, A., Aranda, S., & Di Croce, L. (2020). The Bivalent Genome: Characterization, Structure, and Regulation. *Trends in Genetics : TIG*, *36*(2), 118–131. https://doi.org/10.1016/J.TIG.2019.11.004

Blanco, E., Ruiz-Romero, M., Beltran, S., Bosch, M., Punset, A., Serras, F., & Corominas, M. (2010). *Gene expression following induction of regeneration in Drosophila wing imaginal discs. Expression profile of regenerating wing discs*. http://www.biomedcentral.com/1471-213X/10/94

Bolognesi, R., Beermann, A., Farzana, L., Wittkopp, N., Lutz, R., Balavoine, G., Brown, S. J., & Schröder, R. (2008). Tribolium Wnts: Evidence for a larger repertoire in insects with overlapping expression patterns that suggest multiple redundant functions in embryogenesis. *Development Genes and Evolution*, *218*(3–4), 193–202. https://doi.org/10.1007/s00427-007-0170-3

Bosch, M., Baguñà, J., & Serras, F. (2008). Origin and proliferation of blastema cells during regeneration of Drosophila wing imaginal discs. *International Journal of Developmental Biology*, *52*(8), 1043–1050. https://doi.org/10.1387/ijdb.082608mb

Bosch, M., Serras, F., Martín-Blanco, E., & Baguñà, J. (2005). JNK signaling pathway required for wound healing in regenerating Drosophila wing imaginal discs. *Developmental Biology*, *280*(1), 73–86. https://doi.org/10.1016/j.ydbio.2005.01.002

Bosch, P. S., Ziukaite, R., Alexandre, C., Basler, K., & Vincent, J. P. (2017). Dpp controls growth and patterning in Drosophila wing precursors through distinct modes of action. *ELife*, *6*. https://doi.org/10.7554/ELIFE.22546

Bozek, M., Cortini, R., Storti, A. E., Unnerstall, U., Gaul, U., & Gompel, N. (2019). ATAC-seq reveals regional differences in enhancer accessibility during the establishment of spatial coordinates in the Drosophila blastoderm. *Genome Research*, *29*(5), 771–783. https://doi.org/10.1101/GR.242362.118/-/DC1

Bozek, M., & Gompel, N. (2020). Developmental Transcriptional Enhancers: A Subtle Interplay between Accessibility and Activity: Considering Quantitative Accessibility Changes between Different Regulatory States of an Enhancer Deconvolutes the Complex Relationship between Accessibility and Activity. In *BioEssays* (Vol. 42, Issue 4). John Wiley and Sons Inc. https://doi.org/10.1002/bies.201900188

Brand, A. H., & Perrimon, N. (1993). Targeted gene expression as a means of altering cell fates and generating dominant phenotypes. *Development (Cambridge, England)*, *118*(2), 401–415. https://doi.org/10.1242/DEV.118.2.401

Braun, H., Schmidt, B. M. W., Raiss, M., Baisantry, A., Mircea-Constantin, D., Wang, S., Gross, M. L., Serrano, M., Schmitt, R., & Melk, A. (2012). Cellular senescence limits regenerative capacity and allograft survival. *Journal of the American Society of Nephrology*, *23*(9), 1467–1473. https://doi.org/10.1681/ASN.2011100967

Brennecke, J., Hipfner, D. R., Stark, A., Russell, R. B., & Cohen, S. M. (2003). bantam encodes a developmentally regulated microRNA that controls cell proliferation and regulates the proapoptotic gene hid in Drosophila. *Cell*, *113*(1), 25–36. https://doi.org/10.1016/S0092-8674(03)00231-9

Brown, S., Hu, N., & Hombría, J. C. G. (2001). Identification of the first invertebrate interleukin JAK/STAT receptor, the Drosophila gene domeless. *Current Biology : CB*, *11*(21), 1700–1705. https://doi.org/10.1016/S0960-9822(01)00524-3

Brumby, A. M., & Richardson, H. E. (2005). Using Drosophila melanogaster to map human cancer pathways. In *Nature Reviews Cancer* (Vol. 5, Issue 8, pp. 626–639). https://doi.org/10.1038/nrc1671

Bryant, P. J. (1975). Pattern formation in the imaginal wing disc of Drosophila melanogaster: fate map, regeneration and duplication. *The Journal of Experimental Zoology*, *193*(1), 49–77. https://doi.org/10.1002/JEZ.1401930106

Buecker, C., & Wysocka, J. (2012). Enhancers as information integration hubs in development: Lessons from genomics. In *Trends in Genetics* (Vol. 28, Issue 6, pp. 276–284). https://doi.org/10.1016/j.tig.2012.02.008

Burke, R., & Basler, K. (1996). Dpp receptors are autonomously required for cell proliferation in the entire developing Drosophila wing. *Development (Cambridge, England)*, *122*(7), 2261–2269. https://doi.org/10.1242/DEV.122.7.2261

Calcinotto, A., Kohli, J., Zagato, E., Pellegrini, L., Demaria, M., & Alimonti, A. (2019). Cellular Senescence: Aging, Cancer, and Injury. *Physiol Rev*, *99*, 1047–1078. https://doi.org/10.1152/physrev.00020.2018.-Cellular

Calleja, M., Renaud, O., Usui, K., Pistillo, D., Morata, G., & Simpson, P. (2002). How to pattern an epithelium: Lessons from achaete-scute regulation on the notum of Drosophila. *Gene*, *292*(1–2), 1–12. https://doi.org/10.1016/S0378-1119(02)00628-5

Callejo, A., Culi, J., & Guerrero, I. (2008). Patched, the receptor of Hedgehog, is a lipoprotein receptor. *Proceedings of the National Academy of Sciences of the United States of America*, *105*(3), 912–917. https://doi.org/10.1073/PNAS.0705603105/SUPPL_FILE/05603FIG7.JPG

Calo, E., & Wysocka, J. (2013). Modification of Enhancer Chromatin: What, How, and Why? In *Molecular Cell* (Vol. 49, Issue 5, pp. 825–837). https://doi.org/10.1016/j.molcel.2013.01.038

Cannavò, E., Khoueiry, P., Garfield, D. A., Geeleher, P., Zichner, T., Gustafson, E. H., Ciglar, L., Korbel, J. O., & Furlong, E. E. M. (2016). Shadow Enhancers Are Pervasive Features of Developmental Regulatory Networks. *Current Biology*, *26*(1), 38–51. https://doi.org/10.1016/j.cub.2015.11.034

Cao, X., Rojas, M., & Pastor-Pareja, J. C. (2022). Intrinsic and damage-induced JAK/STAT signaling regulate developmental timing by the Drosophila prothoracic gland. *DMM Disease Models and Mechanisms*, *15*(1). https://doi.org/10.1242/dmm.049160

Carleton, J. B., Berrett, K. C., & Gertz, J. (2017). Multiplex Enhancer Interference Reveals Collaborative Control of Gene Regulation by Estrogen Receptor α-Bound Enhancers. *Cell Systems*, *5*(4), 333-344.e5. https://doi.org/10.1016/j.cels.2017.08.011

Carloni, V., Morganti, E., Galli, A., & Mazzocca, A. (2023). The Adaptability of Chromosomal Instability in Cancer Therapy and Resistance. In *International Journal of Molecular Sciences* (Vol. 24, Issue 1). MDPI. https://doi.org/10.3390/ijms24010245

Carroll, S. B., Weatherbee, S. D., & Langeland, J. A. (1995). Homeotic genes and the regulation and evolution of insect wing number. *Nature*, *375*(6526), 58–61. https://doi.org/10.1038/375058A0

Castellanos, E., Dominguez, P., & Gonzalez, C. (2008). Centrosome Dysfunction in Drosophila Neural Stem Cells Causes Tumors that Are Not Due to Genome Instability. *Current Biology*, *18*(16), 1209–1214. https://doi.org/10.1016/j.cub.2008.07.029

Catarino, R. R., & Stark, A. (2018). *Assessing sufficiency and necessity of enhancer activities for gene expression and the mechanisms of transcription activation*. https://doi.org/10.1101/gad.310367

Cauwelier, B., Dastugue, N., Cools, J., Poppe, B., Herens, C., De Paepe, A., Hagemeijer, A., & Speleman, F. (2006). Molecular cytogenetic study of 126 unselected T-ALL cases reveals high incidence of TCRβ locus rearrangements and putative new T-cell oncogenes. *Leukemia*, *20*(7), 1238–1244. https://doi.org/10.1038/sj.leu.2404243

Cave, J. W., Loh, F., Surpris, J. W., Xia, L., & Caudy, M. A. (2005). A DNA Transcription Code for Cell-Specific Gene Activation by Notch Signaling diate the proper expression pattern specified by that module. Each of these sites is bound by the cognate transcription factor DNA binding proteins, which then. *Current Biology*, *15*, 94–104. https://doi.org/10.1016/j

Chandra, T., Kirschner, K., Thuret, J. Y., Pope, B. D., Ryba, T., Newman, S., Ahmed, K., Samarajiwa, S. A., Salama, R., Carroll, T., Stark, R., Janky, R. S., Narita, M., Xue, L., Chicas, A., Nũnez, S., Janknecht, R., Hayashi-Takanaka, Y., Wilson, M. D., … Narita, M. (2012). Independence of Repressive Histone Marks and Chromatin Compaction during Senescent Heterochromatic Layer Formation. *Molecular Cell*, *47*(2), 203–214. https://doi.org/10.1016/j.molcel.2012.06.010

Childs, B. G., Baker, D. J., Kirkland, J. L., Campisi, J., & Deursen, J. M. (2014). Senescence and apoptosis: dueling or complementary cell fates? *EMBO Reports*, *15*(11), 1139–1153. https://doi.org/10.15252/embr.201439245

Cho, S., & Hwang, E. S. (2012). Status of mTOR activity may phenotypically differentiate senescence and quiescence. *Molecules and Cells*, *33*(6), 597–604. https://doi.org/10.1007/s10059-012-0042-1

Clapier, C. R., Iwasa, J., Cairns, B. R., & Peterson, C. L. (2017). Mechanisms of action and regulation of ATP-dependent chromatin-remodelling complexes. In *Nature Reviews Molecular Cell Biology* (Vol. 18, Issue 7, pp. 407–422). Nature Publishing Group. https://doi.org/10.1038/nrm.2017.26

Claps, G., Cheli, Y., Zhang, T., Scortegagna, M., Lau, E., Kim, H., Qi, J., Li, J. L., James, B., Dzung, A., Levesque, M. P., Dummer, R., Hayward, N. K., Bosenberg, M., Brown, K. M., & Ronai, Z. A. (2016). A Transcriptionally Inactive ATF2 Variant Drives Melanomagenesis. *Cell Reports*, *15*(9), 1884–1892. https://doi.org/10.1016/j.celrep.2016.04.072

Clavier, A., Rincheval-Arnold, A., Colin, J., Mignotte, B., & Guénal, I. (2016). Apoptosis in Drosophila: Which role for mitochondria? In *Apoptosis* (Vol. 21, Issue 3, pp. 239–251). Springer New York LLC. https://doi.org/10.1007/s10495-015-1209-y

Clemente-Ruiz, M., Murillo-Maldonado, J. M., Benhra, N., Barrio, L., Pérez, L., Quiroga, G., Nebreda, A. R., & Milán, M. (2016). Gene Dosage Imbalance Contributes to Chromosomal Instability-Induced Tumorigenesis. *Developmental Cell*, *36*(3), 290–302. https://doi.org/10.1016/j.devcel.2016.01.008

Cohen, B., Simcox, A. A., & Cohen, S. M. (1993). Allocation of the thoracic imaginal primordia in the Drosophila embryo. *Development (Cambridge, England)*, *117*(2), 597–608. https://doi.org/10.1242/DEV.117.2.597

Cohen, S. M. (1990). Specification of limb development in the Drosophila embryo by positional cues from segmentation genes. *Nature*, *343*(6254), 173–177. https://doi.org/10.1038/343173A0

Colombani, J., Andersen, D. S., & Léopol, P. (2012). Secreted peptide Dilp8 coordinates Drosophila tissue growth with developmental timing. *Science (New York, N.Y.)*, *336*(6081), 582–585. https://doi.org/10.1126/SCIENCE.1216689

Coppé, J. P., Desprez, P. Y., Krtolica, A., & Campisi, J. (2010). The senescence-associated secretory phenotype: The dark side of tumor suppression. In *Annual Review of Pathology: Mechanisms of Disease* (Vol. 5, pp. 99–118). https://doi.org/10.1146/annurev-pathol-121808-102144

Cordero, J. B., Stefanatos, R. K., Scopelliti, A., Vidal, M., & Sansom, O. J. (2012). Inducible progenitor-derived Wingless regulates adult midgut regeneration in Drosophila. *The EMBO Journal*, *31*(19), 3901–3917. https://doi.org/10.1038/EMBOJ.2012.248

Cormenier, J., Martin, N., Deslé, J., Salazar-Cardozo, C., Pourtier, A., Abbadie, C., & Pluquet, O. (2018). The ATF6α arm of the Unfolded Protein Response mediates replicative senescence in human fibroblasts through a COX2/prostaglandin E2 intracrine pathway. *Mechanisms of Ageing and Development*, *170*, 82–91. https://doi.org/10.1016/J.MAD.2017.08.003

Correia-Melo, C., Marques, F. D., Anderson, R., Hewitt, G., Hewitt, R., Cole, J., Carroll, B. M., Miwa, S., Birch, J., Merz, A., Rushton, M. D., Charles, M., Jurk, D., Tait, S. W., Czapiewski, R., Greaves, L., Nelson, G., Bohlooly-Y, M., Rodriguez-Cuenca, S., … Passos, J. F. (2016). Mitochondria are required for pro-ageing features of the senescent phenotype. *The EMBO Journal*, *35*(7), 724–742. https://doi.org/10.15252/embj.201592862

Cosolo, A., Jaiswal, J., Csordás, G., Grass, I., Uhlirova, M., & Classen, A. K. (2019). JNK-dependent cell cycle stalling in G2 promotes survival and senescence-like phenotypes in tissue stress. *ELife*, *8*. https://doi.org/10.7554/ELIFE.41036

Couso, J. P., & Arias, A. M. (1994). Notch Is Required for wingless Signaling in the Epidermis of Drosophila. In *Cell* (Vol. 79).

Couso, J. P., Bate, M., & Martinez-Arias, A. (1993). *A wingless-Dependent Polar Coordinate System in Drosophila Imaginal Discs*. https://doi.org/DOI: 10.1126/science.842417

Couso, J. P., Knust, E., & Martinez Arias, A. (1995). Serrate and wingless cooperate to induce vestigial gene expression and wing formation in Drosophila. *Current Biology : CB*, *5*(12), 1437–1448. https://doi.org/10.1016/S0960-9822(95)00281-8

Creyghton, M. P., Cheng, A. W., Welstead, G. G., Kooistra, T., Carey, B. W., Steine, E. J., Hanna, J., Lodato, M. A., Frampton, G. M., Sharp, P. A., Boyer, L. A., Young, R. A., & Jaenisch, R. (2010). Histone H3K27ac separates active from poised enhancers and predicts developmental state. *Proceedings of the National Academy of Sciences of the United States of America*, *107*(50), 21931–21936. https://doi.org/10.1073/pnas.1016071107

Crispatzu, G., Rehimi, R., Pachano, T., Bleckwehl, T., Cruz-Molina, S., Xiao, C., Mahabir, E., Bazzi, H., & Rada-Iglesias, A. (2021). The chromatin, topological and regulatory properties of pluripotency-associated poised enhancers are conserved in vivo. *Nature Communications*, *12*(1). https://doi.org/10.1038/s41467-021-24641-4

Crossman, S. H., Streichan, S. J., & Vincent, J. P. (2018). EGFR signaling coordinates patterning with cell survival during Drosophila epidermal development. *PLoS Biology*, *16*(10). https://doi.org/10.1371/journal.pbio.3000027

Crucianelli, C., Jaiswal, J., Maya, A. V., Nogay, L., Cosolo, A., Grass, I., & Classen, A. K. (2022). Distinct signaling signatures drive compensatory proliferation via S-phase acceleration. *PLoS Genetics*, *18*(12). https://doi.org/10.1371/journal.pgen.1010516

Cruickshanks, H. A., McBryan, T., Nelson, D. M., Vanderkraats, N. D., Shah, P. P., Van Tuyn, J., Singh Rai, T., Brock, C., Donahue, G., Dunican, D. S., Drotar, M. E., Meehan, R. R., Edwards, J. R., Berger, S. L., & Adams, P. D. (2013). Senescent Cells Harbour Features of the Cancer Epigenome. *Nature Cell Biology*, *15*(12), 1495–1506. https://doi.org/10.1038/ncb2879

Cuollo, L., Antonangeli, F., Santoni, A., & Soriani, A. (2020). The senescence-associated secretory phenotype (Sasp) in the challenging future of cancer therapy and age-related diseases. In *Biology* (Vol. 9, Issue 12, pp. 1–16). MDPI AG. https://doi.org/10.3390/biology9120485

Da Silva, S. M., Moutinho-Santos, T., & Sunkel, C. E. (2013). A tumor suppressor role of the Bub3 spindle checkpoint protein after apoptosis inhibition. *Journal of Cell Biology*, *201*(3), 385–393. https://doi.org/10.1083/JCB.201210018

Da Silva-Álvarez, S., Guerra-Varela, J., Sobrido-Cameán, D., Quelle, A., Barreiro-Iglesias, A., Sánchez, L., & Collado, M. (2020). Cell senescence contributes to tissue regeneration in zebrafish. *Aging Cell*, *19*(1). https://doi.org/10.1111/acel.13052

DaCrema, D., Bhandari, R., Karanja, F., Yano, R., & Halme, A. (2021). Ecdysone regulates the Drosophila imaginal disc epithelial barrier, determining the length of regeneration checkpoint delay. *Development (Cambridge)*, *148*(6). https://doi.org/10.1242/dev.195057

Dalle Pezze, P., Nelson, G., Otten, E. G., Korolchuk, V. I., Kirkwood, T. B. L., von Zglinicki, T., & Shanley, D. P. (2014). Dynamic Modelling of Pathways to Cellular Senescence Reveals Strategies for Targeted Interventions. *PLoS Computational Biology*, *10*(8). https://doi.org/10.1371/journal.pcbi.1003728

De Celis, J. F. (2003). Pattern formation in the Drosophila wing: The development of the veins. *BioEssays : News and Reviews in Molecular, Cellular and Developmental Biology*, *25*(5), 443–451. https://doi.org/10.1002/BIES.10258

De Celis, J. F., Garcia-Bellido, A., & Bray, S. J. (1996). Activation and function of Notch at the dorsal-ventral boundary of the wing imaginal disc. *Development (Cambridge, England)*, *122*(1), 359–369. https://doi.org/10.1242/DEV.122.1.359

De Nooij, J. C., Letendre, M. A., & Hariharan, I. K. (1996). A cyclin-dependent kinase inhibitor, dacapo, is necessary for timely exit from the cell cycle during Drosophila embryogenesis. *Cell*, *87*(7), 1237–1247. https://doi.org/10.1016/S0092-8674(00)81819-X

Dekanty, A., Barrio, L., Muzzopappa, M., Auer, H., & Milán, M. (2012). Aneuploidy-induced delaminating cells drive tumorigenesis in Drosophila epithelia. *Proceedings of the National Academy of Sciences of the United States of America*, *109*(50), 20549–20554. https://doi.org/10.1073/pnas.1206675109

Dekanty, A., & Milán, M. (2013). Aneuploidy, cell delamination and tumorigenesis in Drosophila epithelia. *Cell Cycle*, *12*(5), 728–731. https://doi.org/10.4161/cc.23949

Dekker, J., & Heard, E. (2015). Structural and functional diversity of Topologically Associating Domains. In *FEBS Letters* (Vol. 589, Issue 20, pp. 2877–2884). Elsevier B.V. https://doi.org/10.1016/j.febslet.2015.08.044

Demaria, M., Ohtani, N., Youssef, S. A., Rodier, F., Toussaint, W., Mitchell, J. R., Laberge, R. M., Vijg, J., VanSteeg, H., Dollé, M. E. T., Hoeijmakers, J. H. J., deBruin, A., Hara, E., & Campisi, J. (2014). An essential role for senescent cells in optimal wound healing through secretion of PDGF-AA. *Developmental Cell*, *31*(6), 722–733. https://doi.org/10.1016/j.devcel.2014.11.012

Demaria, M., O'Leary, M. N., Chang, J., Shao, L., Liu, S., Alimirah, F., Koenig, K., Le, C., Mitin, N., Deal, A. M., Alston, S., Academia, E. C., Kilmarx, S., Valdovinos, A., Wang, B., De Bruin, A., Kennedy, B. K., Melov, S., Zhou, D., … Campisi, J. (2017). Cellular senescence promotes adverse effects of chemotherapy and cancer relapse. *Cancer Discovery*, *7*(2), 165–176. https://doi.org/10.1158/2159-8290.CD-16-0241

Deng, F., Peng, L., Li, Z., Tan, G., Liang, E., Chen, S., Zhao, X., & Zhi, F. (2018). YAP triggers the Wnt/β-catenin signalling pathway and promotes enterocyte self-renewal, regeneration and tumorigenesis after DSS-induced injury. *Cell Death and Disease*, *9*(2). https://doi.org/10.1038/s41419-017-0244-8

Deplancke, B., Alpern, D., & Gardeux, V. (2016). The Genetics of Transcription Factor DNA Binding Variation. In *Cell* (Vol. 166, Issue 3, pp. 538–554). Cell Press. https://doi.org/10.1016/j.cell.2016.07.012

Despang, A., Schöpflin, R., Franke, M., Ali, S., Jerković, I., Paliou, C., Chan, W. L., Timmermann, B., Wittler, L., Vingron, M., Mundlos, S., & Ibrahim, D. M. (2019). Functional dissection of the Sox9–Kcnj2 locus identifies nonessential and instructive roles of TAD architecture. *Nature Genetics 2019 51:8*, *51*(8), 1263–1271. https://doi.org/10.1038/s41588-019-0466-z

Despres, J., Ramdani, Y., di Giovanni, M., Bénard, M., Zahid, A., Montero-Hadjadje, M., Yvergnaux, F., Saguet, T., Driouich, A., & Follet-Gueye, M. L. (2019). Replicative senescence of human dermal fibroblasts affects struc-

tural and functional aspects of the Golgi apparatus. *Experimental Dermatology*, *28*(8), 922–932. https://doi.org/10.1111/exd.13886

DeVido, S. K., Kwon, D., Brown, J. L., & Kassis, J. A. (2008). The role of Polycomb-group response elements in regulation of engrailed transcription in Drosophila. *Development*, *135*(4), 669–676. https://doi.org/10.1242/dev.014779

Diaz-Benjumea, F. J., & Cohen, S. M. (1995). Serrate signals through Notch to establish a Wingless-dependent organizer at the dorsal/ventral compartment boundary of the Drosophila wing. *Development (Cambridge, England)*, *121*(12), 4215–4225. https://doi.org/10.1242/DEV.121.12.4215

Diaz-Benjumea, F. J., & Garcia-Bellido, A. (1990). *Behaviour of Cells Mutant for an EGF Receptor Homologue of Drosophila in Genetic Mosaics* (Vol. 242, Issue 1303).

Diaz-Benjumea, F. J., & Hafen, E. (1994). The sevenless signalling cassette mediates Drosophila EGF receptor function during epidermal development. *Development (Cambridge, England)*, *120*(3), 569–578. https://doi.org/10.1242/DEV.120.3.569

Díaz-García, S., & Baonza, A. (2013). Pattern reorganization occurs independently of cell division during Drosophila wing disc regeneration in situ. *Proceedings of the National Academy of Sciences of the United States of America*, *110*(32), 13032–13037. https://doi.org/10.1073/pnas.1220543110

Diez Del Corral, R., Aroca, P., Gómez-Skarmeta, J. L., Cavodeassi, F., & Modolell, J. (1999). The Iroquois homeodomain proteins are required to specify body wall identity in Drosophila. *Genes & Development*, *13*(13), 1754–1761. https://doi.org/10.1101/GAD.13.13.1754

Dimri, G. P., Lee, X., Basile, G., Acosta, M., Scott, G., Roskelley, C., Medrano, E. E., Linskens, M., Rubelj, I., Pereira-Smith, O., Peacocke, M., & Campisi, J. (1995). A biomarker that identifies senescent human cells in culture and in aging skin in vivo. *Proceedings of the National Academy of Sciences of the United States of America*, *92*(20), 9363–9367. https://doi.org/10.1073/PNAS.92.20.9363

Dipietro, L. A., Wilgus, T. A., & Koh, T. J. (2021). Macrophages in healing wounds: Paradoxes and paradigms. In *International Journal of Molecular Sciences* (Vol. 22, Issue 2, pp. 1–13). MDPI AG. https://doi.org/10.3390/ijms22020950

Dixon, J. R., Gorkin, D. U., & Ren, B. (2016). Chromatin Domains: The Unit of Chromosome Organization. In *Molecular Cell* (Vol. 62, Issue 5, pp. 668–680). Cell Press. https://doi.org/10.1016/j.molcel.2016.05.018

Dixon, J. R., Selvaraj, S., Yue, F., Kim, A., Li, Y., Shen, Y., Hu, M., Liu, J. S., & Ren, B. (2012). Topological domains in mammalian genomes identified by analysis of chromatin interactions. *Nature*, *485*(7398), 376–380. https://doi.org/10.1038/nature11082

Doumpas, N., Jékely, G., & Teleman, A. A. (2013). Wnt6 is required for maxillary palp formation in Drosophila. *BMC Biology*, *11*. https://doi.org/10.1186/1741-7007-11-104

Druelle, C., Drullion, C., Deslé, J., Martin, N., Saas, L., Cormenier, J., Malaquin, N., Huot, L., Slomianny, C., Bouali, F., Vercamer, C., Hot, D., Pourtier, A., Chevet, E., Abbadie, C., & Pluquet, O. (2016). ATF6α regulates morphological changes associated with senescence in human fibroblasts. *Oncotarget*, *7*(42), 67699–67715. https://doi.org/10.18632/ONCOTARGET.11505

Du, L., Sohr, A., Yan, G., & Roy, S. (2018). Feedback regulation of cytoneme-mediated transport shapes a tissue-specific FGF morphogen gradient. *ELife*, *7*. https://doi.org/10.7554/ELIFE.38137

Dupont, P., Besson, M. T., Devaux, J., & Liévens, J. C. (2012). Reducing canonical Wingless/Wnt signaling pathway confers protection against mutant Huntingtin toxicity in Drosophila. *Neurobiology of Disease*, *47*(2), 237–247. https://doi.org/10.1016/j.nbd.2012.04.007

Eaton, S., & Kornberg, T. B. (1990). Repression of ci-D in posterior compartments of Drosophila by engrailed. *Genes & Development*, *4*(6), 1068–1077. https://doi.org/10.1101/GAD.4.6.1068

Edgar, B. A., & O'Farrell, P. H. (1989). Genetic control of cell division patterns in the Drosophila embryo. *Cell*, *57*(1), 177–187. https://doi.org/10.1016/0092-8674(89)90183-9

Edgar, B. A., & O'Farrell, P. H. (1990). The three postblastoderm cell cycles of Drosophila embryogenesis are regulated in G2 by string. *Cell*, *62*(3), 469–480. https://doi.org/10.1016/0092-8674(90)90012-4

Elchaninov, A., Sukhikh, G., & Fatkhudinov, T. (2021). Evolution of Regeneration in Animals: A Tangled Story. In

Frontiers in Ecology and Evolution (Vol. 9). Frontiers Media S.A. https://doi.org/10.3389/fevo.2021.621686

El-Deiry, W. S., Tokino, T., Velculescu, V. E., Levy, D. B., Parsons, R., Trent, J. M., Lin, D., Mercer, W. E., Kinzler, K. W., & Vogelstein, B. (1993). WAF1, a potential mediator of p53 tumor suppression. *Cell*, *75*(4), 817–825. https://doi.org/10.1016/0092-8674(93)90500-P

Enomoto, M., Siow, C., & Igaki, T. (2018). Drosophila As a Cancer Model. *Advances in Experimental Medicine and Biology*, *1076*, 173–194. https://doi.org/10.1007/978-981-13-0529-0_10

Ertzer, R., Müller, F., Hadzhiev, Y., Rathnam, S., Fischer, N., Rastegar, S., & Strähle, U. (2007). Cooperation of sonic hedgehog enhancers in midline expression. *Developmental Biology*, *301*(2), 578–589. https://doi.org/10.1016/j.ydbio.2006.11.004

Estaquier, J., & Arnoult, D. (2007). Inhibiting Drp1-mediated mitochondrial fission selectively prevents the release of cytochrome c during apoptosis. *Cell Death and Differentiation*, *14*(6), 1086–1094. https://doi.org/10.1038/sj.cdd.4402107

Everetts, N. J., Worley, M. I., Yasutomi, R., Yosef, N., & Hariharan, I. K. (2021). Single-cell transcriptomics of the Drosophila wing disc reveals instructive epithelium-to-myoblast interactions. *ELife*, *10*. https://doi.org/10.7554/ELIFE.61276

Fan, S., Kroeger, B., Marie, P. P., Bridges, E. M., Mason, J. D., McCormick, K., Zois, C. E., Sheldon, H., Khalid Alham, N., Johnson, E., Ellis, M., Stefana, M. I., Mendes, C. C., Wainwright, S. M., Cunningham, C., Hamdy, F. C., Morris, J. F., Harris, A. L., Wilson, C., & Goberdhan, D. C. (2020). Glutamine deprivation alters the origin and function of cancer cell exosomes. *The EMBO Journal*, *39*(16). https://doi.org/10.15252/embj.2019103009

Fan, Y., & Bergmann, A. (2008). Apoptosis-induced compensatory proliferation. The Cell is dead. Long live the Cell! In *Trends in Cell Biology* (Vol. 18, Issue 10, pp. 467–473). https://doi.org/10.1016/j.tcb.2008.08.001

Farley, E. K., Olson, K. M., Zhang, W., Rokhsar, D. S., & Levine, M. S. (2016). Syntax compensates for poor binding sites to encode tissue specificity of developmental enhancers. *Proceedings of the National Academy of Sciences of the United States of America*, *113*(23), 6508–6513. https://doi.org/10.1073/pnas.1605085113

Fernandes, J., Bate, M., & Vijayraghavan, K. (1991). Development of the indirect flight muscles of Drosophila. *Development (Cambridge, England)*, *113*(1), 67–77. https://doi.org/10.1242/DEV.113.1.67

Flavahan, W. A., Gaskell, E., & Bernstein, B. E. (2017). Epigenetic plasticity and the hallmarks of cancer. In *Science* (Vol. 357, Issue 6348). American Association for the Advancement of Science. https://doi.org/10.1126/science.aal2380

Flier, J. S., Underhill, L. H., & Dvorak, H. F. (1986). Tumors: wounds that do not heal. Similarities between tumor stroma generation and wound healing. *The New England Journal of Medicine*, *315*(26), 1650–1659. https://doi.org/10.1056/NEJM198612253152606

Floc'hlay, S., Balaji, R., Christiaens, V., González-Blas, C. B., Winter, S. De, Hulselmans, G., Waegeneer, M. De, Quan, X., Koldere, D., Atkins, M., Halder, G., Classen, A., & Aerts, S. (2022). Shared enhancer gene regulatory networks between wound and oncogenic programs. *BioRxiv*, 2022.06.17.496596. https://doi.org/10.1101/2022.06.17.496596

Fogarty, C. E., Diwanji, N., Lindblad, J. L., Tare, M., Amcheslavsky, A., Makhijani, K., Brückner, K., Fan, Y., & Bergmann, A. (2016). Extracellular Reactive Oxygen Species Drive Apoptosis-Induced Proliferation via Drosophila Macrophages. *Current Biology*, *26*(5), 575–584. https://doi.org/10.1016/j.cub.2015.12.064

Follette, P. J., & O'Farrell, P. H. (1997). Cdks and the Drosophila cell cycle. *Current Opinion in Genetics & Development*, *7*(1), 17. https://doi.org/10.1016/S0959-437X(97)80104-9

Fox, D. T., Cohen, E., & Smith-Bolton, R. (2020). Model systems for regeneration: Drosophila. *Development (Cambridge)*, *147*(7). https://doi.org/10.1242/dev.173781

Frank, S., Gaume, B., Bergmann-Leitner, E. S., Leitner, W. W., Robert, E. G., Catez, F., Smith, C. L., & Youle, R. J. (2001). The Role of Dynamin-Related Protein 1, a Mediator of Mitochondrial Fission, in Apoptosis. *Developmental Cell*, *1*(4), 515–525. https://doi.org/10.1016/S1534-5807(01)00055-7

Franke, M., Ibrahim, D. M., Andrey, G., Schwarzer, W., Heinrich, V., Schöpflin, R., Kraft, K., Kempfer, R., Jerković, I., Chan, W. L., Spielmann, M., Timmermann, B., Wittler, L., Kurth, I., Cambiaso, P., Zuffardi, O., Houge, G., Lambie, L., Brancati, F., … Mundlos, S. (2016). Formation of new chromatin domains determines pathogenicity

of genomic duplications. *Nature*, *538*(7624), 265–269. https://doi.org/10.1038/NATURE19800

Frankel, N., Davis, G. K., Vargas, D., Wang, S., Payre, F., & Stern, D. L. (2010). Phenotypic robustness conferred by apparently redundant transcriptional enhancers. *Nature*, *466*(7305), 490–493. https://doi.org/10.1038/nature09158

Freund, A., Laberge, R. M., Demaria, M., & Campisi, J. (2012). Lamin B1 loss is a senescence-associated biomarker. *Molecular Biology of the Cell*, *23*(11), 2066–2075. https://doi.org/10.1091/mbc.E11-10-0884

Fuchs, Y., & Steller, H. (2011). Programmed cell death in animal development and disease. In *Cell* (Vol. 147, Issue 4, pp. 742–758). Elsevier B.V. https://doi.org/10.1016/j.cell.2011.10.033

Fuchs, Y., & Steller, H. (2015). Live to die another way: Modes of programmed cell death and the signals emanating from dying cells. In *Nature Reviews Molecular Cell Biology* (Vol. 16, Issue 6, pp. 329–344). Nature Publishing Group. https://doi.org/10.1038/nrm3999

Fujioka, M., Emi-Sarker, Y., Yusibova, G. L., Goto, T., & Jaynes, J. B. (1999). Analysis of an even-skipped rescue transgene reveals both composite and discrete neuronal and early blastoderm enhancers, and multi-stripe positioning by gap gene repressor gradients. *Development (Cambridge, England)*, *126*(11), 2527–2538. https://doi.org/10.1242/DEV.126.11.2527

Fujioka, M., & Jaynes, J. B. (2012). Regulation of a duplicated locus: Drosophila sloppy paired is replete with functionally overlapping enhancers. *Developmental Biology*, *362*(2), 309–319. https://doi.org/10.1016/j.ydbio.2011.12.001

Funayama, R., & Ishikawa, F. (2007). Cellular senescence and chromatin structure. In *Chromosoma* (Vol. 116, Issue 5, pp. 431–440). https://doi.org/10.1007/s00412-007-0115-7

Furlong, E. E. M., & Levine, M. (2018). Developmental enhancers and chromosome topology. *Science (New York, N.Y.)*, *361*(6409), 1341–1345. https://doi.org/10.1126/SCIENCE.AAU0320

Fuse, N., Hirose, S., & Hayashi, S. (1996). Determination of wing cell fate by the escargot and snail genes in Drosophila. *Development (Cambridge, England)*, *122*(4), 1059–1067. https://doi.org/10.1242/DEV.122.4.1059

Gagliardi, P. A., Dobrzyński, M., Jacques, M. A., Dessauges, C., Ender, P., Blum, Y., Hughes, R. M., Cohen, A. R., & Pertz, O. (2021). Collective ERK/Akt activity waves orchestrate epithelial homeostasis by driving apoptosis-induced survival. *Developmental Cell*, *56*(12), 1712-1726.e6. https://doi.org/10.1016/j.devcel.2021.05.007

Garcia-Bellido, A., Ripoll, P., & Morata, G. (1973). Developmental compartmentalisation of the wing disk of Drosophila. *Nature: New Biology*, *245*(147), 251–253. https://doi.org/10.1038/NEWBIO245251A0

Garelli, A., Heredia, F., Casimiro, A. P., Macedo, A., Nunes, C., Garcez, M., Dias, A. R. M., Volonte, Y. A., Uhlmann, T., Caparros, E., Koyama, T., & Gontijo, A. M. (2015). Dilp8 requires the neuronal relaxin receptor Lgr3 to couple growth to developmental timing. *Nature Communications*, *6*. https://doi.org/10.1038/ncomms9732

Gebelein, B., Culi, J., Ryoo, H. D., Zhang, W., & Mann, R. S. (2002). Specificity of Distalless repression and limb primordia development by abdominal Hox proteins. *Developmental Cell*, *3*(4), 487–498. https://doi.org/10.1016/S1534-5807(02)00257-5

Gerlach, S. U., Eichenlaub, T., & Herranz, H. (2018). Yorkie and JNK Control Tumorigenesis in Drosophila Cells with Cytokinesis Failure. *Cell Reports*, *23*(5), 1491–1503. https://doi.org/10.1016/j.celrep.2018.04.006

Gerlach, S. U., & Herranz, H. (2020). Genomic instability and cancer: lessons from Drosophila. In *Open Biology* (Vol. 10, Issue 6). Royal Society Publishing. https://doi.org/10.1098/rsob.200060

Gerlach, S. U., Sander, M., Song, S., & Herranz, H. (2019). The miRNA bantam regulates growth and tumorigenesis by repressing the cell cycle regulator tribbles. *Life Science Alliance*, *2*(4). https://doi.org/10.26508/lsa.201900381

Ghosh-Choudhary, S. K., Liu, J., & Finkel, T. (2021). The role of mitochondria in cellular senescence. In *FASEB Journal* (Vol. 35, Issue 12). John Wiley and Sons Inc. https://doi.org/10.1096/fj.202101462R

Gieseler, K., Wilder, E., Mariol, M. C., Buratovitch, M., Bérenger, H., Graba, Y., & Pradel, J. (2001). DWnt4 and wingless elicit similar cellular responses during imaginal development. *Developmental Biology*, *232*(2), 339–350. https://doi.org/10.1006/dbio.2001.0184

Gire, V., & Dulic, V. (2015). Senescence from G2 arrest, revisited. *Cell Cycle (Georgetown, Tex.)*, *14*(3), 297–304.

https://doi.org/10.1080/15384101.2014.1000134

Glise, B., Bourbon, H., & Noselli, S. (1995). hemipterous encodes a novel Drosophila MAP kinase kinase, required for epithelial cell sheet movement. *Cell*, *83*(3), 451–461. https://doi.org/10.1016/0092-8674(95)90123-X

Godwin, J. W., Pinto, A. R., & Rosenthal, N. A. (2013). Macrophages are required for adult salamander limb regeneration. *Proceedings of the National Academy of Sciences of the United States of America*, *110*(23), 9415–9420. https://doi.org/10.1073/pnas.1300290110

Goldman, J. A., & Poss, K. D. (2020). Gene regulatory programmes of tissue regeneration. In *Nature Reviews Genetics* (Vol. 21, Issue 9, pp. 511–525). Nature Research. https://doi.org/10.1038/s41576-020-0239-7

Golembo, M., Schweitzer, R., Freeman, M., & Shilo, B. Z. (1996). Argos transcription is induced by the Drosophila EGF receptor pathway to form an inhibitory feedback loop. *Development (Cambridge, England)*, *122*(1), 223–230. https://doi.org/10.1242/DEV.122.1.223

Gómez-Skarmeta, J. L., Campuzano, S., & Modolell, J. (2003). Half a century of neural prepatterning: the story of a few bristles and many genes. *Nature Reviews. Neuroscience*, *4*(7), 587–598. https://doi.org/10.1038/NRN1142

Gonzalez, C. (2013). Drosophila melanogaster: A model and a tool to investigate malignancy and identify new therapeutics. In *Nature Reviews Cancer* (Vol. 13, Issue 3, pp. 172–183). https://doi.org/10.1038/nrc3461

González-Gualda, E., Baker, A. G., Fruk, L., & Muñoz-Espín, D. (2021). A guide to assessing cellular senescence in vitro and in vivo. *FEBS Journal*, *288*(1), 56–80. https://doi.org/10.1111/febs.15570

Gorgoulis, V., Adams, P. D., Alimonti, A., Bennett, D. C., Bischof, O., Bishop, C., Campisi, J., Collado, M., Evangelou, K., Ferbeyre, G., Gil, J., Hara, E., Krizhanovsky, V., Jurk, D., Maier, A. B., Narita, M., Niedernhofer, L., Passos, J. F., Robbins, P. D., … Demaria, M. (2019). Cellular Senescence: Defining a Path Forward. In *Cell* (Vol. 179, Issue 4, pp. 813–827). Cell Press. https://doi.org/10.1016/j.cell.2019.10.005

Goto, S., & Hayashi, S. (1997). Specification of the embryonic limb primordium by graded activity of Decapentaplegic. *Development (Cambridge, England)*, *124*(1), 125–132. https://doi.org/10.1242/DEV.124.1.125

Goyal, G., Fell, B., Sarin, A., Youle, R. J., & Sriram, V. (2007). Role of Mitochondrial Remodeling in Programmed Cell Death in Drosophila melanogaster. *Developmental Cell*, *12*(5), 807–816. https://doi.org/10.1016/j.devcel.2007.02.002

Gratz, S. J., Rubinstein, C. D., Harrison, M. M., Wildonger, J., & O'Connor-Giles, K. M. (2015). CRISPR-Cas9 genome editing in Drosophila. *Current Protocols in Molecular Biology*, *2015*, 31.2.1-31.2.20. https://doi.org/10.1002/0471142727.mb3102s111

Großhans, J., & Wieschaus, E. (2000). A genetic link between morphogenesis and cell division during formation of the ventral furrow in Drosophila. *Cell*, *101*(5), 523–531. https://doi.org/10.1016/S0092-8674(00)80862-4

Grusche, F. A., Degoutin, J. L., Richardson, H. E., & Harvey, K. F. (2011). The Salvador/Warts/Hippo pathway controls regenerative tissue growth in Drosophila melanogaster. *Developmental Biology*, *350*(2), 255–266. https://doi.org/10.1016/j.ydbio.2010.11.020

Grzeschik, N. A., Parsons, L. M., Allott, M. L., Harvey, K. F., & Richardson, H. E. (2010). Lgl, aPKC, and Crumbs Regulate the Salvador/Warts/Hippo Pathway through Two Distinct Mechanisms. *Current Biology*, *20*(7), 573–581. https://doi.org/10.1016/j.cub.2010.01.055

Guenther, C. A., Wang, Z., Li, E., Tran, M. C., Logan, C. Y., Nusse, R., Pantalena-Filho, L., Yang, G. P., & Kingsley, D. M. (2015). A distinct regulatory region of the Bmp5 locus activates gene expression following adult bone fracture or soft tissue injury. *Bone*, *77*, 31–41. https://doi.org/10.1016/j.bone.2015.04.010

Guillen, I., Mullo, J. L., Capdevila, J., Sanchez-Herrero, E., Morata, G., & Guerrero, I. (1995). The function of engrailed and the specification of Drosophila wing pattern. *Development (Cambridge, England)*, *121*(10), 3447–3456. https://doi.org/10.1242/DEV.121.10.3447

Gunage, R. D., Reichert, H., & VijayRaghavan, K. (2014a). Identification of a new stem cell population that generates Drosophila flight muscles. *ELife*, *3*(August2014), 1–25. https://doi.org/10.7554/eLife.03126

Gunage, R. D., Reichert, H., & VijayRaghavan, K. (2014b). Identification of a new stem cell population that generates Drosophila flight muscles. *ELife*, *3*(August2014), 1–25. https://doi.org/10.7554/eLife.03126

Guo, S., Zhu, X., Huang, Z., Wei, C., Yu, J., Zhang, L., Feng, J., Li, M., & Li, Z. (2023). Genomic instability drives tu-

morigenesis and metastasis and its implications for cancer therapy. In *Biomedicine and Pharmacotherapy* (Vol. 157). Elsevier Masson s.r.l. https://doi.org/10.1016/j.biopha.2022.114036

Guo, Y., Zhao, S., & Wang, G. G. (2021). Polycomb Gene Silencing Mechanisms: PRC2 Chromatin Targeting, H3K27me3 "Readout", and Phase Separation-Based Compaction. In *Trends in Genetics* (Vol. 37, Issue 6, pp. 547–565). Elsevier Ltd. https://doi.org/10.1016/j.tig.2020.12.006

Halder, G., Polaczyk, P., Kraus, M. E., Hudson, A., Kim, J., Laughon, A., & Carroll, S. (1998). *The Vestigial and Scalloped proteins act together to directly regulate wing-specific gene expression in Drosophila*. www.genesdev.org

Halme, A., Cheng, M., & Hariharan, I. K. (2010). Retinoids Regulate a Developmental Checkpoint for Tissue Regeneration in Drosophila. *Current Biology*, *20*(5), 458–463. https://doi.org/10.1016/j.cub.2010.01.038

Hamaguchi, T., Yabe, S., Uchiyama, H., & Murakami, R. (2004). Drosophila Tbx6-related gene, Dorsocross, mediates high levels of Dpp and Scw signal required for the development of amnioserosa and wing disc primordium. *Developmental Biology*, *265*(2), 355–368. https://doi.org/10.1016/j.ydbio.2003.09.034

Hanahan, D. (2022). Hallmarks of Cancer: New Dimensions. In *Cancer Discovery* (Vol. 12, Issue 1, pp. 31–46). American Association for Cancer Research Inc. https://doi.org/10.1158/2159-8290.CD-21-1059

Hanahan, D., & Weinberg, R. A. (2000). The hallmarks of cancer. *Cell*, *100*(1), 57–70. https://doi.org/10.1016/S0092-8674(00)81683-9

Hanssen, L. L. P., Kassouf, M. T., Oudelaar, A. M., Biggs, D., Preece, C., Downes, D. J., Gosden, M., Sharpe, J. A., Sloane-Stanley, J. A., Hughes, J. R., Davies, B., & Higgs, D. R. (2017). Tissue-specific CTCF-cohesin-mediated chromatin architecture delimits enhancer interactions and function in vivo. *Nature Cell Biology*, *19*(8), 952–961. https://doi.org/10.1038/NCB3573

Hariharan, I. K., & Serras, F. (2017). Imaginal disc regeneration takes flight. In *Current Opinion in Cell Biology* (Vol. 48, pp. 10–16). Elsevier Ltd. https://doi.org/10.1016/j.ceb.2017.03.005

Harris, R. E. (2022). Regeneration enhancers: a field in development. In *American Journal of Physiology - Cell Physiology* (Vol. 323, Issue 5, pp. C1548–C1554). American Physiological Society. https://doi.org/10.1152/ajpcell.00403.2022

Harris, R. E., Setiawan, L., Saul, J., & Hariharan, I. K. (2016). *Localized epigenetic silencing of a damage-activated WNT enhancer limits regeneration in mature Drosophila imaginal discs*. https://doi.org/10.7554/eLife.11588.001

Harris, R. E., Stinchfield, M. J., Nystrom, S. L., McKay, D. J., & Hariharan, I. K. (2020). Damage-responsive, maturity-silenced enhancers regulate multiple genes that direct regeneration in drosophila. *ELife*, *9*, 1–26. https://doi.org/10.7554/eLife.58305

Harrison, D. A., McCoon, P. E., Binari, R., Gilman, M., & Perrimon, N. (1998). Drosophila unpaired encodes a secreted protein that activates the JAK signaling pathway. *Genes & Development*, *12*(20), 3252. https://doi.org/10.1101/GAD.12.20.3252

Hatori, R., & Kornberg, T. B. (2020). Hedgehog produced by the Drosophila wing imaginal disc induces distinct responses in three target tissues. *Development (Cambridge)*, *147*(22). https://doi.org/10.1242/dev.195974

Heinz, S., Romanoski, C. E., Benner, C., & Glass, C. K. (2015). The selection and function of cell type-specific enhancers. In *Nature Reviews Molecular Cell Biology* (Vol. 16, Issue 3, pp. 144–154). Nature Publishing Group. https://doi.org/10.1038/nrm3949

Held, L. I. (1993). Segment-polarity mutations cause stripes of defects along a leg segment in Drosophila. *Developmental Biology*, *157*(1), 240–250. https://doi.org/10.1006/DBIO.1993.1128

Henriques, T., Scruggs, B. S., Inouye, M. O., Muse, G. W., Williams, L. H., Burkholder, A. B., Lavender, C. A., Fargo, D. C., & Adelman, K. (2018). Widespread transcriptional pausing and elongation control at enhancers. *Genes and Development*, *32*(1), 26–41. https://doi.org/10.1101/gad.309351.117

Henry, J. J., & Tsonis, P. A. (2010). Molecular and cellular aspects of amphibian lens regeneration. In *Progress in Retinal and Eye Research* (Vol. 29, Issue 6, pp. 543–555). https://doi.org/10.1016/j.preteyeres.2010.07.002

Hernandez-Segura, A., Nehme, J., & Demaria, M. (2018). Hallmarks of Cellular Senescence. *Trends in Cell Biology*, *28*(6), 436–453. https://doi.org/10.1016/J.TCB.2018.02.001

Herr, P., & Basler, K. (2012). Porcupine-mediated lipidation is required for Wnt recognition by Wls. *Developmental Biology*, *361*(2), 392–402. https://doi.org/10.1016/j.ydbio.2011.11.003

Herranz, D., Ambesi-Impiombato, A., Palomero, T., Schnell, S. A., Belver, L., Wendorff, A. A., Xu, L., Castillo-Martin, M., Llobet-Navás, D., Cordon-Cardo, C., Clappier, E., Soulier, J., & Ferrando, A. A. (2014). A NOTCH1-driven MYC enhancer promotes T cell development, transformation and acute lymphoblastic leukemia. *Nature Medicine*, *20*(10), 1130–1137. https://doi.org/10.1038/nm.3665

Herranz, H., Eichenlaub, T., & Cohen, S. M. (2016). Cancer in Drosophila. Imaginal Discs as a Model for Epithelial Tumor Formation. In *Current Topics in Developmental Biology* (Vol. 116, pp. 181–199). Academic Press Inc. https://doi.org/10.1016/bs.ctdb.2015.11.037

Herrera, S. C., & Bach, E. A. (2019). JAK/STAT signaling in stem cells and regeneration: From drosophila to vertebrates. *Development (Cambridge)*, *146*(2). https://doi.org/10.1242/dev.167643

Herrera, S. C., & Bach, E. A. (2021). The emerging roles of jnk signaling in drosophila stem cell homeostasis. *International Journal of Molecular Sciences*, *22*(11). https://doi.org/10.3390/ijms22115519

Herrera, S. C., Martín, R., & Morata, G. (2013). Tissue Homeostasis in the Wing Disc of Drosophila melanogaster: Immediate Response to Massive Damage during Development. *PLoS Genetics*, *9*(4). https://doi.org/10.1371/journal.pgen.1003446

Herrera, S. C., & Morata, G. (2014). Transgressions of compartment boundaries and cell reprogramming during regeneration in Drosophila. *ELife*, *3*. https://doi.org/10.7554/elife.01831

Herz, H. M. (2016). Enhancer deregulation in cancer and other diseases. *BioEssays : News and Reviews in Molecular, Cellular and Developmental Biology*, *38*(10), 1003–1015. https://doi.org/10.1002/BIES.201600106

Heyn, H., Vidal, E., Ferreira, H. J., Vizoso, M., Sayols, S., Gomez, A., Moran, S., Boque-Sastre, R., Guil, S., Martinez-Cardus, A., Lin, C. Y., Royo, R., Sanchez-Mut, J. V., Martinez, R., Gut, M., Torrents, D., Orozco, M., Gut, I., Young, R. A., & Esteller, M. (2016). Epigenomic analysis detects aberrant super-enhancer DNA methylation in human cancer. *Genome Biology*, *17*(1). https://doi.org/10.1186/s13059-016-0879-2

Hieronymus, H., Murali, R., Tin, A., Yadav, K., Abida, W., Moller, H., Berney, D., Scher, H., Carver, B., Scardino, P., Schultz, N., Taylor, B., Vickers, A., Cuzick, J., & Sawyers, C. L. (2018). *Tumor copy number alteration burden is a pan-cancer prognostic factor associated with recurrence and death*. https://doi.org/10.7554/eLife.37294.001

Hnisz, D., Abraham, B. J., Lee, T. I., Lau, A., Saint-André, V., Sigova, A. A., Hoke, H. A., & Young, R. A. (2013). Super-enhancers in the control of cell identity and disease. *Cell*, *155*(4), 934. https://doi.org/10.1016/J.CELL.2013.09.053

Hnisz, D., Weintrau, A. S., Day, D. S., Valton, A. L., Bak, R. O., Li, C. H., Goldmann, J., Lajoie, B. R., Fan, Z. P., Sigova, A. A., Reddy, J., Borges-Rivera, D., Lee, T. I., Jaenisch, R., Porteus, M. H., Dekker, J., & Young, R. A. (2016). Activation of proto-oncogenes by disruption of chromosome neighborhoods. *Science (New York, N.Y.)*, *351*(6280), 1454–1458. https://doi.org/10.1126/SCIENCE.AAD9024

Höhn, A., Weber, D., Jung, T., Ott, C., Hugo, M., Kochlik, B., Kehm, R., König, J., Grune, T., & Castro, J. P. (2017). Happily (n)ever after: Aging in the context of oxidative stress, proteostasis loss and cellular senescence. *Redox Biology*, *11*, 482. https://doi.org/10.1016/J.REDOX.2016.12.001

Holland, A. J., & Cleveland, D. W. (2009). Boveri revisited: Chromosomal instability, aneuploidy and tumorigenesis. In *Nature Reviews Molecular Cell Biology* (Vol. 10, Issue 7, pp. 478–487). https://doi.org/10.1038/nrm2718

Hong, J. W., Hendrix, D. A., & Levine, M. S. (2008). Shadow enhancers as a source of evolutionary novelty. In *Science* (Vol. 321, Issue 5894, p. 1314). https://doi.org/10.1126/science.1160631

Hörnblad, A., Bastide, S., Langenfeld, K., Langa, F., & Spitz, F. (2021). Dissection of the Fgf8 regulatory landscape by in vivo CRISPR-editing reveals extensive intra- and inter-enhancer redundancy. *Nature Communications*, *12*(1). https://doi.org/10.1038/s41467-020-20714-y

Hsu, P. Y., Hsu, H. K., Lan, X., Juan, L., Yan, P. S., Labanowska, J., Heerema, N., Hsiao, T. H., Chiu, Y. C., Chen, Y., Liu, Y., Li, L., Li, R., Thompson, I. M., Nephew, K. P., Sharp, Z. D., Kirma, N. B., Jin, V. X., & Huang, T. H. M. (2013). Amplification of distant estrogen response elements deregulates target genes associated with tamoxifen resistance in breast cancer. *Cancer Cell*, *24*(2), 197–212. https://doi.org/10.1016/j.ccr.2013.07.007

Huang, F., Dambly-Chaudiere, C., & Ghysen, A. (1991). The emergence of sense organs in the wing disc of Dro-

sophila. *Development (Cambridge, England)*, *111*(4), 1087–1095. https://doi.org/10.1242/DEV.111.4.1087

Huang, G. N., Thatcher, J. E., McAnally, J., Kong, Y., Qi, X., Tan, W., DiMaio, J. M., Amatruda, J. F., Gerard, R. D., Hill, J. A., Bassel-Duby, R., & Olson, E. N. (2012). C/EBP Transcription Factors Mediate Epicardial Activation During Heart Development and Injury. *Science (New York, N.Y.)*, *338*(6114), 1599. https://doi.org/10.1126/SCIENCE.1229765

Huang, J., Wu, S., Barrera, J., Matthews, K., & Pan, D. (2005). The Hippo signaling pathway coordinately regulates cell proliferation and apoptosis by inactivating Yorkie, the Drosophila homolog of YAP. *Cell*, *122*(3), 421–434. https://doi.org/10.1016/j.cell.2005.06.007

Huang, Y., Huang, S., Di Scala, C., Wang, Q., Wandall, H. H., Fantini, J., & Zhang, Y. Q. (2018). The glycosphingolipid maccer promotes synaptic bouton formation in drosophila by interacting with Wnt. *ELife*, *7*. https://doi.org/10.7554/ELIFE.38183

Huh, J. R., Guo, M., & Hay, B. A. (2004). Compensatory proliferation induced by cell death in the Drosophila wing disc requires activity of the apical cell death caspase Dronc in a nonapoptotic role. *Current Biology : CB*, *14*(14), 1262–1266. https://doi.org/10.1016/J.CUB.2004.06.015

Igaki, T. (2009). Correcting developmental errors by apoptosis: Lessons from Drosophila JNK signaling. *Apoptosis*, *14*(8), 1021–1028. https://doi.org/10.1007/s10495-009-0361-7

Igaki, T., Kanda, H., Yamamoto-Goto, Y., Kanuka, H., Kuranaga, E., Aigaki, T., & Miura, M. (2002a). Eiger, a TNF superfamily ligand that triggers the Drosophila JNK pathway. *The EMBO Journal*, *21*(12), 3009. https://doi.org/10.1093/EMBOJ/CDF306

Igaki, T., Kanda, H., Yamamoto-Goto, Y., Kanuka, H., Kuranaga, E., Aigaki, T., & Miura, M. (2002b). Eiger, a TNF superfamily ligand that triggers the Drosophila JNK pathway. *The EMBO Journal*, *21*(12), 3009–3018. https://doi.org/10.1093/EMBOJ/CDF306

Igaki, T., & Miura, M. (2004). Role of Bcl-2 family members in invertebrates. In *Biochimica et Biophysica Acta - Molecular Cell Research* (Vol. 1644, Issues 2–3, pp. 73–81). https://doi.org/10.1016/j.bbamcr.2003.09.007

Igaki, T., & Miura, M. (2014). The Drosophila TNF ortholog Eiger: Emerging physiological roles and evolution of the TNF system. In *Seminars in Immunology* (Vol. 26, Issue 3, pp. 267–274). Academic Press. https://doi.org/10.1016/j.smim.2014.05.003

Igaki, T., Pagliarini, R. A., & Xu, T. (2006). Loss of Cell Polarity Drives Tumor Growth and Invasion through JNK Activation in Drosophila. *Current Biology*, *16*(11), 1139–1146. https://doi.org/10.1016/j.cub.2006.04.042

Igea, A., & Nebreda, A. R. (2015). The stress kinase p38α as a target for cancer therapy. In *Cancer Research* (Vol. 75, Issue 19, pp. 3997–4002). American Association for Cancer Research Inc. https://doi.org/10.1158/0008-5472.CAN-15-0173

Iismaa, S. E., Kaidonis, X., Nicks, A. M., Bogush, N., Kikuchi, K., Naqvi, N., Harvey, R. P., Husain, A., & Graham, R. M. (2018). Comparative regenerative mechanisms across different mammalian tissues. In *npj Regenerative Medicine* (Vol. 3, Issue 1). Nature Publishing Group. https://doi.org/10.1038/s41536-018-0044-5

Infante, C. R., Mihala, A. G., Park, S., Wang, J. S., Johnson, K. K., Lauderdale, J. D., & Menke, D. B. (2015). Shared Enhancer Activity in the Limbs and Phallus and Functional Divergence of a Limb-Genital cis-Regulatory Element in Snakes. *Developmental Cell*, *35*(1), 107–119. https://doi.org/10.1016/j.devcel.2015.09.003

Ito, T., & Igaki, T. (2016). Dissecting cellular senescence and SASP in Drosophila. *Inflammation and Regeneration*, *36*(1). https://doi.org/10.1186/S41232-016-0031-4

Ito, T., & Igaki, T. (2021). Yorkie drives Ras-induced tumor progression by microRNA-mediated inhibition of cellular senescence. In *Sci. Signal* (Vol. 14). https://www.science.org

Janson, K., Cohen, E. D., & Wilder, E. L. (2001). Expression of DWnt6, DWnt10, and DFz4 during Drosophila development. *Mechanisms of Development*, *103*(1–2), 117–120. https://doi.org/10.1016/S0925-4773(01)00323-9

Jenett, A., Rubin, G. M., Ngo, T. T. B., Shepherd, D., Murphy, C., Dionne, H., Pfeiffer, B. D., Cavallaro, A., Hall, D., Jeter, J., Iyer, N., Fetter, D., Hausenfluck, J. H., Peng, H., Trautman, E. T., Svirskas, R. R., Myers, E. W., Iwinski, Z. R., Aso, Y., … Zugates, C. T. (2012). A GAL4-Driver Line Resource for Drosophila Neurobiology. *Cell Reports*, *2*(4), 991–1001. https://doi.org/10.1016/j.celrep.2012.09.011

Jeong, Y., El-Jaick, K., Roessler, E., Muenke, M., & Epstein, D. J. (2006). A functional screen for sonic hedgehog

regulatory elements across a 1 Mb interval identifies long-range ventral forebrain enhancers. *Development*, *133*(4), 761–772. https://doi.org/10.1242/dev.02239

Jiang, Y., Seimiya, M., Schlumpf, T. B., & Paro, R. (2018). An intrinsic tumour eviction mechanism in Drosophila mediated by steroid hormone signalling. *Nature Communications*, *9*(1). https://doi.org/10.1038/s41467-018-05794-1

Jindal, G. A., Bantle, A. T., Solvason, J. J., Grudzien, J. L., D'Antonio-Chronowska, A., Lim, F., Le, S. H., Larsen, R. O., Klie, A., Frazer, K. A., & Farley, E. K. (2022). Affinity-optimizing variants within cardiac enhancers disrupt heart development and contribute to cardiac traits. *BioRxiv*, 2022.05.27.493636. https://doi.org/10.1101/2022.05.27.493636

Jindal, G. A., & Farley, E. K. (2021). Enhancer grammar in development, evolution, and disease: dependencies and interplay. In *Developmental Cell* (Vol. 56, Issue 5, pp. 575–587). Cell Press. https://doi.org/10.1016/j.devcel.2021.02.016

John, S., Sabo, P. J., Thurman, R. E., Sung, M. H., Biddie, S. C., Johnson, T. A., Hager, G. L., & Stamatoyannopoulos, J. A. (2011). Chromatin accessibility pre-determines glucocorticoid receptor binding patterns. In *Nature Genetics* (Vol. 43, Issue 3, pp. 264–268). https://doi.org/10.1038/ng.759

Johnson, R. L., Grenier, J. K., & Scott, M. P. (1995). patched overexpression alters wing disc size and pattern: transcriptional and post-transcriptional effects on hedgehog targets. *Development (Cambridge, England)*, *121*(12), 4161–4170. https://doi.org/10.1242/DEV.121.12.4161

Jopling, C., Sleep, E., Raya, M., Martí, M., Raya, A., & Belmonte, J. C. I. (2010). Zebrafish heart regeneration occurs by cardiomyocyte dedifferentiation and proliferation. *Nature*, *464*(7288), 606–609. https://doi.org/10.1038/NATURE08899

Joy, J., Barrio, L., Santos-Tapia, C., Romão, D., Giakoumakis, N. N., Clemente-Ruiz, M., & Milán, M. (2021). Proteostasis failure and mitochondrial dysfunction leads to aneuploidy-induced senescence. *Developmental Cell*, *56*(14), 2043-2058.e7. https://doi.org/10.1016/j.devcel.2021.06.009

Jun, J. Il, & Lau, L. F. (2010). The matricellular protein CCN1 induces fibroblast senescence and restricts fibrosis in cutaneous wound healing. *Nature Cell Biology*, *12*(7), 676–685. https://doi.org/10.1038/ncb2070

Junion, G., Spivakov, M., Girardot, C., Braun, M., Gustafson, E. H., Birney, E., & Furlong, E. E. M. (2012). A transcription factor collective defines cardiac cell fate and reflects lineage history. *Cell*, *148*(3), 473–486. https://doi.org/10.1016/j.cell.2012.01.030

Kaikkonen, M. U., & Adelman, K. (2018). Emerging Roles of Non-Coding RNA Transcription. In *Trends in Biochemical Sciences* (Vol. 43, Issue 9, pp. 654–667). Elsevier Ltd. https://doi.org/10.1016/j.tibs.2018.06.002

Kanda, H., Igaki, T., Kanuka, H., Yagi, T., & Miura, M. (2002). Wengen, a member of the Drosophila tumor necrosis factor receptor superfamily, is required for eiger signaling. *Journal of Biological Chemistry*, *277*(32), 28372–28375. https://doi.org/10.1074/jbc.C200324200

Kang, J., Hu, J., Karra, R., Dickson, A. L., Tornini, V. A., Nachtrab, G., Gemberling, M., Goldman, J. A., Black, B. L., & Poss, K. D. (2016). Modulation of tissue repair by regeneration enhancer elements. *Nature*, *532*(7598), 201–206. https://doi.org/10.1038/NATURE17644

Katainen, R., Dave, K., Pitkänen, E., Palin, K., Kivioja, T., Välimäki, N., Gylfe, A. E., Ristolainen, H., Hänninen, U. A., Cajuso, T., Kondelin, J., Tanskanen, T., Mecklin, J. P., Järvinen, H., Renkonen-Sinisalo, L., Lepistö, A., Kaasinen, E., Kilpivaara, O., Tuupanen, S., … Aaltonen, L. A. (2015). CTCF/cohesin-binding sites are frequently mutated in cancer. *Nature Genetics*, *47*(7), 818–821. https://doi.org/10.1038/ng.3335

Katsuyama, T., Comoglio, F., Seimiya, M., Cabuy, E., & Paro, R. (2015). During Drosophila disc regeneration, JAK/STAT coordinates cell proliferation with Dilp8-mediated developmental delay. *Proceedings of the National Academy of Sciences of the United States of America*, *112*(18), E2327–E2336. https://doi.org/10.1073/pnas.1423074112

Katsuyama, T., & Paro, R. (2011). Epigenetic reprogramming during tissue regeneration. In *FEBS Letters* (Vol. 585, Issue 11, pp. 1617–1624). https://doi.org/10.1016/j.febslet.2011.05.010

Kerr, K. S., Fuentes-Medel, Y., Brewer, C., Barria, R., Ashley, J., Abruzzi, K. C., Sheehan, A., Tasdemir-Yilmaz, O. E., Freeman, M. R., & Budnik, V. (2014). Glial wingless/wnt regulates glutamate receptor clustering and synaptic physiology at the Drosophila neuromuscular junction. *Journal of Neuroscience*, *34*(8), 2910–2920. https://doi.

org/10.1523/JNEUROSCI.3714-13.2014

Khan, S. J., Abidi, S. N. F., Skinner, A., Tian, Y., & Smith-Bolton, R. K. (2017). The Drosophila Duox maturation factor is a key component of a positive feedback loop that sustains regeneration signaling. *PLoS Genetics*, *13*(7). https://doi.org/10.1371/journal.pgen.1006937

Kikuta, H., Laplante, M., Navratilova, P., Komisarczuk, A. Z., Engström, P. G., Fredman, D., Akalin, A., Caccamo, M., Sealy, I., Howe, K., Ghislain, J., Pezeron, G., Mourrain, P., Ellingsen, S., Oates, A. C., Thisse, C., Thisse, B., Foucher, I., Adolf, B., … Becker, T. S. (2007). Genomic regulatory blocks encompass multiple neighboring genes and maintain conserved synteny in vertebrates. *Genome Research*, *17*(5), 545–555. https://doi.org/10.1101/gr.6086307

Kim, J., Irvine, K. D., & Carroll, S. B. (1995). Cell Recognition, Signal Induction, and Symmetrical Gene Activation at the Dorsal-Ventral Boundary of the Developing Drosophila Wing. In *Cell* (Vol. 82).

Kim, J., Sebring, A., Esch, J. J., Kraus, M. E., Vorwerk, K., Magee, J., & Carroll, S. B. (1996). Integration of positional signals and regulation of wing formation and identity by Drosophila vestigial gene. *Nature*, *382*(6587), 133–138. https://doi.org/10.1038/382133A0

Kim, S., & Wysocka, J. (2023). Deciphering the multi-scale, quantitative cis-regulatory code. In *Molecular Cell* (Vol. 83, Issue 3, pp. 373–392). Cell Press. https://doi.org/10.1016/j.molcel.2022.12.032

King, D. M., Hong, C. K. Y., Shepherdson, J. L., Granas, D. M., Maricque, B. B., & Cohen, B. A. (2020). Synthetic and genomic regulatory elements reveal aspects of Cis-regulatory grammar in mouse embryonic stem cells. *ELife*, *9*. https://doi.org/10.7554/eLife.41279

Klebes, A., Sustar, A., Kechris, K., Li, H., Schubiger, G., & Kornberg, T. B. (2005). Regulation of cellular plasticity in Drosophila imaginal disc cells by the Polycomb group, trithorax group and lama genes. *Development*, *132*(16), 3753–3765. https://doi.org/10.1242/dev.01927

Klein, T., & Arias, A. M. (1998). Different Spatial and Temporal Interactions between Notch, wingless, and vestigial Specify Proximal and Distal Pattern Elements of the Wing in Drosophila. In *DEVELOPMENTAL BIOLOGY* (Vol. 194).

Klemm, S. L., Shipony, Z., & Greenleaf, W. J. (2019). Chromatin accessibility and the regulatory epigenome. In *Nature Reviews Genetics* (Vol. 20, Issue 4, pp. 207–220). Nature Publishing Group. https://doi.org/10.1038/s41576-018-0089-8

Kopp, H. G., Hooper, A. T., Shmelkov, S. V., & Rafii, S. (2007). β-galactosidase staining on bone marrow. The osteoclast pitfall. *Histology and Histopathology*, *22*(7–9), 971–976. https://doi.org/10.14670/HH-22.971

Kornberg, T. (1981). engrailed: A gene controlling compartment and segment formation in Drosophila. In *Genetics* (Vol. 78, Issue 2).

Korolchuk, V. I., Miwa, S., Carroll, B., & von Zglinicki, T. (2017). Mitochondria in Cell Senescence: Is Mitophagy the Weakest Link? In *EBioMedicine* (Vol. 21, pp. 7–13). Elsevier B.V. https://doi.org/10.1016/j.ebiom.2017.03.020

Krizhanovsky, V., Yon, M., Dickins, R. A., Hearn, S., Simon, J., Miething, C., Yee, H., Zender, L., & Lowe, S. W. (2008). Senescence of Activated Stellate Cells Limits Liver Fibrosis. *Cell*, *134*(4), 657–667. https://doi.org/10.1016/j.cell.2008.06.049

Kron, K. J., Bailey, S. D., & Lupien, M. (2014). Enhancer alterations in cancer: a source for a cell identity crisis. *Genome Medicine*, *6*(9). https://doi.org/10.1186/S13073-014-0077-3

Kubo, N., Ishii, H., Xiong, X., Bianco, S., Meitinger, F., Hu, R., Hocker, J. D., Conte, M., Gorkin, D., Yu, M., Li, B., Dixon, J. R., Hu, M., Nicodemi, M., Zhao, H., & Ren, B. (2021). Promoter-proximal CTCF binding promotes distal enhancer-dependent gene activation. *Nature Structural and Molecular Biology*, *28*(2), 152–161. https://doi.org/10.1038/s41594-020-00539-5

Kubota, K., Goto, S., Eto, K., & Hayashi, S. (2000). EGF receptor attenuates Dpp signaling and helps to distinguish the wing and leg cell fates in Drosophila. *Development (Cambridge, England)*, *127*(17), 3769–3776. https://doi.org/10.1242/DEV.127.17.3769

Kubota, K., Goto, S., & Hayashi, S. (2003). The role of Wg signaling in the patterning of embryonic leg primordium in Drosophila. *Developmental Biology*, *257*(1), 117–126. https://doi.org/10.1016/S0012-1606(03)00062-9

Kuilman, T., & Peeper, D. S. (2009). Senescence-messaging secretome: SMS-ing cellular stress. *Nature Reviews Cancer 2009 9:2*, *9*(2), 81–94. https://doi.org/10.1038/nrc2560

Kumari, R., & Jat, P. (2021). Mechanisms of Cellular Senescence: Cell Cycle Arrest and Senescence Associated Secretory Phenotype. In *Frontiers in Cell and Developmental Biology* (Vol. 9). Frontiers Media S.A. https://doi.org/10.3389/fcell.2021.645593

Kurada, P., & White, K. (1998). Ras promotes cell survival in Drosophila by downregulating hid expression. *Cell*, *95*(3), 319–329. https://doi.org/10.1016/S0092-8674(00)81764-X

Kuroda, M. I., Kang, H., De, S., & Kassis, J. A. (2020). *Dynamic Competition of Polycomb and Trithorax in Transcriptional Programming*. https://doi.org/10.1146/annurev-biochem-120219

Kurz, D. J., Decary, S., Hong, Y., & Erusalimsky, J. D. (2000). Senescence-associated (beta)-galactosidase reflects an increase in lysosomal mass during replicative ageing of human endothelial cells. *Journal of Cell Science*, *113 (Pt 20)*(20), 3613–3622. https://doi.org/10.1242/JCS.113.20.3613

Kvon, E. Z., Kazmar, T., Stampfel, G., Yáñez-Cuna, J. O., Pagani, M., Schernhuber, K., Dickson, B. J., & Stark, A. (2014). Genome-scale functional characterization of Drosophila developmental enhancers in vivo. *Nature*, *512*(1), 91–95. https://doi.org/10.1038/nature13395

Kvon, E. Z., Waymack, R., Gad, M., & Wunderlich, Z. (2021). Enhancer redundancy in development and disease. In *Nature Reviews Genetics* (Vol. 22, Issue 5, pp. 324–336). Nature Research. https://doi.org/10.1038/s41576-020-00311-x

La Fortezza, M., Schenk, M., Cosolo, A., Kolybaba, A., Grass, I., & Classen, A. K. (2016). JAK/STAT signalling mediates cell survival in response to tissue stress. *Development (Cambridge)*, *143*(16), 2907–2919. https://doi.org/10.1242/dev.132340

La Marca, J. E., & Richardson, H. E. (2020). Two-Faced: Roles of JNK Signalling During Tumourigenesis in the Drosophila Model. In *Frontiers in Cell and Developmental Biology* (Vol. 8). Frontiers Media S.A. https://doi.org/10.3389/fcell.2020.00042

Lagha, M., Bothma, J. P., & Levine, M. (2012). Mechanisms of transcriptional precision in animal development. In *Trends in Genetics* (Vol. 28, Issue 8, pp. 409–416). https://doi.org/10.1016/j.tig.2012.03.006

Lane, M. E., Sauer, K., Wallace, K., Jan, Y. N., Lehner, C. F., & Vaessin, H. (1996). Dacapo, a cyclin-dependent kinase inhibitor, stops cell proliferation during Drosophila development. *Cell*, *87*(7), 1225–1235. https://doi.org/10.1016/S0092-8674(00)81818-8

Laverty, C., Lucci, J., & Akhtar, A. (2010). The MSL complex: X chromosome and beyond. In *Current Opinion in Genetics and Development* (Vol. 20, Issue 2, pp. 171–178). Elsevier Ltd. https://doi.org/10.1016/j.gde.2010.01.007

Lavista-Llanos, S., Centanin, L., Irisarri, M., Russo, D. M., Gleadle, J. M., Bocca, S. N., Muzzopappa, M., Ratcliffe, P. J., & Wappner, P. (2002). Control of the hypoxic response in Drosophila melanogaster by the basic helix-loop-helix PAS protein similar. *Molecular and Cellular Biology*, *22*(19), 6842–6853. https://doi.org/10.1128/MCB.22.19.6842-6853.2002

Lecuit, T., Brook, W. J., Ng, M., Calleja, M., Sun, H., & Cohen, S. M. (1996). Two distinct mechanisms for long-range patterning by Decapentaplegic in the Drosophila wing. *Nature*, *381*(6581), 387–393. https://doi.org/10.1038/381387A0

Lee, N., Maurange, C., Ringrose, L., & Paro, R. (2005). Suppression of Polycomb group proteins by JNK signalling induces transdetermination in Drosophila imaginal discs. *Nature*, *438*(7065), 234–237. https://doi.org/10.1038/nature04120

Lee, S., Jeong, S. Y., Lim, W. C., Kim, S., Park, Y. Y., Sun, X., Youle, R. J., & Cho, H. (2007). Mitochondrial fission and fusion mediators, hFis1 and OPA1, modulate cellular senescence. *Journal of Biological Chemistry*, *282*(31), 22977–22983. https://doi.org/10.1074/jbc.M700679200

Lee, S., & Schmitt, C. A. (2019). The dynamic nature of senescence in cancer. In *Nature Cell Biology* (Vol. 21, Issue 1, pp. 94–101). Nature Publishing Group. https://doi.org/10.1038/s41556-018-0249-2

Legent, K., & Treisman, J. E. (2008). Wingless signaling in Drosophila eye development. In *Methods in Molecular Biology* (Vol. 469, pp. 141–161). https://doi.org/10.1007/978-1-60327-469-2_12

Lehmann, B. D., Paine, M. S., Brooks, A. M., McCubrey, J. A., Renegar, R. H., Wang, R., & Terrian, D. M. (2008). Senescence-associated exosome release from human prostate cancer cells. *Cancer Research*, *68*(19), 7864–7871. https://doi.org/10.1158/0008-5472.CAN-07-6538

Lettice, L. A., Williamson, I., Wiltshire, J. H., Peluso, S., Devenney, P. S., Hill, A. E., Essafi, A., Hagman, J., Mort, R., Grimes, G., DeAngelis, C. L., & Hill, R. E. (2012). Opposing Functions of the ETS Factor Family Define Shh Spatial Expression in Limb Buds and Underlie Polydactyly. *Developmental Cell*, *22*(2), 459–467. https://doi.org/10.1016/j.devcel.2011.12.010

Levine, M. (2010). Transcriptional enhancers in animal development and evolution. In *Current Biology* (Vol. 20, Issue 17). Cell Press. https://doi.org/10.1016/j.cub.2010.06.070

Levine, M. S., & Holland, A. J. (2018). *The impact of mitotic errors on cell proliferation and tumorigenesis*. https://doi.org/10.1101/gad.314351

Lewis, E. B. (1978). A gene complex controlling segmentation in Drosophila. *Nature 1978 276:5688*, *276*(5688), 565–570. https://doi.org/10.1038/276565A0

Li, C., Shen, Y., Huang, L., Liu, C., & Wang, J. (2021). Senolytic therapy ameliorates renal fibrosis postacute kidney injury by alleviating renal senescence. *FASEB Journal*, *35*(1). https://doi.org/10.1096/fj.202001855RR

Li, D., Sun, J., & Zhong, T. P. (2022). Wnt Signaling in Heart Development and Regeneration. In *Current Cardiology Reports* (Vol. 24, Issue 10, pp. 1425–1438). Springer. https://doi.org/10.1007/s11886-022-01756-8

Li, M., Fang, X., Baker, D. J., Guo, L., Gao, X., Wei, Z., Han, S., Van Deursen, J. M., & Zhang, P. (2010). The ATM-p53 pathway suppresses aneuploidy-induced tumorigenesis. *Proceedings of the National Academy of Sciences of the United States of America*, *107*(32), 14188–14193. https://doi.org/10.1073/pnas.1005960107

Li, X. Y., Thomas, S., Sabo, P. J., Eisen, M. B., Stamatoyannopoulos, J. A., & Biggin, M. D. (2011). The role of chromatin accessibility in directing the widespread, overlapping patterns of Drosophila transcription factor binding. *Genome Biology*, *12*(4). https://doi.org/10.1186/gb-2011-12-4-r34

Lim, F., Ryan, G. E., Le, S. H., Solvason, J. J., Steffen, P., & Farley, E. K. (2022). Affinity-optimizing variants within the ZRS enhancer disrupt limb development. *BioRxiv*, 2022.05.27.493789. https://doi.org/10.1101/2022.05.27.493789

Lorberbaum, D. S., Ramos, A. I., Peterson, K. A., Carpenter, B. S., Parker, D. S., De, S., Hillers, L. E., Blake, V. M., Nishi, Y., McFarlane, M. R., Chiang, A. C. Y., Kassis, J. A., Allen, B. L., McMahon, A. P., & Barolo, S. (2016). An ancient yet flexible cis-regulatory architecture allows localized Hedgehog tuning by patched/Ptch1. *ELife*, *5*(MAY2016). https://doi.org/10.7554/ELIFE.13550

Love, N. R., Chen, Y., Ishibashi, S., Kritsiligkou, P., Lea, R., Koh, Y., Gallop, J. L., Dorey, K., & Amaya, E. (2013). Amputation-induced reactive oxygen species are required for successful Xenopus tadpole tail regeneration. *Nature Cell Biology*, *15*(2), 222–228. https://doi.org/10.1038/ncb2659

Lukow, D. A., & Sheltzer, J. M. (2022). Chromosomal instability and aneuploidy as causes of cancer drug resistance. In *Trends in Cancer* (Vol. 8, Issue 1, pp. 43–53). Cell Press. https://doi.org/10.1016/j.trecan.2021.09.002

Ma, C., & Moses, K. (1995). Wingless and patched are negative regulators of the morphogenetic furrow and can affect tissue polarity in the developing Drosophila compound eye. *Development (Cambridge, England)*, *121*(8), 2279–2289. https://doi.org/10.1242/DEV.121.8.2279

Majidinia, M., Aghazadeh, J., Jahanban-Esfahlani, R., & Yousefi, B. (2018). The roles of Wnt/β-catenin pathway in tissue development and regenerative medicine. In *Journal of Cellular Physiology* (Vol. 233, Issue 8, pp. 5598–5612). Wiley-Liss Inc. https://doi.org/10.1002/jcp.26265

Mandaravally Madhavan, M., & Schneiderman, H. A. (1977). Histological analysis of the dynamics of growth of imaginal discs and histoblast nests during the larval development ofDrosophila melanogaster. *Wilhelm Roux's Archives of Developmental Biology*, *183*(4), 269–305. https://doi.org/10.1007/BF00848459

Martín, F. A., Peréz-Garijo, A., & Morata, G. (2009). Apoptosis in Drosophila: Compensatory proliferation and undead cells. In *International Journal of Developmental Biology* (Vol. 53, Issues 8–10, pp. 1341–1347). https://doi.org/10.1387/ijdb.072447fm

Martín, R., & Morata, G. (2018). Regenerative response of different regions of drosophila imaginal discs. *International Journal of Developmental Biology*, *62*(6–8), 507–512. https://doi.org/10.1387/ijdb.170326gm

Martín-Blanco, E., Gampel, A., Ring, J., Virdee, K., Kirov, N., Tolkovsky, A. M., & Martinez-Arias, A. (1998). *puckered encodes a phosphatase that mediates a feedback loop regulating JNK activity during dorsal closure in Drosophila*. www.genesdev.org

Martini, H., & Passos, J. F. (2023). Cellular senescence: all roads lead to mitochondria. In *FEBS Journal* (Vol. 290, Issue 5, pp. 1186–1202). John Wiley and Sons Inc. https://doi.org/10.1111/febs.16361

Mata, J., Curado, S., Ephrussi, A., & Rorth, P. (2000). Tribbles coordinates mitosis and morphogenesis in Drosophila by regulating string/CDC25 proteolysis. *Cell*, *101*(5), 511–522. https://doi.org/10.1016/S0092-8674(00)80861-2

Mattila, J., Omelyanchuk, L., Kyttälä, S., Turunen, H., & Nokkala, S. (2005). Role of Jun N-terminal Kinase (JNK) signaling in the wound healing and regeneration of a Drosophila melanogaster wing imaginal disc. *International Journal of Developmental Biology*, *49*(4), 391–399. https://doi.org/10.1387/ijdb.052006jm

Maurano, M. T., Humbert, R., Rynes, E., Thurman, R. E., Haugen, E., Wang, H., Reynolds, A. P., Sandstrom, R., Qu, H., Brody, J., Shafer, A., Neri, F., Lee, K., Kutyavin, T., Stehling-Sun, S., Johnson, A. K., Canfield, T. K., Giste, E., Diegel, M., … Stamatoyannopoulos, J. A. (2012). Systematic localization of common disease-associated variation in regulatory DNA. *Science (New York, N.Y.)*, *337*(6099), 1190–1195. https://doi.org/10.1126/SCIENCE.1222794

Maurya, S. S. (2021). Role of Enhancers in Development and Diseases. *Epigenomes*, *5*(4). https://doi.org/10.3390/EPIGENOMES5040021

McClure, K. D., Sustar, A., & Schubiger, G. (2008). Three genes control the timing, the site and the size of blastema formation in Drosophila. *Developmental Biology*, *319*(1), 68–77. https://doi.org/10.1016/j.ydbio.2008.04.004

McGuire, S. E., Le, P. T., Osborn, A. J., Matsumoto, K., & Davis, R. L. (2003). Spatiotemporal rescue of memory dysfunction in Drosophila. *Science (New York, N.Y.)*, *302*(5651), 1765–1768. https://doi.org/10.1126/SCIENCE.1089035

Merika, M., & Thanos, D. (2001). Enhanceosomes. *Current Opinion in Genetics & Development*, *11*(2), 205–208. https://doi.org/10.1016/S0959-437X(00)00180-5

Méthot, N., & Basler, K. (1999). Hedgehog controls limb development by regulating the activities of distinct transcriptional activator and repressor forms of Cubitus interruptus. *Cell*, *96*(6), 819–831. https://doi.org/10.1016/S0092-8674(00)80592-9

Meyer, K., Hodwin, B., Ramanujam, D., Engelhardt, S., & Sarikas, A. (2016). *Essential Role for Premature Senescence of Myofibroblasts in Myocardial Fibrosis*.

Michalopoulos, G. K., & DeFrances, M. C. (1997). Liver regeneration. *Science (New York, N.Y.)*, *276*(5309), 60–65. https://doi.org/10.1126/SCIENCE.276.5309.60

Mikhaylichenko, O., Bondarenko, V., Harnett, D., Schor, I. E., Males, M., Viales, R. R., & Furlong, E. E. M. (2018). The degree of enhancer or promoter activity is reflected by the levels and directionality of eRNA transcription. *Genes and Development*, *32*(1), 42–57. https://doi.org/10.1101/gad.308619.117

Milán, M., Clemente-Ruiz, M., Dekanty, A., & Muzzopappa, M. (2014). Aneuploidy and tumorigenesis in Drosophila. In *Seminars in Cell and Developmental Biology* (Vol. 28, pp. 110–115). Elsevier Ltd. https://doi.org/10.1016/j.semcdb.2014.03.014

Miremadi, A., Oestergaard, M. Z., Pharoah, P. D. P., & Caldas, C. (2007). Cancer genetics of epigenetic genes. In *Human Molecular Genetics* (Vol. 16, Issue R1). https://doi.org/10.1093/hmg/ddm021

Mirkovic, M., Guilgur, L. G., Tavares, A., Passagem-Santos, D., & Oliveira, R. A. (2019). Induced aneuploidy in neural stem cells triggers a delayed stress response and impairs adult life span in flies. *PLoS Biology*, *17*(2). https://doi.org/10.1371/journal.pbio.3000016

Mittal, M., Siddiqui, M. R., Tran, K., Reddy, S. P., & Malik, A. B. (2014). Reactive oxygen species in inflammation and tissue injury. In *Antioxidants and Redox Signaling* (Vol. 20, Issue 7, pp. 1126–1167). https://doi.org/10.1089/ars.2012.5149

Miwa, S., Kashyap, S., Chini, E., & von Zglinicki, T. (2022). Mitochondrial dysfunction in cell senescence and aging. In *Journal of Clinical Investigation* (Vol. 132, Issue 13). American Society for Clinical Investigation. https://doi.org/10.1172/JCI158447

Moberg, K. H., & Hariharan, I. K. (2003). Big things from a little RNA. In *Trends in Cell Biology* (Vol. 13, Issue 9, pp. 455–457). Elsevier Ltd. https://doi.org/10.1016/S0962-8924(03)00168-5

Moore, L. D., Le, T., & Fan, G. (2013). DNA methylation and its basic function. In *Neuropsychopharmacology* (Vol. 38, Issue 1, pp. 23–38). https://doi.org/10.1038/npp.2012.112

Morata, G., & Calleja, M. (2020). Cell competition and tumorigenesis in the imaginal discs of Drosophila. In *Seminars in Cancer Biology* (Vol. 63, pp. 19–26). Academic Press. https://doi.org/10.1016/j.semcancer.2019.06.010

Morata, G., & Lawrence, P. A. (1977). The Development of wingless, a Homeotic Mutation of Drosophila. In *DEVELOPMENTAL BIOLOGY* (Vol. 56).

Moreno, E., Yan, M., & Basler, K. (2002). Evolution of TNF signaling mechanisms: JNK-dependent apoptosis triggered by Eiger, the Drosophila homolog of the TNF superfamily. *Current Biology : CB*, *12*(14), 1263–1268. https://doi.org/10.1016/S0960-9822(02)00954-5

Muñoz-Espín, D., & Serrano, M. (2014). Cellular senescence: From physiology to pathology. In *Nature Reviews Molecular Cell Biology* (Vol. 15, Issue 7, pp. 482–496). Nature Publishing Group. https://doi.org/10.1038/nrm3823

Murcia, L., Clemente-Ruiz, M., Pierre-Elies, P., Royou, A., & Milán, M. (2019). Selective Killing of RAS-Malignant Tissues by Exploiting Oncogene-Induced DNA Damage. *Cell Reports*, *28*(1), 119-131.e4. https://doi.org/10.1016/j.celrep.2019.06.004

Muro, I., Hay, B. A., & Clem, R. J. (2002). The Drosophila DIAP1 protein is required to prevent accumulation of a continuously generated, processed form of the apical caspase DRONC. *Journal of Biological Chemistry*, *277*(51), 49644–49650. https://doi.org/10.1074/jbc.M203464200

Musacchio, A., & Salmon, E. D. (2007). The spindle-assembly checkpoint in space and time. In *Nature Reviews Molecular Cell Biology* (Vol. 8, Issue 5, pp. 379–393). https://doi.org/10.1038/nrm2163

Muzzopappa, M., Murcia, L., & Milán, M. (2017). Feedback amplification loop drives malignant growth in epithelial tissues. *Proceedings of the National Academy of Sciences of the United States of America*, *114*(35), E7291–E7300. https://doi.org/10.1073/pnas.1701791114

Mylonas, K. J., O'sullivan, E. D., Humphries, D., Baird, D. P., Docherty, M.-H., Neely, S. A., Krimpenfort, P. J., Melk, A., Schmitt, R., Ferreira-Gonzalez, S., Forbes, S. J., Hughes, J., & Ferenbach, D. A. (2021). Cellular senescence inhibits renal regeneration after injury in mice, with senolytic treatment promoting repair. In *Sci. Transl. Med* (Vol. 13). https://www.science.org

Nakamura, M., Ohsawa, S., & Igaki, T. (2014). Mitochondrial defects trigger proliferation of neighbouring cells via a senescence-associated secretory phenotype in Drosophila. *Nature Communications*, *5*. https://doi.org/10.1038/ncomms6264

Narbonne-Reveau, K., & Maurange, C. (2019). Developmental regulation of regenerative potential in Drosophila by ecdysone through a bistable loop of ZBTB transcription factors. *PLoS Biology*, *17*(2). https://doi.org/10.1371/journal.pbio.3000149

Narciso, C., Wu, Q., Brodskiy, P., Garston, G., Baker, R., Fletcher, A., & Zartman, J. (2015). Patterning of wound-induced intercellular Ca2+ flashes in a developing epithelium. *Physical Biology*, *12*(5). https://doi.org/10.1088/1478-3975/12/5/056005

Narita, M., Nuñ Ez, S., Heard, E., Narita, M., Lin, A. W., Hearn, S. A., Spector, D. L., Hannon, G. J., & Lowe, S. W. (2003). Rb-Mediated Heterochromatin Formation and Silencing of E2F Target Genes during Cellular Senescence. In *Cell* (Vol. 113).

Nellen, D., Burke, R., Struhl, G., & Basler, K. (1996). Direct and long-range action of a DPP morphogen gradient. *Cell*, *85*(3), 357–368. https://doi.org/10.1016/S0092-8674(00)81114-9

Neumann, C. J., & Cohen, S. M. (1996). Distinct mitogenic and cell fate specification functions of wingless in different regions of the wing. *Development (Cambridge, England)*, *122*(6), 1781–1789. https://doi.org/10.1242/DEV.122.6.1781

Neumann, C. J., & Cohen, S. M. (1997). Long-range action of Wingless organizes the dorsal-ventral axis of the Drosophila wing. *Development (Cambridge, England)*, *124*(4), 871–880. https://doi.org/10.1242/DEV.124.4.871

Ng, M., Diaz-Benjumea, F. J., & Cohen, S. M. (1995). Nubbin encodes a POU-domain protein required for proxi-

mal-distal patterning in the Drosophila wing. *Development (Cambridge, England)*, *121*(2), 589–599. https://doi.org/10.1242/DEV.121.2.589

Ng, M., Diaz-Benjumea, F. J., Vincent, J. P., Wu, J., & Cohen, S. M. (1996). Specification of the wing by localized expression of wingless protein. *Nature*, *381*(6580), 316–318. https://doi.org/10.1038/381316A0

Ng M, Diaz-Benjumea FJ, Vincent JP, Wu J, & Cohen SM. (1996). Specification of the wing by localized expression of wingless protein. *Nature*. https://doi.org/10.1038/381316a0

Nishiyama, A., & Nakanishi, M. (2021). Navigating the DNA methylation landscape of cancer. In *Trends in Genetics* (Vol. 37, Issue 11, pp. 1012–1027). Elsevier Ltd. https://doi.org/10.1016/j.tig.2021.05.002

Nora, E. P., Goloborodko, A., Valton, A. L., Gibcus, J. H., Uebersohn, A., Abdennur, N., Dekker, J., Mirny, L. A., & Bruneau, B. G. (2017). Targeted Degradation of CTCF Decouples Local Insulation of Chromosome Domains from Genomic Compartmentalization. *Cell*, *169*(5), 930-944.e22. https://doi.org/10.1016/j.cell.2017.05.004

Nord, A. S., Blow, M. J., Attanasio, C., Akiyama, J. A., Holt, A., Hosseini, R., Phouanenavong, S., Plajzer-Frick, I., Shoukry, M., Afzal, V., Rubenstein, J. L. R., Rubin, E. M., Pennacchio, L. A., & Visel, A. (2013). Rapid and pervasive changes in genome-wide enhancer usage during mammalian development. *Cell*, *155*(7), 1521–1531. https://doi.org/10.1016/j.cell.2013.11.033

Northcott, P. A., Lee, C., Zichner, T., Stütz, A. M., Erkek, S., Kawauchi, D., Shih, D. J. H., Hovestadt, V., Zapatka, M., Sturm, D., Jones, D. T. W., Kool, M., Remke, M., Cavalli, F. M. G., Zuyderduyn, S., Bader, G. D., Vandenberg, S., Esparza, L. A., Ryzhova, M., … Pfister, S. M. (2014). Enhancer hijacking activates GFI1 family oncogenes in medulloblastoma. *Nature*, *511*(7510), 428–434. https://doi.org/10.1038/nature13379

Ollmann, M., Young, L. M., Di Como, C. J., Karim, F., Belvin, M., Robertson, S., Whittaker, K., Demsky, M., Fisher, W. W., Buchman, A., Duyk, G., Friedman, L., Prives, C., & Kopczynski, C. (2000). Drosophila p53 is a structural and functional homolog of the tumor suppressor p53. *Cell*, *101*(1), 91–101. https://doi.org/10.1016/S0092-8674(00)80626-1

O'Neill, E. M., Rebay, I., Tjian, R., & Rubin, G. M. (1994). The activities of two Ets-related transcription factors required for Drosophila eye development are modulated by the Ras/MAPK pathway. *Cell*, *78*(1), 137–147. https://doi.org/10.1016/0092-8674(94)90580-0

Ordóñez-Morán, P., Dafflon, C., Imajo, M., Nishida, E., & Huelsken, J. (2015). HOXA5 Counteracts Stem Cell Traits by Inhibiting Wnt Signaling in Colorectal Cancer. *Cancer Cell*, *28*(6), 815–829. https://doi.org/10.1016/j.ccell.2015.11.001

Osterwalder, M., Barozzi, I., Tissiéres, V., Fukuda-Yuzawa, Y., Mannion, B. J., Afzal, S. Y., Lee, E. A., Zhu, Y., Plajzer-Frick, I., Pickle, C. S., Kato, M., Garvin, T. H., Pham, Q. T., Harrington, A. N., Akiyama, J. A., Afzal, V., Lopez-Rios, J., Dickel, D. E., Visel, A., & Pennacchio, L. A. (2018). Enhancer redundancy provides phenotypic robustness in mammalian development. *Nature*, *554*(7691), 239–243. https://doi.org/10.1038/nature25461

Otera, H., & Mihara, K. (2012). Mitochondrial dynamics: Functional link with apoptosis. In *International Journal of Cell Biology*. https://doi.org/10.1155/2012/821676

Paaby, A. B., & Rockman, M. V. (2013). The many faces of pleiotropy. In *Trends in Genetics* (Vol. 29, Issue 2, pp. 66–73). https://doi.org/10.1016/j.tig.2012.10.010

Pachano, T., Haro, E., & Rada-Iglesias, A. (2022). Enhancer-gene specificity in development and disease. In *Development (Cambridge)* (Vol. 149, Issue 11). Company of Biologists Ltd. https://doi.org/10.1242/dev.186536

Paramos-de-Carvalho, D., Martins, I., Cristóvão, A. M., Dias, A. F., Neves-Silva, D., Pereira, T., Chapela, D., Farinho, A., Jacinto, A., & Saúde, L. (2021). Targeting senescent cells improves functional recovery after spinal cord injury. *Cell Reports*, *36*(1). https://doi.org/10.1016/j.celrep.2021.109334

Parra, A. S., & Johnston, C. A. (2020). Mud Loss Restricts Yki-Dependent Hyperplasia in Drosophila Epithelia. *Journal of Developmental Biology*, *8*(4), 1–20. https://doi.org/10.3390/JDB8040034

Pasini, D., & Di Croce, L. (2016). Emerging roles for Polycomb proteins in cancer. In *Current Opinion in Genetics and Development* (Vol. 36, pp. 50–58). Elsevier Ltd. https://doi.org/10.1016/j.gde.2016.03.013

Passos, J. F., Nelson, G., Wang, C., Richter, T., Simillion, C., Proctor, C. J., Miwa, S., Olijslagers, S., Hallinan, J., Wipat, A., Saretzki, G., Rudolph, K. L., Kirkwood, T. B. L., & Von Zglinicki, T. (2010). Feedback between p21 and reactive oxygen production is necessary for cell senescence. *Molecular Systems Biology*, *6*. https://doi.org/10.1038/

MSB.2010.5

Passos, J. F., Saretzki, G., Ahmed, S., Nelson, G., Richter, T., Peters, H., Wappler, I., Birket, M. J., Harold, G., Schaeuble, K., Birch-Machin, M. A., Kirkwood, T. B. L., & Von Zglinicki, T. (2007). Mitochondrial dysfunction accounts for the stochastic heterogeneity in telomere-dependent senescence. *PLoS Biology*, *5*(5), 1138–1151. https://doi.org/10.1371/journal.pbio.0050110

Pastor-Pareja, J. C., Grawe, F., Martín-Blanco, E., & García-Bellido, A. (2004). Invasive cell behavior during Drosophila imaginal disc eversion is mediated by the JNK signaling cascade. *Developmental Cell*, *7*(3), 387–399. https://doi.org/10.1016/J.DEVCEL.2004.07.022

Patel, P. H., Pénalva, C., Kardorff, M., Roca, M., Pavlović, B., Thiel, A., Teleman, A. A., & Edgar, B. A. (2019). Damage sensing by a Nox-Ask1-MKK3-p38 signaling pathway mediates regeneration in the adult Drosophila midgut. *Nature Communications*, *10*(1). https://doi.org/10.1038/s41467-019-12336-w

Paul, L., Wang, S. H., Manivannan, S. N., Bonanno, L., Lewis, S., Austin, C. L., & Simcox, A. (2013). Dpp-induced Egfr signaling triggers postembryonic wing development in Drosophila. *Proceedings of the National Academy of Sciences of the United States of America*, *110*(13), 5058–5063. https://doi.org/10.1073/pnas.1217538110

Pearson, G., Robinson, F., Gibson, T. B., Xu, B.-E., Karandikar, M., Berman, K., & Cobb, M. H. (2001). *Mitogen-Activated Protein (MAP) Kinase Pathways: Regulation and Physiological Functions**. https://academic.oup.com/edrv/article/22/2/153/2423864

Pellock, B. J., Buff, E., White, K., & Hariharan, I. K. (2007). The Drosophila tumor suppressors Expanded and Merlin differentially regulate cell cycle exit, apoptosis, and Wingless signaling. *Developmental Biology*, *304*(1), 102–115. https://doi.org/10.1016/j.ydbio.2006.12.021

Pereira, P. S., Pinho, S., Johnson, K., Couso, J. P., & Casares, F. (2006). A 3' cis-regulatory region controls wingless expression in the Drosophila eye and leg primordia. *Developmental Dynamics*, *235*(1), 225–234. https://doi.org/10.1002/dvdy.20606

Pérez-Garijo, A., Martín, F. A., & Morata, G. (2004). Caspase inhibition during apoptosis causes abnormal signalling and developmental aberrations in Drosophila. *Development*, *131*(22), 5591–5598. https://doi.org/10.1242/dev.01432

Pérez-Garijo, A., Shlevkov, E., & Morata, G. (2009). The role of Dpp and Wg in compensatory proliferation and in the formation of hyperplastic overgrowths caused by apoptotic cells in the Drosophila wing disc. *Development*, *136*(7), 1169–1177. https://doi.org/10.1242/dev.034017

Perrimon, N. (1994). The Genetic Basis of Patterned Baldness in Drosophila. In *Cell* (Vol. 76).

Perry, M. W., Boettiger, A. N., & Levine, M. (2011). Multiple enhancers ensure precision of gap gene-expression patterns in the Drosophila embryo. *Proceedings of the National Academy of Sciences of the United States of America*, *108*(33), 13570–13575. https://doi.org/10.1073/pnas.1109873108

Petrie, T. A., Strand, N. S., Yang, C.-T., Rabinowitz, J. S., & Moon, R. T. (2015). Macrophages modulate adult zebrafish tail fin regeneration. *Development*, *142*(2), 406–406. https://doi.org/10.1242/dev.120642

Pfeiffer, S., Ricardo, S., Manneville, J. B., Alexandre, C., & Vincent, J. P. (2002). Producing cells retain and recycle Wingless in Drosophila embryos. *Current Biology : CB*, *12*(11), 957–962. https://doi.org/10.1016/S0960-9822(02)00867-9

Phillips, R. G., & Whittle, J. R. S. (1993). wingless expression mediates determination of peripheral nervous system elements in late stages of Drosophila wing disc development. *Development (Cambridge, England)*, *118*(2), 427–438. https://doi.org/10.1242/DEV.118.2.427

Phillips-Cremins, J. E., Sauria, M. E. G., Sanyal, A., Gerasimova, T. I., Lajoie, B. R., Bell, J. S. K., Ong, C. T., Hookway, T. A., Guo, C., Sun, Y., Bland, M. J., Wagstaff, W., Dalton, S., McDevitt, T. C., Sen, R., Dekker, J., Taylor, J., & Corces, V. G. (2013). Architectural protein subclasses shape 3D organization of genomes during lineage commitment. *Cell*, *153*(6), 1281–1295. https://doi.org/10.1016/j.cell.2013.04.053

Pinal, N., Calleja, M., & Morata, G. (2019). Pro-apoptotic and pro-proliferation functions of the JNK pathway of drosophila: Roles in cell competition, tumorigenesis and regeneration. *Open Biology*, *9*(3). https://doi.org/10.1098/rsob.180256

Pinal, N., Martín, M., Medina, I., & Morata, G. (2018). Short-term activation of the Jun N-terminal kinase path-

way in apoptosis-deficient cells of Drosophila induces tumorigenesis. *Nature Communications 2018 9:1*, *9*(1), 1–10. https://doi.org/10.1038/s41467-018-04000-6

Pirotte, N., Stevens, A. S., Fraguas, S., Plusquin, M., Van Roten, A., Van Belleghem, F., Paesen, R., Ameloot, M., Cebrià, F., Artois, T., & Smeets, K. (2015). Reactive oxygen species in planarian regeneration: An upstream necessity for correct patterning and brain formation. *Oxidative Medicine and Cellular Longevity*, *2015*. https://doi.org/10.1155/2015/392476

Pluquet, O., Pourtier, A., & Abbadie, C. (2015). The unfolded protein response and cellular senescence. A review in the theme: Cellular mechanisms of endoplasmic reticulum stress signaling in health and disease. *American Journal of Physiology - Cell Physiology*, *308*(6), 415–425. https://doi.org/10.1152/ajpcell.00334.2014

Popay, T. M., & Dixon, J. R. (2022). Coming full circle: On the origin and evolution of the looping model for enhancer–promoter communication. In *Journal of Biological Chemistry* (Vol. 298, Issue 8). American Society for Biochemistry and Molecular Biology Inc. https://doi.org/10.1016/j.jbc.2022.102117

Pospelova, T. V., Demidenko, Z. N., Bukreeva, E. I., Pospelov, V. A., Gudkov, A. V., & Blagosklonny, M. V. (2009). Pseudo-DNA damage response in senescent cells. In *Cell Cycle* (Vol. 8, Issue 24, pp. 4112–4118). Taylor and Francis Inc. https://doi.org/10.4161/cc.8.24.10215

Pott, S., & Lieb, J. D. (2015). What are super-enhancers? In *Nature Genetics* (Vol. 47, Issue 1, pp. 8–12). Nature Publishing Group. https://doi.org/10.1038/ng.3167

Rada-Iglesias, A., Bajpai, R., Swigut, T., Brugmann, S. A., Flynn, R. A., & Wysocka, J. (2011). A unique chromatin signature uncovers early developmental enhancers in humans. *Nature*, *470*(7333), 279–285. https://doi.org/10.1038/nature09692

Rafel, N., & Milán, M. (2008). Notch signalling coordinates tissue growth and wing fate specification in Drosophila. *Development*, *135*(24), 3995–4001. https://doi.org/10.1242/dev.027789

Rankin Willsey, H., Zheng, X., Carlos Pastor-Pareja, J., Jeremy Willsey, A., Beachy, P. A., & Xu, T. (2016). *Localized JNK signaling regulates organ size during development*. https://doi.org/10.7554/eLife.11491.001

Rao, S. S. P., Huntley, M. H., Durand, N. C., Stamenova, E. K., Bochkov, I. D., Robinson, J. T., Sanborn, A. L., Machol, I., Omer, A. D., Lander, E. S., & Aiden, E. L. (2014). A 3D map of the human genome at kilobase resolution reveals principles of chromatin looping. *Cell*, *159*(7), 1665–1680. https://doi.org/10.1016/j.cell.2014.11.021

Razzell, W., Evans, I. R., Martin, P., & Wood, W. (2013). Calcium flashes orchestrate the wound inflammatory response through duox activation and hydrogen peroxide release. *Current Biology*, *23*(5), 424–429. https://doi.org/10.1016/j.cub.2013.01.058

Rebay, I., & Rubin, G. M. (1995). Yan Functions as a General Inhibitor of Differentiation and Is Negatively Regulated by Activation of the Rasl/MAPK Pathway. In *Cell* (Vol. 81).

Recasens-Alvarez, C., Ferreira, A., & Milán, M. (2017). JAK/STAT controls organ size and fate specification by regulating morphogen production and signalling. *Nature Communications*, *8*. https://doi.org/10.1038/ncomms13815

Reddien, P. W. (2013). Specialized progenitors and regeneration. *Development (Cambridge)*, *140*(5), 951–957. https://doi.org/10.1242/dev.080499

Reiter, F., Wienerroither, S., & Stark, A. (2017). Combinatorial function of transcription factors and cofactors. In *Current Opinion in Genetics and Development* (Vol. 43, pp. 73–81). Elsevier Ltd. https://doi.org/10.1016/j.gde.2016.12.007

Repiso, A., Bergantiños, C., & Serras, F. (2013). Cell fate respecification and cell division orientation drive intercalary regeneration in Drosophila wing discs. *Development (Cambridge)*, *140*(17), 3541–3551. https://doi.org/10.1242/dev.095760

Requena, D., Álvarez, J. A., Gabilondo, H., Loker, R., Mann, R. S., & Estella, C. (2017). Origins and Specification of the Drosophila Wing. *Current Biology*, *27*(24), 3826-3836.e5. https://doi.org/10.1016/j.cub.2017.11.023

Restrepo, S., & Basler, K. (2016). Drosophila wing imaginal discs respond to mechanical injury via slow InsP 3 R-mediated intercellular calcium waves. *Nature Communications*, *7*. https://doi.org/10.1038/ncomms12450

Restrepo, S., Zartman, J. J., & Basler, K. (2014). Coordination of patterning and growth by the morphogen DPP. *Current Biology : CB*, *24*(6). https://doi.org/10.1016/J.CUB.2014.01.055

Rhinn, M., Ritschka, B., & Keyes, W. M. (2019). Cellular senescence in development, regeneration and disease. *Development (Cambridge)*, *146*(20). https://doi.org/10.1242/dev.151837

Richardson, H. E., & Portela, M. (2018). Modelling Cooperative Tumorigenesis in Drosophila. In *BioMed Research International* (Vol. 2018). Hindawi Limited. https://doi.org/10.1155/2018/4258387

Riesgo-Escovar, J. R., Jenni, M., Fritz, A., & Hafen, E. (1996). The Drosophila Jun-N-terminal kinase is required for cell morphogenesis but not for DJun-dependent cell fate specification in the eye. *Genes & Development*, *10*(21), 2759–2768. https://doi.org/10.1101/GAD.10.21.2759

Ring, N. A. R., Valdivieso, K., Grillari, J., Redl, H., & Ogrodnik, M. (2022). The role of senescence in cellular plasticity: Lessons from regeneration and development and implications for age-related diseases. In *Developmental Cell* (Vol. 57, Issue 9, pp. 1083–1101). Cell Press. https://doi.org/10.1016/j.devcel.2022.04.005

Ríos-Barrera, L. D., & Riesgo-Escovar, J. R. (2013). Regulating cell morphogenesis: The drosophila jun N-terminal kinase pathway. In *Genesis* (Vol. 51, Issue 3, pp. 147–162). https://doi.org/10.1002/dvg.22354

Rodier, F., Muñoz, D. P., Teachenor, R., Chu, V., Le, O., Bhaumik, D., Coppé, J. P., Campeau, E., Beauséjour, C. M., Kim, S. H., Davalos, A. R., & Campisi, J. (2011). DNA-SCARS: Distinct nuclear structures that sustain damage-induced senescence growth arrest and inflammatory cytokine secretion. *Journal of Cell Science*, *124*(1), 68–81. https://doi.org/10.1242/jcs.071340

Romão, D., Muzzopappa, M., Barrio, L., & Milán, M. (2021). The Upd3 cytokine couples inflammation to maturation defects in Drosophila. *Current Biology*, *31*(8), 1780-1787.e6. https://doi.org/10.1016/j.cub.2021.01.080

Rowley, M. J., & Corces, V. G. (2016). The three-dimensional genome: Principles and roles of long-distance interactions. In *Current Opinion in Cell Biology* (Vol. 40, pp. 8–14). Elsevier Ltd. https://doi.org/10.1016/j.ceb.2016.01.009

Roy, S., Huang, H., Liu, S., & Kornberg, T. B. (2014). Cytoneme-mediated contact-dependent transport of the Drosophila decapentaplegic signaling protein. *Science (New York, N.Y.)*, *343*(6173). https://doi.org/10.1126/SCIENCE.1244624

Rudrapatna, V. A., Bangi, E., & Cagan, R. L. (2013). Caspase signalling in the absence of apoptosis drives Jnk-dependent invasion. *EMBO Reports*, *14*(2), 172–177. https://doi.org/10.1038/embor.2012.217

Rudrapatna, V. A., Bangi, E., & Cagan, R. L. (2014). A Jnk-Rho-Actin remodeling positive feedback network directs Src-driven invasion. *Oncogene*, *33*(21), 2801–2806. https://doi.org/10.1038/onc.2013.232

Ruiz-Losada, M., Blom-Dahl, D., Córdoba, S., & Estella, C. (2018). Specification and patterning of Drosophila appendages. In *Journal of Developmental Biology* (Vol. 6, Issue 3). MDPI Multidisciplinary Digital Publishing Institute. https://doi.org/10.3390/jdb6030017

Ruiz-Losada, M., González, R., Peropadre, A., Gil-Gálvez, A., Tena, J. J., Baonza, A., & Estella, C. (2022). Coordination between cell proliferation and apoptosis after DNA damage in Drosophila. *Cell Death and Differentiation*, *29*(4), 832–845. https://doi.org/10.1038/s41418-021-00898-6

Ryoo, H. D., Gorenc, T., & Steller, H. (2004). Apoptotic cells can induce compensatory cell proliferation through the JNK and the Wingless signaling pathways. *Developmental Cell*, *7*(4), 491–501. https://doi.org/10.1016/J.DEVCEL.2004.08.019

Sabarís, G., Laiker, I., Preger-Ben Noon, E., & Frankel, N. (2019). Actors with Multiple Roles: Pleiotropic Enhancers and the Paradigm of Enhancer Modularity. In *Trends in Genetics* (Vol. 35, Issue 6, pp. 423–433). Elsevier Ltd. https://doi.org/10.1016/j.tig.2019.03.006

Saito, Y., Chikenji, T. S., Matsumura, T., Nakano, M., & Fujimiya, M. (2020). Exercise enhances skeletal muscle regeneration by promoting senescence in fibro-adipogenic progenitors. *Nature Communications*, *11*(1). https://doi.org/10.1038/s41467-020-14734-x

Sandoval-Guzmán, T., Wang, H., Khattak, S., Schuez, M., Roensch, K., Nacu, E., Tazaki, A., Joven, A., Tanaka, E. M., & Simon, A. (2014). Fundamental differences in dedifferentiation and stem cell recruitment during skeletal muscle regeneration in two salamander species. *Cell Stem Cell*, *14*(2), 174–187. https://doi.org/10.1016/j.stem.2013.11.007

Santabárbara-Ruiz, P., Esteban-Collado, J., Pérez, L., Viola, G., Abril, J. F., Milán, M., Corominas, M., & Serras, F. (2019). Ask1 and Akt act synergistically to promote ROS-dependent regeneration in Drosophila. *PLoS Genetics*,

15(1). https://doi.org/10.1371/journal.pgen.1007926

Santabárbara-Ruiz, P., López-Santillán, M., Martínez-Rodríguez, I., Binagui-Casas, A., Pérez, L., Milán, M., Corominas, M., & Serras, F. (2015). ROS-Induced JNK and p38 Signaling Is Required for Unpaired Cytokine Activation during Drosophila Regeneration. *PLoS Genetics*, *11*(10). https://doi.org/10.1371/journal.pgen.1005595

Sartorelli, V., & Lauberth, S. M. (2020). Enhancer RNAs are an important regulatory layer of the epigenome. In *Nature Structural and Molecular Biology* (Vol. 27, Issue 6, pp. 521–528). Nature Research. https://doi.org/10.1038/s41594-020-0446-0

Saxonov, S., Berg, P., & Brutlag, D. L. (2005). *A genome-wide analysis of CpG dinucleotides in the human genome distinguishes two distinct classes of promoters*. www.pnas.orgcgidoi10.1073pnas.0510310103

Scepanovic, G., Hunter, M. V., Kafri, R., & Fernandez-Gonzalez, R. (2021). p38-mediated cell growth and survival drive rapid embryonic wound repair. *Cell Reports*, *37*(3). https://doi.org/10.1016/j.celrep.2021.109874

Schaub, M. A., Boyle, A. P., Kundaje, A., Batzoglou, S., & Snyder, M. (2012). Linking disease associations with regulatory information in the human genome. *Genome Research*, *22*(9), 1748–1759. https://doi.org/10.1101/gr.136127.111

Schnepp, B., Donaldson, T., Grumbling, G., Ostrowski, S., Schweitzer, R., Shilo, B.-Z., & Simcox, A. (1998). *EGF domain swap converts a Drosophila EGF receptor activator into an inhibitor*. www.genesdev.org

Schott, S., Ambrosini, A., Barbaste, A., Benassayag, C., Gracia, M., Proag, A., Rayer, M., Monier, B., & Suzanne, M. (2017). A fluorescent toolkit for spatiotemporal tracking of apoptotic cells in living Drosophila tissues. *Development (Cambridge)*, *144*(20), 3840–3846. https://doi.org/10.1242/dev.149807

Schubiger, M., Sustar, A., & Schubiger, G. (2010). Regeneration and transdetermination: The role of wingless and its regulation. *Developmental Biology*, *347*(2), 315–324. https://doi.org/10.1016/j.ydbio.2010.08.034

Schuettengruber, B., Bourbon, H. M., Di Croce, L., & Cavalli, G. (2017). Genome Regulation by Polycomb and Trithorax: 70 Years and Counting. In *Cell* (Vol. 171, Issue 1, pp. 34–57). Cell Press. https://doi.org/10.1016/j.cell.2017.08.002

Scully, K. H., Jacobson, E. M., Jepsen, K., Lunyak, V., Viadiu, H., Carriere, C., Rose, D. W., Hooshmand, F., Aggarwal, A. K., & Rosenfeld, M. G. (2000). Allosteric effects of Pit-1 DNA sites on long-term repression in cell type specification. *Science (New York, N.Y.)*, *290*(5494), 1127–1131. https://doi.org/10.1126/SCIENCE.290.5494.1127

Seher, T. C., & Leptin, M. (2000). Tribbles, a cell-cycle brake that coordinates proliferation and morphogenesis during Drosophila gastrulation. *Current Biology : CB*, *10*(11), 623–629. https://doi.org/10.1016/S0960-9822(00)00502-9

Sehring, I., Mohammadi, H. F., Haffner-Luntzer, M., Ignatius, A., Huber-Lang, M., & Weidinger, G. (2022). Zebrafish fin regeneration involvgeneric and regeneration-specifiosteoblast injury responses. *ELife*, *11*. https://doi.org/10.7554/ELIFE.77614

Seifert, A. W., Monaghan, J. R., Smith, M. D., Pasch, B., Stier, A. C., Michonneau, F., & Maden, M. (2012). The influence of fundamental traits on mechanisms controlling appendage regeneration. *Biological Reviews*, *87*(2), 330–345. https://doi.org/10.1111/j.1469-185X.2011.00199.x

Sen, S. (2000). Aneuploidy and cancer. *Current Opinion in Oncology*, *12*(1), 82–88. https://doi.org/10.1097/00001622-200001000-00014

Senger, K., Armstrong, G. W., Rowell, W. J., Kwan, J. M., Markstein, M., & Levine, M. (2004). Immunity regulatory DNAs share common organizational features in Drosophila. *Molecular Cell*, *13*(1), 19–32. https://doi.org/10.1016/S1097-2765(03)00500-8

Serras, F. (2016). The benefits of oxidative stress for tissue repair and regeneration. *Fly*, *10*(3), 128. https://doi.org/10.1080/19336934.2016.1188232

Serras, F. (2022). The sooner, the better: ROS, kinases and nutrients at the onset of the damage response in Drosophila. In *Frontiers in Cell and Developmental Biology* (Vol. 10). Frontiers Media S.A. https://doi.org/10.3389/fcell.2022.1047823

Sexton, T., Yaffe, E., Kenigsberg, E., Bantignies, F., Leblanc, B., Hoichman, M., Parrinello, H., Tanay, A., & Cavalli, G. (2012). Three-dimensional folding and functional organization principles of the Drosophila genome. *Cell*, *148*(3), 458–472. https://doi.org/10.1016/j.cell.2012.01.010

Sharma, R. P. (1973). *wingless- a new mutant in D. melanogaster*.

Sharma, R. P., & Chopra, V. L. (1976). Effect of the Wingless (wg1) Mutation on Wing and Haltere Development in Drosophila melanogaster. In *DEVELOPMENTAL BIOLOGY* (Vol. 48).

Shaw, T., & Martin, P. (2009). Epigenetic reprogramming during wound healing: Loss of polycomb-mediated silencing may enable upregulation of repair genes. *EMBO Reports*, *10*(8), 881–886. https://doi.org/10.1038/embor.2009.102

Shimi, T., Butin-Israeli, V., Adam, S. A., Hamanaka, R. B., Goldman, A. E., Lucas, C. A., Shumaker, D. K., Kosak, S. T., Chandel, N. S., & Goldman, R. D. (2011). The role of nuclear lamin B1 in cell proliferation and senescence. *Genes and Development*, *25*(24), 2579–2593. https://doi.org/10.1101/gad.179515.111

Shimizu, K., Takahama, S., Endo, Y., & Sawasaki, T. (2012). Stress-inducible caspase substrate TRB3 promotes nuclear translocation of procaspase-3. *PLoS ONE*, *7*(8). https://doi.org/10.1371/journal.pone.0042721

Shin, H. Y., Willi, M., Yoo, K. H., Zeng, X., Wang, C., Metser, G., & Hennighausen, L. (2016). Hierarchy within the mammary STAT5-driven Wap super-enhancer. *Nature Genetics*, *48*(8), 904–911. https://doi.org/10.1038/ng.3606

Shlevkov, E., & Morata, G. (2012). A dp53/JNK-dependant feedback amplification loop is essential for the apoptotic response to stress in Drosophila. *Cell Death and Differentiation*, *19*(3), 451–460. https://doi.org/10.1038/cdd.2011.113

Shlyueva, D., Stampfel, G., & Stark, A. (2014). Transcriptional enhancers: From properties to genome-wide predictions. In *Nature Reviews Genetics* (Vol. 15, Issue 4, pp. 272–286). Nature Publishing Group. https://doi.org/10.1038/nrg3682

Simcox, A. A., Grumbling, G., Schnepp, B., Bennington-Mathias, C., Hersperger, E., & Shearn, A. (1996). Molecular, Phenotypic, and Expression Analysis of vein, a Gene Required for Growth of the Drosophila Wing Disc. In *DEVELOPMENTAL BIOLOGY* (Vol. 177).

Simmonds, A. J., Liu, X., Soanes, K. H., Krause, H. M., Irvine, K. D., & Bell, J. B. (1998). *Molecular interactions between Vestigial and Scalloped promote wing formation in Drosophila*. www.genesdev.org

Simões, A. R., Neto, M., Alves, C. S., Santos, M. B., Fernández-Hernández, I., Veiga-Fernandes, H., Brea, D., Durá, I., Encinas, J. M., & Rhiner, C. (2022). Damage-responsive neuro-glial clusters coordinate the recruitment of dormant neural stem cells in Drosophila. *Developmental Cell*, *57*(13), 1661-1675.e7. https://doi.org/10.1016/j.devcel.2022.05.015

Simon, J. A., & Kingston, R. E. (2009). Mechanisms of Polycomb gene silencing: Knowns and unknowns. In *Nature Reviews Molecular Cell Biology* (Vol. 10, Issue 10, pp. 697–708). https://doi.org/10.1038/nrm2763

Singh, A., & Irvine, K. D. (2012). Drosophila as a model for understanding development and disease. In *Developmental Dynamics* (Vol. 241, Issue 1, pp. 1–2). https://doi.org/10.1002/dvdy.23712

Singh, A., Shi, X., & Choi, K. W. (2006). Lobe and Serrate are required for cell survival during early eye development in Drosophila. *Development*, *133*(23), 4771–4781. https://doi.org/10.1242/dev.02686

Slack, J. M. (2017). Animal regeneration: ancestral character or evolutionary novelty? *EMBO Reports*, *18*(9), 1497–1508. https://doi.org/10.15252/embr.201643795

Sluss, H. K., Han, Z., Barrett, T., Davis, R. J., & Ip, Y. T. (1996). A JNK signal transduction pathway that mediates morphogenesis and an immune response in Drosophila. *Genes & Development*, *10*(21), 2745–2758. https://doi.org/10.1101/GAD.10.21.2745

Smith-Bolton, R. K., Worley, M. I., Kanda, H., & Hariharan, I. K. (2009). Regenerative Growth in Drosophila Imaginal Discs Is Regulated by Wingless and Myc. *Developmental Cell*, *16*(6), 797–809. https://doi.org/10.1016/j.devcel.2009.04.015

Song, S., Andrejeva, D., Freitas, F. C. P., Cohen, S. M., & Herranz, H. (2019). DTcf/Pangolin suppresses growth and tumor formation in Drosophila. *Proceedings of the National Academy of Sciences of the United States of America*, *116*(28), 14055–14064. https://doi.org/10.1073/pnas.1816981116

Soto-Gamez, A., Quax, W. J., & Demaria, M. (2019). Regulation of Survival Networks in Senescent Cells: From Mechanisms to Interventions. In *Journal of Molecular Biology* (Vol. 431, Issue 15, pp. 2629–2643). Academic Press. https://doi.org/10.1016/j.jmb.2019.05.036

Spitz, F., & Furlong, E. E. M. (2012). Transcription factors: From enhancer binding to developmental control. In *Nature Reviews Genetics* (Vol. 13, Issue 9, pp. 613–626). https://doi.org/10.1038/nrg3207

Staehling-Hampton, K., Hoffmann, F. M., Baylies, M. K., Rushtont, E., & Bate, M. (1994). dpp induces mesodermal gene expression in Drosophila. *Nature*, *372*(6508), 783–786. https://doi.org/10.1038/372783A0

Staley, B. K., & Irvine, K. D. (2012). Hippo signaling in Drosophila: recent advances and insights. *Developmental Dynamics : An Official Publication of the American Association of Anatomists*, *241*(1), 3–15. https://doi.org/10.1002/DVDY.22723

Staller, M. V., Vincent, B. J., Bragdon, M. D. J., Lydiard-Martin, T., Wunderlich, Z., Estrada, J., & DePace, A. H. (2015). Shadow enhancers enable hunchback bifunctionality in the Drosophila embryo. *Proceedings of the National Academy of Sciences of the United States of America*, *112*(3), 785–790. https://doi.org/10.1073/pnas.1413877112

Stern, D. L. (2000). Evolutionary developmental biology and the problem of variation. *Evolution; International Journal of Organic Evolution*, *54*(4), 1079–1091. https://doi.org/10.1111/J.0014-3820.2000.TB00544.X

Stöckl, P., Zankl, C., Hütter, E., Unterluggauer, H., Laun, P., Heeren, G., Bogengruber, E., Herndler-Brandstetter, D., Breitenbach, M., & Jansen-Dürr, P. (2007). Partial uncoupling of oxidative phosphorylation induces premature senescence in human fibroblasts and yeast mother cells. *Free Radical Biology and Medicine*, *43*(6), 947–958. https://doi.org/10.1016/j.freeradbiomed.2007.06.005

Stocum, D. L. (2012). An Overview of Regenerative Biology. In *Regenerative Biology and Medicine* (pp. 3–20). Elsevier. https://doi.org/10.1016/b978-0-12-384860-4.00001-0

Stratton, M. R., Campbell, P. J., & Futreal, P. A. (2009). The cancer genome. In *Nature* (Vol. 458, Issue 7239, pp. 719–724). https://doi.org/10.1038/nature07943

Strigini, M., & Cohen, S. M. (1999). Formation of morphogen gradients in the Drosophila wing. In *CELL & DEV ELOPMENTAL BI OLOGY* (Vol. 10).

Studencka, M., & Schaber, J. (2017). Senoptosis: non-lethal DNA cleavage as a route to deep senescence. *Oncotarget*, *8*(19), 30656–30671. https://doi.org/10.18632/ONCOTARGET.15693

Sudarsan, V., Anant, S., Guptan, P., Vijayraghavan, K., & Skaer, H. (2001). Myoblast Diversification and Ectodermal Signaling in Drosophila. *Developmental Cell*, *1*(6), 829–839. https://doi.org/10.1016/S1534-5807(01)00089-2

Suen, D. F., Norris, K. L., & Youle, R. J. (2008). Mitochondrial dynamics and apoptosis. In *Genes and Development* (Vol. 22, Issue 12, pp. 1577–1590). https://doi.org/10.1101/gad.1658508

Summerville, J. B., Faust, J. F., Fan, E., Pendin, D., Daga, A., Formella, J., Stern, M., & McNew, J. A. (2016). The effects of ER morphology on synaptic structure and function in Drosophila melanogaster. *Journal of Cell Science*, *129*(8), 1635–1648. https://doi.org/10.1242/jcs.184929

Sun, G., & Irvine, K. D. (2011). Regulation of Hippo signaling by Jun kinase signaling during compensatory cell proliferation and regeneration, and in neoplastic tumors. *Developmental Biology*, *350*(1), 139–151. https://doi.org/10.1016/J.YDBIO.2010.11.036

Sun, G., & Irvine, K. D. (2013). Ajuba Family Proteins Link JNK to Hippo Signaling. *Science Signaling*, *6*(292). https://doi.org/10.1126/SCISIGNAL.2004324

Sur, I. K., Hallikas, O., Vähärautio, A., Yan, J., Turunen, M., Enge, M., Taipale, M., Karhu, A., Aaltonen, L. A., & Taipale, J. (2012). Mice lacking a Myc enhancer that includes human SNP rs6983267 are resistant to intestinal tumors. *Science (New York, N.Y.)*, *338*(6112), 1360–1363. https://doi.org/10.1126/SCIENCE.1228606

Sur, I., & Taipale, J. (2016). The role of enhancers in cancer. In *Nature Reviews Cancer* (Vol. 16, Issue 8, pp. 483–493). Nature Publishing Group. https://doi.org/10.1038/nrc.2016.62

Suzuki, N., & Ochi, H. (2020). Regeneration enhancers: A clue to reactivation of developmental genes. In *Development Growth and Differentiation* (Vol. 62, Issue 5, pp. 343–354). Blackwell Publishing. https://doi.org/10.1111/dgd.12654

Swanson, C., Evans, N., & Barolo, S. (2010). Structural rules and complex regulatory circuitry constrain expression of a Notch- and EGFR-regulated eye enhancer. *Developmental Cell*, *18*(3), 359–376. https://doi.org/10.1016/J.DEVCEL.2009.12.026

Swarup, S., & Verheyen, E. M. (2012). Wnt/wingless signaling in drosophila. *Cold Spring Harbor Perspectives in Biology*, *4*(6), 1–15. https://doi.org/10.1101/cshperspect.a007930

Swygert, S. G., & Peterson, C. L. (2014). Chromatin dynamics: Interplay between remodeling enzymes and histone modifications. In *Biochimica et Biophysica Acta - Gene Regulatory Mechanisms* (Vol. 1839, Issue 8, pp. 728–736). Elsevier. https://doi.org/10.1016/j.bbagrm.2014.02.013

Sykiotis, G. P., & Bohmann, D. (2008). Keap1/Nrf2 Signaling Regulates Oxidative Stress Tolerance and Lifespan in Drosophila. *Developmental Cell*, *14*(1), 76–85. https://doi.org/10.1016/j.devcel.2007.12.002

Symmons, O., Uslu, V. V., Tsujimura, T., Ruf, S., Nassari, S., Schwarzer, W., Ettwiller, L., & Spitz, F. (2014). Functional and topological characteristics of mammalian regulatory domains. *Genome Research*, *24*(3), 390–400. https://doi.org/10.1101/gr.163519.113

Tabata, T., Eaton, S., & Kornberg, T. B. (1992). The Drosophila hedgehog gene is expressed specifically in posterior compartment cells and is a target of engrailed regulation. *Genes & Development*, *6*(12B), 2635–2645. https://doi.org/10.1101/GAD.6.12B.2635

Takasugi, M., Okada, R., Takahashi, A., Virya Chen, D., Watanabe, S., & Hara, E. (2017). Small extracellular vesicles secreted from senescent cells promote cancer cell proliferation through EphA2. *Nature Communications*, *8*. https://doi.org/10.1038/ncomms15728

Takeda, K., Okumura, T., Taniguchi, K., & Adachi-Yamada, T. (2018). Adult Intestine Aging Model. *Advances in Experimental Medicine and Biology*, *1076*, 11–23. https://doi.org/10.1007/978-981-13-0529-0_2

Tan, S. H., & Barker, N. (2015). Stemming Colorectal Cancer Growth and Metastasis: HOXA5 Forces Cancer Stem Cells to Differentiate. In *Cancer Cell* (Vol. 28, Issue 6, pp. 683–685). Cell Press. https://doi.org/10.1016/j.ccell.2015.11.004

Tanaka-Matakatsu, M., Xu, J., Cheng, L., & Du, W. (2009). Regulation of apoptosis of rbf mutant cells during Drosophila development. *Developmental Biology*, *326*(2), 347–356. https://doi.org/10.1016/j.ydbio.2008.11.035

Tang, F., Yang, Z., Tan, Y., & Li, Y. (2020). Super-enhancer function and its application in cancer targeted therapy. In *npj Precision Oncology* (Vol. 4, Issue 1). Nature Research. https://doi.org/10.1038/s41698-020-0108-z

Tao, L., Yu, H. V., Llamas, J., Trecek, T., Wang, X., Stojanova, Z., Groves, A. K., & Segil, N. (2021). Enhancer decommissioning imposes an epigenetic barrier to sensory hair cell regeneration. *Developmental Cell*, *56*(17), 2471-2485.e5. https://doi.org/10.1016/j.devcel.2021.07.003

Taub, R., Kirscht, I., Mortont, C., Lenoir, G., Swans, D., Tronick0, S., Aaronson$, S., & Leder, P. (1982). Translocation of the c-mnc gene into the immunoglobulin heavy chain locus in human Burkitt lymphoma and murine plasmacytoma cells (recombination/chromosome/cancer/DNA). In *Proc. NatL Acad. Sci. USA* (Vol. 79). https://www.pnas.org

Teleman, A. A., & Cohen, S. M. (2000). Dpp gradient formation in the Drosophila wing imaginal disc. *Cell*, *103*(6), 971–980. https://doi.org/10.1016/S0092-8674(00)00199-9

Thandapani, P. (2019). Super-enhancers in cancer. In *Pharmacology and Therapeutics* (Vol. 199, pp. 129–138). Elsevier Inc. https://doi.org/10.1016/j.pharmthera.2019.02.014

Thiagarajah, J. R., Chang, J., Goettel, J. A., Verkman, A. S., & Lencer, W. I. (2017). Aquaporin-3 mediates hydrogen peroxide-dependent responses to environmental stress in colonic epithelia. *Proceedings of the National Academy of Sciences of the United States of America*, *114*(3), 568–573. https://doi.org/10.1073/pnas.1612921114

Thompson, B. J., & Cohen, S. M. (2006). The Hippo Pathway Regulates the bantam microRNA to Control Cell Proliferation and Apoptosis in Drosophila. *Cell*, *126*(4), 767–774. https://doi.org/10.1016/j.cell.2006.07.013

Tian, Y., & Smith-Bolton, R. K. (2021). Regulation of growth and cell fate during tissue regeneration by the two SWI/SNF chromatin-remodeling complexes of Drosophila. *Genetics*, *217*(1). https://doi.org/10.1093/GENETICS/IYAA028

Tong, J. K., Hassig, C. A., Schnitzler, G. R., Kingston, R. E., & Schreiber, S. L. (1998). Chromatin deacetylation by an ATP-dependent nucleosome remodelling complex. *Nature*, *395*(6705), 917–921. https://doi.org/10.1038/27699

Tripathi, B. K., & Irvine, K. D. (2022). The wing imaginal disc. *Genetics*, *220*(4). https://doi.org/10.1093/genetics/iyac020

Tripura, C., Chandrika, N. P., Susmitha, V. N., Noselli, S., & Shashidhara, L. (2011). Regulation and activity of JNK signaling in the wing disc peripodial membrane during adult morphogenesis in Drosophila. *The International Journal of Developmental Biology*, *55*(6), 583–590. https://doi.org/10.1387/IJDB.103275CT

Tseng, A. S., Adams, D. S., Qiu, D., Koustubhan, P., & Levin, M. (2007). Apoptosis is required during early stages of tail regeneration in Xenopus laevis. *Developmental Biology*, *301*(1), 62–69. https://doi.org/10.1016/j.ydbio.2006.10.048

Twig, G., & Shirihai, O. S. (2011). The interplay between mitochondrial dynamics and mitophagy. In *Antioxidants and Redox Signaling* (Vol. 14, Issue 10, pp. 1939–1951). https://doi.org/10.1089/ars.2010.3779

Ugur, B., Chen, K., & Bellen, H. J. (2016). Drosophila tools and assays for the study of human diseases. In *DMM Disease Models and Mechanisms* (Vol. 9, Issue 3, pp. 235–244). Company of Biologists Ltd. https://doi.org/10.1242/dmm.023762

Uhlirova, M., & Bohmann, D. (2006). JNK- and Fos-regulated Mmp1 expression cooperates with Ras to induce invasive tumors in Drosophila. *EMBO Journal*, *25*(22), 5294–5304. https://doi.org/10.1038/sj.emboj.7601401

Vachon, G., Cohen, B., Pfeifle, C., McGuffin, M. E., Botas, J., & Cohen, S. M. (1992). Homeotic genes of the Bithorax complex repress limb development in the abdomen of the Drosophila embryo through the target gene Distal-less. *Cell*, *71*(3), 437–450. https://doi.org/10.1016/0092-8674(92)90513-C

Valon, L., Davidović, A., Levillayer, F., Villars, A., Chouly, M., Cerqueira-Campos, F., & Levayer, R. (2021). Robustness of epithelial sealing is an emerging property of local ERK feedback driven by cell elimination. *Developmental Cell*, *56*(12), 1700-1711.e8. https://doi.org/10.1016/j.devcel.2021.05.006

Van Den Heuvell, M., Harryman-Samos, C., Klingensmith, J., Perrimon2, N., & Nusse3, R. (1993). Mutations in the segment polarity genes wingless and porcupine impair secretion of the wingless protein. In *The EMBO Journal* (Vol. 1, Issue 1).

van Dijk, E., van den Bosch, T., Lenos, K. J., El Makrini, K., Nijman, L. E., van Essen, H. F. B., Lansu, N., Boekhout, M., Hageman, J. H., Fitzgerald, R. C., Punt, C. J. A., Tuynman, J. B., Snippert, H. J. G., Kops, G. J. P. L., Medema, J. P., Ylstra, B., Vermeulen, L., & Miedema, D. M. (2021). Chromosomal copy number heterogeneity predicts survival rates across cancers. *Nature Communications*, *12*(1). https://doi.org/10.1038/s41467-021-23384-6

Varjosalo, M., & Taipale, J. (2007). Hedgehog signaling. *Journal of Cell Science*, *120*(1), 3–6. https://doi.org/10.1242/jcs.03309

Vasileiou, P. V. S., Evangelou, K., Vlasis, K., Fildisis, G., Panayiotidis, M. I., Chronopoulos, E., Passias, P. G., Kouloukoussa, M., Gorgoulis, V. G., & Havaki, S. (2019). Mitochondrial Homeostasis and Cellular Senescence. *Cells*, *8*(7). https://doi.org/10.3390/CELLS8070686

Vasudevan, A., Schukken, K. M., Sausville, E. L., Girish, V., Adebambo, O. A., & Sheltzer, J. M. (2021). Aneuploidy as a promoter and suppressor of malignant growth. In *Nature Reviews Cancer* (Vol. 21, Issue 2, pp. 89–103). Nature Research. https://doi.org/10.1038/s41568-020-00321-1

Venkatesh, S., & Workman, J. L. (2015). Histone exchange, chromatin structure and the regulation of transcription. In *Nature Reviews Molecular Cell Biology* (Vol. 16, Issue 3, pp. 178–189). Nature Publishing Group. https://doi.org/10.1038/nrm3941

Verghese, S., & Su, T. T. (2016). Drosophila Wnt and STAT Define Apoptosis-Resistant Epithelial Cells for Tissue Regeneration after Irradiation. *PLoS Biology*, *14*(9). https://doi.org/10.1371/journal.pbio.1002536

Vizcaya-Molina, E., Klein, C. C., Serras, F., & Corominas, M. (2020). Chromatin dynamics in regeneration epithelia: Lessons from Drosophila imaginal discs. In *Seminars in Cell and Developmental Biology* (Vol. 97, pp. 55–62). Elsevier Ltd. https://doi.org/10.1016/j.semcdb.2019.04.017

Vizcaya-Molina, E., Klein, C. C., Serras, F., Mishra, R. K., Guigó, R., & Corominas, M. (2018). Damage-responsive elements in Drosophila regeneration. *Genome Research*, *28*(12), 1841–1851. https://doi.org/10.1101/gr.233098.117

Von Ohlen, T., Lessing, D., Nusse, R., & Hooper, J. E. (1997). Hedgehog signaling regulates transcription through cubitus interruptus, a sequence-specific DNA binding protein. In *Developmental Biology* (Vol. 94). www.pnas.org.

Walters, H. E., & Yun, M. H. (2020). Rising from the ashes: cellular senescence in regeneration. In *Current Opin-*

ion in Genetics and Development (Vol. 64, pp. 94–100). Elsevier Ltd. https://doi.org/10.1016/j.gde.2020.06.002

Wang, M., Luan, X., Yan, Y., Zheng, Q., Chen, W., & Fang, J. (2021). Wnt6 regulates the homeostasis of the stem cell niche via Rac1-and Cdc42-mediated noncanonical Wnt signalling pathways in Drosophila testis. *Experimental Cell Research*, *402*(1). https://doi.org/10.1016/j.yexcr.2021.112511

Wang, Q., Uhlirova, M., & Bohmann, D. (2010). Spatial restriction of FGF signaling by a matrix metalloprotease controls branching morphogenesis. *Developmental Cell*, *18*(1), 157–164. https://doi.org/10.1016/J.DEVCEL.2009.11.004

Wang, S. H., Simcox, A., & Campbell, G. (2000). Dual role for Drosophila epidermal growth factor receptor signaling in early wing disc development. *Genes and Development*, *14*(18), 2271–2276. https://doi.org/10.1101/gad.827000

Wang, S. L., Hawkins, C. J., Yoo, S. J., Mü, H.-A. J., & Hay, B. A. (1999). The Drosophila Caspase Inhibitor DIAP1 Is Essential for Cell Survival and Is Negatively Regulated by HID The yeast Saccharomyces cerevisiae provides an. In *Cell* (Vol. 98).

Wang, W., Hu, C. K., Zeng, A., Alegre, D., Hu, D., Gotting, K., Granillo, A. O., Wang, Y., Robb, S., Schnittker, R., Zhang, S., Alegre, D., Li, H., Ross, E., Zhang, N., Brunet, A., & Alvarado, A. S. (2020). Changes in regeneration-responsive enhancers shape regenerative capacities in vertebrates. *Science*, *369*(6508). https://doi.org/10.1126/SCIENCE.AAZ3090

Watson, K. L., Justice, R. W., & Bryant, P. J. (1994). Drosophila in cancer research: the first fifty tumor suppressor genes. In *Journal of Cell Science, Supplement* (Vol. 18).

Waymack, R., Fletcher, A., Enciso, G., & Wunderlich, Z. (2020). Shadow enhancers can suppress input transcription factor noise through distinct regulatory logic. *ELife*, *9*, 1–57. https://doi.org/10.7554/ELIFE.59351

Wei, W., Cheng, Y., & Wang, B. (2016). Cancer and Genomic Instability. In *Genome Stability: From Virus to Human Application* (pp. 463–486). Elsevier Inc. https://doi.org/10.1016/B978-0-12-803309-8.00027-6

Whitney, P. H., Shrestha, B., Xiong, J., Zhang, T., & Rushlow, C. A. (2022). Shadow enhancers modulate distinct transcriptional parameters that differentially effect downstream patterning events. *Development (Cambridge)*, *149*(21). https://doi.org/10.1242/dev.200940

Wiel, C., Lallet-Daher, H., Gitenay, D., Gras, B., Le Calvé, B., Augert, A., Ferrand, M., Prevarskaya, N., Simonnet, H., Vindrieux, D., & Bernard, D. (2014). Endoplasmic reticulum calcium release through ITPR2 channels leads to mitochondrial calcium accumulation and senescence. *Nature Communications*, *5*. https://doi.org/10.1038/ncomms4792

Wieschaus, E., & Gehring, W. (1976). Clonal analysis of primordial disc cells in the early embryo of Drosophila melanogaster. *Developmental Biology*, *50*(2), 249–263. https://doi.org/10.1016/0012-1606(76)90150-0

Wiley, C. D., Velarde, M. C., Lecot, P., Liu, S., Sarnoski, E. A., Freund, A., Shirakawa, K., Lim, H. W., Davis, S. S., Ramanathan, A., Gerencser, A. A., Verdin, E., & Campisi, J. (2016). Mitochondrial dysfunction induces senescence with a distinct secretory phenotype. *Cell Metabolism*, *23*(2), 303–314. https://doi.org/10.1016/j.cmet.2015.11.011

Wilkinson, H. N., & Hardman, M. J. (2020). Senescence in Wound Repair: Emerging Strategies to Target Chronic Healing Wounds. In *Frontiers in Cell and Developmental Biology* (Vol. 8). Frontiers Media S.A. https://doi.org/10.3389/fcell.2020.00773

Williams, J. A., Bell, J. B., & Carroll, S. B. (1991). Control of Drosophila wing and haltere development by the nuclear vestigial gene product. *Genes & Development*, *5*(12B), 2481–2495. https://doi.org/10.1101/GAD.5.12B.2481

Wodarz, A., & Näthke, I. (2007). Cell polarity in development and cancer. *Nature Cell Biology 2007 9:9*, *9*(9), 1016–1024. https://doi.org/10.1038/ncb433

Worley, M. I., Everetts, N. J., Yasutomi, R., Chang, R. J., Saretha, S., Yosef, N., & Hariharan, I. K. (2022). Ets21C sustains a pro-regenerative transcriptional program in blastema cells of Drosophila imaginal discs. *Current Biology*, *32*(15), 3350-3364.e6. https://doi.org/10.1016/j.cub.2022.06.040

Wu, J., & Cohen, S. M. (2002). Repression of Teashirt marks the initiation of wing development. *Development (Cambridge, England)*, *129*(10), 2411–2418. https://doi.org/10.1242/DEV.129.10.2411

Wunderlich, Z., Bragdon, M. D. J., Vincent, B. J., White, J. A., Estrada, J., & DePace, A. H. (2015). Krüppel Expression Levels Are Maintained through Compensatory Evolution of Shadow Enhancers. *Cell Reports*, *12*(11), 1740–1747. https://doi.org/10.1016/j.celrep.2015.08.021

Xue, Y., Wong, J., Moreno, G. T., Young, M. K., Côté, J., & Wang, W. (1998). NURD, a novel complex with both ATP-dependent chromatin-remodeling and histone deacetylase activities. *Molecular Cell*, *2*(6), 851–861. https://doi.org/10.1016/S1097-2765(00)80299-3

Yang, K., & Kang, J. (2019). Tissue Regeneration Enhancer Elements: A Way to Unlock Endogenous Healing Power. *Developmental Dynamics*, *248*, 34–42. https://doi.org/10.1002/dvdy

Yoon, Y. S., Yoon, D. S., Lim, I. K., Yoon, S. H., Chung, H. Y., Rojo, M., Malka, F., Jou, M. J., Martinou, J. C., & Yoon, G. (2006). Formation of elongated giant mitochondria in DFO-induced cellular senescence: Involvement of enhanced fusion process through modulation of Fis1. *Journal of Cellular Physiology*, *209*(2), 468–480. https://doi.org/10.1002/jcp.20753

Yu, J. J. S., Maugarny-Calès, A., Pelletier, S., Alexandre, C., Bellaiche, Y., Vincent, J. P., & McGough, I. J. (2020). Frizzled-Dependent Planar Cell Polarity without Secreted Wnt Ligands. *Developmental Cell*, *54*(5), 583-592.e5. https://doi.org/10.1016/j.devcel.2020.08.004

Yu, Q., Walters, H. E., Pasquini, G., Singh, S. P., León-Periñán, D., Petzold, A., Kesavan, P., Subiran, C., Garteizgogeascoa, I., Knapp, D., Wagner, A., Bernardos, A., Alfonso, M., Nadar, G., Dahl, A., Busskamp, V., Martínez-Máñez, R., & Yun, M. H. (2022). Cellular senescence modulates progenitor cell expansion during axolotl limb regeneration. *BioRxiv*, 2022.09.01.506196. https://doi.org/10.1101/2022.09.01.506196

Yuen, A. C., Prasad, A. R., Fernandes, V. M., & Amoyel, M. (2022). A kinase translocation reporter reveals real-time dynamics of ERK activity in Drosophila. *Biology Open*, *11*(5). https://doi.org/10.1242/BIO.059364

Yun, M. H., Davaapil, H., & Brockes, J. P. (2015). Recurrent turnover of senescent cells during regeneration of a complex structure. *ELife*, *4*(MAY). https://doi.org/10.7554/ELIFE.05505

Zaret, K. S., & Carroll, J. S. (2011). Pioneer transcription factors: Establishing competence for gene expression. In *Genes and Development* (Vol. 25, Issue 21, pp. 2227–2241). https://doi.org/10.1101/gad.176826.111

Zecca, M., Basler, K., & Struhl, G. (1995). Sequential organizing activities of engrailed, hedgehog and decapentaplegic in the Drosophila wing. *Development (Cambridge, England)*, *121*(8), 2265–2278. https://doi.org/10.1242/DEV.121.8.2265

Zecca, M., Basler, K., & Struhl, G. (1996). Direct and Long-Range Action of a Wingless Morphogen Gradient. In *Cell* (Vol. 87).

Zecca, M., & Struhl, G. (2002a). Control of growth and patterning of the Drosophila wing imaginal disc by EGFR-mediated signaling. *Development (Cambridge, England)*, *129*(6), 1369–1376. https://doi.org/10.1242/DEV.129.6.1369

Zecca, M., & Struhl, G. (2002b). Subdivision of the Drosophila wing imaginal disc by EGFR-mediated signaling. *Development (Cambridge, England)*, *129*(6), 1357–1368. https://doi.org/10.1242/DEV.129.6.1357

Zeitlinger, J., & Bohmann, D. (1999). Thorax closure in Drosophila: involvement of Fos and the JNK pathway. *Development*, *126*(17), 3947–3956. https://doi.org/10.1242/DEV.126.17.3947

Zeitlinger, J., Zinzen, R. P., Stark, A., Kellis, M., Zhang, H., Young, R. A., & Levine, M. (2007). Whole-genome ChIP-chip analysis of Dorsal, Twist, and Snail suggests integration of diverse patterning processes in the Drosophila embryo. *Genes and Development*, *21*(4), 385–390. https://doi.org/10.1101/gad.1509607

Zentner, G. E., & Henikoff, S. (2013). Regulation of nucleosome dynamics by histone modifications. In *Nature Structural and Molecular Biology* (Vol. 20, Issue 3, pp. 259–266). https://doi.org/10.1038/nsmb.2470

Zentner, G. E., Tesar, P. J., & Scacheri, P. C. (2011). Epigenetic signatures distinguish multiple classes of enhancers with distinct cellular functions. *Genome Research*, *21*(8), 1273–1283. https://doi.org/10.1101/gr.122382.111

Zhang, P., Torres, K., Liu, X., Liu, C., & E. Pollock, R. (2016). An Overview of Chromatin-Regulating Proteins in Cells. *Current Protein & Peptide Science*, *17*(5), 401–410. https://doi.org/10.2174/1389203717666160122120310

Zhang, R., Poustovoitov, M. V., Ye, X., Santos, H. A., Chen, W., Daganzo, S. M., Erzberger, J. P., Serebriiskii, I. G., Canutescu, A. A., Dunbrack, R. L., Pehrson, J. R., Berger, J. M., Kaufman, P. D., & Adams, P. D. (2005). Formation

of macroH2A-containing senescence-associated heterochromatin foci and senescence driven by ASF1a and HIRA. *Developmental Cell*, *8*(1), 19–30. https://doi.org/10.1016/j.devcel.2004.10.019

Zhang, X., Choi, P. S., Francis, J. M., Imielinski, M., Watanabe, H., Cherniack, A. D., & Meyerson, M. (2016). Identification of focally amplified lineage-specific super-enhancers in human epithelial cancers. *Nature Genetics*, *48*(2), 176–182. https://doi.org/10.1038/NG.3470

Zhao, Z., & Shilatifard, A. (2019). Epigenetic modifications of histones in cancer. In *Genome Biology* (Vol. 20, Issue 1). BioMed Central Ltd. https://doi.org/10.1186/s13059-019-1870-5

Zhou, W., Chang, J., Wang, X., Savelieff, M. G., Zhao, Y., Ke, S., & Ye, B. (2014). GM130 is required for compartmental organization of dendritic Golgi outposts. *Current Biology*, *24*(11), 1227–1233. https://doi.org/10.1016/j.cub.2014.04.008

Zhou, X., & Sigmund, C. D. (2008). Chorionic enhancer is dispensable for regulated expression of the human renin gene. *American Journal of Physiology. Regulatory, Integrative and Comparative Physiology*, *294*(2). https://doi.org/10.1152/AJPREGU.00780.2007

Zhu, F., Li, Y., Zhang, J., Piao, C., Liu, T., Li, H. H., & Du, J. (2013). Senescent cardiac fibroblast is critical for cardiac fibrosis after myocardial infarction. *PloS One*, *8*(9). https://doi.org/10.1371/journal.pone.0074535

Ziegler, D. V., Wiley, C. D., & Velarde, M. C. (2015). Mitochondrial effectors of cellular senescence: Beyond the free radical theory of aging. In *Aging Cell* (Vol. 14, Issue 1, pp. 1–7). https://doi.org/10.1111/acel.12287

Zielke, N., Korzelius, J., vanStraaten, M., Bender, K., Schuhknecht, G. F. P., Dutta, D., Xiang, J., & Edgar, B. A. (2014). Fly-FUCCI: A Versatile Tool for Studying Cell Proliferation in Complex Tissues. *Cell Reports*, *7*(2), 588–598. https://doi.org/10.1016/j.celrep.2014.03.020

Zirin, J. D., & Mann, R. S. (2007). Nubbin and Teashirt mark barriers to clonal growth along the proximal-distal axis of the Drosophila wing. *Developmental Biology*, *304*(2), 745–758. https://doi.org/10.1016/J.YDBIO.2007.01.025

Annex

seqnames	start	end	width	strand	score.avg	score.max	cons.avg	cons.max	pv.min	pv.max	TF	Merged BS	Nrs in Figures	Mutations	wg^1 region
chr2L	7324347	7324356	10	*	0,75	**0,75**	1	1	0,00202891	0,00202891	MEME_fly_factor_survey-pointed_FBgn0003118	ETS BS α1			
chr2L	7324379	7324390	12	*	0,71	**0,71**	1	1	0,0016605	0,0016605	MEME_fly_factor_survey-ci_FBgn0004859	Ci BS α1	Ci-1*		
chr2L	7324397	7324406	10	*	0,74	**0,74**	0,9982	0,9982	0,0023733	0,0023733	MEME_fly_factor_survey-pointed_FBgn0003118	ETS BS α2			
chr2L	7324411	7324418	8	*	0,74	**0,74**	0,934	0,934	0,00539244	0,00539244	Jaspar_2020_MA0026.1-Eip74EF	ETS BS α3			
chr2L	7324468	7324477	10	*	0,7	**0,7**	1	1	0,00374811	0,00374811	MEME_fly_factor_survey-pointed_FBgn0003118	ETS BS α4			
chr2L	7324486	7324499	14	*	0,74	**0,74**	0,99914286	0,99914286	0,00086389	0,00086389	MEME_fly_factor_survey-ci_FBgn0004859_2	Ci BS α2	Ci-2*		α
chr2L	7324514	7324525	12	*	0,735	**0,76**	1	1	0,00422431	0,01004987	Jaspar_2020_MA0026.1-Eip74EF	ETS BS α5			
chr2L	7324555	7324564	10	*	0,87	**0,87**	1	1	0,00011746	0,00011746	MEME_fly_factor_survey-yan_FBgn0000097				
chr2L	7324555	7324564	10	*	0,88	**0,88**	1	1	0,00012691	0,00012691	MEME_fly_factor_survey-pointed_FBgn0003118	ETS BS α6			
chr2L	7324556	7324563	8	*	0,83	**0,83**	1	1	0,00165395	0,00165395	Jaspar_2020_MA0026.1-Eip74EF				
chr2L	7324568	7324575	8	*	0,74	**0,74**	0,70975	0,70975	0,00539244	0,00539244	Jaspar_2020_MA0026.1-Eip74EF	ETS BS α7			
chr2L	7324904	7324915	12	*	0,73	**0,73**	0,99983334	0,99983334	0,00108345	0,00108345	MEME_fly_factor_survey-ci_FBgn0004859	Ci BS β1	Ci-3*		
chr2L	7325021	7325033	13	*	0,78	**0,83**	0,9994375	0,99975	0,00165395	0,00711399	Jaspar_2020_MA0026.1-Eip74EF	ETS BS β1			
chr2L	7325057	7325066	10	*	0,71	**0,71**	0,9966	0,9966	0,00368844	0,00368844	MEME_fly_factor_survey-yan_FBgn0000097	ETS BS β1			
chr2L	7325057	7325066	10	*	0,74	**0,74**	0,9966	0,9966	0,0023733	0,0023733	MEME_fly_factor_survey-pointed_FBgn0003118				
chr2L	7325093	7325102	10	*	0,77	**0,77**	1	1	0,0011357	0,0011357	MEME_fly_factor_survey-yan_FBgn0000097	ETS BS β2			
chr2L	7325093	7325102	10	*	0,79	**0,79**	1	1	0,00081947	0,00081947	MEME_fly_factor_survey-pointed_FBgn0003118				
chr2L	7325094	7325101	8	*	0,78	**0,78**	1	1	0,00337067	0,00337067	Jaspar_2020_MA0026.1-Eip74EF				
chr2L	7325147	7325156	10	*	0,71	**0,71**	0,9475	0,9475	0,00327765	0,00327765	MEME_fly_factor_survey-pointed_FBgn0003118	ETS BS β3			
chr2L	7325148	7325155	8	*	0,78	**0,78**	0,9775	0,9775	0,00337067	0,00337067	Jaspar_2020_MA0026.1-Eip74EF				β
chr2L	7325171	7325180	10	*	0,74	**0,74**	0,9106	0,9106	0,0023733	0,0023733	MEME_fly_factor_survey-pointed_FBgn0003118				
chr2L	7325171	7325180	10	*	0,84	**0,84**	0,9106	0,9106	0,00023386	0,00023386	MEME_fly_factor_survey-yan_FBgn0000097	ETS BS β4	ETS-1*		
chr2L	7325172	7325179	8	*	0,91	**0,91**	0,920125	0,920125	0,00022737	0,00022737	Jaspar_2020_MA0026.1-Eip74EF				
chr2L	7325204	7325211	8	*	0,73	**0,73**	1	1	0,00711399	0,00711399	Jaspar_2020_MA0026.1-Eip74EF	ETS BS β5			
chr2L	7325280	7325289	10	*	0,78	**0,78**	1	1	0,00101152	0,00101152	MEME_fly_factor_survey-pointed_FBgn0003118				
chr2L	7325280	7325289	10	*	0,8	**0,8**	1	1	0,00063708	0,00063708	MEME_fly_factor_survey-yan_FBgn0000097	ETS BS β6			
chr2L	7325281	7325288	8	*	0,83	**0,83**	1	1	0,00165395	0,00165395	Jaspar_2020_MA0026.1-Eip74EF				
chr2L	7325361	7325368	8	*	0,82	**0,82**	0,99900001	0,99900001	0,00168166	0,00168166	Jaspar_2020_MA0026.1-Eip74EF	ETS BS β7			
chr2L	7325644	7325656	13	*	0,705	**0,71**	0,9216	1	0,00368844	0,00422571	MEME_fly_factor_survey-yan_FBgn0000097				
chr2L	7325645	7325655	11	*	0,81	**0,84**	0,9510625	1	0,00089647	0,00337067	Jaspar_2020_MA0026.1-Eip74EF	ETS BS γ1			
chr2L	7325647	7325656	10	*	0,74	**0,74**	1	1	0,0023733	0,0023733	MEME_fly_factor_survey-pointed_FBgn0003118				
chr2L	7325656	7325663	8	*	0,71	**0,71**	1	1	0,01004987	0,01004987	Jaspar_2020_MA0026.1-Eip74EF	ETS BS γ2			
chr2L	7325720	7325733	14	*	0,775	**0,82**	0,9981	1	0,00037506	0,0025622	MEME_fly_factor_survey-yan_FBgn0000097				
chr2L	7325721	7325738	18	*	0,81333333	**0,9**	0,979125	1	0,00031723	0,01004987	Jaspar_2020_MA0026.1-Eip74EF	ETS BS γ3	ETS-2*		
chr2L	7325724	7325733	10	*	0,76	**0,76**	0,9962	0,9962	0,00182321	0,00182321	MEME_fly_factor_survey-pointed_FBgn0003118				
chr2L	7325793	7325815	23	*	0,735	**0,74**	0,95821429	0,99878572	0,00086389	0,00106933	MEME_fly_factor_survey-ci_FBgn0004859_2	Ci BS γ1	Ci-4*		
chr2L	7325796	7325812	17	*	0,72	**0,74**	0,97312501	0,9985	0,0008713	0,00203686	MEME_fly_factor_survey-ci_FBgn0004859				
chr2L	7325825	7325834	10	*	0,81	**0,81**	0,9982	0,9982	0,00046499	0,00046499	MEME_fly_factor_survey-yan_FBgn0000097				
chr2L	7325825	7325834	10	*	0,87	**0,87**	0,9982	0,9982	0,00019415	0,00019415	MEME_fly_factor_survey-pointed_FBgn0003118	ETS BS γ4			
chr2L	7325826	7325836	11	*	0,745	**0,78**	0,999125	1	0,00337067	0,01004987	Jaspar_2020_MA0026.1-Eip74EF				
chr2L	7325843	7325850	8	*	0,71	**0,71**	0,99625	0,99625	0,01004987	0,01004987	Jaspar_2020_MA0026.1-Eip74EF	ETS BS γ5			
chr2L	7325856	7325863	8	*	0,77	**0,77**	1	1	0,0035508	0,0035508	Jaspar_2020_MA0026.1-Eip74EF	ETS BS γ6			
chr2L	7325879	7325888	10	*	0,74	**0,74**	1	1	0,00202387	0,00202387	MEME_fly_factor_survey-yan_FBgn0000097	ETS BS γ7			
chr2L	7325880	7325887	8	*	0,78	**0,78**	1	1	0,00337067	0,00337067	Jaspar_2020_MA0026.1-Eip74EF				
chr2L	7326069	7326078	10	*	0,73	**0,73**	1	1	0,0025622	0,0025622	MEME_fly_factor_survey-yan_FBgn0000097				
chr2L	7326069	7326078	10	*	0,77	**0,77**	1	1	0,0015053	0,0015053	MEME_fly_factor_survey-pointed_FBgn0003118	ETS BS γ8			
chr2L	7326070	7326077	8	*	0,78	**0,78**	1	1	0,00337067	0,00337067	Jaspar_2020_MA0026.1-Eip74EF				γ
chr2L	7326078	7326090	13	*	0,735	**0,74**	1	1	0,00539244	0,00711399	Jaspar_2020_MA0026.1-Eip74EF	ETS BS γ9			
chr2L	7326082	7326091	10	*	0,71	**0,71**	1	1	0,00368844	0,00368844	MEME_fly_factor_survey-yan_FBgn0000097	ETS BS γ10			
chr2L	7326123	7326130	8	*	0,73	**0,73**	0,9995	0,9995	0,00711399	0,00711399	Jaspar_2020_MA0026.1-Eip74EF	ETS BS γ11			
chr2L	7326165	7326172	8	*	0,71	**0,71**	0,984875	0,984875	0,01004987	0,01004987	Jaspar_2020_MA0026.1-Eip74EF	ETS BS γ12			
chr2L	7326173	7326180	8	*	0,76	**0,76**	0,99924999	0,99924999	0,00422431	0,00422431	Jaspar_2020_MA0026.1-Eip74EF	ETS BS γ13			
chr2L	7326182	7326195	14	*	0,7	**0,7**	0,99442857	0,99442857	0,00199642	0,00199642	MEME_fly_factor_survey-ci_FBgn0004859_2	Ci BS γ2	Ci-5*		
chr2L	7326185	7326196	12	*	0,74	**0,74**	0,98066667	0,98066667	0,0008713	0,0008713	MEME_fly_factor_survey-ci_FBgn0004859				
chr2L	7326328	7326337	10	*	0,82	**0,82**	1	1	0,0003074	0,0003074	MEME_fly_factor_survey-pointed_FBgn0003118				
chr2L	7326328	7326337	10	*	0,83	**0,83**	1	1	0,00028828	0,00028828	MEME_fly_factor_survey-yan_FBgn0000097	ETS BS γ14	ETS-3*		
chr2L	7326329	7326339	11	*	0,845	**0,95**	1	1	9,6575E-05	0,00539244	Jaspar_2020_MA0026.1-Eip74EF				
chr2L	7326343	7326350	8	*	0,73	**0,73**	1	1	0,00711399	0,00711399	Jaspar_2020_MA0026.1-Eip74EF	ETS BS γ15			
chr2L	7326343	7326356	14	*	0,82	**0,82**	1	1	0,00012201	0,00012201	MEME_fly_factor_survey-ci_FBgn0004859_2	Ci BS γ3	Ci-6*	Ci mut	
chr2L	7326346	7326359	14	*	0,785	**0,86**	0,99825	1	3,6678E-05	0,0016605	MEME_fly_factor_survey-ci_FBgn0004859				
chr2L	7326388	7326398	11	*	0,715	**0,73**	0,87995	0,9012	0,0025622	0,00422571	MEME_fly_factor_survey-yan_FBgn0000097				
chr2L	7326389	7326398	10	*	0,74	**0,74**	0,8587	0,8587	0,0023733	0,0023733	MEME_fly_factor_survey-pointed_FBgn0003118	ETS BS γ16			
chr2L	7326389	7326397	9	*	0,76	**0,78**	0,9339375	0,991375	0,00337067	0,00539244	Jaspar_2020_MA0026.1-Eip74EF				
chr2L	7326432	7326441	10	*	0,72	**0,72**	1	1	0,00277568	0,00277568	MEME_fly_factor_survey-yan_FBgn0000097	ETS BS γ17			
chr2L	7326433	7326440	8	*	0,73	**0,73**	1	1	0,00711399	0,00711399	Jaspar_2020_MA0026.1-Eip74EF				

Region	Start	End	Num bp
α	7323135	7324749	1614
β	7324770	7325443	673
γ	7325445	7326565	1120
δ	7326565	7327855	1290

ETS Score	Ci Score
1-0,95	0,90-0,85
0,94-0,90	0,84-0,80
0,89-0,85	0,79-0,75
0,84-0,80	0,74-0,70
0,79-0,75	
0,74-0,70	

Table Annex 1. Ci and ETS predicted binding sites present in the *wg*^{1}-enhancer sequence. Table containing information on the bioinformatically-predicted Ci (in green) and ETS (in brown) binding sites identified in *wg*^{1}-enhancer. The table includes the genomic coordinates, the PWMs used and the statistical parameters on conservation and match. Same binding sites found by different PWMs have been merge as a single binding site and the highest score have been taken as the score of the binding site (Merged BS). A colour code was used to easily identify the different score-ranges of the binding sites (ETS and Ci score table). The binding sites depicted in the figures or mutated are indicated.

seqnames	start	end	width	strand	score.avg	score.max	cons.avg	cons.max	pv.min	pv.max	TF	Merged BS	Nrs in Figures	wg^1 region
chr2L	7324312	7324323	12	*	0,70	**0,7**	1	1	0,00424065	0,00424065	MEME_fly_factor_survey-Ap1_FBgn0001291	AP1 BS α1		
chr2L	7324312	7324323	12	*	0,70	**0,7**	1	1	0,00424065	0,00424065	MEME_fly_factor_survey-Ap1_FBgn0001297			
chr2L	7324314	7324321	8	*	0,70	**0,7**	1	1	0,01182806	0,01182806	Jaspar_2020_MA0099.2-FOS::JUN			
chr2L	7324334	7324345	12	*	0,70	**0,7**	1	1	0,00424065	0,00424065	MEME_fly_factor_survey-Ap1_FBgn0001291	AP1 BS α2		
chr2L	7324334	7324345	12	*	0,70	**0,7**	1	1	0,00424065	0,00424065	MEME_fly_factor_survey-Ap1_FBgn0001297			
chr2L	7324336	7324343	8	*	0,75	**0,75**	1	1	0,00446246	0,00446246	Jaspar_2020_MA0099.2-FOS::JUN			α
chr2L	7324476	7324483	8	*	0,70	**0,7**	1	1	0,01182806	0,01182806	Jaspar_2020_MA0099.2-FOS::JUN	AP1 BS α3		
chr2L	7324476	7324484	9	*	0,76	**0,76**	1	1	0,0031645	0,0031645	Jaspar_2020_MA0099.1-JUN::FOS			
chr2L	7324499	7324506	8	*	0,70	**0,7**	1	1	0,01182806	0,01182806	Jaspar_2020_MA0099.2-FOS::JUN	AP1 BS α4		
chr2L	7324510	7324520	11	*	0,71	**0,71**	1	1	0,00338315	0,00338315	Jaspar_2020_MA0099.3-FOS::JUN	AP1 BS α5		
chr2L	7324512	7324519	8	*	0,71	**0,71**	1	1	0,0094282	0,0094282	Jaspar_2020_MA0099.2-FOS::JUN			
chr2L	7324903	7324914	12	*	0,75	0,76	1	1	0,00119911	0,00193183	MEME_fly_factor_survey-Ap1_FBgn0001291	AP1 BS β1		
chr2L	7324903	7324914	12	*	0,75	0,76	1	1	0,00119911	0,00193183	MEME_fly_factor_survey-Ap1_FBgn0001297			
chr2L	7324904	7324914	11	*	0,76	0,76	1	1	0,0012434	0,0012434	Jaspar_2020_MA0099.3-FOS::JUN			
chr2L	7324905	7324912	8	*	0,72	0,72	1	1	0,00811457	0,00811457	Jaspar_2020_MA0099.2-FOS::JUN			
chr2L	7324948	7324959	12	*	0,85	**0,85**	1	1	0,00012603	0,00018019	Jaspar_2020_MA0099.3-FOS::JUN	AP1 BS β2	AP1-1*	
chr2L	7324948	7324959	12	*	0,84	**0,85**	1	1	0,00012837	0,00020339	MEME_fly_factor_survey-Ap1_FBgn0001291			
chr2L	7324948	7324959	12	*	0,84	**0,85**	1	1	0,00012837	0,00020339	MEME_fly_factor_survey-Ap1_FBgn0001297			
chr2L	7324949	7324958	10	*	0,87	**0,89**	1	1	0,00021105	0,00058112	Jaspar_2020_MA0099.1-JUN::FOS			
chr2L	7324950	7324957	8	*	0,91	**0,93**	1	1	0,0001111	0,00040154	Jaspar_2020_MA0099.2-FOS::JUN			
chr2L	7325003	7325010	8	*	0,76	0,76	0,9875	0,9875	0,00344073	0,00344073	Jaspar_2020_MA0099.2-FOS::JUN	AP1 BS β3		β
chr2L	7325099	7325110	12	*	0,70	0,7	0,90383333	0,90383333	0,00424065	0,00424065	MEME_fly_factor_survey-Ap1_FBgn0001291	AP1 BS β4		
chr2L	7325099	7325110	12	*	0,70	0,7	0,90383333	0,90383333	0,00424065	0,00424065	MEME_fly_factor_survey-Ap1_FBgn0001297			
chr2L	7325100	7325108	9	*	0,71	0,71	0,87222222	0,87222222	0,00780907	0,00780907	Jaspar_2020_MA0099.1-JUN::FOS			
chr2L	7325101	7325108	8	*	0,70	0,7	0,85625	0,85625	0,01182806	0,01182806	Jaspar_2020_MA0099.2-FOS::JUN			
chr2L	7325216	7325224	9	*	0,70	0,7	1	1	0,00904082	0,00904082	Jaspar_2020_MA0099.1-JUN::FOS	AP1 BS β5		
chr2L	7325217	7325224	8	*	0,72	0,72	1	1	0,00811457	0,00811457	Jaspar_2020_MA0099.2-FOS::JUN			
chr2L	7325315	7325322	8	*	0,70	0,7	0,999875	0,999875	0,01182806	0,01182806	Jaspar_2020_MA0099.2-FOS::JUN			
chr2L	7325330	7325340	11	*	0,72	0,72	1	1	0,00273281	0,00273281	Jaspar_2020_MA0099.3-FOS::JUN	AP1 BS β6		
chr2L	7325331	7325339	9	*	0,71	0,71	1	1	0,00780907	0,00780907	Jaspar_2020_MA0099.1-JUN::FOS			
chr2L	7325332	7325339	8	*	0,75	0,75	1	1	0,00446246	0,00446246	Jaspar_2020_MA0099.2-FOS::JUN			
chr2L	7325605	7325616	12	*	0,75	**0,75**	0,84508334	0,84508334	0,00147232	0,00193183	MEME_fly_factor_survey-Ap1_FBgn0001291	AP1 BS γ1		
chr2L	7325605	7325616	12	*	0,75	**0,75**	0,84508334	0,84508334	0,00147232	0,00193183	MEME_fly_factor_survey-Ap1_FBgn0001297			
chr2L	7325605	7325616	12	*	0,76	**0,77**	0,8775	0,92109091	0,00099343	0,0018502	Jaspar_2020_MA0099.3-FOS::JUN			
chr2L	7325606	7325615	10	*	0,78	**0,8**	0,95138889	0,995	0,00159953	0,0031645	Jaspar_2020_MA0099.1-JUN::FOS			
chr2L	7325607	7325614	8	*	0,78	**0,81**	0,995125	0,995125	0,00141349	0,00446246	Jaspar_2020_MA0099.2-FOS::JUN			
chr2L	7325625	7325636	12	*	0,85	**0,89**	0,96886364	0,97063637	4,2495E-05	0,00046578	Jaspar_2020_MA0099.3-FOS::JUN	AP1 BS γ2	AP1-2*	
chr2L	7325625	7325636	12	*	0,89	**0,89**	0,958	0,958	3,501E-05	5,6267E-05	MEME_fly_factor_survey-Ap1_FBgn0001291			
chr2L	7325625	7325636	12	*	0,89	**0,89**	0,958	0,958	3,501E-05	5,6267E-05	MEME_fly_factor_survey-Ap1_FBgn0001297			
chr2L	7325626	7325635	10	*	0,95	**1**	0,98727778	0,98888889	1,2488E-05	0,00021105	Jaspar_2020_MA0099.1-JUN::FOS			
chr2L	7325627	7325644	18	*	0,82	**1**	0,84607501	0,994	4,4315E-05	0,01182806	Jaspar_2020_MA0099.2-FOS::JUN			
chr2L	7325636	7325644	9	*	0,72	**0,72**	0,71833334	0,71833334	0,00682458	0,00682458	Jaspar_2020_MA0099.1-JUN::FOS			
chr2L	7325695	7325703	9	*	0,73	**0,73**	0,99955555	0,99955555	0,00537512	0,00537512	Jaspar_2020_MA0099.1-JUN::FOS	AP1 BS γ3	AP1-3*	
chr2L	7325695	7325719	25	*	0,75	**0,86**	0,999425	1	0,00084239	0,01182806	Jaspar_2020_MA0099.2-FOS::JUN			
chr2L	7325710	7325721	12	*	0,75	**0,78**	0,99983334	0,99983334	0,00076315	0,00284148	MEME_fly_factor_survey-Ap1_FBgn0001291	AP1 BS γ4		
chr2L	7325710	7325721	12	*	0,75	**0,78**	0,99983334	0,99983334	0,00076315	0,00284148	MEME_fly_factor_survey-Ap1_FBgn0001297			
chr2L	7325710	7325721	12	*	0,78	**0,83**	0,99990909	1	0,00022497	0,00226953	Jaspar_2020_MA0099.3-FOS::JUN			
chr2L	7325711	7325720	10	*	0,82	**0,84**	1	1	0,00070995	0,00159953	Jaspar_2020_MA0099.1-JUN::FOS			
chr2L	7325762	7325769	8	*	0,70	**0,7**	1	1	0,01182806	0,01182806	Jaspar_2020_MA0099.2-FOS::JUN	AP1 BS γ5		
chr2L	7325762	7325770	9	*	0,75	**0,75**	1	1	0,00408322	0,00408322	Jaspar_2020_MA0099.1-JUN::FOS			
chr2L	7325773	7325783	11	*	0,74	**0,74**	1	1	0,0018502	0,0018502	Jaspar_2020_MA0099.3-FOS::JUN	AP1 BS γ6		
chr2L	7325773	7325784	12	*	0,74	**0,74**	1	1	0,00193183	0,00193183	MEME_fly_factor_survey-Ap1_FBgn0001291			
chr2L	7325773	7325784	12	*	0,74	**0,74**	1	1	0,00193183	0,00193183	MEME_fly_factor_survey-Ap1_FBgn0001297			
chr2L	7325774	7325782	9	*	0,77	**0,77**	1	1	0,00241001	0,00241001	Jaspar_2020_MA0099.1-JUN::FOS			
chr2L	7325775	7325782	8	*	0,71	**0,71**	1	1	0,0094282	0,0094282	Jaspar_2020_MA0099.2-FOS::JUN			
chr2L	7325895	7325902	8	*	0,70	**0,7**	1	1	0,01182806	0,01182806	Jaspar_2020_MA0099.2-FOS::JUN	AP1 BS γ7		
chr2L	7325912	7325920	9	*	0,72	**0,72**	1	1	0,00682458	0,00682458	Jaspar_2020_MA0099.1-JUN::FOS	AP1 BS γ8		
chr2L	7325912	7325919	8	*	0,76	**0,76**	1	1	0,00344073	0,00344073	Jaspar_2020_MA0099.2-FOS::JUN			
chr2L	7325936	7325946	11	*	0,71	**0,71**	0,99890909	0,99890909	0,00338315	0,00338315	Jaspar_2020_MA0099.3-FOS::JUN	AP1 BS γ9		
chr2L	7325937	7325946	10	*	0,74	**0,76**	0,99883334	0,99900001	0,0031645	0,00682458	Jaspar_2020_MA0099.1-JUN::FOS			
chr2L	7325938	7325945	8	*	0,79	**0,84**	0,99887501	0,99887501	0,00106875	0,00590571	Jaspar_2020_MA0099.2-FOS::JUN			
chr2L	7326061	7326068	8	*	0,70	**0,7**	0,999625	0,999625	0,01182806	0,01182806	Jaspar_2020_MA0099.2-FOS::JUN	AP1 BS γ10		γ
chr2L	7326202	7326210	9	*	0,73	**0,73**	0,81411111	0,81411111	0,00537512	0,00537512	Jaspar_2020_MA0099.1-JUN::FOS	AP1 BS γ11		
chr2L	7326202	7326209	8	*	0,73	**0,73**	0,790875	0,790875	0,00712114	0,00712114	Jaspar_2020_MA0099.2-FOS::JUN			
chr2L	7326210	7326221	12	*	0,79	**0,79**	1	1	0,00060747	0,00076315	MEME_fly_factor_survey-Ap1_FBgn0001291	AP1 BS γ12	AP1-4*	
chr2L	7326210	7326221	12	*	0,79	**0,79**	1	1	0,00060747	0,00076315	MEME_fly_factor_survey-Ap1_FBgn0001297			
chr2L	7326210	7326221	12	*	0,78	**0,82**	1	1	0,00028163	0,0018502	Jaspar_2020_MA0099.3-FOS::JUN			
chr2L	7326211	7326220	10	*	0,81	**0,86**	1	1	0,00038984	0,0031645	Jaspar_2020_MA0099.1-JUN::FOS			
chr2L	7326212	7326219	8	*	0,82	**0,86**	1	1	0,00084239	0,00264099	Jaspar_2020_MA0099.2-FOS::JUN			
chr2L	7326271	7326288	18	*	0,77	**0,81**	0,99948148	1	0,00106899	0,00780907	Jaspar_2020_MA0099.1-JUN::FOS	AP1 BS γ13		
chr2L	7326272	7326279	8	*	0,78	**0,83**	0,999125	0,999125	0,00116134	0,00712114	Jaspar_2020_MA0099.2-FOS::JUN			
chr2L	7326278	7326289	12	*	0,73	**0,73**	1	1	0,00230048	0,00230048	MEME_fly_factor_survey-Ap1_FBgn0001291			
chr2L	7326278	7326289	12	*	0,73	**0,73**	1	1	0,00230048	0,00230048	MEME_fly_factor_survey-Ap1_FBgn0001297			
chr2L	7326280	7326291	12	*	0,74	**0,75**	1	1	0,00446246	0,00712114	Jaspar_2020_MA0099.2-FOS::JUN			
chr2L	7326370	7326380	11	*	0,70	**0,7**	0,91045455	0,91045455	0,00408307	0,00408307	Jaspar_2020_MA0099.3-FOS::JUN	AP1 BS γ14		
chr2L	7326370	7326381	12	*	0,70	**0,7**	0,91791667	0,91791667	0,00424065	0,00424065	MEME_fly_factor_survey-Ap1_FBgn0001291			
chr2L	7326370	7326381	12	*	0,70	**0,7**	0,91791667	0,91791667	0,00424065	0,00424065	MEME_fly_factor_survey-Ap1_FBgn0001297			
chr2L	7326372	7326379	8	*	0,73	**0,73**	0,99700001	0,99700001	0,00712114	0,00712114	Jaspar_2020_MA0099.2-FOS::JUN			
chr2L	7326382	7326393	12	*	0,71	**0,71**	1	1	0,00338997	0,00338997	MEME_fly_factor_survey-Ap1_FBgn0001291	AP1 BS γ15		
chr2L	7326382	7326393	12	*	0,71	**0,71**	1	1	0,00338997	0,00338997	MEME_fly_factor_survey-Ap1_FBgn0001297			
chr2L	7326384	7326391	8	*	0,75	**0,78**	1	1	0,00264099	0,00811457	Jaspar_2020_MA0099.2-FOS::JUN			
chr2L	7326384	7326392	9	*	0,80	**0,8**	1	1	0,00159953	0,00159953	Jaspar_2020_MA0099.1-JUN::FOS			
chr2L	7326404	7326415	12	*	0,80	**0,81**	1	1	0,00036329	0,00060847	Jaspar_2020_MA0099.3-FOS::JUN	AP1 BS γ16	AP1-5*	
chr2L	7326404	7326415	12	*	0,81	**0,85**	1	1	0,00012837	0,00119911	MEME_fly_factor_survey-Ap1_FBgn0001291			
chr2L	7326404	7326415	12	*	0,81	**0,85**	1	1	0,00012837	0,00119911	MEME_fly_factor_survey-Ap1_FBgn0001297			
chr2L	7326405	7326414	10	*	0,89	**0,93**	1	1	7,4097E-05	0,00058112	Jaspar_2020_MA0099.1-JUN::FOS			
chr2L	7326406	7326413	8	*	0,91	**0,93**	1	1	0,0001111	0,00040154	Jaspar_2020_MA0099.2-FOS::JUN			
chr2L	7326417	7326424	8	*	0,70	**0,7**	1	1	0,01182806	0,01182806	Jaspar_2020_MA0099.2-FOS::JUN	AP1 BS γ17		
chr2L	7326438	7326446	9	*	0,72	**0,72**	1	1	0,00682458	0,00682458	Jaspar_2020_MA0099.1-JUN::FOS	AP1 BS γ18		
chr2L	7326439	7326446	8	*	0,70	**0,7**	1	1	0,01182806	0,01182806	Jaspar_2020_MA0099.2-FOS::JUN			
chr2L	7326453	7326461	9	*	0,70	**0,7**	1	1	0,00904082	0,00904082	Jaspar_2020_MA0099.1-JUN::FOS	AP1 BS γ19		
chr2L	7326454	7326461	8	*	0,75	**0,75**	1	1	0,00446246	0,00446246	Jaspar_2020_MA0099.2-FOS::JUN			

Region	Start	End	Num bp
α	7323135	7324749	1614
β	7324770	7325443	673
γ	7325445	7326565	1120
δ	7326565	7327855	1290

AP1 Score
1-0,91
0,90-0,85
0,84-0,80
0,79-0,75
0,74-0,70

Table Annex 2. AP1 predicted binding sites present in the *wg*^{1}-enhancer sequence. Table containing information on the bioinformatically-predicted AP1 (in blue) binding sites identified in *wg*^{1}-enhancer. The table includes the genomic coordinates, the PWMs used and the statistical parameters on conservation and match. Same binding sites found by different PWMs have been merge as a single binding site and the highest score have been taken as the score of the binding site (Merged BS). A colour code was used to easily identify the different score-ranges of the binding sites. The binding sites depicted in the figures or mutated are indicated.

Publications

nature communications

Article

https://doi.org/10.1038/s41467-022-32400-2

A single WNT enhancer drives specification and regeneration of the *Drosophila* wing

Received: 3 February 2022

Accepted: 28 July 2022

Published online: 22 August 2022

Check for updates

Elena Gracia-Latorre[1,4], Lidia Pérez[1,3,4], Mariana Muzzopappa[1] & Marco Milán[1,2]

Wings have provided an evolutionary advantage to insects and have allowed them to diversify. Here, we have identified in *Drosophila* a highly robust regulatory mechanism that ensures the specification and growth of the wing not only during normal development but also under stress conditions. We present evidence that a single wing-specific enhancer in the *wingless* gene is used in two consecutive developmental stages to first drive wing specification and then contribute to mediating the remarkable regenerative capacity of the developing wing upon injury. We identify two evolutionary conserved cis-regulatory modules within this enhancer that are utilized in a redundant manner to mediate these two activities through the use of distinct molecular mechanisms. Whereas Hedgehog and EGFR signalling regulate Wingless expression in early primordia, thus inducing wing specification from body wall precursors, JNK activation in injured tissues induce Wingless expression to promote compensatory proliferation. These results point to evolutionarily linked conservation of wing specification and regeneration to ensure robust development of the wing, perhaps the most relevant evolutionary novelty in insects.

The evolutionarily conserved Wnt/β-catenin pathway is classically known for its fundamental role in governing key developmental decisions during embryonic development[1,2]. However, in the last two decades, it has been shown that this pathway is also used by vertebrates and invertebrates to drive cell proliferation upon tissue injury[3–6], and that its chronic activation is relevant in the development of cancer[7]. Identifying the molecular mechanisms by which the expression of Wnt ligands is regulated in space and time will contribute to the understanding of their roles in regulating developmental decisions, driving regeneration or causing cancer. Gene expression is governed mainly by enhancers, which are regions of non-coding DNA that recruit transcriptional factors and fully activate the transcription of a gene by interaction with its promoter[8]. The spatio-temporal expression of genes is determined by the activation of specific pathways in response to particular inputs plus the accessibility of the enhancer. *Drosophila* Wingless (Wg) is the founding member of the Wnt family. It was not until 1973 that wingless flies were found in a stock by serendipity, and this mutation, named *wingless*[1] (*wg*[1]), was mapped to the second chromosome[9]. Despite the highly pleiotropic effects of Wg in the development of most fly tissues (reviewed in ref. 10), the phenotype of *wg*[1] flies was remarkably restricted to the absence of wings.

In this work, we present evidence that the *wg*[1] phenotype is due to the loss of a highly conserved 1.8-kb-long enhancer, which is functionally restricted to the developing wing primordium. In young larvae, signalling molecules present in the wing primordium act on this enhancer to drive the expression of *wg* to the most distal part, where it induces wing fate specification. The combination of CRISPR/Cas9-mediated deletions and reporter assays allowed us to functionally identify and narrow down the wing-specific enhancer to two highly

[1]Institute for Research in Biomedicine (IRB Barcelona), The Barcelona Institute of Science and Technology, Baldiri Reixac, 10, 08028 Barcelona, Spain. [2]Institució Catalana de Recerca i Estudis Avançats (ICREA), Pg. Lluís Companys 23, 08010 Barcelona, Spain. [3]Present address: Hubrecht Institute, University Medical Centre Utrecht, Utrecht, The Netherlands. [4]These authors contributed equally: Elena Gracia-Latorre, Lidia Pérez.
e-mail: marco.milan@irbbarcelona.org

evolutionarily conserved *cis*-regulatory modules (CRMs) that are used in a redundant manner by Hedgehog and Vein, a ligand of the Epidermal Growth Factor receptor (EGFR), to mediate wing fate specification. In older larvae and once wing specification is underway, this enhancer remains silent but accessible to transcription factor binding in growing wing primordia[11,12]. Upon injury, this enhancer is activated by JNK signalling to drive regeneration[13]. We present evidence that the two CRMs present in the wing-specific enhancer are activated in a redundant manner not only in injured tissues to mediate Wg expression and wing regeneration but also in malignant tumours to drive unlimited proliferation. The use of a single wing-specific enhancer of the *wg* gene to drive wing specification and regeneration in two consecutive developmental stages unravels highly linked evolutionary conservation of these two activities. The functional redundancy of the two existing CRMs in mediating these two processes unveils a highly robust mechanism to guarantee proper wing development.

Results

A genomic region required for wing specification

In 1973, Dr. Sharma observed that the phenotype of wg^1 mutant flies was markedly restricted to the absence of wings and was associated with a duplication of the notum, the dorsal side of the body wall that arises from the same larval primordium, the wing disc[9]. Fourteen years later, wg^1 was shown to be linked to a small deficiency downstream of the *wg* gene[14] (Fig. 1a and named hereafter as Δwg^1 for simplicity). Unfortunately, though, it was not certain that this deletion was responsible for the mutant phenotype. The penetrance of the wg^1 phenotype was not complete and only 40% of the heminota (half of a notum) lacked the appendage[15]. Similar results were recently obtained with the same allele, but penetrance was shown to be even lower (below 20%[13]). Given the observed reduction in the penetrance of the phenotype over time, we backcrossed the Δwg^1-carrying chromosome twice into the w^{1118} genetic background to remove potential genetic suppressors. To characterise the potential contribution of the region deleted in the wg^1 allele to the adult wingless phenotype, we crossed wg^1 mutant flies with flies carrying either an independently generated overlapping deletion (*ΔBRV118*[13], see Fig. 1a) or larger chromosomal deficiencies (Supplementary Table 1). The penetrance of the wingless phenotype was over 90% in most transheterozygous conditions over large deficiencies and, most interestingly, it was up to 80% in $\Delta BRV118/\Delta wg^1$ heterozygous flies (Fig. 1b, c). We observed the presence of a duplicated notum (nt) in all cases (Fig. 1c).

Wg is expressed in a highly dynamic manner in the developing larval wing disc (Figs. 1d and 2a). Early in development (in second instar, L2), Wg is expressed in a ventral anterior wedge (Figs. 1d and 2a, ref. 16), where it signals locally to specify the progenitors of the adult wing[17]. In third instar (L3), wing discs contain the progenitors of the adult wing and notum, and Wg expression at this developmental stage promotes wing growth and notum patterning, respectively (Figs. 1d and 2a, refs. 18–21). Interestingly, $\Delta BRV118/\Delta wg^1$ individuals lacked Wg expression in second instar wing discs and the resulting mature wing discs showed loss of wing progenitors and duplication of notal precursors (Fig. 1d). The wg^1-associated deletion is placed between two *wnt* genes, namely *wg* and *wnt6*, and we observed that *wnt6* was expressed in the same pattern as *wg*, not only in late third instar wing discs[22,23], where it potentiates Wg-driven tissue growth[18], but also in second instar wing discs (Fig. 1e). However, several observations indicate that Wg, but not Wnt6, is the main ligand driving wing fate specification. Transheterozygous conditions of *ΔBRV118* or Δwg^1 with wg^{CX4} (a null allele of *wg* deleting the first coding exon, ref. 24, shown in Fig. 1a) or with wg^{CX3} (a 17kb-long insertion allele of *wg* located between the wg^1-enhancer and the *wg* gene, ref. 24, depicted in Fig. 1a) gave rise to adult flies lacking wings (Fig. 1b). We found that the penetrance was lower than $\Delta BRV118/\Delta wg^1$ or *ΔBRV118* homozygous flies, most probably because of potential interactions in trans (transvection) between the wg^1-enhancer and the *wg* promoter of homologous chromosomes. By contrast, adult flies homozygous for $wnt6^{KO}$ (a null allele of *wnt6* lacking the first coding exon, Fig. 1a) and transheterozygous flies of $wnt6^{KO}$ over large chromosomal deficiencies developed wings (Fig. 1b). Remarkably, ectopic expression of Wg, but not Wnt6, was able to induce secondary wings in the notum (Supplementary Fig. 1a). All these results indicate that the genomic region deleted in the wg^1 mutation is required in early wing discs to drive Wg expression and wing fate specification, and they point to the presence of a wing-specifying enhancer in this region.

The wg^1 deletion contains an early enhancer

We next used a transgenic reporter gene assay to address whether the genomic region deleted in the wg^1 mutation was sufficient to drive *lacZ* reporter expression in a pattern that reproduced the early pattern of Wg expression in the ventral anterior wedge of the wing disc. A *lacZ* reporter containing the genomic region deleted in the wg^1 mutation (wg^1-*lacZ*) reproduced the early expression pattern of Wg in the ventral anterior wedge of the wing disc (Fig. 2e). However, this expression pattern persisted in older wing discs, although at lower levels, thereby suggesting that the regulatory elements responsible for turning it off during normal development are not present in this region. Similar results were obtained with a *lacZ* reporter containing the overlapping *BRV118* region (Fig. 2f). By contrast, a *lacZ*-enhancer trap placed in the promoter of the *wg* gene (Fig. 2b) recapitulated the dynamic expression pattern of Wg in the wing disc during larval development (Fig. 2d). These results indicate that the genomic region deleted in the wg^1 mutation contains an enhancer that drives the characteristic expression of Wg in second instar wing discs.

In early wing discs, Hedgehog (Hh) coming from posterior (P) cells induces Wg expression in anterior (A) cells[17] (Fig. 2c). Consistent with this, we identified several bioinformatically predicted binding sites of the transcription factor Ci, the most downstream component of the Hh signalling pathway (Gli in vertebrates), in the wg^1 genomic region (green bars in Fig. 2b, see Supplementary Fig. 2b, c, Supplementary Tables 2 and 4, and Methods for details). Despite the presence of two other high-score Ci binding sites in other regions close to the *wg* and *wnt6* genes, they did not drive restricted expression to the A compartment of the wing disc (Supplementary Fig. 3a). We next genetically manipulated Hh expression and signalling with the use of the *sd-gal4* driver, which is ubiquitously expressed in the early wing primordia (Fig. 2h), and addressed the impact on the expression of the wg^1-lacZ reporter. Interestingly, the expression pattern of this reporter was expanded throughout the A compartment upon ubiquitous expression of Hh and reduced upon ubiquitous overexpression of Ptc (Fig. 2g), which is known to block Hh signalling when overexpressed[25]. Surprisingly, we observed that expression of wg^1-lacZ was not abolished upon Ptc overexpression (Fig. 2g, arrows), suggesting that Hh signalling is not an absolute requirement for the expression of Wg in early wing discs. Consistently, only a small proportion of the Ptc-overexpressing adult flies lacked wings and showed duplicated notal structures (Fig. 2k). The presence of vestigial wings in these animals (Fig. 2j, arrows and magnification) is most probably a consequence of reduced expression of the growth-promoting and Hh-regulated morphogen Dpp in late third instar wing discs (reviewed in ref. 26). These results suggest that, early in development, the enhancer present in the wg^1 region integrates Hh-dependent and -independent inputs to drive the early expression of Wg responsible for wing fate specification.

The mature wing disc contains the primordia of the adult wing and notum, and this subdivision is generated in second instar by the combined activities of three signalling molecules, namely Wg[17], EGFR ligand Vein (Vn, ref. 27), and Unpaired (Upd) ligand, the latter activating the JAK/STAT pathway[28] (Fig. 2c). While the opposing activities of Wg and Vn, which are expressed in the most distal and proximal portions of the wing disc, specify wing and notum fate respectively, the

https://doi.org/10.1038/s41467-022-32400-2

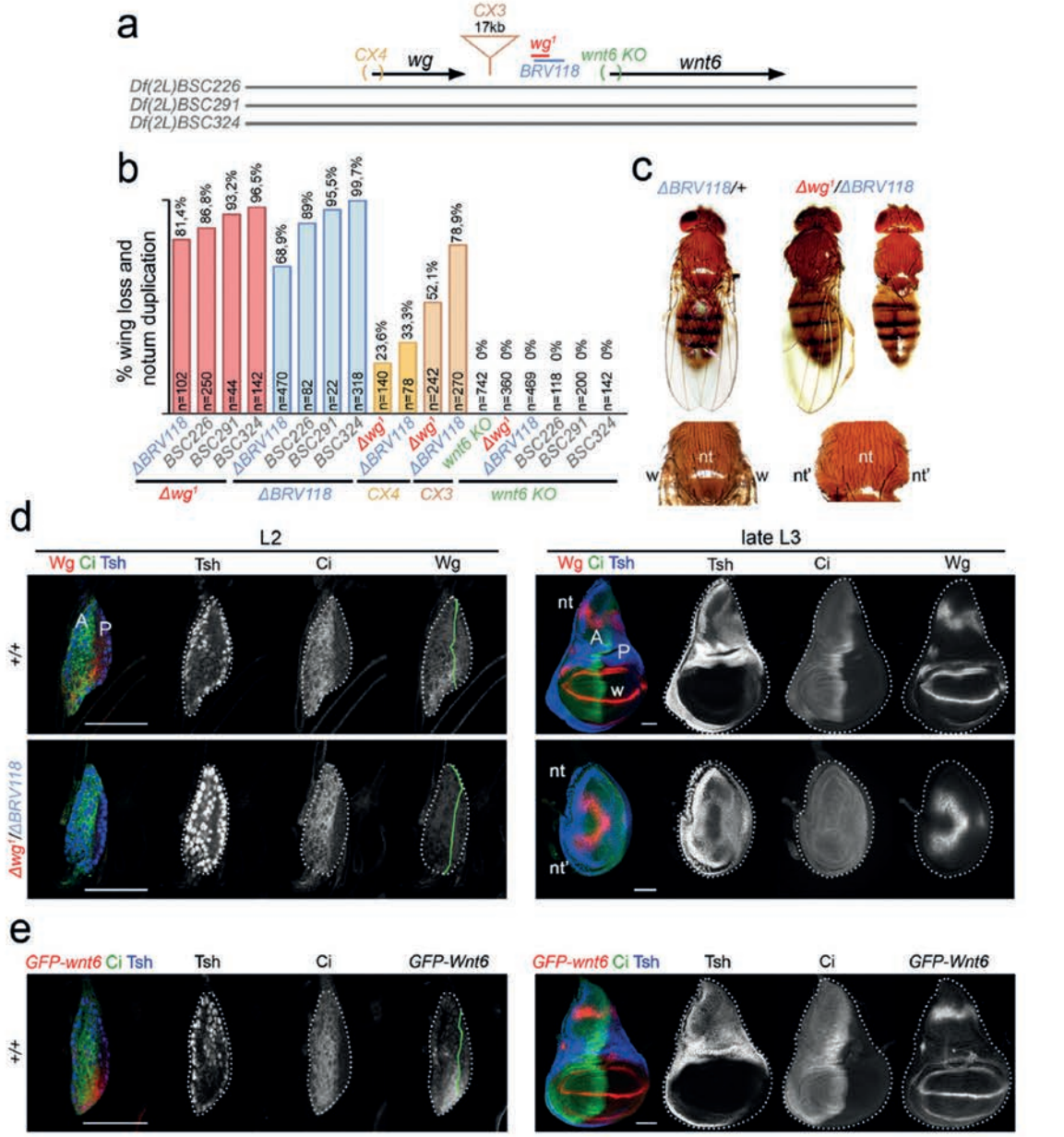

Fig. 1 | A genomic region required to drive early expression of Wg and wing specification. a Cartoon depicting the genomic location of the *wg*^{1}*/BRV118* enhancer between the *wg* and the *wnt6* genes and the deficiencies and mutations affecting these elements. **b** Histogram showing the percentage of wingless flies with duplicated nota of the indicated genotypes. The number of scored heminota are shown. **c** Examples of notum duplications in adult flies of the indicated genotypes. **d**, **e** Second (L2) and late third (L3) instar wing discs of larvae of the indicated genotypes and stained for Wingless (Wg, red or white, **d**), *GFP-wnt6* transcriptional reporter (red or white, **e**), Ci (green or white, **d**, **e**), and Teashirt (Tsh, blue or white, **d**, **e**). Wing disc contour and the AP boundary are labelled by white and green lines, respectively. Progenitors of wing (w), endogenous notum (nt) and duplicated notum (nt') are marked in (**c**), (**d**). Scale bars, 50 μm. See also Supplementary Fig. 1 and Supplementary Tables 1 and 6.

expression of Upd in the distal portion of the wing disc contributes indirectly to wing fate specification by counteracting the activity of Vn. The observation that *wg*^{1}-lacZ expression is restricted to the distal portion of the wing disc suggests that it might be negatively regulated by Vn activity in the proximal portion. Consistent with this proposal, expression of a Vn antagonist—a chimeric protein between Vn and the secreted EGFR antagonist Argos (Vein::Argos, ref. 27)—in the early wing disc gave rise to a proximal expansion in the expression domain of *wg*^{1}-lacZ (Fig. 2i arrows), and three high-score binding sites for the ETS-family of *Drosophila* transcription factors Yan and Pointed (the most downstream regulator of the EGFR pathway) were identified in the *wg*^{1} region (red bars in Fig. 2b, see Supplementary Fig. 2b, c,

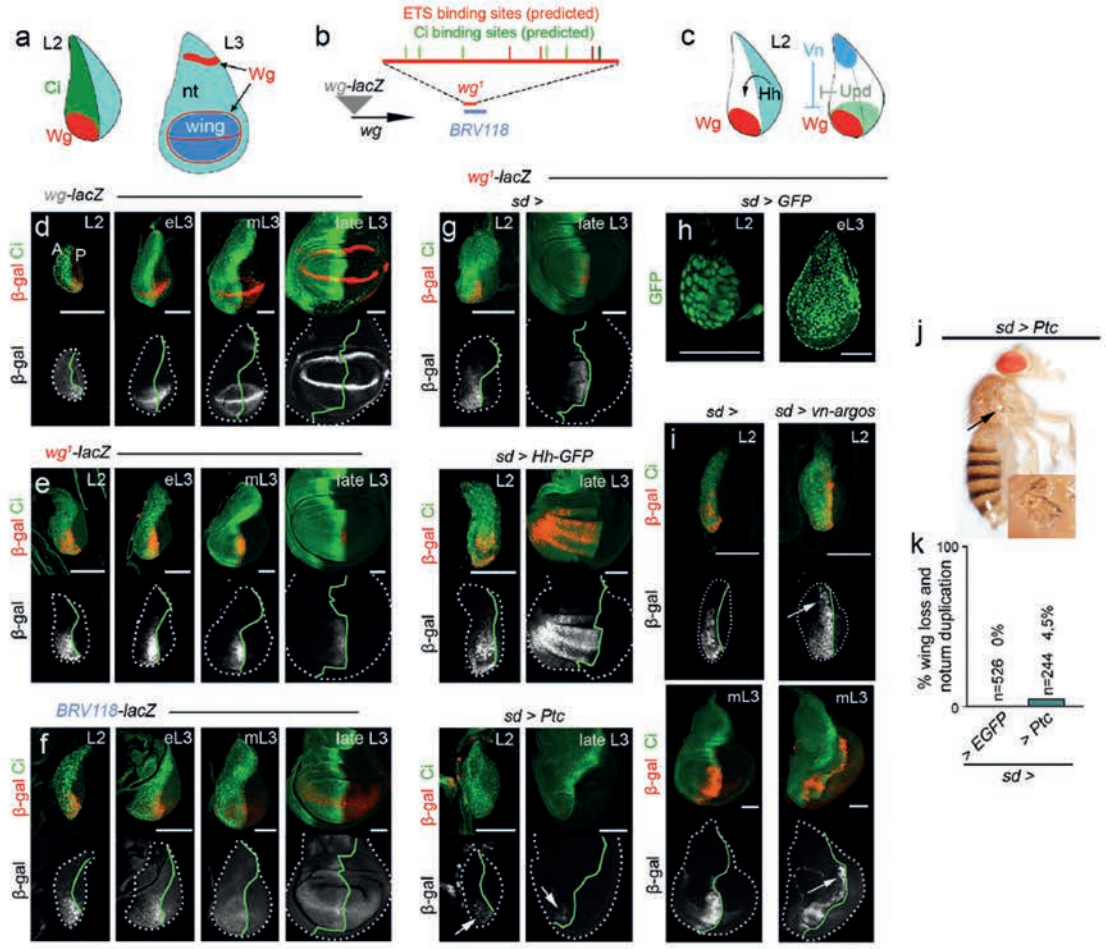

Fig. 2 | Regulation of the *wg¹*-enhancer by Hh-dependent and -independent mechanisms. a–c Cartoons depicting the expression of Wg in second (L2) and third (L3) instar wing discs (in **a**), the genomic location of the *wg¹*-enhancer, the Ci (in green) and ETS (in red) binding sites present in it, and the *wg-lacZ* insertion with respect to the *wg* gene (in **b**), and the regulation of *wg* expression in L2 discs by the pre-existing signalling molecules (in **c**). **d–i** Second (L2), early (eL3), mid (mL3) and late third (late L3) instar wing discs of larvae, bearing the *wg-lacZ* enhancer trap (**d**), or the *wg¹-lacZ* (**e**, **g**, **i**) and *BRV118-lacZ* (**f**) reporter constructs and stained in (**d–g**) and (**i**) for ß-galactosidase (red or white) and Ci (green) and in h for GFP (green). In **g–i**, larvae expressed the indicated transgenes under the control of the *sd-gal4* driver. Wing disc contour and the AP boundary are labelled by white and green lines, respectively. Arrows in **g** point to the presence of some lacZ-expressing cells upon Ptc-overexpression and in **i** to the ectopic expression of the lacZ reporters. Scale bars, 50 μm. **j** Adult fly of the indicated genotype showing the most representative phenotype: a vestigial wing (arrow, see also high magnification). **k** Percentages of wingless flies of the indicated genotypes with duplicated nota. Number of scored nota are shown. See also Supplementary Figs. 2 and 3 and Supplementary Tables 1–4 and 6.

Supplementary Tables 3, 4 and Methods for details). These results indicate that the enhancer located in the *wg¹* deletion is regulated in early wing discs by the combined activities of the Hh and Vn signalling molecules.

The *wg¹*-enhancer is comprised of two *cis*-regulatory modules

On the basis of sequence conservation with other *Drosophila* species (Supplementary Fig. 2a), we subdivided a 4.7-kb-long region containing the *wg¹* deletion into four fragments [*Alpha* (α), *Beta* (β), *Gamma* (γ) and *Delta* (δ); Fig. 3a] and generated reporter constructs carrying them. The *Alpha* fragment drove expression of *lacZ* to the notum of mature wing discs while *Delta* did not induce the expression of *lacZ* at any time during development (Fig. 3c). The *Gamma* fragment, which contains a high-score Ci binding site (Supplementary Fig. 2b, c), reproduced the expression pattern of the *wg¹-lacZ* reporter in early and late wing discs (Fig. 3c) and was subjected to regulation by Hh signalling. Thus, the expression pattern of the *Gamma-lacZ* reporter was expanded throughout the A compartment upon ubiquitous expression of Hh and abolished upon ubiquitous overexpression of Ptc (Fig. 3g). The latter observation indicates that Hh signalling is an absolute requirement for the expression of *Gamma* in early wing discs. Further subdivision of *Gamma* into two evolutionarily conserved fragments (Fig. 3b and Supplementary Fig. 2a) allowed us to identify a 590-bp-long fragment containing the Ci binding site with the highest score (dark green bar in Fig. 3a, b) that was sufficient to reproduce the expression pattern of the *wg¹-lacZ* reporter (Fig. 3d). Mutating this Ci binding site compromised, but did not completely abolish, the ability of *Gamma* and the 590-bp-long fragment to drive sustained and restricted expression of *lacZ* to the ventral anterior wedge of early wing discs (Fig. 3d). This observation suggests that a second Ci binding site present in this region but with a lower score (light green bar in Fig. 3a, b, Supplementary Fig. 2b and Supplementary Table 2) is

https://doi.org/10.1038/s41467-022-32400-2

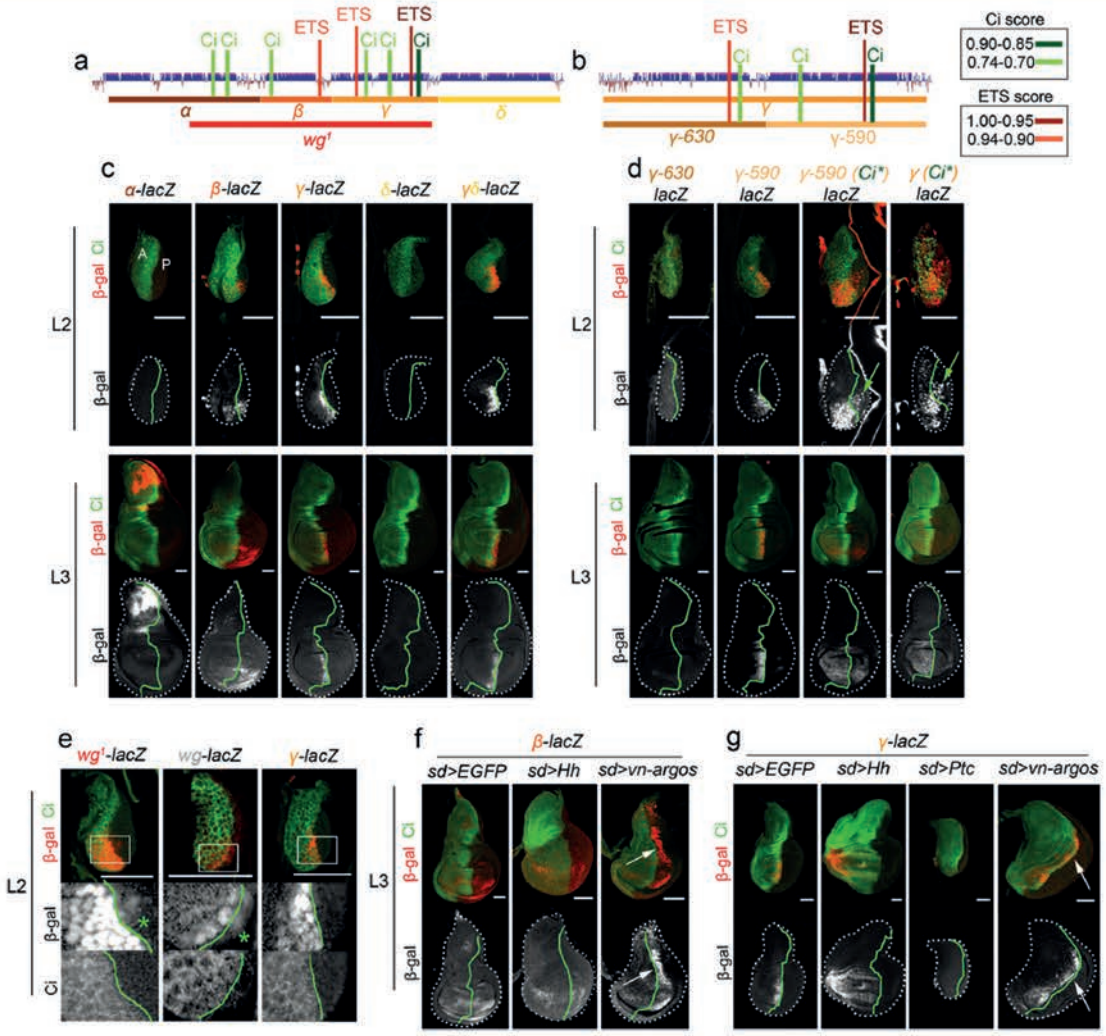

Fig. 3 | Two independent CRMs within the *wg*^{1}-enhancer. a, b Cartoons depicting the evolutionarily conserved modules spanning the *wg*^{1}-enhancer and the presence of bioinformatically predicted Ci (in green) and ETS (in red) binding sites with the scores shown in the table. **c–g** Second (L2) and late third (L3) instar wing imaginal discs of larvae bearing the indicated reporters and stained for ß-galactosidase (red or white) and Ci (green). Green arrows in (**d**) and green stars in (**e**) mark lacZ-expressing cells in the P compartment. In **f, g**, larvae also expressed the indicated transgenes under the control of the *sd-gal4* driver, and arrows point to the ectopic expression of the lacZ reporters. Wing disc contour and the AP boundary are labelled by white and green lines, respectively. Scale bars, 50 μm. See also Supplementary Fig. 2 and Supplementary Tables 1–4.

functionally relevant in regulating Wg expression. Despite the presence of a predicted low-score Ci binding site in the 630-bp-long fragment (light green bar in Fig. 3a, b, and Supplementary Table 2), this fragment did not drive expression in this context (Fig. 3d), thereby suggesting that this site is not functional in the wing disc. As with the *wg*^{1}-lacZ reporter, expression of *Gamma-lacZ* was restricted to the distal portion of the wing (Fig. 3c), suggesting that this CRM responds to the activity of Vn. Consistently, expression of Vn::Argos in the early wing disc gave rise to proximal expansion in the expression of *Gamma-lacZ* (Fig. 3g, arrows), and two high-score binding sites for the ETS transcription factors Yan and Pointed were identified in this CRM (red bars in Fig. 3a, b and Supplementary Tables 3 and 4). These results indicate that *Gamma* is a CRM that integrates the positive input of Hh and negative input of Vn to drive expression of Wg to a ventral anterior wedge in the early wing disc.

The *Beta* fragment drove expression of *lacZ* to the most distal region of early and late wing discs (Fig. 3c), thereby suggesting that the Vn-dependent input into the *wg*^{1}-lacZ reporter might be also mediated by this CRM. Indeed, expression of Vn::Argos in the early wing disc gave rise to a proximal expansion in the expression pattern driven by *Beta* (Fig. 3f), and one high-score binding site for Yan and Pointed was identified in this CRM (red bars in Fig. 3a, b and Supplementary Tables 3 and 4). Despite the presence of a predicted low-score Ci binding site in *Beta* (light green bar in Fig. 3a, b, Supplementary Fig. 2b and Supplementary Table 2), this fragment drove expression of *lacZ* to both A and P cells in wild-type larvae (Fig. 3c), and this expression was not expanded throughout the A compartment upon ubiquitous expression of Hh (Fig. 3c), thereby indicating that this binding site is not functionally relevant in this context. All these results show that the activities of the *Gamma* and *Beta* CRMs are restricted to the distal part

of the wing disc by Vn to drive Wg expression and wing fate specification in the distal part of the wing primordium, and that *Gamma* and *Beta* CRMs integrate Hh-dependent and -independent inputs, respectively. Consistently, we observed that wg^1-lacZ (containing the two CRMs) and the *wg-lacZ* enhancer trap (responding to the two CRMs) drove expression of *lacZ* not only to A but also to P cells (Fig. 3e), and that expression of *Gamma-lacZ* was restricted to the A compartment (Fig. 3e). We noticed that expression of *lacZ* driven by *Beta* and *Gamma* CRMs in second instar wing discs persisted in later stages even in the presence of *Delta* (Fig. 3c), a genomic region that has been shown to block the activity of this enhancer upon tissue damage in mature wing discs[13]. These results suggest that the regulatory elements responsible for turning *Gamma* and *Beta* CRMs off during normal development are not present in these genomic regions.

The two CRMs act redundantly to drive wing specification

The above results also suggest that Wg expression in the early wing disc is regulated in a redundant manner by two independent CRMs: *Gamma*, which responds to the combined activities of Hh and Vn; and *Beta*, which responds only to the negative input of Vn. To experimentally confirm the biological relevance of this proposal and the functional redundancy of the two CRMs in driving Wg expression and wing fate specification, we used the CRISPR/Cas9 technique to generate targeted deletions within the *Gamma* and *Beta* CRMs (Fig. 4a, b). Targeted mutation of the highest-score Ci binding site in *Gamma* or deletion of the 590-bp-long fragment (Δγ-590) did not cause a wingless phenotype in adults when homozygous, and only 0.39% of flies lacking the whole *Gamma* CRM showed a wingless phenotype (Fig. 4c). Similarly, deletion of *Beta*, which drove expression in the distal side of the early wing disc, did not cause any overt phenotype in adults (Fig. 4c). It was necessary to delete both *Beta* and *Gamma* to induce a wingless phenotype in adults (Fig. 4c, d). Interestingly, the penetrance of the wingless phenotype was up to 80% upon deletion of both *Beta* and *Gamma* (in Δβγ homozygous or Δβγ/*ΔBRV118* transheterozygous flies, Fig. 4c). As expected, the early expression of Wg was lost in Δβγ homozygous wing discs, thus causing mature wing discs to lack wing progenitors and duplicate the notum primordium (Fig. 4d, e). The deletion of *Gamma* over larger deletions containing the wg^1-enhancer (in Δγ/Δβγ or Δγ/*ΔBRV118* flies) induced a wingless adult phenotype, although at a lower penetrance (12% in Δγ/Δβγ flies and 37% in Δγ/*ΔBRV118* flies, Fig. 4c). Even deletion of the 590-bp-long fragment over *ΔBRV118* was able to cause this phenotype, but in this case penetrance was extremely low (1.65%, Fig. 4c). In contrast, deletions of *Beta* did not cause a reproducible wingless adult phenotype over the same deletions (Fig. 4c). Taken together, these results demonstrate the functional redundancy of *Gamma* and *Beta* CRMs in driving the expression of Wg in early wing discs and in specifying the wing. We observed that the penetrance of the wingless adult phenotype was higher in Δγ than in Δγ-590 transheterozygous (Fig. 4c) pointing to a potential role of the remaining 630-bp-long fragment in the regulation of *wingless* expression despite its inability to drive *lacZ* expression (Fig. 3d). Whether this fragment contributes to transcription factor accessibility, enhancer-promoter interactions or chromatin conformation remains to be further investigated.

Adult flies mutant for the original wg^1 deletion, which covers the *Gamma* and *Beta* CRMs and part of the *Alpha* region, presented a small effect on the shape of the eyes (Supplementary Fig. 4a, see also ref. 29). Also, some wg^1 mutant individuals lost notum structures in the adult and beared very small wing and haltere imaginal discs (Supplementary Fig. 4b, c, see also ref. 15). Interestingly, none of these phenotypes occurred in Δβγ homozygous flies (Fig. 4d and Supplementary Fig. 4a, c). The phenotypes observed in wg^1 individuals are consistent with the fact that the wg^1-*lacZ* reporter is expressed in other parts of the developing fly, including the eye-imaginal primordium and the larval notum (Supplementary Fig. 2b). Interestingly, the expression pattern of the eye-imaginal primordium was also reproduced by the *Alpha* and *Beta* regions, and *Alpha* drove expression also to the presumptive notum in the developing wing (Supplementary Fig. 4d–f). Although *Alpha* and *Gamma* drove expression of the reporter in the leg discs (Supplementary Fig. 4d, f), no overt phenotype was observed in the adult appendage of wg^1 mutant flies (not shown). These results point to the presence of three partially overlapping functional enhancers in this region (Supplementary Fig. 4g) and unravel a 1.8-kb-long wing-specific enhancer comprised of the *Beta* and *Gamma* CRMs.

The two CRMs respond to JNK to drive wing regeneration

Later in development and once the wing primordium has been specified, Wg, emerging from a central stripe that corresponds to the future wing margin, acts as mitogenic molecule and drives wing growth[18,19]. Wnt6, which is also expressed in the future wing margin (Fig. 1e), but is less efficient at activating the canonical pathway than Wg[30], also contributes to wing growth[18]. Tissue injury induces the expression of these two ligands as a consequence of JNK signalling acting on the wg^1-enhancer, which is populated by five bioinformatically predicted high-score AP1 binding sites (blue bars in Fig. 5a, Supplementary Fig. 2b, c and Supplementary Table 5), and Wg has been shown to play a functional role in driving compensatory proliferation and regeneration of the developing wing[4,13,31]. However, experimental settings to genetically induce ablation of the wing primordium by different means came up with opposite observations and conclusions on the role of Wg in wing regeneration[32–34]. In some cases, functional experiments to deplete Wg expression and address its role in wing regeneration upon injury were also unable to completely circumvent the developmental requirements of Wg in wing fate specification and wing growth. No attempt to analyse the specific contribution of Wnt6 to wing regeneration was reported either. Thus, using our collection of expression reporters and CRISPR/Cas9-targeted deletions, we decided to revisit the role of Wg, Wnt6, the wg^1-enhancer and the newly identified CRMs in regeneration.

Two distinct experimental settings were used to address whether Wg is required for tissue regeneration upon ablation. Overexpression of the *Drosophila* TNF-α homologue Eiger was used in refs. 4,13, to activate the JNK pathway and induce the apoptosis of most wing pouch cells. Overexpression of the pro-apoptotic gene *reaper* was used in ref. 32 to directly induce apoptosis. In both cases, transgene expression was driven by the *rotund-gal4* (*rn-gal4*) driver, which is expressed in those cells that will give rise to the adult wing (Fig. 5b, region coloured in yellow). The GAL4/UAS system was combined with the temperature-sensitive version of the Gal4 repressor Gal80 ($Gal80^{ts}$) to drive transgene expression during a discrete period of time in early third instar wing discs and to analyse the capacity of the remaining tissue to give rise to a normal adult wing as a consequence of compensatory proliferation. We used two different transactivation systems (Gal4/UAS and LexA/LexO) and shortened the induction period to 11 h (in the case of Reaper) or 16 h (in the case of Eiger) in early third instar larvae (Fig. 5b). We used *rn-gal4* to drive Eiger expression and *spalt-lexA*, which is expressed in a central region of the presumptive wing (Fig. 5b, region coloured in brown), to drive *reaper* expression. We first compared the ability of these two transgenes to drive ectopic activation of wg^1-lacZ and expression of the Wg and Wnt6 genes. Both transgenes triggered robust activation of wg^1-lacZ, and ectopic expression of an endogenous Wg-GFP fusion protein, the *wnt6* gene, and MMP1, a bona fide target gene of JNK in *Drosophila*[35] (Fig. 5c–g). All these reporters were expressed mainly in apoptotic cells, as visualised by their pyknotic nuclei.

The ability of the wg^1-enhancer to drive lacZ expression upon Eiger expression was drastically compromised when mutating four out of the five existing AP1 binding sites (Fig. 6b, mutated AP1 binding sites are marked with stars in Fig. 6a, see 'Methods' for details). We observed that the developmental expression of the wg^1-enhancer was largely

https://doi.org/10.1038/s41467-022-32400-2

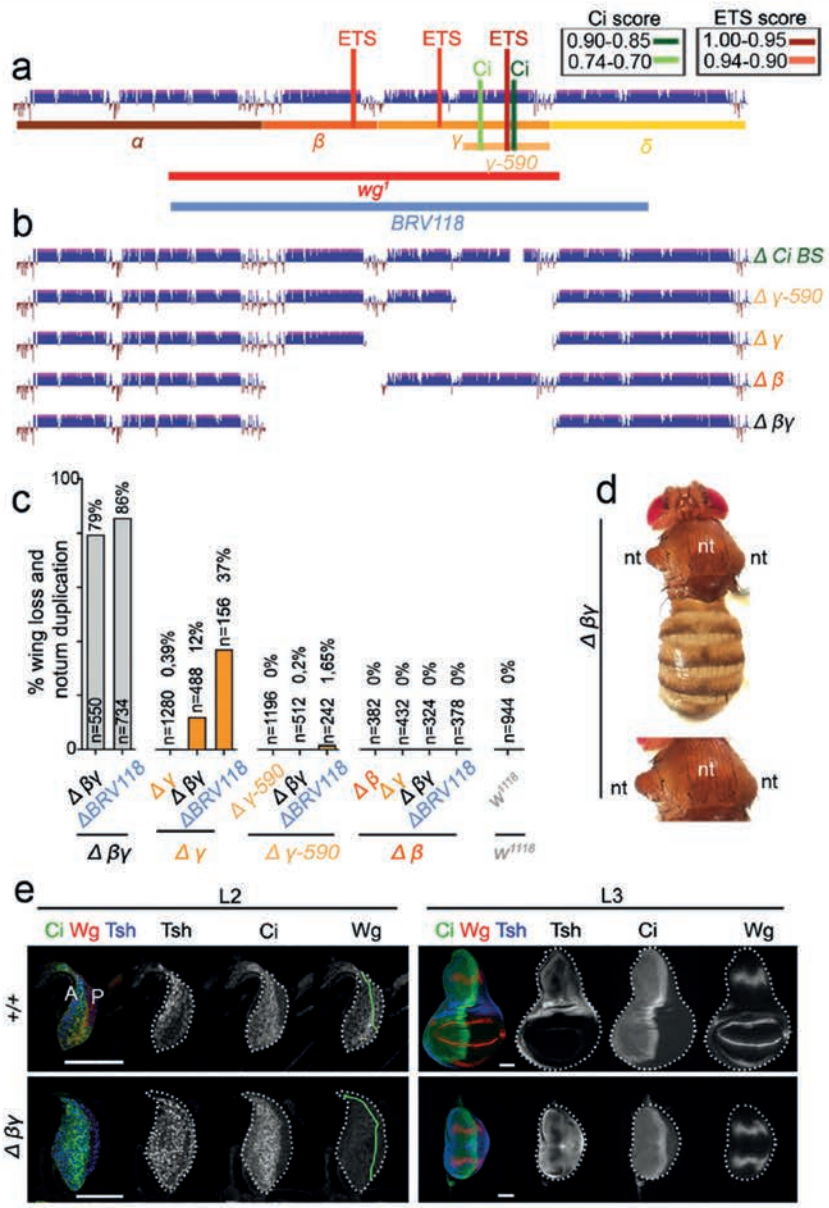

Fig. 4 | Functional redundancy within the *wg*^{1}-enhancer to drive wing fate specification. **a**, **b** Cartoons depicting in **a** the evolutionarily conserved modules spanning the *wg*^{1}-enhancer and the presence of bioinformatically predict predicted Ci (in green) and ETS (in red) binding sites with the scores shown in the table, and in **b** the CRISPR/Cas9-induced deletions of the indicated elements. **c** Histogram plotting the percentage of wing loss and notum duplication in flies of the indicated genotypes. The number of scored heminota is also shown. **d** Examples of notum duplication of an adult fly of the indicated genotype. **e** Second (L2) and late third (L3) instar wing discs of larvae of the indicated genotypes and stained for Wg (red or white), Ci (green or white), and Teashirt (Tsh, blue or white). Wing disc contour and the AP boundary are labelled by white and green lines, respectively. Scale bars, 50 μm. See also Supplementary Figs. 2 and 4 and Supplementary Tables 1–4 and 6.

unaffected by these mutations (Supplementary Fig. 4e). We next used our *lacZ*-reporter constructs carrying the evolutionarily conserved *Alpha*, *Beta*, *Gamma* and *Delta* genomic regions to further validate the bioinformatically predicted AP1 binding sites, and targeted deletions of these fragments to functionally address their contribution to JNK-driven expression of Wg and Wnt6 and to wing regeneration. Our results indicate that only *Beta* and *Gamma* are induced in wing discs expressing Eiger, and that JNK has an impact on both the 630-bp- and 590-bp-long fragments comprising the *Gamma* CRM (Fig. 6b). The levels of Wg expression induced by Eiger were significantly reduced in Δβγ homozygous flies and partially reduced in flies where either the *Gamma* or *Beta* CRMs were deleted (Fig. 6c, d). These findings thus point to the functionally independent role of these CRMs in mediating JNK-driven Wg expression. Interestingly, Eiger was able to cause ectopic expression of Wg even upon deletion of these two CRMs, thus indicating the presence of other genomic regions acting on Wg and

https://doi.org/10.1038/s41467-022-32400-2

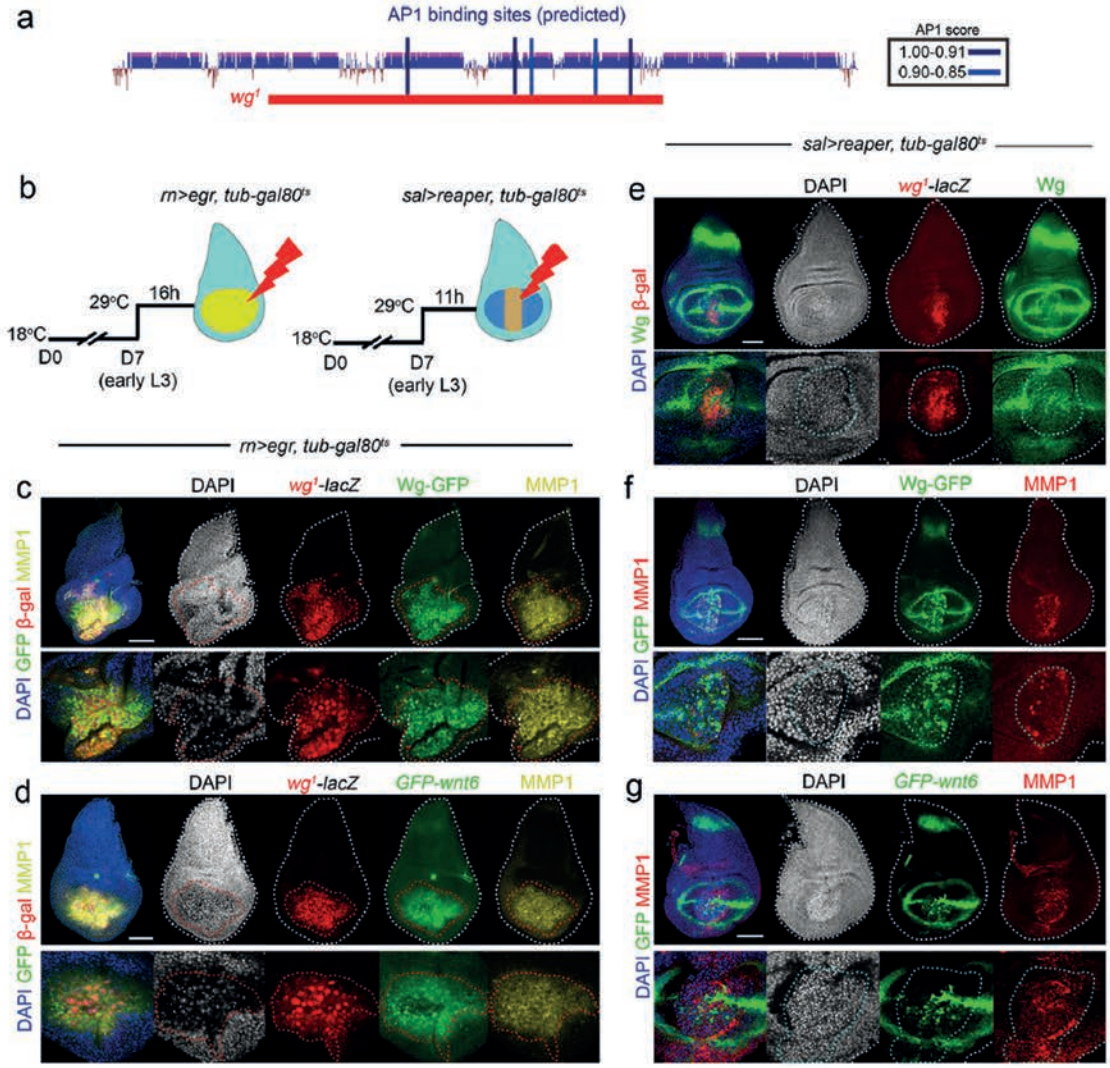

Fig. 5 | The *wg*^{1}-enhancer is activated in apoptotic cells upon tissue injury. **a** Cartoon depicting the presence of bioinformatically predicted high-score AP1 binding sites (in blue) in the *wg*^{1}-enhancer with the scores shown in the table. **b** Schematic representation of the Eiger- and Reaper-dependent wing ablation systems. Larvae were raised at 18 °C for 7 days (D7) and switched to 29 °C for 16 h (**c**, **d**) or 11 h (**e**–**g**) to visualise gene expression. **c**–**g** Third instar wing discs of larvae bearing the indicated reporters, after Eiger (**c**, **d**) or Reaper (**e**–**g**) expression and stained for *wg*^{1}*-lacZ* expression (antibody to ß-galactosidase in red, **c**, **d**, **e**), Wg-GFP (green, **c**, **f**), *GFP-Wnt6* (green, **d**, **g**), Wg (green, **e**), MMP1 (yellow in **c**, **d**, and red in **f**, **g**), and DAPI (blue or white). Wing disc contours are labelled by a white line, cells expressing the *wg*^{1}-enhancer by a red line (**c**, **d**) and apoptotic cells by a blue line (**e**–**g**). Higher magnification of the wing pouch is shown in lower panels. Scale bars, 50 μm. See also Supplementary Fig. 2 and Supplementary Tables 1 and 5.

responding to JNK. The presence of Gal80^{ts} also allowed us to express Eiger in the wing pouch for a short period (16 h, Fig. 6e), thus killing a good fraction of developing wing cells, and to address the regenerative capacity of the remaining tissue in flies where the *Gamma* or *Beta* CRMs had been deleted. Deletion of either CRM in homozygosis did not cause any wing phenotype by themselves (Fig. 4c) but significantly reduced the regenerative capacity of the wing (Fig. 6f, g). This capacity was even more compromised when both CRMs were deleted in homozygosis (Fig. 6f, g). In this case, those flies presenting a notum duplication and absence of wing tissue, as a result of the developmental role of both CRMs in wing fate specification, were not scored.

Wg is a potent mitogenic molecule in wing pouch cells[18,19] and Wnt6 contributes to positively regulate this mitogenic activity[18]. Consistently, Wg expression levels and mitotic activity in wing discs subjected to Eiger expression, which is increased when compared to undamaged discs[4], were reduced in Δγ, Δβ and Δβγ homozygous individuals (Fig. 6c, d). Similar results were obtained when monitoring cells in S-phase (Fig. 6c, d). Not only Wg but also Wnt6 contributed to the regenerative capacity of the wing, as RNAi-mediated depletion of Wnt6 compromised this capacity and reduced the mitotic activity observed in regenerating wing primordia (Fig. 6h, i). All these results indicate that the two evolutionarily conserved CRMs of the wing-specific enhancer respond to JNK and contribute, in a functionally redundant manner, to tissue regeneration, thus reinforcing the role of Wg as a mitogen and Wnt6 as a positive modulator[18].

https://doi.org/10.1038/s41467-022-32400-2

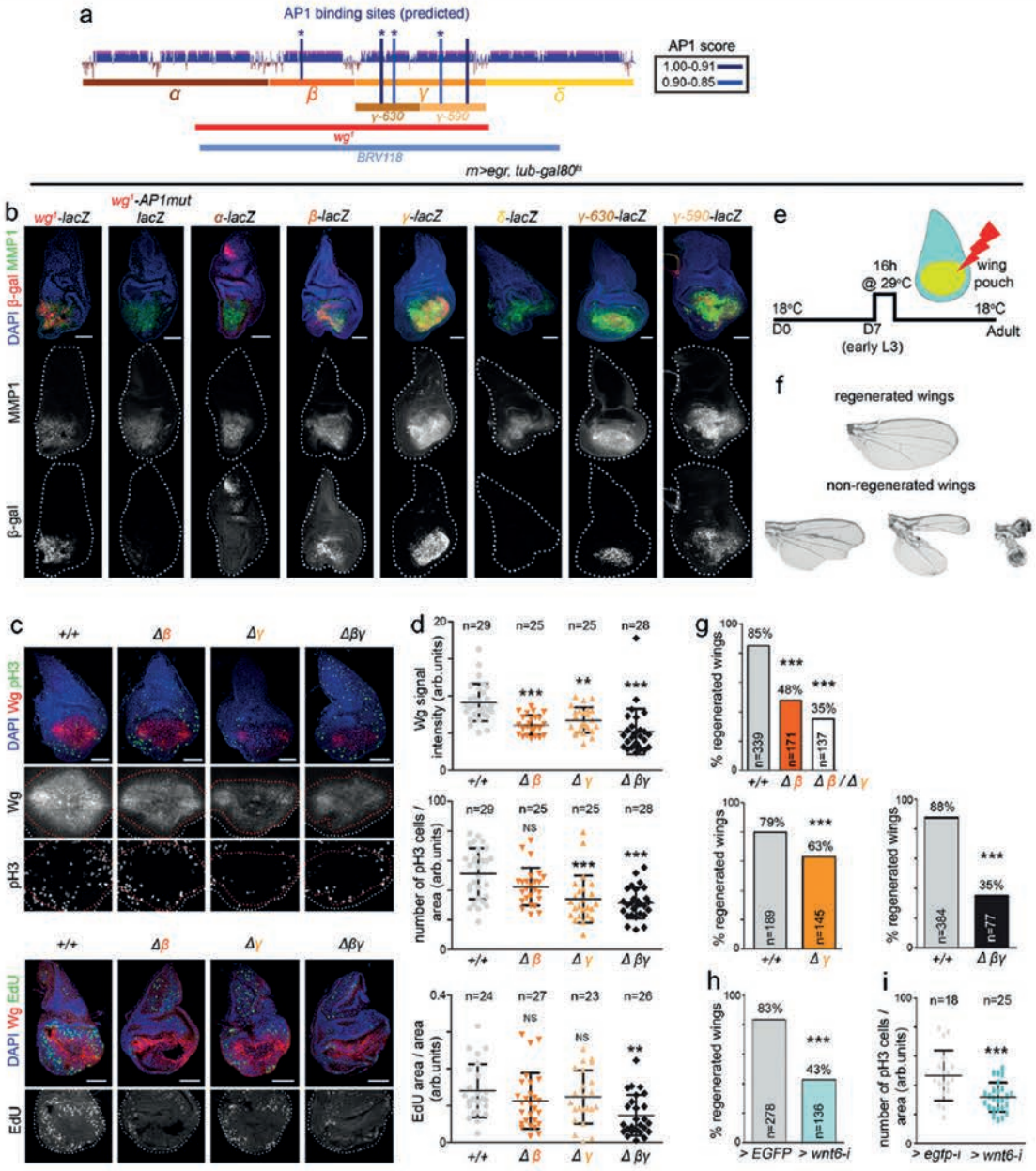

The two CRMs respond to JNK to drive malignant overgrowth

Vertebrate and invertebrate tissues with strong regenerative capacity, such as the mammalian liver and fly wing primordium, use almost the same signalling molecules to regenerate a missing part or to induce tumorigenesis in situations in which deleterious cells have not been removed by apoptosis. In the case of the developing fly wing, JNK-driven expression of Wg and Wnt6 induces compensatory proliferation and wing regeneration upon tissue injury (above results and ref. 13), and JNK-driven expression of Wg in tissues subjected to chromosomal instability (CIN)—a high rate in the gain or loss of chromosomes during mitosis and a hallmark or most solid tumours in humans—contributes to the production of tumour-like overgrowths upon additional blockage of the apoptotic pathway[36,37]. We decided to analyse whether the two ligands and the wing-specific enhancer were activated in CIN tissues, and whether the two CRMs also contributed to the resulting tumour-like overgrowths in a functionally redundant manner. Interestingly, not only Wg but also Wnt6 was ectopically induced in CIN tissues (Fig. 7a), wg^1-lacZ, *Beta* and *Gamma* CRMs, and the 630-bp- and 590-bp-long fragments comprising the *Gamma* CRM were activated (Fig. 7b) and their expression levels were drastically reduced by expressing a dominant negative version of JNK (Bsk in *Drosophila*, Fig. 7c). Mutating four out of the five existing AP1 binding sites in the wg^1-enhancer (labelled with a star in Fig. 6a) compromised its ability to drive *lacZ* expression in CIN tissues (Fig. 7b). Deletion of either *Beta* or *Gamma* in homozygosis significantly reduced the CIN-induced tissue overgrowth, as well as the levels of Wg expression

Fig. 6 | Functionally redundant CRMs in the *wg*^{1}-enhancer respond to JNK and contribute to wing regeneration. **a** Cartoon depicting the evolutionarily conserved modules spanning the *wg*^{1}-enhancer and the presence of bioinformatically predicted AP1 binding sites (in blue) with the scores shown in the table. Stars mark mutated AP1 binding sites in the *wg*^{1}*-AP1mut-lacZ* reporter. **b**, **c** Third instar wing discs of larvae, subjected to the expression of Eiger under the control of the *rn-gal4* driver for 16 h, bearing the indicated reporters in **b**, and stained for ß-galactosidase (red or white, **b**), MMP1 (green or white, **b**), Wg (red or white, **c**), pH3 (green or white, **c** top panels), EdU (green or white, **c** bottom panels), and DAPI (blue). Wing disc contours are labelled by white lines in (**b**). Scale bars, 50 µm. **d**, **g**, **h**, **i** Scattered plots (**d**, **i**) representing Wg signal intensity (in arbitrary units, **d**), number of pH3-positive cells per area (in arbitrary units, **d**, **i**), and EdU incorporation per area (in arbitrary units, **d**), and histograms (**g**, **h**) plotting the percentages of fully regenerated wings of individuals of the indicated genotypes. The number of scored wing discs or wings is shown in (**d**, **g**, **h**, **i**), and the area where mitotic activity was quantified in (**d**, **h**, **i**) is labelled by a red line in (**c**). Mean and SD (**d**, **i**) are shown. All statistical tests (Anova in **d**, **i**, logistic regression/Wald test statistic in **g**, **h**) are two-tailed and, in case of more than two conditions, Dunnett's multiple comparison correction against a common control was performed. Statistically significant differences are shown: NS, $p > 0.05$; $^{**}p < 0.01$; $^{***}p < 0.001$. p values **d**: Wg = 0.00002 (Δβ/Δβ), 0.0016 (Δγ/Δγ), 4.5×10^{-11} (Δβγ/Δβγ); pH3 = 0.2 (Δβ/Δβ), 0.00007 (Δγ/Δγ), 0.000002 (Δβγ/Δβγ), EdU = 0.2 (Δβ/Δβ), 0.53 (Δγ/Δγ), 0.001 (Δβγ/Δβγ), **i**: pH3 = 0.0006. **e** Schematic representation of the Eiger-dependent wing ablation and regeneration system. Larvae were raised at 18 °C for 7 days (D7), switched to 29 °C for 16 h and allowed to develop at 18 °C until adulthood. **f** Examples of the resulting fully regenerated and non-regenerated adult wings. See also Supplementary Fig. 2, Supplementary Tables 1, 5 and 7. Source data are provided as Source data file.

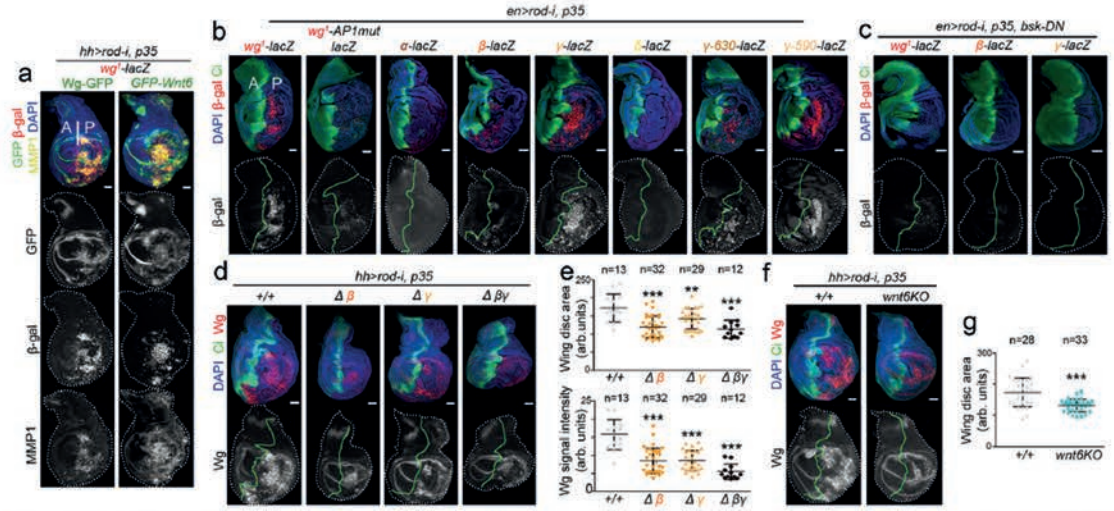

Fig. 7 | Functionally redundant CRMs in the *wg*^{1}-enhancer respond to JNK and contribute to the growth of Chromosomal Instability-induced tumours. **a**–**d**, **f** Third instar wing discs of larvae bearing the indicated reporters, subjected to the expression of the indicated transgenes under the control of the *en-gal4* (**b**, **c**) or *hh-gal4* (**a**, **d**, **f**) drivers for four days and stained GFP (**a**, green or white), ß-galactosidase (**a**, **b**, **c**, red or white), MMP1 (**a**, yellow or white), Wg (**d**, **f**, red or white), Ci (**b**, **c**, **d**, **f**, green), and DAPI (blue). Gal4 drivers are expressed in the posterior (P) compartment and Ci is used to label the anterior (A) compartment. Wing disc contours are labelled by white lines and the AP boundary by a green line. Scale bars, 50 µm. **e**, **g** Scattered plots representing wing disc area and Wg signal intensity (in arbitrary units) of the indicated genotypes. Mean and SD are shown. Number of wing discs is shown. All statistical tests are two-tailed Anova tests and, in case of more than two conditions, Dunnett's multiple comparison correction against a common control was performed. Statistically significant differences are shown: NS, $p > 0.05$; $^{**}p < 0.01$; $^{***}p < 0.001$. p values **e**: Wing disc area = 4.2×10^{-6} (Δβ/Δβ), 0.009 (Δγ/Δγ), 0.00001 (Δβγ/Δβγ); Wg = 1.1×10^{-7} (Δβ/Δβ), 7.4×10^{-6} (Δγ/Δγ), 2.5×10^{-12} (Δβγ/Δβγ), **g**: Wing disc area = 0.000018. See also Supplementary Table 7. Source data are provided as Source data file.

(Fig. 7d–f). The effects on tissue overgrowth and Wg expression were even stronger when both fragments were deleted simultaneously (in Δβγ larvae, Fig. 7d–e, we obviously selected those mutant wing discs bearing a wing primordium). Not only Wg[36] but also Wnt6 contributed to the CIN-induced tissue overgrowth, as monitored by the effects on tissue size of a null allele of *wnt6* (Fig. 7f, g). All these results indicate that the two evolutionarily conserved CRMs of the wing-specific enhancer respond to JNK and contribute, in a functionally redundant manner, to CIN-induced tissue overgrowth by driving the expression of both Wg and Wnt6.

Discussion

A *wingless* enhancer devoted to wing specification

Since the serendipitous discovery of *wg*^{1} 50 years ago[9], one of the most remarkable aspects of this mutation is the restriction of its phenotype to the absence of wings, hence its name *wingless* and that of the whole family of Wnts (a fusion of *wingless* and the vertebrate homologue, *integrated* or *int-1*). After five decades of research, this wing-specific phenotype contrasts with the highly pleiotropic effects of the *wingless* gene during the embryonic and larval development of the fly. Here we have solved this conundrum by presenting experimental evidence that the *wg*^{1} phenotype is due to the loss of an enhancer whose functional requirement is restricted to the developing wing primordium. We combined CRISPR/Cas9-mediated deletions and reporter assays to identify and narrow down the wing-specific enhancer to a 1.8-kb-long genomic region that drives Wg expression and wing fate specification in early wing discs. This enhancer contains two highly evolutionarily conserved CRMs, *Beta* and *Gamma*, which are activated in a redundant manner by a combination of pre-existing signalling molecules (Fig. 8a). Whereas Vn/EGFR signalling emanating from the most proximal part of the wing disc restricts the expression of *Beta* and *Gamma* to the most distal portion of the wing, Hh emanating from P cells induces the expression of *Gamma* in A cells (Fig. 8a). The redundant use of pre-existing signals acting independently on these two evolutionarily conserved CRMs to trigger Wg expression and wing fate specification reveals a highly robust mechanism to ensure wing development.

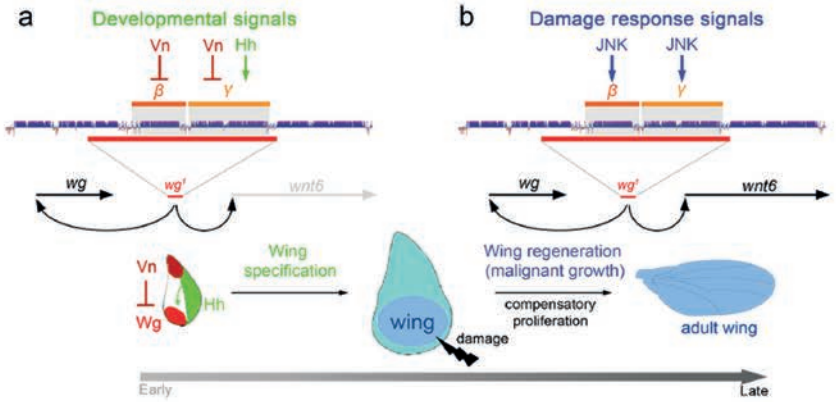

Fig. 8 | A Wnt enhancer devoted to wing fate specification, regeneration and malignant growth. a, b Cartoons depicting the redundant roles of Beta and Gamma CRMs of the *wg*^{1}-enhancer in responding to developmental (**a**) or damage response signals (**b**), and in driving wing specification through the activity of Wingless (**a**), and wing regeneration or malignant growth through the activities of Wingless and Wnt6 (**b**). Wnt6 has no major role in wing specification despite the fact that it is expressed during development in the same expression pattern as Wg.

Identification of a wing-specific enhancer driving Wg expression and wing fate specification from body wall cells in the early larval wing disc reinforces the proposal that insect wings evolved in evolution as an extension of the dorsal thorax and not directly from a proximal leg component[38,39].

Functional redundancy in driving wing regeneration

Wnts can act not only as cell fate determinants but also as mitogenic molecules. In the developing wing primordium of *Drosophila*, these two activities are separated in time and take place in two consecutive developmental stages. Whereas Wg drives wing fate specification at early larval stages[17], it promotes wing growth at later stages by mediating the organising activity of the signalling centre located in the developing wing margin[18,20]. Research carried out in the wing primordium pointed to a role of Wg in compensatory proliferation upon tissue injury[4,31], but this proposal was subsequently disputed[32,34]. The identification of the wing-specific enhancer as the one responding to the activation of the stress-induced signalling pathway JNK upon several types of tissue injuries, such as Eiger induction, physical damage or ionizing radiation-induced DNA damage, contributed to reinforcing the mitogenic role of Wg in injured tissues[13]. Unfortunately, though, functional experiments to deplete Wg expression and address its role in wing regeneration upon injury did not fully circumvent the developmental requirements of Wg in wing fate specification and growth[13,32]. Here we combined the use of CRISPR/Cas9-mediated deletions, which have no major effects on wing fate specification or growth, and reporter assays to demonstrate that the two highly evolutionarily conserved CRMs, *Beta* and *Gamma*, are activated by JNK and are functionally required in a redundant manner to drive Wg expression and compensatory proliferation upon tissue damage (Fig. 8b). The redundant and shared use of the same regulatory elements in wing fate specification and regeneration unravels a highly evolutionarily robust mechanism to ensure the development of the wing, probably the most important evolutionary innovation in insects, not only during normal development but also under stress conditions.

Wing regeneration and tumorigenesis: commonalities

Vertebrate and invertebrate tissues with strong regeneration capacity, such as the *Drosophila* wing primordium, use almost the same signalling molecules to regenerate a missing part or to induce tumorigenesis when harmful cells are maintained in the tissue upon apoptosis inhibition. In the last few years, our lab has underscored the deleterious consequences of maintaining CIN- or DNA damage-induced highly aneuploid cells in the wing epithelium[36]. CIN or DNA damage causes tumour-like overgrowths upon blockade of the apoptotic machinery, and this tumorigenic response relies mainly on the production of highly aneuploid cells that delaminate from the epithelium and activate a JNK-dependent transcriptional response. Here we present evidence that the wing-specific enhancer of the *wg* gene is activated in the same types of cells in regenerating and tumorigenic tissues. Whereas it is activated in dying cells within regenerating tissues, this activation takes place in highly deleterious aneuploid cells within CIN-tissues expressing the apoptosis inhibitor p35. JNK-driven activation of the enhancer in both cases is shown to promote Wg expression and the proliferation and growth of the wing epithelium (Fig. 8b). These results reinforce the proposal that the same type of cells (apoptotic or deleterious cells), the same molecular actor (JNK), and the same molecules (Wingless and Wnt6) mediate both tissue regeneration and tumorigenesis. The main difference between the two cases is the amount of time deleterious cells spend in the tissue before being removed by immune cells. Interestingly, similar phenomena take place in vertebrate epithelia and exactly the same actors appear to be in place[40].

A role of Wnt6 in proliferative growth

The fly wing primordium has served as a useful model system to visualise how Wg acts as fate determinant and mitogenic molecule in two consecutive developmental time points. Here we present evidence that Wnt6, which is expressed in the same cells as Wg throughout the development of the wing disc in both early and late stages, has no major role in wing fate specification but contributes to driving compensatory proliferation upon tissue damage and to producing tumour-like overgrowths upon CIN induction and additional blockage of the apoptotic pathway (Fig. 8). The mitogenic activity of Wnt6 was also identified in wing discs during normal development but only upon the depletion of Wg, the main driver of proliferative growth in these cells[18]. These data indicate that Wg activity levels might be saturated during normal development and that Wnt6 acts as a positive modulator of Wg only when a sharp increase in its activity levels is required to drive compensatory proliferation under stress conditions.

Methods

Fly maintenance, husbandry and transgene expression

Strains of *Drosophila melanogaster* were maintained on standard medium (4% glucose, 55 g/L yeast, 0.65% agar, 28 g/L wheat flour, 4 ml/L propionic acid and 1.1 g/L nipagin) at 25 °C in light/dark cycles of 12 h. The sex of experimental larvae was not considered relevant to

this study and was not determined. The strains used are summarised in Supplementary Table 8.

Expression of reporter lines in development

Flies carrying the corresponding lacZ reporters were allowed to lay eggs for 24 h at 25 °C. For those experiments aimed at monitoring the developmental dynamics in expression pattern, flies were allowed to lay eggs for 6 h. Flies carrying GAL4/UAS transgenes were switched to 29 °C or were otherwise kept at 25 °C. Second instar (L2) or early third instar (eL3), mild third instar (mL3) and late third instar (L3) larvae were dissected at day 3, 4 or 5, respectively.

Expression of reporter lines in regeneration

In the case of Eiger-induced cell death, females of the following genotype *wg^{1}-lacZ/CyO,GFP; rotund-GAL4,tubulin-GAL80^{ts},UAS-egr/TM6B,tubulin-GAL80* were crossed with males of the following genotype: *GFP-Wg* or *nls-wnt6-GFP* and allowed to lay eggs for 24 h at 18 °C. Developing animals were kept at 18 °C until day 7 when they were switched to 29 °C for 16 h and dissected immediately after to isolate wing discs for immunostainings. In the case of Reaper-induced cell death, females of the following genotypes *wg^{1}-lacZ/CyO,GFP; spalt-lexA,tub-Gal80^{ts}*, or *GFP-Wg/CyO,GFP; spalt-lexA,tub-Gal80^{ts}*, or *nls-wnt6-GFP/CyO,GFP; spalt-lexA,tub-Gal80^{ts}* were crossed with males carrying the *lexO-reaper* transgene (genotype: *lexO-rpr/Cyo; MKRS/TM6B*) and allowed to lay eggs for 24 h at 18 °C. Developing animals were kept at 18 °C until day 7 when they were switched to 29 °C for 11 h and dissected immediately after to isolate wing discs for immunostainings.

Regeneration experiments

Flies were allowed to lay eggs for 6 h at 18 °C. Developing animals of the following genotypes: (1) *+/+; rotund-GAL4,tubulin-GAL80^{ts},UAS-egr/+*, (2) *Δβ/Δβ; rotund-GAL4,tubulin-GAL80^{ts},UAS-egr/+* (3) *ΔɣΔɣ; rotund-GAL4,tubulin-GAL80^{ts},UAS-egr/+*, (4) *ΔβɣΔβɣ; rotund-GAL4,tubulin-GAL80^{ts},UAS-egr/+;* (5) *+/+; rotund-gal4, tubulin-GAL80^{ts}, UAS-egr/UAS-egfp-i*, (6) *+/+; rotund-gal4, tubulin-GAL80^{ts}, UAS-egr/UAS-wnt6-i, (7) Δβ/Δɣ; rotund-GAL4, tubulin-GAL80, UAS-egr/+*, were kept at 18 °C until day 7 when they were switched to 29 °C to induce *eiger* expression for 16 h. Larvae were either dissected immediately after to isolate wing discs for immunostainings to analyse Wg intensity, number of pH3-positive cells and EdU incorporation, or returned to 18 °C until adulthood to allow regeneration. Experimental flies and control individuals were grown in parallel.

Standard induction of CIN

Flies were allowed to lay eggs on standard fly food for 24 h (for the expression of reporter lines) or 8 h (for the quantification of tissue size) at 25 °C, larvae kept at 25 °C for an additional day, switched to 29 °C and dissected 4 days thereafter. Experimental flies and control individuals were grown in parallel. The larval genotypes used in Fig. 7 were the following: (1) *wg^{1}-lacZ/ wg:GFP; hh-GAL4 /UAS-rod-RNAi, UAS-p35* (Fig. 7a); (2) *wg^{1}-lacZ/ GFP-Wnt6; hh-GAL4/UAS-rod-RNAi, UAS-p35/+* (Fig. 7a); (3) *en*-GAL4*/reporter-lacZ; UAS-rod-RNAi, UAS-p35/+* (Fig. 7b); (4) *UAS-bsk-DN/+; en-GAL4*/reporter-lacZ; *UAS-rod-RNAi, UAS-p35/+* (Fig. 7c); (5) *+/+; hh-GAL4/UAS-rod-RNAi, UAS-p35* (Fig. 7d, e); (6) *Δβ/Δβ; hh-GAL4/UAS-rod-RNAi, UAS-p35* (Fig. 7d, e); (7) *ΔɣΔɣ; hh-GAL4/UAS-rod-RNAi, UAS-p35* (Fig. 7d, e); (8) *ΔβɣΔβɣ; hh-GAL4/UAS-rod-RNAi, UAS-p35* (Fig. 7d, e); and (9) *wnt6KO/wnt6KO; hh-GAL4/UAS-rod-RNAi, UAS-p35* (Fig. 7f, g).

Immunohistochemistry

Wing, haltere, and leg imaginal discs, brains and ring glands of the indicated larval stage were dissected in cold PBS, fixed in 4% formaldehyde for 20 min, washed three times in PBT (PBS1%, 0.2% Triton), blocked for 45 min in BBT (PBS1X, 0.3% BSA, 0.2% Triton, 250 mM NaCl), and incubated overnight with the following antibodies (see also Supplementary Table 8): mouse anti-MMP1 (1:50; 14A3D2, Developmental Studies Hybridoma Bank, DSHB); goat polyclonal anti-GFP (1:300; ab6673, Abcam); rabbit anti-β-galactosidase (1:600; 0855976, Cappel (MP Biochemicals)); mouse anti-β-galactosidase (40.1a, DSHB); rabbit anti-PH3 (1:1000; Merk Millipore); rat anti-Ci (1:10; 2A1, DSHB); mouse anti-Wg (1:50; 4D4, DSHB); mouse anti-Nubbin (1:50; nub2D4, DSHB); and rabbit anti-Tsh (1:100) kindly provided by S. Cohen. Discs were rinsed with BBT and incubated with secondary antibodies [Cy2, Cy3 and Cy5 (1:400), Jackson ImmunoResearch] and DAPI for 90 min. After 4 washes with PBT, discs were kept on mounting media (80 ml glycerol + 10 ml PBS 10x + 0.8 ml N-propyl-gallate 50%). The most representative images are shown in all experiments. At least 10–15 wing discs per genotype were imaged.

DNA synthesis

Click-iT™ Plus EdU Alexa Fluor™ 647 Imaging Kit from Invitrogen (C10640) was used to measure DNA synthesis (S phase) in regenerating wing discs, following the manufacturer's indications. EdU (5-ethynyl-2′-deoxyuridine) provided in the kit is a nucleoside analogue of thymidine and is incorporated into DNA during active DNA synthesis. Time of incubation with EdU: 10 min. Experiments were carried out 3 consecutive days and 23–27 wing discs per genotype were imaged.

Analysis of sequence conservation

Conservation of the CRMs spanning the *wg^{1}*-enhancer (*Alpha*, *Beta*, *Gamma* and *Delta*, Supplementary Fig. 2) was performed at the University of California Santa Cruz (UCSC) Genome Browser on *Drosophila melanogaster* (BDGP Release 6). In brief, multiple alignments of 27 insect species (23 *Drosophila* species, and *Musca Domestica*, *Anopheles gambiae*, *Apis melifera* and *Tribolium castaneum*) and measurements of evolutionary conservation used two methods (phastCons[41] and phyloP) from the PHAST package (http://compgen.cshl.edu/phast/), for all 27 species. Multiz and other tools in the UCSC/Penn State Bioinformatics comparative genomics alignment pipeline (http://www.bx.psu.edu/miller_lab/) were used to generate multiple alignments. For more details, see description of methods at https://genome-euro.ucsc.edu/index.html.

Generation of *lacZ*-reporter lines

Different regions of the *wg^{1}*-containing enhancer named *Alpha* to *Delta*, *wnt6 Intron* and *SpdFlag* (Supplementary Table 1) were amplified by PCR from genomic DNA extracted from *w^{1118}* flies, using the suitable primers detailed in Supplementary Table 8. PCR products were digested with EcoRI/KpnI or KpnI/NotI restriction enzymes, gel-purified (NZYGelpure) and ligated into the pHs43nLacz vector previously digested with the same enzymes. Final constructs were checked by restriction, sequenced and sent for injection for transgenic generation in the *w^{1118}* background. At least six independent insertions per construct were analysed and shown to drive a reproducible expression pattern.

Prediction of transcription factor binding sites

Predictions of binding sites in the *wg^{1}* region (see Supplementary Table 1 for coordinates) were performed using the Matscan software[42]. Position weight matrices were obtained from JASPAR 2020-all organisms[43], and MEME v12.21 Fly Factor Survey collection (https://meme-suite.org/meme/db/motifs). Matrix logos were plotted using the seqLogo R package (https://bioconductor.org/packages/release/bioc/html/seqLogo.html). Conservation score was taken from the evolutionary conservation track from UCSC (https://genome.ucsc.edu/index.html) for 26 species close to *Drosophila melanogaster* (DM6). Method of computation for conservation score: phastCons[41]. *p*-values were computed by permutation test in 1000 random genomic sequences of the same length as the analysed query sequence(s).

Predicted binding sites that overlapped using the same position weight matrix were merged and presented in Supplementary Tables 2–5, where maximum and average match score (score.max, score.avg), maximum and average conservation score (cons.max, cons.avg), and minimum and maximum permutation test *p*-value (pv.min, pv.max) for all individual hits within the overlapping region are shown.

Generation of *Gamma* and *Gamma*-590 reporters carrying mutations in the Ci binding site

To introduce the Ci mutation in the *Gamma*-LacZ reporter, two independent PCRs were performed using the pHsnLacZ-*Gamma* as a template. The first PCR introduced the mutation GCGT**G**T**G**GTCT → GCGT**A**T**A**GTCT in the Reverse primer (see PCR1 wg-*Gamma*Ci mut on Supplementary Table 8) and the second PCR introduced the same mutation on the Fwd primer (see PCR2 wg-*Gamma*Ci mut on Supplementary Table 8). A third PCR was performed on the mixed PCR1 and PCR2 products using the wg-*Gamma* Fwd and wg-*Gamma* Rev primers. The final product was 1145 bp long bearing the mutation in the Ci binding site. The wg-*Gamma*-mut was digested and cloned into the pHsnLacZ vector. To obtain the *Gamma*-590Cimut-LacZ reporter, a PCR with the *Gamma*590-Fwd and *Gamma*-Rev was performed using the pHsnLacZ-*Gamma*Cimut construct as a template. The PCR product was digested and cloned in the pHsnLacZ vector. Final constructs were checked by restriction, sequenced and sent for injection for transgenic generation in the w^{1118} background.

Generation of wg^1-reporter carrying mutations in AP1 binding sites

Five AP1 binding sites were present in the wg^1-enhancer and AP1 binding sites 1 to 4 (oriented 5′ to 3′ in Fig. 6a) were mutated (labelled with stars in Fig. 5a). These four AP1 binding sites were mutated introducing XbaI restriction sites in oligos. For sites 1 and 4 the following mutations were introduced: CGCGCTTATGTTTCTA**TGAT TC**AGCAGCCAGATT → CGCGCTTATGTTTCTA**TCTAGA**AGCAGCCAG ATT. TCTCTGCTGGCTGACGT**TTAGTC**ATAAAATATTCCA → TCTCTG CTGGCTGACGT**TCTAGA**ATAAAATATTCCA. The two oligos were annealed to vector pBS-wg^1 followed by PCR polymerase reaction, Klenow blunt, ligation, DpnI digestion and transformation. Minipreps were checked by XbaI restriction. Mutations 2 and 3 were introduced performing independent PCRs using pBSK-wg^1 Mut1&4 as a template. For Mutation 2 the first PCR introduced the mutation TAGC**TGACT-C**ACTC → TAGC**TCTAGA**ACTC on the Reverse primer and the second PCR introduced the same mutation on the Forward primer. A third PCR was performed on the mixed PCRs products using wg-AP1 Fwd and wg-AP1 Rev primers. For Mutation 3 the same strategy was used introducing mutation AGTC**TGACTA**ATAC → AGTC**TCTAGA**ATAC. The final vector pBSK-wg^1 Mut1,2,3&4 was sequenced, digested KpnI/NotI and cloned into the pHsnLacZ vector.

Generation of wg^1-enhancer deletions with the CRISPR/Cas9 technique

gRNAs Up and Down to generate the different wg^1-enhancer deletions were cloned in the pBFv-U6.2B vector in three steps as follows:

1. gRNA_Up was designed, and sticky ends for BbsI were added to the 5′ end of the Fwd (CTTC) and Rev (AAAC) oligos (see Supplementary Table 8). 9.5 µl of Fwd and Rev oligos at a concentration of 100 µM were mixed with 1 µl of SSC20X, boiled for 5 min and allowed to cool down overnight in a 1 L water bath for efficient annealing. 1 µl of 1/20 dilution of the mix was used to ligate with the pBFv-U6.2 plasmid previously digested with BbsI. Ligation was transformed into DH5*Alpha* competent bacteria and 3 colonies were selected for DNA miniprep and sequencing with the T3 primer.

2. gRNA-Down was designed, and sticky ends for BbsI were added to the 5′ end of the Fwd (CTTC) and Rev (AAAC) oligos (see Supplementary Table 8). Fwd and Rev oligos were annealed and ligated in the pBFv-U6.2B plasmid previously digested with BbsI. Ligation was transformed and 3 positive colonies were selected for checking and sequencing.

3. pBFv-U6.2-gRNA_Up was digested with EcoRI/NotI and the gRNA_Up insert was gel-purified and ligated with the pBFv-U6.2B-gRNA_Down, previously digested with EcoRI/NotI. Five colonies were selected for plasmid preparation and sequenced with the T3 primer.

One positive colony pBFv-U6.2B-gRNA_Up+Down was selected for Maxiprep and the DNA was used for injection into *y¹v¹P{nos-phiC31\int.NLS}X; P{CaryP}attP40* (BL 25709) flies. Trangenics were identified as *v+* individuals.

gRNAup+down transgenic flies were then crossed to *y¹ cho v¹; attP40.nosCas9/Cyo* flies to generate the deletions in the germline. Five males from the progeny that carried gRNAUp+Down and the Cas9 were individually crossed with *v¹; Sco/SM6a* (BL137) females. In a second step, 5 to 10 males from each cross were selected and individually backcrossed with *v¹; Sco/SM6a* females. 2–3 individuals from each established stock were used for genomic extraction and PCR checking to identify the mutant lines (see Supplementary Table 8).

Molecular characterisation of deletions

To identify CRISPR mutants, genomic DNA was extracted from individuals of 10–15 different candidate lines. For this purpose, 2–3 flies from each line were squashed in 300 µL of homogenizing buffer (0.1 M Tris-HCl pH 9, 0.1 M EDTA, 1% SDS) and the mix incubated at 65 °C for 30 min. After incubation, 67.8 µl of KAc was added and tubes were kept on ice for 30 min. Samples were centrifuged for 10 min at 4 °C, the supernatant was transferred to a new tube and DNA was precipitated by adding 0.5 volumes of isopropanol, incubated 5 min at RT and centrifuged again for 5 min at RT. The pellet was washed with 70% EtOH and resuspended in 50 µl of TE. 1 µl was then used to perform a PCR with the suitable primers (see Supplementary Table 8). PCR products from samples that showed the expected deletions were gel-purified and sent for Sanger sequencing to characterise indels.

Quantification

(1) Wing to notum transformation: each heminotum was considered an independent event. The percentage of wing to notum transformation (loss of wings and appearance of an ectopic heminotum where bristles showed reverse polarity) was calculated by dividing the number of transformed heminota by the total number of heminota (% wing to notum transformation = (*n* transformed heminota/*n* total heminota) × 100). Representative pictures of the phenotype were obtained.

(2) Adult wing regeneration: Adult flies were collected in SH buffer (75% glycerol, 25% ethanol) and wings were dissected in water and mounted in Faure's mounting medium. Regenerated wings were scored using Fiji Software (NIH, USA). They were considered regenerated when they were capable of reaching a regular size. No patterning problems were considered when assessing the regenerative potential. The percentage of regenerated wings was calculated by dividing the number of regenerated wings by the total number of scored wings (% regenerated wings = (*n* regenerated wings/*n* total wings) × 100).

(3) Wing disc size upon CIN: The sizes of the whole wing disc (based on DAPI staining) were measured manually using Fiji Software (NIH, USA) on Z-projection of the wing disc obtained using a Zeiss LSM780 confocal microscope at ×25 glycerol immersion objective with 1.5 µm per optical section covering the entire thickness of each disc.

(4) Wingless signal intensity: Wingless areas in the pouch of regenerating wing discs and in the pouch and hinge of the P compartment of wing discs subjected to CIN (based on the absence of Ci expression) were selected using the polygonal tool of Fiji Software (NIH, USA). Wingless intensity (in arbitrary units, a.u.) was measured upon setting a fluorescence threshold for the corresponding channel.

Image stacks were obtained using a Zeiss LSM780 confocal microscope at ×40 oil immersion objective with 1.5 µm per optical section for regenerating discs, and at ×25 glycerol immersion objective with 1.5 µm per optical section for wing discs subjected to CIN. The entire thickness of each disc was covered in both cases. Maximum intensity Z-projection was performed on the stacks prior to quantification.

(5) Mitotic activity: Mitosis was measured by counting mitotic cells (pH3-positive cells) present in an area slightly broader to the one of the Wg expression domain (red lines in Fig. 6c) of regenerating wing discs using the Fiji Software (NIH, USA). Image stacks were obtained using a Zeiss LSM780 confocal microscope under a ×40 oil immersion objective with 1.5 µm per optical section to cover the entire thickness of each disc. The ratio between the number of mitotic cells and Wg area (sizes measured in arbitrary units, a.u., using the polygonal tool on Fiji) was calculated.

(6) EdU incorporation: The region comprising the wing pouch and hinge primordia was selected using the polygonal tool of Fiji and the area was quantified. EdU positive area within this region was measured using a Macro created in Fiji. The ratio between the areas of EdU incorporation and wing pouch and hinge regions (sizes measured in arbitrary units, a.u.) was calculated. Experiments were carried out in parallel in all the genotypes analysed and experiments were repeated three times.

Microscopy

Larval discs or tissues were analysed and scanned with a LSM 780 Zeiss confocal microscope. Adult wings, nota and eyes were analysed and pictured with an Olympus MVX10 macroscope. Regenerating wings were imaged using an ECLIPSE E600 microscope coupled to a NIKON DSRi2 camera.

Statistics and reproducibility

The statistical analysis for comparison of means was performed by linear regression using the experimental batch as adjusting variable. Normality assumption was tested for every fitted model, applying a log2-transformation of the data when necessary. However, for clarity of representation, data are shown in the original scale. The statistical analysis for comparison of percentages of regenerated wings was performed by logistic regression using the experimental batch as adjusting variable. In both types of models, Dunnett's multiple comparisons correction was applied when comparing the means/percentages of several experimental groups with a common control. Differences were considered significant when adjusted p values were <0.001 (***), 0.01 (**) or 0.05 (*). Statistical analysis was carried out with the multcomp[44] R package. All genotypes included in each histogram or scatter plot were subjected to the same experimental conditions (temperature and time of transgene induction) and analysed in parallel, and all experimental quantifications were carried out at least three times in different days with at least 12 wing discs, 27 adult wings and 22 heminota per genotype. Information about the n values, p values, and statistical tests used can be found in the figure legends and in Supplementary Tables 6, 7. Representative micrographs of at least 10 different wing discs of the indicated age, genotype and immunostaining are shown in the figures.

Reporting summary

Further information on research design is available in the Nature Research Reporting Summary linked to this article.

Data availability

Source data are provided with this paper.

References

1. Clevers, H. Wnt/beta-catenin signaling in development and disease. *Cell* **127**, 469–480 (2006).
2. Logan, C. Y. & Nusse, R. The Wnt signaling pathway in development and disease. *Annu. Rev. Cell Dev. Biol.* **20**, 781–810 (2004).
3. Kawakami, Y. et al. Wnt/beta-catenin signaling regulates vertebrate limb regeneration. *Genes Dev.* **20**, 3232–3237 (2006).
4. Smith-Bolton, R. K., Worley, M. I., Kanda, H. & Hariharan, I. K. Regenerative growth in *Drosophila* imaginal discs is regulated by Wingless and Myc. *Dev. Cell* **16**, 797–809 (2009).
5. Lengfeld, T. et al. Multiple Wnts are involved in Hydra organizer formation and regeneration. *Dev. Biol.* **330**, 186–199 (2009).
6. Chera, S. et al. Apoptotic cells provide an unexpected source of Wnt3 signaling to drive hydra head regeneration. *Dev. Cell* **17**, 279–289 (2009).
7. Zhan, T., Rindtorff, N. & Boutros, M. Wnt signaling in cancer. *Oncogene* **36**, 1461–1473 (2016).
8. Shlyueva, D., Stampfel, G. & Stark, A. Transcriptional enhancers: from properties to genome-wide predictions. *Nat. Rev. Genet.* **15**, 272–286 (2014).
9. Sharma, R. P. Wingless—a new mutant in *D. melanogaster*. *D. I. S.* **50**, 134 (1973).
10. Bejsovec, A. Wingless signaling: a genetic journey from morphogenesis to metastasis. *Genetics* **208**, 1311–1336 (2018).
11. Vizcaya-Molina, E. et al. Damage-responsive elements in *Drosophila* regeneration. *Genome Res.* **28**, 1852–1866 (2018).
12. Harris, R. E., Stinchfield, M. J., Nystrom, S. L., McKay, D. J. & Hariharan, I. K. Damage-responsive, maturity-silenced enhancers regulate multiple genes that direct regeneration in *Drosophila*. *Elife* **9**, 1–26 (2020).
13. Harris, R. E., Setiawan, L., Saul, J. & Hariharan, I. K. Localized epigenetic silencing of a damage-activated WNT enhancer limits regeneration in mature *Drosophila* imaginal discs. *Elife* **5**, e11588 (2016).
14. Baker, N. E. Molecular cloning of sequences from wingless, a segment polarity gene in Drosophila: the spatial distribution of a transcript in embryos. *EMBO J.* **6**, 1765–1773 (1987).
15. Sharma, R. P. & Chopra, V. L. Effect of the wingless (wg1) mutation on wing and haltere development in Drosophila melanogaster. *Dev. Biol.* **48**, 461–465 (1976).
16. Couso, J. P., Bate, M. & Martinez Arias, A. A wingless-dependent polar coordinate system in the imaginal discs of *Drosophila*. *Science* **259**, 484–489 (1993).
17. Ng, M., Diaz-Benjumea, F. J., Vincent, J. P., Wu, J. & Cohen, S. M. Specification of the wing by localized expression of wingless protein. *Nature* **381**, 316–318 (1996).
18. Barrio, L. & Milán, M. Regulation of anisotropic tissue growth by two orthogonal signaling centers. *Dev. Cell* **52**, 659–672.e3 (2020).
19. Baena-Lopez, L. A., Franch-Marro, X. & Vincent, J. P. Wingless promotes proliferative growth in a gradient-independent manner. *Sci. Signal* **2**, ra60 (2009).
20. Diaz-Benjumea, F. J. & Cohen, S. M. Serrate signals through Notch to establish a Wingless-dependent organizer at the dorsal/ventral compartment boundary of the *Drosophila* wing. *Development* **121**, 4215–4225 (1995).
21. Phillips, R. & Whittle, J. R. S. wingless expression mediates determination of peripheral nervous system elements in late stages of *Drosophila* wing disc development. *Development* **118**, 427–438 (1993).
22. Yu, J. J. S. et al. Frizzled-dependent planar cell polarity without secreted Wnt ligands. *Dev. Cell* **54**, 583–592.e5 (2020).
23. Ewen-Campen, B., Comyn, T., Vogt, E. & Perrimon, N. No evidence that Wnt ligands are required for planar cell polarity in *Drosophila*. *Cell Rep.* **32**, 08121 (2020).
24. van den Heuvel, M., Harryman-Samos, C., Klingensmith, J., Perrimon, N. & Nusse, R. Mutations in the segment polarity genes wingless and porcupine impair secretion of the wingless protein. *EMBO J.* **12**, 5293–5302 (1993).

25. Johnson, R. L., Grenier, J. K. & Scott, M. P. Patched overexpression alters wing disc size and pattern: transcription and post-transcriptional effects on hedgehog targets. *Development* **121**, 4161–4170 (1995).
26. Restrepo, S., Zartman, J. J. & Basler, K. Coordination of patterning and growth by the morphogen DPP. *Curr. Biol.* **24**, R245–R255 (2014).
27. Wang, S. H., Simcox, A. & Campbell, G. Dual role for *Drosophila* epidermal growth factor receptor signaling in early wing disc development. *Genes Dev.* **14**, 2271–2276 (2000).
28. Recasens-Alvarez, C., Ferreira, A. & Milan, M. JAK/STAT controls organ size and fate specification by regulating morphogen production and signalling. *Nat. Commun.* **8**, 13815 (2017).
29. Morata, G. & Lawrence, P. A. The development of wingless, a homeotic mutation of *Drosophila*. *Dev. Biol.* **56**, 227–240 (1977).
30. Doumpas, N., Jékely, G. & Teleman, A. A. Wnt6 is required for maxillary palp formation in *Drosophila*. *BMC Biol.* **11**, 104 (2013).
31. Ryoo, H. D., Gorenc, T. & Steller, H. Apoptotic cells can induce compensatory cell proliferation through the JNK and the Wingless signaling pathways. *Dev. Cell* **7**, 491–501 (2004).
32. Herrera, S. C., Martín, R. & Morata, G. Tissue homeostasis in the wing disc of *Drosophila melanogaster*: immediate response to massive damage during development. *PLoS Genet.* **9**, e1003446 (2013).
33. Perez-Garijo, A. et al. The role of Dpp and Wg in compensatory proliferation and in the formation of hyperplastic overgrowths caused by apoptotic cells in the *Drosophila* wing disc. *Development* **136**, 1169–1177 (2009).
34. Díaz-García, S. & Baonza, A. Pattern reorganization occurs independently of cell division during *Drosophila* wing disc regeneration in situ. *Proc. Natl Acad. Sci. USA* **110**, 13032–13037 (2013).
35. Uhlirova, M. & Bohmann, D. JNK- and Fos-regulated Mmp1 expression cooperates with Ras to induce invasive tumors in *Drosophila*. *EMBO J.* **25**, 5294–5304 (2006).
36. Dekanty, A., Barrio, L., Muzzopappa, M., Auer, H. & Milan, M. Aneuploidy-induced delaminating cells drive tumorigenesis in *Drosophila epithelia*. *Proc. Natl Acad. Sci. USA* **109**, 20549–20554 (2012).
37. Muzzopappa, M., Murcia, L. & Milan, M. Feedback amplification loop drives malignant growth in epithelial tissues. *Proc. Natl Acad. Sci. USA* **114**, E7291–E7300 (2017).
38. Bruce, H. S. & Patel, N. H. Knockout of crustacean leg patterning genes suggests that insect wings and body walls evolved from ancient leg segments. *Nat. Ecol. Evol.* **4**, 1703–1712 (2020).
39. Clark-Hachtel, C. M. & Tomoyasu, Y. Two sets of candidate crustacean wing homologues and their implication for the origin of insect wings. *Nat. Ecol. Evol.* **4**, 1694–1702 (2020).
40. Ankawa, R. et al. Apoptotic cells represent a dynamic stem cell niche governing proliferation and tissue regeneration. *Dev. Cell* **56**, 1900–1916.e5 (2021).
41. Siepel, A. et al. Evolutionarily conserved elements in vertebrate, insect, worm, and yeast genomes. *Genome Res.* **15**, 1034–1050 (2005).
42. Blanco, E., Messeguer, X., Smith, T. F., Guigo, R. & Guigó, R. Transcription factor map alignment of promoter regions. *PLoS Comput. Biol.* **2**, e49 (2006).
43. Khan, A. et al. JASPAR 2018: update of the open-access database of transcription factor binding profiles and its web framework. *Nucleic Acids Res.* **46**, D1284 (2018).
44. Hothorn, T., Bretz, F. & Westfall, P. Simultaneous inference in general parametric models. *Biometrical J.* **50**, 346–363 (2008).

Acknowledgements

We thank I. Guerrero, I. Hariharan, R.E. Harris, J.P. Vincent, G. Schubiger, F. Serras, A. Teleman, and the Bloomington *Drosophila* Stock Center (USA), the Vienna Drosophila Resource Center (Austria), and the Developmental Studies Hybridoma Bank (USA) for flies and antibodies, Lara Barrio and Elena Fusari for comments on the manuscript, and the IRB Advanced Digital Microscopy (ADM) and Biostatistics and Bioinformatics Facilities for support. This work was funded by the *BFU2016-77587-P* and *PID2019-110082GB-I00* grants to M.Milán from the Spanish Ministry of Science and Competitiveness, and ERDF "Una manera de hacer Europa". We gratefully acknowledge institutional funding from the Spanish Ministry of Science and Competitiveness through the Centres of Excellence Severo Ochoa Award, and from the CERCA Programme of the Government of Catalonia.

Author contributions

E.G., L.P., M.Muzzopappa and M.Milán conceived and designed the experiments, E.G., L.P. and M.Muzzopappa performed the experiments, all authors analysed the data, and M.Milán wrote the paper.

Competing interests

The authors declare no competing interests.

Additional information

Supplementary information The online version contains supplementary material available at https://doi.org/10.1038/s41467-022-32400-2.

Correspondence and requests for materials should be addressed to Marco Milán.

Peer review information *Nature Communications* thanks Salvador Herrera and the other, anonymous, reviewer(s) for their contribution to the peer review of this work. Peer reviewer reports are available.

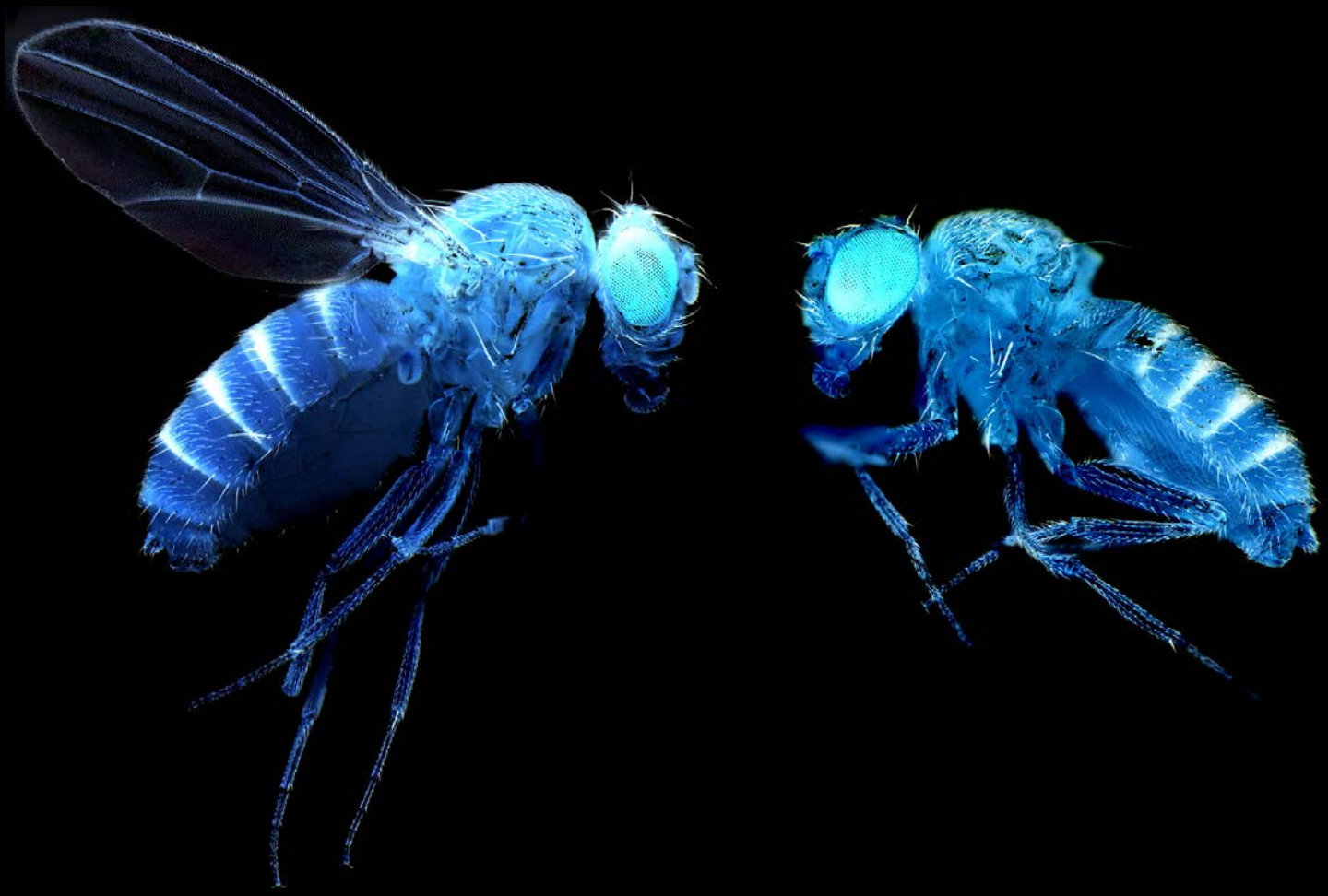

UNIVERSITAT DE BARCELONA